



Universidade do Minho
Escola de Engenharia

Javier Ortega Heras Reduction of the seismic vulnerability of vernacular
architecture with traditional strengthening solutions

Javier Ortega Heras

Reduction of the seismic vulnerability of
vernacular architecture with traditional
strengthening solutions



Universidade do Minho
Escola de Engenharia

Javier Ortega Heras

Reduction of the seismic vulnerability of
vernacular architecture with traditional
strengthening solutions

Tese de Doutoramento
Engenharia Civil

Trabalho efetuado sob a orientação do
Professor Graça Vasconcelos
Professor Hugo Rodrigues
Professor Mariana Correia

March, 2018

STATEMENT OF INTEGRITY

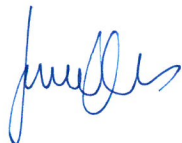
I hereby declare having conducted my thesis with integrity. I confirm that I have not used plagiarism or any form of falsification of results in the process of the thesis elaboration.

I further declare that I have fully acknowledged the Code of Ethical Conduct of the University of Minho.

University of Minho, March 28th 2018

Full name: Javier Ortega Heras

Signature:

A handwritten signature in blue ink, appearing to read 'Javier Ortega Heras', written in a cursive style.

ACKNOWLEDGEMENTS

First of all, I would like to thank my supervisors for all the support and guidance. I am very grateful to Professor Graça Vasconcelos for making this work possible by sharing her knowledge, her time and her attention, but also because of the opportunity that she gave me to participate in many other activities within the group. I am also thankful to Professor Hugo Rodrigues for his guidance, which has been essential for the development of this work, for his permanent availability to discuss and for his constant support. I would like to thank Professor Mariana Correia for being also part of this work and greatly contribute with her always appropriate suggestions, as well as words of support. Thank you all for your involvement in this research. It has been a real pleasure working with you all. I hope we can continue doing so in the future.

To Professor Paulo Lourenço, I would like to express my deepest gratitude for the opportunity he gave me to work in the historical masonry research group at the University of Minho. It has been an outstanding environment to develop this work. Many of the colleagues within the group have contributed to this research. I am particularly thankful to Dr. Tiago Ferreira, who has provided essential information to develop this thesis, but also to Dr. Nuno Mendes, for his help with the numerical part of the work, and to Dr. Tiago Miranda, whose contribution on the statistical part has been crucial for accomplishing the thesis objectives.

Many thanks to all my colleagues and friends from the University I was lucky to work with and from whom I learned a lot. These years have been also full of good times and amazing memories thanks to them. Thanks to Worajak Janwaen, Chrysl Aranha, Susana Moreira, Federica Freco, Angelo Gaetani, João Almeida, Leonardo Rodrigues, Luis Silva and others that contribute to make these wonderful years. Particularly, I would like to thank Giorgos Karanikoloudis for all the discussion and his interest in my work and support. Some of the best ideas for the thesis arose from those conversations we had.

Special thanks to my parents and sister for their endless support, encouragement and love.

To Marieta, thank you for being always there.

Finally, I would like to dedicate this thesis to Dr. Savvas Saloustros for stealing his name.

ABSTRACT

The valorization and preservation of vernacular architecture, as well as traditional construction techniques and materials, is a key-element for cultural identity. As part of this essential objective, the present thesis focuses on vernacular architecture earthquake preparedness, with a particular focus on the Portuguese case. Conservation efforts are often mainly focused on historical constructions and monuments. Furthermore, more detailed and sophisticated seismic vulnerability assessment approaches typically used for monumental buildings require time, cost and resources that are not commonly assigned to the study of vernacular architecture. Earthquakes come unexpectedly, endangering in-use vernacular architecture and the population who inhabits it. That is why the development of a simplified method for the seismic vulnerability assessment of vernacular architecture is of paramount importance.

The present research establishes four clear objectives that are accomplished through the development of four research tasks structured along the nine chapters that composed this document. The first part of the thesis is dedicated to the investigation of traditional strengthening construction techniques developed empirically by local communities to protect their built-up environment, based on literature review and on-site visits. The second part deals with the development of two seismic vulnerability assessment methods for vernacular architecture: (1) Seismic Vulnerability Index for Vernacular Architecture (SVIVA); and (2) Seismic Assessment of the Vulnerability of Vernacular Architecture Structures (SAVVAS). The development of these two methods composes the main body of the thesis, which is carried out on the basis of an extensive numerical modeling campaign that also helped to gain a deeper quantitative knowledge on the seismic behavior of representative examples of existing Portuguese vernacular architecture.

The third part of the thesis addresses the numerical investigation of traditional strengthening construction solutions identified within the first part. It is mainly intended to validate their efficiency in mitigating the seismic vulnerability of vernacular architecture for their eventual application. Finally, the thesis deals with the application of the two methods in two different case studies. This part allows calibrating the two methods, as well as validating their applicability as first level seismic vulnerability assessment approaches.

Keywords: vernacular architecture, local seismic culture, traditional earthquake resistant techniques, seismic retrofitting, pushover analysis, numerical parametric study, seismic vulnerability assessment methods, seismic loss assessment

RESUMO

A valorização e conservação da arquitetura vernácula, assim como das técnicas e materiais tradicionais de construção, é um elemento chave de identidade cultural. A presente tese centra-se na arquitetura vernácula e na sua preparação para fazer face aos terremotos, em particular no caso português. Os esforços de conservação centram-se em geral nas construções históricas. Abordagens muito detalhadas e sofisticadas para a avaliação da vulnerabilidade sísmica são, sobretudo, aplicáveis em edifícios históricos e monumentais, porque requerem um tempo, um custo e uma quantidade de recursos que não podem ser atribuídos ao estudo da arquitetura vernácula. Contudo, os sismos são inesperados e põem em risco a arquitetura vernácula e os seus habitantes. É por isso que o desenvolvimento de um método simplificado para a avaliação da vulnerabilidade sísmica da arquitetura vernácula é de suma importância.

A presente investigação estabelece quatro objetivos que são atingidos através do desenvolvimento de quatro tarefas organizadas em nove capítulos que compõem este documento. A primeira parte da tese centra-se no estudo de técnicas tradicionais de reforço desenvolvidas por comunidades locais empiricamente, com o objetivo de proteger os seus edifícios das ações sísmicas. Esta parte inclui a revisão da literatura e a investigação *in-situ*. A segunda parte dedica-se a desenvolver dois métodos para a avaliação da vulnerabilidade sísmica da arquitetura vernácula: (1) *Seismic Vulnerability Index for Vernacular Architecture* (SVIVA); e (2) *Seismic Assessment of the Vulnerability of Vernacular Architecture Structures* (SAVVAS). O desenvolvimento destes métodos compõe o corpo principal da tese, baseado num extenso trabalho de modelação numérica, que também contribui para se obter um melhor conhecimento do comportamento sísmico de exemplos existentes e representativos da arquitetura vernácula portuguesa.

A terceira parte aborda a investigação numérica das soluções de reforço tradicionais identificadas previamente e destina-se principalmente à validação da sua eficiência na mitigação da vulnerabilidade sísmica da arquitetura vernácula, para assim poder ser aplicadas em edifícios existentes. A tese é concluída com a aplicação dos dois métodos desenvolvidos, em dois casos de estudo. Esta parte contribui para a calibração dos métodos, além da validação da sua aplicabilidade como abordagem de primeiro nível na avaliação da vulnerabilidade sísmica.

Palavras-chave: arquitetura vernácula, cultura sísmica local, técnicas tradicionais sismo-resistentes, reforço sísmico, análise *pushover*, estudo paramétrico numérico, métodos de avaliação da vulnerabilidade sísmica, avaliação de perdas sísmicas

TABLE OF CONTENTS

Chapter 1 Introduction

1.1. Background and motivation	1
1.2. Thesis objectives	4
1.3. Research methodology	5
1.4. Outline and organization of the thesis	9

Chapter 2 Traditional earthquake resistant techniques for vernacular architecture and local seismic culture

2.1. Introduction	13
2.2. Basic concepts	15
2.2.1. Vernacular architecture and local seismic culture	15
2.2.2. Earthquake performance of vernacular constructions	17
2.2.2.1. Poor connection between structural elements	18
2.2.2.2. Out-of-plane wall collapse	18
2.2.2.3. Delamination of wall leaves	19
2.2.2.4. In-plane shear failure	20
2.2.2.5. Poor workmanship and maintenance	20
2.3. Traditional seismic resistant building practices	21
2.3.1. Techniques improving the connections between structural elements	23
2.3.2. Techniques stabilizing structural elements and buildings	28
2.3.2.1. Masonry walls	28
2.3.2.2. Floors and roofs	31
2.3.2.3. Timber frames as earthquake resistant systems	32
2.3.3. Techniques allowing partial collapse of structural elements	33
2.3.4. Techniques counteracting horizontal loads	35
2.3.4. Summary	37
2.4. Seismic-V project: Vernacular seismic culture in Portugal	38
2.5. Conclusions	39

Chapter 3 Definition of a seismic vulnerability assessment method for vernacular architecture

3.1. Introduction	41
3.2. Overview of the existing methods	45
3.2.1. The vulnerability index method	45
3.2.2. The macroseismic method	47
3.2.3. Combination of the vulnerability index and the macroseismic method	48
3.3. Proposed seismic vulnerability assessment methods for vernacular architecture	50
3.4. Definition of seismic vulnerability assessment parameters	51
3.5. Numerical strategy adopted for the parametric study	55
3.5.1. Definition of limit states	56
3.5.2. Reference numerical model	57
3.5.3. Numerical model details	59
3.5.4. Parameters variation	61
3.5.4.1. Wall slenderness	61
3.5.4.2. Maximum wall span	61
3.5.4.3. Type of material	62
3.5.4.4. Wall-to-wall connections	63
3.5.4.5. Horizontal diaphragms	64
3.5.4.6. Roof thrust	66
3.5.4.7. Wall openings	67
3.5.4.8. Number of floors	68
3.5.4.9. Previous structural damage	68
3.5.4.10. In-plane index	69
3.6. Conclusions	70

Chapter 4 Definition of seismic vulnerability classes

4.1. Introduction	71
4.2. Methodology adopted for the seismic vulnerability classes definition	72
4.3. Seismic vulnerability classes according to the wall slenderness (P1)	77
4.4. Seismic vulnerability classes according to the maximum wall span (P2)	84
4.5. Seismic vulnerability classes according to the type of material (P3)	89
4.6. Seismic vulnerability classes according to the wall-to-wall connections (P4)	96

4.7. Seismic vulnerability classes according to the horizontal diaphragms (P5)	101
4.8. Seismic vulnerability classes according to the roof thrust (P6)	117
4.9. Seismic vulnerability classes according to the wall openings (P7)	122
4.10. Seismic vulnerability classes according to the number of floors (P8)	130
4.11. Seismic vulnerability classes according to the previous structural damage (P9)	139
4.12. Seismic vulnerability classes according to the in-plane index (P10)	147
4.13. Conclusions	155

Chapter 5 Definition of seismic vulnerability assessment parameters weight

5.1. Introduction	157
5.2. Construction of the database for the seismic vulnerability assessment methods	159
5.2.1. Methodology adopted for the seismic vulnerability assessment parameters weight definition	159
5.2.2. Methodology adopted for the development of the SAVVAS method	161
5.2.3. Preliminary data analysis and extension of the database	163
5.3. Definition of the parameters weights based on statistical analysis	168
5.3.1. Regression coefficients	169
5.3.2. Vulnerability index weights	170
5.4. Definition of the parameters weights based on expert opinion	172
5.4.1. Questionnaire survey and Analytical Hierarchy Process (AHP) methodology	172
5.4.2. Definition of the weights	174
5.4.3. Comparison with the numerical results	177
5.5. Seismic vulnerability index for vernacular architecture (SVIVA) formulation	179
5.6. Conclusions	179

Chapter 6 Development of a new seismic vulnerability assessment method

6.1. Introduction	183
6.2. Development of the SAVVAS method	183
6.2.1. Analysis of the database and variables transformation	186
6.2.2. Multiple regression models	189
6.2.3. Artificial Neural Networks	196
6.2.4. ANN regression models and comparison among data mining techniques	197
6.3. Validation of the regression models	199
6.4. SAVVAS formulation	208

6.5. Conclusions	209
------------------	-----

Chapter 7 Numerical evaluation of traditional earthquake resistant techniques

7.1. Introduction	211
7.2. Traditional earthquake resistant techniques for vernacular architecture	212
7.2.1. Ring beams	214
7.2.2. Corner braces	221
7.2.3. Quoins	228
7.2.4. Ties	231
7.2.5. Timber elements within the masonry	235
7.2.6. Wall subdivisions	238
7.2.7. Buttresses	242
7.2.8. Walls thickening	249
7.2.9. Summary	251
7.3. Updated definition of the seismic vulnerability classes for P4	252
7.4. Updated formulation of the SAVVAS method	253
7.5. Conclusions	254

Chapter 8 Calibration and application of the proposed seismic vulnerability assessment methods

8.1. Introduction	255
8.2. Calibration of the methods based on the damage data after the 1998 Azores earthquake	257
8.2.1. Building stock characterization	258
8.2.2. Damage classification	258
8.2.3. Calibration and validation of the proposed methods	261
8.2.3.1. Vulnerability index (SVIVA) method	261
8.2.3.2. SAVVAS method	265
8.2.3.3. Comparison between both methods	271
8.3. Application of the methods in Vila Real de Santo António	274
8.3.1. Building characterization	276
8.3.2. Seismic vulnerability assessment	279
8.3.2.1. Vulnerability index (SVIVA) method	280
8.3.2.2. SAVVAS method	285
8.3.2.3. Historical vs current condition	291
8.3.2.4. Mitigation of the seismic vulnerability with different building retrofitting strategies	295

8.3.3. Loss assessment	300
8.3.3.1. Collapsed and unusable buildings	300
8.3.3.2. Human casualties and homelessness	302
8.3.3.3. Economic loss and repair cost estimation	303
8.4. Conclusions	305
Chapter 9 Conclusions and future research	
9.1. Introduction	309
9.2. Summary of conclusions	310
9.2.1. Quantitative evaluation of the seismic behavior of representative examples of Portuguese vernacular architecture (Research objective 1)	311
9.2.2. Development of a seismic vulnerability assessment method for vernacular architecture (Research objective 2)	311
9.2.3. Assessment of the efficiency of traditional strengthening solutions to mitigate the seismic vulnerability of in-use vernacular architecture (Research objective 3)	314
9.2.4. Recommendations of traditional strengthening solutions to reduce the seismic vulnerability of in-use vernacular architecture (Research objective 4)	315
9.2.5. Thesis outcomes	319
9.3. Future research	320
References	323
Annex A Database for the SVIVA method	339
Annex B Database for the SAVVAS method	353
Annex C Expert survey	369
Annex D Guidelines for application of the SAVVAS method	385

CHAPTER 1

INTRODUCTION

Chapter outline

- 1.1. [Background and motivation](#)
- 1.2. [Thesis objectives](#)
- 1.3. [Research methodology](#)
- 1.4. [Outline and organization of the thesis](#)

1.1. Background and motivation

Vernacular architecture is the result of a tight relation between humans and the environment. When local communities have to build their dwellings, satisfying their needs and ambitions, they respond to their surrounding environment and climate, through empirical knowledge acquired along generations. This inherited way of building is an accumulation of knowledge, understanding and intuition, considering the best use of the available local material. Vernacular architecture reflects the tradition and life style of a community, and the inhabitants' bonding with the natural environment. It is an architecture that is intimately associated with the place, the territory and its history. Thus, on one side, there are social key factors that determine the form of vernacular architecture, including ritual, economics, defensive, religious and cultural factors. On the other side, there are physical determinants influencing the vernacular form, which mainly include the climate, the natural hazards, the locally available materials and the available technology of the community through time.

As a result, vernacular architecture is extremely heterogeneous, responding to local conditions. However, the use of technological and standardized modern materials has homogenized the way of building throughout the world, providing an architecture that can be observed in any geography, jeopardizing the local building culture and vernacular architecture. For this reason, the valorization and preservation of the vernacular heritage, as well as the traditional construction techniques and materials is crucial, not only as a key element of cultural identity and a witness of the past, but also as a privileged factor for local development, boosting local economies (Fernandes and Mateus 2012; Correia 2017). The revival of small industries of

traditional local materials can also reduce waste and energy consumptions in production and transportation.

Vernacular architecture located in seismic prone areas can be particularly vulnerable to earthquakes due to a scarcity of resources in generally poor communities, resulting in inadequate overall structural layout of the construction, the use of poor materials, the lack of proper constructive details and a poor maintenance. Portugal, in spite of being considered a moderate seismic hazard country, has suffered several devastating earthquakes, such as in 1755, 1909, 1969 and 1998 (LNEC 1986; Sousa 2015; Neves et al. 2012). Therefore, it is susceptible to significant occurrences in the future. Earthquakes come unexpectedly, endangering in-use vernacular architecture and the population who inhabits it. Vernacular buildings are a significant part of the building stock. Oliver (1997) estimated that around 90% of the constructions around the world were considered to be vernacular. Nowadays, more recent research estimates that around 50% of the total population inhabits vernacular architecture (Correia 2017). There is a critical gap in knowledge regarding vernacular architecture earthquake preparedness, since research in vernacular architecture has predominantly been focused on building typologies and spatial organization. The study of the seismic behavior and vulnerability of representative vernacular construction systems has traditionally been ignored, and conservation efforts have been mainly placed on historical architecture and monuments.

The seismic assessment of the built vernacular heritage requires a deep knowledge and investigation of the place, traditional techniques and materials. However, the time, cost and resources required to obtain a sufficient in-depth level of information of the analyzed structure are not commonly assigned to the study of vernacular architecture. Seismic vulnerability assessment methods play an important role on risk mitigation because they are the main components of models capable of predicting damage to the built environment and estimating losses in future earthquakes. There is a big variety of methods available in the literature and the selection of one over another depends on the goal, scale and nature of the study. That is why the development of an expedite method for the seismic vulnerability assessment of vernacular architecture is of paramount importance, since more detailed and sophisticated approaches are typically restricted for individual monumental buildings. Thus, research in the seismic vulnerability assessment of vernacular architecture, including the estimation of economic and social losses for possible future earthquakes, is relevant and can eventually save lives through risk prevention mitigation, as well as contribute to the preservation of the built heritage.

Even though vernacular buildings are especially vulnerable to earthquakes, due to the long-term exposure to earthquake hazard, local communities can eventually adapt to this hazard and protect their built-up environment developing traditional seismic resistant techniques. Ferruccio Ferrigni at Centro Universitario per i Beni Culturali (CUEBC), recognized the existence of a 'Local Seismic Culture' and carried out the first research project aimed at reducing the seismic

vulnerability of vernacular constructions based on the rediscovery of this local know-how (Ferrigni 1990; Ferrigni et al. 2005). A local seismic culture has been identified in many seismic prone regions, such as Italy (Pierotti and Uliveri 2001), Greece (Touliatos 1992), Algeria (Foufa and Benouar 2005), India (Langenbach 2009) and Nepal (Gautam et al. 2016). The gap in knowledge regarding the identification of traditional earthquake-resistant features in Portuguese vernacular architecture and the reflection on the existence of a local seismic culture in Portugal was addressed by the research project ‘Seismic-V: Vernacular Seismic Culture in Portugal’ (Correia et al. 2014).

Considering that vernacular architecture is an outstanding inheritance that bears important lessons on hazard mitigation, the identification and update of traditional architectural solutions that local population developed to prevent or repair earthquake damage can lead to their eventual application and contribute to preserve and retrofit surviving examples without prejudice for its identity. Besides the loss of authenticity of vernacular architecture, there is another undesirable effect resulting from the current global urbanization tendency. Traditional building materials are being systematically replaced with new modern alien techniques and technologies, enabling structures to be erected quickly and cheaply, but not necessarily safely (Degg and Homan 2005). This phenomenon increases the vulnerability of the communities because they do not have any longer their own tools to prevent earthquake damage. They become extremely dependent on external agents, circumstance that ends up diluting the local seismic culture. Indigenous construction practices acquired from their ancestors and based on their experience are thus being gradually abandoned and replaced, because local communities rely less on them (Halvorson and Hamilton 2007).

Nevertheless, since vernacular architecture and local seismic culture are based on empiric knowledge transference, the origin of the solution is sometimes lost and implemented strengthening solutions do not present a satisfactory improvement in the resistance of the construction. Therefore, an increase in knowledge of local seismic culture and the study of the efficiency and confirmation of the positive effect of traditional seismic strengthening solutions identified in vernacular architecture is justified. The use of effective traditional techniques can also prevent further changes in the existing buildings that increase of seismic vulnerability by avoiding inadequate construction practices that can result from an inappropriate juxtaposition of old and new technologies.

The present research work intends to give a step towards the preservation of vernacular heritage. The risk of vernacular heritage to disappear due to this economic, cultural and architectural homogenization was already highlighted by ICOMOS (1999). Traditional building knowledge, technologies and materials face subsequently problems of obsolescence in a parallel way (May 2010). As a result of this progressive abandonment, there is an increasing vulnerability of vernacular architecture facing natural disasters, including earthquakes. A proper expedite

easy-to-use seismic vulnerability assessment method adapted to the specific characteristics of vernacular architecture can be an essential tool for determining building fragilities, since it can be used to evaluate the need for retrofitting solutions and to assess the efficiency in reducing the seismic vulnerability of proposed structural interventions (Vicente et al. 2011). At the same time, the definition and the recommendations on seismic retrofitting strategies for vernacular buildings should be based on traditional strengthening solutions that are proven to be efficient in reducing the seismic vulnerability of vernacular architecture. The adoption of traditional building practices associated with vernacular architecture fulfills minimum intervention and respect for the authenticity criteria recommended by accepted preservation charters (ICOMOS 1964). Moreover, it can ensure the continuity of old building traditions in the vernacular building culture, which is a key principle of conservation of the built vernacular heritage (ICOMOS 1999).

1.2. Thesis objectives

Based on the established gap in knowledge and the challenges identified in the previous section, the main objective of the present PhD research is to contribute to the awareness and protection of the vernacular heritage located in earthquake prone areas. For that matter, the main research question of the project deals with vernacular architecture earthquake preparedness with a main focus on the Portuguese context. It should be noted that the targeted Portuguese vernacular architectural heritage includes stone masonry, fired brick masonry, adobe masonry and rammed earth constructions, which, in spite of their particularities, share many characteristics with other vernacular constructions throughout the world, especially in the south Mediterranean region. This is particularly evident at a structural level, since the structural system is in most cases conceptually the same and consists of load bearing walls as the main vertical resisting elements. Therefore, the results obtained in this work may be extrapolated to other similar structures outside the Portuguese context.

In order to address the aforementioned research question concerning vernacular architecture earthquake preparedness, there is a need to: (a) gain a better insight of the seismic behavior of vernacular architecture; and (b) assess traditional strengthening solutions identified within a local seismic culture in order to understand how their eventual application can contribute to the preservation of the vernacular heritage. For this purpose, this work embraces the following four specific and fundamental objectives:

Objective 1: Evaluate quantitatively the seismic behavior of representative examples of existing Portuguese vernacular architecture.

Objective 2: Develop a seismic vulnerability assessment method for vernacular architecture.

Objective 3: Assess the efficiency of traditional strengthening solutions to mitigate the seismic vulnerability of vernacular architecture.

Objective 4: Propose recommendations of traditional strengthening solutions to reduce the seismic vulnerability of in-use vernacular architecture.

1.3. Research methodology

The accomplishment of the thesis objectives is achieved by adopting a variety of qualitative and quantitative research methods for the data collection and analysis, including: literature review, field observations, historical analysis, numerical analysis, statistical analysis and expert opinion. A special emphasis is placed on the quantitative analysis, since the main core of the work embraces an important numerical contribution for the better insight of the structural behavior of vernacular architecture typologies under seismic loading. This can be considered one of the main contributions of this research work, in the sense that: (1) there is no sufficient numerical data about the seismic behavior of vernacular buildings; (2) there is not a clear analytical insight on the effect of different traditional strengthening and earthquake resistant solutions in reducing the seismic vulnerability of vernacular architecture; and (3) this numerical data constitutes the basis for the development of the two seismic vulnerability assessment methods for vernacular architecture that are proposed. Therefore, four distinct tasks were developed to fulfill the research objectives, see Figure 1.1.

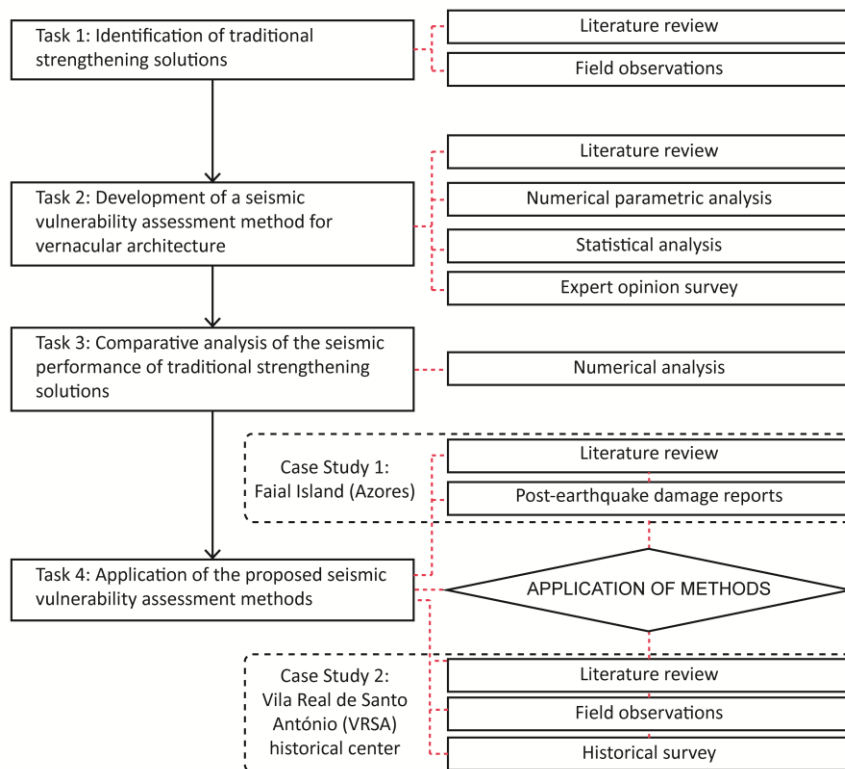


Figure 1.1: Research tasks and research methods applied

Task 1: Identification of traditional strengthening solutions

The first task of the research work involves the identification of traditional strengthening construction techniques in seismic prone Portuguese regions, based on literature review and on-site surveys of selected case studies. The literature review is meant to provide an overview of the most common strengthening techniques traditionally used around the world and already identified to be a result of an existing local seismic culture. The survey visits and field observations were carried out alongside with the aforementioned research project ‘Seismic-V’. One of the shared objectives with this project was the recognition and systematization of earthquake resistant reinforcement techniques traditionally implemented in Portuguese earthquake prone areas.

The literature review, together with the on-site inspection, carried out during this first part provides fundamental information for the development of the thesis. First of all, the identification of geometrical features, materials and construction techniques representative of the Portuguese vernacular architecture helps to define and prepare the reference models for the numerical analysis to be developed within Task 2. Secondly, the understanding of the structural behavior and construction principles of the identified earthquake resistant construction techniques and solutions is required for the numerical work that is performed within Task 3. Thirdly, the on-site research led also to the selection of one of the case studies used within Task 4: Vila Real de Santo António. Finally, the knowledge acquired is also essential for the definition of different building retrofitting strategies that are evaluated during Task 4.

Task 2: Development of a seismic vulnerability assessment method for vernacular architecture

The second task is considered to be the main body of the present thesis and is directly associated with the first and second established objectives. This part of the research work involves the development of an extensive numerical modeling campaign for the evaluation of the seismic behavior of vernacular buildings, which resulted in the development of two seismic vulnerability assessment methods: (1) Vulnerability index method, which is considered to be an adaption of existing vulnerability index methods for vernacular architecture and is denominated as Seismic Vulnerability Index for Vernacular Architecture (SVIVA); and (2) a novel method called Seismic Assessment of the Vulnerability of Vernacular Architecture Structures (SAVVAS) method, which is based on the estimation of the maximum seismic capacity of the building in terms of base shear or load factor.

Both methods are focused on the identification and characterization of constructive and material characteristics that are more influential in the seismic response of the building. Classical vulnerability index methods select seismic vulnerability parameters based on post-earthquake damage observations and expert judgment. In this work, the identification of the parameters was extracted from information available in the literature, but their influence on the

seismic behavior of vernacular buildings is further validated through a numerical parametric study. Besides obtaining a sound understanding of the seismic behavior of vernacular architecture by means of advanced numerical analysis, this thorough parametric study provides the basis for the development of the two seismic vulnerability assessment methods.

Current existing methods are mainly based solely on empiric observation. Detailed finite element (FE) modeling and nonlinear static (pushover) analysis were used to perform the extensive parametric study. The influence of the different selected parameters is thus evaluated and quantified numerically. The strategy consists of modifying a reference model according to the different parameters considered. The variations on the seismic performance of the structure are analyzed and compared in order to define each parameter influence. From the extensive numerical analysis, classes of increasing seismic vulnerability could be established. The definition of these classes is required for the two proposed seismic vulnerability assessment methods.

Besides the key vulnerability parameters and corresponding seismic vulnerability classes, vulnerability index methods also require the definition of weights for each parameter, which reflect the relative importance of each parameter in defining the seismic vulnerability of the structure. For the definition of the weights, two approaches were followed: (1) statistical analysis, based on the database built with the results of the parametric analysis, which allows performing a regression analysis that led to assess the relative importance of the different parameters; and (2) expert opinion collected by means of a questionnaire prepared and distributed among a group of international experts in the field, from around the world. The SVIVA method is defined and completed with the determination of the parameters classes and weights.

The statistical approach used for the definition of the weights was also followed for the development of the new proposed SAVVAS method, which is based on quantitative data analysis through Knowledge Discovery in Databases (KDD) and Data Mining (DM) techniques. The regression models provide an expression intended to predict the seismic capacity of vernacular structures in terms of load factor, using as inputs simple variables based on the key vulnerability parameters. These regression models constitute the core of the proposed method. The DM techniques applied for regression analysis include multiple linear regression and artificial neural networks (ANN). The use of an analytical process instead of an empirical one for the development of an expedite method for the seismic vulnerability assessment of vernacular structures is considered a step forward in the contribution for scientific knowledge.

Task 3: Comparative analysis of the seismic performance of traditional strengthening solutions

This task is directly associated with the third research objective. This part of the research work is devoted to the evaluation of the capacity and performance of traditional strengthening techniques resulting from a local seismic culture (identified in Task 1) to reduce the seismic vulnerability of

vernacular buildings. This task is developed based on detailed FE models and nonlinear static analysis. Traditional strengthening solutions are modeled and their effect is assessed quantitatively, by means of comparison between the variations on the seismic performance of the structures with or without the different techniques.

As a result of this task, both seismic vulnerability assessment methods are updated to consider the effect of traditional strengthening solutions. This is an important output, since most of the existing methods available to characterize the buildings vulnerability do not take into account the effect of traditional strengthening solutions. These updates are also fundamental for the definition of the building retrofitting strategies (Task 4), as well as for the preparation of recommendations.

Task 4: Application of the proposed seismic vulnerability assessment methods

Task 4 corresponds to the application of the methods developed in Task 2 on two selected case studies, for their calibration and validation. The first case study selected was the island of Faial, in Azores, which was used to calibrate both seismic vulnerability assessment methods. The reason behind the selection of this case study was twofold: (a) because of the seismicity and the high number of traditional stone masonry buildings existing in the region; and (b) because of the availability of significant amount of information and post-earthquake reports of the building stock before and after the 1998 Azores earthquake (Neves et al. 2012; Ferreira et al. 2016). Besides the characterization of the post-earthquake damage, this data also allowed a reliable characterization of a significant amount of vernacular buildings scattered throughout the island, which was a necessary step to perform the seismic risk assessment.

The application of both seismic vulnerability assessment methods was intended to evaluate their performance in estimating the seismic damage after the 1998 earthquake. For that matter, the seismic hazard is correlated with the building vulnerability, in order to estimate the level of damage that a building is prone to suffer, when subjected to the defined seismic event. A risk scenario equivalent to the one observed for the 1998 earthquake was considered. This resulted in estimating the damage scenario using the two proposed methods, which were compared with the results from the post-earthquake observation for their calibration and validation.

After the calibration, both methods were applied to a different case study to perform a complete seismic vulnerability and loss assessment. Following the survey visits carried out within Task 1, the historical city center of Vila Real de Santo António (VRSA) was selected as the second case study mainly due to its location and the type of construction. The city of VRSA was initially conceived as part of an original rigorously designed plan, which took into consideration seismic resistant provisions. Even though the buildings within the historical city center were the result of this plan and might not be considered strictly vernacular in the origin, most of the buildings have been either substituted or subjected to continuous modifications because of the new needs of the

users. Thus, it can be considered as a representative example of how this designed plan has been continuously modified by anonymous and customary forces without any principled changes, leading to the current unplanned spontaneous occupation and alteration of the urban layout. Most of the original buildings were substituted or highly altered and few buildings still preserve their original characteristics in terms of volume, construction characteristics and opening distribution in elevation. In summary, the main objectives of applying the seismic vulnerability assessment methods to VRSA are: (1) understanding if this deep alteration of the city at an urban and building level has compromised the seismic vulnerability of VRSA and to what extent, which is why the assessment includes a comparison with the historical condition of the city; and (2) studying the effects of the different strengthening solutions evaluated in Task 3 on mitigating the seismic vulnerability of vernacular buildings.

The historical condition of the city was obtained based on literature review and historical research. Survey sheets were prepared to collect information about the remaining original buildings and the structural alterations suffered along their history. Data collection is based on on-site observation and existing documentation, namely books and existing reports provided by city halls and other institutions. The application of the seismic vulnerability assessment methods for different retrofitting scenarios considered can be used for a comparative analysis of the performance of different strengthening strategies. An estimation of the losses for the different scenarios is also performed, based on the probability of the buildings to reach the different damage levels, particularly the collapse and loss of functionality. As a result, the economic losses can also be estimated and a cost-benefit analysis of the retrofitted strategies is presented and discussed. These models can also be used for the estimation of fatalities and injuries. The results obtained are also useful to exemplify the applicability and the potential of the two seismic vulnerability assessment methods for technicians and decision-makers.

1.4. Outline and organization of the thesis

This thesis is structured in nine chapters and includes four annexes. The present chapter 1 introduces the background of the thesis, identifies the gap in knowledge and establishes the main research objectives and the tasks defined to accomplish them. This introductory chapter also presents the research methods adopted and the outline and organization of the document.

Chapter 2 presents a literature review on traditional earthquake resistant techniques for vernacular architecture and local seismic culture. The chapter thus firstly identifies the basic concepts for the development of the research. An overview of traditional seismic resistant practices throughout the world is also provided. Additionally, it identifies the use of these techniques in the Portuguese vernacular heritage.

Chapters 3 to 6 deal with the development of the two seismic vulnerability assessment methods for vernacular architecture. Chapter 3 firstly introduces the topic of seismic vulnerability assessment, followed by a brief state-of-the art review where the main methods existing in the literature are discussed, with a particular focus on the seismic vulnerability index and the macroseismic method on which the two proposed methods are based. Secondly, the different parameters used by the existing methods are reviewed and compared. As a result of this literature review, the chapter presents the selection of the parameters to be studied and used in the proposed methods. Finally, the chapter introduces the numerical strategy followed in the succeeding chapters, including the reference numerical model that is used on the parametric study and the definition of the limit states that are used to quantify the variations in the seismic performance of the buildings.

Chapter 4 focuses on the definition of the parameters classes. This chapter presents the results of the thorough numerical parametric study conducted to characterize the influence of the different vulnerability parameters selected in Chapter 3. Each key parameter is analyzed independently. First, the variations on the reference model according to each parameter are presented. The discussion of the results includes: (1) the variations in the damage patterns and failure mechanisms; (2) the variations in the seismic capacity in terms of base shear or load factor for the different limit states previously defined. Finally, the definition of the vulnerability classes is based on the variations obtained.

Chapter 5 addresses the definition of the parameters weights required to complete the SVIVA method. The results from the whole parametric study are compiled and gathered in an extensive database that is used to perform the regression statistical analysis intended to estimate the parameters weight. This database is provided as an important output of the thesis in Annexes A and B. A brief literature review on values proposed by other authors is presented and compared with the results obtained from the statistical analysis. Additionally, the weights are also calculated based on a survey research carried out to collect the opinion of experts in the field. The questionnaire prepared for the survey is provided for reference in Annex C. The differences among the weights calculated using the expert opinion survey and the results from the statistical analysis are then critically discussed.

Chapter 6 presents the development of the new SAVVAS method for the seismic vulnerability assessment of vernacular architecture, which is mainly intended to estimate the seismic load factors that would cause a building to reach different damage limit states and can help to define the seismic response of vernacular buildings to a specific event. Thus, this method can be later used to correlate directly the Peak Ground Acceleration (PGA) with the foreseen damage. A brief introduction of the statistical methods is provided, mainly presenting the data mining techniques that were used for the extraction of useful knowledge from the extensive database resulting from Chapter 4. The results obtained from this statistical analysis led to the definition of the

regression models that constitute the SAVVAS method. The validation of the regression models obtained was carried out by means of using them to estimate the load factors of several masonry constructions that have been either tested at the shaking table or numerically. Several examples were thus gathered from the literature and the results obtained using the regression models were compared with the results from the literature in order to validate the models.

Chapter 7 is focused on the numerical evaluation of the efficiency of traditional strengthening solutions to reduce the seismic vulnerability of vernacular architecture identified in Chapter 2. After the selection of several strengthening techniques, a numerical study was conducted. Similarly to Chapter 4, each technique is assessed independently. A description of the new models constructed to simulate the different strengthening solutions is provided. Afterwards, the chapter discusses the results of the numerical study and the effect of the different solutions on the seismic behavior of the building by comparing damage patterns, failure mechanisms and seismic capacity of the structures with or without the different techniques. Finally, based on the results obtained, the chapter proposes the calibration of the seismic vulnerability assessment methods in order to include the effect of traditional strengthening techniques.

Chapter 8 is focused on the calibration and validation of the two proposed seismic vulnerability assessment methods using two case studies. The chapter introduces the island of Faial as the first case study where the methods are calibrated. The set of data collected includes information of the stone masonry building stock and post-earthquake damage observation in the sequence of the 1998 Azores earthquake. The methods are applied on the database for the estimation of the seismic damage and confronted with the observed damage. A discussion and comparison of the performance of the two methods is provided. The second case study of Vila Real de Santo António historical center is then presented and discussed, mainly in terms of the historical research carried out. The building characterization was based on on-site collected data regarding the current condition of the city, particularly focusing on the alterations carried out throughout the years. The seismic vulnerability and the loss assessment of VRSA is then carried out by using the two seismic vulnerability assessment methods, in order to compare them and prove their applicability. The historical condition of the city center is also assessed, in order to understand and quantify the increment of its the seismic vulnerability, since the city was originally designed to be particularly earthquake resistant. The assessment also includes the application of different building retrofitting strategies on the existing building stock, aiming at the evaluation of their efficiency in reducing the seismic vulnerability of the buildings. The demonstration of the application of the SAVVAS method is provided for reference in Annex D as a set of guidelines.

Finally, chapter 9 presents a summary of the work conducted and the main conclusions drawn from the obtained results. As one of the main outcomes of the thesis, this chapter presents recommendations on traditional strengthening solutions to reduce the seismic vulnerability of

vernacular architecture. Suggestions for further research are recommended for the continuation of the present research work.

Figure 1.2 shows a diagram of the organization of the thesis that outlines the sequence of the chapters and their relationship with the research objectives.

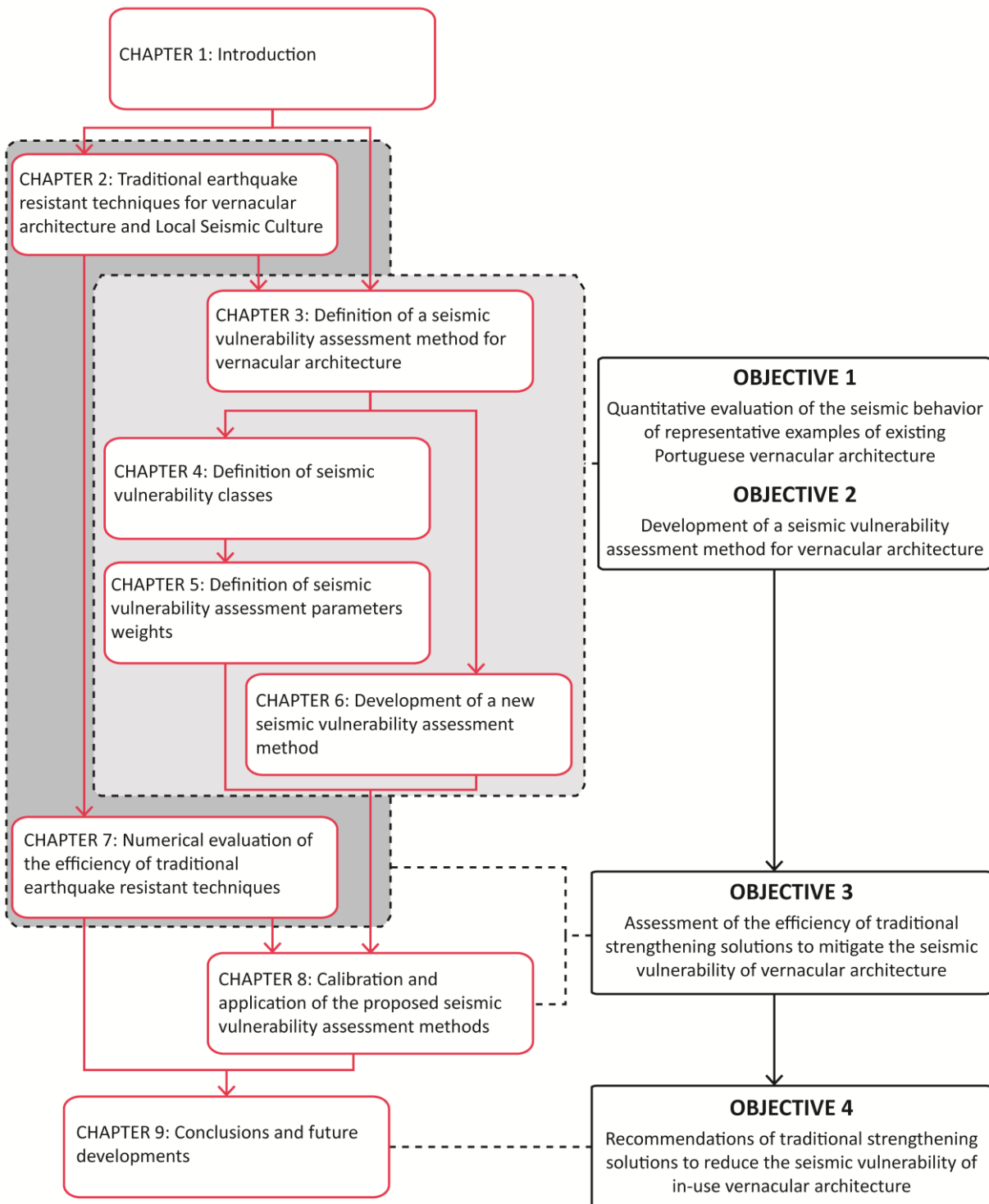


Figure 1.2: Thesis outline and relationship between chapters and research objectives

CHAPTER 2

TRADITIONAL EARTHQUAKE RESISTANT TECHNIQUES FOR VERNACULAR ARCHITECTURE AND LOCAL SEISMIC CULTURE

Chapter outline

- 2.1. [Introduction](#)
- 2.2. [Basic concepts](#)
 - 2.2.1. [Vernacular architecture and local seismic culture](#)
 - 2.2.2. [Earthquake performance of vernacular constructions](#)
 - 2.2.2.1. [Poor connection between structural elements](#)
 - 2.2.2.2. [Out-of-plane wall collapse](#)
 - 2.2.2.3. [Delamination of wall leaves](#)
 - 2.2.2.4. [In-plane shear failure](#)
 - 2.2.2.5. [Poor workmanship and maintenance](#)
- 2.3. [Traditional seismic resistant building practices](#)
 - 2.3.1. [Techniques improving the connections between structural elements](#)
 - 2.3.2. [Techniques stabilizing structural elements and buildings](#)
 - 2.3.2.1. [Masonry walls](#)
 - 2.3.2.2. [Floors and roofs](#)
 - 2.3.2.3. [Timber frames as earthquake resistant systems](#)
 - 2.3.3. [Techniques allowing partial collapse of structural elements](#)
 - 2.3.4. [Techniques counteracting horizontal loads](#)
 - 2.3.5. [Summary](#)
- 2.4. [Seismic-V Project: Vernacular seismic culture in Portugal](#)
- 2.5. [Conclusions](#)

2.1. Introduction

Specific architectural elements can be identified in constructions located in regions frequently exposed to earthquakes. These earthquake resistant features were developed empirically by local communities to protect their built-up environment. Research in these traditional practices, resulting from a local seismic culture, is a relevant and positive approach, since it focuses on the strength of the system rather than on its weaknesses. Its integration into current vernacular building practices can help to preserve and retrofit surviving in-use examples while respecting

their authenticity. This chapter presents a comprehensive overview of traditional earthquake resistant techniques and practices that can be typically observed around the world, aiming in particular at a better understanding of their structural role. This overview was developed under the framework of the research project ‘Seismic-V: Vernacular Seismic Culture in Portugal’, which specifically focused on the identification of seismic retrofitting techniques for vernacular buildings in Portugal. Therefore, the chapter also elaborates on the Portuguese context by indicating which techniques can also be recognized within Portuguese vernacular architecture, so that it can additionally contribute to the reflection on the existence of a local seismic culture in Portugal. A summary and description of the main outcomes of the aforementioned research project is outlined at the end of the chapter.

Earthquakes are naturally occurring events that affect negatively people and their environment by causing loss of life, injury, property damage, social and economic disruptions or environmental damage. Since they seriously disrupt the functioning of a community, local builders have thus often integrated seismic risk as a determinant for construction, adopting different strategies to protect the population from these natural disasters. They have developed rich and varied knowledge resulting in singular construction techniques, building details and temporary technical devices aimed at reducing the vulnerability of structures. A local seismic culture thus emerges from the need of local population to react to earthquakes and from the efforts made for the physical community to survive. People can either undertake preventive measures, repairing and refurbishing their personal properties in order to minimize future losses in the following earthquakes, or they can respond to earthquakes just in the immediate aftermath of the event, with no future orientation, developing a reactive response behavior (Correia and Merten 2001). In any case, traditional seismic resistant construction techniques arise from this need to repair earthquake damage to both personal and public buildings. These efforts made by local populations as a reaction to earthquakes gave rise to the development of a local seismic culture, which is a key element for the preservation of cultural identity and vernacular construction practices.

The existence of a local seismic culture was recognized and firstly investigated by Ferrigni (1990). From that moment on, a local seismic culture has been identified in many countries throughout the world frequently exposed to earthquakes, such as Italy (Pierotti and Uliveri 2001) Greece (Touliatos 1992), Turkey (Homan 2004), Algeria (Foufa and Benouar 2005), Iran (Naderzadeh 2009), India (Langenbach 2009), Nepal (Gautam et al. 2016), Japan (Okubo 2016), Haiti (Audefroy 2011) and Colombia (Mogollón 2002). Other organizations such as CRAterre have developed risk management programs including the construction of traditional seismic resistant housing in El Salvador and the development of guidelines for reconstruction based on the local seismic culture in Kashmir (Garnier and Moles 2012). The World Housing Encyclopedia (Brzev et al. 2004) is another project of the Earthquake engineering research institute (EERI) and the

International association for earthquake engineering (IAEE) that collects existing construction practices in earthquake regions, with a focus on vernacular building typologies. Its main objectives are to understand the seismic vulnerability of these construction systems and the reasons for their good or poor seismic performance, as well as to provide recommendations for strengthening (Blondet et al. 2011; Bothara and Brzev 2012).

Research in seismic strengthening solutions has for a long time addressed monumental architecture instead of the vernacular heritage, which has traditionally been ignored and underestimated. However, in the last years, there has been a growing interest on the experimental characterization of the seismic behavior of representative vernacular construction systems (Vasconcelos and Lourenço 2009a; Vasconcelos and Lourenço 2009b; Varum et al. 2011; Neves et al. 2012), as well as on seismic strengthening solutions for vernacular constructions based on modern techniques and materials (Tomazevic 1999; Vargas et al. 2009; D'Ayala 2014). Still, little research has focused on traditional strengthening solutions emerging from vernacular architecture (Correia 2005). Therefore, the present chapter addresses the gap in knowledge on the most common measures adopted by local communities to repair and restore their dwellings. It is considered that a better awareness of traditional earthquake resistant measures is important to protect and reduce the seismic vulnerability of the built vernacular heritage by encouraging local communities to recognize and readopt techniques emerging from a local seismic culture.

2.2. Basic concepts

2.2.1. Vernacular architecture and local seismic culture

The object of this overview is the vernacular architectural heritage, which comprises dwellings and other buildings built by the people. Vernacular buildings are usually owner or community built. They are not designed by specialists but, on the contrary, are part of a process that involves many people over many generations and are based on empirical knowledge. This is why vernacular architecture is often called communal, popular or folk architecture and even '*architecture without architects*' (Rudofsky 1964). Following the same reasoning, vernacular architecture has often been defined as the opposite of high or monumental architecture. Still, vernacular is the most common term used by academics (Rapoport 1969; Oliver 1997) and professionals (ICOMOS 1999).

Earthquakes striking cities and devastating communities have been reported since ancient times. However, in spite of the constant threat that earthquakes represent, far from abandoning these seismic prone regions, people have proven to be exceedingly attached to the places where they have always lived and have remained living under these dangerous circumstances, in spite of being continuously exposed to seismic hazard. Consequently, it seems reasonable that people coexisting with earthquakes are forced to learn how to protect themselves from them and have

developed preventive measures for earthquake mitigation. This is the origin of a local seismic culture. Considering that the built up environment is the most vulnerable element to earthquake forces and the major cause for the economic and human toll, most of the efforts have been dedicated to improve the seismic resistance of constructions, aiming at minimizing the earthquake catastrophic effects.

As part of the vernacular practice, Local Seismic Cultures make use of locally available materials, skills and resources but, more importantly, they are culturally sensitive to the local building tradition and effective in resisting earthquakes. This type of knowledge derives from centuries of trial and error and generally uses low-level technology. However, it is frequently disregarded and rarely documented or scientifically explained. For this reason, research in hazard mitigation through vernacular building practices resulting from local seismic culture is relevant.

The main factor that leads to the development of a seismic culture is earthquake hazard awareness, which is strictly correlated with the seismic hazard of the region or the probability of occurrence of an earthquake in a given area. In addition to the seismic hazard, the impact of the earthquake on the built-up environment is of great importance. In this way, methods and construction solutions proved as dangerous after an earthquake are either abandoned or modified, while reconstruction works will copy those construction techniques that have withstood the event, as a sort of natural selection.

There is a close correlation between the development of seismic resistant building practices and the earthquake frequency (Touliatos 1992). Earthquakes must be frequent in a region so the people can remember the seismic behavior of the empirically devised techniques. At least one important earthquake during the life period of a generation is needed to keep the local seismic culture level high, resulting in a 'culture of prevention', and enhancing the quality of aseismic construction (Figure 2.1). If earthquakes are not frequent and there are long periods of time between the seismic events, larger than the average generation life time, the function of different techniques implemented after an earthquake will be forgotten and gradually abandoned, developing a 'culture of repairs'. This loss of the collective memory of past events eventually leads to the abandonment and erosion of seismic cultures.

The development of a seismic culture is not only related with the frequency of the earthquakes but also with their intensity. As an example, Portugal has a moderate seismicity characterized by small events, but several devastating earthquakes have sporadically struck the country throughout its history. This has led to the development of important reactive responses in which seismic resistant constructions were devised and implemented after earthquakes, such as the well-known *Pombalino* buildings after the 1755 Lisbon earthquake. However, due to a progressive loss of seismic awareness, *Pombalino* buildings were replaced by the *Gaioleiro* buildings, with a much worse construction quality and where the initially devised seismic

resistant measures were neglected, increasing their vulnerability (Mendes and Lourenço 2010). A similar example can be found in India, where the seismicity of some regions is also characterized by a relative high frequency of large earthquakes and low frequency of moderate earthquakes. According to Jain (1998), this has led to the development of seismic resistant construction typologies, such as the ‘Assam-type’ timber-frame houses developed after the 1897 Assam Earthquake. They showed an excellent performance in subsequent earthquakes but were again abandoned because of the lack of seismic concern.

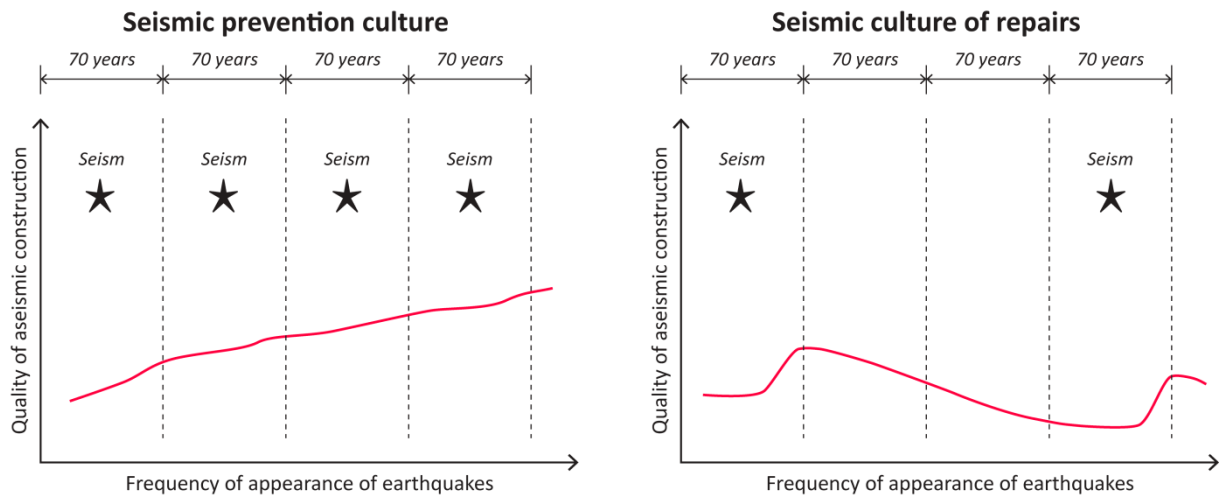


Figure 2.1: Evolution of the quality of aseismic construction related with earthquake frequency (Touliatos 1992)

2.2.2. Earthquake performance of vernacular constructions

The serious aftermaths of earthquakes, such as human fatalities, are caused mainly by the collapse of poorly constructed or unsafe buildings and other man-made structures. Therefore, the seismic risk directly depends on the seismic vulnerability of the constructions, which can be defined as their intrinsic proneness to suffer damage as a result of a seismic event of a given intensity. Other factors, such as the level of exposure (e.g. density of population or time of the day of the earthquake occurrence) and the seismic hazard of the region can also reduce or increase the risk. However, since the earthquake action cannot be reduced, efforts should be made on identifying the building fragilities and on repairing and strengthening the building stock, addressing an essential aspect in which the engineering research can intervene. For that purpose, understanding the earthquake effects on buildings is of major importance.

Vernacular buildings are mainly constructed with traditional materials using low cost and simple construction technology. Thus, they respond very poorly to earthquake ground shakings, even to moderate ones. The seismic deficiencies of vernacular constructions are mainly caused by the poor quality of building materials, workmanship and maintenance, generally resulting from economic constraints and lack of proper training of local masons. Examples of the poor performance of vernacular architecture that led to significant human and economic losses include:

the 2005 Kashmir and 2001 Bhuj earthquakes, where most of the deaths were attributed to the collapse of stone masonry dwellings (Bothara and Brzev 2012); and the 2001 El Salvador, 2003 Bam and 2007 Pisco earthquakes, where many people died and were left without shelter after the collapse of earthen dwellings (Blondet et al. 2011). Vernacular stone masonry buildings can show insufficient construction quality to withstand seismic loads because of the use of round, unshaped stones, the absence of connection between leaves, the lack of adhesion and cohesion of the mortar, or the presence of voids. Earthen buildings seismic failure is mainly due to its own characteristics as a building material, such as its low strength and brittleness. In this section, a brief overview of common earthquake damages patterns associated to poor building practices will be provided.

2.2.2.1 Poor connection between structural elements

The lack of structural integrity due to poor connection between structural elements is one of the main causes of earthquake damage in vernacular buildings. Proper connections are required to ensure the 'box-behavior' of the building so that inertial forces can be transferred between the structural elements and in-plane resisting mechanisms can develop in the masonry walls, which are typically the main structural elements in masonry buildings. This is one of the main earthquake resistant construction concepts, since the in-plane stiffness of the masonry is significantly higher than its out-of-plane stiffness (Lourenço et al. 2011). However, a full multi-connected box is often very far from reality in vernacular architecture given the absence of rigid floors, causing the single walls to work separately.

Deficient walls connections lead to out-of-plane failures due to the separation of walls at the corners. When seismic forces are transferred between perpendicular walls, there is a concentration of tensile and shear stresses at the connection that instigates vertical cracking and ultimately the global overturning of external walls (Figure 2.2a). Additionally, if the anchorage between horizontal diaphragms (floors and roofs) and walls is not adequate, walls are free to vibrate independently and are more susceptible to topple (Figure 2.2b). Inadequate wall-to-roof and wall-to-floor connections also lead to the separation of roofs and floors from walls. The loss of support often causes the partial and sometimes even the complete collapse of the roof and floors (Figure 2.2c), which is one of the major causes of fatalities during earthquakes.

2.2.2.2 Out-of-plane wall collapse

Other out-of-plane failure patterns associated to the bending of the masonry walls can also develop. The damage pattern varies according to the geometry and boundary conditions of the walls. It can consist of vertical cracks at the wall intersections preceding the tilting and collapse of big portions of the walls, sometimes even the entire wall. If the free length of the wall is significant (i.e. the distance between intermediate transversal supports), the out-of-plane mechanism typically consists of horizontal cracking in the base or intermediate height, together

with vertical cracks (Figure 2.3a). Failure mechanisms in shorter walls are usually formed by vertical cracks in the center of the wall and diagonal cracking, coupled with the separation of the walls at the corners (Figure 2.3b). Other out-of-plane mechanisms can also involve specific structural elements of the buildings, such as the out-of-plane collapse of corners (Figure 2.3c). Buildings with gable walls tend to vibrate as freestanding cantilevers and are susceptible to their out-of-plane partial collapse (Figure 2.3d). These failures are facilitated at top floors in multi-story buildings, where earthquake accelerations are intensified and there are lower axial loads.

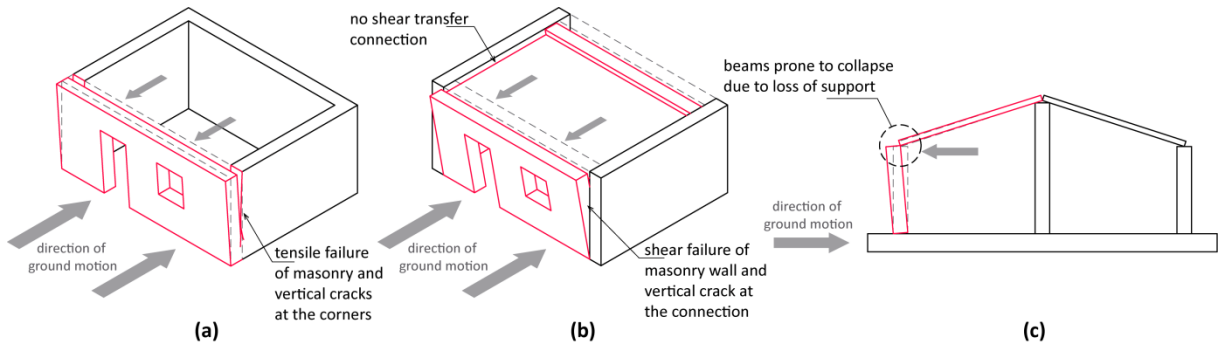


Figure 2.2: (a) Global overturning of the external walls; (b) lack of anchorage between walls and horizontal diaphragms leading to the toppling of walls; and (c) separation of floors and roofs from the walls

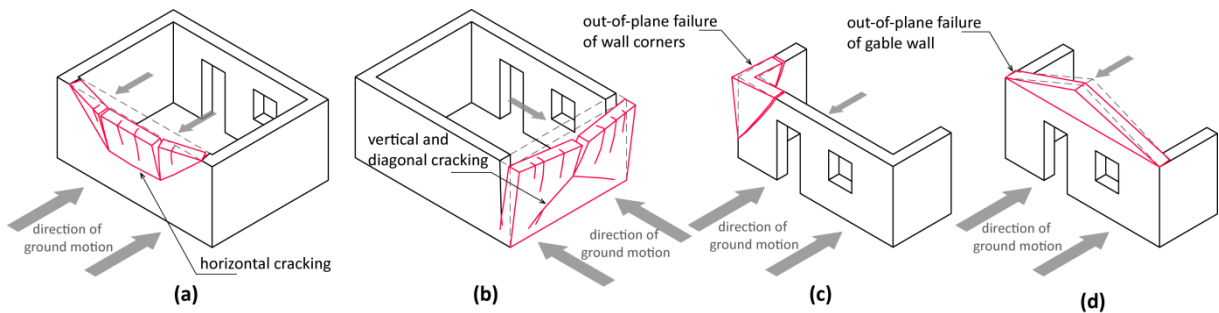


Figure 2.3: (a) Out-of-plane mechanism in long walls (AIS 2005); (b) out-of-plane mechanism in short walls (AIS 2005); (c) out-of-plane collapse of the corner; and (d) out-of-plane collapse of the gable

2.2.2.3 Delamination of wall leaves

Another common damage concerning multiple-leaf stone masonry walls is the bulging of the external leaf or delamination (Figure 2.4a). This type of failure is typically caused by poor quality of the masonry because of the lack of through-stones or ‘diatons’, which are larger stones that cross the entire thickness of the wall and allow the adequate bracing between leaves. Moreover, the space between the wall leaves is usually filled with small stones and rubble, which can exert thrust from inside and push the leaves outward, causing the bulging and either partial or total collapse of the wall (Figure 2.4b). This usually occurs at the upper parts of the wall, where the lack of weight allows the masonry to vibrate more independently (Bothara and Brzev 2012). The

use of low quality building materials such as poorly placed irregular stones also tends to induce localized damage and partial collapses (Figure 2.4c).

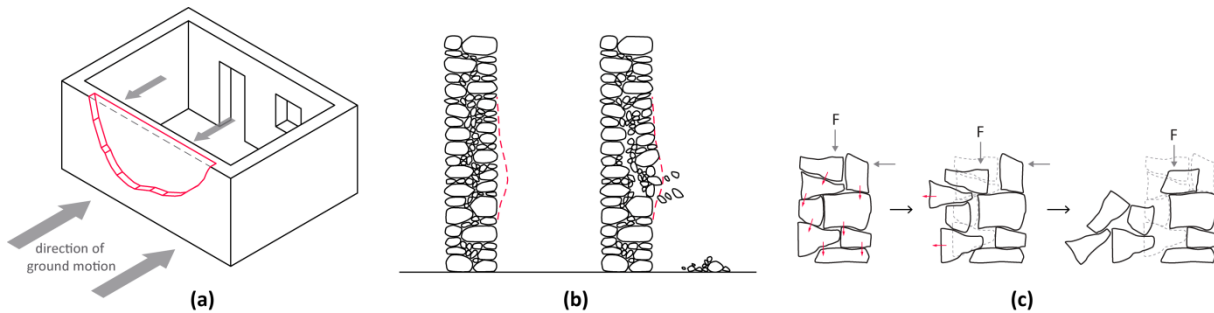


Figure 2.4: (a) Delamination of the wall leaf; (b) inner leaf causing the bulging of the exterior wall leaf (Giuffrè 1993); and (c) wall failure caused by the irregularity of stones (Bothara and Hıçılmaz 2008)

2.2.2.4 In-plane shear failure

Seismic events may also cause in-plane shear failure, which is mainly characterized by diagonal or X-cracking in the direction of the wall length (Figure 2.5a). This failure is due to excessive shear efforts and low material shear strength. In-plane failures also highly depend on the geometry of the walls, such as the length to height ratio and the wall thickness. The presence of openings facilitates in-plane cracking, which typically arises from the opening edges, where a greater concentration of stress is present (Figure 2.5b). In the case of slender piers, rocking may occur, which consists of the rotation of the piers and results in the crushing of the pier end zones (Bothara and Brzev 2012), see Figure 2.5c.

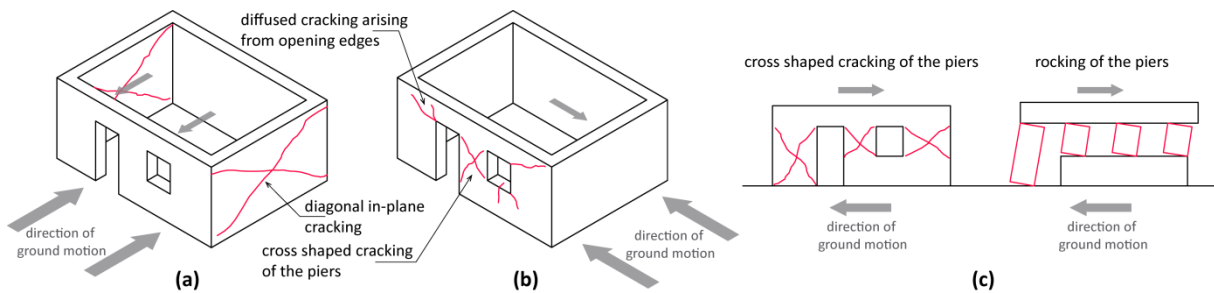


Figure 2.5: (a) In-plane shear failure in the direction of the wall length; (b) shear cracking around the openings; and (c) shear cracking versus rocking of the piers (Bothara and Brzev 2012)

2.2.2.5 Poor workmanship and maintenance

Poor construction practices commonly observed in vernacular architecture increase the earthquake damage previously described. For example, openings that are too large or bad positioned (e.g. very close to each other or to the edges of the building) lead to excessively slender piers in the wall, enabling in-plane damage. Additionally, an irregular distribution of openings leads to an uneven distribution of stiffness and shear capacity among the piers so that some

might be more vulnerable than others (D'Ayala and Paganoni 2011). The thrust exerted by heavy roofs also greatly facilitates out-of-plane and in-plane mechanisms to take place. Parapets and other freestanding nonstructural elements prone to out-of-plane collapse are also potential seismic deficiencies of vernacular buildings.

Moreover, vernacular architecture has a distinctly open-ended and spontaneous nature so it is strongly characterized by its transformation process. Vernacular buildings are thus subjected to continuous modifications that are a normal consequence of the changes in the use of the buildings and of the new needs of the users. These alterations on the original structures are a common source of vulnerability because they usually compromise the seismic performance of the buildings. The most common structural alterations include the addition of new floors, the opening of new windows and doors, the enlargement of the original openings, and the replacement of structural elements, such as floors and roofs.

2.3. Traditional seismic resistant building practices

Many different seismic resilient local building practices and constructive traditions can be recognized throughout the world and history, involving just some basic structural members of the building or consisting of an entire building structural system. The most successful ones have lasted for centuries and have survived numerous seismic events, proving their validity. Indeed, they were actually efficient in enhancing the structural performance of buildings during earthquakes and they have become recognized as evidences of a local seismic culture. Given the unchangeable nature of earthquakes, similar techniques following the same earthquake resistant principles can be observed in different seismic prone regions of the world, despite the use of different materials and techniques more adapted to each local situation and practice (Figure 2.6).

Traditionally, the best and costliest materials, as well as the most advanced techniques, were traditionally reserved for temples and monumental buildings, as they were the buildings conceived to last over time. The sturdiest types of masonry were used to build bulky constructions that were able to resist very large earthquakes based solely on the strength, stiffness and good quality of the materials. The well-known Inca cyclopean masonry walls composed by large stones very precisely cut to fit perfectly one another are a good example. Another example is Roman monumental architecture whose massive walls and foundations work as rigid monolithic constructions thanks to the use of pozzolanic materials. However, these techniques required a high consumption of materials and massive labor force, which limited their use only for monuments and great buildings.

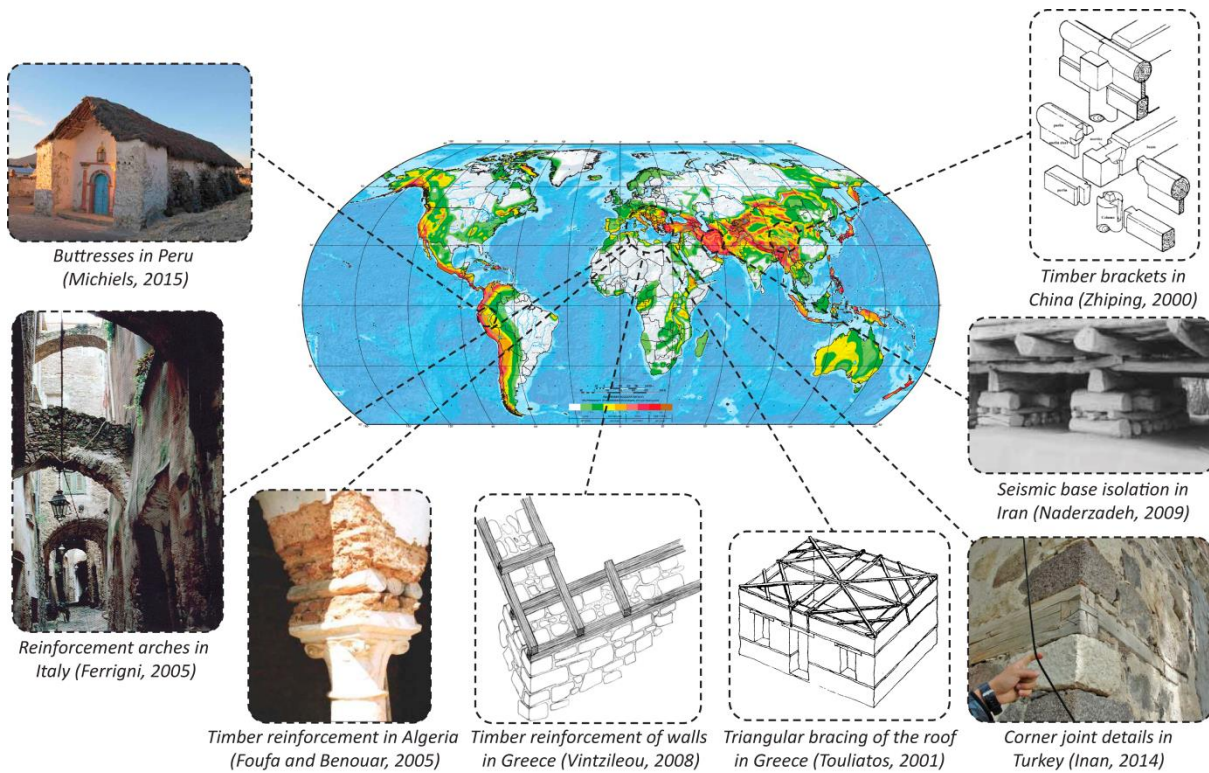


Figure 2.6: Examples of earthquake resistant techniques and traces of local seismic culture throughout the world in relation to the Global Seismic Hazard Map (Giardini et al. 1999)

Ordinary constructions and dwellings belonging to vernacular architecture could not replicate the technologies used in monumental architecture because they had to make use of more affordable and locally available materials. The basic seismic resistant concepts that eventually took root in the vernacular building culture of a seismic prone region had to be necessarily different. Local populations acknowledged and accepted that it is not economically viable to construct every building to resist earthquakes without suffering deformation and damage but the collapse of the structure must always be avoided. Thus, the main construction efforts traditionally made by vernacular builders consist of improving the capacity of the structures to undergo deformation and damage but maintaining enough load-carrying capacity to prevent global collapse. Traditional earthquake resistant techniques mainly follow four main resisting principles:

- (a) Improving the connections between the structural elements and enhancing the global behavior of the structure by forming closed contours in vertical and horizontal planes so that stress concentrations are avoided and forces are transmitted from one component to another even through large deformations.
- (b) Stabilizing structural elements and buildings by imparting resistance and deformation capacity to the brittle stone masonry or earthen walls, and by improving the diaphragm action of floors and roofs.

(c) Allowing partial collapse by means of redundancy of structural elements so that the failure of certain members is tolerated.

(d) Counteracting horizontal loads exerted by the buildings during the shaking by adding extra resistance to the lateral thrust with the help of new structural elements.

This section presents different traditional construction solutions and detailing that improve the seismic performance of vernacular architecture and can be considered as examples of a local seismic culture throughout the world. Additionally, an effort is carried out in order to identify signs of earthquake resistant traditional construction in Portugal that supports the existence of a Portuguese local seismic culture.

2.3.1. Techniques improving the connections between structural elements

As previously mentioned, the lack of connection between structural elements is one of the main causes of earthquake induced damage in buildings and, as shown by past earthquakes, this can be significantly reduced when building components are properly connected and the construction behaves like a monolithic box (Bothara and Brzev 2012). Therefore, many traditional earthquake resistant construction techniques are aimed at improving the connections between the different structural elements: wall-to-wall, wall-to-floor and wall-to-roof.

One of the most effective and widespread traditional techniques used to ensure the structural integrity of stone masonry and earthen buildings is the construction of timber ring beams, also known as bond or collar beams. Traditionally, ring beams are built using a pair of longitudinal parallel planks joined together with small transversal members in a ladder-like configuration (Figure 2.7), but sometimes they simply consist of a rough timber grid of horizontal timber trunks or tree branches lying longitudinally and transversally. They are usually placed continuously at the lintel level, at the roof level or, in the case of multi-story buildings, at the floor levels. The introduction of this type of beams at different levels within the height of the walls improves the connections between the different structural elements, tying the building and improving its 'box-behavior'. In order to be more effective, ring beams should be continuous around the entire building. A proper connection between timber elements at the wall intersections should be ensured, by means of different timber joint details or even steel dowels or straps. The connection between the beam and the wall should also be ensured but it has been traditionally achieved solely by friction.

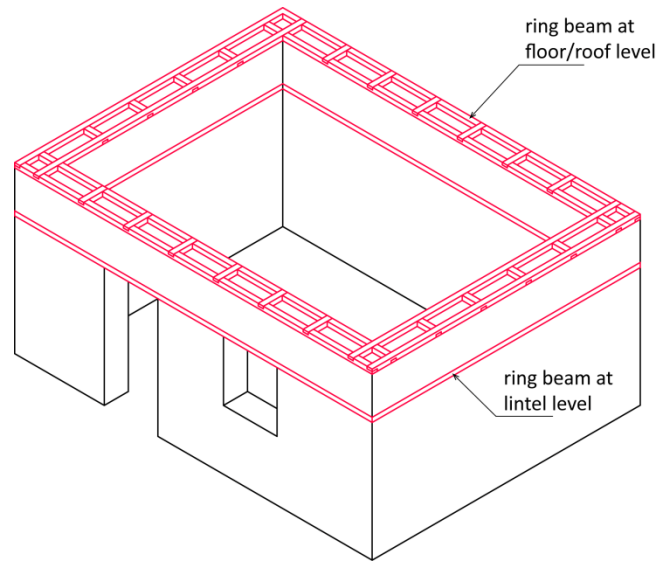


Figure 2.7: Traditional timber ring beam reinforcement

Ring beams can prevent the overturning of the wall by providing out-of-plane strength and stiffness. In addition, since they are usually built running across the entire thickness of the wall, they can also help to tie the leaves of multiple-leaf masonry walls and prevent their separation. This technique does not avoid the formation of cracks, which still initiates for a loading similar to that observed in unreinforced structures (Michiels 2015). However, it can greatly improve the seismic performance of the building in its inelastic range, maintaining its load-carrying capacity and being able to undergo larger deformations without collapsing. The use of ring beams as a strengthening technique in existing buildings is quite difficult, since their installation might require the raising and removal of the roof.

Timber ring beams can be observed in many highly seismic regions of the world and have been used for a long time in both monumental and vernacular architecture. For example, they have been used in Greece during the last 35 centuries and have nowadays become endemic of vernacular constructions in many regions of the country, being part of their local seismic culture (Vintzileou 2011). It is also a common practice in other countries, such as Turkey, Nepal, Pakistan and India. Moreover, in recognition of this ancient traditional wisdom, their use has been included in present-day codes of some of these countries as a way of improving the earthquake resistance of low strength masonry and earthen buildings; see the Indian Standards (IS-13827 1993; IS-13828 1993) and the Nepalese code (NBC-203 1994; NBC-204 1994).

The connection between the ring beams at the wall intersections has also been typically ensured by means of corner braces or corner keys. Traditional braces are timber stiffening elements placed usually diagonally at the corners that help to reinforce the wall-to-wall connections of the building (Figure 2.8a). Nevertheless, these braces are not always necessarily attached to ring beams but are also used independently, particularly in earth buildings (Figure 2.8b). If they are applied independently, timber wedges are usually used to attach the diagonal

struts to the walls in order to limit their movement (Angulo-Ibáñez et al. 2012). Corner braces can simply consist of longitudinal timber beams embedded within the walls at the corners, properly connected (Figure 2.8c). This technique also improves the post-elastic performance of the walls because it will keep the walls working together even when the joints between perpendicular walls crack during an earthquake. Given the ease of application of this technique as a strengthening solution, it has been traditionally applied in many seismic prone countries, such as Chile, Morocco and Peru (Angulo-Ibáñez et al. 2012). Timber corner braces can also be found in some regions of Portugal (Figure 2.8d), but its use is scarce.

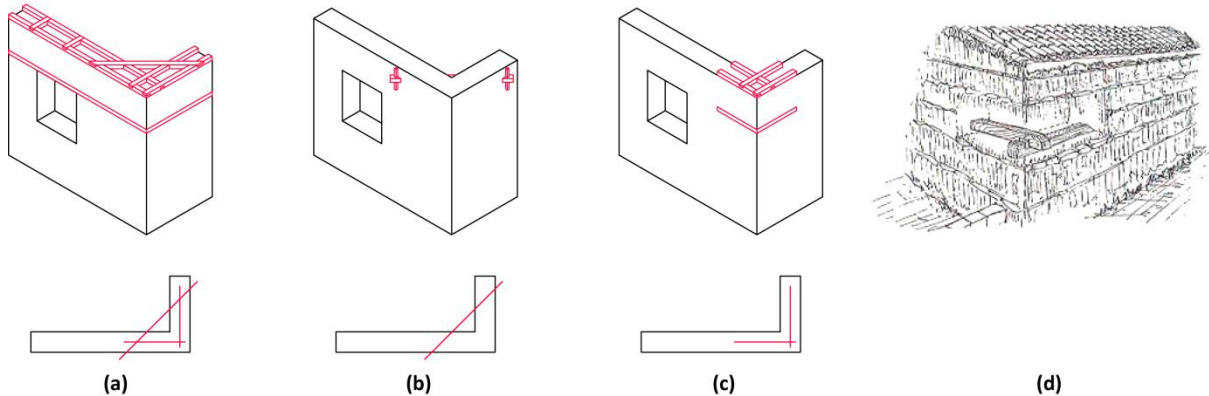


Figure 2.8: Different types of corner braces: (a) stiffening ring beams; (b) independent corner brace attached to the wall with wedges; (c) partial ring beam at the corner; and (d) timber corner brace in rammed earth building in Alentejo, Portugal (Correia 2007)

The need of strengthening buildings at the corners was already emphasized by Leon Battista Alberti (1404-1472) in his treatise *De re aedificatoria*. He recommended thickening the walls at the corners by adding pilasters to reinforce the area (Tavares et al. 2014). Another common and efficient traditional technique of reinforcing wall-to-wall connections, mainly at the façades, is the construction of quoins. This technique consists of using the best quality large squared stone blocks at the corners, carefully bonded to the orthogonal walls by creating an efficient overlapping of the ashlars with the rest of the wall (Figure 2.9a). However, the efficacy of quoins is limited when coupled with poor fabric or internally unconnected masonry which tends to become loose (D’Ayala and Paganoni 2011). Quoins can be made of other materials, such as brick masonry, when used together with earthen walls. This technique is practically impossible to be implemented other than at the time of construction or during partial reconstruction. Quoins can be commonly found in many stone masonry vernacular buildings composing the historic city centers of many seismic prone regions, such as Italy, Greece and Algeria. There are also many examples in Portugal, whose old city centers are mainly constructed with stone masonry (Figure 2.9b-c). Moreover, quoins can also be recognized in earthen buildings in some cases in Portugal, where pieces of schist or brick are introduced at the corners as reinforcement (Correia 2007).



Figure 2.9: (a) Traditional ashlar stone masonry quoin; (b) stone masonry quoin in Lagos, Portugal; and (c) ashlar stone masonry quoin in Vila Real de Santo António, Portugal

Many technical construction manuals that arose during the nineteenth and early twentieth century in Italy described detailed methods on how to properly connect the floors to the vertical resisting walls (Barbisan and Laner 1995). They acknowledged the importance of this aspect in seismic resistant construction in order to prevent the global overturning of the walls. Eventually, these technical solutions were also widely applied in vernacular architecture. A tight connection between the roof and floor beams and walls has been traditionally ensured by using beams going through the whole width of the wall and wooden wedges anchoring the beam (Figure 2.10a-b). Transition elements, such as perimeter timber resting plates and stone brackets, are also applied to provide a better support for the beams, redistribute stresses and improve their connection with the walls (Figure 2.10c). Metallic anchoring devices and ties are typically implemented as strengthening solutions (Figure 2.10d). Reinforced connections can be commonly found in vernacular architecture in many seismic countries, including Portugal (Figure 2.10e).

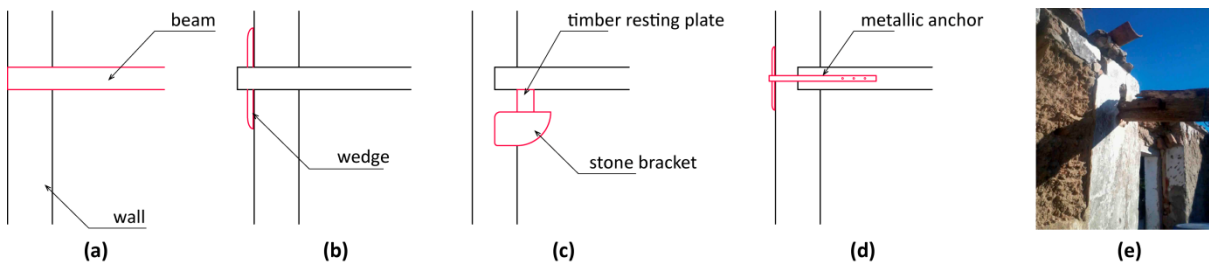


Figure 2.10: Different types of reinforced floor/roof-to-wall connections: (a) timber beam resting on the whole width of the wall; (b) timber wedges; (c) timber resting plates and stone brackets; (d) metallic anchoring devices; and (e) roof timber beam strengthened with metal bracket in Melides, Portugal (photo by CI-ESG 2013)

The use of ties for making effective links to hold together the different structural elements of the building is another ancient practice. Traditionally, ties might be the most often adopted technique to ensure the 'box-behavior' of the building and improve its structural integrity. Steel tie rods and wooden tie beams can be systematically observed in highly seismic regions as a reinforcement measure to connect perpendicular load bearing walls, load bearing walls to interior walls, parallel load bearing walls, walls to floors, and walls to roofs (Figure 2.11). Ties connecting

parallel walls are intended to avoid their out-of-plane collapse but can also constrain the floors and facilitate a better load redistribution among the different walls, improving the overall performance of the system. They are usually placed at the floor and roof levels. Actually, a common vernacular practice is the use of the floor timber joists as ties connecting parallel walls by means of using solutions such as the ones previously described to reinforce their connection with the walls.

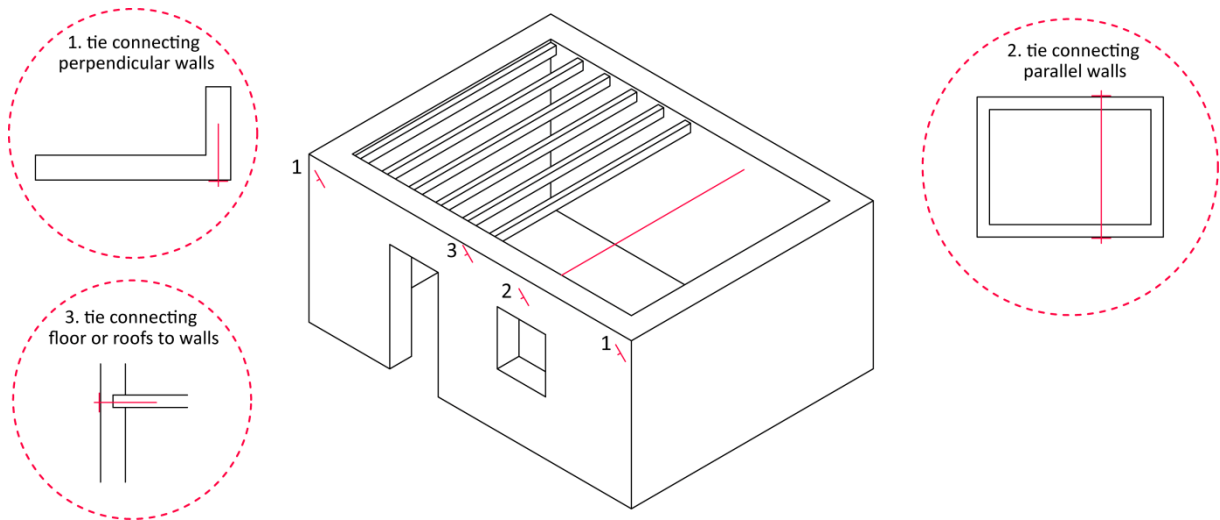


Figure 2.11: Different possible locations of ties

Ties have to be well fastened at the ends typically using steel anchor plates in the case of steel tie rods and timber wedges in the case of wooden tie beams. If not properly connected, they can actually be counterproductive and induce significant stress concentrations, causing cracking (Tolles et al. 2000). Given the fact that ties are easy to implement in existing structures before or after earthquake damage, they have been widely used for many centuries. Wooden tie beams are more frequently used in earthen buildings due to the compatibility of materials, and they can be commonly observed in many seismic prone regions, such as Peru (Michiels 2015). Steel tie rods are very commonly used to strengthen stone masonry buildings across the Mediterranean region. Their use is also widespread in Portuguese vernacular architecture (Figure 2.12).

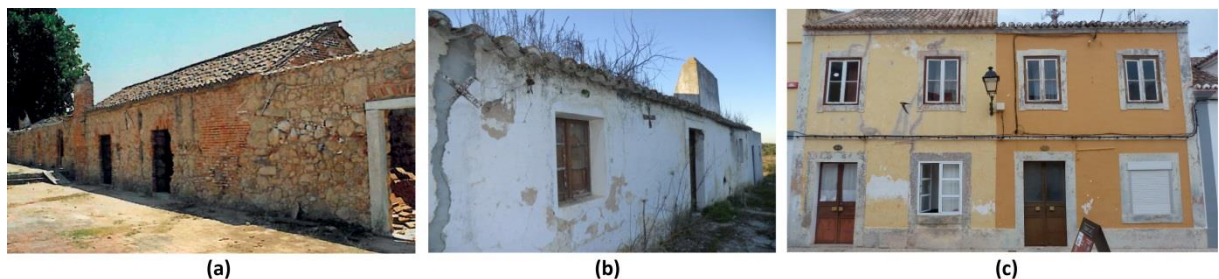


Figure 2.12: Ties in Portuguese vernacular architecture: (a) Alcácer do Sal (photo by Mariana Correia 1997); (b) Melides (photo by CI-ESG 2013); and (c) Vila Real de Santo António

2.3.2. Techniques stabilizing structural elements and buildings

2.3.2.1 Masonry walls

Besides the widespread use of timber ring beams at the top of the loadbearing walls aiming at improving the global behavior of masonry buildings, the insertion of timber elements within the masonry can also be clearly seen as a strengthening method (Figure 2.13a). Timber elements are applied due to their excellent tensile properties, becoming successful slip planes in the horizontal direction and helping to dissipate great amounts of energy. This horizontal reinforcement usually runs continuously around the entire building, holding the walls together. Furthermore, it improves the out-of-plane bending and in-plane shear resistance because, by confining portions of masonry walls, it enhances their compressive strength, shear strength and deformability properties (Vintzileou 2008). Since timber bands are typically inserted within the entire thickness of the walls, they can also avoid the separation of the leaves in multiple-leaf stone masonry walls and prevent crack propagation.

This is a very common vernacular construction practice in many seismic prone areas such as in Greece, in Turkey, where the resulting timber-laced masonry is generally known as *hatil*, and in India, where it is known as *taq* (Figure 2.13b-d). In the case of earthen buildings, bamboo or reed elements can be placed inside the walls as internal reinforcement instead of timber. Timber elements can sometimes be inserted as reinforcement of structural elements other than walls. As an example, logs are inserted on top of the column capital, working as imposts from which the arches are built, in some buildings in the Casbah of Algiers, in Algeria. The presence of the logs allows some slip movement or rolling, providing ductility and energy dissipation in the occurrence of an earthquake (Benouar and Foufa 2008).

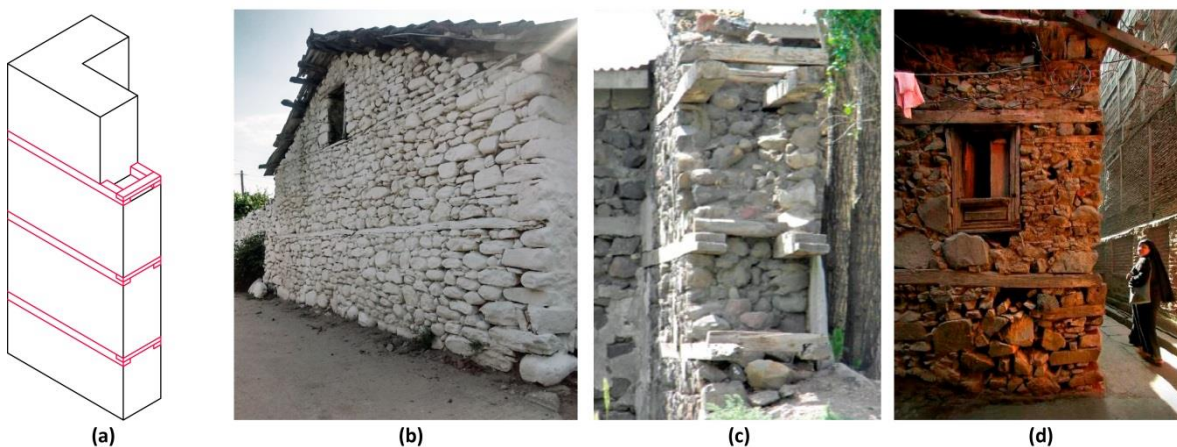


Figure 2.13: (a) Traditional way of inserting horizontal timber elements within the masonry walls; (b) timber-laced wall in Greece; (c) timber-laced wall or *hatil* in Turkey (Inan 2014); and (d) timber-laced wall or *taq* in India (Langenbach 2009)

Vernacular builders used other ways of providing ductility to the structural walls without timber. Most of them are based on the same concept of subdivision of the wall, interrupting its structural homogeneity in order to allow relative displacements of the subdivided elements and thus absorb large amounts of energy (Figure 2.14). The subdivision of the wall is also beneficial because it arrests crack development. Among the techniques and materials applied for this subdivision, the use of brick horizontal courses that extend through the thickness of the wall is the most common. Rush mats or layers of reed in-between the masonry or between lifts of rammed earth constructions have also been historically used for the same purpose of creating slip planes (Kirikov 1992). Horizontal courses of brick masonry can sometimes be recognized in the Portuguese vernacular practice (Correia 2007). This common traditional technique is only practically applicable at the time of construction or during partial reconstruction.

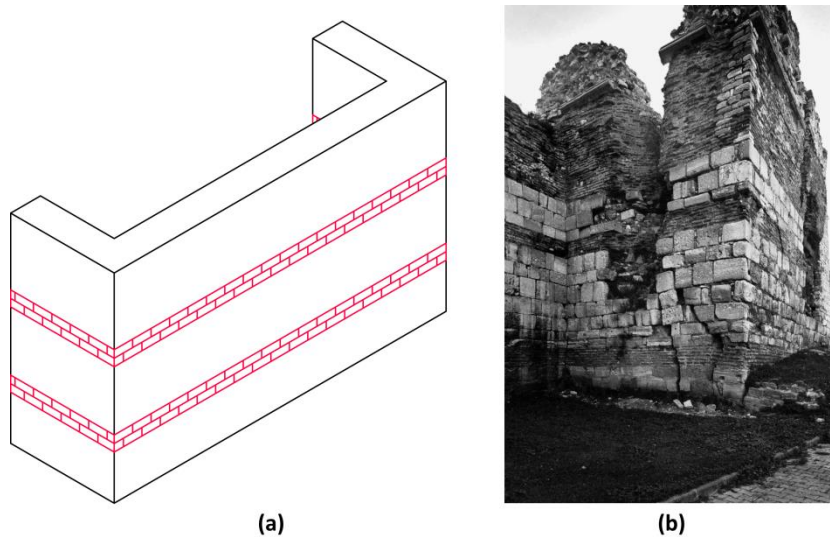


Figure 2.14: (a) Subdivision of the wall with brick horizontal courses; and (b) original city wall constructed using horizontal brick masonry bands in Istanbul, Turkey (Langenbach 2007)

One of the most common earthquake resistant provisions for masonry walls in vernacular buildings is the use of through-stones, also known as bond stones or ‘diatons’ (Figure 2.15a). As previously defined, through-stones are long stones placed across the full wall thickness. They help to prevent the separation of the wall leaves, and they provide the walls with greater stability by improving its monolithic behavior due to a better distribution of efforts through the whole section. They can also be placed at wall intersections to improve the connections between walls. The morphology of the wall cross section has a pronounced influence on the stability and bending resistance of the wall. Particularly, the number and position of through-stones can greatly improve the wall structural behavior for both in-plane and out-of-plane seismic action (de Felice 2011). Through-stones can usually only be implemented at the moment of the construction or during partial reconstruction (Figure 2.15b). Timber or metal elements can also be used as transversal ties to connect the masonry leaves and are usable as a strengthening technique.

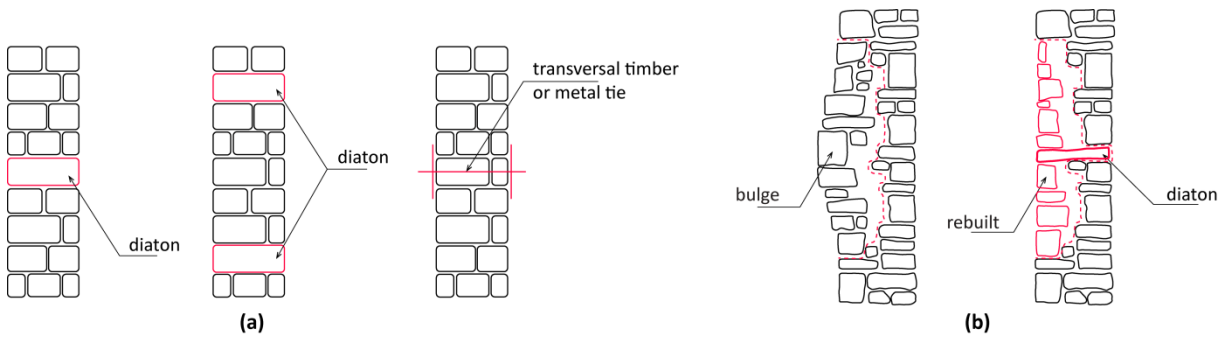


Figure 2.15: (a) Use of through-stones or 'diatons' and transversal elements; and (b) partial reconstruction of masonry wall using through-stones (Tomazevic 1999)

Post-earthquake repairs such as mended cracks intend to restore the wall integrity and stabilize it. Many techniques can be traditionally applied to repair cracks. Partial reconstructions are used to recover heavily damaged parts of the masonry and fill cracks. However, they are labor-intensive and not very widespread as a traditional repairing technique. In the case of rammed earth structures, an ancient repair technique is soft stitching (Figure 2.16a), which mainly consists of cutting chases both internally and externally around the cracks and re-filling them with rammed earth (Hurd 2009). A common vernacular solution that can be found also in Portugal is the application of metallic staples at the cracks (Figure 2.16b-c).

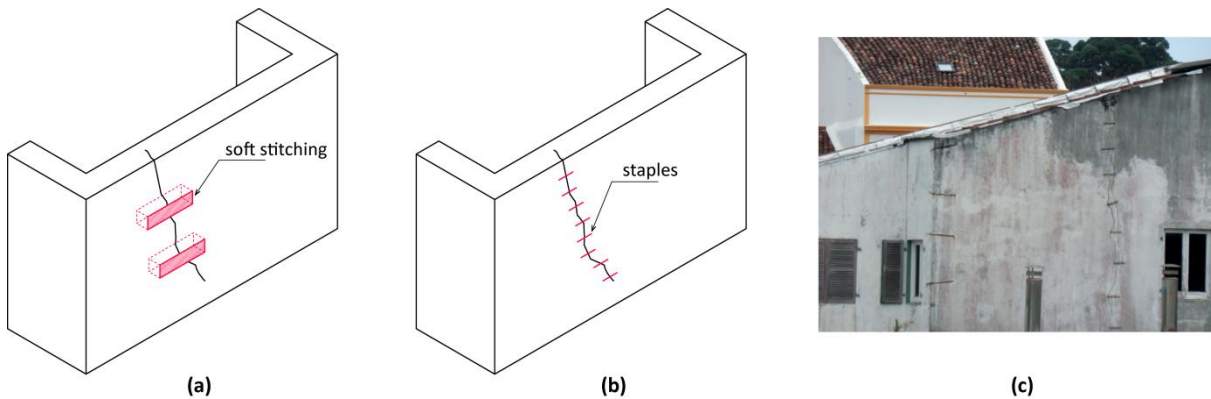


Figure 2.16: (a) soft stitching, characteristic of rammed earth constructions; (b) use of staples, characteristic of masonry constructions; and (c) example of mended cracks in Azores, Portugal (photo by Mariana Correia 2013)

The presence of openings in load bearing walls always indicates a potential seismic vulnerability of the building. A bad positioning, such as openings near the edges, causes stress concentration and cracks to arise, while too many openings or openings with oversized dimensions can greatly reduce the shear capacity of the walls. In order to reduce this seismic vulnerability, vernacular constructions usually present a reduced number of openings and symmetry in their layout. Closed openings can be commonly identified in seismic prone areas, showing the inhabitants awareness of the vulnerability of these elements.

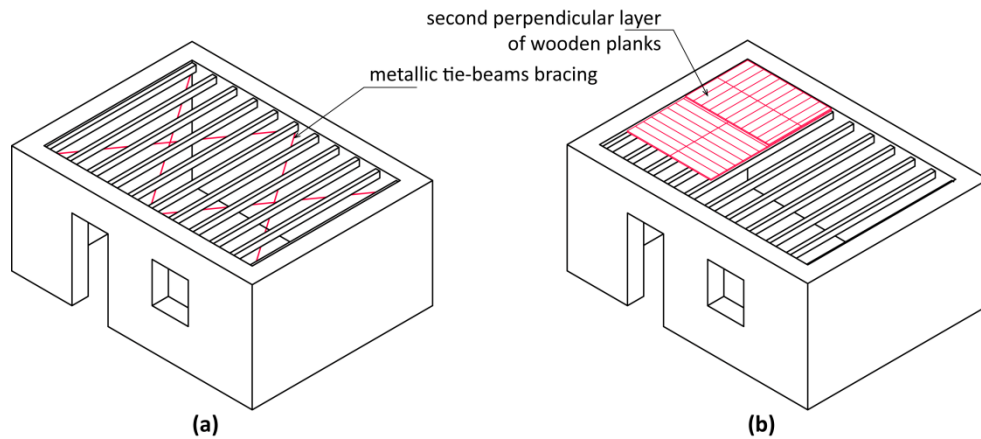


Figure 2.18: (a) Traditional way of stiffening floors and roofs by diagonal bracing; and (b) floor stiffening by adding an extra floor layer consisting of wooden planks placed perpendicular to the existing ones

2.3.2.3 Timber frames as earthquake resistant systems

The use of structural timber frames in vernacular architecture can be observed in many places around the world, where they are acknowledged as earthquake resistant construction systems. They can be found in Greece, in Turkey, where they are known as *himis*, in Northern Pakistan, known as *cator and cribbage* (Hughes 2000), or in Kashmir, known as *dhajji-dewari* (Langenbach 2009). Even in Central and South America, timber or bamboo frame constructions have been used since Pre-Hispanic times in rural houses and are known as *bahareque* in Colombia, Ecuador and El Salvador, *quincha* in Peru, or *taquezal* in Nicaragua. The good seismic performance of timber frame traditional structures has been reported in many past earthquakes, such as the 1988 Armenian earthquake (Jigyasu 2002), the 1999 Marmara earthquake in Turkey (Gülhan and Güney 2000), the 2005 Kashmir earthquake (Langenbach 2009), or the 2010 Haiti earthquake (Langenbach et al. 2010). In all these cases, they performed overall better than many new reinforced concrete buildings.

In Portugal, there is a particular case of timber frame construction known as *Pombalino*, which can be highlighted as the most representative example of a Portuguese seismic culture. A complex reconstruction process introducing new urban, architectural and structural concepts was devised by the government and mandatorily introduced after the 1755 Lisbon earthquake. It introduced what can be considered the first technical prescriptions regarding seismic resistance (Cardoso et al. 2004). This process has been widely studied (Lopes dos Santos 1994; Mascarenhas 1996), and the most relevant seismic resistant provision was the inclusion of a three-dimensional braced timber structure named *gaiola pombalina* as the internal structure of the building.

The *gaiola* is a resistant and flexible cage, whose walls are composed by horizontal, vertical and diagonal timber elements usually filled with rubble or brick masonry and plastered. The external walls of *Pombalino* buildings are made of stone masonry and the walls composing the

gaiola, which are known as *frontal* walls, act as the shear walls of the building. They are supposed to resist horizontal loads by providing a bracing function, avoiding an out-of-plane premature collapse of the exterior masonry walls while dissipating substantial amounts of energy (Figure 2.19a). A minimal timber skeleton is occasionally also present in the inner face of the exterior masonry walls, facilitating the connection with the floors and the inner shear walls.

This constructive system was adopted by local communities as a model of earthquake resistant construction. Its use spread around the country, eventually taking root in the vernacular way of building and becoming part of the Portuguese local seismic culture. Nowadays, *frontal* walls can be identified in many vernacular constructions scattered across the country (Figure 2.19b-d). A relevant example is the case of the town of Benavente, where this seismic resistant construction system was chosen for the reconstruction works of the city after the 1909 devastating earthquake, based on the Lisbon experience. According to Vieira (2009), all the rebuilt districts of the town have buildings with a timber skeleton. A similar experience took place in Calabria (Italy), where the government developed another similar timber frame earthquake resistant system, known as *casa baraccata*, after the 1783 earthquake (Tobriner 1983; Dipasquale 2015). Again, the imposed reconstruction solution with timber frame buildings was eventually adopted by vernacular builders and several buildings testify to its widespread application in the region.

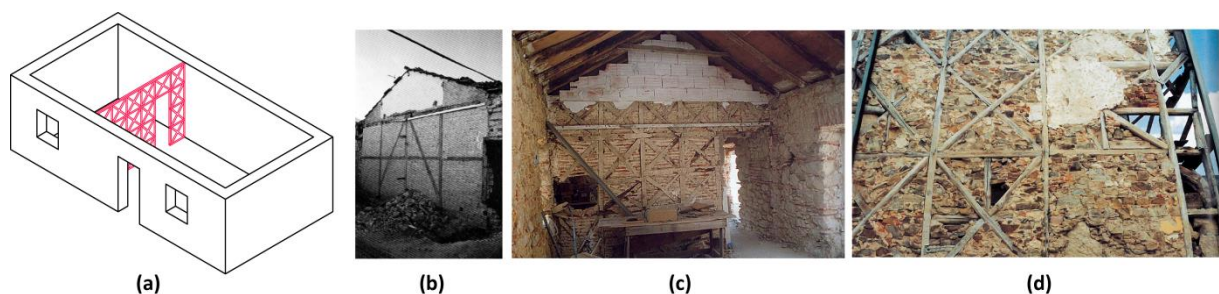


Figure 2.19: (a) Traditional structural timber frame *frontal* wall; (b) *frontal* wall in Benavente, Portugal (Vieira 2009); (c) *frontal* wall in Alcácer do Sal, Portugal (Correia and Merten 2001); and (d) *frontal* wall in Vila Real de Santo António, Portugal (Figueiras 1999)

2.3.3. Techniques allowing partial collapse of structural elements

A key aspect for a building to sustain damage without total collapse is the redundancy of structural elements so that the failure of certain members does not mean the failure of the building. Structural redundancy is a very efficient seismic resistant technique that was traditionally achieved by the simultaneous use of timber and masonry structural elements (Figure 2.20). The most representative example of this technique and illustrative of the development of a local seismic culture can be observed in the island of Lefkas, in Greece. The periodic recurrence of earthquake in the island led the inhabitants to improve the seismic

resistance of their constructions and to work out an indigenous structural system that effectively resisted earthquake loading. This system is thus a consequence of the practical need of inhabitants to respond to the local conditions, and it emerged from a long traditional practice (Porphyrios 1971). Additionally, after the 1825 destructive earthquake, its use was also imposed by the English government, which occupied the island at the time (Touliatos 1992).

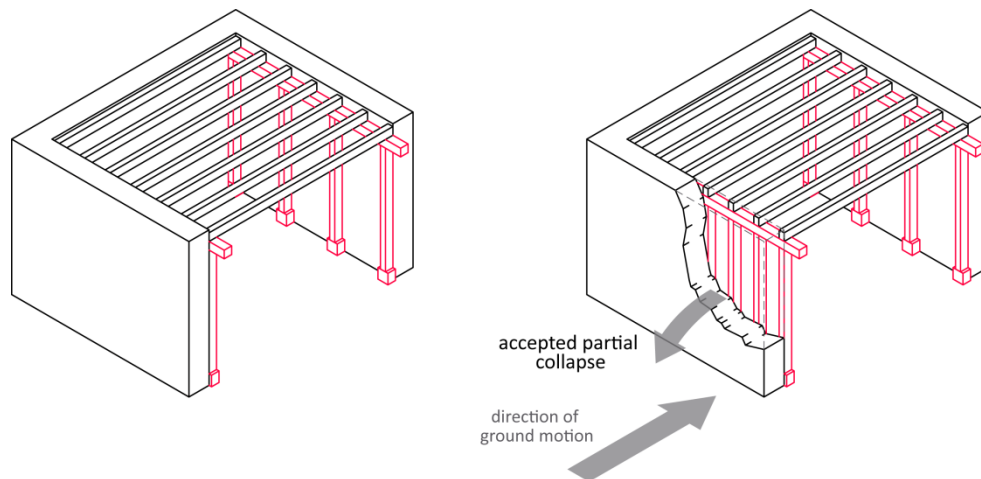


Figure 2.20: Structural redundancy: the use of a dual load bearing structure allows the partial collapse of some elements while keeping the construction standing

The structural system includes a highly perfected timber frame but the most significant resistant characteristic is the structural redundancy. The ground floor of the buildings is constructed with load bearing thick masonry walls but timber structural columns are also present as a secondary structure, independent from the first one. In this way, the masonry walls can collapse in the event of an earthquake and tend to be thrown towards the exterior due to the presence of the timber structure in the interior. The timber structure does not collapse because it is supported by the timber columns and keeps the building standing with the timber frame second floor and the roof intact. As a result, the people inside the building are more protected and the masonry walls can be easily and rapidly repaired. Today, this system is still common and widespread in the island and has proven to behave well against earthquakes. In the 2003 earthquake, none of these traditional buildings suffered total collapse, even though some three-story reinforced concrete buildings did, and just several of them suffered partial collapse of the timber frame masonry infill or the ground floor masonry walls (Karakostas et al. 2005).

The redundancy of structural elements is also a characteristic feature of some Chinese traditional buildings, in which timber beams and columns are the main structural elements, but heavy masonry walls made of adobe or brick are also commonly built in between columns. These walls highly increase the stiffness of the building but, due to their poor shear strength, are vulnerable to earthquakes. According to Zhiping (2000), their collapse during an earthquake reduces the earthquake action and therefore it is accepted and expected. In addition, as there is

no link between the walls and the columns, it does not endanger the timber frame, keeping the building standing. It should be mentioned that this is also a characteristic feature of the previously discussed *pombalino* buildings. During a seismic event, the heavy masonry façade can fall, together with the roof tiles and the plaster of the inner walls, but the inner timber skeleton is supposed to keep standing, avoiding the complete collapse of the building. Nevertheless, all these construction typologies were conceived at the time of the construction of the building. Therefore, they can only be implemented as a strengthening technique by introducing new structural elements in the building, which can be rather invasive and unacceptable.

2.3.4. Techniques counteracting horizontal loads

Techniques based on providing a counteracting effect against the buckling tendency of a wall are very common in most seismic prone regions (Pierotti and Uliveri 2001). The most common and widespread traditional strengthening technique used for resisting and counterbalancing seismic horizontal forces is the construction of buttresses or counterforts. They can also be known as pilasters if they are embedded within the walls in rammed earth buildings. They can be built at the same time as the building, as a deliberated feature, or they can be added as a reinforcement measure. They consist of pier-like, massive local additions typically of masonry, whose working principle is to counter the rotation of the façade thanks to their sheer mass (Figure 2.21).

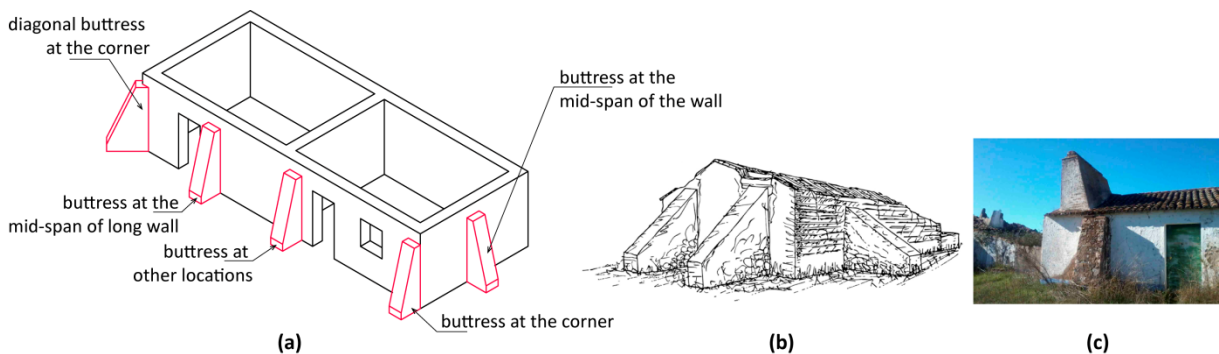


Figure 2.21: (a) Different possible locations of buttresses; (b) buttresses in Redondo, Portugal (Correia 2007); and (c) buttress in the region of Évora, Portugal (photo by CI-ESG 2013)

When adding a buttress as reinforcement, special attention should be put at its connection with the original walls. If they are not properly connected, they add little or no stability to the building, acting independently and only when the wall moves towards the buttress. They can even be prone to rock against the wall if the movement is the opposite, imposing an extra load. Therefore, it is recommended to tie the buttresses to the walls using, for example, cross ties (Michiels 2015). Buttresses should be placed at critical locations, such as the mid-span of long walls, which are the most vulnerable elements to the effects of out-of-plane earthquake vibrations, and at the corners, in order to avoid the separation of the walls. They can be found in most seismic prone regions, such as Peru and Italy, but are also very common in Portugal (Figure

2.22). Buttresses are also very common in an urban environment, and are distinctly a reinforcement measure because, when added to the buildings, they invade the public space, sacrificing the comfort of the inhabitants in pursuit of the seismic safety (Figure 2.22a). Sometimes, other urban structures, such as external stairs, can also achieve a similar role of counteracting the rotation of the walls (Figure 2.22c).



Figure 2.22: (a) Buttress invading the side walk in Samora Correia (Correia and Merten 2001); (b) two-floor buttress in Évora (Correia and Merten 2001); and (c) external staircase in Benavente (Correia and Merten 2001)

Another traditional seismic resistant concept is to lower the center of gravity of the buildings. This has been traditionally achieved by using scarp walls, decreasing the thickness of the upper floors walls, and using light timber floors and roofs. The combination of two different structural systems, using the lighter one on the upper floors, is also common. Usually, the ground floor is built with stone masonry and a timber frame system is used in the upper floors. This is a common practice in Turkey and Greece, but also in Portugal (Ferreira et al. 2013a). A traditional strengthening technique aimed at lowering the center of gravity of the building consists of thickening the walls by means of adding mass to the ground floor walls (Figure 2.23). This technique increases the resisting area of the walls and reduces their height-to-thickness ratio, which improves their out-of-plane resistance and reduces the possibility of overturning.

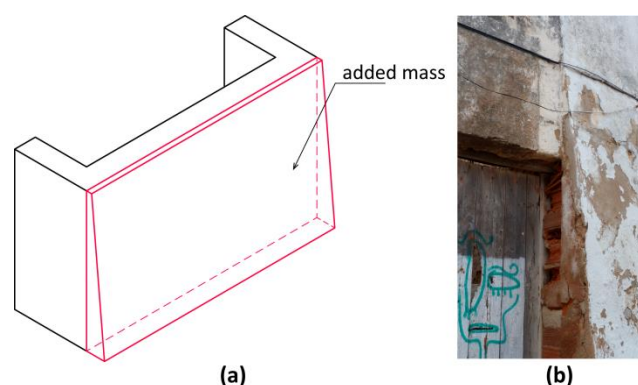


Figure 2.23: (a) Traditional thickening of the wall by adding mass and increasing the resisting cross section; (b) example of thickened wall in Lagos, Portugal

In urban environments, other common reinforcement elements are urban reinforcing arches, also known as buttressing arches. They are usually made of masonry and span the streets, joining

facing buildings at the level of their floors (Figure 2.24a). These alterations of the historical built-up areas effectively lead to the collaborative action of neighboring constructions, enabling the horizontal movements to be redistributed among their structural elements. In order to perform an effective reinforcing function, reinforcing arches should be properly connected with the old structures, and they should avoid differences in the level of the floors or ceilings, which may lead to dangerous eccentricities. Similarly to the buttresses, these arches work as propping structures and do not have an influence under static conditions. They are the typical historical solution to avoid the development of out-of-plane mechanisms at an urban level in villages built mainly of stone masonry, such as Italians, and have become part of their historical fabric. They can also be recognized in many Portuguese cities, such as Lisbon, Évora and Lagos (Figure 2.24b-d).

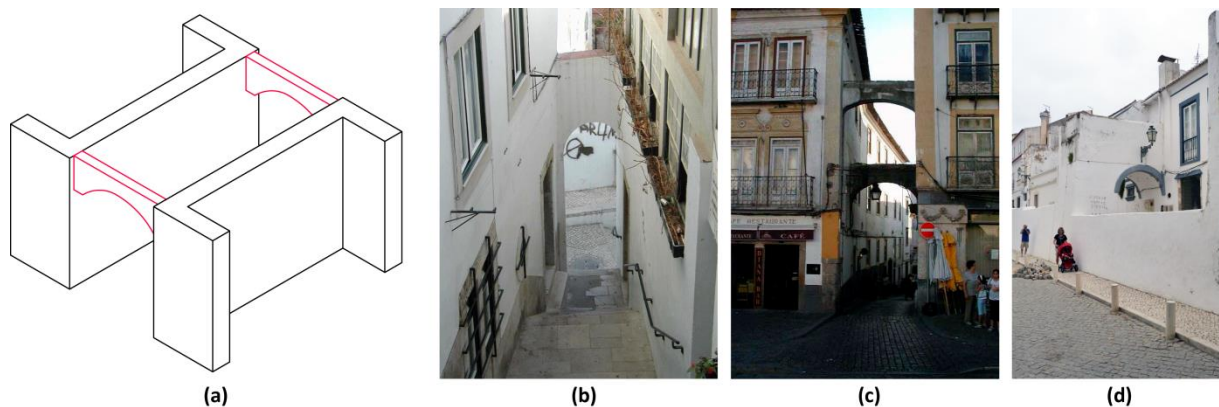


Figure 2.24: (a) Masonry reinforcing arches; (b) reinforcement arch in Alfama, Lisbon (Correia and Merten 2001); (c) reinforcement arches in Évora (Correia and Merten 2001); and (d) vaulted passage in Lagos, Portugal

Urban reinforcement arches and buttresses can eventually transform into other urban elements that accommodate new uses, since their construction can result in an increase in volume and in new space available for the building. In this way, these added structures can eventually become habitable and turn into loggias, vaulted passageways or arcades, fulfilling simultaneously a structural and a functional role, with the addition of new paths and rooms. The use of these elements can be counterproductive if the reinforced buildings have insufficient thick walls and thus are not able to produce counterthrust that centers the new horizontal forces exerted by the arcades and habitable buttresses (Niglio and Ulivieri 2005).

2.3.5. Summary

Aiming at providing a general overview of the earthquake resistant techniques observed in vernacular architecture, a summary is presented in Table 2.1. The table highlights the type of damage that can be avoided applying each technique, as well as the applicability of the different techniques as strengthening solutions, which refers to the ease of use of the technique in existing buildings. ‘Difficult’ indicates that the technique should be better implemented at the time of the

construction or during partial reconstruction, and ‘practical’ indicates that the technique can be and have been successfully applied for strengthening.

Table 2.1: Summary of traditional earthquake resistant techniques classified according to the typologies defined and highlighting: (a) type of damage avoided; and (b) applicability as a strengthening technique

Technique	Damage prevention				Applicability as strengthening technique	
	Separation	Out-of-plane	Delamination	In-plane	Difficult	Practical
1. Techniques improving the connection between structural elements						
Ring beams	X	X	X	X	X	
Corner braces	X					X
Quoins	X				X	
Reinforced floor-to-wall and roof-to-wall connections		X				X
Ties	X	X				X
2. Techniques stabilizing structural elements and buildings						
Timber elements within the masonry	X	X	X	X	X	
Wall subdivision		X	X	X	X	
Through-stones	X	X	X	X		X
Mended cracks		X		X		X
Reinforcing openings		X		X	X	
Stiffening floors and roofs	X	X		X		X
Wall structural timber frame	X	X	X	X	X	
3. Techniques allowing partial collapse of structural elements						
Redundancy of structural elements ¹					X	
4. Techniques counteracting horizontal loads						
Buttresses	X	X				X
Walls thickening		X		X		X
Urban reinforcing arches		X				X

¹ Damage of certain structural elements is tolerated, such as the out-of-plane collapse of the walls

2.4. Seismic-V Project: Vernacular seismic culture in Portugal

The research project ‘Seismic-V: Vernacular seismic culture in Portugal’ (Correia et al. 2014) was primarily aimed at contributing to the reflection on the existence of a local seismic culture in Portugal through the identification of strategies and earthquake resistant elements incorporated in the local constructive culture of different Portuguese regions. This main research objective laid the foundations of the present PhD thesis and provides its general framework.

As part of the research methodology, the project included the definition of several Portuguese regions as study areas, followed by survey missions intended to the *in-situ* identification of earthquake resistant solutions in vernacular architecture. The overview of traditional seismic resistant practices shown in the present chapter has been illustrated with examples observed during these survey missions. Moreover, based on the results from the field observations, one study area was selected as a case study for the present thesis: Vila Real de Santo António

(VRSA), which belongs to the region of Algarve, in the south of Portugal. The two seismic vulnerability assessment methods developed will be applied in Chapter 8 in VRSA.

The research project's outcomes were presented in different publications (Correia and Carlos 2015; Correia et al. 2015) and a website. One of the fundamental issues was to attract research interest towards vernacular architecture and its contribution to seismic risk mitigation. The emerged findings brought consistent outcomes. The main reinforcement and retrofitting elements identified in the vernacular architecture at each region were analyzed and systematized. Furthermore, the project findings also involved the identification and definition of the most frequent constructive errors that lead to an increase in the seismic vulnerability of vernacular architecture, as well as the most efficient solutions for the mitigation of the seismic vulnerability. As a result, a set of recommendations for the seismic retrofitting of vernacular architecture was provided. The project outcomes thus suppose an important contribution to understand the seismic behavior of vernacular buildings and can help to the safety and survival of local communities in the event of an earthquake.

2.5. Conclusions

This chapter provides an overview of the most common seismic resistant provisions traditionally used in vernacular architecture associated with a local seismic culture, and classifies them according to the damage prevention and their possible applicability as strengthening measures. Earthquake resistant techniques traditionally used throughout the world have been presented and discussed, with a parallel analysis of the Portuguese context. Sometimes, it can be difficult to associate changes or innovations in the construction techniques to the existence of a seismic culture. However, even if they were or not consciously developed to minimize damages produced by an earthquake, a sort of natural selection of the successful designs that have continually proven to withstand earthquakes have most likely occurred. If something has become traditional is because it has been effective in resisting past seismic events in the region and, moreover, it can resist seismic events in the future. As a result, a commonality in the use of specific seismic resistant features can be observed in highly seismic regions across the world.

Most of the reviewed techniques can also be identified in Portugal, particularly where past earthquakes took place in the past, namely in Lisbon and other cities located in the south region of Portugal, which is also considered as a moderate seismic hazard region. However, signs of seismic culture in these regions seem to become scarcer and essentially abandoned. Portugal seismicity is distinguished by large periods of time without seismic events and this has led to the development of a reactive response behavior in which local communities usually just respond to earthquakes in the immediate aftermath of the event. This means that there has been a seismic concern and awareness at particular times in the past. Important measures and seismic resistant

construction techniques, such as the *Pombalino* construction system, were devised and implemented after the infrequent destructive earthquakes, and they eventually became part of the indigenous knowledge. Nevertheless, the large periods of time without earthquakes resulted in the removing and abandonment of these elements, particularly in rehabilitation processes or in the adaptation of the buildings to other uses. Therefore, Portugal is considered to belong to those cases where there has been an abandonment of a local seismic culture led by the loss of seismic awareness of the population.

The appreciation and successful protection of the vernacular heritage is a demand of the modern societies, but it highly depends on the involvement and support of the community. Thus, the dissemination of local seismic culture is a must in order to contribute to the reawakening of the risk awareness of local communities. Local communities should be encouraged to readopt some of the reviewed traditional techniques in order to reduce the seismic vulnerability of their constructions. Research in these traditional provisions and in its possible use as seismic strengthening for existing in-use vernacular architecture is, therefore, justified. Besides, the use of traditional solutions is in accordance with the modern principles of preservation of the vernacular heritage regarding compatibility and authenticity, since they use similar materials and techniques. Following the presented identification of the most typical solutions, Chapter 7 will deal with the understanding of their structural behavior by means of numerical analysis, aiming at their validation for their eventual application for strengthening in-use vernacular architecture.

CHAPTER 3

DEFINITION OF A SEISMIC VULNERABILITY ASSESSMENT METHOD FOR VERNACULAR ARCHITECTURE

Chapter outline

- 3.1. [Introduction](#)
- 3.2. [Overview of the existing methods](#)
 - 3.2.1. [The vulnerability index method](#)
 - 3.2.2. [The macroseismic method](#)
 - 3.2.3. [Combination of the vulnerability index and the macroseismic method](#)
- 3.3. [Proposed seismic vulnerability assessment methods for vernacular architecture](#)
- 3.4. [Definition of seismic vulnerability assessment parameters](#)
- 3.5. [Numerical strategy adopted for the parametric study](#)
 - 3.5.1. [Definition of limit states](#)
 - 3.5.2. [Reference numerical model](#)
 - 3.5.3. [Numerical models details](#)
 - 3.5.4. [Parameters variations](#)
 - 3.5.4.1. [Wall slenderness](#)
 - 3.5.4.2. [Maximum wall span](#)
 - 3.5.4.3. [Type of material](#)
 - 3.5.4.4. [Wall-to-wall connections](#)
 - 3.5.4.5. [Horizontal diaphragms](#)
 - 3.5.4.6. [Roof thrust](#)
 - 3.5.4.7. [Wall openings](#)
 - 3.5.4.8. [Number of floors](#)
 - 3.5.4.9. [Previous structural damage](#)
 - 3.5.4.10. [In-plane index](#)
- 3.6. [Conclusions](#)

3.1. Introduction

Considering that vulnerability can be broadly defined as the potential for loss (Cutter 1996), the seismic vulnerability of a structure can be defined as its intrinsic proneness to suffer damage as a result of a seismic event. Therefore, the main objective of seismic vulnerability assessments is to

measure the probability of a specific building to reach a given level of damage when subjected to a seismic action with specified characteristics (Barbat et al. 1996; Calvi 2006). Seismic vulnerability assessment methods for the built environment, together with hazard analysis (evaluation of the probability of exceedance of a certain level of seismic intensity) and exposure data (inventory of the elements at risk), is one of the main tools used in earthquake loss models (Azizi-Bondarabadi 2016). Earthquake loss models are meant to predict the consequences of an earthquake quantitatively, in terms of economic impact (e.g. probability of collapsed and unusable buildings), repair cost and human casualties. They are an essential tool for seismic risk mitigation because they can be important for evaluating different mitigation policies and planning immediate emergency response and disaster recovering.

The present thesis focuses on the development of a method for the seismic vulnerability assessment of vernacular architecture, acknowledging that these methods can be also capable of identifying building fragilities and thus can address an essential aspect in which the engineering research can intervene (Vicente et al. 2011). The evaluation of the seismic vulnerability of existing constructions can be used to: (1) evaluate the need of retrofitting solutions; (2) assess the efficiency of proposed structural interventions in reducing the seismic vulnerability of the buildings; and (3) evaluate different building retrofitting strategies through cost/benefit studies. In conclusion, the seismic vulnerability assessment of vernacular buildings can lead to the definition and optimization of building retrofitting strategies based on traditional practices emerging from vernacular architecture as a consequence of a local seismic culture, which is one of the main objectives of the present research.

There exists a wide range of seismic vulnerability assessment methods available in the literature, suitable for different types of analysis with different goals. First of all, the selection of a specific method depends on the scale of the analysis and the level of detail required for the targeted buildings in the area of study (Vicente 2008). First level approaches are based on less exhaustive inspection and qualitative information comprising few parameters that can be also treated statistically. They are particularly well suited for large scale analyses, e.g. urban or national scale, which comprise large numbers of buildings. Second level approaches require a higher quality of information including geometrical and mechanical aspects of the evaluated structures. Finally, third level approaches are particularly adequate for individual buildings because they demand rigorous surveys for the compilation of precise quantitative data, which is required for the preparation of complex numerical models.

The type of method used for a seismic vulnerability assessment can be also distinguished based on the approach adopted to obtain information about the probability of a building to suffer a certain damage level for a given earthquake intensity: (a) empirical; (b) analytical; or (c) expert judgment. The empirical approach relies on qualitative information mainly based on data gathered from post-earthquake damage observation. After the analysis of the data, correlations

can be extracted between the damage observed on different building typologies and a given ground motion intensity, leading to damage-motion relationships, as termed by Calvi (2006). There are different ways of expressing this relationship in the literature. For instance, damage probability matrices (DPM) are formulated in a discrete form based on the concept that a particular structural typology has a similar probability of reaching a given damage state after an earthquake of a given intensity. They were firstly proposed by Whitman et al. (1973) based on post-earthquake observation after the 1971 San Fernando earthquake, but have been later applied and updated after different earthquakes by different authors, using different intensity and damage scales (Braga et al. 1982; Grünthal 1998; Dolce et al. 2003; Di Pasquale et al. 2005). Another possibility of describing the damage-motion relationship is through continuous vulnerability functions, first developed by Spence et al. (1992). The main problem to overcome for their derivation is that both earthquake intensity and damage are typically expressed in a discrete form and not as continuous variables. However, different authors used different ways to describe the earthquake action and the damage in order to develop empirical vulnerability or fragility curves after post-earthquake surveys (Sabetta et al. 1998; Rota et al. 2006). Empirical methods require a large set of post-earthquake damage data which is not always available, but are adequate for large scale analyses because they can make use of simpler qualitative data that can be obtained from an expedite evaluation of the buildings based on visual observation.

Analytical approaches use models representing buildings or building components and perform structural analysis to evaluate the seismic effect on the structures, in terms of damage. There are many methods that can range different degrees of complexity depending on the type of model selected to simulate the structure and the analytical procedure adopted to perform the analysis. Analytical vulnerability curves can then be derived through regression analysis on the damage distribution data obtained after performing a large number of analyses on the models. Some common analytical methods existing in the literature are based on simplified mechanical models and limit state analysis (Calvi 1999) or kinematic limit analysis (D'Ayala and Speranza 2003). Others make use of more sophisticated models and nonlinear static analysis procedures (ATC-40 1996; Fajfar 1999). Many recent studies use the equivalent frame model (Lagomarsino et al. 2013) and perform a high number of nonlinear dynamic and static analyses in order to obtain vulnerability curves for different masonry building typologies (Erberick 2008; Pasticier et al. 2008; Rota et al. 2010). Analytical approaches are suitable to overcome the lack of post-earthquake damage observations, but they require more detailed information and a better understanding of construction details and materials to prepare the models. Thus, they can be very computationally expensive to use on large-scale analysis comprising areas with buildings showing diverse construction characteristics. Moreover, they highly depend on the analytical model considered. For example, some of the mentioned equivalent frame models disregard the out-of-plane behavior of the walls, which is a common failure mechanism for unreinforced

masonry buildings. On the other hand, the use of complex numerical modeling also allows taking into account the effect of constructive and material characteristics that cannot be typically considered in empirical methods, meaning that it is an appropriate tool to carry out parametric studies. It should be noted that analytical methods should be always validated with empirical observations.

Methods based on expert judgments emerged as a result of the limited post-earthquake damage data in terms of different building typologies and the high costs related to analytical approaches (Jaiswal et al. 2012). On the basis of expert opinion and previous knowledge, they estimate the damage that a certain structure can suffer for a given seismic intensity by analyzing the structural characteristics of the constructions and classifying them into different building typologies (ATC-13 1985; HAZUS 1999). Finally, there are also hybrid approaches that result from a combined use of the previously described approaches, such as the vulnerability index method (Benedetti and Petrini 1984) and the macroseismic method (Lagomarsino and Giovinazzi 2006), which are supported by statistical studies of post-earthquake damage information, but also rely on expert opinion.

The present thesis focuses on the seismic vulnerability assessment of the vernacular architectural heritage. While vernacular buildings can show significant variations on structural, construction and material characteristics, there is a typical lack of resources (mainly economic) that can be assigned to the study of a traditionally underestimated and precarious heritage. That is why a method for the seismic vulnerability assessment of vernacular architecture should be based on empirical post-earthquake surveys and expert judgments and, making use of qualitative data that can be rapidly obtained from simple visual inspections of the buildings. This research work intends to develop two methods that are based on the combination of the vulnerability index and the macroseismic methods, following the approach proposed by Vicente (2008), but are specifically adapted to the characteristics of vernacular architecture. An overview of the methods that are considered as reference is provided in the present chapter.

Two important aspects need to be clarified in relation to the developed methods. First of all, they require the identification of some key parameters related to geometrical, structural, constructive or material features of the buildings that are considered to influence the seismic response of the building. A review of parameters selected by existing vulnerability index methods is presented in this chapter. This is followed by the presentation of the parameters that are used for the present research, whose selection is based on literature review, but takes as basis the particularities of vernacular building typologies. Secondly, a thorough parametric numerical simulation based on FE modeling was designed to support the analysis of the influence of the selected key parameters on the seismic behavior of vernacular buildings. This numerical study is thus aimed at: (a) obtaining a deep understanding of the seismic behavior of vernacular constructions; and (b) quantitatively evaluating the importance of the key parameters in the

definition of the seismic vulnerability of vernacular buildings. It should be mentioned that few studies have combined analytical approaches, such as numerical analysis, to add robustness to mostly empirical methods (Shakya 2014). The numerical strategy that will be followed in the succeeding chapters for the development of the two proposed seismic vulnerability assessment methods is also introduced within this chapter.

3.2. Overview of the existing methods

The methods that are used as basis for the initial development of the two seismic vulnerability assessment methods for vernacular architecture are described in the following subsections.

3.2.1. The vulnerability index method

The vulnerability index method was originally proposed by Benedetti and Petrini (1984) specifically for masonry buildings. It can be considered as a hybrid approach because it is based on a vast set of post-seismic damage survey data and on expert judgment for the identification of constructive aspects that are more influential in the seismic structural behavior of the building, which results in the definition of several qualitative and quantitative parameters. The original formulation accounted for a total of eleven parameters including, among others, the type of vertical structural system, the type of horizontal diaphragms, the plan configuration and the conservation state. The parameters are related to four classes corresponding to increasing vulnerability, from A (lowest) to D (highest), which are associated with a qualification coefficient (C_{vi}). A weight factor (p_i) is also included to emphasize the relative importance of each parameter. Each parameter can be qualified individually, and the overall vulnerability of the building is calculated as the weighted sum of the parameters, expressed by means of a vulnerability index (I_v). As an example, Table 3.1 shows the parameters, qualification coefficients and weight factors proposed by Benedetti and Petrini (1984). It should be noted that the vulnerability index is typically normalized to fall within a range between 0 (very low vulnerability) and 100 (very high). The vulnerability index can thus be understood as a measure of the building safety under seismic loads (Barbat et al. 1996).

Post-earthquake records can be used to calibrate vulnerability functions relating the vulnerability index to a damage factor (d) for a particular seismic event, expressed either by means of macroseismic intensity or peak ground acceleration (PGA). The damage factor is an economic index that ranges from 0 to 1 and represents the structural state of the building after an earthquake taking into account the expected repair cost. The damage-motion relationship proposed by Guagenti and Petrini (1989) assumes a linear variation of the damage factor between two PGA threshold values. Both threshold values represent the initial acceleration that leads to the onset of damage and the acceleration that causes the collapse of the building. The damage-motion relationship can be defined for a given normalized vulnerability indexes using empirically

developed formulations calibrated after post-earthquake damage observations. The original vulnerability curves shown in Figure 3.1 were calibrated after data from the 1976 Friuli and 1984 Abruzzo earthquakes. The use of PGA to express the severity of the seismic event allows using a continuous parameter instead of a discrete one, such as macroseismic intensity.

Table 3.1: Vulnerability index original formulation (Benedetti and Petrini 1984)

Parameter	Class (C_{vi})				Weight (p_i)	Vulnerability index	
	A	B	C	D			
P1. Type and organization of resisting system	0	5	20	45	1.00	$I_V = \sum_{i=1}^{11} C_{vi} \times p_i$ $0 \leq I_V \leq 382.5$	
P2. Quality of resisting system	0	5	25	45	0.25		
P3. Conventional resistance	0	5	25	45	1.50		
P4. Building position and type of foundations	0	5	25	45	0.75		
P5. Type of horizontal structural system	0	5	15	45	1.00		
P6. Plan configuration	0	5	25	45	0.50		
P7. Elevation configuration	0	5	25	45	1.00		
P8. Maximum distance between walls	0	5	25	45	0.25		
P9. Type of roofing structural system	0	15	25	45	1.00		Normalized index
P10. Non-structural elements	0	0	25	45	0.25		$0 \leq I_V \leq 100$
P11. Conservation state	0	5	25	45	1.00		

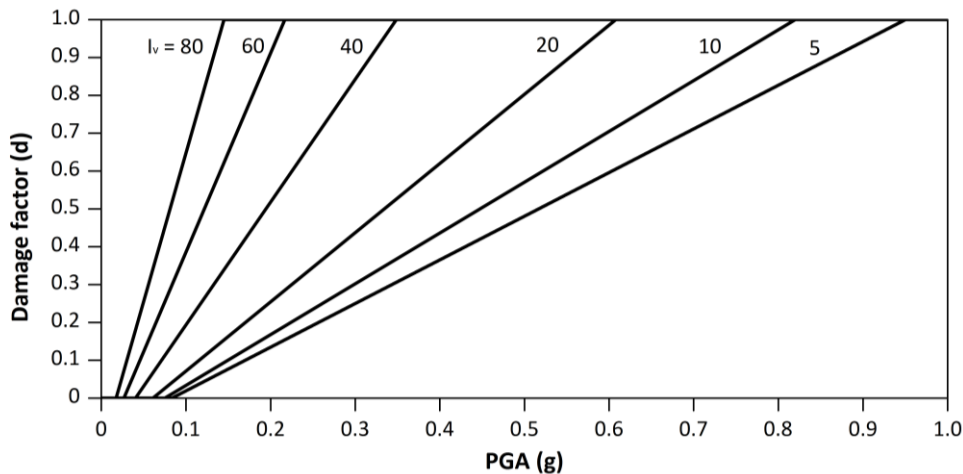


Figure 3.1: Vulnerability curves relating damage factor (d) and PGA for different values of the vulnerability index (I_v) (Guagenti and Petrini 1989)

With the application of this method, vulnerability curves can be developed, and the damage suffered by a building or a group of buildings presenting a specific vulnerability index can be evaluated in a fast and simple way for a given seismic event. Therefore, it constitutes a reliable large-scale assessment and has been extensively applied in Italy, with the development of the GNDT II level method (GNDT 1994). The vulnerability evaluation can be also important in the

identification of critical buildings for which a more detailed assessment is required, as well as for the definition of priorities for retrofitting. The mapping of risk scenarios can also help to foresee the impact of different retrofitting strategies in the reduction of the seismic vulnerability and the consequent economic losses.

3.2.2. The macroseismic method

The macroseismic method was developed by Lagomarsino and Giovinazzi (2006), based on the EMS-98 macroseismic scale defined by Grünthal (1998). The EMS-98 scale differentiates types of buildings into six classes of decreasing vulnerability (from A to F), based on expert judgment and provides the probability of a type of building of belonging to a specific class. It also defines five seismic damage grades, from negligible (Grade 1) to complete destruction (Grade 5). Finally, the EMS-98 indicates qualitatively the expected damage for buildings belonging to different vulnerability classes for a given macroseismic intensity (from I to XII). Therefore, the expected damage is classified through linguistic terms (“few”, “many” and “most”): e.g. ‘few buildings of vulnerability class A and B will suffer damage of grade 1 for an earthquake with a macroseismic intensity of V’. As a result, empirical damage probability matrices (DPM) can be constructed for the different vulnerability classes (Table 3.2).

Table 3.2: Damage matrices constructed based on the definitions provided by EMS-98 (Grünthal 1998) for buildings belonging to vulnerability classes A and C

Vulnerability class A						Vulnerability class C						
Damage Level Intensity	Damage grade					Damage Level Intensity	Damage grade					
	1	2	3	4	5		1	2	3	4	5	
V	Few					V						
VI	Many	Few				VI	Few					
VII			Many	Few			VII	Few				
VIII				Many	Few	VIII	Many		Few			
IX					Many	IX	Many			Few		
X						X					Many	Few
XI						XI				Most	Many	
XII						XII						

The macroseismic method intends to overcome the problems of incompleteness (missing information for all damage grades for a given intensity) and imprecision (qualitative description) of the DPM resulting from the EMS-98. This method uses probability theory assuming a beta distribution for the damage in order to give a numerical interpretation and complete the distribution of damage grades in the DPM. The vagueness of the correlation between intensity and damage is addressed by using the fuzzy set theory (Dubois and Parade 1980), which mathematically describes the overlapping ranges of the linguistic definitions in terms of membership functions. A vulnerability index (V) is also introduced as a score (ranging from 0 to 1)

that represents a measure of the weakness of the building to the earthquake (Giovinazzi and Lagomarsino 2004). This index is initially defined based on the EMS-98 vulnerability table, which identifies a most likely, probable and less probable vulnerability class for each building typology. The vulnerability classes are numerically translated into vulnerability indexes by using again the fuzzy set theory. The vulnerability index can be subsequently affected by behavior modifier factors in order to include particular characteristics of the building stock and regional construction practices. These factors include, among others, the state of conservation, the number of floors and the aggregate building position. They are chosen on an empirical basis after observation of typical damage patterns and expert judgment.

Through the use of these numerical definitions, damage distributions, mean damage grade values and vulnerability curves can be derived based on the EMS-98 matrices for each vulnerability class and for a given macroseismic intensity. The interpolation of the calculated vulnerability curves resulted in the definition of an analytical expression that correlates the expected mean damage grade (μ_D) and the seismic input, as a function of the building vulnerability:

$$\mu_D = 2.5 \left[1 + \tanh \left(\frac{I + 6.25V - 13.1}{Q} \right) \right] \quad (3.1)$$

where I is the seismic input in terms of macroseismic intensity, V is the vulnerability index and Q is the ductility index, which is an empirically defined index that takes into account the ductility of a determined construction typology, typically ranging from 1 to 4. This analytical expression can be used to build vulnerability curves for different masonry typologies. Figure 3.2a shows an example of vulnerability curves derived from the original expression (using Eq. 3.1) for different masonry building typologies (M1 to M7) that are defined in the EMS-98 scale. Fragility curves can be also generated based on the probability mass function of the binomial distribution adopted to complete the distribution of the damage grades, see Figure 3.2b. They express the probability ($P[D_k]$) for a specific building typology of exceeding a fixed damage grade (D_k) as a function of the earthquake macroseismic intensity. This method was validated by comparing estimated and observed damage data from past earthquakes (Giovinazzi 2005). Several authors have applied this method for the seismic risk assessment of several city centers, such as Faro (Oliveira et al. 2004), Barcelona (Lantada et al. 2004) and Lisbon (Oliveira et al. 2005).

3.2.3. Combination of the vulnerability index and the macroseismic method

Both methods described above express the vulnerability curves using different parameters. The vulnerability index method relate the variations of the damage factor (d) as a function of the PGA, while the macroseismic method provides the variation of the mean damage grade (μ_D) as a function of the EMS-98 macroseismic intensity. The vulnerability indexes used in both methods are also different. Vicente (2008) proposed a relationship between the measures of vulnerability

used by the two methods. For that purpose, a correlation between the two measures of the seismic input and between the two measures of damage had to be addressed.

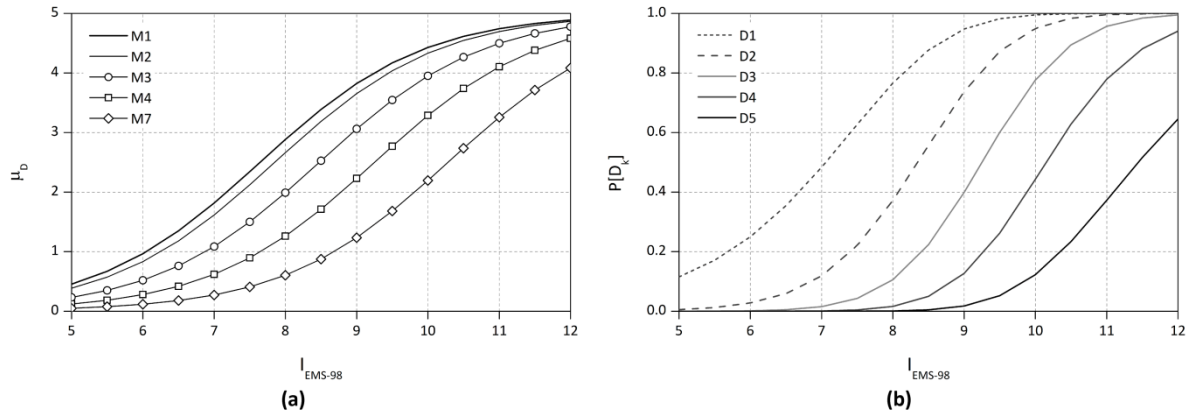


Figure 3.2: (a) Vulnerability curves derived for different masonry building typologies relating mean damage grade (μ_D) and EMS-98 macroseismic intensity; and (b) fragility curves for the masonry building typology M4 as a function of the EMS-98 macroseismic intensity (Giovinazzi and Lagomarsino 2004)

There are several formulations in the literature relating seismic intensity and PGA (Guagenti and Petrini 1989; Margottini et al. 1992; Wald et al. 1999). The expression proposed by Guagenti and Petrini (1989) was adopted by Vicente (2008):

$$\ln(y) = 0.602 \times I_{MCS} - 7.073 \quad (3.2)$$

where y represents the PGA, I_{MCS} is the intensity according to the Mercalli-Cancani-Sieberg (MCS) scale. It should be noted that the PGA is a physical parameter of the ground motion related to local site conditions and the macroseismic intensity is a qualitative measure associated to the damage consequences of earthquakes based on expert opinion. Thus, the relationships existing in the literature are developed based on post-earthquake observations and will always incorporate some degree of subjectivity (Azizi-Bondarabadi et al. 2016). The correlation between the EMS-98 intensity scale and the MCS scale is obtained using the relationship proposed by Margottini et al. (1992), taking into account the equivalence between the Medvédev-Sponheuer-Kárník (MSK) scale (Medvédev 1962) and the EMS-98 scale ($I_{MSK} = I_{EMS-98}$):

$$I_{MSK} = 0.734 + 0.814 \times I_{MCS} \quad (3.3)$$

Concerning the two measures of damage, the mean damage grade (μ_D) used in the macroseismic method has a physical meaning and represents a mean value of a discrete damage distribution ranging from 0 to 5, while the damage factor (d) used by the vulnerability index method is an economic index ranging from 0 to 1. There are several studies relating level of damage and economic damage indexes in the literature, all based on empirical loss data

(Whitman et al. 1973; ATC-13 1985; Brammerini et al. 1995; HAZUS 1999; Timchenko 2002; Roca et al. 2006). The variations in the equivalences proposed by the authors respond to the differences in regional economic factors (Azizi-Bondarabadi et al. 2016). Vicente (2008) proposed the analytical expression based on the correlations between level of damage and economic damage index defined by HAZUS (1999):

$$\mu_D = 4 \times d^{0.45} \quad (3.4)$$

Once these relationships are established, vulnerability curves using both methods can be prepared in the same format, relating mean damage grade and EMS-98 macroseismic intensity. As a result, the curves can be compared and a final correlation between the vulnerability indexes is achieved. An analytical expression was proposed (Vicente 2008) so that the vulnerability index (I_v) can be easily transformed into the vulnerability index used in the macroseismic method (V):

$$V = 0.56 + 0.0064 \times I_v \quad (3.5)$$

The combination of the two methods presented allows calculating the mean damage grade using Eq. 3.1 proposed by the macroseismic method and the subsequent evaluation of damage and estimation of losses. The vulnerability index formulation can be used to estimate the seismic vulnerability of the building using predefined parameters, as shown in Table 3.1. This allows an individual evaluation of the buildings instead of using a general vulnerability class for a specific building typology, which is an improvement in terms of accuracy. This approach combining the seismic vulnerability index formulation with the macroseismic method has been recently implemented for the seismic vulnerability assessment of Portuguese masonry structures in several historic city centers (Vicente et al. 2011; Neves et al. 2012; Ferreira et al. 2013b; Ferreira et al. 2017), obtaining useful and reliable results as a first level approach. It has also been adapted for other particular structures, such as Nepalese pagoda temples (Shakya 2014).

3.3. Proposed seismic vulnerability assessment methods for vernacular architecture

Two seismic vulnerability assessment methods for vernacular architecture are developed and validated within the present thesis, being both of them based on the previously described methods. The first method proposed can be considered as an adaptation of the approach followed by Vicente (2008), in order to accommodate the particularities of vernacular architecture. Thus, it makes use of the vulnerability index method to evaluate the seismic vulnerability vernacular buildings. It is referred as Seismic Vulnerability Index for Vernacular Architecture (SVIVA). Three steps were necessary for its development: (1) to identify and define a number of parameters that represent appropriately distinctive characteristics of vernacular buildings that influence their seismic behavior; (2) to obtain seismic vulnerability classes for each parameter; and (3) to

estimate the weights for each parameter. Once these three tasks are completed, an updated vulnerability index formulation (similar to the one presented in Table 3.1) is proposed with vernacular structures as its specific target. Then, through the use of the analytical expression shown in Eq. 3.5 (Vicente 2008) to estimate the mean damage grade, the macroseismic method can be applied to perform the seismic vulnerability assessment, damage estimation and the seismic loss evaluation.

The identification of the parameters, which will be described in the present chapter, is based on literature review. The definition of the parameters classes will be addressed by means of advanced numerical analysis and an extensive parametric study. The numerical strategy adopted is presented within this chapter, but the definition of the classes is presented in Chapter 4. Finally, the definition of the parameters weights is performed through a statistical analysis of the results obtained from the parametric study. The parameters weights, together with the resulting vulnerability index formulation of the SVIVA method, are presented in Chapter 5.

The second method that is proposed is called Seismic Assessment of the Vulnerability of Vernacular Architecture Structures (SAVVAS). This method intends to provide a value of the seismic capacity of the building expressed in terms of base shear coefficient or load factor. This value can be compared in a straightforward way with an expected seismic event expressed in terms of PGA. This method is considered analytical because it is exclusively developed from a wide parametric study based on detailed finite element modeling and nonlinear static analyses. The parametric study is carried out according to the parameters selected for the seismic vulnerability index method. As a result of the pushover analyses, load factors are associated with different structural limit states, which can be correlated with the damage suffered by a structure. Thus, for each numerical model corresponding to the variation of a certain parameter, seismic load factors are obtained for the different limit states considered. This information is gathered from each model used in the nonlinear parametric study, composing a wide database that relates the parameters with the load factors defining the limit states previously defined. Through a statistical analysis of the database using Data Mining techniques, regression models are derived, allowing the calculation of the seismic capacity of the building in terms of load factors defining structural limit states, using as the input the set of parameters considered. The vulnerability functions resulting from the SAVVAS method relate the seismic input in terms of PGA with limit states of the building, which can be correlated with damage levels for the seismic loss assessment.

3.4. Definition of seismic vulnerability assessment parameters

In the case of masonry structures, the parameters that are usually considered to be influential in the seismic behavior refer to different geometrical, structural, constructive and material aspects, such as: (a) the presence and effectiveness of the connection between orthogonal walls; (b)

the ultimate shear strength of the vertical elements, which mainly takes into account the distribution of the structural walls and the area of resisting walls in each orthogonal direction; (c) the type and quality of the material, namely the material properties, masonry arrangement, size of units or the presence of mortar; (d) plan regularity and configuration; (e) efficiency of the connections between walls and horizontal diaphragms; (f) roof typology, weight and trust; (g) number of floors and floor height; (h) type of foundations; (i) number and location of wall openings; (j) previous damage, alterations and conservation state; and (k) for buildings in an urban environment, the interaction with neighboring buildings, considering mainly the relative position within the block and the relative height with the adjacent buildings.

These are decisive parameters that define the seismic behavior of a building and are common to most of the applications of the vulnerability index method that can be observed in the literature. As an example, Table 3.1 showed the parameters used in the original formulation (Benedetti and Petrini 1984). Other studies have adapted this formulation to specific structure typologies, identifying the most relevant parameters and discarding others that are not considered remarkably significant for those structural types. For example, Sepe et al. (2008) eliminated two parameters from the original formulation to create the VULNeT method for large-scale vulnerability assessment of slender structures, particularly addressing Italian historic towers. Boukri and Bensaibi (2008) also adapted the methodology to the characteristics of the masonry constructions in Algiers, including a new parameter and redefining existing ones to depict typical construction details in the region. Vicente et al. (2011) also redefined the parameters shown in Table 3.1 to better represent typical construction features in masonry buildings in urban areas at Portuguese old city centers, particularly at the level of the interaction between buildings (structural aggregates). Following these studies, Ferreira et al. (2014) defined a set of parameters intended to evaluate the seismic response of masonry façade walls. Similarly, Shakya (2014) proposed new adjustments of the parameters for the application of the method to the study of slender structures and, more specifically, Nepalese pagoda temples.

Based on the work developed by these authors and on the review of the earthquake performance of vernacular constructions on past earthquakes shown in Chapter 2, a new set of parameters is proposed for this research study. The research work initially addressed Portuguese vernacular architecture, whose structural system typically consists on load bearing masonry or earthen walls coupled with horizontal timber diaphragms. Parameters are selected according to the singular behavior of this structural typology, acknowledging that many vernacular constructions around the world share a similar concept at the structural level and, thus, the seismic vulnerability assessment methods developed are not restricted to the Portuguese context. The selected ten parameters are listed below together with a brief description of each of them.

P1. Wall slenderness: This parameter can be defined as the ratio between the height of the wall and its thickness (h/t). Given the traditional materials commonly used for the walls (stone and

earth), vernacular buildings typically presents low slenderness ratio below 9, being rare to find ratios over 12.

P2. Maximum wall span: This parameter takes into account the maximum length of a wall prone to out-of-plane movements, which is the wall spanning the maximum distance between two in-plane earthquake resistant walls.

P3. Type of material: This parameter takes into account the type of material used for the vertical structural elements of the buildings. In the cases included in this study, earthen and masonry (brick and stone) materials are considered. Materials can vary from adobe masonry or irregular not worked stone masonry to workmanlike constructed dressed stone masonry.

P4. Wall-to-wall connection: This parameter takes into account the quality of the connection between the structural walls. The quality may vary from visible separation between orthogonal walls to efficiently built connections with good interlocking between the masonry units at the corners in the case of masonry buildings.

P5. Horizontal diaphragms: This parameter takes into account the type of horizontal diaphragm (floors and roofs), focusing on the quality of its connection to the load bearing walls and on its in-plan stiffness. Typically, the diaphragms may vary from diaphragms of negligible stiffness with beams poorly connected to the walls to rigid timber diaphragms well-connected to the walls.

P6. Roof thrust: This parameter takes into account the possible thrust that the roof may exert to the load bearing walls. Roofs may vary from thrusting types with considerable weight and low inclination to non-thrusting types.

P7. Wall openings: This parameter takes into account the number and area of wall openings, which can be measured as a percentage of the total area of each wall.

P8. Number of floors: This parameter takes into account the number of floors of the studied building. Vernacular buildings rarely present more than three stories.

P9. Previous structural damage: This parameter takes into account the state of conservation of the building, but focuses on the existing damage that can be observed, mainly addressing the state of degradation of the structural elements of the building (i.e. the walls). A poor maintenance and abandonment is common in many vernacular buildings, which may present an advanced state of deterioration of the materials and widespread cracking at the walls.

P10. In-plane index: This parameter can be defined as the ratio between the in-plan area of earthquake resistant walls in each main direction and the total in-plan area of earthquake resistant walls. This ratio provides direct information about the in-plane stiffness of the structure along each main direction. Values that deviate significantly from 0.5 will indicate that one

direction is clearly predominant and that there is an asymmetry in the amount of earthquake resistant walls in each main direction.

It should be mentioned that the ten parameters were confirmed to have a significant influence on the seismic behavior of vernacular buildings based on previous tentative parametric analyses. Other parameters that are commonly used in existing seismic vulnerability index methods were initially considered as well, such as the plan configuration, elevation irregularities, structural alterations and those parameters related with the interaction between adjacent buildings. The influence of the plan configuration, which is commonly taken into account because irregular plans may cause torsional effects in the building in the event of an earthquake, was finally disregarded because its influence in the seismic behavior of the vernacular building typology under study was found to be minor. Since load bearing walls are the main resisting elements of the structure and concentrate most of the mass of the buildings that typically present light and flexible floors, the main damage patterns are related to out-of-plane walls mechanisms. Only when the diaphragm is rigid enough or the walls present low shear strength, in-plane damage patterns can also be observed, but the in-plan irregularity was observed not to be decisive for this type of structures.

With respect to elevation irregularities, preliminary analyses investigated the influence of the irregularity in elevation, mainly resulting from variations of the lateral stiffness and the mass of the individual stories because of: (a) the use of different materials along the height; (b) variations of the wall thickness along the height; or (c) variations of the opening distribution along the height. This parameter is also highly related with the structural alterations that vernacular constructions are typically subjected to, which include the addition of new floors, the replacement of existing floors and roofs with concrete slabs or the enlargement of openings. Even though results confirmed their influence in the seismic behavior of vernacular buildings, they were initially deemed to be out of the scope of this research work. This decision was made for the sake of simplification, since they are complex parameters that are difficult to characterize into simple seismic vulnerability classes. There is also a higher complexity derived from the nonlinear numerical analysis of structures showing different materials and the interaction between them, which would demand a rigorous approach for the quantitative assessment of their influence that is left for future work. The methods proposed thus focus on more simple buildings showing fewer alterations and few stories, leaving no room for significant structural irregularities along the height. Nevertheless, it is also noted that some of the conditions of irregularity can be taken into account by assuming the worst case to be on the safe side, e.g. when evaluating a building showing different materials along the height, the material showing poorer characteristics can be assumed for the seismic assessment.

Similarly, the parameters related with the interaction between adjacent buildings have been also left out of the scope of this research work. Vernacular buildings in urban centers are the result of the progressive growth of the cities and do not behave independently but are structurally

connected with the adjacent ones, eventually composing structural units known as building aggregates. The assessment of the seismic behavior of aggregate structural units involves the study of specific parameters which may include: (a) the position of the building within the aggregate; (b) the relative height of the building within the aggregate; (c) the presence of staggered floors; (d) the typological heterogeneity among adjacent units; and (e) the difference in percentage of opening areas among adjacent façades. This matter has been tackled by some authors (Formisano et al. 2011; Cardani et al. 2015) but is still a wide unexplored research field. Again, because of the high complexity related to the study of these important aspects by means of nonlinear numerical analysis, it was considered necessary to leave it for future work. It is worth highlighting that assuming no interaction between adjacent buildings would usually represent the most unfavorable condition for a building so results of this research work will tend to be on the safe side. This was observed within preliminary analyses performed on a case study (Vong 2016), where considering the buildings within the aggregate in isolation proved to be conservative because the seismic behavior of the aggregate is greatly governed by the most vulnerable parts within the block. The influence of the aggregate was observed to be less important when failure of the individual parts is governed by out-of-plane walls mechanisms, which is typically the case for vernacular masonry and earthen buildings.

3.5. Numerical strategy adopted for the parametric study

As aforementioned, an extensive parametric numerical study aiming at the assessment and quantification of the influence of the different parameters in the seismic behavior of vernacular buildings was designed. The numerical analysis is based on FE modeling and pushover analysis. The parametric analysis models the variations of the parameters previously selected as influential on the seismic behavior of vernacular buildings. This helps to understand the seismic behavior and resisting mechanisms of vernacular constructions showing different characteristics in terms of construction, geometry and materials.

FE modeling following a common macro-model approach has already been extensively and successfully applied with the aim of analyzing the seismic behavior of complex masonry and rammed earth structures (Lourenço et al. 2007; Mallardo et al. 2008; Lourenço et al. 2011; Saloustros et al. 2014; Lourenço et al. 2016). Pushover analyses with distribution of forces proportional to the mass is also a generally accepted and recommended tool used for the seismic assessment of existing masonry buildings without box behavior (Lourenço et al. 2011). It mainly consists of simulating the seismic loading as static horizontal forces that are constant with respect to the building height. This distribution of forces tends to be overestimated at the lower level of the building (Betti and Vignoli 2011), but it is common in the analysis of masonry structures. The loads in a pushover analysis are applied incrementally on the structure until its collapse. This approach is simpler than other methods of analysis like nonlinear dynamic time-

history analysis and allows determining the ability of the building to resist the characteristic horizontal loading caused by the seismic actions taking into account the material nonlinear behavior. The response of the structure is described by the capacity or pushover curve, given as a relation between the base shear coefficient or load factor (i.e. the ratio between the horizontal forces at the base and the self-weight of the structure) and the displacement at the control point, which is usually the point where the highest displacements take place. Despite the limitations of simulating the earthquake loading as a set of equivalent static forces, pushover analysis is a powerful tool to assess the seismic behavior of buildings, since it can be performed with relatively low computational efforts in comparison with other more sophisticated nonlinear analysis. Besides allowing the estimation of damage patterns and failure mechanisms of the building, it also provides an insight on the seismic capacity of the structure. The pushover curves are also used for the identification and definition of different limit states, which can be correlated with different damage levels. Each limit state is associated to a seismic load factor, which allows having a common basis for a quantitative comparison of the seismic response of the buildings, taking into account the variation of the different parameters.

3.5.1. Definition of limit states

Performance levels and structural limit states were defined based on the capacity curves in order to quantitatively compare the performance of the building according to the variations defined for each parameter. Several methods have been proposed in the literature for a quantitative definition of limit states associated to a certain damage level exhibited by the structure based on the results of nonlinear analyses (Rota et al. 2010; Ferreira et al. 2012; Mouyiannou et al. 2014). In this work, four limit states (LS) are identified from the global response of each building evaluated, described with the pushover curve obtained in the numerical analysis (Figure 3.3):

LS1: Represents the onset of cracking and the end of the elastic behavior. It can be defined also as Light Damage or Immediate Occupancy limit state. Until this limit, the behavior of the building is essentially elastic and the structure can be considered as fully operational. The beginning of cracking is assumed to start when there is a reduction of the initial stiffness of the wall up to 2%. This reduction was defined after observing the first cracks that appeared in the numerical models, which are visible after a reduction of the initial stiffness of around this value, characterizing the end of the elastic behavior. It is noted that the value is relatively low, but is related to the low tensile strength of the materials considered in this study.

LS2: It can be defined as the limit state corresponding to damage limitation. This limit state tries to depict the transition between a point where the structure is still functional and retains most of its original stiffness and strength, showing minor structural damage and cracks, and a state where significant damage is visible so that the building could not be used after without significant repair. The definition of the point depicting LS2 in the pushover curve is made based

on two criteria: (1) the first energy criterion assumes that the area below the three-linear curve formed by LS1, LS2 and LS3 coincides with the area below the pushover curve from LS1 to LS3; and (2) the second criterion assumes that the point is on the slope associated to the secant stiffness corresponding to 70% of the maximum strength.

LS3: Defined by the base shear coefficient (or load factor) and displacement corresponding to the attainment of the building maximum strength. The building shows significant structural damage. It is usually denominated as Life Safety limit state. At this stage, the building has lost a significant amount of its original stiffness, but retains some lateral strength and margin against collapse even if it cannot be used after the earthquake.

LS4: This ultimate limit state is related to the collapse of the building and corresponds to the point where the building resistance deteriorates below an acceptable limit, which is set at the 80% of the maximum strength. It is known as Near Collapse limit state. Repairing the building after reaching this limit state may be neither possible nor economically reasonable.

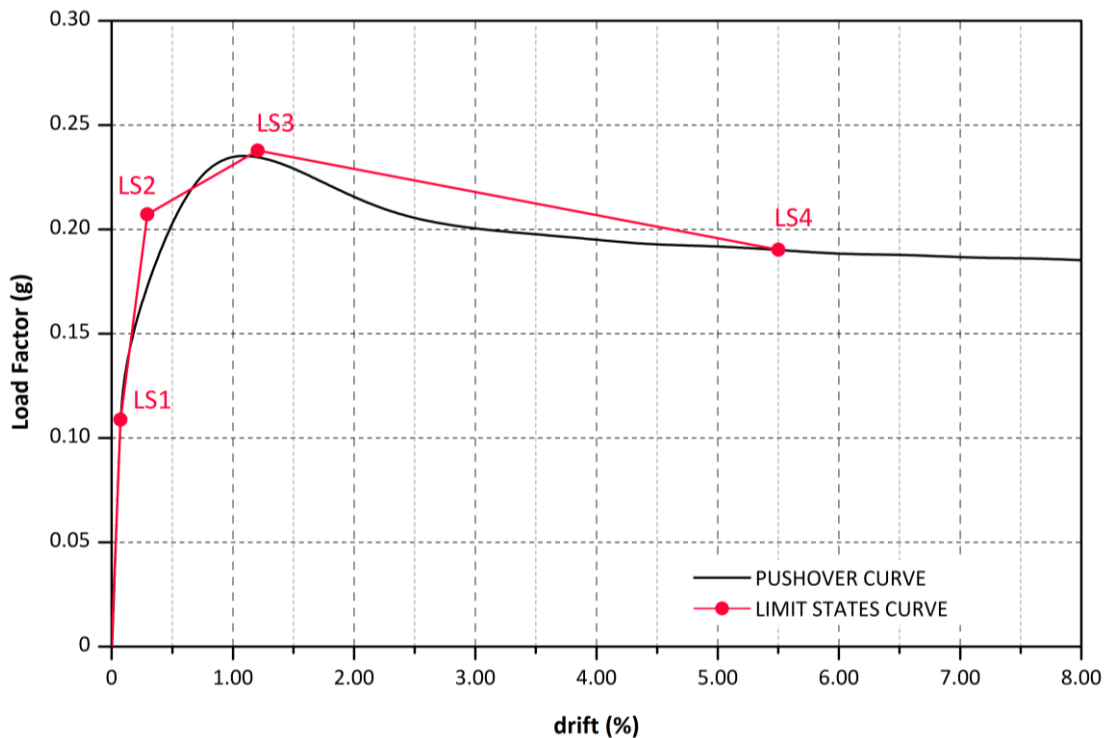


Figure 3.3: Identification and definition of the four considered limit states on an exemplary pushover curve

3.5.2. Reference numerical model

The initial step to perform the parametric study was based on the definition of a reference model that is representative of vernacular architecture. This reference model will serve as basis for comparison of the seismic behavior of different buildings showing variations according to the previously selected key parameters. For all parameters, the starting reference model is based on

representative vernacular rammed earth constructions commonly found in the South Portuguese region of Alentejo. Rammed earth construction, known as *taipa* in Portugal, has traditionally been the most widespread construction technique in this region and is still in use in some places. Traditional dwellings in Alentejo have generally small dimensions, simple rectangular shape and from one to two floors (Correia 2002). They are simple regarding their plan configuration, little compartmentalized and present massive walls with few or no openings, other than a single door, as a measure of protection for the hot summers. Rammed earth walls are usually around 0.5 m thick and present a base course or *soco* built in stone masonry, aimed at protecting the rammed earth from the humidity and rain penetration, by preventing the action of rising damp. Timber lintels are usually placed over windows and doors. Roofs are commonly mono-pitched roofs or gable roofs, usually presenting low slope, and made with a simple framework of timber beams. Figure 3.4 presents some examples of this vernacular typology. More detailed information about geometry, structural solutions, construction materials and detailing of this type of construction can be found in Correia (2007).



Figure 3.4: (a) traditional rural one-floor rammed earth vernacular construction in Alentejo, Portugal (Correia 2007); and (b) traditional urban two-floor rammed earth construction in Alentejo, Portugal (Correia 2002)

The reference models were slightly simplified with respect to the buildings on which they were based, so that they can represent generic vernacular buildings and can easily accommodate the variations required to assess the influence of the different parameters. Figure 3.5 shows the three main reference models finally prepared for the parametric analysis. The reference models thus show different materials and number of floors. When considering earthen constructions, one and two floors are considered for the reference models, while in the case of masonry constructions, the reference models can present up to three floors. The reference models with two and three floor are slightly simplified with respect to the one-floor model regarding the geometry and in-plan

configuration, so that the computing time can be significantly reduced. It should be noted that for some parameters, extra reference models were prepared. For example, for evaluating the influence of the type of material (P3), another reference model was built assuming that the building presents a rigid diaphragm and a different opening distribution. The description of these additional reference models will be specifically addressed in Chapter 4, when evaluating each parameter independently. They were built in order to evaluate the influence of some parameters for different combinations of the other parameters.

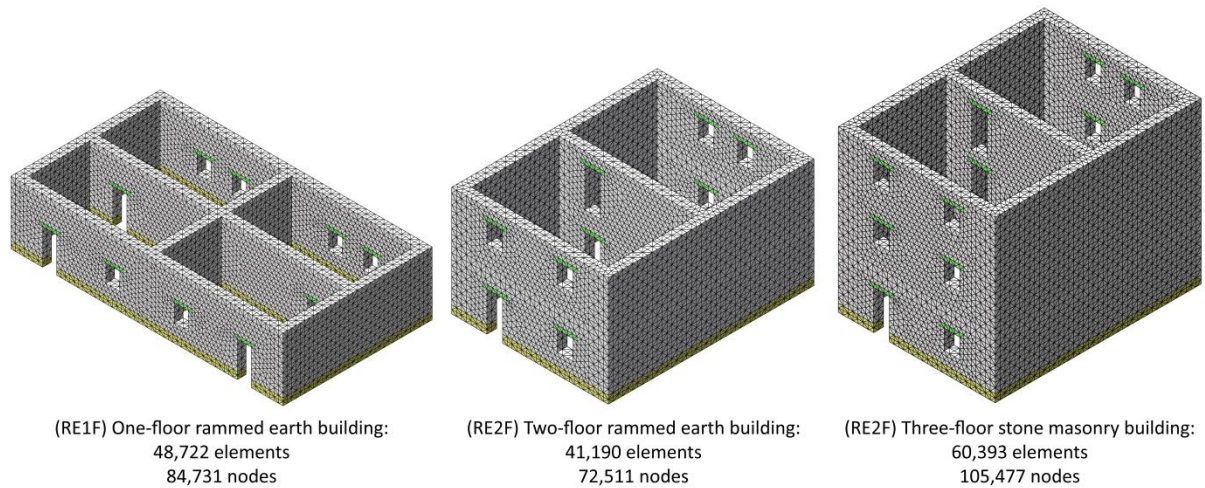


Figure 3.5: Example of reference numerical models constructed for the parametric study

3.5.3. Numerical models details

The software selected to perform the numerical parametric analysis was DIANA software (TNO 2011). The walls are simulated with ten-node isoparametric 3D solid tetrahedron elements (CTE30), with four-point integration scheme over the volume, and have at least two elements within the thickness. The displacements of the walls elements at the base are fully restrained. Three different materials were initially considered for the reference models. Rammed earth or stone masonry is used for the interior and exterior structural walls. Stone masonry is used for the abovementioned base course on rammed earth buildings, whose height is set at 0.4 m and it is assumed to be built with irregular schist or granite masonry. The same material properties used for the base course are given to the walls of the reference models in stone masonry. Timber is used for the lintels over all the openings.

The material model adopted to represent the nonlinear behavior of the rammed earth and masonry is a standard isotropic Total Strain Rotating Crack Model (TSRCM). The model describes the tensile and compressive behavior of the material with one stress-strain relationship and assumes that the crack direction rotates with the principal strain axes. It has been selected due to its robustness and simplicity, and because it is very well suited for materials whose mechanical behavior is predominantly governed by cracking or crushing. The tension softening

function selected is exponential and the compressive function selected to model the crushing behavior is parabolic, see Figure 3.6. This constitutive model has been already successfully applied in previous analysis of complex stone masonry structures (Lourenço et al. 2007; Lourenço et al. 2015). Regarding earthen constructions, few studies have adopted this type of models taking into account the nonlinear behavior of the material (Angulo-Ibáñez et al. 2012; Miccoli et al. 2014), but it proved to provide good results on complex earthen structures (Lourenço et al. 2016).

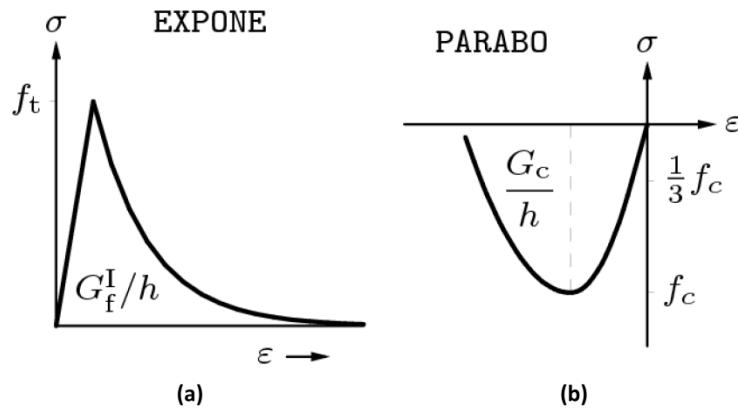


Figure 3.6: Stress-strain diagrams adopted for the nonlinear behavior of the rammed earth and masonry in: (a) tension; and (b) compression (TNO 2009)

The material properties required to define the constitutive model were based on data collected from different authors. Timber was considered to present only an elastic behavior, as structural nonlinearities are not expected to concentrate in these elements. An elasticity modulus of 10 GPa and a Poisson's ratio of 0.2 were used (Gomes et al. 2011). The stone masonry compressive strength and specific weight were obtained from the reference values provided by the Italian code (NTC 2008), assuming a low-quality masonry class: an irregular masonry composed of stone units of different sizes and shapes. A compressive strength of 1 MPa was adopted for the rammed earth, which is in the range of the scattered values provided in the literature (Bui et al. 2008; Jaquin 2008; Braga and Estevão 2010; Gomes et al. 2011; Angulo-Ibáñez 2012; Gallego and Arto 2014; Miccoli et al. 2014). The elastic properties of the rammed earth were also based on values proposed in the same set of literature. An elasticity modulus of 300 MPa and a Poisson's ratio of 0.3 were adopted. The remaining nonlinear properties of both the masonry and rammed earth were computed directly from the compressive strength through recommendations given by Lourenço (2009). The compressive fracture energy was obtained by considering a ductility factor d , defined as the ratio between the fracture energy and the ultimate compressive strength, of 1.6 mm. The tensile strength was estimated as 1/10 of the compressive strength. Finally, an average value of 0.012 N/mm is adopted for the mode I fracture energy. Table 3.3 presents the material properties adopted for the reference models.

Table 3.3: Mechanical properties adopted for the three materials used in the reference models

Material	E (MPa)	ν	f_c (MPa)	G_{fc} (N/mm)	f_t (MPa)	G_{ft} (N/mm)	W (kN/m ³)
Stone masonry	1500	0.2	1.5	2.4	0.15	0.012	20
Rammed earth	300	0.3	1	1.6	0.1	0.012	20
Timber	10000	0.2	-	-	-	-	6

3.5.4. Parameters variations

This section presents a detailed description of the selected parameters considered to affect the seismic behavior of vernacular buildings addressing: (1) their structural role on the global seismic behavior of vernacular buildings; and (2) the ranges of variation considered in the parametric numerical analysis, whose results are used for the development of the two seismic vulnerability assessment methods that are proposed.

3.5.4.1 Wall slenderness

The wall slenderness (λ) is a geometrical parameter that can be defined as the ratio between the effective wall inter-story height (h) and its thickness (t), see Figure 3.7. The slenderest elements are always the most vulnerable to the seismic action. The slenderness particularly affects the out-of-plane behavior of walls and several authors have already used this parameter to assess the seismic vulnerability of masonry walls (Spence and D'Ayala 1999; Lourenço et al. 2013; Ferreira et al. 2014). Vernacular buildings walls are typically very thick. They are rarely thinner than 0.45-0.5 m and can easily reach 0.6-0.7 m thick. The maximum wall height is more variable, even though vernacular buildings tend to be rather compact and present small height dimensions. Taking into account these aspects, the definition of a new set of models with varying wall slenderness is straightforward in order to perform the parametric study to evaluate the influence of this parameter. The range of variation considered for the wall slenderness varied between 4 and 22.5, which may exceed typical values for vernacular constructions but were adopted for the study to be more comprehensive.

3.5.4.2 Maximum wall span

The maximum wall span (s) is another geometrical parameter governing the out-of-plane response of the walls. The longest elements without intermediate supports can be particularly vulnerable to the seismic action and increase the probability of occurrence of out-of-plane collapse. Vulnerability index methods that include this parameter propose the classification of this parameter in terms of span to thickness ratio (Vicente 2008). However, since the wall thickness is already taking into account in the previous parameter, it was decided to consider simply the variation of the maximum wall span (s), measured in meters, see Figure 3.8. The maximum wall span is much variable for vernacular buildings and thus, the parametric analysis included a wide range of variation that went from 4 and 12.

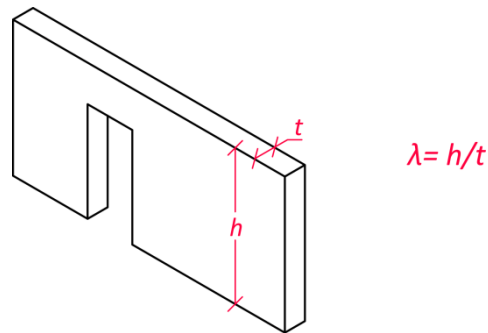


Figure 3.7: Definition of the wall inter-story height (h) and wall thickness (t) to evaluate the influence of the wall slenderness (λ) on the seismic behavior of vernacular buildings

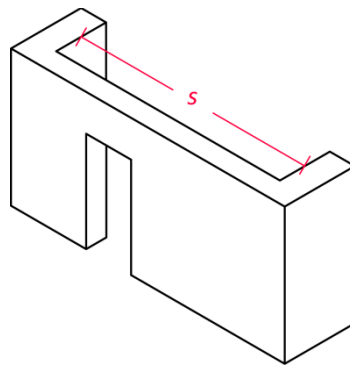


Figure 3.8: Definition of the maximum wall span (s) to evaluate its influence on the seismic behavior of vernacular buildings

3.5.4.3 Type of material

This parameter reflects the nature of the material used to build the walls, which are the main vertical load bearing elements of vernacular buildings. Walls typologies may primarily differ in the constituent material, usually consisting of stone, brick, adobe and rammed earth. Undoubtedly, the material affects the seismic performance of the building under an earthquake, since the mechanical properties of the materials may vary highly from one another and they have an important role in the seismic performance of the structure. With respect to masonry fabric typologies, there can be also significant variations in the morphology of the masonry wall: (a) on the type, shape and size of the masonry units (ashlar stone masonry, irregular rubble stone masonry, roughly shaped stone masonry, brick masonry, etc.); (b) on the masonry layout (irregular/regular horizontal courses, presence of several leaves, lack of connection between the leaves, etc.); or (c) on the type of mortar used, if any. These aspects determine the quality of the masonry and, thus, the capacity of the building to withstand horizontal forces resulting from the seismic load, as reported by many authors after post-earthquake observations (Giuffrè 1993; Binda and Penazzi 2000; Binda and Saisi 2001).

The mechanical properties of typical vernacular materials have been studied widely and characterized experimentally. Table 3.4 shows the values of different material properties collected from the literature that will be used as a reference within this thesis. According to these representative values, ranges of variation of the material properties can be defined to perform a parametric study and evaluate the influence of this parameter in the seismic behavior of vernacular buildings.

Table 3.4: Mechanical properties of different materials typically used for the construction of walls in vernacular architecture

Material	Type	E (MPa)		f _c (MPa)		τ ₀ (MPa)		G (MPa)		W (kN/m ³)
		Min	Max	Min	Max	Min	Max	Min	Max	
Masonry (NTC08 2009)	Irregular stone masonry	690	1050	0.6	0.9	0.15	0.012	115	175	19
	Uncut stone masonry	1020	1440	1.1	1.55	0.035	0.051	170	240	20
	Cut stone masonry	1500	1980	1.5	2	0.056	0.074	250	330	21
	Soft stone masonry	900	1260	0.8	1.2	0.028	0.042	150	210	16
	Dressed stone masonry	2340	2820	3	4	0.078	0.098	390	470	22
	Solid brick masonry	1800	2400	1.8	2.8	0.06	0.092	300	400	18
Rammed earth (Gallego and Arto 2014)		100	500	0.6	1.5	0.03	0.08	74	200	20
Adobe masonry (Tarque 2008)		117	189	0.8	1.1	0.021	0.07	30	78	-

3.5.4.4 Wall-to-wall connections

The quality of the wall-to-wall connections is a parameter that takes into account the organization of the vertical structural system and, more specifically, the level of connection between orthogonal walls. Damage observation after earthquakes has shown how the failure mode of the building is characterized many times by vertical cracks at the wall intersections, leading to the out-of-plane overturning or bending failure of the walls. The low tensile strength of stone masonry and rammed earth results in the detachment of the façade walls from the transversal ones. In addition, the level of connection between perpendicular walls, namely at the building corner and at the connection between external and internal walls, is a key aspect regarding the seismic behavior of the building. Particularly, concerning stone masonry buildings, the level of interlocking between the stones at the corner, mainly defined by the size and arrangement of the units, may have a decisive influence in advancing or delaying the formation of a failure mechanism consisting of the separation of the walls at the corners. Because of this, the presence of stones or other elements bracing perpendicular walls is typical in vernacular buildings. As an example, pieces of schist or timber can be found within rammed earth walls at the corners.

In order to evaluate the influence of this parameter in a simple way, the mechanical strength of the elements at the corners is reduced to simulate weak connections that are more prone to fail and allow the perpendicular walls to behave independently. This way of simulating weak connections at rammed earth buildings represent the difficulty of creating corners inside the

frameworks and poor joints with vertical recess solution (Angulo-Ibáñez 2012). For stone masonry buildings, this reduction of the material properties would represent the presence of vertical joints and, thus, the lack of proper interlocking between orthogonal walls.

3.5.4.5 Horizontal diaphragms

This parameter addresses construction solutions and materials used to build the horizontal structural elements of the buildings. Timber floors are the most common horizontal diaphragms used in vernacular architecture. They have a critical role in transmitting the lateral earthquake loads to the vertical resisting elements of the structure. The flexibility of traditional timber floors in unreinforced masonry and earthen vernacular buildings leads to significant bending and shear deformations under horizontal loads (Mendes and Lourenço 2015), which affects the distribution of the forces among the vertical elements. This excessive deformability or lack of proper connections with the load bearing walls forces the walls to work independently, resulting in their local out-of-plane failure when the building is subjected to earthquake loading. However, when effective diaphragm-to-wall connections are ensured, and the in-plane stiffness of the diaphragm is enough to redistribute the horizontal forces engaging the walls parallel to the seismic load, the seismic behavior of vernacular buildings relies on the in-plane response of the walls.

Therefore, the seismic response of vernacular buildings is strongly dependent on the characteristics of timber diaphragms. In particular, it depends on: (a) the in-plane stiffness of timber diaphragms; and (b) the quality of the connection between the diaphragms and the load bearing walls. Timber floor construction in vernacular architecture is usually very simple, consisting of wooden beams covered with cross boards directly nailed to the beams composing the sheathing (Figure 3.9a). When larger spans are required, two-way floors are commonly used, which add a secondary set of timber joists perpendicular to the main beams (Figure 3.9b). The overall in-plane flexibility of this type of single sheathing timber floors results from the contribution of the flexural and shear deformation of the single cross boards and the rigid rotation of the board due to nail slip (Brignola et al. 2008).

Since timber beams are the main structural element composing traditional horizontal diaphragms, the behavior of the diaphragm is clearly different in the two orthogonal directions: perpendicular and parallel to the main beam axis. Likewise, in terms of construction, there are different ways of achieving a proper diaphragm-to-wall connection in both directions. In existing timber floors, primary beams are usually only linked with the perpendicular walls by means of partial embedment of the timber beams within the masonry or rammed earth walls. Nevertheless, different traditional ways of ensuring a tight connection between both elements exists and were shown in Chapter 2 (Figure 2.10).

Proper detailing is also required to ensure shear transfer connection between the diaphragm and the load bearing walls parallel to the primary timber beams. Many times, the connection

between both elements is barely nonexistent. A beam is placed adjacent to the wall but there is no structural element linking diaphragm and wall (Figure 3.10a) and their connection relies solely on friction. Metallic anchor keys and ties have been traditionally applied with the purpose of connecting two or three consecutive beams to the wall, see Figure 3.10b (Lozano and Lozano 1995). Perimeter steel elements can also further or alternatively ensure the diaphragm-to-wall connection (Figure 3.10c). In cases where there is a change in the section of the wall, the beam can typically rest on the set-back, which provides a better support and helps to transfer the shear through friction (Figure 3.10d). For two-way floors, the secondary set of timber joists perpendicular to the main beams can be properly connected to the walls by means of partial embedment or by any of the solutions previously discussed in Chapter 2 (Figure 2.10) for connecting beams to perpendicular walls (Figure 3.10e).

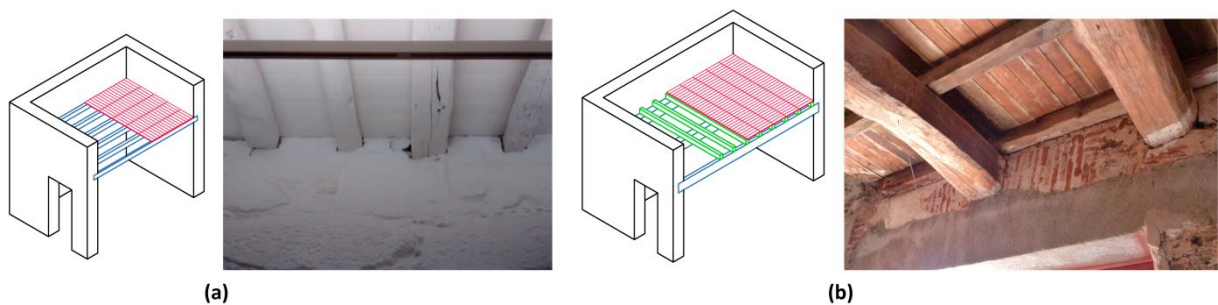


Figure 3.9: (a) Typical layout of traditional timber floors: wooden beams and board sheathing – example observed in Porto, Portugal; and (b) two-way traditional timber floor with secondary set of timber joists – example observed in Vila Real de Santo António, Portugal

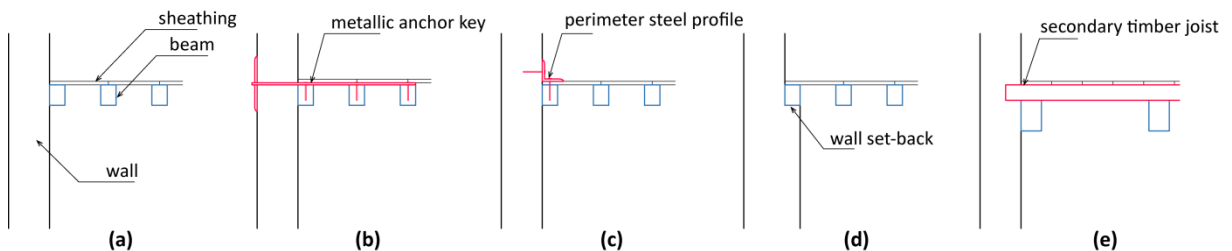


Figure 3.10: (a) Typical lack of connection between the beams and the parallel walls; (b) metallic anchor keys anchoring the beams to the wall; (c) use of perimeter steel profiles; (d) beams resting on the set-back of the wall; and (e) secondary timber joists partially embedded within the wall

Traditional horizontal diaphragms are always difficult to characterize and increases the complexity of numerical models, since there is not so much information on how to simulate their effects on the seismic behavior of vernacular buildings. The overall stiffness of the diaphragm is considered by Brignola et al. (2008) as the combination of the in-plane stiffness of the diaphragm and the stiffness of the diaphragm-to-wall connection. The influence of the quality of the diaphragm-to-wall connection can be evaluated based on the typical structural solutions previously discussed. Taking into account that vernacular diaphragm structural systems typically

consist of wooden beams and timber board sheathing, the influence of the quality of the connection between the main beams and the perpendicular walls and between the whole diaphragm and the perimeter walls will be assessed independently. The influence of the stiffness of the beams can also be evaluated. In summary, four aspects can be considered as the most critical in defining the seismic behavior of horizontal diaphragms (Figure 3.11): (a) level of connection between timber beams and walls (k_c); (b) stiffness of the beams (k_b); (c) stiffness of the diaphragm (k_d); and (d) level of connection between the diaphragm and the walls (k_{dc}).

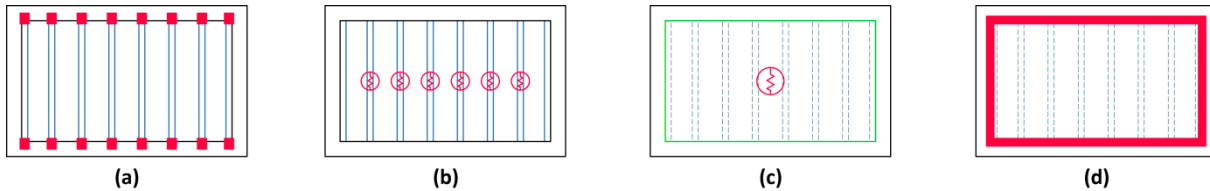


Figure 3.11: Details of the characterization of horizontal diaphragms: (a) level of connection between timber beams and walls (k_c); (b) stiffness of the beams (k_b); (c) stiffness of the diaphragm (k_d); and (d) level of connection between the diaphragm and the walls (k_{dc})

3.5.4.6 Roof thrust

This parameter evaluates the influence of the type of roofing system, specifically taking into account the thrust exerted by the roof, which may anticipate the out-of-plane collapse mechanism of the load bearing walls supporting the roof. There are particular types of roofing structural system that can be typically observed in vernacular buildings that exert lateral thrust. This thrust-exerting roof types are mainly composed by rafters with no intermediate support, whose feet are fixed at a wall plate but are not properly connected among them at the ridge. Thus, rafters subjected to vertical loads push the supporting walls outwards at their top (Figure 3.12).

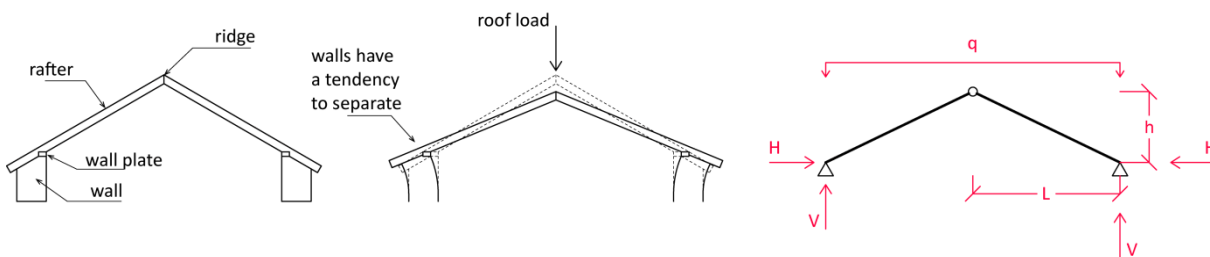


Figure 3.12: Common behavior of thrust exerting roofing structural systems under vertical loading

Other roof structural types do not exert lateral thrust simply because of their geometry or because of the addition of specific structural elements. Collar roofs with tie beams or ceiling joists can make use of horizontal roof elements to absorb the horizontal thrust (Figure 3.13a-b). Truss roofs use the structural framework and the different diagonal and horizontal elements to exert only vertical loads on the supporting walls (Figure 3.13c). Shed roofs (Figure 3.13d) or single roof systems composed only by rafters but having an intermediate support (Figure 3.13e) can also

highly reduce the thrust because of the proper vertical support at the ridge. The presence of other structural elements, such as ring beams at the top of the wall, tying the rafters together, can also help in reducing the detrimental effects of thrust-exerting roofing systems.

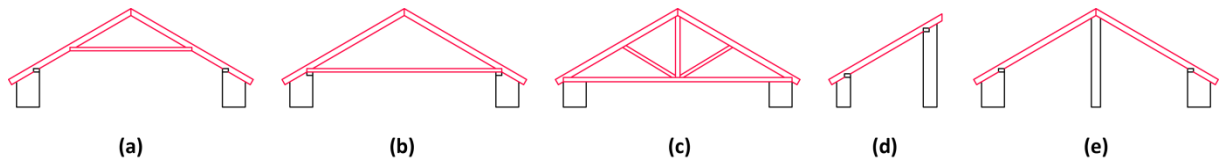


Figure 3.13: (a-c) Different non-thrust exerting roofing structural system; and (d-e) semi-thrusting roof types

Post-earthquake damage observation has shown how the failure mode of the buildings many times involves the out-of-plane bending failure of exterior walls. The additional horizontal load created by an incorrectly designed roof can certainly anticipate this failure. This horizontal loading can also increase the stresses at the corners and induce damage at these points. Therefore, the type of roof and its ability to exert or not thrust onto the supporting walls is a key aspect regarding the seismic behavior of buildings. As shown in the diagram of Figure 3.12, the thrust exerted by the roof depends on: (a) the span covered by the roof ($2L$); (b) the load of the roof (q), which mainly consists of its self-weight; and (c) the inclination of the roof (L/h). The variation of these features inducing different levels of roof thrust will be considered in the parametric study to evaluate the influence of this parameter in the seismic behavior of vernacular buildings.

3.5.4.7 Wall openings

The amount of wall openings is a geometrical parameter that can be measured as the ratio between the area of wall openings and the total area of the wall in terms of percentage. The presence of wall openings in earthquake resistant walls can always compromise their in-plane resistance. This can be particularly significant when the building is prone to suffer in-plane damage, such as when presently sufficiently stiff diaphragms able to avoid premature out-of-plane collapses. Damage patterns observed after earthquakes show that crack lines often follow the distribution of the façade openings, revealing the vulnerability induced by these elements. Vernacular buildings in rural areas generally present a reduced area of wall openings, but it is very variable and the area of wall openings can increase significantly if the building is located in an urban environment. A wide range of variation of the area of wall openings is thus considered for the parametric analysis, going from 2%, assuming a building presenting almost no openings, to 63%, assuming that the façade walls are perforated with large openings. With this respect, it is important to mention that the study should focus on the evaluation of the influence of openings in the earthquake resistant walls (i.e. the walls parallel to the loading direction), since openings mainly affect the in-plane behavior. Therefore, this parameter is specifically measured as the ratio between the total area of wall openings in all earthquake resistant walls in one main direction and the total area of the walls in that same direction, see Figure 3.14.

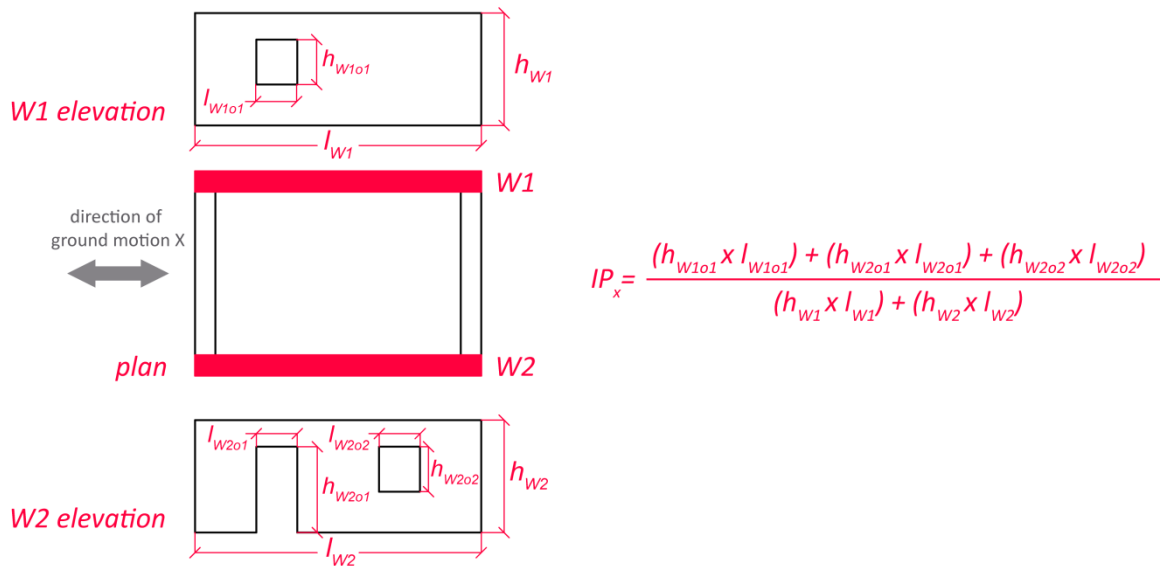


Figure 3.14: Definition of the ratio adopted to evaluate the influence of wall openings on the seismic behavior of vernacular buildings according to the seismic loading direction

3.5.4.8 Number of floors

The number of floors is a parameter that usually has an important influence on the seismic behavior of a building. Taller buildings tend to be more vulnerable to earthquakes because the center of gravity is raised and, thus, the lateral loads on the bearing walls increase during the seismic action. Vernacular buildings are typically not too high. In the rural environment, rammed earth constructions usually extend horizontally and are composed by a single story, but in the urban context they rarely present more than two stories (Figure 3.4). Stone masonry vernacular buildings in the urban context can easily present up to four stories, particularly when arranged in aggregates, such as in most European historical city centers. The parametric study can be very straightforward just by varying number of floors of buildings according to the walls constructive system. It should be noted that taking into account the former considerations, the range of variation must be narrow, particular for rammed earth constructions. It can vary between 1 and 3 floors for the rammed earth models and between 1 and 4 for the stone masonry models.

3.5.4.9 Previous structural damage

This parameter takes into account the degree of deterioration existing in the building and the weakening signs that may aggravate damage in the event of an earthquake, increasing its vulnerability. Generally, a critical reason for the vernacular heritage to be so vulnerable to earthquakes is the fact that they are in an advance state of deterioration, as a result of poor maintenance and abandonment. This abandonment results in previous structural damage often going unrepaired. Existing cracks increase the vulnerability of specific parts of the structure and can anticipate its failure. This parameter is specifically focused on the state of degradation of the

load bearing walls of the building. The state of conservation can be simulated by imposing an initial level of damage to the structure before carrying out the pushover analysis. The numerical models were thus firstly loaded in one direction until reaching a certain degree of damage, and then the pushover analysis can be performed in the perpendicular direction. The degree of damage can be measured according to the maximum crack size. In this work, the level of damage is defined according to the maximum crack size, following recommendations by Masciotta et al. (2016), see Table 3.5. Taking this classification into account, a range of variation of the initial level of damage can be established to perform the parametric study and evaluate the influence of this parameter on the seismic response of vernacular buildings.

Table 3.5: Classification of damage according to existing cracks according to Masciotta et al. (2016)

Degree of damage	Description	Crack width
No visible damage	No visible damage	-
Slight damage	Hairline and fine cracks	~ 1 mm
Moderate damage	Moderate cracks	~ 1 mm to 5 mm
Severe damage	Large cracks impairing functionality	> 5 mm

3.5.4.10 In-plane index

This parameter takes into account the conventional shear strength of the walls, addressing their distribution. The seismic capacity of a building may be jeopardized when it presents an unbalanced area of resisting walls in the two orthogonal directions. This parameter gives a measure of the in-plane stiffness of the structure in each main direction and, thus, it can be considered as an indicator of the feasible seismic performance of the building (Lourenço et al. 2013). The in-plane index (γ_i) is here defined as the ratio between the in-plane area of earthquake resistant walls in each main direction (A_{wi}) and the total in-plane area of earthquake resistant walls (A_w), see Figure 3.15.

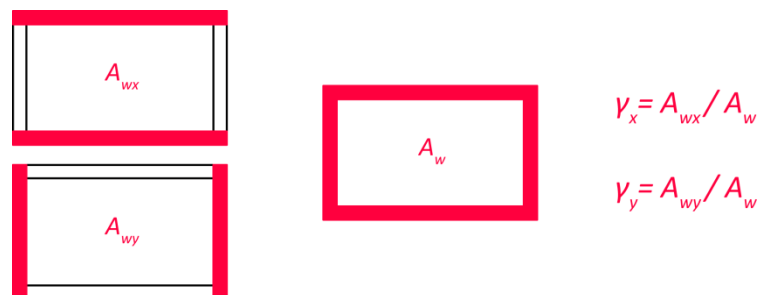


Figure 3.15: Definition of the in-plan area of earthquake resistant walls in each main direction (A_{wi}) to evaluate the influence of the in-plane index (γ_i) on the seismic behavior of vernacular buildings

This ratio provides an estimation of the shear strength in each orthogonal directions. For values close to 0.5 the walls are well-balanced, while an in-plane index that deviates from 0.5 shows that the building has a weaker direction. This index can be very variable in vernacular buildings, indicating very different plan configurations. The evaluation of the influence of the

area of resisting walls in each direction is carried out by varying this ratio. It is noted that this index can be considered as an indicator of the in-plan irregularity of a building.

3.6. Conclusions

A brief review of seismic vulnerability assessment methods existing in the literature was presented in this chapter, with a particular focus on the vulnerability index method and the macroseismic method. These two methods serve as basis for the development of two seismic vulnerability assessment methods for vernacular architecture. The chapter discusses and justifies the selection of the methods that are developed within this research work: (1) SVIVA; and (2) SAVVAS. In particular, the chapter identifies two aspects that need to be defined for both methods: (a) seismic vulnerability assessment parameters; and (b) seismic vulnerability classes. The SVIVA method requires, in addition, the definition of the parameters weights for the determination of the vulnerability index formulation.

The chapter presents and discusses the parameters that are considered to be more influential on the seismic performance of vernacular architecture. The selection of the parameters is based on previous works available in the literature, but its definition takes into account the particularities of vernacular buildings. Some parameters that are commonly selected in similar vulnerability assessment methods existing in the literature were disregarded because preliminary analysis showed that they were not relevant in defining the seismic behavior of vernacular architecture. Other set of parameters that were indeed observed to be influential on the seismic behavior of vernacular constructions were considered out of the scope of the present work because of the complexity that would require their analysis. Therefore, the evaluation of their influence was left for future work. This is for example the case of those parameters related with the position of the building within the urban aggregate.

The information required for the definition of all the selected key parameters can be obtained easily through expedited surveys that can be carried out even solely by means of simple visual inspection. That is why it is considered that both methods proposed for the seismic vulnerability assessment of vernacular architecture will provide the possibility of performing a fast primary seismic safety assessment and obtaining an indicator of the seismic performance of a building or group of buildings even with limited resources.

Finally, the chapter introduces the numerical approach that will be carried out in the following chapters to support the development of the SVIVA and the SAVVAS method. The parametric study presented is based on FE modeling and pushover analysis. Limit states are defined from the pushover curves in order to compare the seismic performance of the buildings in a quantitative way. The numerical reference model and the specifications of the nonlinear analysis, namely software, element type and material constitutive model are also presented.

CHAPTER 4

DEFINITION OF SEISMIC VULNERABILITY CLASSES

Chapter outline

- [4.1. Introduction](#)
- [4.2. Methodology adopted for the seismic vulnerability classes definition](#)
- [4.3. Seismic vulnerability classes according to the wall slenderness \(P1\)](#)
- [4.4. Seismic vulnerability classes according to the maximum wall span \(P2\)](#)
- [4.5. Seismic vulnerability classes according to the type of material \(P3\)](#)
- [4.6. Seismic vulnerability classes according to the wall-to-wall connections \(P4\)](#)
- [4.7. Seismic vulnerability classes according to the horizontal diaphragms \(P5\)](#)
- [4.8. Seismic vulnerability classes according to the roof thrust \(P6\)](#)
- [4.9. Seismic vulnerability classes according to the wall openings \(P7\)](#)
- [4.10. Seismic vulnerability classes according to the number of floors \(P8\)](#)
- [4.11. Seismic vulnerability classes according to the previous structural damage \(P9\)](#)
- [4.12. Seismic vulnerability classes according to the in-plane index \(P10\)](#)
- [4.13. Conclusions](#)

4.1. Introduction

As discussed in Chapter 3, the development of a seismic vulnerability assessment method for vernacular architecture based on the vulnerability index formulation requires the definition of seismic vulnerability classes for the ten key parameters already defined. Existing methods have defined vulnerability classes on the basis of empirical knowledge and expert judgment. This research work proposes to define the classes by means of a wide parametric analysis that is performed using detailed FE modeling and pushover analysis and whose details were specified in Chapter 3. The extensive numerical campaign will also contribute to obtain a better and quantifiable understanding of the influence of the different parameters on the seismic behavior of vernacular constructions, which is essential for the development of the novel SAVVAS method.

The chapter firstly introduces the methodology adopted for the definition of the seismic vulnerability classes. The chapter is then structured in ten sections showing the analysis of each parameter independently, following the methodology defined. All sections present the results according to the same structure. The presentation of the reference numerical models prepared to carry out the parametric analysis is followed by the discussion of the results in terms of: (1)

variations on damage patterns and damage mechanisms; (2) building of capacity curves and identification of limit states; and (3) analysis of the load factor variations. The final classification of each parameter into four classes of increasing seismic vulnerability is defined based on the variations of load factor. It should be noted that other classifications have been proposed by other authors as a part of the development of similar seismic vulnerability assessment methods based on the vulnerability index method, as reviewed in chapter 3 (Benedetti and Petrini 1984; GNDT 1994; Vicente 2008; Shakya 2014). They are also taken as a reference in the definition of the seismic vulnerability classes. Each section closes providing a table with the description of the seismic vulnerability classes for each parameter. The table will serve as a reference when performing a building survey to carry out the seismic vulnerability assessment.

4.2. Methodology adopted for the seismic vulnerability classes definition

The definition of the seismic vulnerability classes will be carried out following a methodology consisting of seven clearly defined steps. This methodology will be used consistently for all the ten key parameters selected and discussed in Chapter 3.

Step 1: Preparation of reference models

The three main reference models used in the parametric analysis were explained in Chapter 3 (see Figure 3.5). However, for the evaluation of each parameter, extra reference models were prepared assuming different initial conditions and combinations of the remaining parameters, for example, varying the type of material, the type of horizontal diaphragm, the distribution of wall openings or the number of floors. This is meant to provide a more comprehensive understanding of the influence of each parameter and to better validate the influence of each parameter on buildings showing different characteristics. For example, for the analysis of parameter P2 (maximum wall span), two reference models were prepared, see Figure 4.1: (1) one-floor rammed earth building with flexible diaphragm (*RE1F*); and (2) two-floor rammed earth building with rigid diaphragm (*RE2Fd1*). The use of these two clearly differentiated building typologies as reference models allows understanding the influence of the maximum wall span when the building is expected to behave differently under seismic loading. In the case of the model with flexible diaphragm, the parametric analysis evaluates the influence of the maximum wall span for a building more prone to show an out-of-plane failure mode. On the other hand, in the case of the model with the rigid diaphragm, the analysis is meant to evaluate the influence of the maximum wall span for a building that is more prone to present in-plane collapse mechanisms.

Step 2: Modelling the variations according to each parameter

On the basis of the reference models selected, the second step consists of preparing the rest of the models according to the variations defined for each parameter. A range of variation was

determined for each parameter taking into account the characteristics of vernacular architecture, as shown in Chapter 3. Thus, a set of models is prepared departing from each reference model according to this range, constituting the base of the parametric analysis. For example, in the same case of parameter P2, the range of maximum wall span established went from 4 m to 12 m. The maximum wall span of the reference model was 7 m. The span was thus decreased and increased by 1 m until covering the whole range defined. As a result, two sets of 9 models were prepared (Figure 4.1). They will be evaluated independently in order to evaluate the influence of the maximum wall span for different types of buildings.

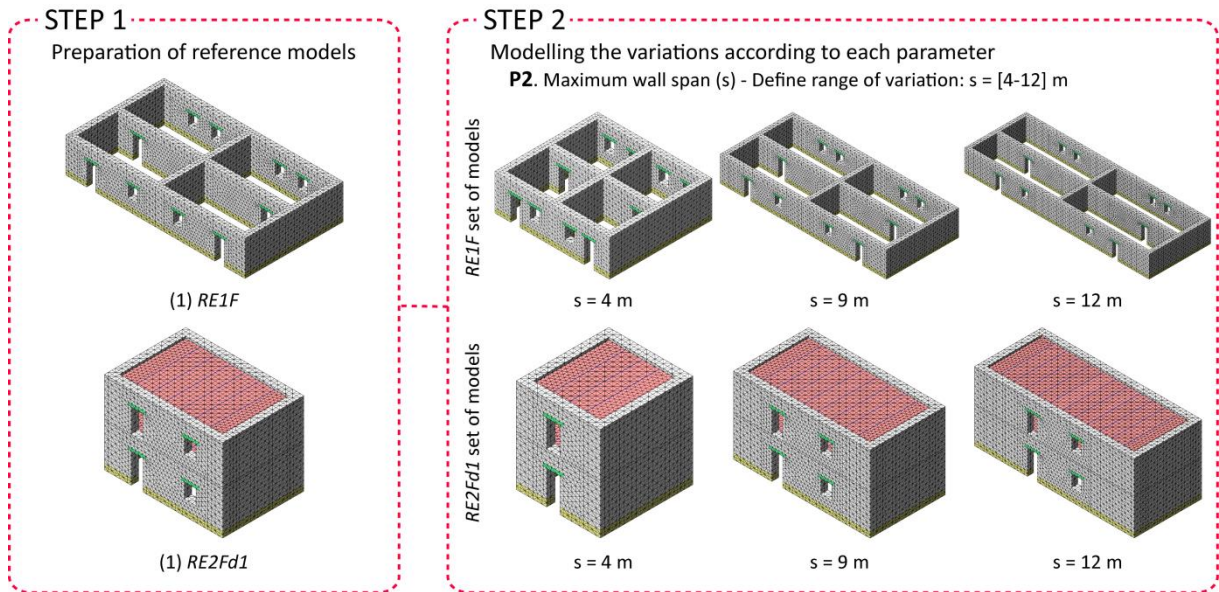


Figure 4.1: Steps 1 and 2 from the methodology adopted for the definition of the seismic vulnerability classes using P2 (maximum wall span) as an example

Step 3: Pushover analysis

Once all the models are constructed, a pushover analysis is performed on each of them. The direction selected to perform the pushover analyses depends on the expected response and failure mode of the buildings. Each set of models is tested in the same direction, which is commonly the one in which the buildings are assumed to be more vulnerable. However, in some cases, the models are tested in the direction in which the parameter under evaluation is supposed to have a greater influence. For example, when assessing the influence of wall openings, since they mainly affect the in-plane resistance of the earthquake resistant walls, the buildings are tested in the direction parallel to the walls where the amount of wall openings varies. Continuing with the example above, parameter P2 evaluates the variations in the response of the building when the maximum length of a wall prone to out-of-plane movements varies. Thus, the direction selected for the pushover analyses had to be perpendicular to the walls whose span is being modified. The direction perpendicular to the walls presenting the maximum wall span is referred to as Y

direction and the opposite perpendicular direction as X, see Figure 4.2. This nomenclature is common to all the analysis performed within the parametric study.

Step 4: Analysis of variations in the damage patterns and failure mechanisms

While this step is not strictly necessary for the definition of the seismic vulnerability classes, it contributes to another main objective of the work, which aims at obtaining a better understanding of the seismic behavior of vernacular buildings. The pushover analyses carried out on each model from the set, allows performing a comparison among them in terms of variations in the crack patterns at the ultimate limit state of the building (LS4). It should be mentioned that this limit state is considered to be close to the collapse of the building, which allows a comparison also in terms of failure mechanisms. This step helps to understand how the seismic response of the building changes according to the variations in the parameter under evaluation. Results are discussed and the failure modes are presented in terms of: (a) maximum total displacements; and (b) crack pattern; see Figure 4.2. It should be noted that, given the great amount of models analyzed, it would be impossible to show all the results from the analyses performed. Thus, only the most representative failure mechanisms and variations will be presented for each parameter.

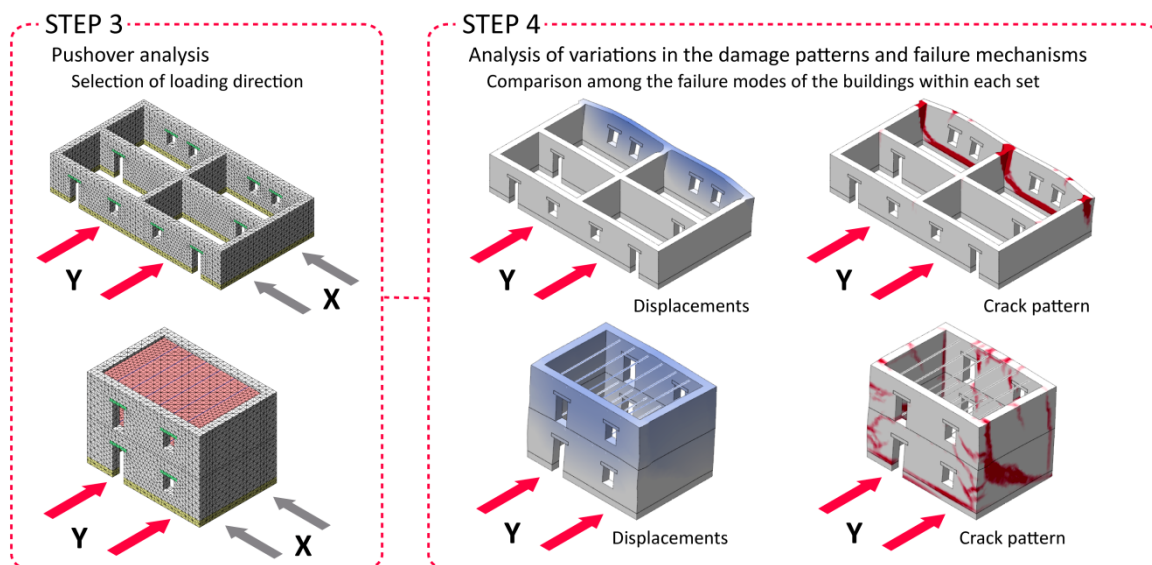


Figure 4.2: Steps 3 and 4 from the methodology adopted for the definition of the seismic vulnerability classes using P2 (maximum wall span) as an example

Step 5: Building of four-linear capacity curves

The pushover analysis allows describing the seismic response of the structure in terms of the capacity or pushover curve. Using the procedure explained in Chapter 3 (Figure 3.3), this curve can be transformed into a four-linear capacity curve by determining the points associated to the four structural limit states (LS) already defined. Each LS is thus associated with a specific value of load factor (ratio between horizontal forces at the base and self-weight of the structure) and

drift at the node showing the highest displacements. It should be noted that this node usually varies according to the collapse mechanism obtained, which differs between buildings. Thus, the curves are representative of the global structural behavior of the different buildings subjected to horizontal loading, not individual structural elements composing the buildings. As a result, the seismic behavior of each building is described by four load factors that make it reach the four LS, but also provides information about the deformation capacity of the model. Therefore, these equivalent curves allow an easier and quantitative comparison between the structural response of the models from each set in terms of capacity, stiffness and ductility. Figure 4.3 shows the procedure that is followed for step 5.

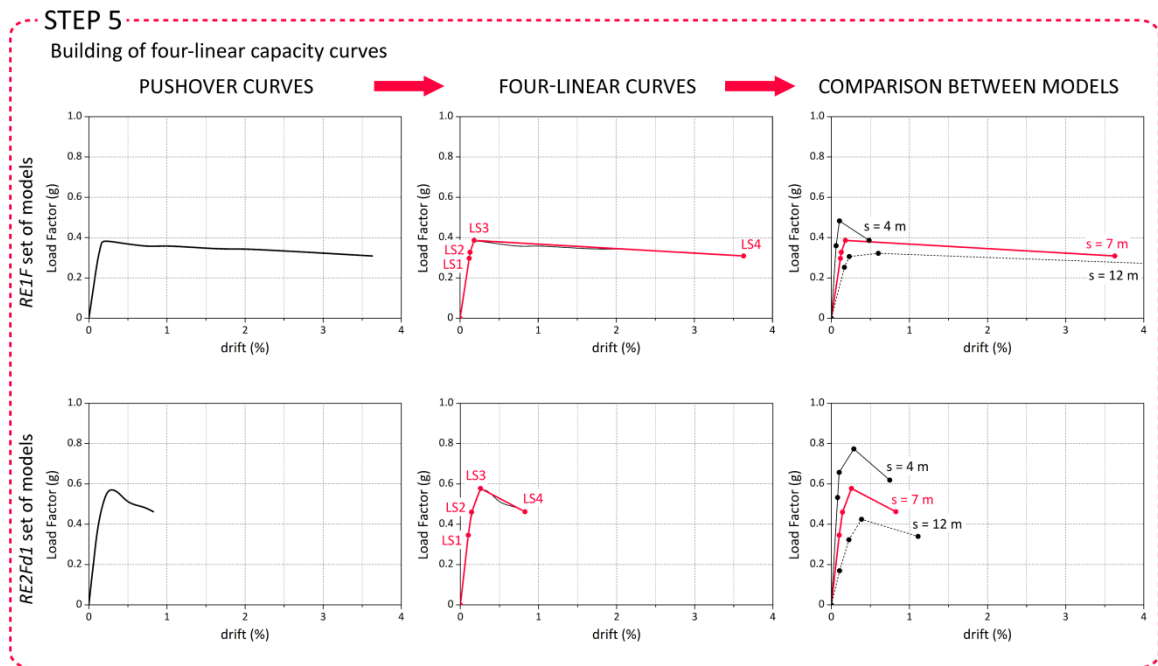


Figure 4.3: Step 5 from the methodology adopted for the definition of the seismic vulnerability classes using P2 (maximum wall span) as an example

Step 6: Analysis of load factor variations

The previous step allows obtaining load factors defining the four LS for all models in each set. Since the load factors can be directly associated to equivalent static horizontal loads that the buildings can withstand before reaching the LS, they are adopted as the basis of comparison among the buildings in each set in order to quantitatively evaluate their relative seismic vulnerability. The values of load factor corresponding to LS1, LS2 and LS3 for the different models are compared in order to have a better insight on the variation of the capacity of the building as a function of the variations defined for each parameter. LS4 is not included because the load factor defining LS4 is, by definition, 80% of the load factor corresponding to the attainment of LS3, so the variation is the same. The load factor variations for each LS can be

expressed in terms of percentage. To normalize, the value of load factor obtained for each model of the set (i) is divided by the maximum value of load factor obtained among the buildings analyzed. This operation is repeated for the three LS:

$$LS1(\%)_i = \frac{LS1(g)_i}{LS1(g)_{max}} \quad (4.1)$$

$$LS2(\%)_i = \frac{LS2(g)_i}{LS2(g)_{max}} \quad (4.2)$$

$$LS3(\%)_i = \frac{LS3(g)_i}{LS3(g)_{max}} \quad (4.3)$$

Continuing with the example of P2, for both set of models, the building with $s = 4$ m showed the maximum capacity and the highest values of load factor defining LS1 and LS2. Therefore, these three values of load factor defining the three LS are used for the normalization of the load factors obtained for the remaining models of the set ($LS1(\%)_{s=4\text{ m}} = 100\%$; $LS2(\%)_{s=4\text{ m}} = 100\%$; and $LS3(\%)_{s=4\text{ m}} = 100\%$). Three curves can be constructed this way showing the variation of the load factor defining each LS as a function of the wall span, see Figure 4.4. The curves can show in a clear manner the influence of the parameter in the global seismic behavior of the buildings, which can understood in comparative terms.

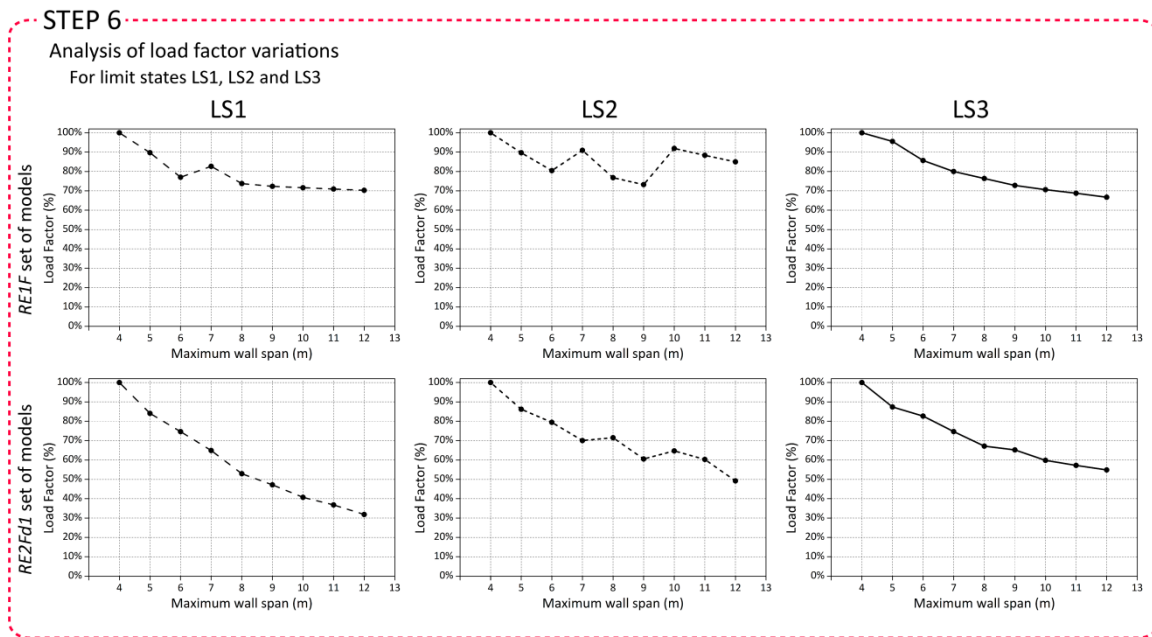


Figure 4.4: Step 6 from the methodology adopted for the definition of the seismic vulnerability classes using P2 (maximum wall span) as an example

Step 7: Definition of seismic vulnerability classes

The trends of variation evaluated in the previous step are the basis for the definition of the seismic vulnerability classes. The final classification is defined according to the variation of the

load factor corresponding to the attainment of the maximum capacity of the building (LS3). The criterion followed for the definition of the typical four vulnerability classes of increasing vulnerability (A, B, C and D) consists of dividing equally the total range of variation ($LS3(\%)_{max} - LS3(\%)_{min}$) within each into four parts. Each interval is thus associated with a vulnerability class and the buildings are classified according to the interval they lie within. Figure 4.5 illustrates this process using as an example the definition of the classes of P2. It is noted that the ranges of variation obtained for each set always differ, which sometimes results in differences in the definition of the seismic vulnerability classes. In these cases, the most unfavorable class is always considered. As an example, in the definition of the classes for P2 (Figure 4.5), within the *RE1F* set of models, the building with $s = 5$ m classifies as A, whereas within the *RE2Fd1* set of models, the building with $s = 5$ m classifies as B. The final classification is made taking into account these discrepancies by adopting the most unfavorable class. Thus, buildings with $s = 5$ m are considered as class B, see Figure 4.5. With this step, the definition of the seismic vulnerability classes according to each parameter concludes. Nevertheless, the final classification obtained for each parameter is also compared with other classifications existing in the literature that are based on post-earthquake damage observation for reference purposes.

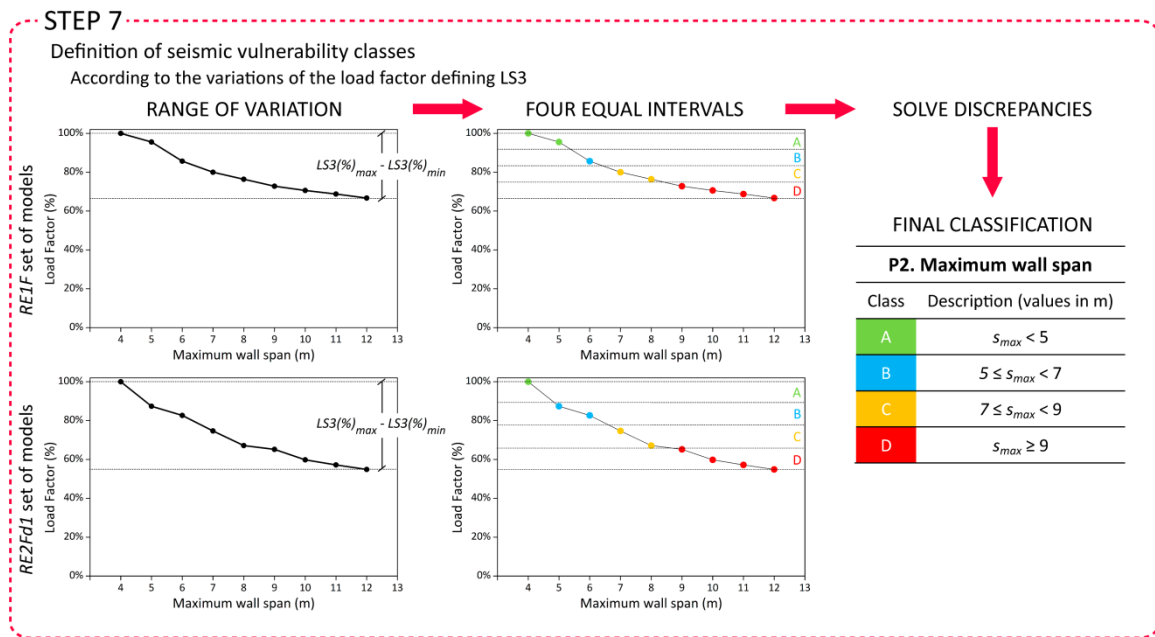


Figure 4.5: Final step 7 from the methodology adopted for the definition of the seismic vulnerability classes using P2 (maximum wall span) as an example

4.3. Seismic vulnerability classes according to the wall slenderness (P1)

Three reference models were prepared for the analysis of the influence of P1 using three different values of maximum wall span (s) perpendicular to the loading direction (Figure 4.6): (1) one-floor rammed earth building with $s = 7$ m, a height $h = 3$ m and a thickness $t = 0.5$ m ($s7h3t5$); (2) one-

floor rammed earth building with $s = 5$ m, a height $h = 3$ m and a thickness $t = 0.5$ m ($s5h3t5$); and (3) one-floor rammed earth building with $s = 3.5$ m, a height $h = 3$ m and a thickness $t = 0.5$ m ($s3_5h3t5$). The three buildings are assumed to present flexible diaphragms and the roof load is modelled as distributed load along the walls. In plan, model $s7h3t5$ has 15.5×8.5 m², model $s5h3t5$ has 11.5×8.5 m² and model $s3h3t5$ has 8×8.5 m². The resulting value of wall slenderness ($\lambda = h/t$) of the reference models is 6. In order to assess the influence of this parameter, λ is modified based on values of wall inter-story height and thickness observed in typical vernacular buildings, as previously discussed in Chapter 3. The height varies in a range between 2.4 and 4.5 m, while the thickness varies between 0.2 and 0.6 m. Thus, the values of slenderness vary between 4 and 22.5.

Both $s7h3t5$ and $s5h3t5$ sets of models were analyzed in the direction perpendicular to the walls with the maximum wall span (Y). However, in order to evaluate if the reduction of the in-plan area of the wall can also compromise its in-plane resistance, the models from the $s3_5h3t5$ set were analyzed in the orthogonal direction (X). It is noted that the in-plan dimensions of the models from this third set are the same as those from the $s7h3t5$ set, but their in-plan configuration was simplified to reduce the computing time. Table 4.1 presents a summary of the 38 models constructed and Figure 4.6 shows some of the models prepared with variations of λ .

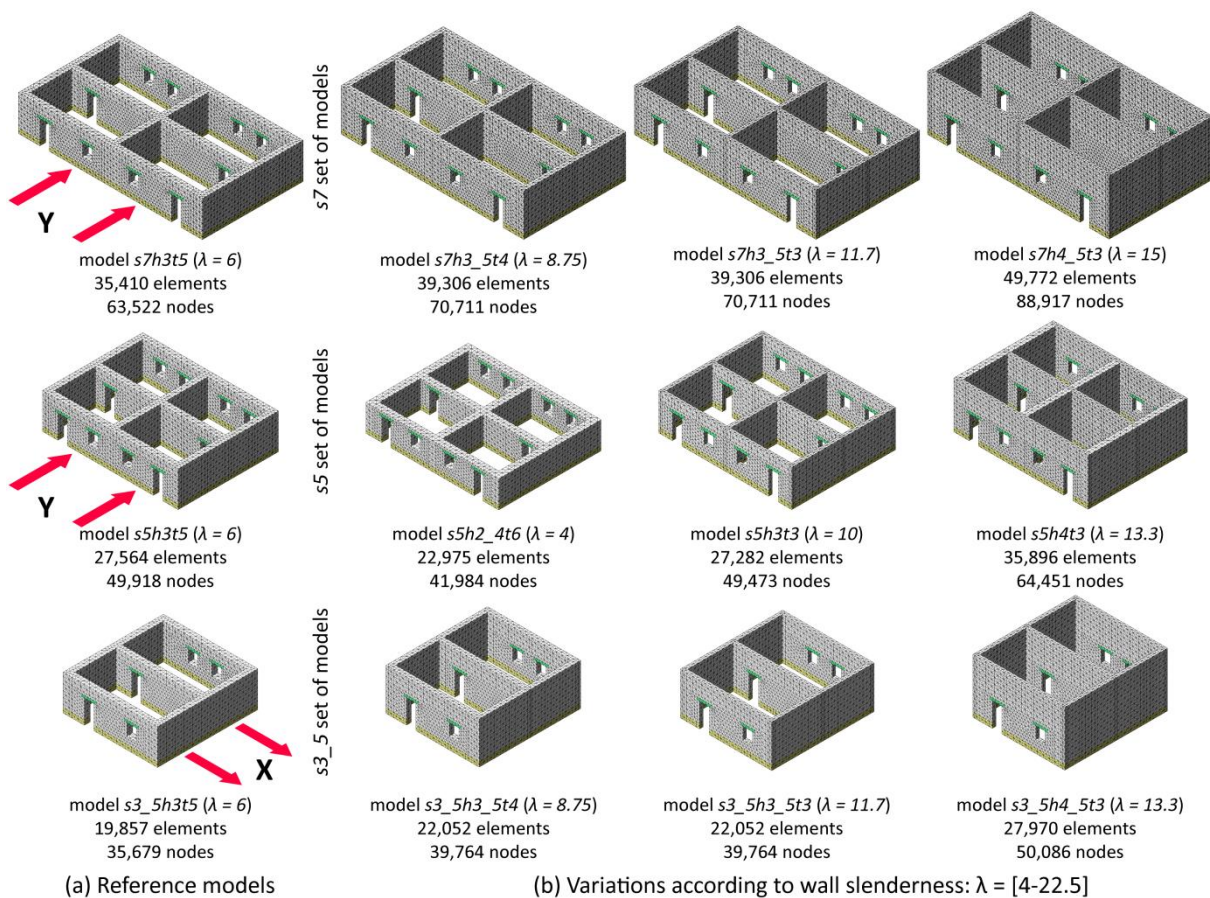


Figure 4.6: Numerical models built in order to assess the influence of the wall slenderness (λ) on the seismic behavior of vernacular buildings: (a) reference models; (b) examples of variations of wall slenderness modelled

Table 4.1: Summary of the 38 different models built in order to assess the influence of the wall slenderness (λ) on the seismic behavior of vernacular buildings

Model Name	Set of models			Height, h (m)	Variations	
	$s = 7$ m	$s = 5$ m	$s = 3.5$ m		Thickness, t (m)	Wall slenderness, λ
<i>h2_4t6</i>	X	X	X	2.4	0.6	4
<i>h3t6</i>	X	X	X	3	0.6	5
<i>h3t5 (Ref)</i>	X	X	X	3	0.5	6
<i>h3_5t5</i>	X		X	3.5	0.5	7
<i>h3t4</i>	X	X	X	3	0.4	7.5
<i>h3_5t4</i>	X		X	3.5	0.4	8.75
<i>h3t3</i>	X	X	X	3	0.3	10
<i>h4t4</i>	X		X	4	0.4	10
<i>h3_5t3</i>	X		X	3.5	0.3	11.67
<i>h4t3</i>	X	X	X	4	0.3	13.33
<i>h4_5t3</i>	X		X	4.5	0.3	15
<i>h3t2</i>	X	X	X	3	0.2	15
<i>h3_5t2</i>	X		X	3.5	0.2	17.5
<i>h4t2</i>	X	X	X	4	0.2	20
<i>h4_5t2</i>	X		X	4.5	0.2	22.5

4.3.1. Variations on damage patterns and failure mechanisms

The most representative failure mechanisms for the three sets of models analyzed are shown in Figure 4.7 in terms of maximum total displacements and crack pattern at the ultimate limit state (LS4). The crack and deformation patterns show that the global behavior of the buildings is mainly governed by out-of-plane resisting mechanisms of the exterior walls perpendicular to the seismic load, presenting only some small variations in the damage pattern observed. The wall slenderness thus mainly influences the bending resistance of the walls. For lower values of wall slenderness, collapse is mainly driven by the failure at the connection between perpendicular walls, showing vertical cracks at the wall intersections and extensive cracking at the base, which leads to the overturning of the wall. When the wall slenderness increases, collapse is mainly determined by the out-of-plane bending failure of the walls, characterized by diagonal and vertical cracks at the mid-span of the wall. Nevertheless, it should be mentioned that a combination of both types of damage patterns can be observed in all cases.

4.3.2. Building of four-linear capacity curves and analysis of load factor variations

The four-linear capacity curves derived from the pushover curves obtained in the parametric analysis are shown in Figure 4.8, grouped by set of models with varying maximum wall span. As it could be expected, the initial stiffness of the models significantly decreases when increasing the wall slenderness. The graphs show very similar variations in the behavior of the buildings when varying the wall slenderness for the three sets. The most severe difference in terms of load factor in all cases occurs for the model with a slenderness ratio of $\lambda = 4$, whose maximum capacity

almost doubles the capacity of the model with $\lambda = 6$. Apart from this, the differences in the response of the building according to the variation of λ are more gradual, but they confirm the influence of the parameter in the seismic behavior of the buildings.

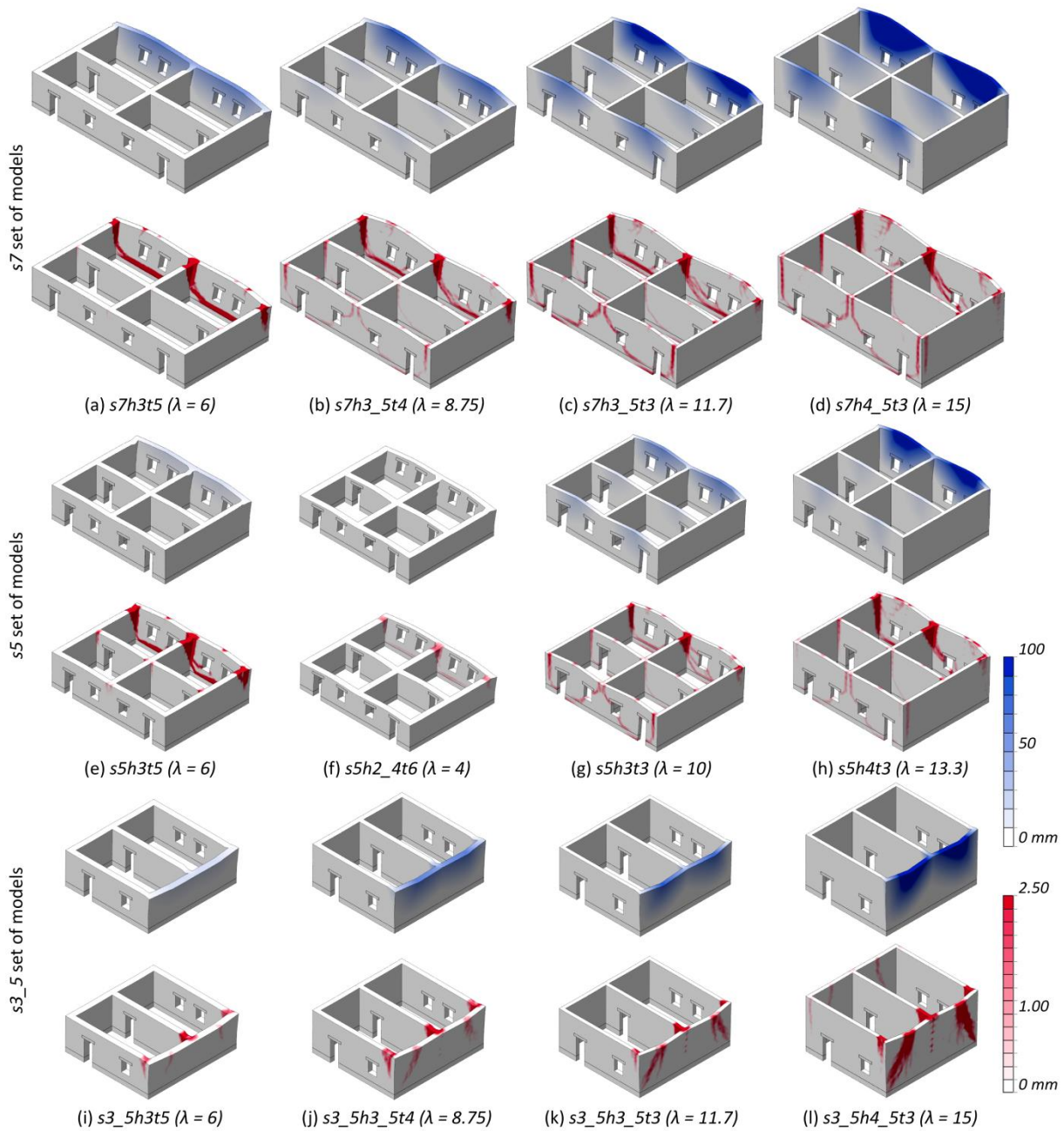


Figure 4.7: Representative failure modes at ultimate limit state (LS4) obtained for several buildings with varying wall slenderness (λ) within each of the three sets of models analyzed: (blue) maximum total displacements; and (red) crack pattern (crack width scale)

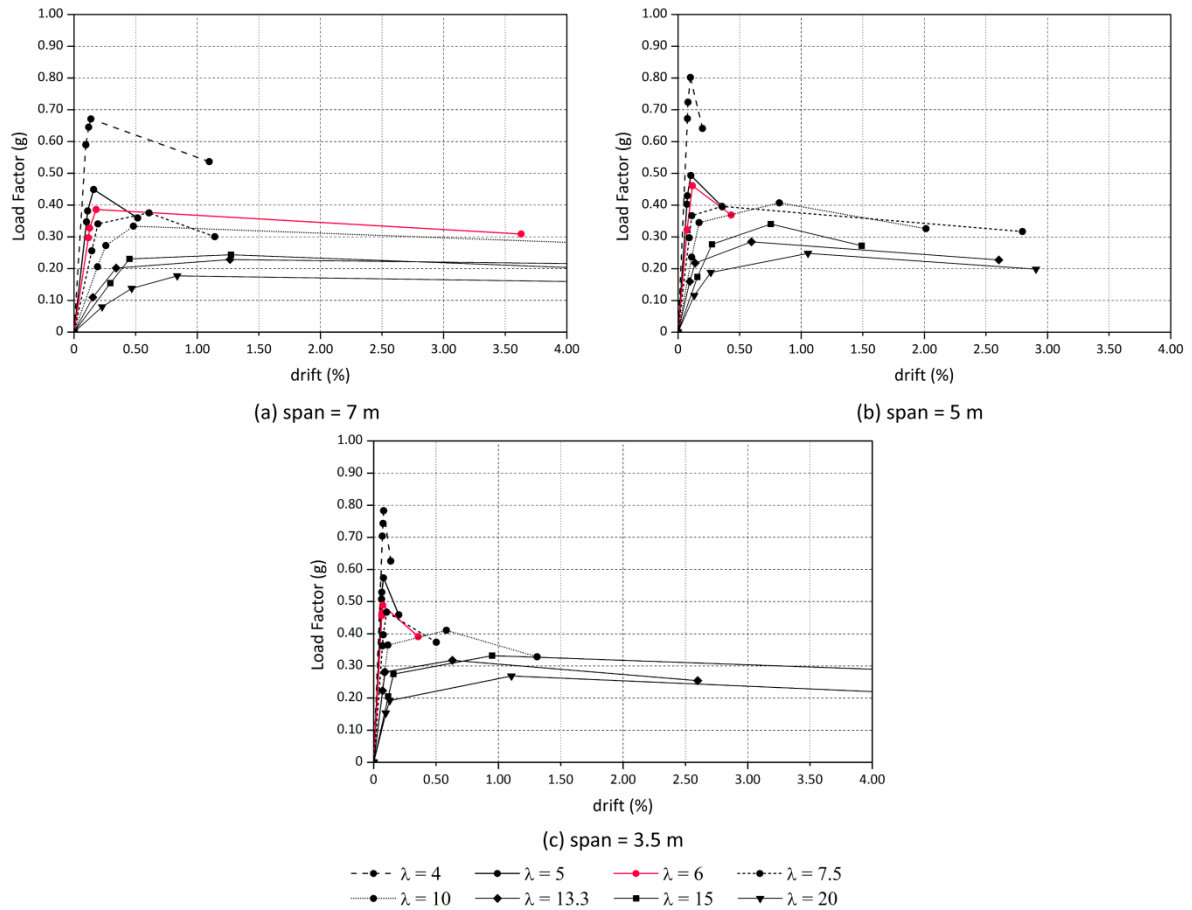


Figure 4.8: Four-linear capacity curves for the three sets of models with varying wall span: (a) $s = 7$ m; (b) $s = 5$ m; and (c) $s = 3.5$ m

The seismic response of the buildings is also very variable in terms of ductility. Those buildings with low values of slenderness show a very pronounced softening, in contrast with the smooth post-peak behavior shown by the curves from the buildings with high values of λ . The differences are particularly evident for the buildings with the lower values of span ($s5$ and $s3_5$). This can be explained by the failure modes observed in the buildings. For example, models $s5h2_4t6$ or $s3_5h3t5$ behave very rigidly because of the thick walls and the low values of height and span. This increases their out-of-plane resistance, but their collapse mechanism is brittle and sudden. The buildings do not suffer significant deformations until damage occurs at the wall intersections and at the base, which leads to the overturning of the walls (Figure 4.7f and i). On the other hand, for the buildings with high values of λ , the damage is much more widespread and involves several structural elements of the building, which leads to high displacements at LS4, see Figure 4.7d, h and l. Nevertheless, their resistance is considerably lower.

The variations of the load factors defining each limit state are shown in Figure 4.9, grouped by set of models. For the three sets, the models with a slenderness value (λ) of 4 showed the maximum capacity and were used for the normalization. Results indicate a clear variation of the

load factors according to the slenderness ratio. In general, as expected, the different limit states are attained for decreasing load factors as the wall slenderness increases. This trend is similar for the three sets with varying maximum wall span. The highest variations occur for the load factor defining LS1, meaning that slender walls are prone to suffer damage for lower seismic loads.

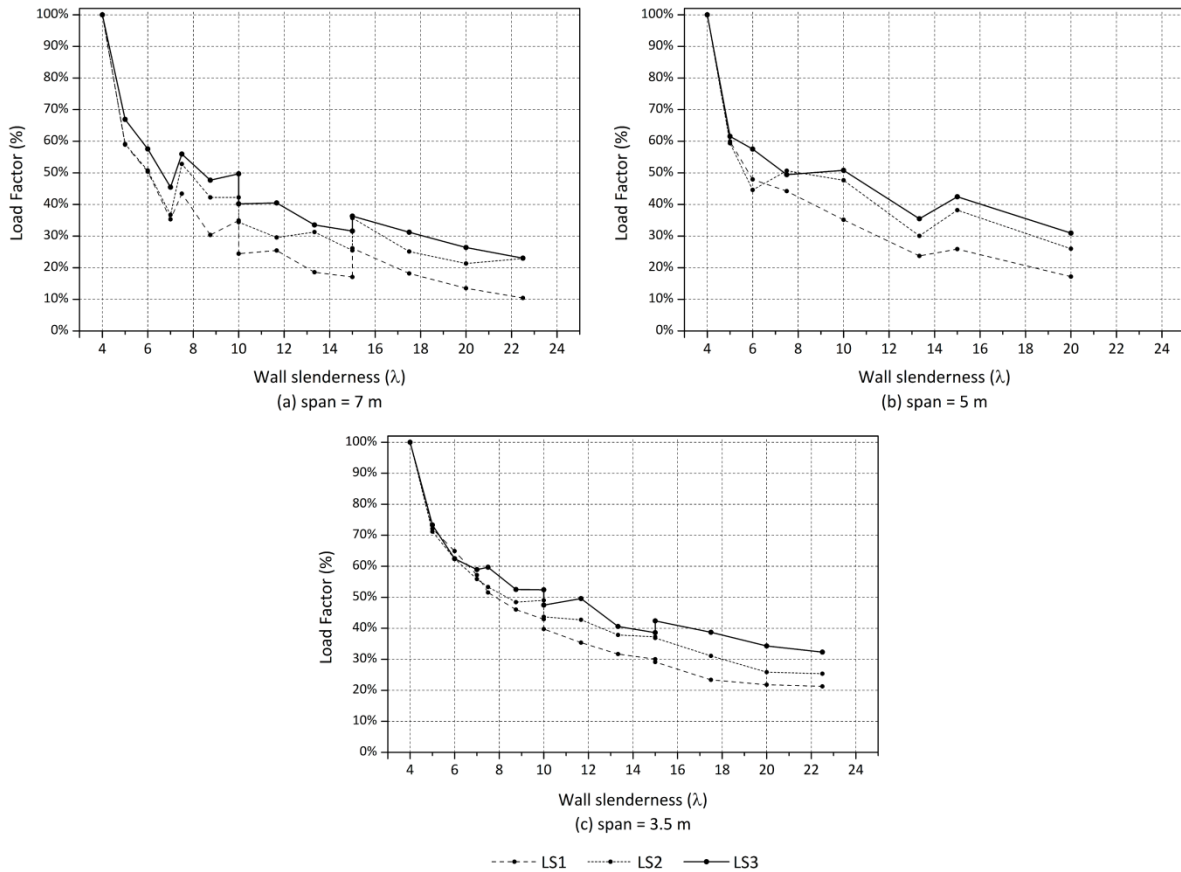


Figure 4.9: Load factor variations for each LS for the three set of models with varying wall span: (a) $s = 7$ m; (b) $s = 5$ m; and (c) $s = 3.5$ m

4.3.3. Definition of seismic vulnerability classes

The four seismic vulnerability classes are defined from the variation of the load factor corresponding to the attainment of LS3. The difference between the model with $\lambda = 4$ and the remaining models was deemed exceptionally high (see Figure 4.9) so it was not taken into account for the definition of the classes. Instead, the model with $\lambda = 5$ was used for the normalization of the load factor variations that led to the definition of the classes. Figure 4.10 shows the variation of the load factor defining LS3 for the three sets of models and the four intervals associated to the four vulnerability classes (A, B, C and D). The three sets lead to very similar classifications. Nevertheless, the discrepancies observed were solved by adopting the most unfavorable class obtained. For example, for $s = 5$, the building with $\lambda = 10$ lies within class B, but the same model lies within class C when $s = 5$ or $s = 7$. Therefore, $\lambda = 10$ is finally considered within class C.

Table 4.2 provides the range of values of wall slenderness that delimits each seismic vulnerability class. The threshold values of wall slenderness (λ) obtained here are lower than values observed in classifications proposed by other authors in existing seismic vulnerability index formulations that have taken into account the wall slenderness as a parameter (Vicente 2008; Ferreira 2009). Table 4.3 shows a comparison of the values proposed here with other values from the literature. This is attributed to the low wall slenderness ratios that can be typically observed in vernacular stone masonry and earthen buildings. The high values of λ proposed by other authors are not representative for vernacular buildings. Therefore, this new classification is adapted the typical characteristics of vernacular architecture.

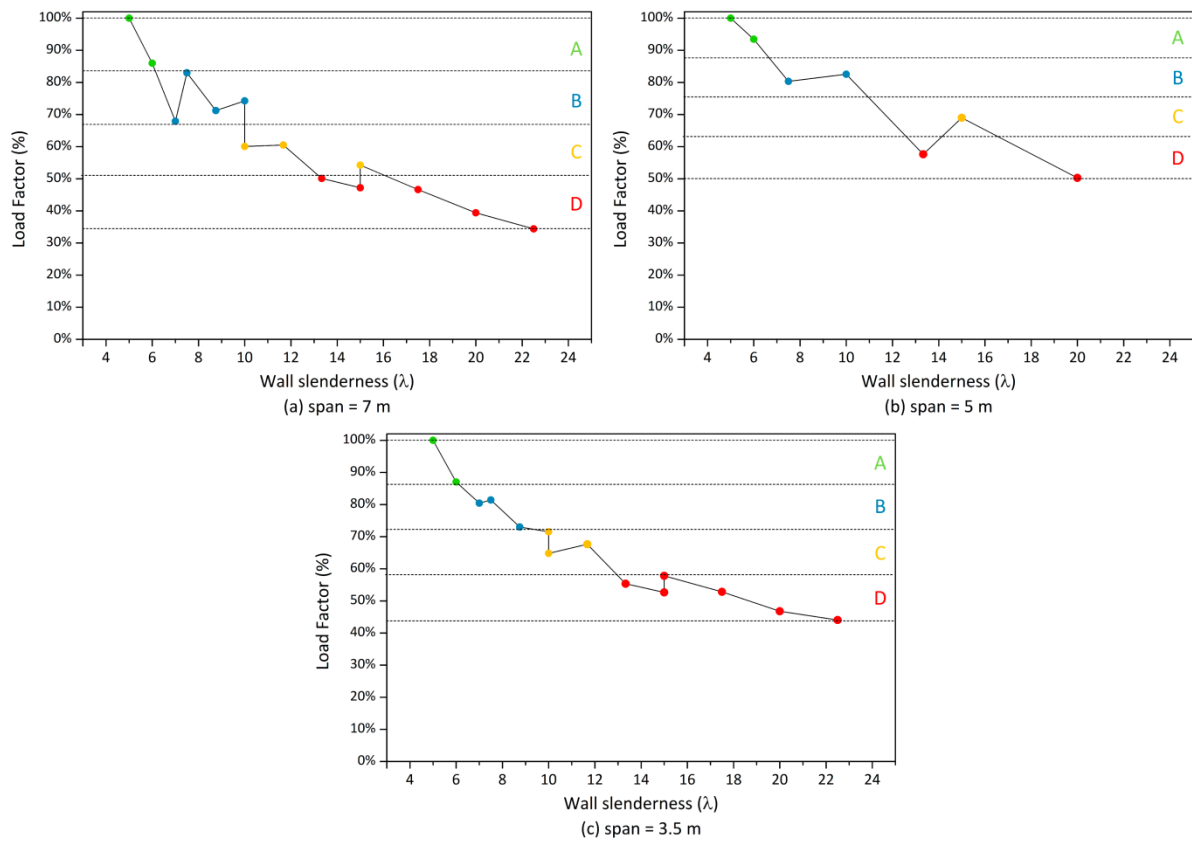


Figure 4.10: Variation of the load factor leading to the attainment of the maximum capacity (LS3) for the three sets of models evaluated with different values of maximum wall span: (a) $s = 7$ m; (b) $s = 5$ m; and (c) $s = 3.5$ m

Table 4.2: Vulnerability classes proposed according to the wall slenderness (λ)

P1. Wall slenderness	
Class	Description
A	$\lambda \leq 6$
B	$6 < \lambda \leq 9$
C	$9 < \lambda \leq 12$
D	$\lambda > 12$

Table 4.3: Comparison among vulnerability classes proposed by other authors for similar vulnerability index formulations that have taken into account the wall slenderness (λ) as a parameter

P1. Wall slenderness			
Class	Classification proposed	Vicente (2008)	Ferreira (2009)
A	$\lambda \leq 6$	$\lambda \leq 10$	$\lambda \leq 9$
B	$6 < \lambda \leq 9$	$10 < \lambda \leq 15$	$9 < \lambda \leq 15$
C	$9 < \lambda \leq 12$	$15 < \lambda \leq 20$	$15 < \lambda \leq 20$
D	$\lambda > 12$	$\lambda > 20$	$\lambda > 20$

4.4. Seismic vulnerability classes according to the maximum wall span (P2)

Two reference models with varying number of floors and type of diaphragm were prepared for the analysis of the influence of P2 (Figure 4.11): (a) one-floor rammed earth building with flexible diaphragm and 0.5 m thick walls (*RE1F*); and (b) two-floor rammed earth building with rigid diaphragm and 0.5 m thick walls (*RE2Fd1*). The walls of the one-floor models are 3 m high and the in-plan area varies according to the span. The maximum wall span of the one-floor reference model is 7 m and its in-plan area is 15.5x8.5 m². The ground floor walls of the two-floor models are 3 m high, while the walls at the upper floor are 2.6 m high. The wall span of the two-floor reference model is 7 m and its in-plan area is 8x5.5 m². In both cases, the roof load is modelled as distributed load along the walls. In order to assess the influence of the maximum wall span (s) on the seismic behavior of vernacular buildings, s is increased and decreased within a range between 4 and 12. The range is established based on typical values for vernacular buildings, as discussed in Chapter 3. The two sets of models were analyzed in the direction perpendicular to the walls whose maximum wall span (s) is being modified (Y). This direction was selected because P2 evaluates the variations in the response of the building when the maximum length of a wall prone to out-of-plane movements varies. Table 4.4 presents a summary of the 18 models constructed and Figure 4.11 shows some of the models prepared with variations of s .

The rigid diaphragm in the *RE2Fd1* set of models is composed by timber beams and cross-board sheathing. The timber beams are simulated using three-node beam elements (CL18B) and the mechanical properties of the timber shown in Table 3.3 are assigned to them. The cross section considered for the timber beams is 0.3x0.225 m² with a spacing of 1 m. The beams are considered fully embedded within the wall, going through the whole thickness. The cross boards are modelled using six-node triangular shell elements (CT30S), aiming at simulating the in-plane deformability (Mendes and Lourenço 2015). Only the elastic properties are considered for the diaphragm and timber beams, since the failure and nonlinearities are expected to take place in the walls. An elasticity modulus (E_d) of 200 MPa and a Poisson's ratio of 0.3 were adopted. The thickness of the diaphragm cross boards (t_d) is considered as 0.036 m and the specific mass is set

at 750 kg/m³. The connections between the board sheathing and the walls are assumed to share all degrees of freedom.

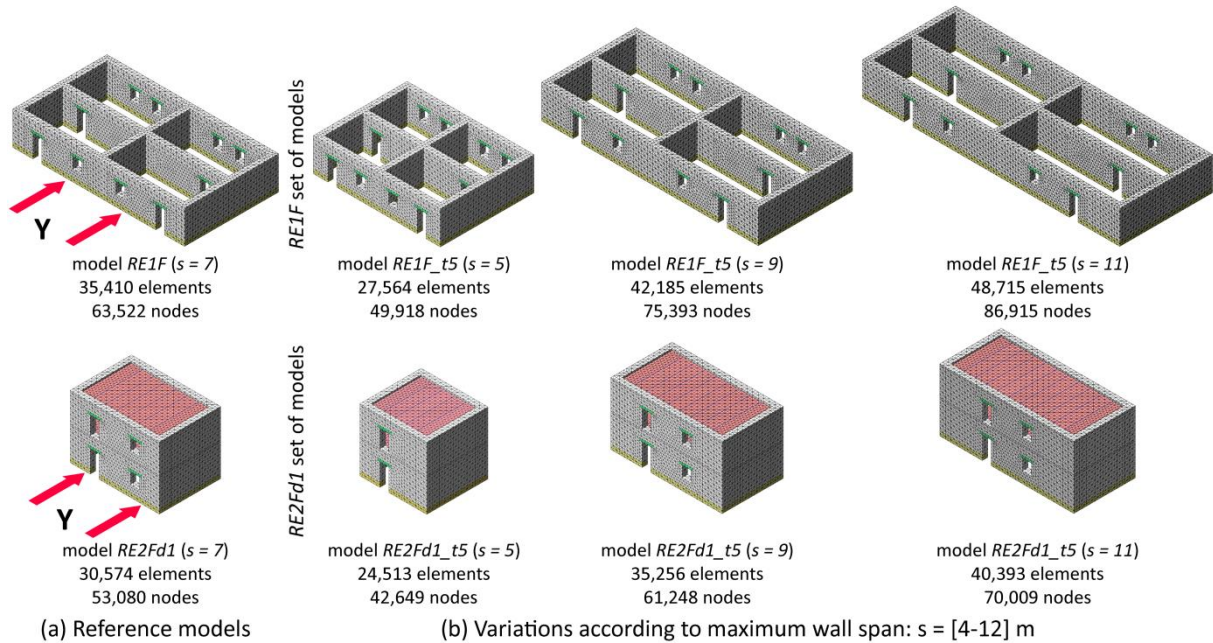


Figure 4.11: Numerical models built in order to assess the influence of the maximum wall span (s) on the seismic behavior of vernacular buildings: (a) reference models; (b) examples of variations of s modelled

Table 4.4: Summary of the 18 different models built in order to assess the influence of the maximum wall span (s) on the seismic behavior of vernacular buildings

Set of models	Maximum wall span, s (m)									
	4	5	6	7	8	9	10	11	12	
RE1F	X	X	X	X (Ref)	X	X	X	X	X	
RE2Fd1	X	X	X	X (Ref)	X	X	X	X	X	

4.4.1. Variations on damage patterns and failure mechanisms

The most representative failure mechanisms obtained for the two sets of models analyzed are shown in Figure 4.12. The models from the *RE1F* set, which disregard the diaphragm effect, showed clear out-of-plane failure modes. In this case, the crack patterns corresponding to the limit state close to collapse developed at the connection between perpendicular walls and at the base, indicating the overturning of the exterior walls perpendicular to the seismic load. The only significant variation in the damage pattern observed concerns those models presenting higher values of wall span (over 9 m), which show significant damage at all the walls perpendicular to the seismic load, see Figure 4.12c and d. On the other hand, those models with walls spanning shorter distances only show important damage at the back walls perpendicular to the seismic load, see Figure 4.12a and b. As it could be expected, the confinement imposed by the wall-to-wall connections is more effective when the span is shorter.

With respect to the models presenting a rigid diaphragm (*RE2Fd1* set of models), their global response is mostly governed by the in-plane failure of the walls parallel to the seismic load. Since the diaphragm has been modelled rigid enough to redistribute the load among the resisting elements, damage is more widespread throughout the building. Nevertheless, there is also important out-of-plane bending damage at the walls perpendicular to the loading direction, as well as damage at the connection between perpendicular walls. For this set of models, there are no significant variations in the failure mode when varying the wall span, see Figure 4.12e-h.

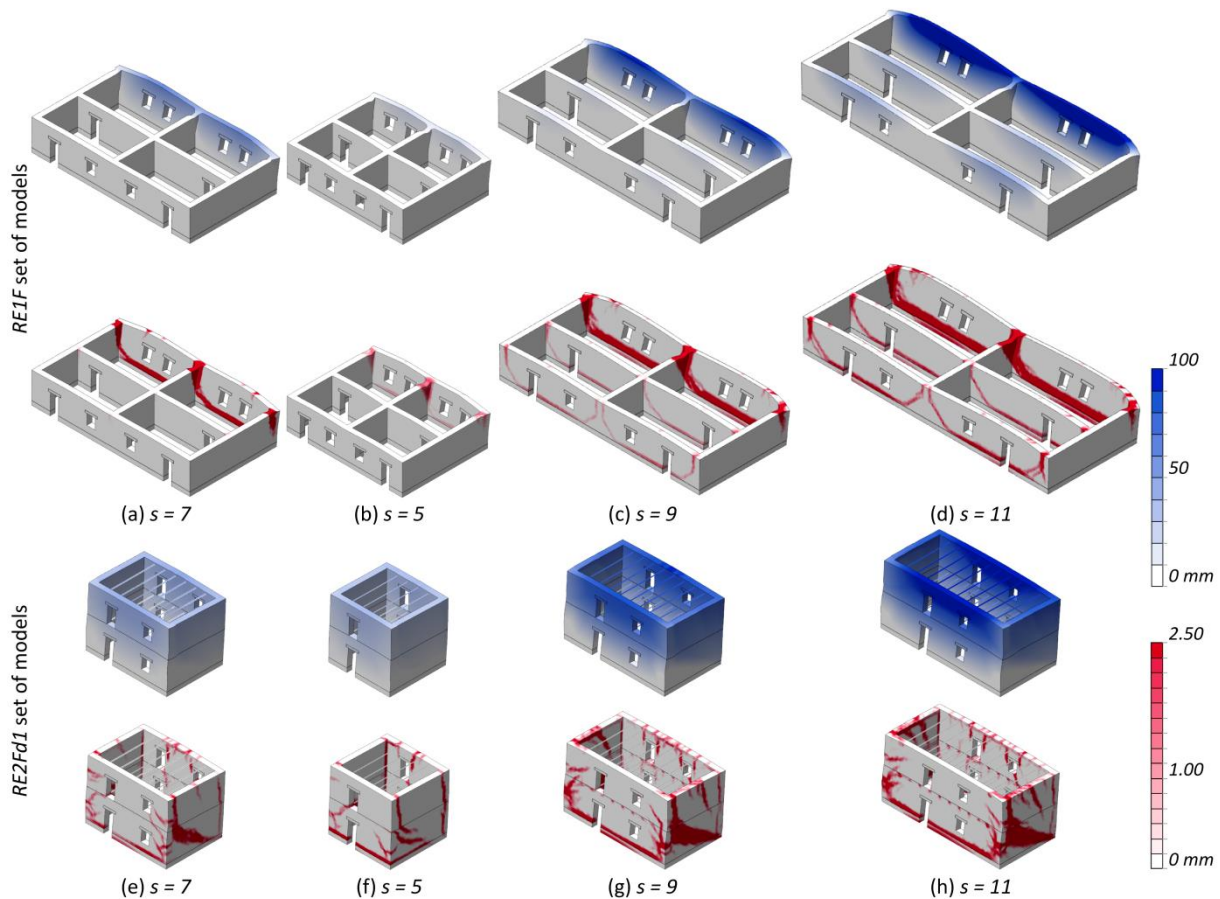


Figure 4.12: Representative failure modes at ultimate limit state (LS4) obtained for several buildings with varying maximum wall span (s) within the *RE1F* and *RE2Fd1* sets of models analyzed: (blue) maximum total displacements; and (red) crack pattern (crack width scale)

4.4.2. Building of capacity curves and analysis of load factor variations

Figure 4.13 presents the four-linear capacity curves constructed from the pushover analyses performed, grouped by set of models. In both sets of models, there are variations in both the maximum capacity and initial stiffness of the building, which decrease gradually when increasing the maximum wall span perpendicular to the seismic loading. However, the graphs show that influence of the maximum wall span (s) is not the same for both sets of models. For the *RE1F* set of models, the variation of s results in a range of variation of the load factor defining LS3 between

0.32g and 0.48g. This range of variation is wider for the *RE2Fd1* set of models, which varies between 0.42g and 0.77g. This means that the influence of this parameter is sensitive to variations of the other parameters, such as the number of floors and type of horizontal diaphragm, revealing the interdependence among the different parameters. It should be also taken into account that when varying the maximum wall span of the building, other geometrical parameters are subsequently modified, such as the area of wall openings (P7) or the in-plan index (P10). In any case, the influence of this specific parameter on the seismic behavior of the building seems clear.

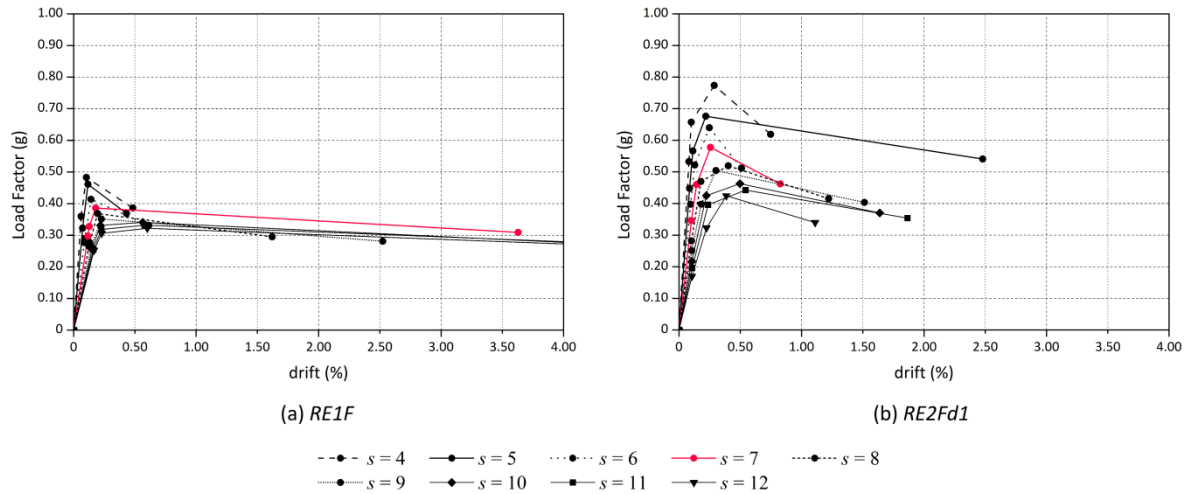


Figure 4.13: Four-linear capacity curves for the two sets of models: (a) *RE1F*; and (b) *RE2Fd1*

For the *RE1F* set of models, there is also a noticeable variation in the seismic response of the buildings in terms of ductility. The buildings increase their out-of-plane resistance when decreasing the maximum wall span, but the response is notably more brittle and show a more pronounced softening. Thus, the graphs confirm the variations in the failure mode of the building observed in Figure 4.12a-d. The boundary conditions, which are more restrictive for the walls with shorter spans, result in this brittle failure of the back walls perpendicular to the seismic load. On the other hand, when the walls span longer distances, the buildings suffer larger deformations before reaching the collapse and the damage is more widespread, involving all the walls of the building perpendicular to the seismic load. This is not the case for the *RE2Fd1* set of models, whose failure mode, as previously discussed, remains mainly unaltered. Therefore, there are not significant differences in the four-linear curves obtained in terms of ductility.

The variations of the load factors defining each limit state obtained for the two sets of models are shown in Figure 4.14. The variations were normalized using the models with $s = 4$ m, which showed the maximum capacity. The diagrams from both sets of models confirm the influence of the maximum wall span (s) on the global seismic behavior of the buildings. The results of the parametric study show a clear decrease of the capacity of the building when increasing the maximum wall span, but the range of variation is notably wider for the *RE2Fd1* set of models for

all the limit states. The highest variations occur for the load factor defining LS1 in models *RE2Fd1*, which means that walls spanning long distances without intermediate supports are prone to suffer damage, even if the building presents a sufficiently stiff diaphragm.

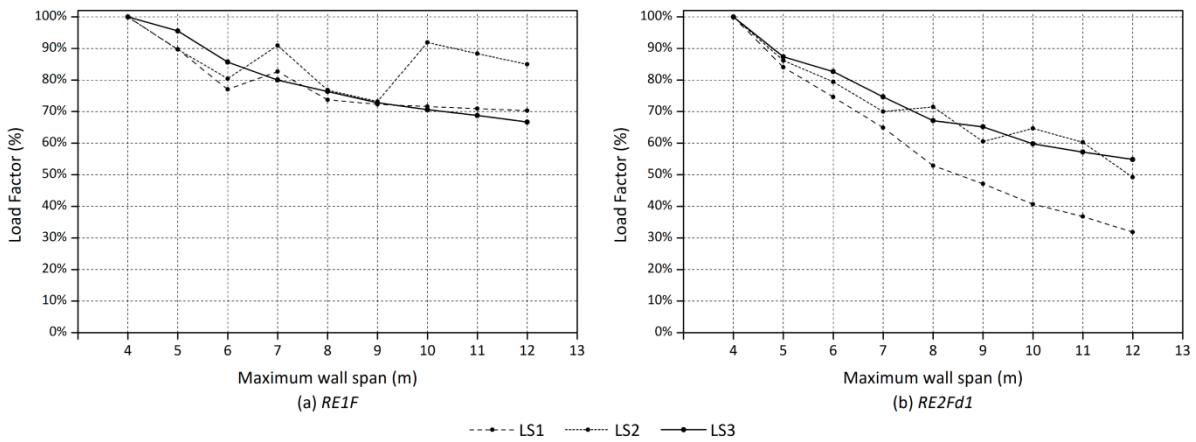


Figure 4.14: Load factor variations for each LS for the two sets of models: (a) *RE1F*; and (b) *RE2Fd1*

4.4.3. Definition of seismic vulnerability classes

The four seismic vulnerability classes are defined according to the variation of the load factor corresponding to the attainment of LS3. Figure 4.15 shows the variation of the load factor defining LS3 for the two sets of models and the four intervals associated to the four vulnerability classes (A, B, C and D). Even if the range of variation is notably lower for the model with no diaphragm effect, the vulnerability classes obtained for both sets do not differ significantly. Nonetheless, in case of discrepancies, it is noted that the most unfavorable class is considered. For example, for *RE1F*, the building with $s = 5$ lies within class A, but the same building lies within class B for *RE2Fd1*. Therefore, $s = 5$ is finally considered within class B.

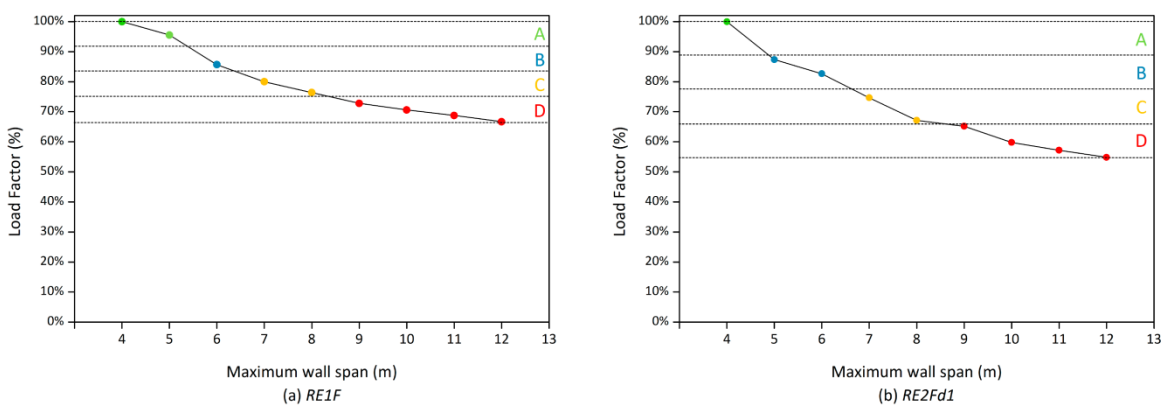


Figure 4.15: Variation of the load factor leading to the attainment of the maximum capacity (LS3) for the two sets of models evaluated: (a) *RE1F*; and (b) *RE2Fd1*

Table 4.5 provides the range of values of maximum wall span (s) that delimits each seismic vulnerability class. The classification proposed by Vicente (2008) expresses the maximum wall span parameter according to the span to thickness ratio (s/t). However, since the wall thickness was already taken into account in the previous parameter (P1), it was decided to adopt only the maximum wall span (measured in meters) for the definition of the vulnerability classes. Table 4.6 shows the classification proposed by Vicente (2008) and the new classification proposed, transformed into s/t for three different typical values of wall thickness (t), in order to allow a direct comparison. Even though this comparison is done for only two values of t , the new classification proposed is generally stricter. This can be again attributed to the low values of s that can be typically observed in vernacular architecture, which generally have small dimensions.

Table 4.5: Vulnerability classes proposed according to the maximum wall span (s)

P2. Maximum wall span	
Class	Description (values in m)
A	$s_{max} < 5$
B	$5 \leq s_{max} < 7$
C	$7 \leq s_{max} < 9$
D	$s_{max} \geq 9$

Table 4.6: Comparison with the classes according to the maximum wall span (s/t) proposed by Vicente (2008)

P2. Maximum wall span				
Class	Classification proposed ($t = 0.6\text{ m}$)	Classification proposed ($t = 0.5\text{ m}$)	Classification proposed ($t = 0.4\text{ m}$)	Vicente (2008)
A	$(s/t)_{max} < 8.33$	$(s/t)_{max} < 10$	$(s/t)_{max} < 12.5$	$(s/t)_{max} \leq 15$
B	$8.33 \leq (s/t)_{max} < 11.67$	$10 \leq (s/t)_{max} < 14$	$12.5 \leq (s/t)_{max} < 17.5$	$15 < (s/t)_{max} \leq 18$
C	$11.67 \leq (s/t)_{max} < 15\text{ m}$	$17.5 \leq (s/t)_{max} < 18$	$17.5 \leq (s/t)_{max} < 22.5$	$18 < (s/t)_{max} \leq 25$
D	$(s/t)_{max} \geq 15\text{ m}$	$(s/t)_{max} \geq 18$	$(s/t)_{max} \geq 22.5$	$(s/t)_{max} > 25$

4.5. Seismic vulnerability classes according to the type of material (P3)

Two reference models with varying number of floors, type of diaphragm and distribution of wall openings were prepared for the analysis of the influence of P3 (Figure 4.16): (a) one-floor rammed earth building with flexible diaphragm, 0.5 m thick walls and reduced number of wall openings (*RE1F*); and (b) two-floor rammed earth building with rigid diaphragm, 0.5 m thick walls and high number of wall openings (*RE2Fd1*). The walls of the one-floor models are 3 m high and the maximum wall span is 7 m. The in-plan area is 8x10.5 m². The ground floor walls of the two-floor models are 3 m high, while the upper floor walls are 2.6 m high. The maximum wall span is 7 m and the in-plan area is 8x5.5 m². In both sets, the roof load is modelled as distributed load along the walls. The *RE1F* set of models was analyzed in the direction perpendicular to the walls with the maximum wall span (Y), in order to understand the influence of the material when the

building is expected to show an out-of-plane failure mode. The *RE2Fd1* set of models was analyzed in the direction parallel to the walls with openings (X), in order to understand the influence of the material when the building is prone to present an in-plane collapse mechanism.

In order to assess the influence of the type of material on the seismic behavior of vernacular buildings, the material properties of the walls were modified. Particularly, the mechanical properties defining the compressive and tensile material laws of the TSRCM model adopted for the nonlinear analysis were varied, namely the Young's modulus (E), the compressive strength (f_c) and the tensile strength (f_t). The values for the compressive fracture energy (G_{fc}) vary in proportion with the compressive strength, and the mode I fracture energy (G_{fI}) was kept constant for all the models. The ranges of variation considered for the different mechanical properties are established based on representative values obtained from the literature (NTC 2008; Gallego and Arto 2014; Tarque 2008), as discussed in Chapter 3 (Table 3.4). Table 4.7 presents a summary of the 50 models finally built for the evaluation of this parameter. The different combinations of the material properties can be associated to eight different materials that are commonly applied in vernacular buildings for the construction of the walls.

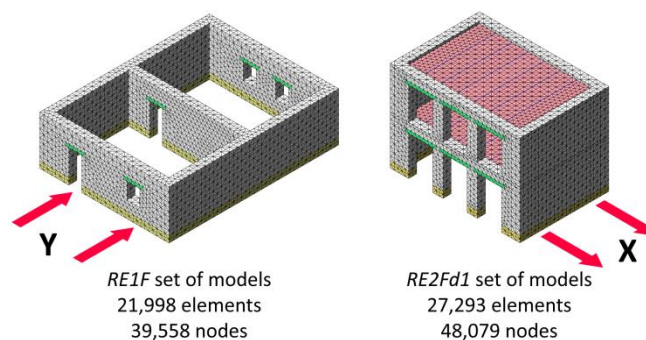


Figure 4.16: Numerical models built in order to assess the influence of the type of material on the seismic behavior of vernacular buildings

4.5.1. Variations on damage patterns and failure mechanisms

The failure mode observed in all models from the *RE1F* set consists of the out-of-plane overturning mechanism of the exterior walls, see Figure 4.17. The main variation in the damage pattern observed is that it is much more widespread for the models with lower values of the mechanical properties. In particular, the variations in f_t and E have a significant influence on this aspect. When poorer quality material properties are adopted, for example simulating adobe masonry (Figure 4.17a), the models show significant damage since early stages of loading at all the walls perpendicular to the seismic load. At the ultimate limit state, extensive out-of-plane bending damage is visible, together with the characteristic overturning of the exterior back wall perpendicular to the seismic load. However, when the material properties adopted are associated to better quality materials, such as dressed stone masonry (Figure 4.17d), the damage is more

localized and prevented almost until reaching the maximum capacity of the building. Thus, collapse is more sudden and mainly consists of the overturning of the exterior back wall, illustrated by vertical cracks at the wall intersections and horizontal cracking at the base.

Table 4.7: Summary of the 50 different models built in order to assess the influence of the type of material on the seismic behavior of vernacular buildings

Model Name	Set of models		Mechanical properties			Material associated
	RE1F	RE2Fd1	E (MPa)	f _c (MPa)	f _t (MPa)	
150-10-005	X				0.05	
150-10-010	X	X	150	1.0	0.1	Rammed earth / adobe masonry
150-10-020	X				0.2	
300-06-005	X	X		0.6	0.05	
300-06-010	X				0.1	
300-10-005	X				0.05	
300-10-010 (Ref)	X	X	300	1.0	0.1	Rammed earth
300-10-020	X				0.2	
300-15-010	X			1.5	0.1	
300-15-015	X				0.15	
500-06-010	X	X	500	0.6	0.1	Rammed earth / irregular stone masonry
500-10-010	X			1.0	0.1	
500-15-010	X		500	1.5	0.1	Rammed earth
500-15-015	X				0.15	
1000-06-005	X	X			0.05	
1000-06-010	X			0.6	0.1	Irregular stone masonry
1000-06-020	X				0.2	
1000-10-005	X				0.05	
1000-10-010	X	X	1000	1.0	0.1	Soft stone masonry
1000-10-020	X				0.2	
1000-15-010	X				0.1	
1000-15-015	X	X		1.5	0.15	Uncut stone masonry
1000-15-030	X				0.3	
1500-15-015	X	X	1500	1.5	0.15	Uncut stone masonry / cut stone masonry
1500-20-020	X	X	1500	2.0	0.2	Cut stone masonry
2000-20-010	X				0.1	
2000-20-020	X	X		2.0	0.2	Cut stone masonry / full brick masonry
2000-20-040	X		2000		0.4	
2000-30-030	X			3.0	0.3	
2500-20-020	X			2.0	0.2	Full brick masonry
2500-30-015	X				0.15	
2500-30-030	X	X	2500	2.5	0.3	Full brick masonry / dressed stone masonry
2500-30-060	X				0.6	
3000-30-030	X	X		3.0	0.3	
3000-40-015	X				0.15	
3000-40-030	X		3000	4.0	0.3	Dressed stone masonry
3000-40-060	X	X			0.6	

The two-floor models showed how the rigid diaphragm is able to activate in-plane resisting mechanisms that contribute to the global stability of the buildings. As a result, the failure mode observed for all models from the *RE2Fd1* set consists of a typical in-plane shear failure, see Figure 4.17. The failure is significantly aggravated because of the presence of openings of large dimensions. The characteristic diagonal shear cracks follow the distribution of the openings. For this set of models, there are not significant variations in the failure mode when varying the material properties. Only the damage is slightly more widespread when poorer material properties are adopted for the walls (Figure 4.17e).

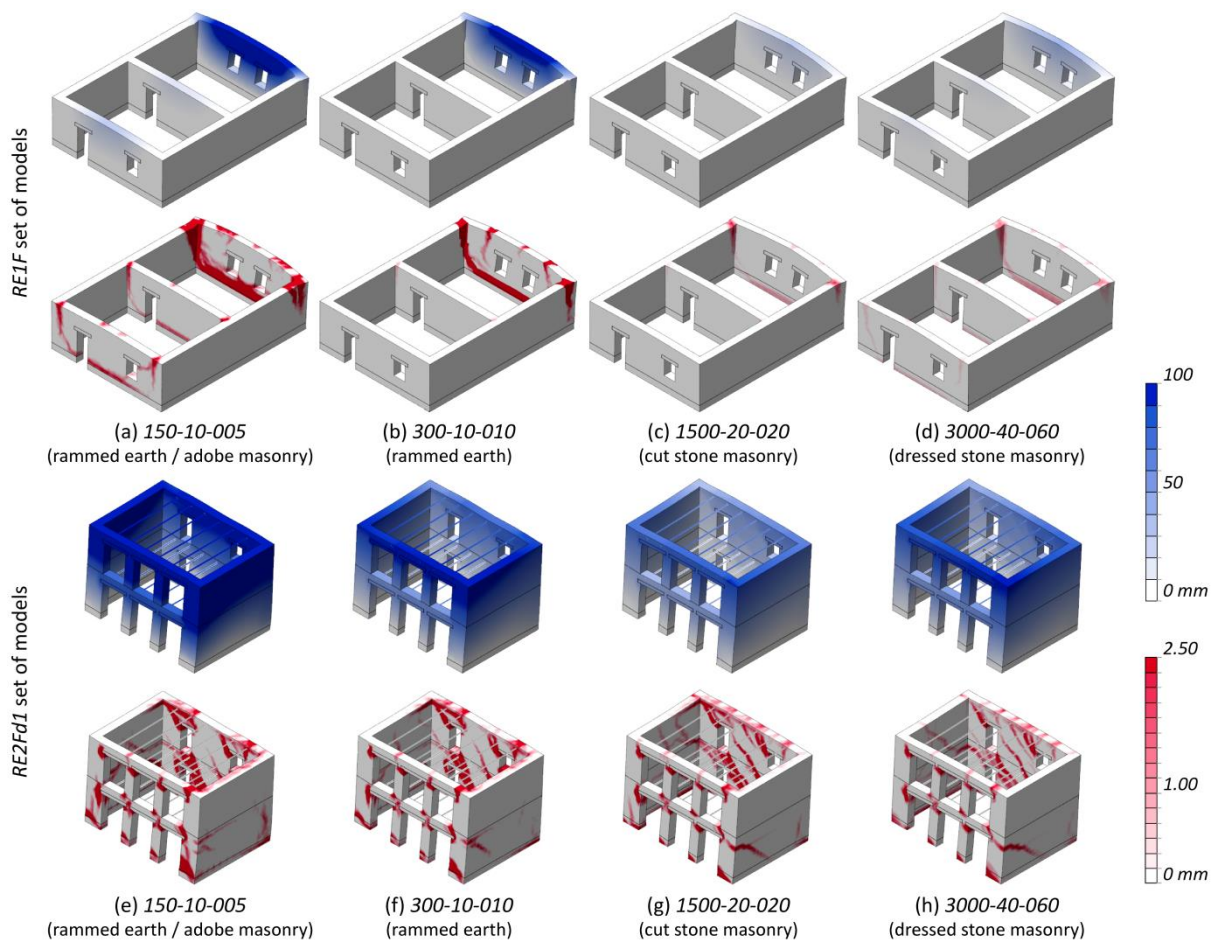


Figure 4.17: Representative failure at ultimate limit state (LS4) obtained for several buildings with varying material properties within the *RE1F* and *RE2Fd1* set of models analyzed: (blue) maximum total displacements; and (red) crack pattern (crack width scale)

4.5.2. Building of capacity curves and analysis of load factor variations

Figure 4.18 shows the four-linear capacity curves constructed from the pushover analyses performed, grouped by set of models. Each curve represents one of the eight different materials considered (Table 4.7). They were constructed using average values obtained from the results of all the models that can be associated to each material. In both sets of models, there is a clear the

variation of the capacity of the building according to the different material properties considered, confirming the influence of this parameter. Both sets of buildings are sensitive to the variation of the material properties in terms of maximum capacity, which decrease gradually when decreasing the material properties of the resisting walls. The range of variation is also similar for both sets, but is slightly wider for the *RE1F* set, which ranges between 0.33g and 0.80g, while the *RE2Fd1* ranges between 0.41g and 0.70g.

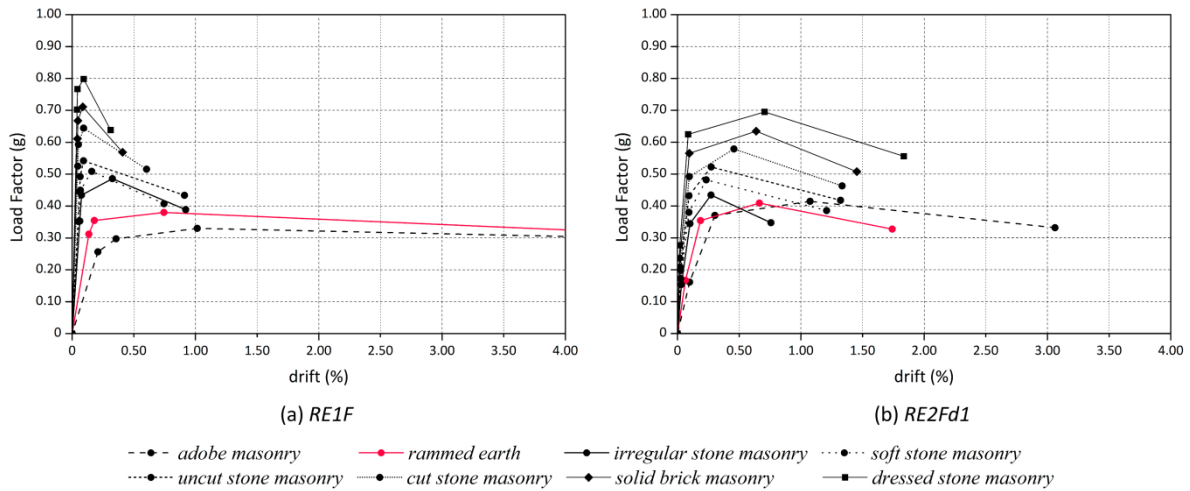


Figure 4.18: Four-linear capacity curves for the two sets of models: (a) *RE1F*; and (b) *RE2Fd1*

It is worth highlighting that the *RE1F* set of models, where the diaphragm is not modelled, is particularly sensitive to the variations in terms of initial stiffness and ductility. Materials like adobe or rammed earth, which are usually associated to low values of Young’s modulus (E), show an expected significantly less stiff behavior, showing high displacements for low values of load. The differences among the models within the set are also very evident in the post-peak behavior of the building. The adoption of poorer quality material properties for the walls led to the development of damage since very early stages of loading at several structural elements of the buildings (Figure 4.17a). As a consequence, at ultimate limit state (LS4), damage is extensively widespread, which also results in high values of drift (Figure 4.18a). This ductile behavior contrast with the brittle failure observed in buildings constructed with good quality materials. The enhanced material properties lead to an important increase in the out-of-plane resistance. Thus, the building does not suffer damage or deformations until very high values of load. However, when the maximum capacity is reached and localized damage arises at the wall intersections and at the base of the exterior back wall (Figure 4.17d), the building resistance shows a sudden drop (Figure 4.18a).

These significant variations of the seismic response of the building in terms of ductility and initial stiffness are not significant for the *RE2Fd1* set of models. This was expected, since Figure 4.17 showed that there are not significant variations in the failure mode when varying the material properties of the two-floor buildings with rigid diaphragm. The ability of the diaphragm

to involve all the walls in the structural response of the building avoids the appearance of the localized brittle failure that occurs for the *RE1F* models built with materials with high mechanical properties. Also in terms of initial stiffness the variations are lower for this set because of the same effect of the diaphragm activating several structural elements in the seismic response of the building. Thus, it is less dependent on the mechanical properties of a single wall.

The variations of the load factors defining each limit state obtained for the two sets of models are shown in Figure 4.19. The variations were normalized using the average results of the models with mechanical properties associated to dressed stone masonry, which showed the maximum capacity. The diagrams from both sets of models confirm the influence of the type of material on the global seismic behavior of the buildings. The results show an almost linear decreasing trend in the capacity of the buildings when reducing the material properties of the walls. The one-floor model with no diaphragm effect shows a wider range of variation for all the limit states, but the trend is similar for both models.

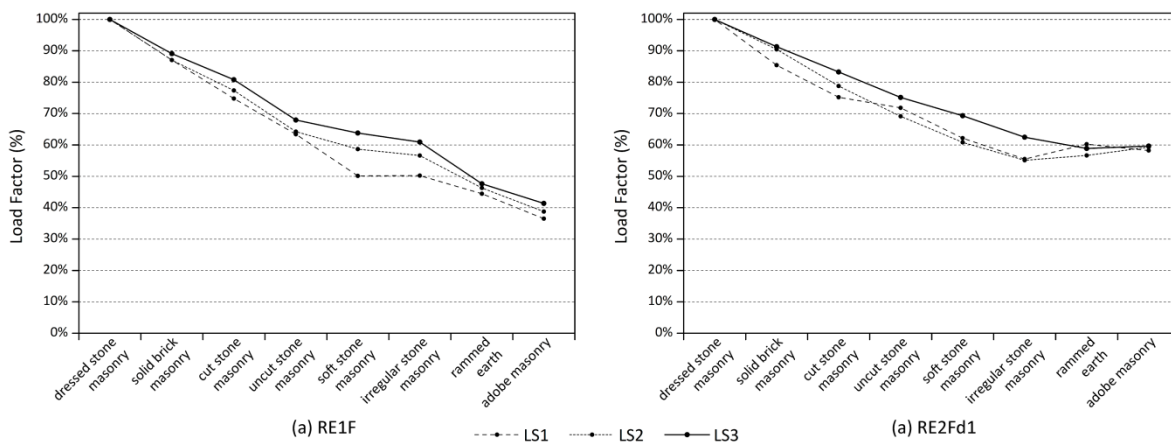


Figure 4.19: Load factor variations for each LS for the two sets of models: (a) *RE1F*; and (b) *RE2Fd1*

4.5.3. Definition of seismic vulnerability classes

The four seismic vulnerability classes are defined according to the variation of the load factor corresponding to the attainment of LS3. Figure 4.20 shows the variation of the load factor defining LS3 for the two sets of models and the four intervals associated to the four vulnerability classes (A, B, C and D). Although the range of variation for the *RE1F* set of models is wider, both sets of models lead to a very similar definition of classes. The only difference occurs in the case of irregular stone masonry buildings, which belong to vulnerability class C for the *RE1F* set, whereas it falls into vulnerability class D for the *RE2Fd1* set. Since the most unfavorable class is always considered, irregular stone masonry buildings are finally considered within class D.

Table 4.8 shows the final classification proposed for P3. The classification is made according to the variation of the type of material applied to build the walls, which is associated to a range of material properties. Therefore, the table provides the range of values of mechanical properties

that delimits each seismic vulnerability class. These quantitative ranges can be useful in case that an experimental campaign can also be performed along with the survey or if quantitative data is available. It is worth highlighting that, during this sensitivity analysis, it was noted that the variation of the Young's modulus (E) led to the highest differences in terms of maximum capacity of the building. Thus, if this value of the material property is known, it may provide relevant information about the seismic performance of a building. Nevertheless, a qualitative description of the type of material belonging to each seismic vulnerability class is also provided, similarly to what is available in other classifications from other vulnerability index methods (Benedetti and Petrini 1984; Vicente 2008; Ferreira 2009; Shakya 2014). This description is particularly important when only data based on visual inspection is available.

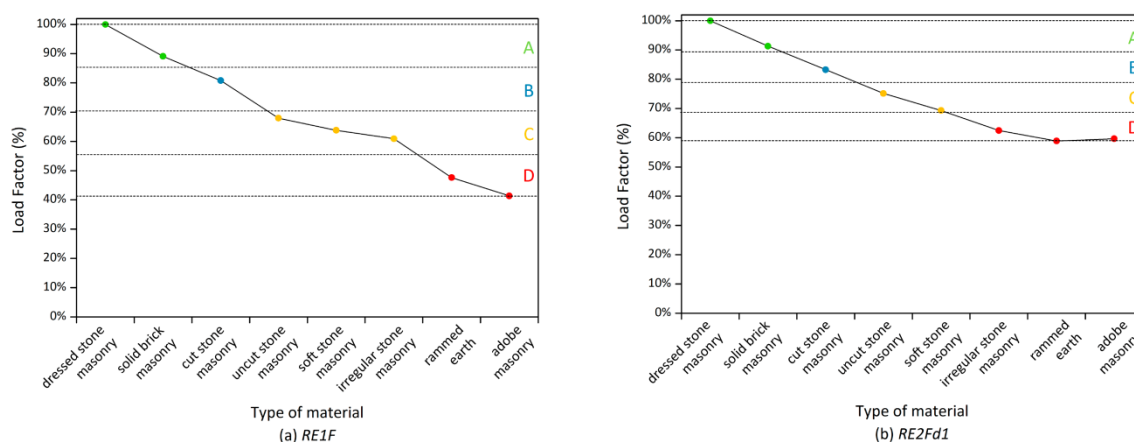


Figure 4.20: Variation of the load factor leading to the attainment of the maximum resistance (LS3) for the two sets of models evaluated: (a) $RE1F$; and (b) $RE2Fd1$

Table 4.8: Vulnerability classes proposed according to the type of material

P3. Type of material				
Class	Description	Reference material properties		
		E (MPa)	f_c (MPa)	f_t (MPa)
A	Stone masonry consisting of well-cut homogeneous units in terms of material and dimensions with parallelepiped shape. Carefully worked horizontal courses with not-aligned mortar head joints. The mortar has good quality and properly fills vertical and horizontal joints. Proper transversal connection among wall leaves using through-stones or stones or brick bands crossing the entire wall thickness. Brick masonry with well-arranged vertical and horizontal joints and good quality mortar	2000-3000	2-4	0.1-0.6
B	Non-homogeneous stone masonry in terms of materials and dimensions but well-arranged longitudinally and transversally with generally respected horizontal courses, not-aligned mortar head joints and good quality mortar. Proper transversal connection among the wall leaves using through-stones or stone or brick bands crossing the entire wall thickness. Brick masonry with well-arranged joints and average quality mortar	1500-2000	1.5-2	0.1-0.4
C	Coarsely carved stone masonry irregularly shaped with poor arrangement of the stones and weak or average quality mortar. Few or no transversal connection elements. The core of multiple-leaf walls has a reasonably consistency.	1000-1500	1-1.5	0.05-0.3
D	Irregular not worked stone masonry of low quality, with not respected horizontal courses or aligned mortar head joints. Poor quality mortar. There are no transversal connection elements. Multi-leaf masonry with partially unstable empty core showing voids. Adobe masonry and rammed earth walls are also included within this class	150-1000	0.6-1.5	0.05-0.2

4.6. Seismic vulnerability classes according to the wall-to-wall connections (P4)

Three reference models with varying number of floors, type of diaphragm and distribution of wall openings were prepared for the analysis of the influence of P4 (Figure 4.21): (a) one-floor rammed earth building with flexible diaphragm, 0.5 m thick walls and reduced number of wall openings (*RE1F*); (b) two-floor rammed earth building with flexible diaphragm, 0.5 m thick walls and high number of wall openings (*RE2F*); and (c) two-floor rammed earth building with rigid diaphragm, 0.5 m thick walls and high number of wall openings (*RE2Fd1*). The one-floor model walls are 3 m high and the maximum wall span is 7 m. The in-plan area is 15.5x8.5 m². The ground floor walls of the two-floor models are 3 m high, while the upper floor walls are 2.6 m high. The maximum wall span is 7 m and the in-plan area is 8x5.5 m². In all three cases, the roof load is modelled as distributed load along the walls. The *RE1F* and *RE2F* sets of models were analyzed in the direction perpendicular to the walls with the maximum wall span (Y), in order to understand the influence of the material when the building is prone to fail out-of-plane. The *RE2Fd1* set of models was analyzed in the direction parallel to the walls with openings (X) to understand the influence of the material when the building is prone to develop in-plane resisting mechanisms.

In order to assess the influence of the quality of the wall-to-wall connections on the seismic behavior of vernacular buildings, the mechanical properties of the rammed earth walls at the corners were progressively reduced. This intends to simulate increasingly weaker connections that are more prone to fail, allowing the walls to behave independently from each other. Thus, a ratio (*c*) is defined that simulates the integrity of the wall-to-wall connections. This ratio is expressed in terms of percentage of the reference mechanical properties adopted for the rammed earth wall that were presented in Chapter 3 (Table 3.3). It ranges from 100% (no reduction), simulating a full workmanlike connection between orthogonal walls to 10%, simulating barely non-existent or highly degraded wall-to-wall connections. Figure 4.21 shows the three reference models constructed, marking the elements with reduced material properties in red. Table 4.9 presents a summary of the 18 models constructed with the variations of the *c* ratio assumed.

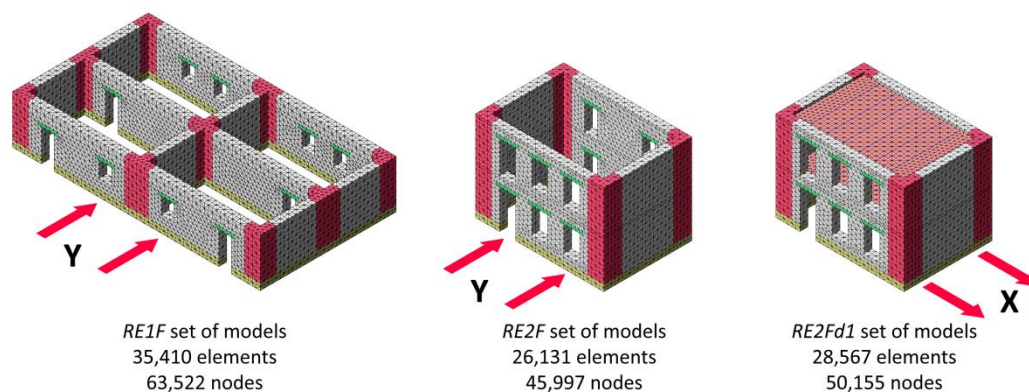


Figure 4.21: Numerical models built in order to assess the influence of the quality of the wall-to-wall connections on the seismic behavior of vernacular buildings

Table 4.9: Summary of the 18 different models built in order to assess the influence of the quality of the wall-to-wall connections on the seismic behavior of vernacular buildings

Set of models	c (%)					
	100	80	60	40	20	10
<i>RE1F</i>	X (Ref)	X	X	X	X	X
<i>RE2F</i>	X (Ref)	X	X	X	X	X
<i>RE2Fd1</i>	X (Ref)	X	X	X	X	X

4.6.1. Variations on damage patterns and failure mechanisms

The most representative failure mechanisms obtained for the three sets of models analyzed are shown in Figure 4.22. The models from the *RE1F* and *RE2F* sets, which disregard the diaphragm effect, showed clear out-of-plane failure modes. When the integrity of the wall-to-wall connections is not compromised and the mechanical properties of the corner elements are not reduced, the collapse of the building is driven by a combination of: (a) the out-of-plane bending failure of the walls, characterized by diagonal and vertical cracks at the mid-span of the wall; and (b) the failure at the connection between perpendicular walls, showing vertical cracks at the wall intersections and extensive cracking at the base (Figure 4.22a,e). When the mechanical properties of the corner elements are highly reduced, the damage concentrates at the connection between perpendicular walls, resulting in their separation and subsequent overturning. In this case, the out-of-plane bending damage at the center of the wall completely disappears, particularly in the *RE1F* model, see Figure 4.22d,h.

There are also significant variations in the failure mode of the two-floor models with rigid diaphragm when reducing the quality of the wall-to-wall connections. The failure mode for all the models from the set is mainly determined by the activation of in-plane resisting mechanisms of the walls parallel to the seismic load (Figure 4.22i,j). Nevertheless, when the properties at the connections are highly reduced, the importance of the out-of-plane resisting mechanism becomes greater. In this case, the crack patterns corresponding to the limit state close to the collapse of the building also developed at the connection between perpendicular walls (Figure 4.22l). There is also important damage occurring at the mid-height of the exterior upper floor wall perpendicular to the loading direction. This damage is related to the wall bulging due to out-of-plane bending. While the lateral bounds are not effective restraining the wall out-of-plane movement, the upper and lower bounds represented by the diaphragms effectively prevent the global overturning of the wall. This is a common situation in masonry buildings.

4.6.2. Building of capacity curves and analysis of load factor variations

The four-linear capacity curves derived from the pushover curves obtained in the parametric analysis are shown in Figure 4.23, grouped by set of models. The three sets clearly show the variation in the capacity of the building when reducing the mechanical properties of the elements

at the connections between perpendicular walls. As it could be expected, the buildings where the diaphragms are not modelled appear to be slightly more sensitive to the variations in the quality of the wall-to-wall connections. Since a poor wall-to-wall connection mainly anticipates the out-of-plane failure of the wall and facilitates its global overturning, those buildings whose seismic response is more dependent on the out-of-plane resisting mechanisms of the walls are definitely more affected by variations in the c ratio.

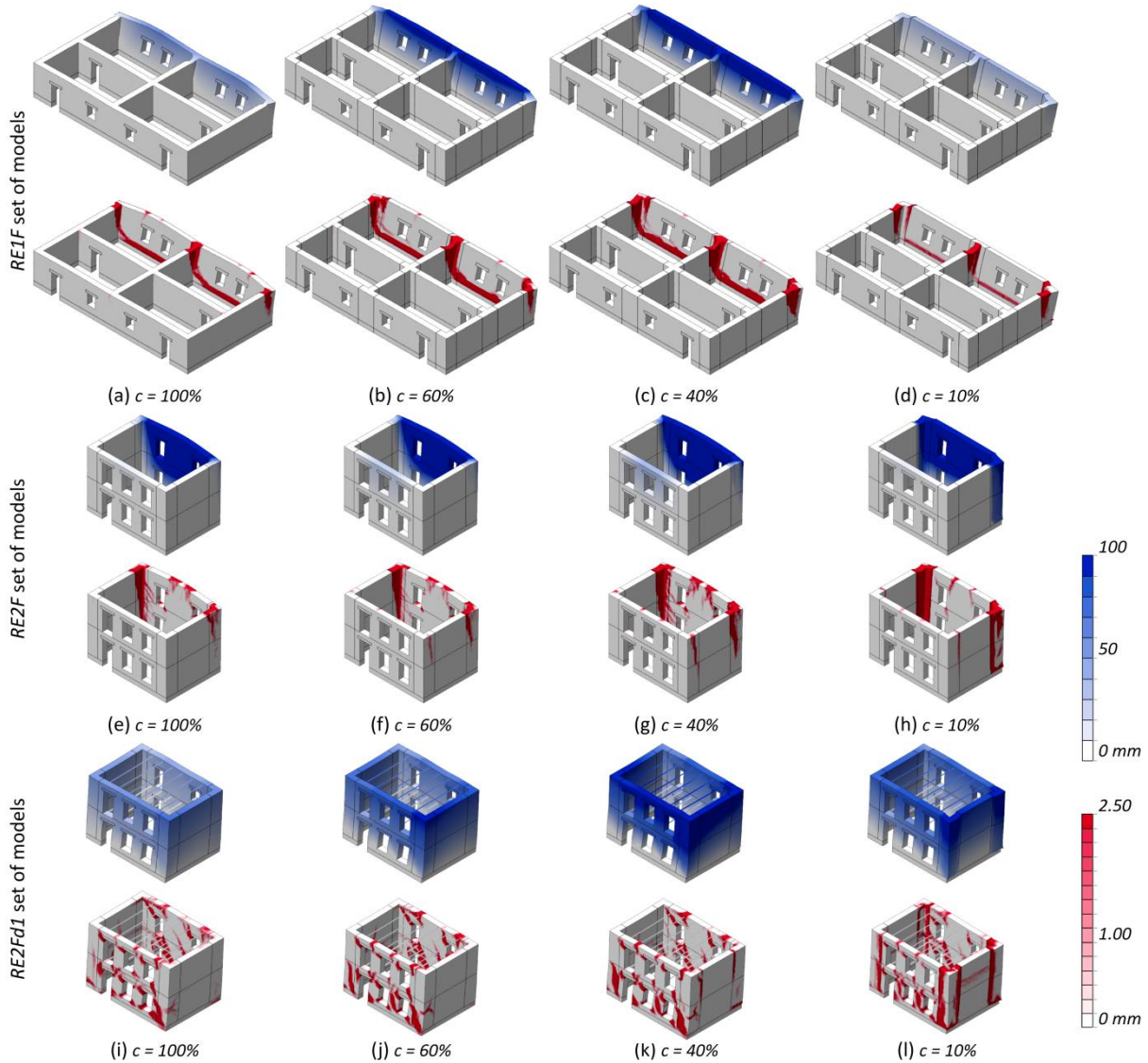


Figure 4.22: Representative failure modes at ultimate limit state (LS4) obtained for several buildings with varying quality of the wall-to-wall connection within each of the three sets of models analyzed: (blue) maximum total displacements; and (red) crack pattern (crack width scale)

There are no such significant variations in terms of ductility or initial stiffness for any of the three sets evaluated. When comparing the two sets of two-floor buildings, the maximum capacity of the buildings with rigid diaphragms is significantly higher than the capacity of the buildings with no diaphragms and unrestrained walls. However, the latter show a more fragile behavior,

which can be associated to the predominance of in-plane shear resisting mechanisms observed in Figure 4.22i-l. Nevertheless, this type of behavior is not altered when varying c .

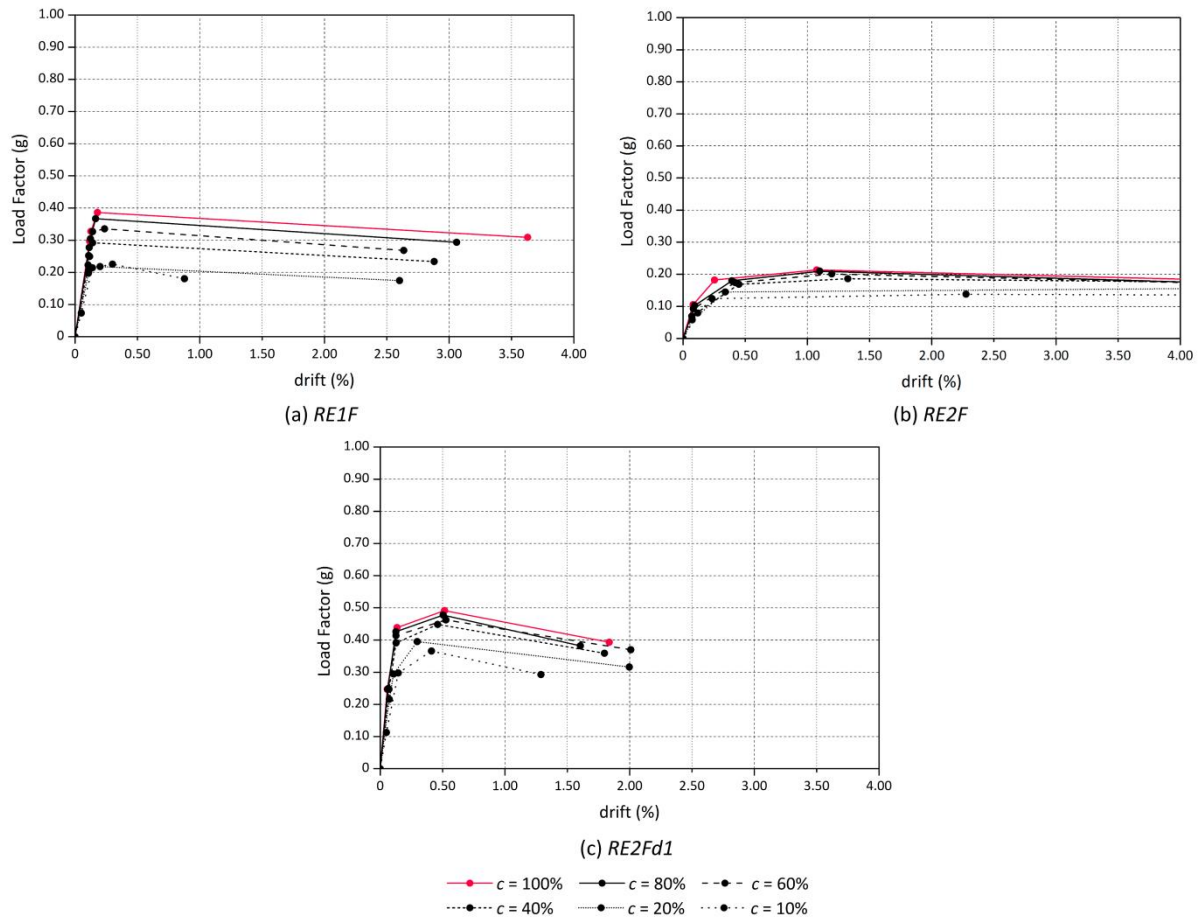


Figure 4.23: Four-linear capacity curves for the three sets of models: (a) *RE1F*; (b) *RE2F*; and (c) *RE2Fd1*

The variations of the load factors defining each limit state are shown in Figure 4.24, grouped by set of models. For the three sets, the reference models that keep the integrity of the material properties at the corner elements ($c = 100\%$) showed the maximum capacity and were used for the normalization. Results show the clear decreasing trend of the normalized load factors when reducing the quality of the wall-to-wall connection in the three sets. However, the two sets of models considering no diaphragm effect show greater variations. With respect to the one-floor model, there is no variation in the maximum capacity of the building between the model with $c = 20\%$ and the model with $c = 10\%$. This means that for such level of reduction of the material properties, the walls are almost completely unrestrained and behave independently, essentially as a cantilever. The highest variations for the three sets of models occur for the load factor defining LS1. This can be explained by the fact that the onset of cracking is very sensitive to the reduction of the material properties at the connection. For poor wall-to-wall connections, such as the ones simulated by the models with $c = 10\%$, the separation of the walls, which in this case is represented by the cracking, is likely to occur for low values of horizontal load.

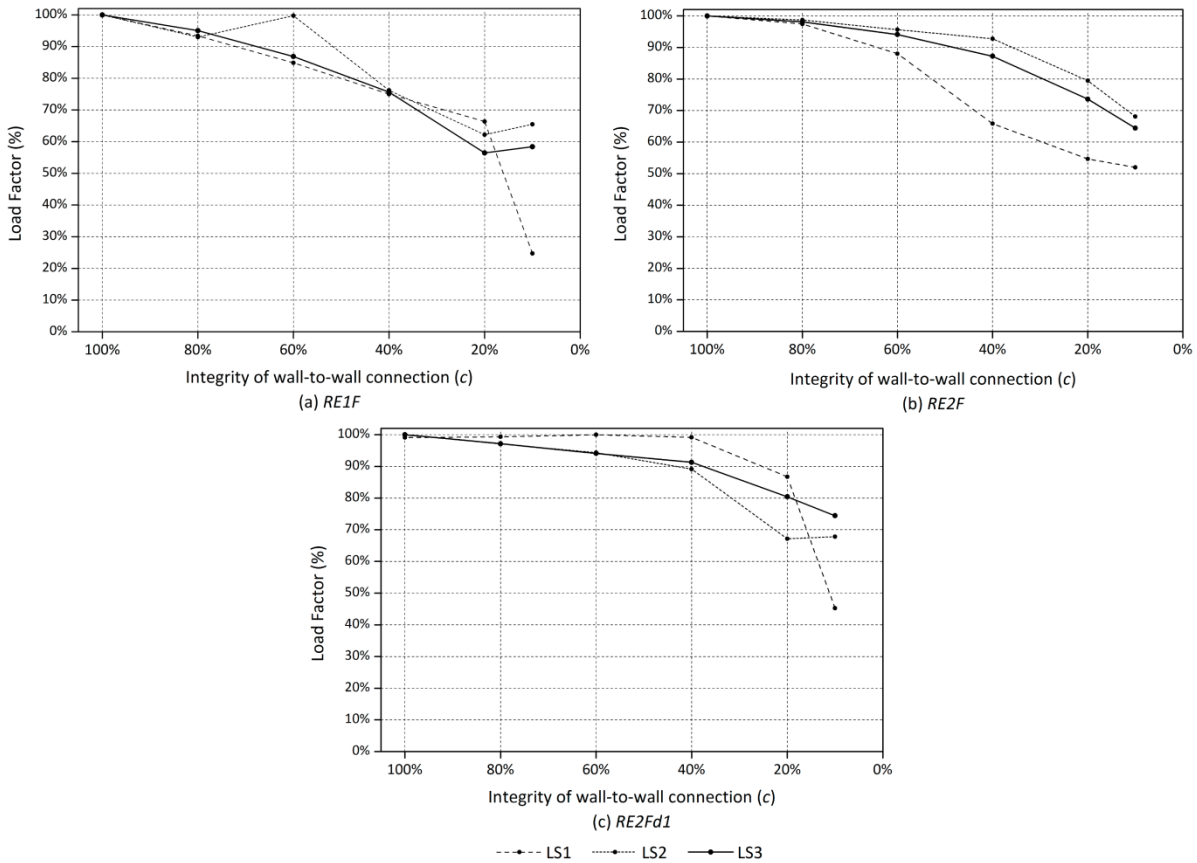


Figure 4.24: Load factor variations for each LS for the three sets of models: (a) *RE1F*; (b) *RE2F*; and (c) *RE2Fd1*

4.6.3. Definition of seismic vulnerability classes

The four seismic vulnerability classes are defined according to the variation of the load factor corresponding to the attainment of LS3. Figure 4.25 shows the variation of the load factor defining LS3 for the three sets of models and the four intervals associated to the four vulnerability classes (A, B, C and D). The difference in terms of range of variation between the *RE2Fd1* set of models and the two sets of models considering no diaphragm effect is evident and there are some discrepancies in the vulnerability classes obtained for the three sets, particularly with the models with $c = 60\%$ and $c = 40\%$. These differences in the definition of the classes were again solved by considering the most unfavorable class is considered. Thus, the buildings with $c = 60\%$ were considered as class B and the buildings with $c = 40\%$ as class C.

The final classification proposed for P4 is shown in Table 4.10. The classification is made according to the reduction of the c ratio that defines the integrity of the wall-to-wall connection and intends to simulate different quality levels of the wall-to-wall connections. Thus, a qualitative description is assigned to each vulnerability level. It should be mentioned that previous classifications from other vulnerability index methods have also provided a qualitative description for this parameter, which is sometimes referred as organization of the vertical

structural system (Benedetti and Petrini 1984) or type of resisting system (Vicente 2008; Shakya 2014). It is also noted that this is necessary for the survey, since it is the only way of characterizing the wall-to-wall connection by means of visual inspection.

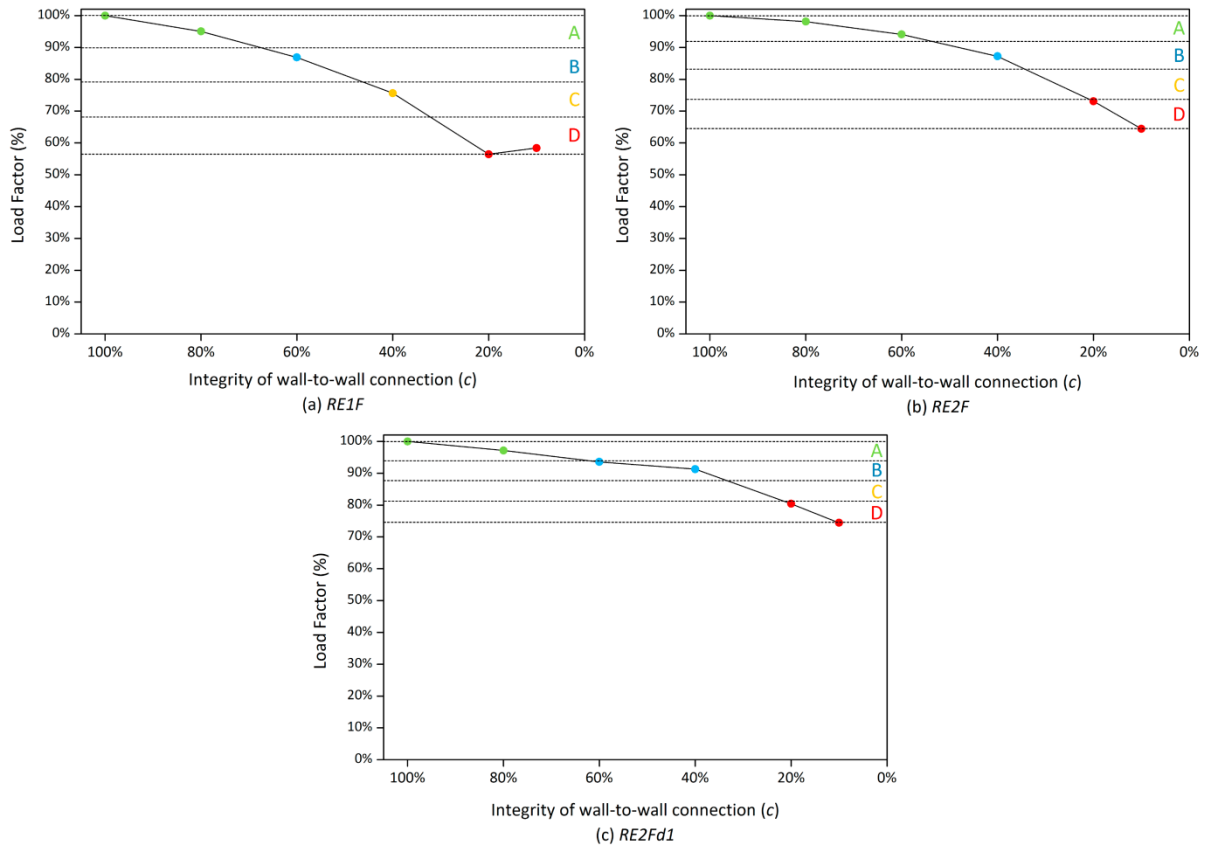


Figure 4.25: Variation of the load factor leading to the attainment of the maximum capacity (LS3) for the three sets of models evaluated: (a) RE1F; (b) RE2F; and (c) RE2Fd1

Table 4.10: Vulnerability classes proposed according to the wall-to-wall connections

P4. Wall-to-wall connections	
Class	Description
A	All wall-to-wall connections are workmanlike built. There is no weakening signs or construction deficiencies. In case of masonry buildings, there is a good interlocking between the masonry units at the corners. In case of earthen buildings, there are no vertical joints at the corners
B	Some wall-to-wall connections show either construction deficiencies, such as lack of efficient interlocking of the masonry units in case of masonry buildings or vertical joints in case of earthen construction, or weakening signs
C	Many wall-to-wall connections are deficient or degraded because of construction deficiencies, such as vertical joints, and/or weakening signs, such as cracks or detachments
D	Most wall-to-wall connections are barely non-existent because of poor construction practices or are highly degraded with important signs of separation and vertical cracks

4.7. Seismic vulnerability classes according to the horizontal diaphragms (P5)

Three reference models with varying number of floors and walls material were prepared for the analysis of the influence of P5: (a) one-floor rammed earth building (RE1F); (b) two-floor rammed

earth building (*RE2F*); and (c) three-floor stone masonry building (*STM3F*). The walls of the reference model are 0.5 m thick. The walls of the one-floor models are 3.6 m high and the maximum wall span is 7 m. The in-plan area is 15.5x8.5 m². The ground floor walls of the two-floor models are 3 m high, while the upper floor walls are 2.6 m high. The maximum wall span is 7 m and the in-plan area is 8x10.5 m². The floor load of the three buildings is simply modeled as distributed load along the walls.

4.7.1. Modelling the variations on the type of horizontal diaphragm

The reference models consider no diaphragm effect (Figure 4.26a). Thus, the possible beneficial effects of transferring the inertial forces among the orthogonal walls are not taken into consideration. This is a conservative approach but it is relevant because vernacular buildings commonly present flexible diaphragms and weak diaphragm-to-wall connections. As a result, walls are free to vibrate independently, which typically results in local out-of-plane mechanisms. The variations introduced in the models intend to compare the response of structures presenting different types of horizontal diaphragm with the response of the reference model, which represents the worst case scenario in which a null influence of the diaphragm effect is assumed. As previously discussed in Chapter 3 (Figure 3.11), the variations that are considered for this parameter are based on the characteristics of the horizontal diaphragm assumed to be influential on the seismic performance of vernacular structures: (a) beams-to-wall connection (k_c); (b) beams stiffness (k_b); (c) diaphragm stiffness (k_d); and (d) diaphragm-to-wall connection (k_{dc}).

4.7.1.1 Beams-to-wall connection (k_c)

Firstly, only the timber beams are modelled, assuming that the diaphragm cross board sheathing is so flexible that is not able to redistribute the loads among the walls and has no structural role (Figure 4.26b). It is noted that the beams are simulated using the approach discussed for the analysis of P2 and adopting the material properties of the timber shown in Chapter 3 (Table 3.3). In order to assess the influence of the beams-to-wall connection (k_c), different levels of embedment of the beam within the wall were simulated, based on the traditional constructive solutions presented in Chapter 2 (Figure 2.10). Variations on the beams-to-wall connection thus represent only specific constructive details of the numerical model at the connections between the beams and the walls elements. The following different conditions at the connection were considered:

- k_{c1} : The timber beams are connected with the walls, but there is no embedment within the wall. It simulates a beam supported by a timber plate or stone bracket and fixed. The connection provides equal translation of degrees of freedom between the beam and the wall. It should be noted that the connection between the beam element and the 3D solid element of the wall can only take place at one node, which is not realistic. An auxiliary horizontal beam element is simulated at this connection to redistribute the load among the surrounding nodes and avoid

extremely local effects. This allows also simulating more realistically that the connection does not take place at one node, but at an area equal to the cross section of the timber beam. This auxiliary element is used for the rest of the models where the timber beams are simulated.

- *kc2-4*: The timber beams are partially embedded within the walls with different levels of embedment going through the 25%, 50% and 75% of the wall thickness. It should be mentioned that full connection between the embedded beam elements and the wall 3D solid elements is considered for the models.

- *kc5*: The timber beams go through the whole thickness of the wall.

- *kc6*: The timber beams pierce the walls through the whole thickness and are anchored at the external part, simulating a traditional wooden wedge.

4.7.1.2 Beams stiffness (k_b)

In order to assess the influence of the stiffness of the beams (k_b), the Young's modulus adopted for the timber beams (E_b) was divided and multiplied by two and five. The model that assumes that the timber beams are resting on the whole width of the wall (*kc5*) is taken as the reference model and considers the reference material properties (Table 3.3). Four models are additionally built for the comparison: (a) $0.2E_b$ (*kc5b2*); (b) $0.5E_b$ (*kc5b3*); (c) $2E_b$ (*kc5b4*); and (d) $5E_b$ (*kc5b5*).

4.7.1.3 Diaphragm stiffness (k_d)

In a second step, the structural influence of the cross-board sheathing was taken into account and modelled (Figure 4.26c). The cross-board sheathing is simulated using the approach discussed for the analysis of P2 and adopting the same material properties: an elasticity modulus (E_d) of 200 MPa and a Poisson's ratio of 0.3. These values are based on typical values observed in the literature where the diaphragm is modelled in a similar way. For example, Mendes and Lourenço (2015) proposed a value of E_d of 160 MPa after calibration of a numerical model using the results of an experimental shaking table test. Nevertheless, these values are also in agreement with other values observed in the literature, where E_d typically lies within the range 80 to 350 MPa (Whitney and Agrawal 2015). It should be noted that the characterization of the in-plane stiffness of typical vernacular timber diaphragms is complex, as it depends on many factors resulting from the contributions from the nails and the timber floorboard elements (Brignola et al. 2012; Wilson et al. 2013). Here, the in-plane behavior is simply defined by the assigned elastic material properties. Also, the characteristic orthotropic behavior of timber diaphragms given by the direction of the beams (Giongo et al. 2014) is partially simulated by modelling the beams independently. That is why an isotropic material is considered for the diaphragm. The beams are initially considered to go through the whole thickness of the wall, using model *kc5* as a reference. The beams and the diaphragm shell elements are considered to be fully connected, sharing

common nodes. The connections between the board sheathing and the walls are also assumed to share all degrees of freedom. These simplifications are intended to reduce the amount of variables under study, while providing an insight of the variability in the seismic performance of the building due to changes in the global stiffness of its diaphragm.

In order to assess the influence of the diaphragm stiffness (k_d), different conditions were simulated. First, since the stiffness of the diaphragm can vary to a great extent, the reference value of the Young's modulus (E_d) was multiplied by five (model *kc5d2*) and divided by five and twenty (models *kc5d3* and *kc5d4* respectively). These variations provide values ranging from diaphragms being essentially rigid to almost totally flexible. Secondly, the in-plane stiffness of the diaphragms was decreased and increased by doubling and halving its thickness (models *kc5d5* and *kc5d6* respectively). Two extra models were also constructed assuming a poor beam-to-wall connection, using model *kc1* as a reference, and varying the diaphragm stiffness: (a) E_d (*kc1d1*); and (b) $0.05E_d$ (*kc1d4*).

4.7.1.4 Diaphragm-to-wall connection (k_{dc})

The low values of Young's modulus used for the study of the influence of the stiffness board sheathing already include indirectly the effect of a poor connection between the diaphragm and the walls (Mendes and Lourenço 2015). The stiffness of the diaphragm-to-wall connection and the diaphragm stiffness can be combined into an equivalent diaphragm stiffness accounting for both contributions (Brignola et al. 2008). Nevertheless, in order to assess independently the influence of the diaphragm-to-wall connection (k_{dc}), new models were constructed assuming an inexistent connection between the cross boards and the walls. The board sheathing was still modeled adopting the same geometry and material properties previously described, but a gap was left between the diaphragm and the walls (Figure 4.26d). This way, the sliding of the diaphragm with respect to the walls that was restrained in the previous models can occur, while the effect of a rigid diaphragm can still be taken into account. This simulates typical traditional constructive solutions, as shown in Chapter 3 (Figure 3.10a). The variations on the diaphragm-to-wall connection thus only involve changes in the model construction. It is noted that, since the beams are modelled, the diaphragm is supported solely by the beams, assuming the full connection between the diaphragm and the beam nodes previously referred.

Four models were prepared assuming this type of diaphragm. The first two models consider a good beam-to-wall connection, with the beams going through the whole thickness of the wall, using model *kc5* as a reference, and varying the diaphragm stiffness: (a) E_d (*kc5d1_kdc0*); and (b) $0.05E_d$ (*kc5d4_kdc0*). The two additional models are prepared assuming a poor beam-to-wall connection, using model *kc1* as a reference, and varying the diaphragm stiffness: (a) E_d (*kc1d1_kdc0*); and (b) $0.05E_d$ (*kc1d4_kdc0*).

4.7.1.5 Summary

Figure 4.26 shows the most representative models constructed. The three sets of models were analyzed in both directions: (1) parallel to the direction of the beams and perpendicular to the walls with the maximum wall span (Y); and (2) perpendicular to the beams direction (X). Both directions were evaluated because significant variations in the failure mode presented by the different models within each set are expected, given the great variations in the characteristics of the diaphragm previously introduced that were simulated. The summary of the 49 models constructed according to the variations previously described is shown in Table 4.11.

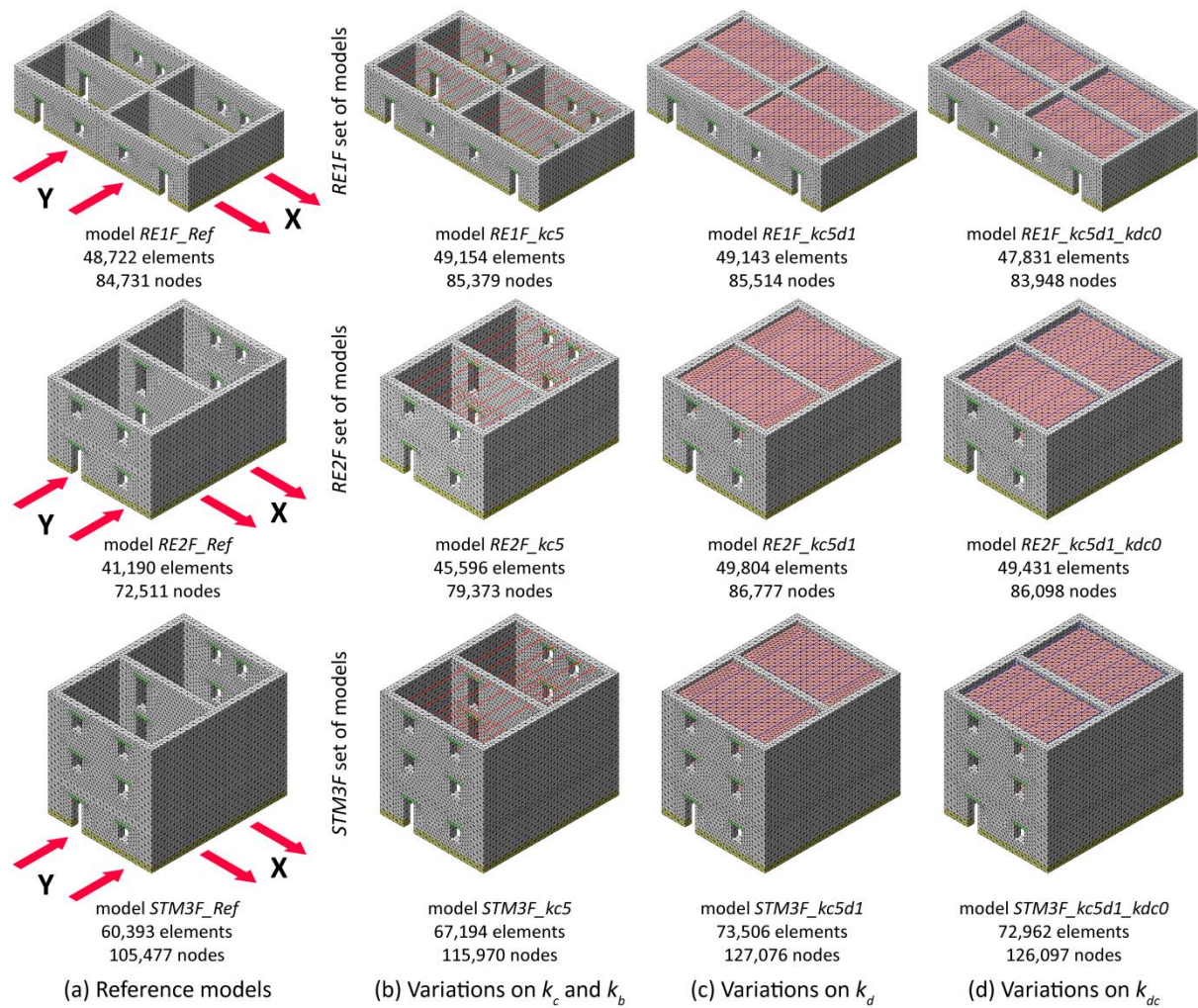


Figure 4.26: Numerical models built in order to assess the influence of the type of horizontal diaphragm on the seismic behavior of vernacular buildings: (a) reference models; (b) examples of variations only considering the timber beams to evaluate the influence of k_c and k_b ; (c) examples of variations also including the cross-board sheathing to evaluate the influence of k_d ; and (d) examples of variations allowing the sliding of the diaphragm with respect to the walls to evaluate the influence of k_{dc}

Table 4.11: Summary of the 49 different models built in order to assess the influence of the type of horizontal diaphragm on the seismic behavior of vernacular buildings

Name	Set of models	Variations																								
		Beams connection (k_c)						Beams stiffness (k_b)					Diaphragm stiffness (k_d)					Diaphragm-to-wall connection (k_{dc})								
		$kc1$	$kc2$	$kc3$	$kc4$	$kc5$	$kc6$	$kb1$	$kb2$	$kb3$	$kb4$	$kb5$	$kd1$	$kd2$	$kd3$	$kd4$	$kd5$	$kd6$	$kdc0$	$kdc1$						
		Variations of beams embedment within the wall						Variation of beams Young's modulus (E_b)					Variation of diaphragm Young's modulus (E_d) and thickness (t_d)													
		0%	25%	50%	75%	100%	100%+ wedge	E_b	$0.2E_b$	$0.5E_b$	$2E_b$	$5E_b$	E_d	t_d	$5E_d$	t_d	$0.2E_d$	t_d	$0.05E_d$	t_d	E_d	$2t_d$	E_d	$0.5t_d$		
Ref	STM3F RE2F RE1F	X	X	X	X	X																			Not modelled	100%
kc1		X						X																	Not modelled	
kc2			X					X																	Not modelled	
kc3				X				X																	Not modelled	
kc4					X			X																	Not modelled	
kc5						X		X																	Not modelled	
kc6							X	X																	Not modelled	
kc5b2								X																	Not modelled	
kc5b3								X																	Not modelled	
kc5b4								X																	Not modelled	
kc5b5								X																	Not modelled	
kc5d1								X																	Not modelled	X
kc5d2								X																	Not modelled	X
kc5d3								X																	Not modelled	X
kc5d4								X																	Not modelled	X
kc5d5								X																	Not modelled	X
kc5d6								X																	Not modelled	X
kc1d1								X																	Not modelled	X
kc1d4								X																	Not modelled	X
kc5d1_kdc0								X																	Not modelled	X
kc5d4_kdc0								X																	Not modelled	X
kc1d1_kdc0								X																	Not modelled	X
kc1d4_kdc0								X																	Not modelled	X

4.7.2. Variations on damage patterns and failure mechanisms

As expected, the variations on the type of horizontal diaphragm significantly affected the failure mode of the building. Within each set of models, buildings presented from clear out-of-plane failure modes, when disregarding the diaphragm effect, to the typical in-plane shear failure of the walls parallel to the seismic load, when showing an effective diaphragm action. The different variations modelled on the buildings also led in some cases to failures driven by a combination of in-plane and out-of-plane resisting mechanisms. A summary of the damage patterns and failure mechanisms modes obtained for the different model is presented in Table 4.12.

Table 4.12: Summary of the failure modes obtained for each model showing different horizontal diaphragms

Failure mode	Models	
	Y direction	X direction
Out-of-plane overturning and bending failure of the exterior wall perpendicular to the seismic load	Ref	Ref kc1 kc5 kc5d4_kdc0 kc1d1_kdc0 kc1d4_kdc0
		kc1 kc2-7 kc5b2-5 kc5d4_kdc0 kc1d1_kdc0 kc1d4_kdc0
Out-of-plane overturning and bending failure of walls perpendicular to the seismic load, collapsing simultaneously	kc5d3-4 kc1d4 kc5d1_kdc0	
Out-of-plane overturning and bending failure of walls perpendicular to the seismic load, collapsing simultaneously. Walls parallel to the seismic load show significant in-plane damage	kc5d1-2 kc5d5-6 kc1d1	kc5d3-4 kc1d4
In-plane failure of the walls parallel to the seismic load. Walls perpendicular to the seismic load show significant out-of-plane damage		kc5d1-2 kc1d1
In-plane failure of the walls parallel to the seismic load		kc5d1_kdc0
Out-of-plane overturning and bending failure of the exterior wall perpendicular to the seismic load. Walls parallel to the seismic load show significant in-plane damage		

The most representative failure mechanisms for the three sets of models analyzed in Y direction are shown in Figure 4.27 in terms of maximum total displacements and crack pattern at the ultimate limit state (LS4). The failure mode of the reference buildings, where the diaphragm is simply modeled as concentrated mass, consists of the out-of-plane bending failure of the exterior walls, which is characterized by extensive cracking at the base, big vertical cracks at the wall intersections, and vertical cracks in the center of the wall (Figure 4.27a,e,i). When beams are modelled, the failure mode involves the simultaneous out-of-plane collapse of all transversal walls (Figure 4.27b,f,j). Modelling the cross-board sheathing with enough in-plane stiffness to transfer the load to the walls parallel to the horizontal load led to a significant change of the failure mode involving the in-plane collapse of the walls parallel to the seismic load, showing the characteristic diagonal shear cracking (Figure 4.27c,g,k). When the diaphragm is flexible or the diaphragm is poorly connected to the walls, the main failure mode consists again of the walls collapsing out-of-plane simultaneously, even though relevant in-plane damage also takes place (Figure 4.27d,h,l).

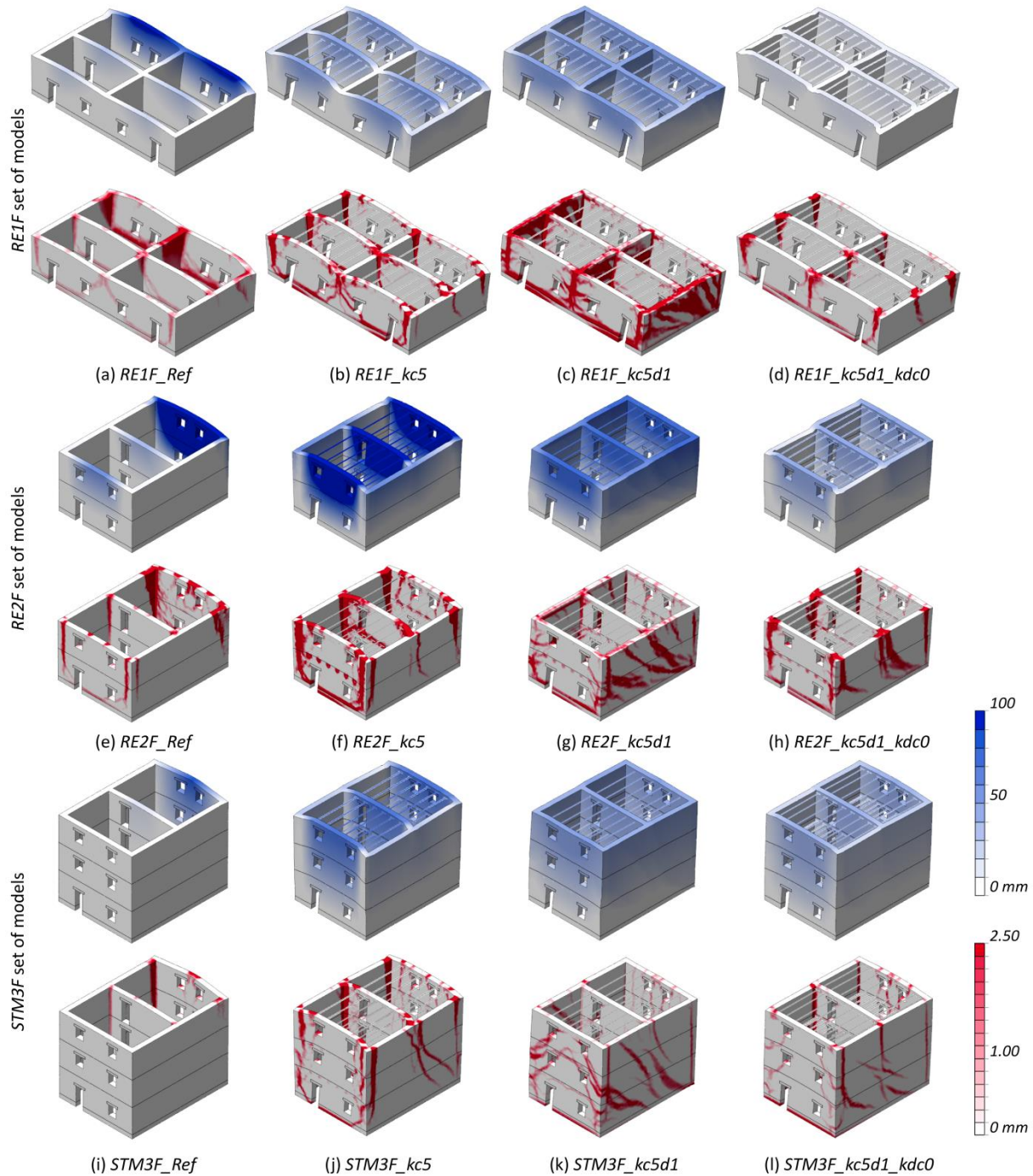


Figure 4.27: Representative failure modes at ultimate limit state (LS4) obtained for several buildings with varying type of horizontal diaphragm within each of the three sets of models analyzed in Y direction: (blue) maximum total displacements; and (red) crack pattern (crack width scale)

Figure 4.28 shows the most representative failure mechanisms for the three sets of models analyzed in X direction. The failure mode obtained for the reference model is led by the out-of-plane overturning of the exterior walls, characterized by vertical cracks at the connection and the horizontal crack at the base of the wall (Figure 4.28a,e,i). Significant vertical cracks at the mid-span of the wall also show out-of-plane bending damage. The three-floor stone masonry model

shows significant in-plane shear damage even if the diaphragms are not modelled (Figure 4.28i). This exemplifies the influence of the material properties in defining the failure mode of the building. The improved material properties of the stone masonry, when compared with the other materials, together with the good connection considered between perpendicular walls, activate the resisting mechanism that involves the in-plane walls in the seismic response of the building.

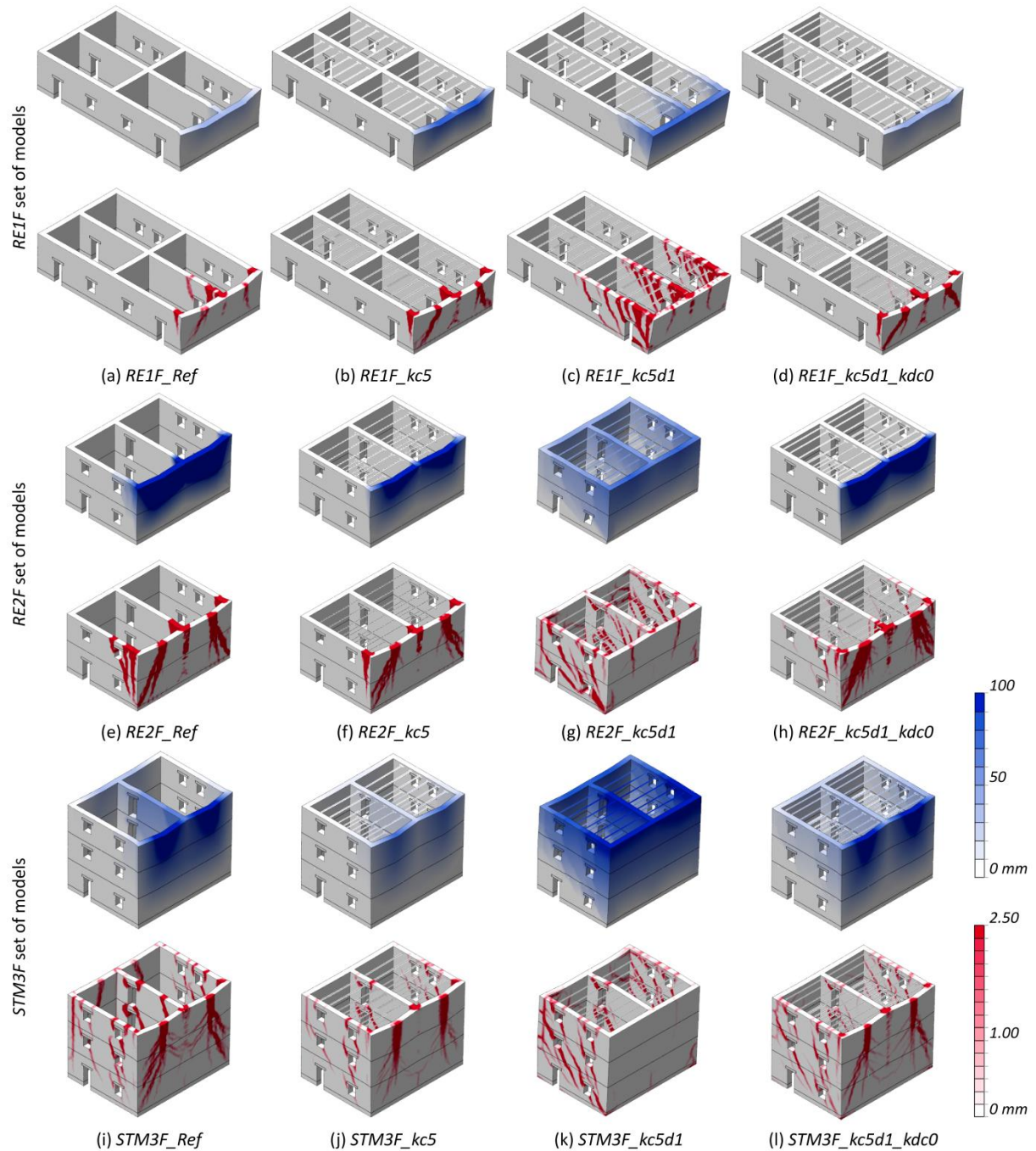


Figure 4.28: Representative failure modes at ultimate limit state (LS4) obtained for several buildings with varying type of horizontal diaphragm within each of the three sets of models analyzed in X direction: (blue) maximum total displacements; and (red) crack pattern (crack width scale)

Since the loading direction is perpendicular to the beams, their influence is almost negligible and they do not have the beneficial coupling action observed in the transversal direction. The failure mode obtained for the models where only the beams are modelled does not vary and is governed by the out-of-plane failure of the exterior walls perpendicular to the seismic load (Figure 4.28b,f,j). Modelling the whole diaphragm with enough stiffness to transfer the load to the walls parallel to the seismic load transforms the failure mode into a very clear in-plane failure characterized by diagonal cracking in the direction of the wall length, arising from the edges of the openings (Figure 4.28c,g,k). In this case, the damage at the connection between perpendicular walls is highly reduced and a greater number of walls are involved in the seismic response. When the diaphragms are flexible or poorly connected to the walls, the main failure mode consists again of the out-of-plane overturning of the walls perpendicular to the seismic load (Figure 4.28d,h,l). Nevertheless, the diaphragms partially activate the walls parallel to the seismic load and relevant in-plane damage can be observed, particularly in the models with two and three floors.

4.7.3. Building of capacity curves and analysis of load factor variations

The four-linear curves derived for the pushover analysis in Y direction for the one-floor rammed earth building are shown in Figure 4.29. As previously discussed in Chapter 3, the four-linear curves are built using the node showing the highest displacements. However, it should be noted that this node varies according to the collapse mechanism obtained, which differs when the building present different types of horizontal diaphragms (Table 4.12). Thus, the curves are representative of the global structural behavior of the different buildings subjected to horizontal loading, not individual structural elements composing the buildings.

Figure 4.29 shows the results in Y direction for the *REIF* set of models, which evaluates independently the influence of the four variations defined for horizontal timber diaphragms: (a) influence of the beams-to-wall connection (k_c); (b) influence of the beams stiffness (k_b); (c) influence of the diaphragm stiffness (k_d) according to the variation of the diaphragm Young's modulus (E_d); (d) influence of the diaphragm stiffness (k_d) according to the variation of the diaphragm thickness (t_d); and (e) influence of the diaphragm-to-wall connection for different levels of beams-to-wall connection and variable diaphragm stiffness.

Results clearly show the influence of the different levels of beams-to-wall connection on the seismic resistance of the building (Figure 4.29a). Considering proper connections of the beams going through the whole section of the wall led to an increase of approximately 75% on the capacity of the building with respect to the model without effective beams-to-wall connections. By increasing its embedment length, the beams manage to activate a bigger portion of the wall and are able to take greater axial force before causing the tensile failure of the portion of earthen wall surrounding the connection with the beam. This is known as cone failure. On the other hand, the variation of the stiffness of the beams barely varies the behavior (Figure 4.29b).

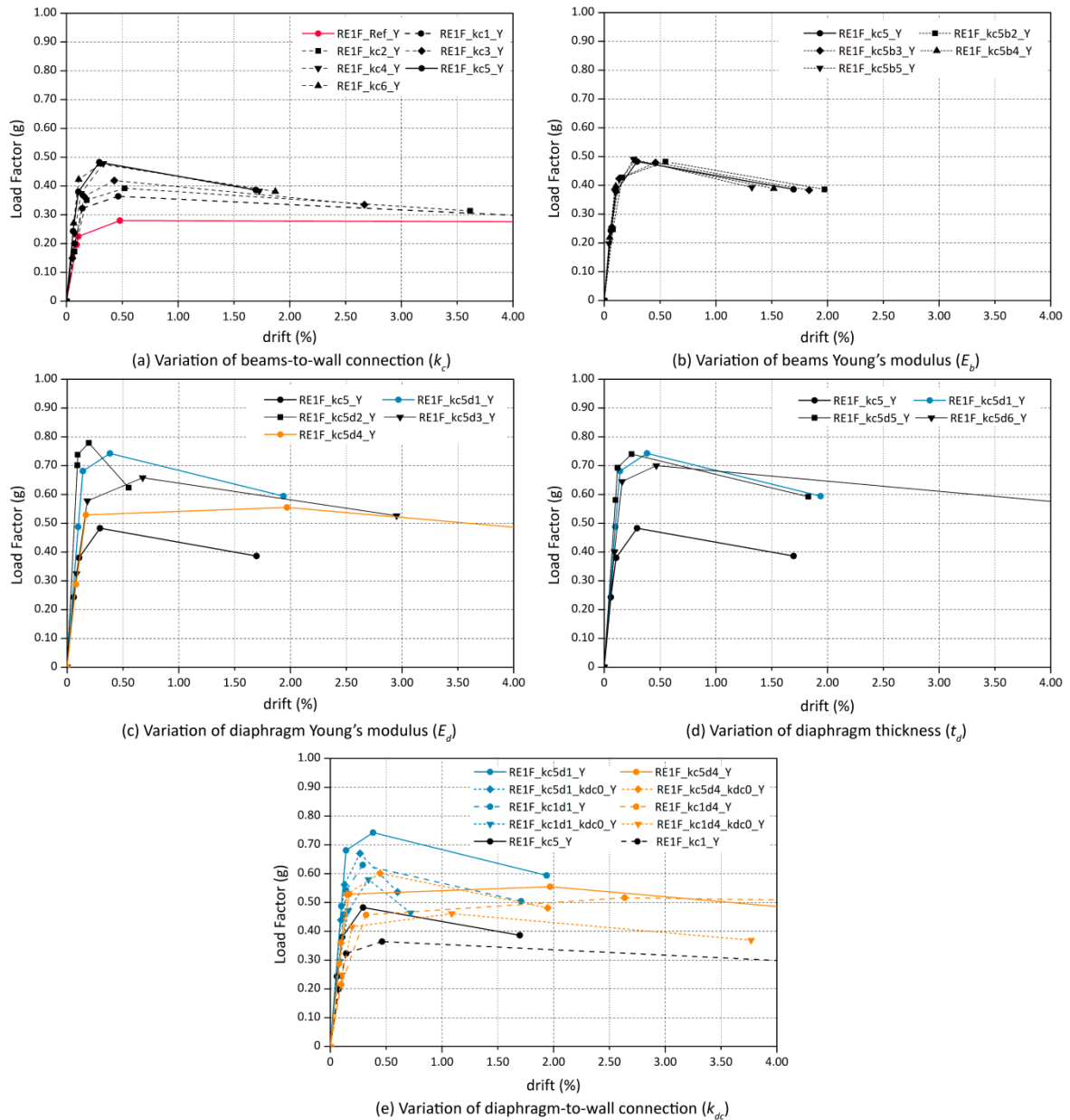


Figure 4.29: Four-linear capacity curves for the RE1F set of models analyzed in Y direction

As expected, the diaphragm action that is achieved by modelling also the cross-boards has a great influence on the seismic behavior of the buildings. The presence of a rigid diaphragm almost doubles the capacity of the model in which only the timber beams are considered. Figure 4.29c shows the sensitivity of the building to the variations in the diaphragm stiffness in terms of E_d . Even if the simulated diaphragm is very flexible, the capacity of the building increases with respect to the models that disregard the diaphragm action because the walls parallel to the horizontal loading are also activated in the response and show significant in-plane damage. On the other hand, the variation of t_d has a lesser influence on the building response (Figure 4.29d), which is attributed to a lower increment and decrease of the diaphragm stiffness. Finally, Figure

4.29e shows the decreasing capacity of the structure when the level of connection between the structural elements is compromised. For example, the model with a rigid diaphragm well-connected to the walls, but beams poorly coupled with the walls presents a lower capacity than the model presenting a well-connected rigid diaphragm. If, additionally, the sheathing is poorly connected to the walls, the seismic capacity of the structure is further reduced.

Figure 4.30 shows the results of the parametric analysis grouped by set of models and loading direction (X and Y). For the analysis in Y direction, the three set of models show similar patterns of variation, even in terms of percentage of variation. The maximum difference in the maximum capacity between the reference model and the model presenting a rigid diaphragm well-connected to the walls (*kc5d2*) is almost the same for the three models and ranges between 30% and 40%. There are no significant variations in the seismic response of the buildings in terms of initial stiffness, but the variation is noticeable in terms of ductility. The diaphragmatic action does not only manage to increase the capacity of the building, but also increase their ductility. This is achieved by involving more structural elements in the seismic response. The buildings are thus able to suffer larger deformations before reaching the collapse, showing a more widespread damage, see Figure 4.27c,g.

With respect to the X direction, results confirm that the beam-to-wall connection has almost no influence when subjected to lateral loading perpendicular to the beams. Results barely vary for all models where the diaphragm is not modeled or the diaphragm-to-wall connection is considered to be negligible. As shown in Table 4.12, the failure mode does not vary between them and always consisted of the out-of-plane failure of the exterior wall perpendicular to the seismic load. However, the influence of modeling the diaphragm sheathing is still critical. For example, the maximum capacity of model *RE2F_kc5d2* in the longitudinal direction more than doubles the capacity of model *RE2F_kc5*, in which only the timber beams are considered. Figure 4.30b and d show that the variation of the stiffness of the diaphragm results in significant differences in the seismic capacity in terms of load factor. The response of the model with rigid or flexible diaphragm well-connected to the walls is basically the same if the beams are properly or poorly coupled with the walls, see models *RE2F_kc5d1* and *RE2F_kc1d1*. This confirms again that the influence of the beams-to-wall connection is almost zero for the analysis in this direction. In the case of the three-floor stone masonry model, the influence of the diaphragm stiffness on the seismic behavior of the building is lower when compared to the other two models. This can be explained by the ability of the longitudinal walls to contribute to the seismic resistance of the building developing in-plane resisting mechanisms even when the timber diaphragms are not modeled, as shown in Figure 4.28. This is related with the better material properties assumed for the stone masonry and the full connection considered between perpendicular walls. These characteristics are enough to avoid the premature out-of-plane collapse of the walls and activate the in-plane behavior of the walls in the seismic response of the building.

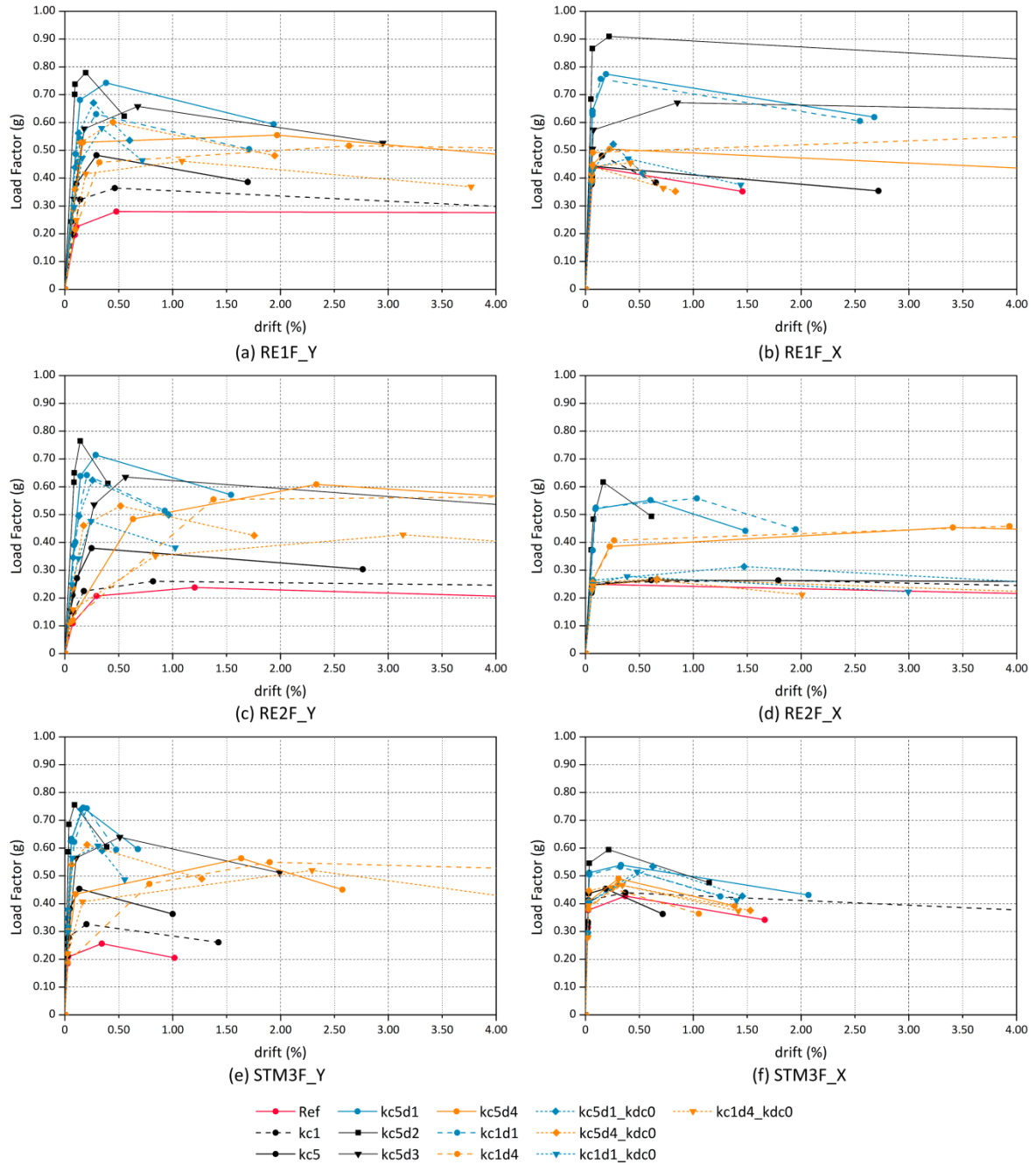


Figure 4.30: Four-linear capacity curves for the three sets of models in both X and Y directions

The variations of the load factors defining each limit state obtained for the three sets of models and the two directions analyzed are shown in Figure 4.31. The variation were normalized using the model presenting the most rigid diaphragm well-connected to the walls (model *kc5d2*), which showed the maximum capacity. The diagrams from the three sets confirm the great influence of the type of horizontal diaphragm on the global seismic behavior of the buildings. They show the decreasing capacity of the building when deviating from this ideal condition in terms of the characteristics of the horizontal diaphragm. However, it is noted that the variations

are notably lower for the load factor defining LS1. The onset of cracking is thus not avoided by the presence of the diaphragm unless this is significantly stiff. Figure 4.31 also confirms that the absence of the beneficial coupling effect of the beams in X direction results in almost the same seismic response for all models presenting a very flexible or a poorly connected diaphragm. Indeed, all models presenting a poor diaphragm-to-wall connection led to similar values of the load factors defining the three different limit states.

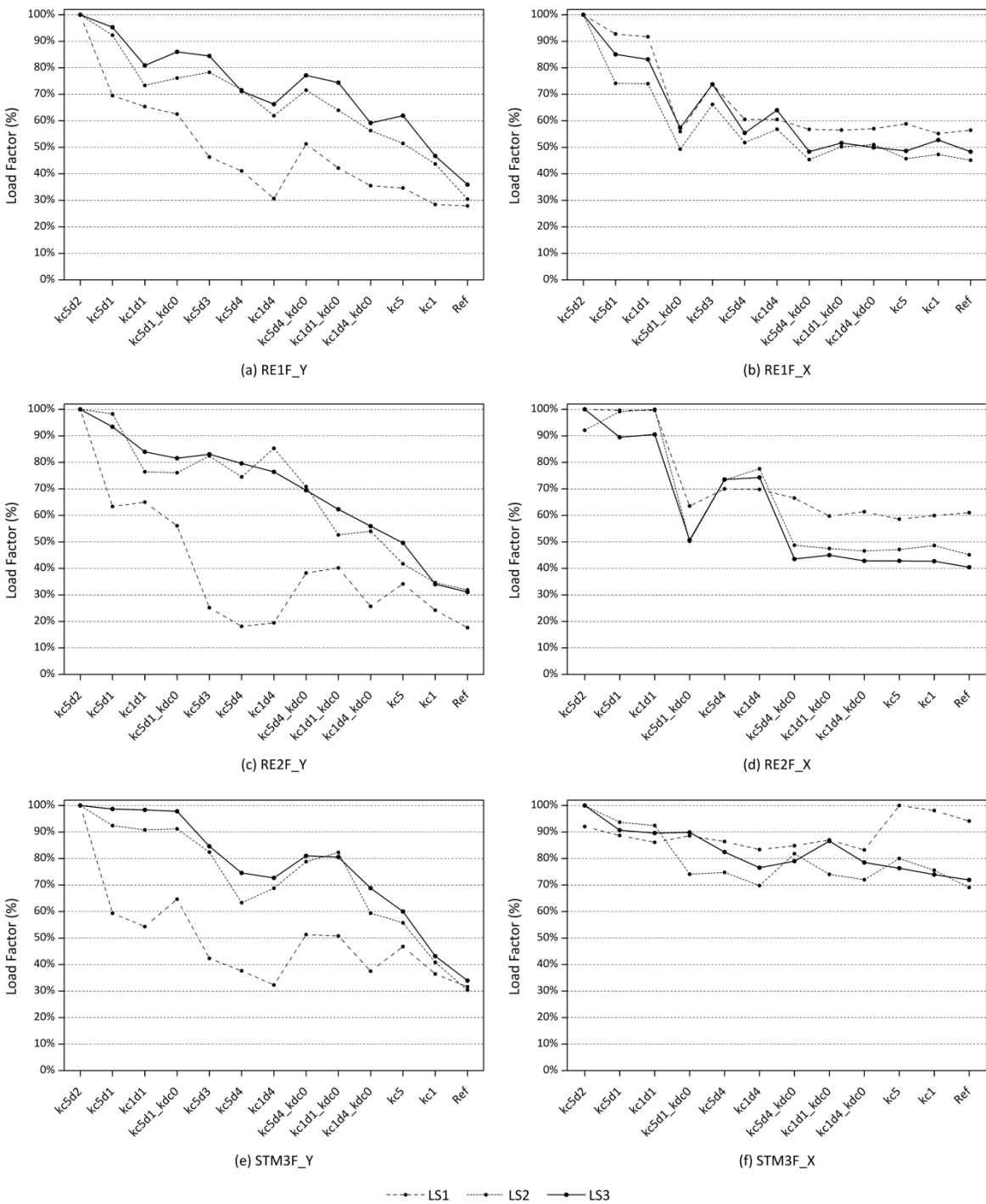


Figure 4.31: Load factor variations for each limit state for the three sets of models in X and Y direction

4.7.4. Definition of seismic vulnerability classes

The four seismic vulnerability classes are defined according to the variation of the load factor corresponding to the attainment of LS3. Figure 4.31 showed that the buildings were significantly more sensitive to the variations on the characteristics of the timber diaphragm when the building was loaded in the Y direction. In addition, the beneficial effect of the constructive characteristics of the diaphragms previously defined, such as the beams coupling effect between parallel walls, was only noticeable when the building was loaded in the direction parallel to the beams (Y). That is why the definition of the vulnerability classes according to the type of diaphragm is based on the results in Y direction. Figure 4.32 shows the variation of the load factor defining LS3 for the three sets of models and the four intervals associated to the four vulnerability classes (A, B, C and D). Even though the range of variation is very similar, the definition of the vulnerability classes for the three sets led to some discrepancies. It is noted that the most unfavorable class was always considered in these cases. For example, model *kc1d1* belongs to vulnerability class A in the *RE2F* and *STM3F* sets of buildings, but to class B in the *RE1F* set. Thus, this type of diaphragm was finally considered as class B. Similar decisions were made for other discrepancies.

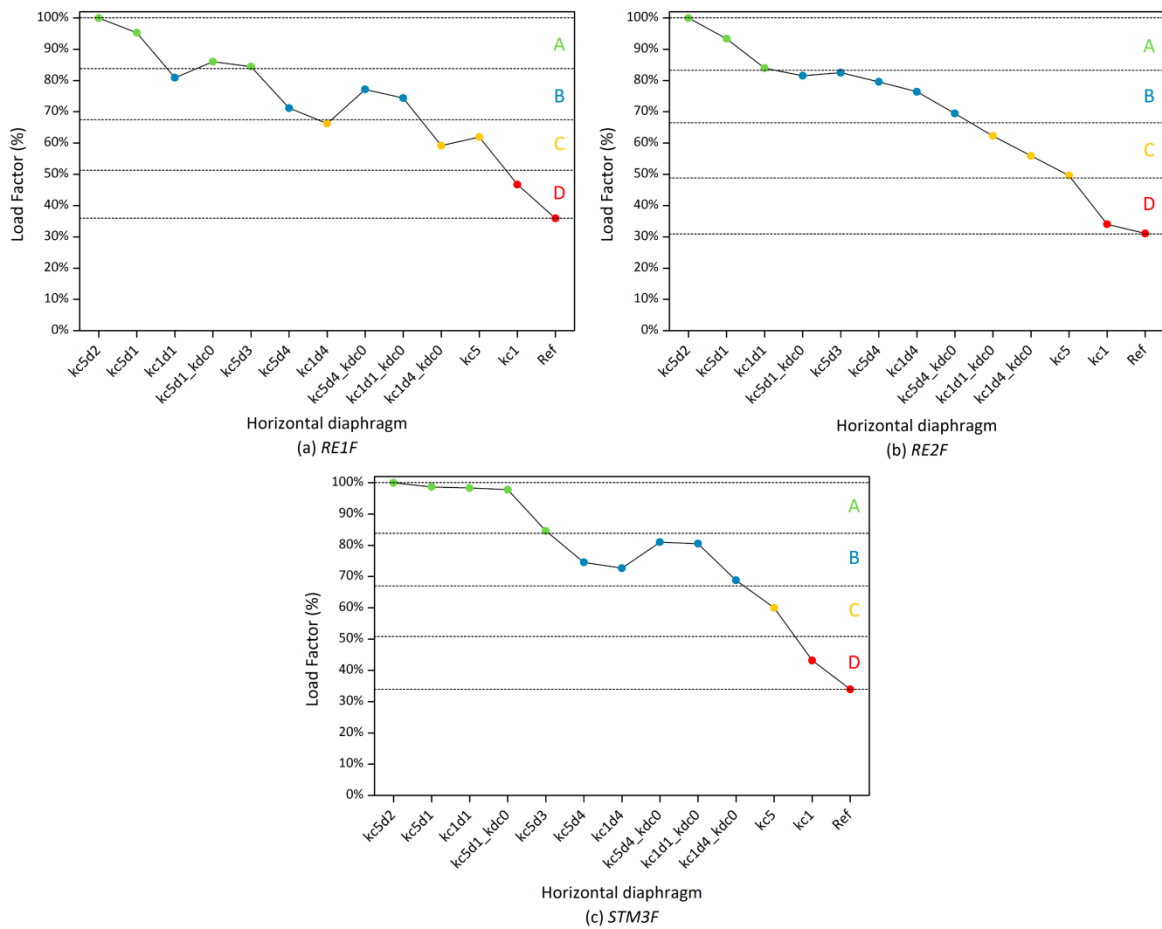


Figure 4.32: Variation of the load factor leading to the attainment of the maximum capacity (LS3) for the three sets of models evaluated in Y direction: (a) *RE1F*; (b) *RE2F*; and (c) *STM3F*

Table 4.13 shows the final classification proposed for P5. The classification is made according to the variation of the type of horizontal diaphragm considered in the building according to the three variations defined that were observed to be influential: (a) beams-to-wall connection (k_c); (b) diaphragm stiffness (k_d); and (c) diaphragm-to-wall connection. Therefore, the classification is structured according to this, providing simple qualitative linguistic definitions for these characteristics: “good” or “poor” for the connections; and “rigid”, “flexible” or “negligible” (left in blank in the table) for the stiffness. This simplification is made acknowledging that the buildings are most likely surveyed only by means of visual inspection and further distinctions are difficult to characterize. This is also the reason why the classification provides, as a reference, a qualitative description of the type of horizontal diaphragm that belongs to each class.

Nevertheless, given the results in X direction, attention should be paid to the direction of the beams. If there are walls prone to out-of-plane collapse that are not coupled with the beams and the floor is not well connected, the possible beneficial coupling effect of the beams cannot be taken into account and the building should always classify as class D. The classification suggested in Table 4.13 is generally in agreement with previous classifications from other vulnerability index methods existing in the literature that are also expressed in qualitative terms (Benedetti and Petrini 1984; Vicente 2008; Shakya 2014). However, the new classification provides more detailed information about the characteristics of the elements composing horizontal timber diaphragms and their level of connection with other structural elements.

Table 4.13: Vulnerability classes proposed according to the horizontal diaphragms

P5. Horizontal diaphragms				
Class	Description	Beam-to-wall connection (k_c)	Diaphragm connection (k_{dc})	Diaphragm stiffness (k_d)
A	Rigid diaphragm well-connected to the walls	Good	Good	Rigid
B	Flexible diaphragm well-connected to the walls. Rigid diaphragm well-connected to the walls but beams poorly coupled with the walls. Rigid diaphragm poorly connected to the walls but beams properly coupled with the walls. Poor connections can be either due to construction deficiencies or because of signs of deterioration and decay of the timber elements, such as rotting or biological attacks	Good	Good	Flexible
		Poor	Good	Rigid
		Good	Poor	Rigid
C	Flexible diaphragm well-connected to the walls but beams poorly coupled with the walls. Rigid and flexible diaphragms poorly connected to the walls with beams poorly coupled with the walls. Flexible diaphragms poorly connected to the walls but beams properly coupled with the walls. Diaphragms of negligible stiffness with beams well-connected to the walls achieving a coupling effect. Poor connections can be either due to construction deficiencies or because of signs of deterioration and decay of the timber elements, such as rotting or biological attacks	Poor	Good	Flexible
		Poor	Poor	Rigid
		Good	Poor	Flexible
		Poor	Poor	Flexible
D	Diaphragms of negligible stiffness with beams poorly connected to the walls. Poor connections can be either due to construction deficiencies or because of signs of deterioration and decay of the timber elements, such as rotting or biological attacks	Good	-	-
		Poor	-	-

4.8. Seismic vulnerability classes according to the roof thrust (P6)

Two reference models with varying number of floors and distribution of wall openings were prepared for the analysis of the influence of P6 (Figure 4.33): (a) one-floor rammed earth building with flexible diaphragm, 0.5 m thick walls and reduced number of wall openings (*RE1F*); and (b) two-floor rammed earth building with flexible diaphragm, 0.5 m thick walls and high number of wall openings (*RE2F*). The walls of the one-floor models are 2.4 m high and the maximum wall span is 7 m. The in-plan area is 15.5x6 m². The ground floor walls of the two-floor models are 3 m high, while the walls at the upper floor are 2.6 m high. The maximum wall span is 7 m and the in-plan area is 8x5.5 m². For the reference models of both sets, the roof and the floor loads are simply modelled as vertical distributed loads along the top of the walls and no thrust is considered, assuming that they present a non-thrust exerting roof type.

In order to assess the influence of the roof thrust on the seismic behavior of vernacular buildings, a thrust-exerting roofing structural system is considered and the thrust exerted is progressively increased. As previously discussed and shown in Chapter 3 (Figure 3.12), the thrust exerted by the roof mainly depends on the span covered by the roof, on its weight and on its inclination. Since the span (L) is kept the same for all analyses, the weight (q) and inclination (L/h) will be modified to obtain different levels of thrust. This variation results in a progressive increase of the horizontal load (H) that is initially applied simulating the roof thrust. The two sets of models were analyzed in the direction perpendicular to the walls with the maximum wall span (Y), which is also the direction parallel to the roof thrust. Therefore, the analysis is performed in two steps: (1) first, the thrust horizontal load (H) of the roof is applied at the beginning of each analysis at the top of the walls (marked in blue in Figure 4.33); and (2) the pushover analysis load is applied progressively in Y direction parallel to the roof thrust loading direction (marked in red in Figure 4.33). This phased analysis is performed in order to understand how the application of the initial thrust load can anticipate the out-of-plane collapse. Table 4.14 presents a summary of the 12 models constructed with varying roof weight and inclination.

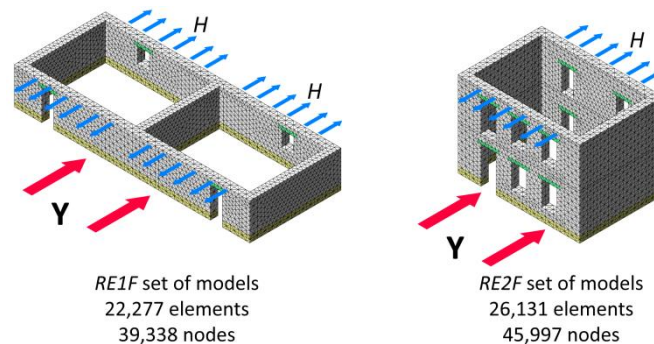


Figure 4.33: Numerical models built in order to assess the influence of the roof thrust on the seismic behavior of vernacular buildings

Table 4.14: Summary of the 12 different models built in order to assess the influence of the roof thrust on the seismic behavior of vernacular buildings

Model Name	Set of models			Variations		
	RE1F	RE2F	q (kN/m ²)	L/h	H	Description
<i>Ref</i>	X	X	0	-	0	Non-thrust exerting roof
<i>R1</i>	X	X	0.6	1.0	H_0	Light roof with high inclination (45°)
<i>R2</i>	X	X	0.6	1.5	$1.5H_0$	Light roof with medium-high inclination (35°)
<i>R3</i>	X	X	0.6 / 1.2	2.0 / 1.0	$2H_0$	Light roof with medium inclination (26°) or heavy roof with high inclination (45°)
<i>R4</i>	X	X	0.6 / 1.2	3.0 / 1.5	$3H_0$	Light roof with low inclination (20°) or heavy roof with medium-high inclination (35°)
<i>R5</i>	X	X	1.2	2	$4H_0$	Heavy roof with medium inclination (26°)

4.8.1. Variations on damage patterns and failure mechanisms

The failure mode remained unaltered when increasing the roof thrust. For both sets of models, the damage pattern observed consists of the typical out-of-plane failure and overturning of the exterior walls perpendicular to the seismic load, see Figure 4.34. Nevertheless, there are some differences in the damage pattern observed that should be highlighted. In the case of the RE1F set of models, when the building is considered to present a non-thrust exerting roof type (model *Ref*), significant damage is observed at the two walls perpendicular to the seismic load (Figure 4.34a). Taking into consideration the roof thrust anticipates the out-of-plane failure due to the initial outwards thrust applied at the walls. The damage at the front wall is avoided because, at this wall, the roof thrust counteracts the seismic load. On the other hand, damage at the exterior wall is increased because the roof and seismic load are applied in the same direction. Damage in this case particularly concentrates at the connection between perpendicular walls. As it could be expected, the additional horizontal load increases the stresses at the corners. For high values of thrust, damage at these points is imposed since the beginning of the analysis, which leads to an anticipated more sudden failure. However, the type of failure does not vary when the roof thrust is increased (Figure 4.34b-d).

With respect to the two-floor set of models (*RE2F*), the variations in the damage pattern obtained are less evident. Nevertheless, damage is also more localized at the wall-to-wall connections when increasing the initial roof thrust, as in the case of the *RE1F* set of models. Even though the crack pattern did not vary significantly, the widespread out-of-plane bending damage at the center of the wall shown in the reference model (Figure 4.34e) is gradually less extensive when increasing the roof thrust (Figure 4.34f-h).

4.8.2. Building of capacity curves and analysis of load factor variations

The four-linear capacity curves derived from the pushover curves obtained in the parametric analysis are shown in Figure 4.35, grouped by set of models. The two sets clearly show the

decrease in the capacity of the building when applying an increasing roof horizontal load. This confirms the previously observed influence of the roof thrust, mainly by anticipating the out-of-plane collapse mechanism. The range of variation is also similar for both sets. All the models from the same set present a very similar behavior. Since the roof thrust is imposed before carrying out the pushover analysis, the curves are mainly shifted according to this imposed initial drift resulting from the thrust. As an example, for the models with a heavy roof and medium inclination (*R5*), the initial drift is high enough for the building to present a nonlinear response from the beginning, since it already induces initial damage to the structure.

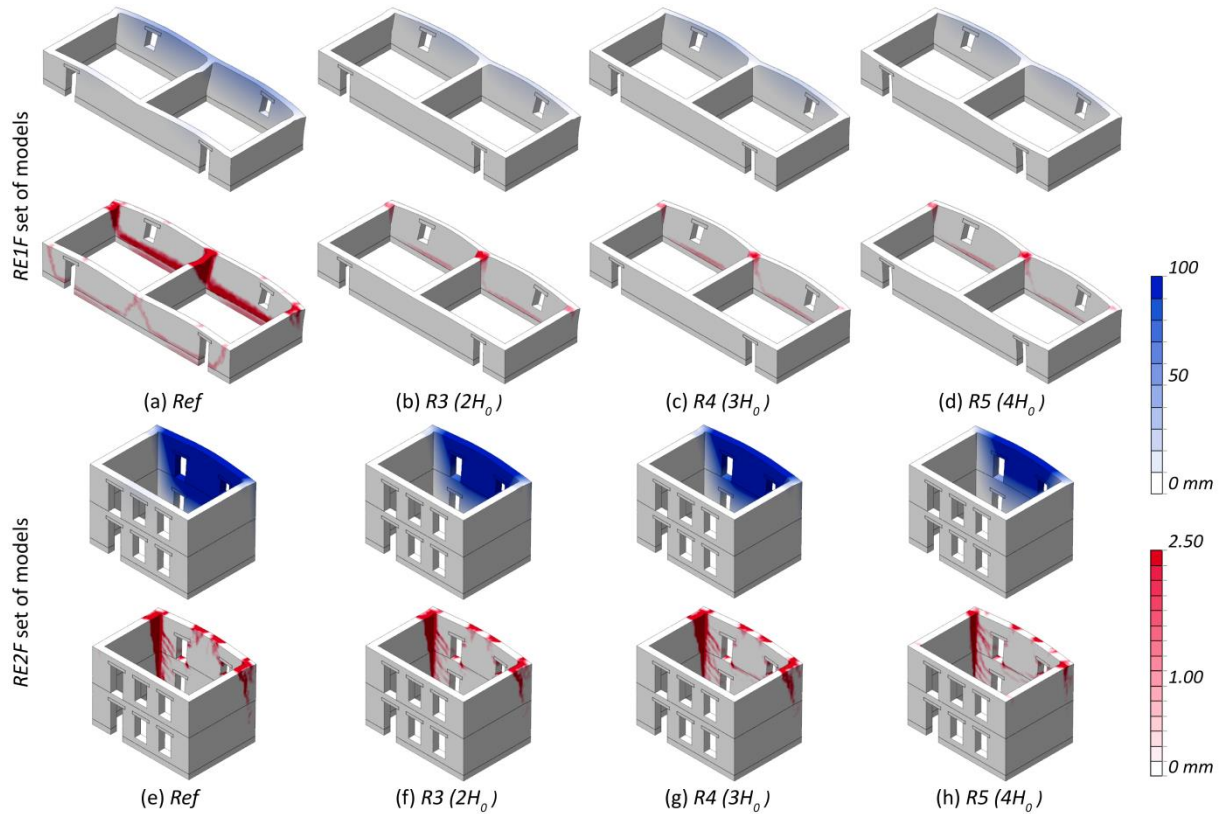


Figure 4.34: Representative failure modes at ultimate limit state (LS4) obtained for several buildings with varying roof thrust within the *RE1F* and *RE2F* sets of models analyzed: (blue) maximum total displacements; and (red) crack pattern (crack width scale)

Because of the similar behavior observed in all the models from each set, there are no significant variations in terms of initial stiffness among the models. However, for the *RE1F* set of models, there is an important variation in terms of ductility between the reference model (*Ref*), where the roof thrust is not taken into account, and the remaining models from the set, where the thrust is considered. The widespread damage at the two walls perpendicular to the seismic load observed in Figure 4.34a is a consequence of the building effectively redistributing the stresses among several structural elements. Thus, the building shows a relatively ductile post-peak behavior. On the other hand, the accumulation of stresses at the wall-to-wall connections

resulting from the initial application of the roof thrust leads to the previously discussed localized damage at the corners at the ultimate limits state (Figure 4.34b-d). This eventually results in a sudden failure, which is confirmed by the pronounced softening observed in Figure 4.35. These differences in terms of ductility are not noticeable in the *RE2F* set of models, since there are not either such significant differences in the failure modes obtained from the models within this set.

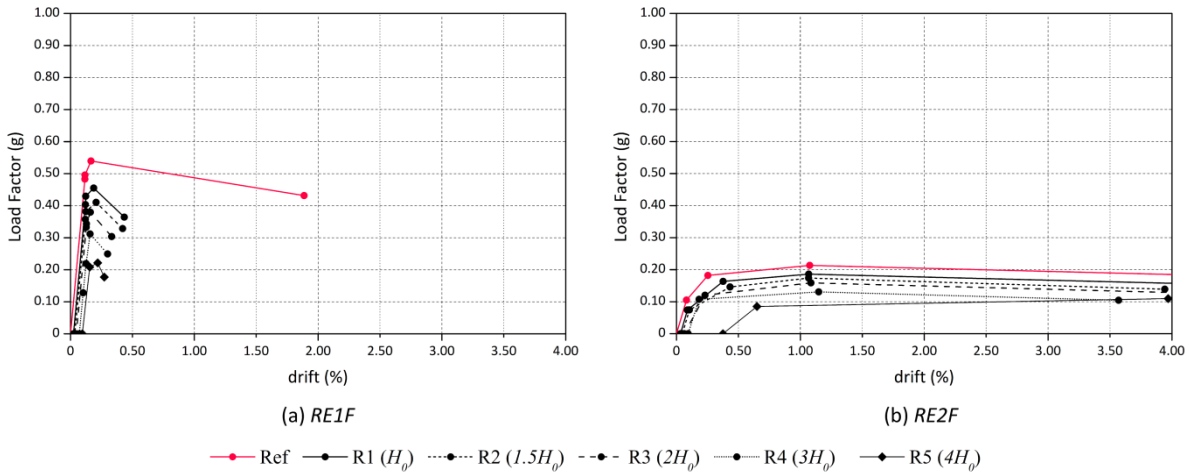


Figure 4.35: Four-linear capacity curves for the two sets of models: (a) *RE1F*; and (b) *RE2F*

The variations of the load factors defining each limit state are shown in Figure 4.36, grouped by set of models. For both sets, the models with a non-thrust exerting roof (*Ref* models) showed the maximum capacity and were used for the normalization. Results indicate a clear variation of the load factors according to the roof thrust. As expected, the diagrams show that the different limit states are attained for decreasing load factors when increasing the thrust exerted by the roofing system. The trend is similar for both sets of models. Because of the abovementioned initially imposed drift resulting from the phased analysis where the roof load is applied before carrying out the pushover analysis, some models present an initial level of damage and thus reach LS1 since the beginning. That is why the load factor defining LS1 is 0 for some models.

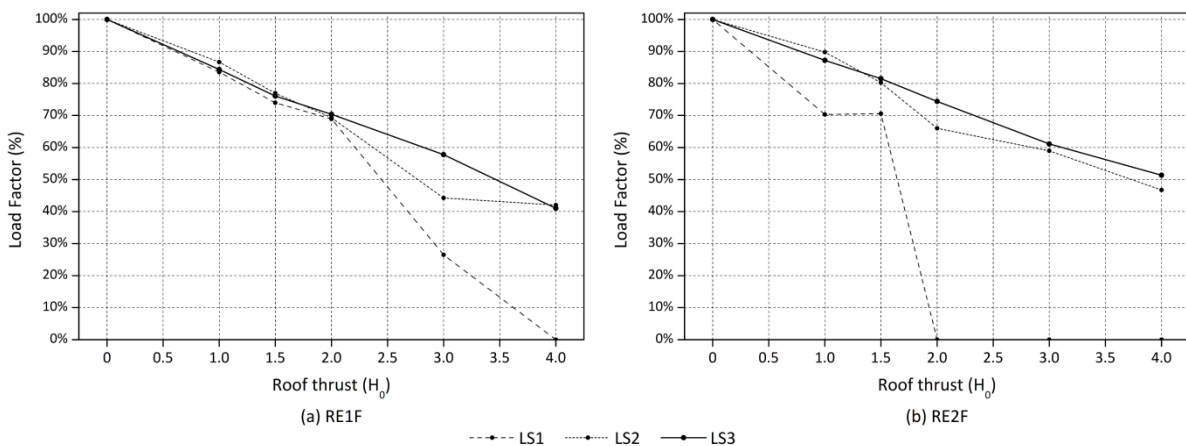


Figure 4.36: Load factor variations for each limit state for the two sets of models: (a) *RE1F*; and (b) *RE2F*

4.8.3. Definition of seismic vulnerability classes

The four seismic vulnerability classes are defined according to the variation of the load factor corresponding to the attainment of LS3. Figure 4.37 shows the variation of the load factor defining LS3 for the two sets of models and the four intervals associated to the four vulnerability classes (A, B, C and D). As aforementioned, the lateral thrust induced by the roof is more determining for the *RE1F* building, which results also in a wider range of variation. Nevertheless, both sets of models lead to a very similar definition of classes. The only discrepancy occurs in the case of the model simulating a light roof with low inclination or a heavy roof with medium-high inclination ($3H_0$). This model lies within class C for the *RE1F* set, whereas it falls into vulnerability class D for the *RE2F* set. Thus, it was finally considered as class D.

Table 4.15 shows the final classification proposed for P6. The classification is made according to the variation on the characteristics of the roofing system according to: (a) the thrusting nature of the roofing system; (b) the roof weight (w); and (c) its inclination (α). Taking as reference other classifications existing in the literature (Benedetti and Petrini 1984; Vicente 2008; Ferreira 2009), semi-thrusting roof types are also included in the classification as a middle ground between non-thrust exerting and exerting roofing systems.

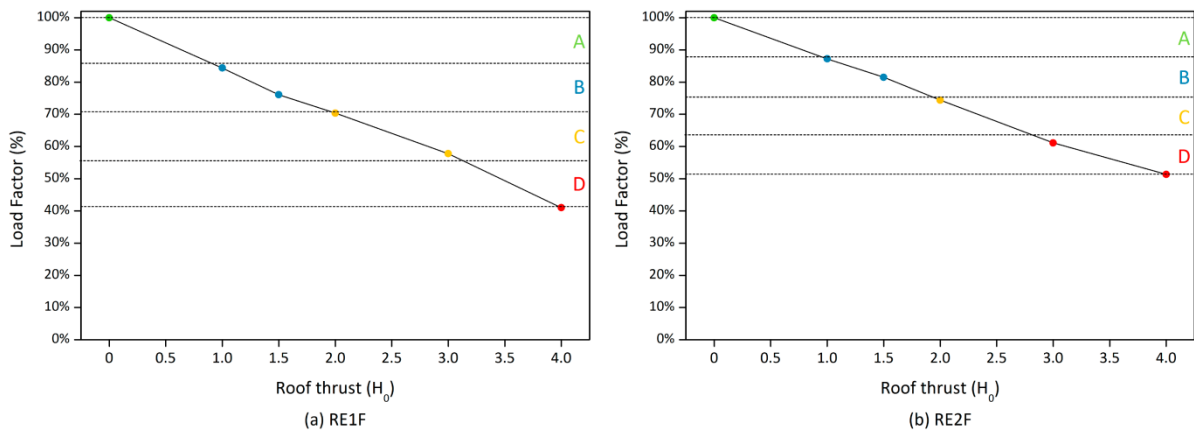


Figure 4.37: Variation of the load factor leading to the attainment of the maximum resistance (LS3) for the two set of models evaluated: (a) *RE1F*; and (b) *RE2F*

Table 4.15: Vulnerability classes proposed according to the roof thrust

P6. Roof thrust	
Class	Description
A	Non-thrusting roof types and semi-thrusting roof types with light-weight and high inclination
B	Thrusting roof types with light-weight ($w < 0.9 \text{ kN/m}^2$) and high inclination ($\alpha > 35^\circ$). Semi-thrusting roof types with light-weight and low inclination ($\alpha < 20^\circ$) or heavy roof types ($w > 0.9 \text{ kN/m}^2$) with high inclination ($\alpha > 35^\circ$)
C	Thrusting roof types with light-weight ($w < 0.9 \text{ kN/m}^2$) and medium inclination ($20^\circ < \alpha < 35^\circ$) or heavy roof types ($w > 0.9 \text{ kN/m}^2$) with high inclination ($\alpha > 35^\circ$). Semi-thrusting heavy roof types ($w > 0.9 \text{ kN/m}^2$) with medium-high inclination ($20^\circ < \alpha < 35^\circ$)
D	Thrusting roof types with light-weight ($w < 0.9 \text{ kN/m}^2$) and low inclination ($\alpha < 20^\circ$) or heavy roof types ($w > 0.9 \text{ kN/m}^2$) with medium-high inclination ($\alpha < 35^\circ$)

4.9. Seismic vulnerability classes according to the wall openings (P7)

Four reference models with varying number of floors and type of diaphragm were prepared for the analysis of the influence of P7 (Figure 4.38): (a) one-floor rammed earth building with flexible diaphragm (*RE1F*); (b) one-floor rammed earth building with rigid diaphragm (*RE1Fd1*); (c) two-floor rammed earth building with flexible diaphragm (*RE2F*); and (d) two-floor rammed earth building with rigid diaphragm (*RE2Fd1*). The walls of the one-floor models are 3 m high and 0.5 m thick. The maximum wall span is 7 m and the in-plan area is $8 \times 5.5 \text{ m}^2$. The ground floor walls of the two-floor models are 3 m high, while the walls at the upper floor are 2.6 m high. All walls are 0.5 m thick. The maximum wall span is 7 m and the in-plan area is $8 \times 5.5 \text{ m}^2$. For all the models, the roof is simply modelled as distributed load along the walls and, for those models where the diaphragm is not modelled, the floor is also simply simulated as a vertical distributed load applied on top of the walls. With respect to the amount and area of wall openings of the reference models, the one-floor buildings have two openings in the two parallel walls presenting the maximum wall span: (a) a door with $2.1 \times 0.8 \text{ m}^2$ (height x length); and (b) a window with $1 \times 0.8 \text{ m}^2$. The two-floor buildings present the same two openings at the walls with the maximum wall span, both at the ground floor and the upper floor.

In order to assess the influence of wall openings on the seismic behavior of vernacular buildings, three characteristics concerning the openings of the reference models are modified: (a) the number of openings; (b) the area of the wall openings; and (c) the configuration of the wall openings. Situations where there is an unbalanced distribution of openings among the different walls were also considered. As previously discussed in Chapter 3, the amount of wall openings can be measured as the ratio between the area of wall openings and the total surface area of the wall. Additionally, the presence of wall openings mainly compromises the in-plane resistance of the walls. That is why the four sets of models were analyzed in the direction parallel to the walls with openings (X), in order to understand the influence of wall openings in the earthquake resistant walls. The ratio used to quantitatively measure this parameter is the ratio between the total area of wall openings in all earthquake resistant walls in one main direction and the total surface area of the walls in that same direction, as specified in Chapter 3 (Figure 3.14). This in-plane ratio is referred as *IP* and varies within a wide range, from buildings presenting almost no openings ($IP = 2\%$) to buildings where most of the façade is perforated with large openings ($IP = 63\%$). Since the building is more prone to suffer in-plane damage when presently sufficiently stiff diaphragms able to avoid premature out-of-plane collapses, the sets are prepared considering two possibilities, namely: (1) whether the building presents diaphragms rigid enough to redistribute the load to the resisting walls parallel to the seismic load (*RE1Fd1* and *RE2Fd1*); and (2) whether the diaphragm is assumed to be very flexible and is not modeled (*RE1F* and *RE2F*). Table 4.16 presents a summary of the 40 models finally built for the evaluation of this parameter.

Table 4.16: Summary of the 40 different models built in order to assess the influence of the wall openings on the seismic behavior of vernacular buildings

Model Name	Set of models				Variations								IP (%)
					Front wall				Back wall				
	RE1F	RE1Fd1	RE2F	RE2Fd1	Size of openings height (m) x length (m)			Number of openings	Size of openings height (m) x length (m)				
					O1	O2	O3		O1	O2	O3		
IP2			X	X	1	2.1x0.8	-	-	0	-	-	-	2
IP4	X	X			1	2.1x0.8	-	-	0	-	-	-	4
IP11 (Ref)	X	X	X	X	2	2.1x0.8	1x0.8	-	2	2.1x0.8	1x0.8	.	11
IP19	X	X	X	X	3	2.1x0.8	1.6x1	1.6x1	2	2.1x0.8	1x0.8	.	19
IP26	X	X	X	X	3	2.4x1.5	1.6x1.5	1.6x1.5	2	2.1x0.8	1x0.8	.	26
IP27	X	X			3	2.1x0.8	1.6x1	1.6x1	3	2.1x0.8	1.6x1	1.6x1	27
IP28			X	X	3	2.1x0.8	1.6x1	1.6x1	3	2.1x0.8	1.6x1	1.6x1	28
IP31	X	X	X	X	3	2.4x1.5	2.4x1.5	2.4x1.5	2	2.1x0.8	1x0.8	.	31
IP38	X	X	X	X	3	2.5x1.8	2.5x1.8	2.5x1.8	2	2.1x0.8	1x0.8	.	38
IP40	X	X			3	2.4x1.5	1.6x1.5	1.6x1.5	3	2.4x1.5	1.6x1.5	1.6x1.5	40
IP41			X	X	3	2.4x1.5	1.6x1.5	1.6x1.5	3	2.4x1.5	1.6x1.5	1.6x1.5	41
IP51	X	X	X	X	3	2.4x1.5	1.6x1.5	1.6x1.5	3	2.4x1.5	1.6x1.5	1.6x1.5	51
IP63			X	X	3	2.5x1.8	2.5x1.8	2.5x1.8	3	2.5x1.8	2.5x1.8	2.5x1.8	63
IP64	X	X			3	2.5x1.8	2.5x1.8	2.5x1.8	3	2.5x1.8	2.5x1.8	2.5x1.8	64

4.9.1. Variations on damage patterns and failure mechanisms

The most representative failure mechanisms obtained for the four sets of models analyzed are shown in Figure 4.39. Clear variations were observed in the damage patterns and failure mechanisms observed for the different models with varying distribution of wall openings within each set. The failure mode observed in the sets of models where a flexible diaphragm is considered (*RE1F* and *RE2F*) varies from the typical out-of-plane mechanism leading to the overturning of the exterior walls perpendicular to the seismic load (Figure 4.39a,k) to a clear in-plane failure of the walls parallel to the seismic load, when the area of wall openings in the resisting walls is significantly increased (Figure 4.39e,o). The out-of-plane observed in the models with a reduced number of wall openings is localized at the connection between perpendicular walls, showing vertical cracks at the wall intersections, and at the center of the wall, showing out-of-plane bending damage at the walls perpendicular to the loading direction (Figure 4.39a,b,k,l). Increasing the amount and area of wall openings gradually avoids the formation of the out-of-plane mechanism, confirming that the presence of openings facilitate the development of in-plane mechanisms (Figure 4.39d,e,n,o). This is particularly evident in the case of the two-floor models, where damage arising at the edge of the openings gains significance when increasing the number of openings, while the out-of-plane bending damage at the walls perpendicular to the loading direction gradually disappears (Figure 4.39n,o).

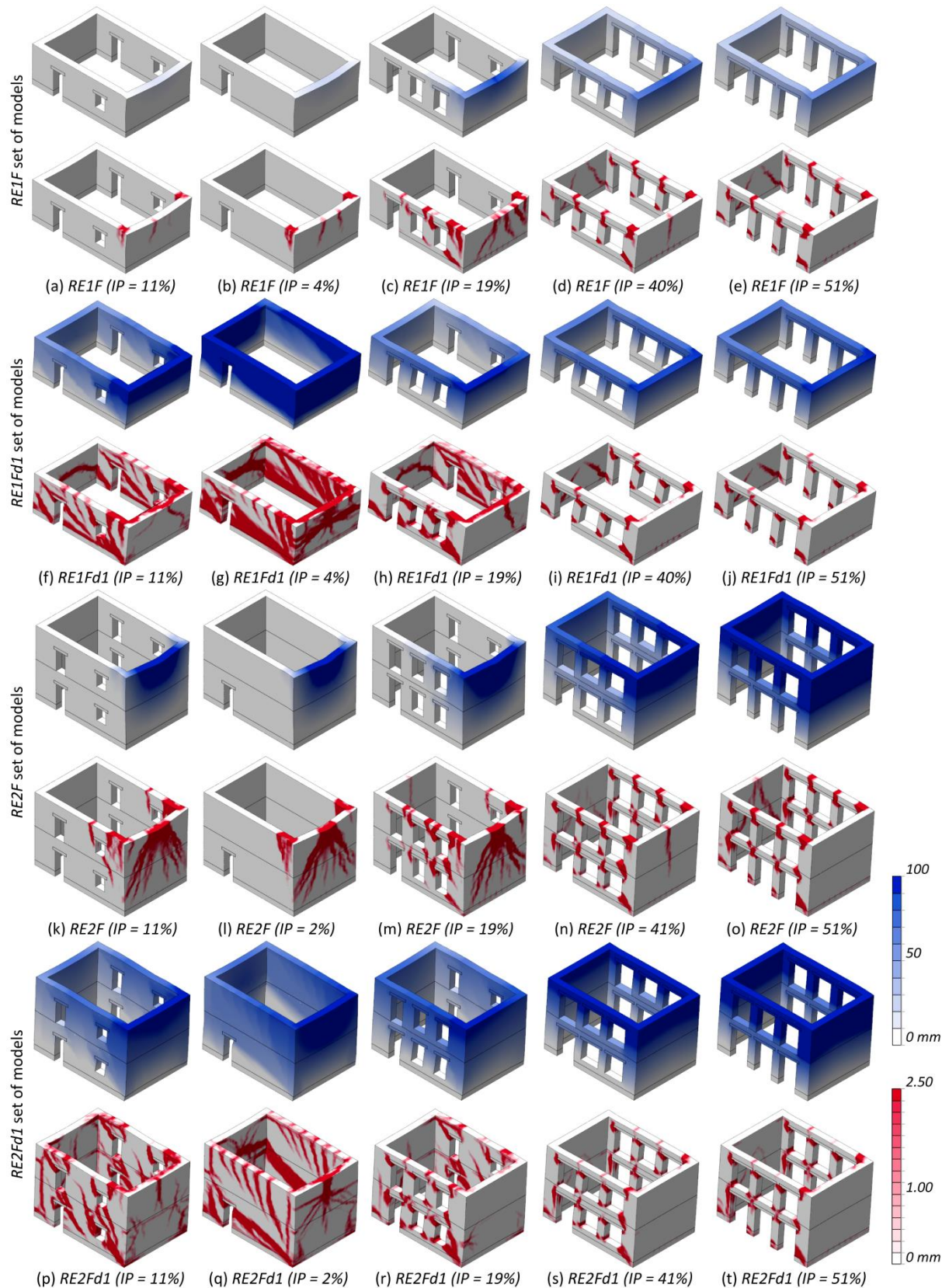


Figure 4.39: Representative failure modes at ultimate limit state (LS4) obtained for several buildings with varying number and area of wall openings within each of the four sets of models analyzed: (blue) maximum total displacements; and (red) crack pattern (crack width scale)

With respect to the sets of models with a rigid diaphragm (*RE1Fd1* and *RE2Fd1*), the failure mode invariably consists of the in-plane mechanism of the walls parallel to the seismic load, showing great concentration of damage at the edge of the openings and the development of the characteristic diagonal shear cracking (Figure 4.39f-i,p-t). The diaphragm is rigid enough to engage all the resisting walls parallel to the seismic load in the seismic response of the buildings. Whereas the failure mode always consists of in-plane mechanisms of the earthquake resisting walls, increasing the area of wall openings implies the reduction of the surface area of the walls, which leads to a severe concentration of damage at the edges of the openings (Figure 4.39i,j,s,t). Additionally, for both sets, damage progressively spreads since earlier stages of the analysis when increasing the area of wall openings, confirming that the presence of openings highly compromises the in-plane performance of the buildings.

4.9.2. Building of capacity curves and analysis of load factor variations

Figure 4.40 shows the four-linear capacity curves derived from the pushover analyses performed, grouped by set of models. As aforementioned, the quantitative measure used for the analysis of the influence of the wall openings on the global seismic behavior of vernacular buildings is the area of wall openings in the in-plane walls ratio (*IP*). The four sets clearly show the variation in the capacity of the building for an increasing area of wall openings in the earthquake resistant walls. As it was expected, the variation of the maximum capacity of the buildings is significantly more relevant when they have a diaphragm that is rigid enough to redistribute the load to the in-plane walls (Figure 4.40b,d). The in-plane capacity of the resisting walls reduces gradually according to the increase in the area of openings. As a consequence, if the global response of the buildings depends on the in-plane capacity of the walls, it is severely compromised when increasing the area of wall openings.

This is clear when observing the failure modes presented in Figure 4.39. For example, for the *RE1Fd1* set of models, the in-plane mechanism developed by the models presenting barely any openings involves the whole area of the wall (Figure 4.39g), while the in-plane mechanism of the models with a high number of openings (Figure 4.39i) is much localized at the edges of the openings, only involving a small portion of the walls. This has a direct influence on the maximum capacity of the building, which is highly reduced. The difference in the maximum capacity between the model with $IP = 4\%$ and the model with $IP = 64\%$ is very high, reaching 30%. Another example of this can be observed in Figure 4.40, which shows that if the area of wall openings is exceptionally high ($IP = 63\%$), the seismic behavior of the building with or without a rigid diaphragm is very similar. This indicates that the rigid diaphragm is not effective when the in-plane capacity of the walls is such reduced that they cannot withstand the load redistributed by the diaphragm. In this case, the out-of-plane resistance of the walls perpendicular to the seismic load is even higher than the in-plane resistance of the walls parallel to the seismic load.

This highlights the importance of the interaction among different parameters in the seismic response of the building, namely horizontal diaphragms and area of wall openings in this case.

For the *RE1F* set of models, there is also a noticeable variation in terms of ductility, which is related to the variation in the failure mode presented by the buildings within the set previously discussed. The failure shown by the model with almost no openings is a clear out-of-plane mechanism with significant cracking taking place locally at the connections between perpendicular buildings (Figure 4.39a). The out-of-plane capacity of the building is high, given the short span and the relatively large thickness. Thus, damage arises for high values of load, but once the building reaches its maximum capacity, it shows a brittle response and a sudden drop in the resistance. On the other hand, the presence of openings leads to a reduction in both the initial stiffness of the building and the capacity of the buildings. Damage arises from lower values of load, but is more widespread among the different structural elements (Figure 4.39c,d,e). This results in the more ductile behavior. For the two sets of models simulating a rigid diaphragm (*RE1Fd1* and *RE2Fd1*), there are similar differences in terms of initial stiffness, but not in terms of ductility, since the failure mode observed in the buildings within each set do not vary.

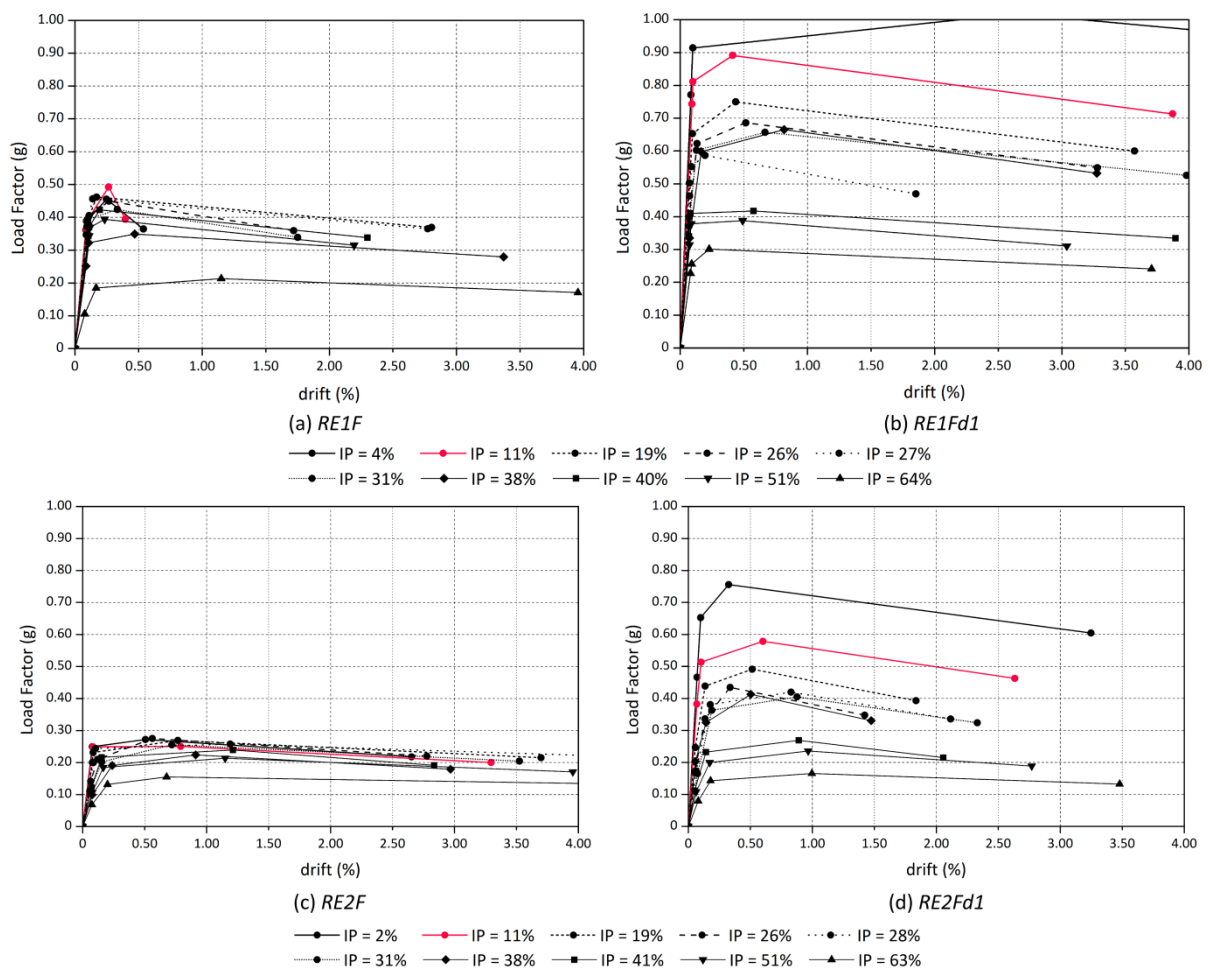


Figure 4.40: Four-linear capacity curves for the four sets: (a) *RE1F*; (b) *RE1Fd1*; (c) *RE2F*; and (d) *RE2Fd1*

The variations of the load factors defining each limit state obtained for the four sets of models are shown in Figure 4.41. The variations were normalized using the average results of the models with almost no openings ($IP = 2\%$), which showed the maximum capacity. There is a clear decreasing trend of the load factor when increasing IP for all sets. However, the influence of the openings is notably greater when the building has stiff diaphragms. When the in-plane resisting walls have a low IP , the rigid diaphragm is very effective in avoiding the premature out-of-plane collapse of the walls perpendicular to the seismic load. On the other hand, for high values of IP , the in-plane capacity of the wall is much compromised and the in-plane resisting mechanism is very weak. In this case, the out-of-plane capacity of the walls perpendicular to the seismic load is higher than the in-plane capacity of the walls parallel to the seismic load. Thus, the building presents a similar performance with and without rigid diaphragm. Until reaching high values of IP , the variations are much lower when buildings have flexible diaphragms. However, because of the previously discussed compromised in-plane capacity of the wall for high values of IP , there is a great decrease on the load factors obtained for the three different LS for $IP > 40\%$. The variations for the load factor defining LS1 appear to be higher for the two-floor sets of models. This reveals that buildings with many openings are typically more prone to suffer damage for low values of seismic load.

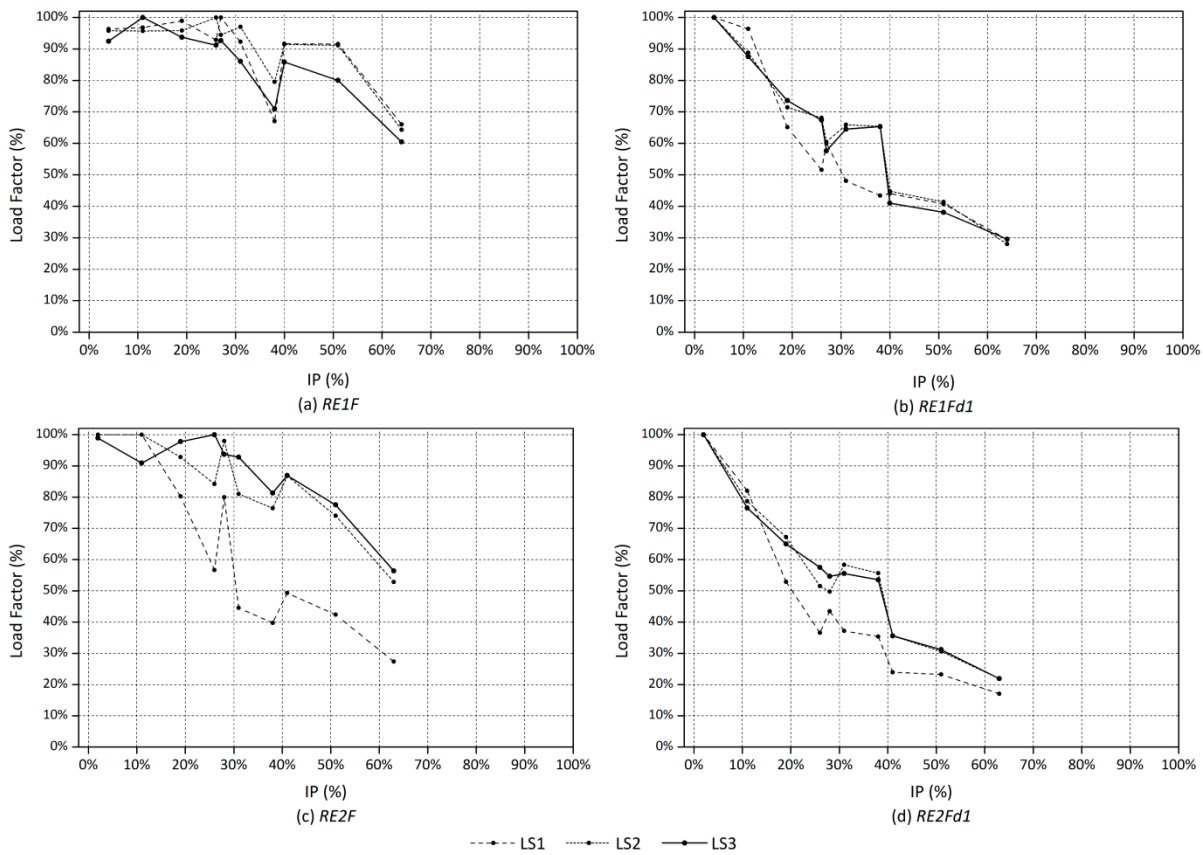


Figure 4.41: Load factor variations for the four sets: (a) *RE1F*; (b) *RE1Fd1*; (c) *RE2F*; and (d) *RE2Fd1*

4.9.3. Definition of seismic vulnerability classes

The four seismic vulnerability classes are defined according to the variation of the load factor corresponding to the attainment of LS3. Figure 4.42 shows the variation of the load factor defining LS3 for the four sets of models and the four intervals associated to the four vulnerability classes (A, B, C and D). The graphs show the great differences between the ranges of variation obtained from the sets of models assuming a flexible diaphragm (*RE1F* and *RE2F*) and those from the sets of buildings with rigid diaphragm (*RE1Fd1* and *RE2Fd1*). The seismic vulnerability classes are primarily defined based on the load factor variations from the *RE1Fd1* and *RE2Fd1* sets because the wall openings has a greater influence when the buildings present a rigid diaphragm and they lead to the most unfavorable definition of the classes. The range of variation is also wider for the *RE2Fd1* set of models and there are some small discrepancies among the classes obtained using one set or the other. The most unfavorable class is always adopted. For example, for *RE1Fd1*, the building with $IP = 38\%$ lies within Class B, but the same model lies within Class C for *RE2Fd1*. Therefore, $IP = 38\%$ is finally considered within Class C.

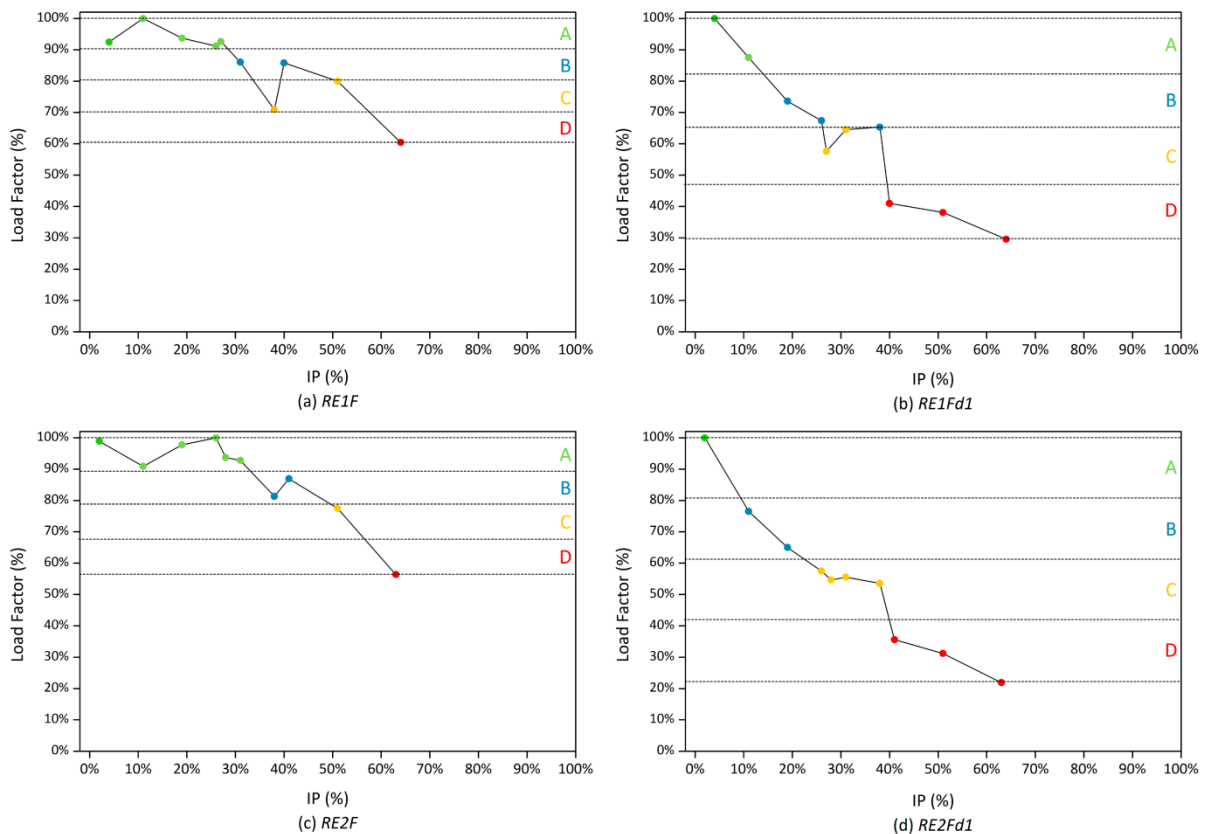


Figure 4.42: Variation of the load factor leading to the attainment of the maximum resistance (LS3) for the four sets of models evaluated: (a) *RE1F*; (b) *RE1Fd1*; (c) *RE2F*; and (d) *RE2Fd1*

Table 4.17 provides the range of values of the previously defined ratio of openings in the in-plane walls (IP) that delimits each seismic vulnerability class. Since this ratio can be calculated

in each loading direction, the final class of the building should be determined for the most unfavorable one, i.e. the direction presenting the greatest percentage of wall openings. The threshold values of IP obtained here are lower than values observed in classifications proposed by other authors in existing seismic vulnerability index formulations (Vicente 2008; Ferreira 2009; Shakya 2014). Table 4.18 shows a comparison of the values proposed here with other values from the literature. Similarly to what occurred for P1 (wall slenderness), this can be attributed to the typically reduced area of wall openings that vernacular buildings present. The high values of IP proposed by other authors are not so representative for vernacular buildings. Therefore, this new classification is adapted the typical characteristics of vernacular architecture.

Table 4.17: Vulnerability classes proposed according to the wall openings

P7. Wall openings	
Class	Description
A	$IP < 10\%$
B	$10\% \leq IP < 25\%$
C	$25\% \leq IP < 40\%$
D	$IP \geq 40\%$

Table 4.18: Comparison among vulnerability classes proposed by other authors for similar vulnerability index formulations that have taken into account the amount of wall openings (IP) as a parameter

P7. Wall openings				
Class	Classification proposed	Vicente (2008)	Ferreira (2009)	Shakya (2014)
A	$IP < 10\%$	$IP < 20\%$	$IP < 20\%$	$IP < 18\%$
B	$10\% \leq IP < 25\%$	$20\% \leq IP < 35\%$	$20\% \leq IP < 35\%$	$18\% \leq IP < 36\%$
C	$25\% \leq IP < 40\%$	$35\% \leq IP < 60\%$	$35\% \leq IP < 60\%$	$36\% \leq IP < 50\%$
D	$IP \geq 40\%$	$IP \geq 60\%$	$IP \geq 60\%$	$IP \geq 50\%$

4.10. Seismic vulnerability classes according to the number of floors (P8)

Eight reference models combining two walls materials with four types of horizontal diaphragm were prepared for the analysis of the influence of P8 (Figure 4.43): (a) rammed earth and stone masonry buildings where the diaphragm effect is not considered and floors are simply simulated with distributed vertical loads applied on top of the walls (RE and STM); (b) rammed earth and stone masonry buildings where only the timber beams are modelled, poorly connected with the walls (RE_{kc1} and STM_{kc1}); (c) rammed earth and stone masonry buildings where only the timber beams are modelled, properly connected with the walls (RE_{kc5} and STM_{kc5}); and (d) rammed earth and stone masonry buildings with rigid diaphragm and beams well-connected to the walls ($REd1_{kc5}$ and $STMd1_{kc5}$). It is noted that the nomenclature of the models followed

the one used for parameter P5 (horizontal diaphragms). The ground floor walls of the models are 3 m high, while the walls at the upper floor are 2.6 m high. The maximum wall span is 7 m and the in-plan area is 8x10.5 m². For all the models, the roof is modelled as distributed load along the walls. In order to assess the influence of the number of floors (N) on the seismic behavior of vernacular buildings, N is increased within a range between 1 and 3 floors for the rammed earth models and between 1 and 4 for the stone masonry models. These narrow ranges are established based on typical values observed for vernacular buildings, as discussed in Chapter 3.

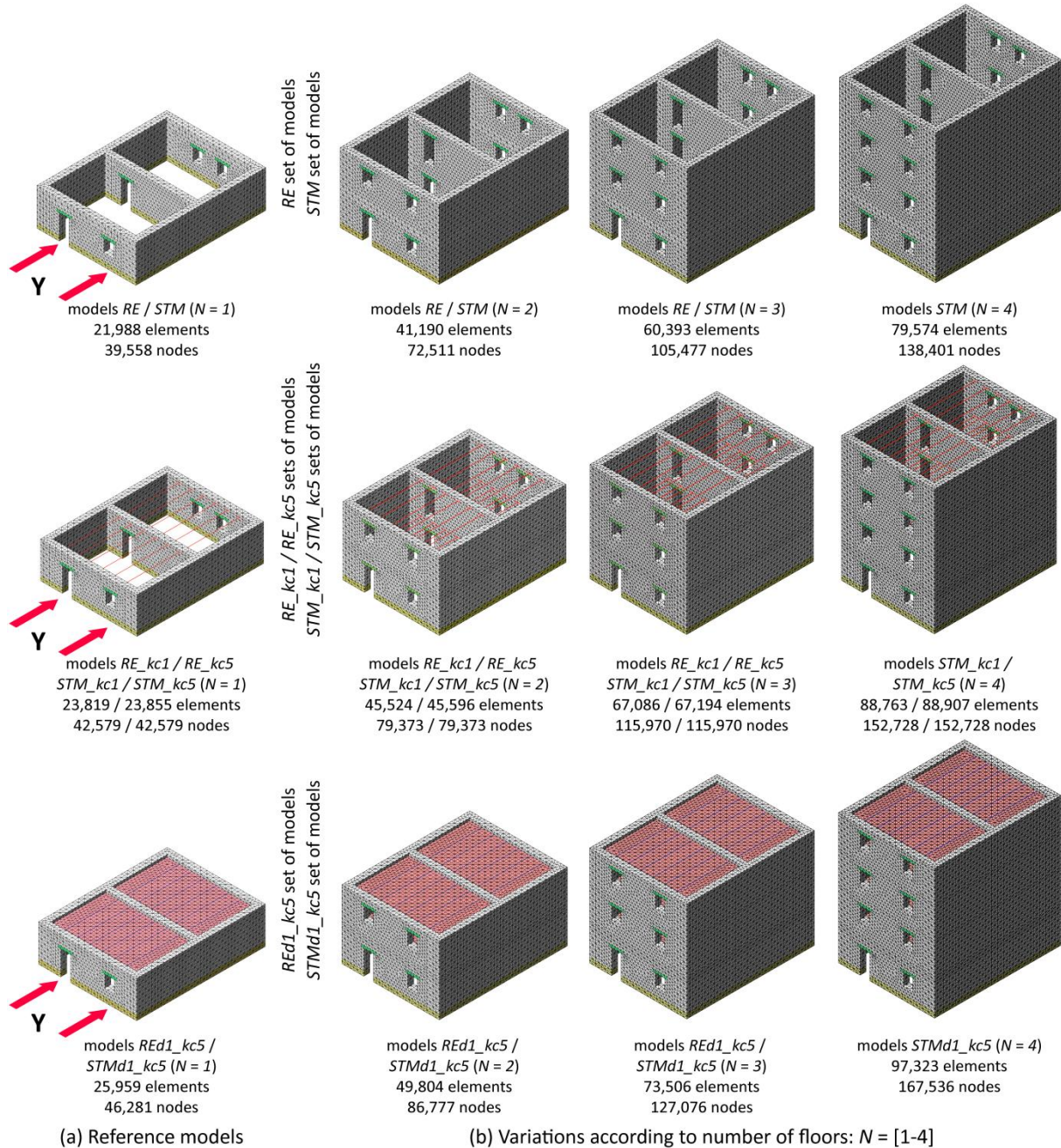


Figure 4.43: Numerical models built in order to assess the influence of the number of floors in the seismic behavior of vernacular buildings: (a) reference models; (b) variations modelled

It should be noted that the sets of models with types of diaphragm *kc1* and *kc5* only vary in the level of embedment of the beams within the wall. Models with diaphragm type *kc5* assume that the beams go through the whole thickness of the wall, while models with diaphragm type *kc1* assumed no embedment. That is why they are shown within the same group in Figure 4.43. The eight sets of models were analyzed in the direction parallel to the direction of the beams (Y) because this is the direction where beams have a more significant influence on the seismic behavior of the building. Table 4.19 presents a summary of the 28 models built for the evaluation of the influence of the number of floors on the seismic behavior of vernacular buildings.

Table 4.19: Summary of the 28 different models built in order to assess the influence of the number of floors on the seismic behavior of vernacular buildings

Model Name	Material		Number of floors <i>N</i>	Type of horizontal diaphragm			Diaphragm
				Beams connection (<i>k_c</i>)			
				Variation of beams embedment within the wall			
				<i>kc1</i>	<i>kc5</i>		
	Rammed earth	Stone masonry		0%	100%		
<i>RE1F</i>	X		1	-	-	-	
<i>STM1F</i>		X	1	-	-	-	
<i>RE1F_kc1</i>	X		1	X	-	-	
<i>STM1F_kc1</i>		X	1	X	-	-	
<i>RE1F_kc5</i>	X		1	-	X	-	
<i>STM1F_kc5</i>		X	1	-	X	-	
<i>RE1Fd1_kc5</i>	X		1	-	X	X	
<i>STM1Fd1_kc5</i>		X	1	-	X	X	
<i>RE2F</i>	X		2	-	-	-	
<i>STM2F</i>		X	2	-	-	-	
<i>RE2F_kc1</i>	X		2	X	-	-	
<i>STM2F_kc1</i>		X	2	X	-	-	
<i>RE2F_kc5</i>	X		2	-	X	-	
<i>STM2F_kc5</i>		X	2	-	X	-	
<i>RE2Fd1_kc5</i>	X		2	-	X	X	
<i>STM2Fd1_kc5</i>		X	2	-	X	X	
<i>RE3F</i>	X		3	-	-	-	
<i>STM3F</i>		X	3	-	-	-	
<i>RE3F_kc1</i>	X		3	X	-	-	
<i>STM3F_kc1</i>		X	3	X	-	-	
<i>RE3F_kc5</i>	X		3	-	X	-	
<i>STM3F_kc5</i>		X	3	-	X	-	
<i>RE3Fd1_kc5</i>	X		3	-	X	X	
<i>STM3Fd1_kc5</i>		X	3	-	X	X	
<i>STM4F</i>		X	4	-	-	-	
<i>STM4F_kc1</i>		X	4	X	-	-	
<i>STM4F_kc5</i>		X	4	-	X	-	
<i>STM4Fd1_kc5</i>		X	4	-	X	X	

4.10.1. Variations on damage patterns and failure mechanisms

The most representative failure mechanisms obtained for the eight sets of models analyzed are shown in Figure 4.44. The failure modes obtained vary significantly according to the material used for the walls and type of diaphragm used in the different models. However, the type of

failure did not seem to depend on the number of floors. All the buildings within each set present very similar collapse mechanisms. For example, when the diaphragms are not modelled (Figure 4.44a,b), the failure of the models consists of the typical out-of-plane mechanism leading to the overturning of the exterior walls perpendicular to the seismic load. The failure mode is the same when the building presents one, two, three and four floors. However, there are slight variations in the damage patterns. For example, the models within the *RE* set with more than one floor present widespread damage at all the walls perpendicular to the seismic load. Thus, increasing the height of the walls favors the development out-of-plane mechanisms at all these walls, even if the rotation occurs inwards. This failure is avoided in the one-floor model because the boundary conditions are more restrictive (Figure 4.44a). Similarly, the four-floor model within the *STM* set presents a vertical crack at the in-plane walls parallel to the seismic load that cannot be seen in the rest of the buildings within the set (Figure 4.44b). This reveals an increase in the vulnerability of the walls presenting a significant height and no horizontal restriction (diaphragm effect), which are more prone to develop out-of-plane mechanisms.

For the two sets where only timber beams poorly connected to the walls are modelled, the failure mode observed for all the buildings consists of the out-of-plane overturning and bending failure of the walls perpendicular to the seismic load, collapsing simultaneously (Figure 4.44c,d). The beams are able to couple parallel walls and involve all of them in the seismic response of the building. There are not significant variations in the damage pattern when increasing the number of floors. When the timber beams are assumed to be properly connected to the walls (*RE_kc5* and *STM_kc5* sets of models), the failure mode is also driven by the out-of-plane overturning and bending failure of the walls perpendicular to the seismic load (Figure 4.44e,f). Nevertheless, there are slight variations in the damage patterns. The buildings with more than one floor in both sets show additional in-plane damage in the walls parallel to the seismic load. This damage is not observed in the building with one-floor. Increasing the number of floors thus promotes the development of a combined in-plane and out-of-plane resisting mechanisms.

Finally, when the buildings present a rigid diaphragm (*REd1_kc5* and *STMd1_kc5* sets of models), they are able to develop in-plane resisting mechanisms at the walls parallel to the seismic load. This is the main failure mode observed, but the walls perpendicular to the seismic load also show significant out-of-plane damage (Figure 4.44g,h). Even though this failure mode is again not affected by the variation of the number of floors, there are some variations in the damage pattern observed. Since the diaphragm has been modelled rigid enough to redistribute the load among the resisting elements, damage is much widespread throughout the building. However, the extension of the damage is gradually reduced when increasing the number of floors. Whereas the in-plane damage for the one-floor and two-floor models is smeared along the in-plane walls, cracks at the buildings with three and four walls follow much clearer lines that appear to indicate a global overturning of big structural portions of the buildings.

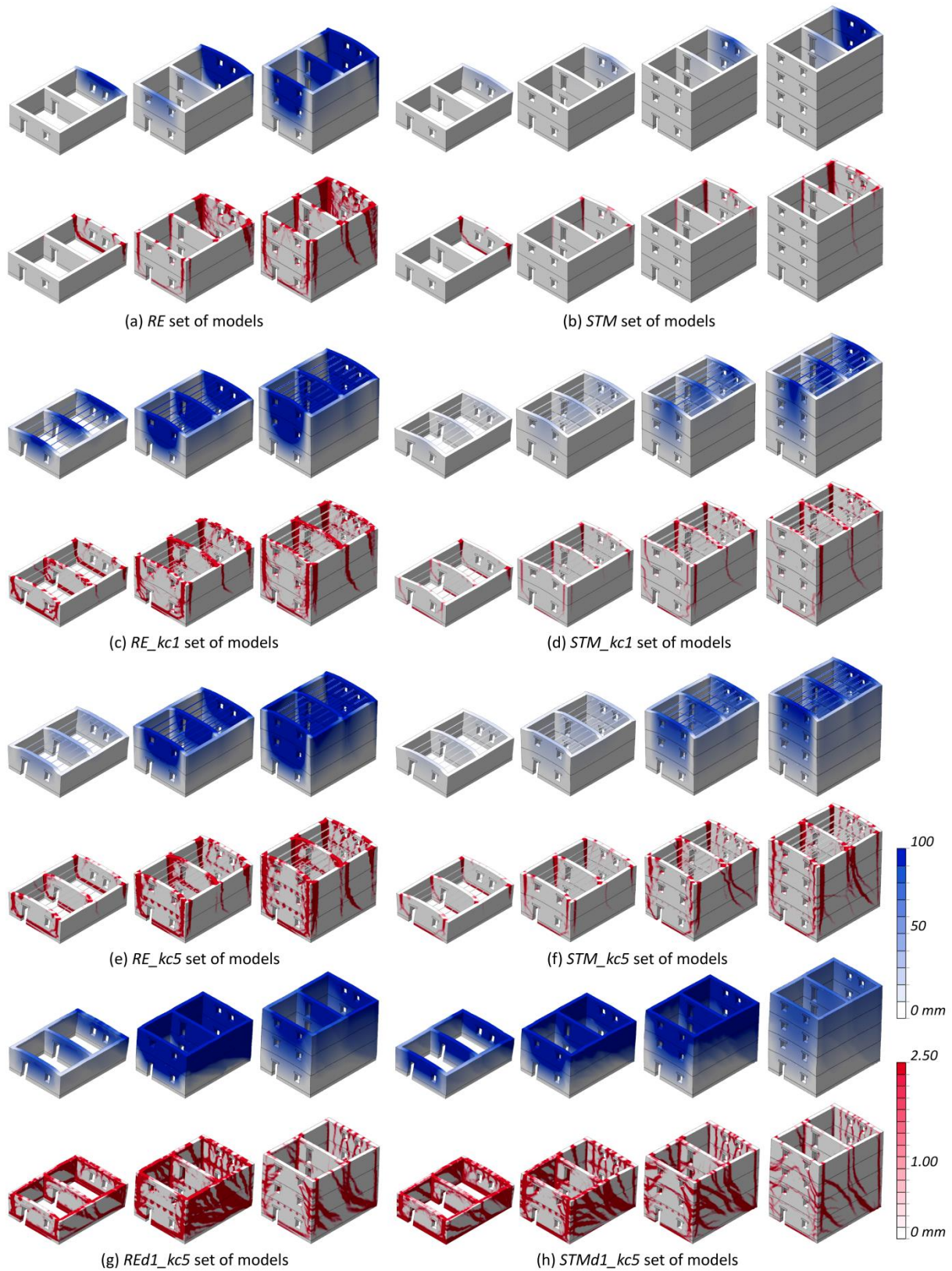


Figure 4.44: Representative failure modes at ultimate limit state (LS4) obtained for the buildings with varying number of floors (N) within the each of the eight sets of models analyzed: (blue) maximum total displacements; and (red) crack pattern (crack width scale)

4.10.2. Building of capacity curves and analysis of load factor variations

Figure 4.45 presents the four-linear capacity curves constructed from the pushover analyses performed, grouped by set of models. For all set of models, there is an important decrease in the capacity when increasing the number of floors. The level of variation is similar for the eight sets. The maximum capacity observed for the models with three floors ranges between 50-60% the maximum capacity of the model with one floor and the same type of diaphragm. In the case of the stone masonry sets of models, where buildings with four floors are also modelled, the maximum capacity of the four-floor models is around 40-50% the maximum capacity of the one-floor models for the four sets.

As previously detected, there are not significant variations in the failure mode of the buildings within the sets. Therefore, there are not meaningful variations in the seismic response of the buildings in terms of ductility and initial stiffness. There are slight variations in those models that also showed variations in the damage pattern observed. For example, for the *RE* set of models, the buildings with more than one floor present more widespread damage at all walls perpendicular to the seismic load, while the one-floor model of the same set is more localized only at the exterior wall perpendicular to the seismic load (Figure 4.44a). In terms of capacity curves, this variation in the behavior is reflected by a more ductile behavior for the two and three-floor models, which suffer larger deformations before reaching the collapse of the building. On the other hand, the one-floor model presents an almost linear behavior until reaching the maximum capacity, suffering light damage and little deformation (Figure 4.45a). This gradually more ductile behavior is also observable in the *RE_kc5* set of models and, to a lesser extent, in the *STM_kc5* set (Figure 4.45e,f). For the *REd1_kc5* and *STMd1_kc5*, the opposite happens. Figure 4.44g,h showed that the extension of the damage is greater for the one-floor models and gradually reduces when increasing the number of floors. Again, these variations in the development of the damage pattern are reflected in the four-linear capacity curves, which show a gradually less ductile behavior for greater number of floors (Figure 4.45g,h).

The variations of the load factors defining each limit state obtained for the eight sets of models are shown in Figure 4.46. The variations were normalized using the model with one floor, which showed the maximum capacity. Results show the influence of the number of floors (N) on the global seismic behavior of the buildings and the clear decrease of the load factor when increasing the number of floors. As previously mentioned, the decreasing trend is practically the same for the eight sets of models, showing similar ranges of variation. For all sets, the variation of the load factor defining LS3 is also clearly not linear. There is a major decrease in the seismic capacity of the building when the number of floors increases from one to two, but this decrease is notably lower when increasing from two to three and from three to four. The variations defining LS1 in all sets are generally higher, which means that the buildings with greater number of floors are prone to suffer damage for lower values of seismic load.

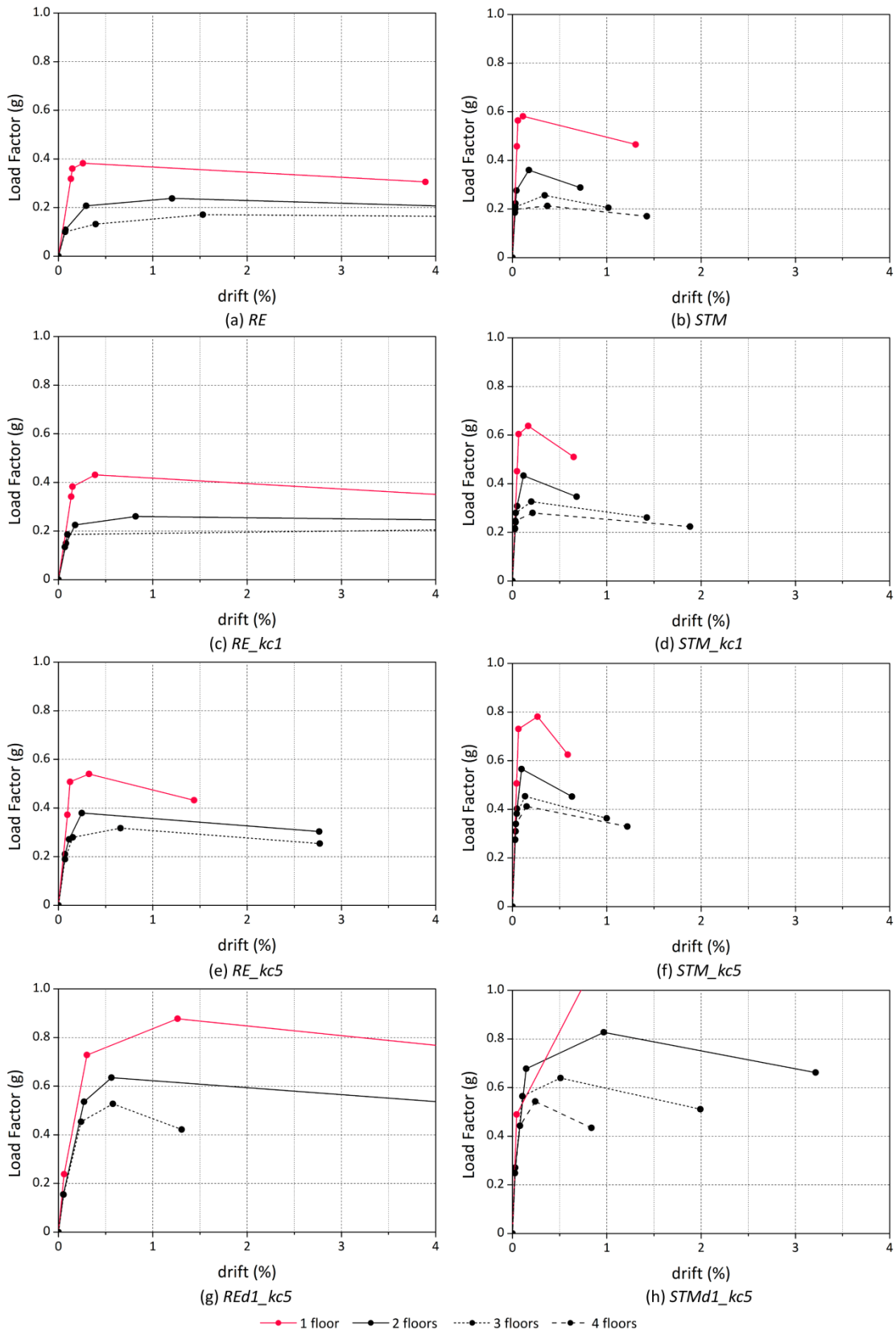


Figure 4.45: Four-linear capacity curves constructed for the eight sets of models: (a) *RE*; (b) *STM*; (c) *RE_kc1*; (d) *STM_kc1*; (e) *RE_kc5*; (f) *STM_kc5*; (g) *REd1_kc5*; and (h) *STMd1_kc5*

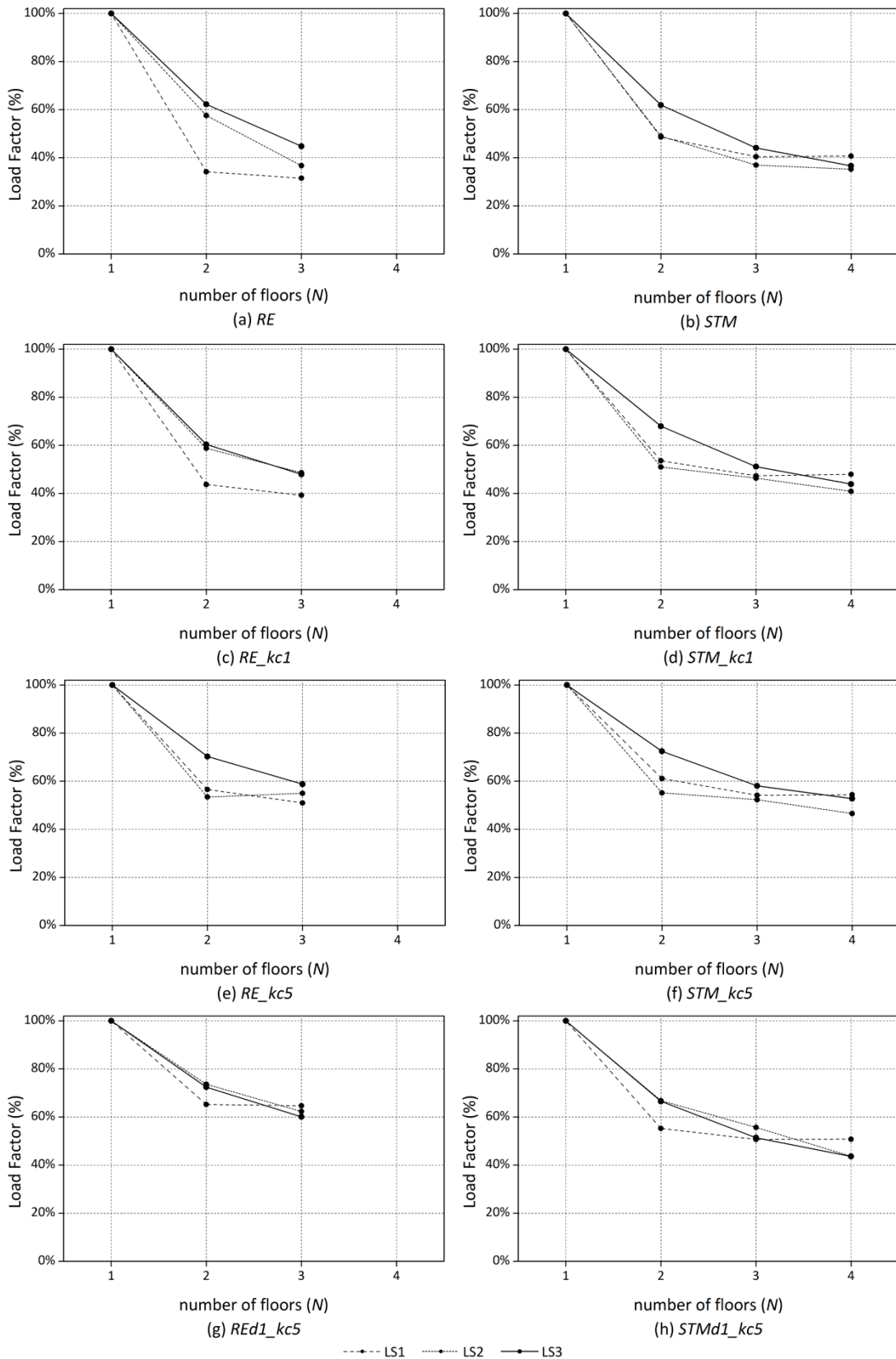


Figure 4.46: Load factor variations for each LS for the eight sets of models: (a) RE; (b) STM; (c) RE_kc1; (d) STM_kc1; (e) RE_kc5; (f) STM_kc5; (g) REd1_kc5; and (h) STMd1_kc5

4.10.3. Definition of seismic vulnerability classes

The four seismic vulnerability classes are defined according to the variation of the load factor corresponding to the attainment of LS3. Figure 4.47 shows the variation of the load factor defining LS3 for the eight sets of models and the four intervals associated to the four vulnerability classes (A, B, C and D). The range of variation is not exactly the same for all the sets of models. The models that do not take into account the diaphragm effect (*RE* and *STM* sets of models) are the most sensitive to the variations of the number of floors and show the widest ranges. However, the ranges are rather similar for all sets and they lead to the same definition of the seismic vulnerability classes. There are no discrepancies that had to be solved.

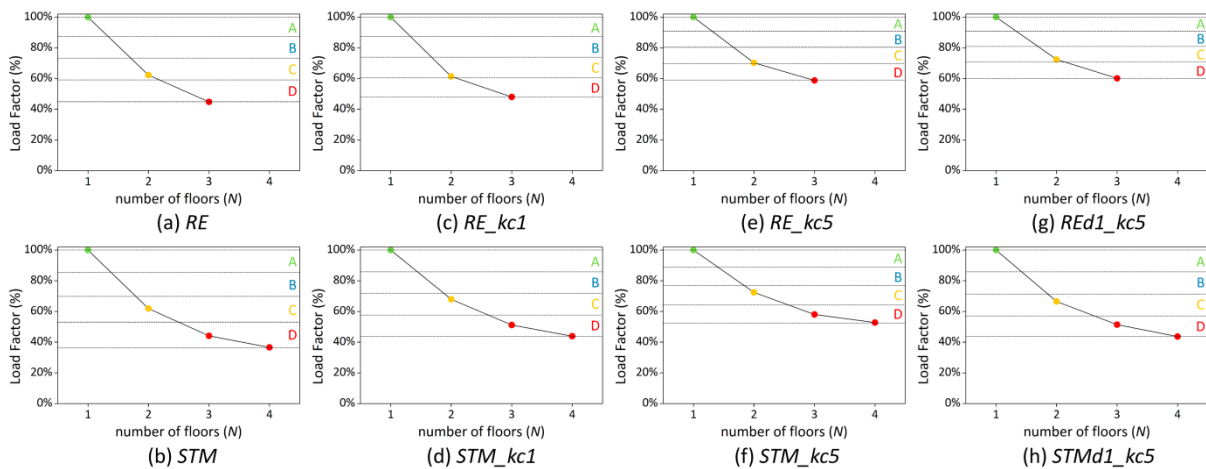


Figure 4.47: Variation of the load factor leading to the attainment of the maximum capacity (LS3) for the eight sets of models evaluated: (a) *RE*; (b) *STM*; (c) *RE_kc1*; (d) *STM_kc1*; (e) *RE_kc5*; (f) *STM_kc5*; (g) *REd1_kc5*; and (h) *STMd1_kc5*

Table 4.20 provides the range of number of floors (N) that delimits each seismic vulnerability class. The values used to define the proposed classification range between 1 and 4 floors, since this is the typical range that can be observed in vernacular architecture. It should be remarked that the present classification is far more restrictive than others proposed by other authors (Vicente 2008). Table 4.21 shows a comparison of the values proposed here with the values proposed by Vicente (2008), who also took into consideration the number of floor of the buildings as a parameter. This is due to the fact that vernacular buildings are usually made of traditional materials and rarely raise more than three or four stories. The higher number of floors typically proposed by other authors is again not representative for vernacular buildings. This is also the reason why the classification was reduced down to three classes, since two-floor buildings already present a highly reduced maximum capacity when compared with one-floor buildings. Thus, they are considered directly as Class C. Similarly, three-floor buildings cannot be considered higher than class D as they greatly reduce the maximum capacity of the building. This way the new classification proposed is adapted the typical characteristics of vernacular architecture.

Table 4.20: Vulnerability classes proposed according to the number of floors (N)

P8. Number of floors	
Class	Description
A	1 floor
B	-
C	2 floors
D	≥ 3 floors

Table 4.21: Comparison among vulnerability classes proposed by other authors for similar vulnerability index formulations that have taken into account the number of floors (N) as a parameter

P8. Number of floors		
Class	Classification proposed	Vicente (2008)
A	$N = 1$	$N = 1$
B	-	$2 \leq N \leq 3$
C	$N = 2$	$4 \leq N \leq 5$
D	$N \geq 3$	$N \geq 6$

4.11. Seismic vulnerability classes according to the previous structural damage (P9)

Six reference models with varying number of floors, type of diaphragm and distribution of wall openings were prepared for the analysis of the influence of P9 (Figure 4.48): (a) one-floor rammed earth building with flexible diaphragm and reduced number of wall openings (*RE1F_IP9*); (b) one-floor rammed earth building with flexible diaphragm and moderate number of wall openings (*RE1F_IP18*); (c) one-floor rammed earth building with rigid diaphragm and high number of wall openings (*RE1Fd1_IP26*); (d) two-floor rammed earth building with flexible diaphragm and high number of wall openings (*RE2F_IP32*); (e) two-floor rammed earth building with flexible diaphragm and very high number of wall openings (*RE2F_IP39*); and (f) two-floor rammed earth building with rigid diaphragm and high number of wall openings (*RE2Fd1_IP31*). The walls of all models are 0.5 m thick. The ground floor walls of the models are 3 m high, while the walls at the upper floor of the two-floor buildings are 2.6 m high. The in-plan area is variable. The in-plan area of the models with flexible diaphragm (*RE1F_IP9*, *RE1F_IP18*, *RE2F_IP32* and *RE2F_IP39*) is $8 \times 5.5 \text{ m}^2$ and the in-plan area of the models with rigid diaphragm (*RE1Fd1_IP26* and *RE2Fd1_IP31*) is $8 \times 10.5 \text{ m}^2$. For all the models, the roof is simply modelled as distributed load along the walls and, for those models where the diaphragm is not modelled, the floor is also simply simulated as a vertical distributed load applied on top of the walls.

As previously discussed in Chapter 3, previous cracks at the structural load bearing walls increase their vulnerability and can anticipate the failure of the building. Thus, in order to assess

the influence of this parameter, a fixed initial level of damage is firstly imposed on the structural walls before carrying out the pushover analysis. Three different levels of damage are initially imposed to each reference model by means of another pushover analysis performed in the perpendicular direction. The levels of damage imposed are based on the classification of damage according to existing cracks shown in Chapter 3 (Table 3.5): (a) the structure is loaded until the development of fine cracks below 1 mm (slight damage); (b) the structure is loaded until moderate cracks between 1 and 5 mm develop (moderate damage); and (c) the structure is loaded until large cracks over 5 mm develop (severe damage). In summary, a phased analysis is performed in two steps: (1) first, a pushover analysis is carried out in one direction gradually until reaching a specific level of damage (marked in blue in Figure 4.48); and (2) the pushover analysis load is applied progressively in the perpendicular direction until failure (marked in red in Figure 4.48). The application of an initial load in the direction perpendicular to the main direction of the analysis is intended to impose a level of damage on the building that do not activate the same resisting mechanisms that will be activated during the main analysis. Thus, the initial level of damage is not directly related with the damage that will be caused by the main pushover analysis and tries to simulate random damage that can be observed in existing buildings.

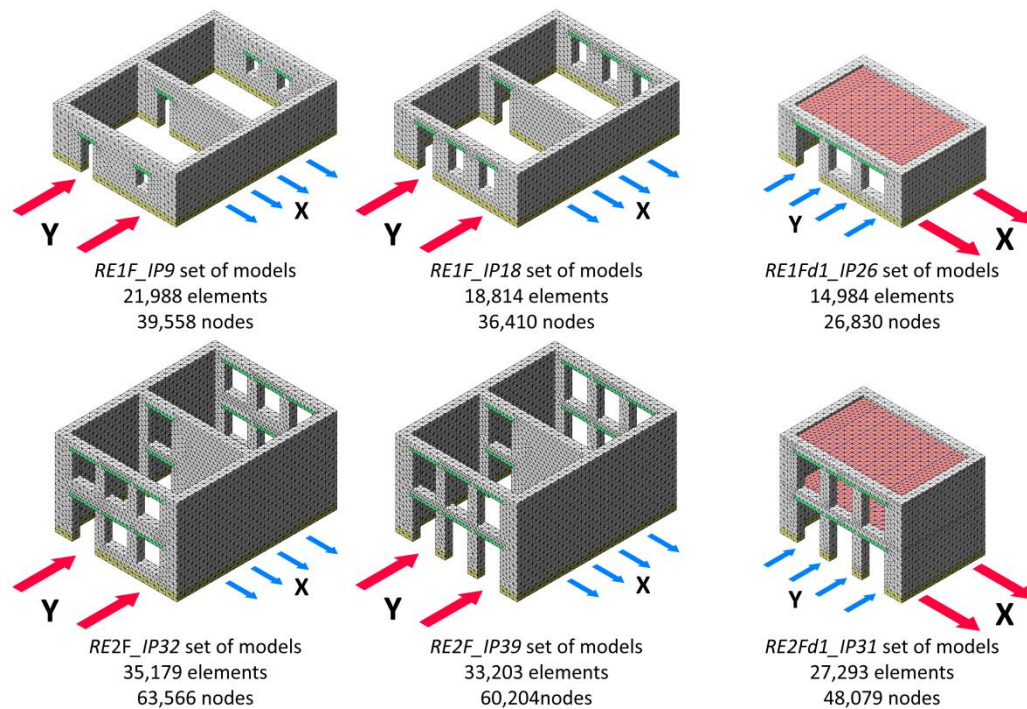


Figure 4.48: Numerical models built in order to assess the influence of the previous structural damage on the seismic behavior of vernacular buildings

The four sets of models with flexible diaphragm (*RE1F_IP9*, *RE1F_IP18*, *RE2F_IP32* and *RE2F_IP39*) were analyzed in the direction perpendicular to the walls with the maximum wall span (Y), in order to understand the influence of previous structural damage when the building is expected to show an out-of-plane failure mode. Therefore, the initial load is applied by means of a

pushover analysis in X direction. The two sets of models with rigid diaphragm (*RE1Fd1_IP26* and *RE2Fd1_IP31*) were analyzed in the direction parallel to the walls with openings (X), in order to understand the influence of the previous structural damage when the building is more prone to present in-plane collapse mechanisms. Therefore, the initial load is applied by means of a pushover analysis in Y direction. Table 4.22 presents a summary of the 24 models finally built for the evaluation of the previous structural damage.

Table 4.22: Summary of the 24 different models built in order to assess the influence of the previous structural damage on the seismic behavior of vernacular buildings

Set of models	Number of floors		In-plane area of wall openings	Previous structural damage			
	(N)	Type of diaphragm		Maximum crack width, <i>w</i> (mm)			
			IP (%)	0	0-1	1-5	>5
<i>RE1F_IP9</i>	1	Flexible	9	X (Ref)	X	X	X
<i>RE1F_IP18</i>	1	Flexible	18	X (Ref)	X	X	X
<i>RE1Fd1_IP26</i>	1	Rigid	26	X (Ref)	X	X	X
<i>RE2F_IP32</i>	2	Flexible	32	X (Ref)	X	X	X
<i>RE2F_IP39</i>	2	Flexible	39	X (Ref)	X	X	X
<i>RE2Fd1_IP31</i>	2	Rigid	31	X (Ref)	X	X	X

4.11.1. Variations on damage patterns and failure mechanisms

The most representative failure mechanisms obtained for the six sets of models analyzed are shown in Figure 4.49. The resisting mechanisms observed in the different buildings depend greatly on the distribution of wall openings and the type of horizontal diaphragm. Since the initial level of damage is also imposed by means of a pushover analysis, the main cracks defining this damage also depend on initial geometrical and constructive characteristics of the different models. For the six sets, the prevailing failure mode does not vary for the four models within each set. Nevertheless, when increasing the level of initial damage induced, the damage at the ultimate limit state of the analysis is more widespread and involves more structural elements. The integrity of some structural elements is compromised due to the imposed initial damage. When the building is initially loaded in a specific direction, the resisting elements in that direction exhibit significant damage and incipient failure mechanisms that did not take place when the analysis is carried out on the initially undamaged building. Indeed, if this initial level of damage is severe, some structural elements are incapable of performing their resisting role when loaded in the perpendicular direction, resulting in changes in the damage patterns and failure mechanisms obtained.

For example, for the *RE1F_IP9* set of models, the failure mode observed for the undamaged building ($w = 0$) is the clear out-of-plane mechanism leading to the overturning of the exterior wall perpendicular to the seismic load (Figure 4.49a). However, the initial damage imposed in X direction induced cracking at all the walls parallel to this direction. As a result, the resisting

capacity of these walls is compromised and they also show significant out-of-plane damage at the ultimate limit state when performing the pushover analysis in Y direction, see buildings with $0 < w < 1 \text{ mm}$ and $w > 5 \text{ mm}$ in Figure 4.49a. Very similar variations in the damage patterns occurs for the *RE1F_IP18* set of models.

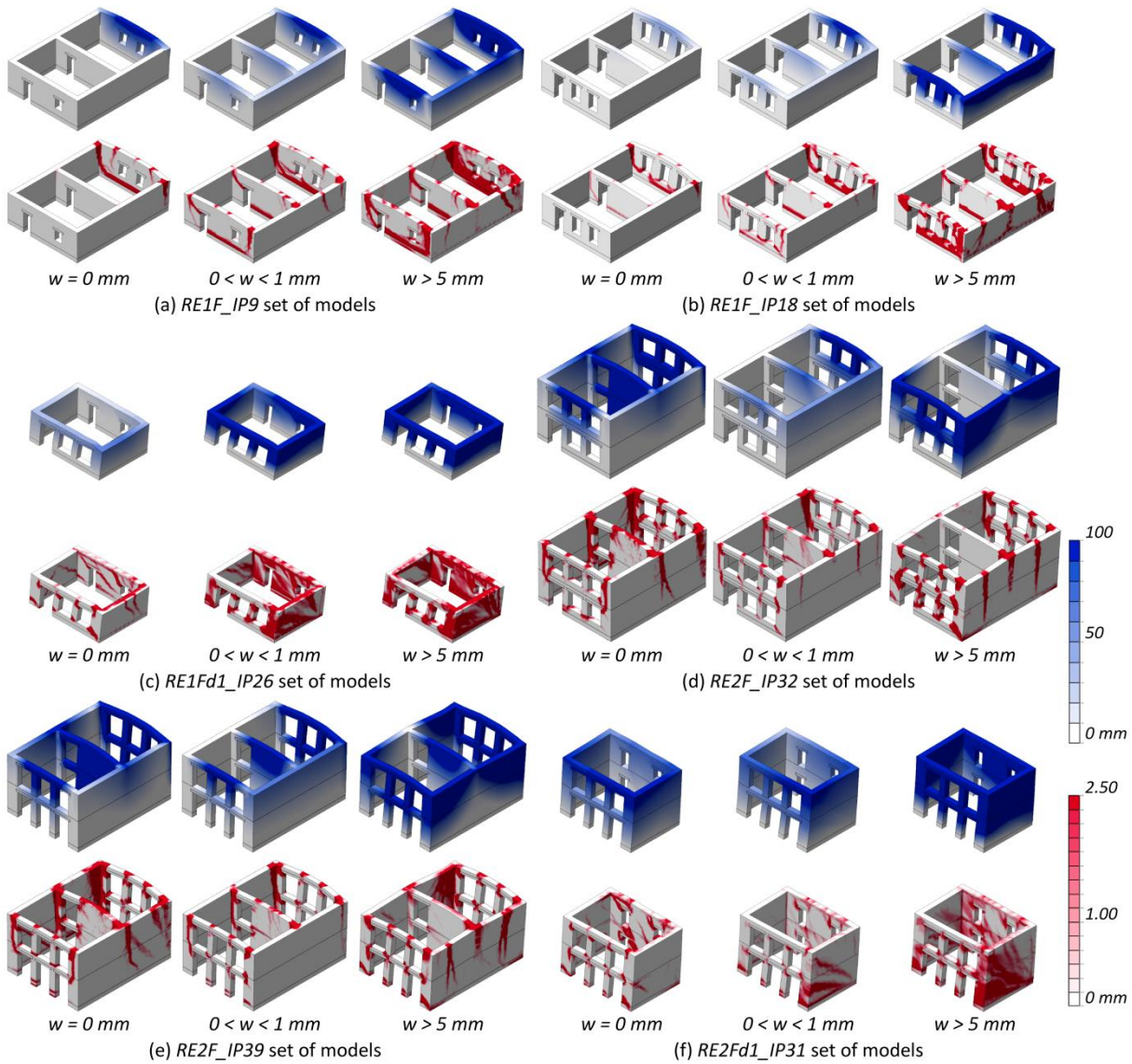


Figure 4.49: Representative failure modes at ultimate limit state (LS4) obtained for several buildings with varying initial level of damage (according to maximum initial crack size, w) within each of the six sets of model analyzed: (blue) maximum total displacements; and (red) crack pattern (crack width scale)

In the case of the two-floor sets of models with flexible diaphragm (*RE2F_IP32* and *RE2F_IP39*), the imposed initial damage caused significant widespread in-plane damage at the walls due to the high number of wall openings. As a result, the capacity of these walls is compromised and show extensive out-of-plane bending damage at the ultimate states, instead of the characteristic cracking at the connection between perpendicular walls observed in undamaged models (Figure 4.49d,e). For the models presenting a rigid diaphragm (*RE1Fd1_IP26* and

RE2Fd1_IP31), the main consequence of imposing an initial level of damage to the buildings is the extension of the damage, which is much more widespread. Damage can be observed at all the walls, not only at those parallel to the seismic load, but failure is governed by in-plane mechanisms in all cases (Figure 4.49c,f).

4.11.2. Building of capacity curves and analysis of load factor variations

Figure 4.50 shows the four-linear capacity curves derived from the pushover analyses performed, grouped by set of models. The quantitative measure used for the assessment of the influence of the previous structural damage on the global seismic behavior of vernacular buildings is the maximum initial crack size imposed to the model. The patterns of variation differ between the six sets of models, but it is clear that the seismic behavior is greatly affected when considering different levels of initial damage. The maximum capacity of the buildings decreases progressively when increasing the initial level of damage. The range of variation is wider for some sets than others. For instance, the *RE1F_IP9* set of models is less sensitive to the variations in the previous structural damage than the others (Figure 4.50a). This is probably due to the fact that the initial cracks imposed during the first part of the analysis are more localized and do not affect the resisting mechanisms that the building develops in the second part of the analysis, when loaded in the perpendicular direction. For the remaining sets of models, the damage initially imposed in the building is much widespread (either due to the rigid diaphragm or the high number of wall openings). Thus, the resisting mechanisms of the buildings are weakened and their maximum capacity decreases more significantly.

As expected, the initial stiffness is also greatly affected by the level of initial level of damage imposed to the building. This damage is typically enough for the building to present a nonlinear response from the beginning. As a result, there is a gradual loss of stiffness when increasing the initial level of damage. For example, this is very evident for the *RE1Fd1_IP26*, *RE2F_IP32* and *RE2F_IP39* sets of models (Figure 4.50c,d,e). The extensive damage imposed at all the structural elements of the building at the first part of the analysis ($w > 5$ mm) causes the building to be on the inelastic range since the beginning, with the consequent notable loss of initial stiffness.

There are also notable differences in post-peak behavior of the building, which illustrates the changes in the failure mechanisms previously observed. For example, the undamaged building within the *RE1F_IP18* set shows a greater out-of-plane resistance than the remaining models from the set. However, the failure mode observed is much localized and only involves the out-of-plane overturning of the exterior wall perpendicular to the seismic load (Figure 4.49b). When the initial level of damage increases, the resisting capacity of the other walls perpendicular to the seismic load decreases and they also show significant out-of-plane damage at failure. As a result, all the walls are involved in the resisting mechanism, which show larger deformations before reaching the collapse and the damage is more widespread. This leads to the gradually more

ductile behavior that can be observed when increasing the initial level of damage in the models within the *RE1F_IP18* set (Figure 4.50b).

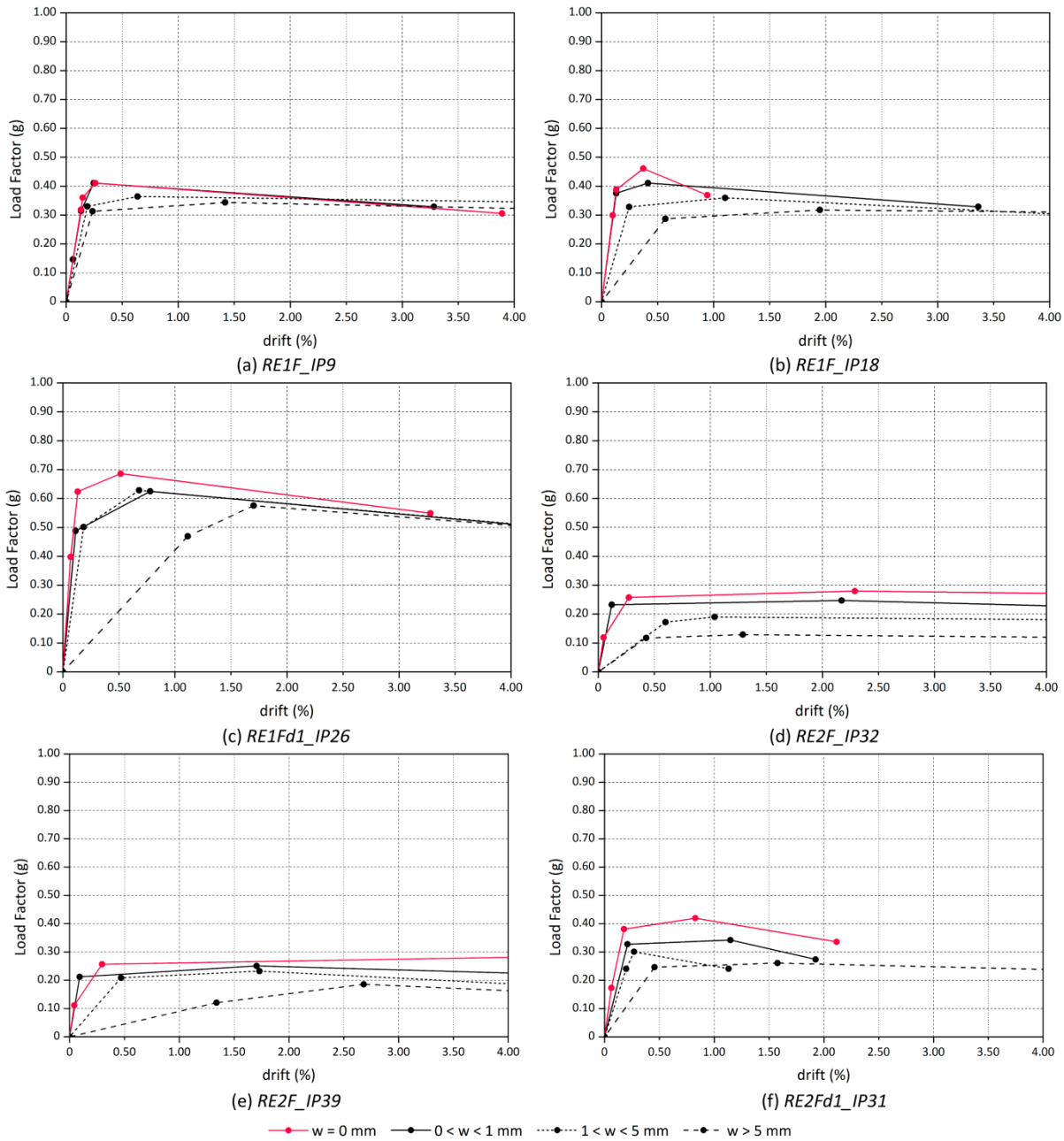


Figure 4.50: Four-linear capacity curves constructed for the six sets of models: (a) *RE1F_IP9*; (b) *RE1F_IP18*; (c) *RE1Fd1_IP26*; (d) *RE2F_IP32*; (e) *RE2F_IP39*; and (f) *RE2Fd1_IP31*

The variations of the load factors defining each limit state obtained for the six sets of models are shown in Figure 4.51. The variations were normalized using the initially undamaged models, which showed the maximum capacity. The diagrams show the decrease in the load factor when increasing the initial damage imposed to the structure and confirm its influence on the global seismic behavior of the buildings. Nevertheless, the level of variation differs among the different

models. This can be mainly attributed to the damage imposed initially, which, for some sets of models, affects structural elements that are critical in resisting the seismic load applied in the second part of the analysis.

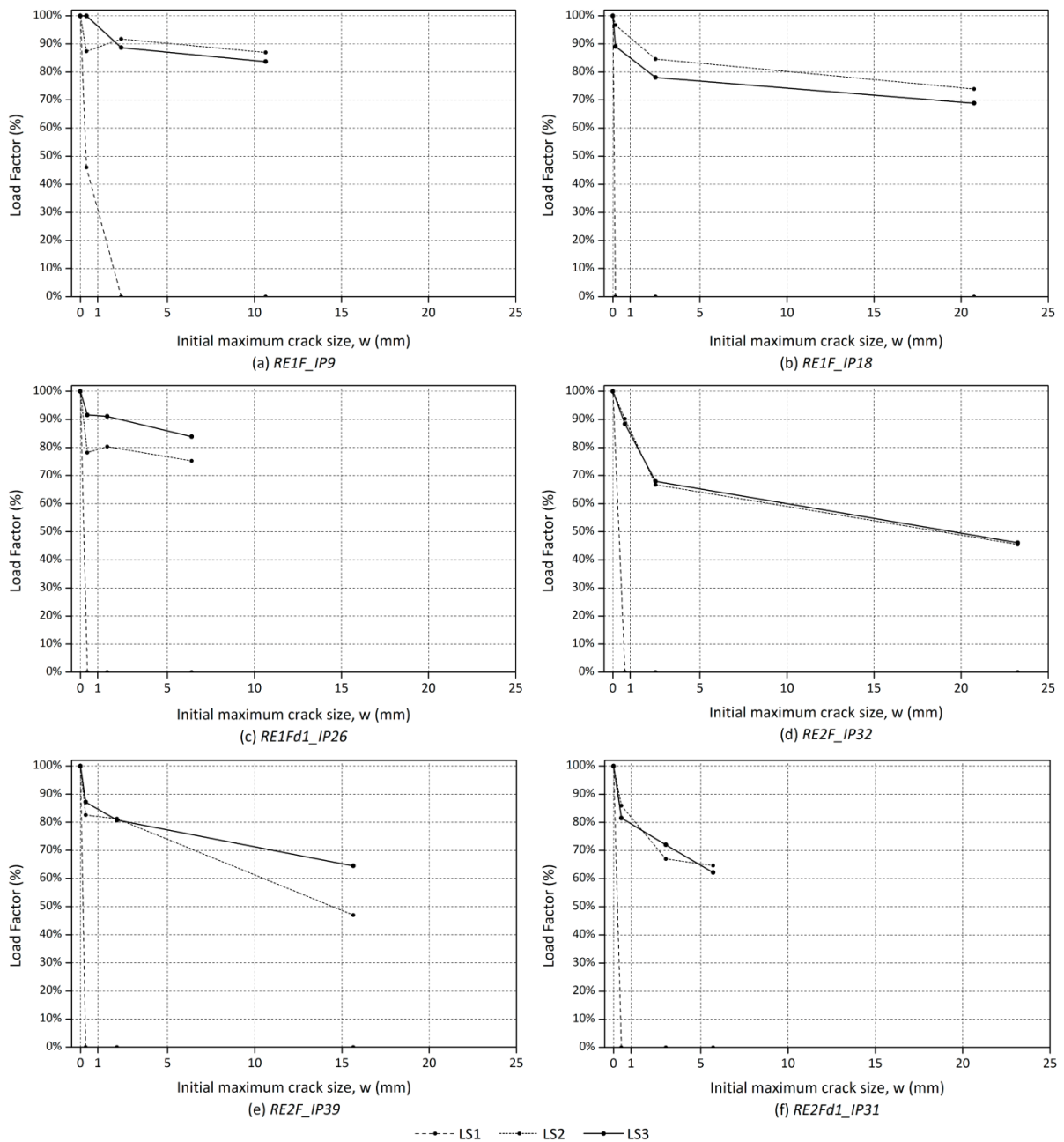


Figure 4.51: Load factor variations for each limit state for the six sets of models: (a) *RE1F_IP9*; (b) *RE1F_IP18*; (c) *RE1Fd1_IP26*; (d) *RE2F_IP32*; (e) *RE2F_IP39*; and (f) *RE2Fd1_IP31*

As an example, in the case of the previously discussed *RE1F_IP9* set, the initially imposed damage does not affect the most important structural elements resisting the seismic load in the orthogonal direction and the capacity of the building is not as much compromised, leading to a narrower range of variation (Figure 4.51a). On the other hand, for the sets of models with two-

floor buildings, where the initially imposed damage is widespread and affects several structural elements that are critical in resisting the seismic load in the perpendicular direction, there is a significant decrease in the maximum capacity of the building and more important variations in terms of load factors (Figure 4.51d,e,f). It should be noted that because of the initial level of structural damage, some models reach LS1 since the beginning of the analysis. That is why the load factor defining LS1 is 0 except for the initially undamaged model.

4.11.3. Definition of seismic vulnerability classes

The four seismic vulnerability classes are defined according to the variation of the load factor corresponding to the attainment of LS3. Figure 4.52 shows the variation of the load factor defining LS3 for the two sets of models and the four intervals associated to the four vulnerability classes (A, B, C and D). Even if the range of variation is very variable, the vulnerability classes obtained for the different sets of models are mainly the same. In the case of some of the discrepancies encountered, the most unfavorable class was considered. For example, for the *RE1F_IP9* and *RE2F_IP32* sets, the building with $0 < w < 1$ mm lies within class A, but the same building lies within class B for the *RE1F_IP18*, *RE1Fd1_IP26*, *RE2F_IP39* and *RE2Fd1_IP31* sets. Therefore, previous structural damage with small cracks ($0 < w < 1$) are finally considered within class B.

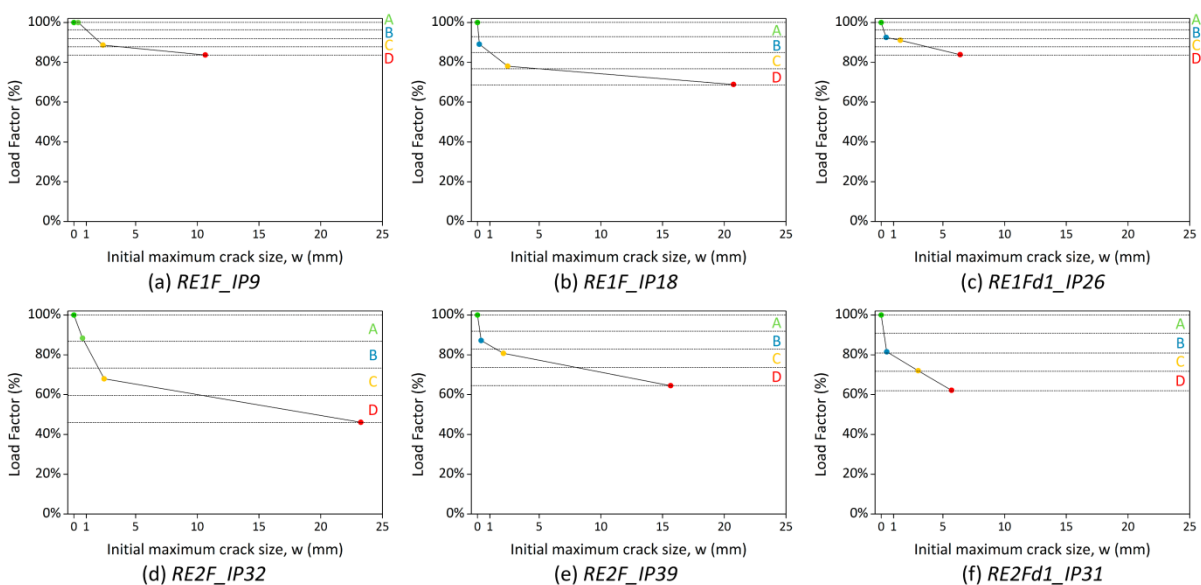


Figure 4.52: Variation of load factor leading to the attainment of the maximum capacity (LS3) for the six sets of models: (a) *RE1F_IP9*; (b) *RE1F_IP18*; (c) *RE1Fd1_IP26*; (d) *RE2F_IP32*; (e) *RE2F_IP39*; and (f) *RE2Fd1_IP31*

Table 4.23 shows the final classification proposed for P9. The classification is defined in terms of the visible damage observed in the building. A qualitative description of the damage that is associated to each seismic vulnerability class is thus provided. Additionally, the table specifies a range of values with an estimation of the crack widths that delimit each seismic vulnerability

class (in mm). The visual inspection of the buildings should thus be carried along with a proper damage survey of the building. The threshold values are compared in Table 4.24 with other classifications proposed by other authors in existing seismic vulnerability index formulations that provide this information (Benedetti and Petrini 1984; Vicente 2008; Shakya 2014). Despite slight differences, the classifications show a good agreement with the classification proposed here.

Table 4.23 :Vulnerability classes proposed according to the previous structural damage

P9. Previous structural damage	
Class	Description
A	Structural load bearing walls are in good condition with no visible damage
B	Structural load bearing walls present not widespread hairline and small cracks (≈ 1 mm or less) , and/or slight signs of deformation in the structural elements (drifts below 0.1%)
C	Structural load bearing walls present a poor state of conservation showing moderate cracks ($\approx 1-5$ mm) and/or relevant signs of deformation in the structural elements (drifts between 0.1-0.5%)
D	Structural load bearing walls present a state of severe deterioration with widespread damage. There are large structurally compromising cracks (> 5 mm) at critical locations, such as near the corners, indicating a sign of disconnection between orthogonal walls. There are severe signs of deformation in the structural elements, such as out-of-plumb walls or bulging of the load bearing walls (drifts over 0.5%)

Table 4.24: Comparison among vulnerability classes proposed by other authors for similar vulnerability index formulations that have taken into account the previous structural damage as a parameter and provided range of values of crack width (w) to delimit the classes

P9. Previous structural damage				
Class	Classification proposed	Benedetti and Petrini (1984)	Vicente (2008)	Shakya (2014)
A	$w = 0$	$w = 0$	$w = 0$	$w = 0$
B	$0 < w \leq 1$	-	$0 < w \leq 0.5$	$0 < w \leq 0.5$
C	$1 < w \leq 5$	$w = 2-3$	$w = 2-3$	$w = 2-3$
D	$w > 5$	-	-	-

4.12. Seismic vulnerability classes according to the in-plane index (P10)

Four reference models with varying maximum wall span perpendicular to the loading direction, number of floors and distribution of wall openings were prepared for the analysis of the influence of P10 (Figure 4.53): (a) one-floor rammed earth without wall openings in the in-plane walls and maximum wall span of 7 m (*RE1Fd1*); (b) two-floor rammed earth building without wall openings in the in-plane walls and maximum wall span of 7 m (*RE2Fd1*); (c) two-floor rammed earth building with 35% of wall openings in the in-plane walls and maximum wall span of 4.5 m (*RE2Fd1_IP35*); and (d) two-floor rammed earth building with 55% of wall openings in the in-plane walls and maximum wall span of 4.5 m (*RE2Fd1_IP55*). The walls of the one-floor models are 3 m high. The ground floor walls of the two-floor models are 3 m high, while the walls at the upper floor are 2.6 m high. All walls are 0.5 m thick and the in-plan area of the reference models is 8×5.5 m². For all the models, the roof is simply modelled as distributed load on top of the walls.

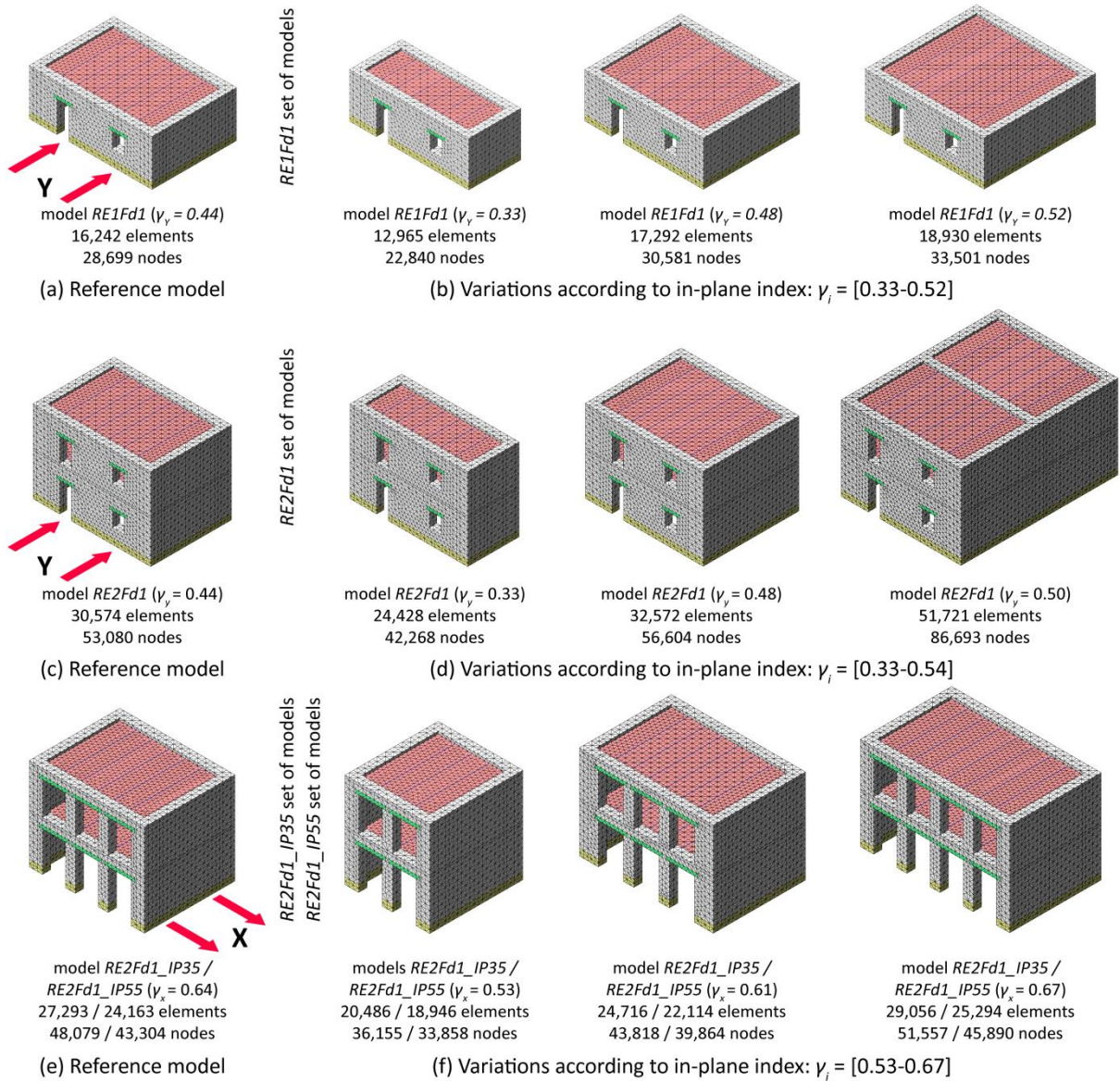


Figure 4.53: Numerical models built in order to assess the influence of the in-plane index (γ_i) on the seismic behavior of vernacular buildings: (a) reference models; (b) examples of variations of in-plane index modelled

As previously discussed in Chapter 3, the in-plan index (γ_i) intends to characterize the ability of a vernacular building to resist the seismic action through the development of in-plane resisting mechanisms of the shear walls parallel to the seismic load. It was defined as the ratio between the in-plane area of earthquake resistant walls in the direction under evaluation and the total in-plane area of earthquake resistant walls. Generally, these shear walls are only effective in contributing to the global seismic resistance of the building if premature out-of-plane failure mechanisms are prevented. This is typically only possible in cases where the building presents sufficiently stiff diaphragms that allow involving all walls in the seismic response of the building, ensuring the activation of the in-plane resisting walls. That is why the four reference models were prepared considering rigid diaphragms (Figure 4.53).

In order to assess the influence of the in-plane index (γ_i) on the seismic behavior of vernacular buildings, γ_i is increased and decreased within a range between 0.33 and 0.67 by increasing or decreasing the length of the earthquake resistant walls parallel to the loading direction. Thus, the in-plan area of the different models within the set varies along with the variations of the in-plan index. It should be noted that the whole range of variation is not covered by all the sets because it would lead to unreal geometrical configurations. Thus, for example, the γ_i from the *RE1Fd1* set of models only varies within a range between 0.33 and 0.52 (Figure 4.53b), while the *RE2Fd1_IP35* varies between 0.53 and 0.67 (Figure 4.53f). It should be also mentioned that *RE2Fd1_IP55* set only differs from *RE2Fd1_IP35* set in the amount of walls in the back wall and that is why they are shown together in Figure 4.53e,f. The models were analyzed in the direction parallel to the walls whose length is being modified. This direction was selected in order to vary the in-plan index, while keeping fixed the maximum wall span (s) of the wall prone to out-of-plane movements. Thus, *RE1Fd1* and *RE2Fd1* were analyzed in Y direction, while *RE2Fd1_IP35* and *RE2Fd1_IP55* were analyzed in X direction. Table 4.25 presents a summary of the 23 models finally built for the evaluation of this parameter.

Table 4.25: Summary of the 23 different models built in order to assess the influence of the in-plane index (γ_i) on the seismic behavior of vernacular buildings

Model name	Set of models				In-plan area length x width (m ²)	In-plan index (γ_i)
	<i>RE1Fd1</i>	<i>RE2F1</i>	<i>RE2Fd1_IP35</i>	<i>RE2Fd1_IP55</i>		
<i>L2_5</i>	X	X			8 x 3.5	0.33
<i>L3_5</i>	X	X			8 x 4.5	0.39
<i>L4_5 (Ref)</i>	X	X			8 x 5.5	0.44
<i>L3_5x2</i>		X			8 x 8.5	0.45
<i>L5_5</i>	X	X			8 x 6.5	0.48
<i>L4_5x2</i>		X			8 x 10.5	0.50
<i>L6_5</i>	X	X			8 x 7.5	0.52
<i>L5_5x2</i>		X			8 x 12.5	0.54
<i>L4</i>			X	X	5 x 5.5	0.53
<i>L5</i>			X	X	6 x 5.5	0.57
<i>L6</i>			X	X	7 x 5.5	0.61
<i>L7 (Ref)</i>			X	X	8 x 5.5	0.64
<i>L8</i>			X	X	9 x 5.5	0.67

4.12.1. Variations on damage patterns and failure mechanisms

The most representative failure mechanisms for the four sets of models analyzed are shown in Figure 4.54. The failure modes obtained vary depending on the geometry of the different models and the direction of the load. Nevertheless, for the four sets, the prevailing failure mode does not vary for the different models within each set, varying γ_i . Given the presence of the rigid diaphragms in all buildings, the failure mode typically involves the development of in-plane mechanisms at the walls parallel to the seismic load.

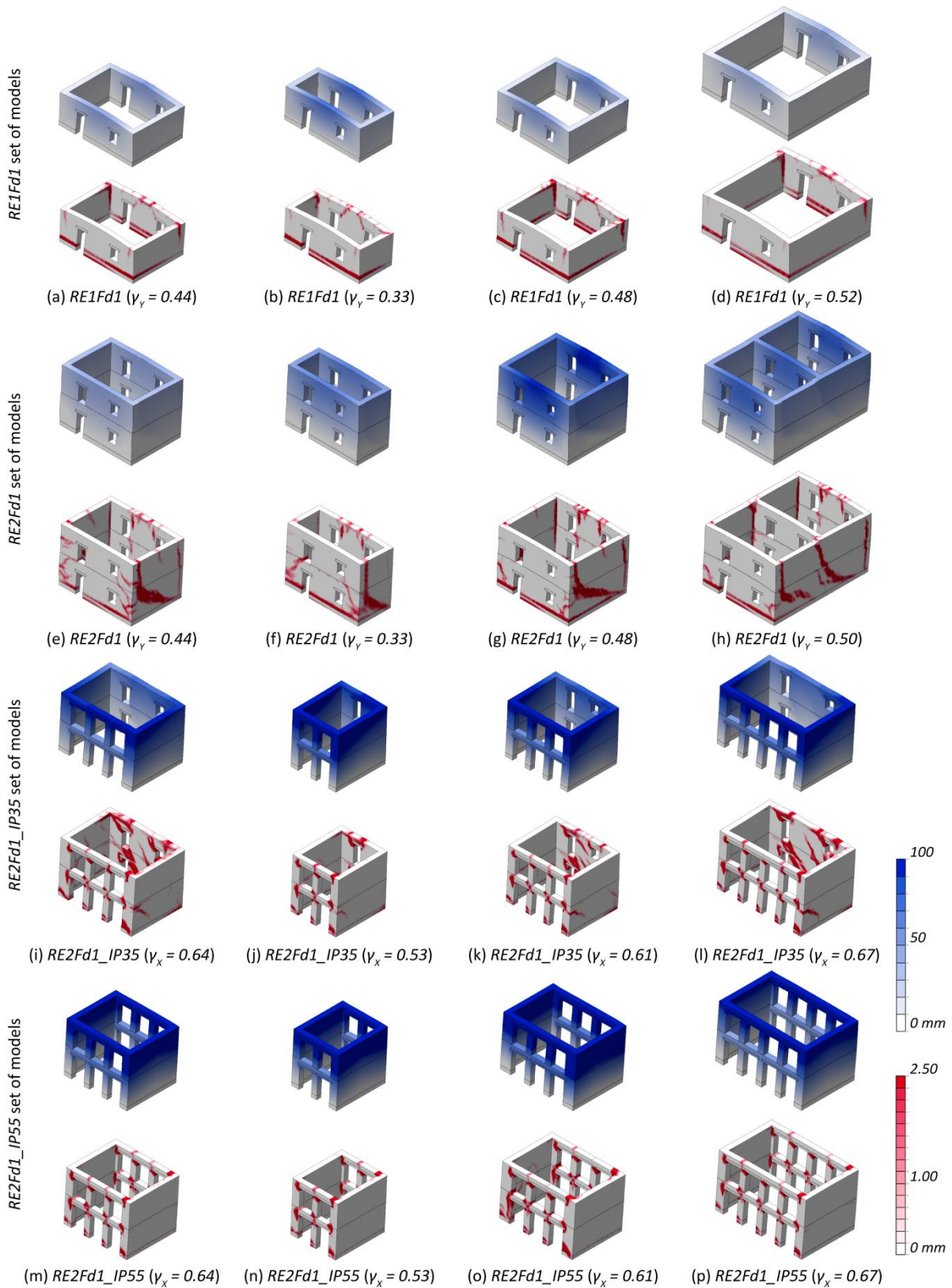


Figure 4.54: Representative failure modes at ultimate limit state (LS4) obtained for several buildings with varying in-plane index (γ_i) within the four sets of models analyzed: (blue) maximum total displacements; and (red) crack pattern (crack width scale)

The characteristic shear failure is particularly evident when the buildings present a high number of wall openings at the in-plane walls (*RE2Fd1_IP35* and *RE2Fd1_IP55* sets of models), where the cracks follow the distribution of the openings (Figure 4.54i-p). The models within the *RE2Fd1* set also show the characteristic diagonal shear cracking at the walls parallel to the seismic load, illustrating the development of an in-plane mechanism. However, there is also widespread out-of-plane bending damage at the walls perpendicular to the seismic load and a significant horizontal crack at the base (Figure 4.54e-h). This crack illustrates that the rigid diaphragm is inducing a global overturning mechanism of the whole building. The type of failure does not vary for the different models within the set. For the *RE1Fd1* set, there are not variations in the damage pattern or failure mechanism observed in the different models, but the failure mode does not consist of an in-plane type. Because of the reduced dimensions and the presence of the diaphragm, the buildings behave as a unit and show a global rotation as the main failure mechanism. This is again illustrated by the horizontal crack at the connection between the rammed earth walls and the stone masonry base which also extends throughout the walls parallel to the seismic load (Figure 4.54a-d).

4.12.2. Building of capacity curves and analysis of load factor variations

Figure 4.55 presents the four-linear capacity curves constructed from the pushover analyses performed, grouped by set of models. There are variations in the seismic capacity of the buildings within the four sets of models evaluated. The capacity decreases gradually when decreasing the in-plane index (γ_i). However, apart from the seismic load capacity, the diagrams indicate that there are no significant changes in the behavior of the buildings when decreasing γ_i , in terms of ductility or initial stiffness. This can be also related to the fact that there were no variations in the failure mode observed at the different buildings within each set (Figure 4.54).

The variation is much more relevant in the case of the sets where the buildings have shear walls without openings (Figure 4.55a,b). As an example, increasing γ_i from 0.33 to 0.55 in the *RE2Fd1* set of models leads to double the maximum capacity of the building. On the other hand, the range of variation obtained for the models with a high number of openings (*RE2Fd1_IP35* and *RE2Fd1_IP55*) is notably narrower (Figure 4.55c,d). The in-plane index ratio mainly takes into account the global shear resistance of the building, which is mainly given by the shear capacity of the resisting walls parallel to the loading direction. The introduction of a high number of wall openings in the shear walls reduces their in-plane resistance, which increases their vulnerability to seismic actions. As a result, increasing the length of the earthquake resisting walls does not have such a strong influence on increasing the seismic load capacity of the building, since their shear capacity is severely compromised by the presence of openings. This is even more evident in the case of the *RE2Fd1_IP55* set of models, where the influence of the in-plane index (γ_i) is minor, given the great amount of wall openings at the walls.

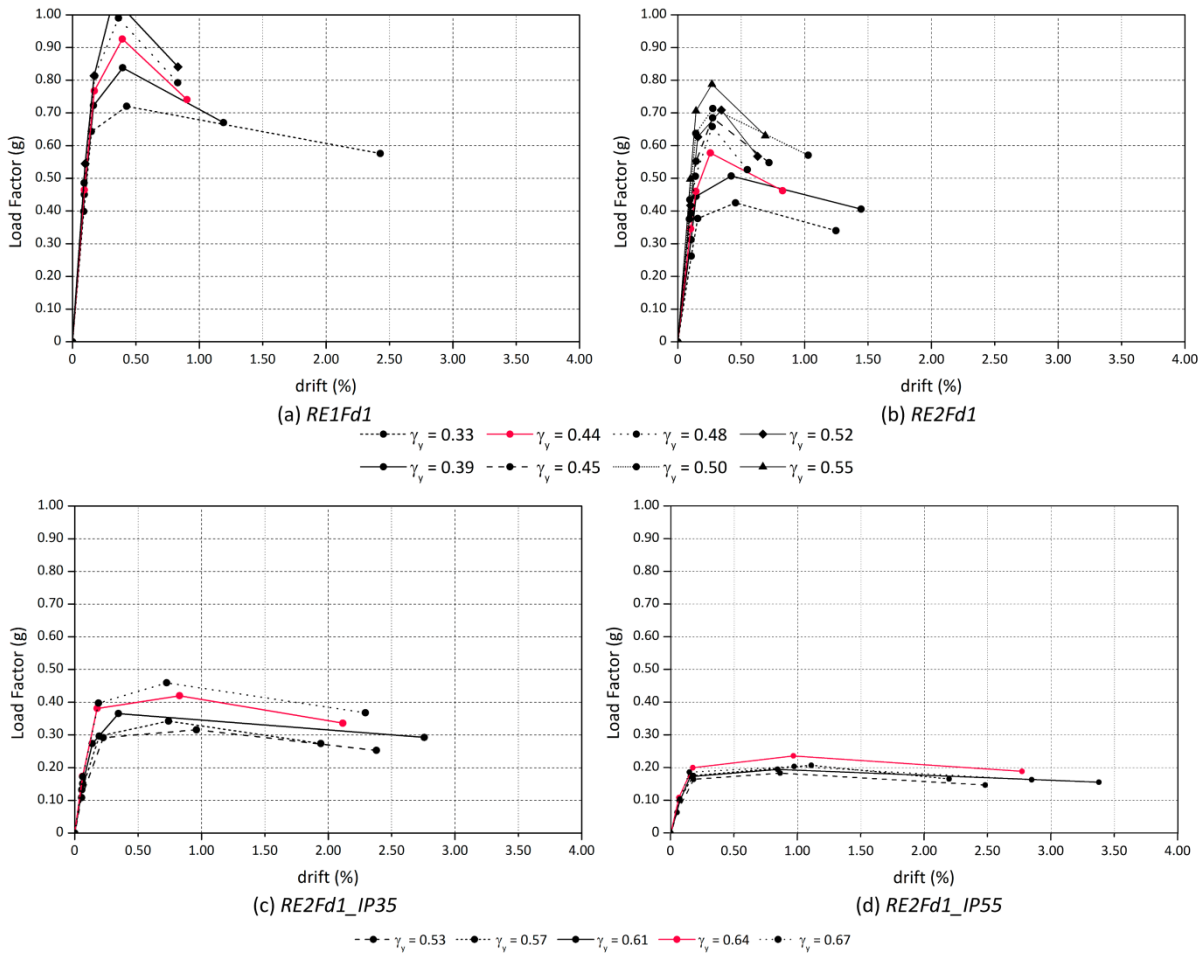


Figure 4.55: Four-linear capacity curves for the four sets of models: (a) *RE1Fd1*; (b) *RE2Fd1*; (c) *RE2Fd1_IP35*; and (d) *RE2Fd1_IP55*

The variations of the load factors defining each limit state obtained for the four sets of models are shown in Figure 4.56. The variations were normalized using the models that showed the maximum capacity within in each set. This model is typically the one with the maximum in-plane index in the evaluated direction for all sets except for the *RE2Fd1_IP55* set. As previously mentioned, for this set, the effect of varying γ_i is marginal. Additionally, the maximum capacity of the model with $\gamma_i = 0.64$ is slightly higher than the maximum capacity of the model with $\gamma_i = 0.67$ (Figure 4.56d). This can be due to the influence of other parameters on the seismic behavior of the building. It should be also taken into account that when varying γ_i , other geometrical parameters are subsequently modified, such as the area of wall openings (P7). The slightly higher ratio of wall openings in the in-plane walls (*IP*) might have led to this small difference. In any case, for the other three sets of models, results show the clear abovementioned decrease of the load factor when decreasing the in-plane index, verifying the influence of this parameter on the seismic behavior of the building. As abovementioned, the decreasing rate is higher in the case of the building presenting walls openings (Figure 4.56a,b).

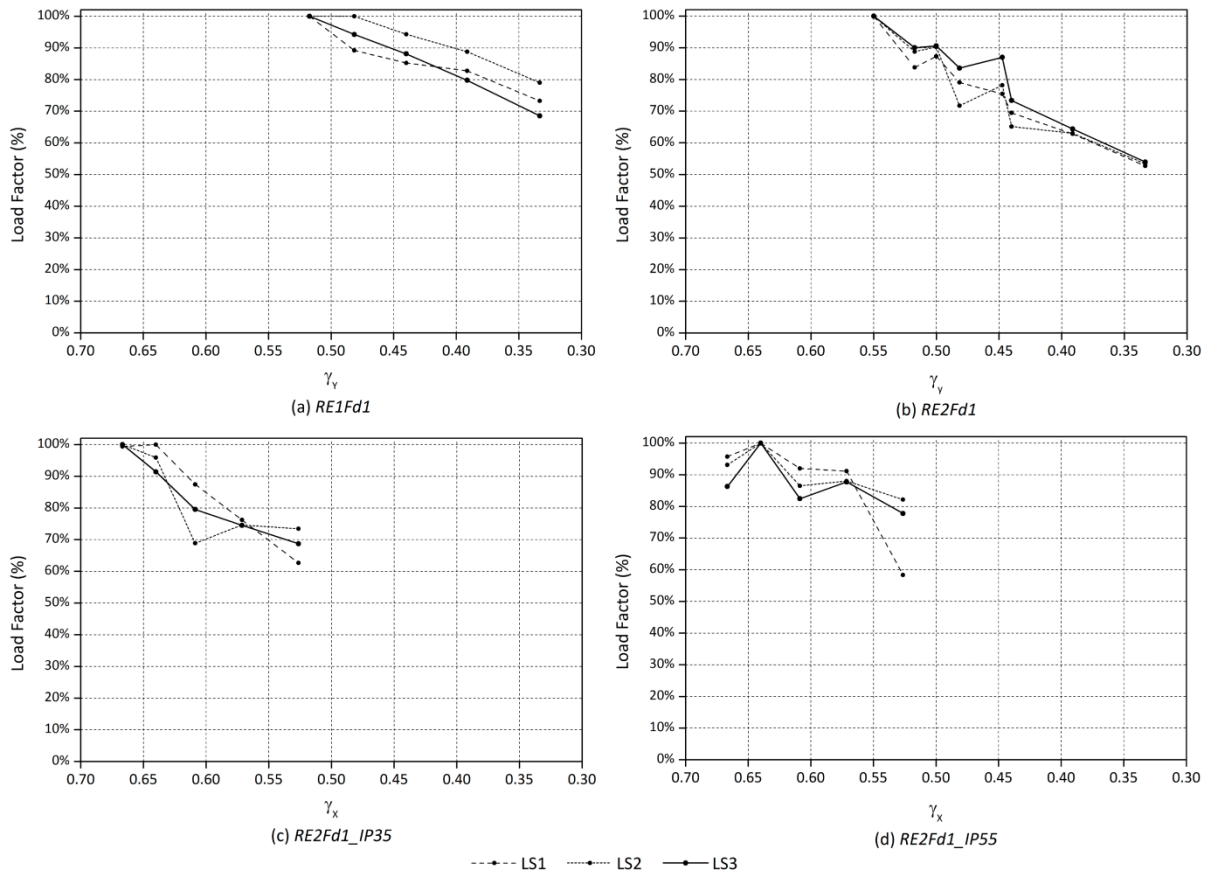


Figure 4.56: Load factor variations for the four sets of models analyzed: (a) *RE1Fd1*; (b) *RE2Fd1*; (c) *RE2Fd1_IP35*; and (d) *RE2Fd1_IP55*

4.12.3. Definition of seismic vulnerability classes

The four seismic vulnerability classes are defined according to the variation of the load factor corresponding to the attainment of LS3. The definition of the four seismic vulnerability classes for vernacular buildings according to the in-plane index (γ_i) is shown in Figure 4.57. As abovementioned, each set by itself cannot cover the full range of variation established for γ_i (between 0.33 and 0.67). That is why the four sets are included within the same graph. This index provides information about the in-plane stiffness of the structure along each main direction. An index of 0.5 indicates that there is a balance in the amount of earthquake resistant walls in each direction. That is why the load factors are re-normalized using the results of the models with $\gamma_i = 0.5$ in the assessed direction in each set. Figure 4.57 shows the variation of the load factor defining LS3 for the four sets of models and the four intervals associated to the four vulnerability classes (A, B, C and D). It should be noted that the model with $\gamma_i = 0.67$ within the *RE2Fd1_IP55* set is not taken into account for the definition of the classes because of the previously commented irregularity that is not considered representative, i.e. it shows a lower maximum capacity than the model with $\gamma_i = 0.64$ (Figure 4.56d). The few discrepancies found are solved by adopting the most unfavorable class. For example, for *RE1Fd1*, the building with $\gamma_i = 0.44$ lies within Class C,

but the same model lies within Class D for *RE2Fd1*. Therefore, $\gamma_i = 0.44$ is finally considered within Class D.

Table 4.26 provides the range of values of the in-plane ratio (γ_i) that delimits each seismic vulnerability class. Since this ratio can be calculated in each loading direction, the final class of the building should be determined for the most unfavorable one, i.e. the direction presenting the lowest in-plane index. It is worth highlighting that, as previously mentioned, the classification is made considering rigid diaphragms, since this is the scenario for which this parameter is relevant. The classification according to this seismic vulnerability parameter implies to know roughly the geometry of the walls, which can be easily obtained from a field visual inspection. It is finally noted that this classification is not directly compared with other classifications from the literature because this parameter is typically taken into account in different ways. Most authors consider the effect of the in-plane index in an indirect way and evaluate it partially when assessing the in-plan irregularities (Benedetti and Petrini 1984; Vicente 2008; Shakya 2014).

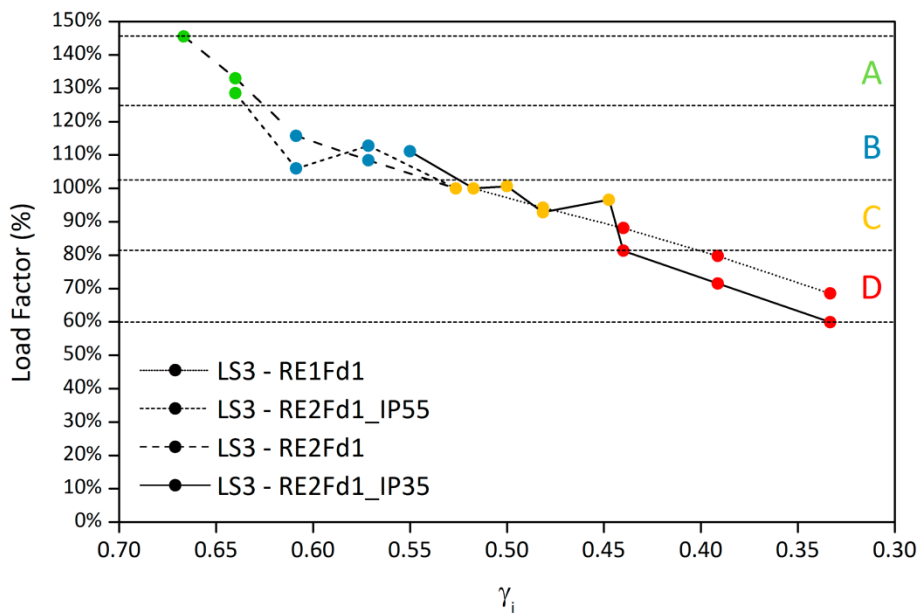


Figure 4.57: Variation of the load factor leading to the attainment of the maximum resistance (LS3) for the four sets of models evaluated

Table 4.26: Vulnerability classes proposed according to the in-plane index (γ_i)

P10. In-plane index	
Class	Description
A	$\gamma_i \geq 0.65$
B	$0.55 \leq \gamma_i < 0.65$
C	$0.45 \leq \gamma_i < 0.55$
D	$\gamma_i < 0.45$

4.13. Conclusions

The influence of the different seismic vulnerability assessment parameters previously selected on the seismic behavior of vernacular buildings has been thoroughly evaluated within this chapter. An extensive numerical parametric study that included the preparation of 277 numerical models has been presented. This study has been primarily useful in two ways. First of all, it helps to validate the selection of the parameters done in the previous chapter, based on expert judgment and literature review. Secondly, the advanced numerical analysis performed on the many models constructed showing different constructive, geometrical and material characteristics that can be typically observed on vernacular structures has been deeply discussed. Thus, this chapter can be considered as a contribution for a better insight of the seismic structural behavior of vernacular buildings, which is one of the objectives of the thesis initially established.

Nevertheless, the main objective of the chapter is to use the results of the numerical analyses to provide a quantitative definition of seismic vulnerability classes for each parameter. Each of the ten parameters has been individually addressed within this chapter from P1 to P10, showing the most representative results obtained in terms of: (a) damage patterns and failure mechanisms; (b) capacity curves and identification of limit states; and (c) load factor variations. As a result of each section, the seismic vulnerability classes were defined and a table was provided showing the classification for each parameter. These tables are meant to serve as reference when performing the seismic vulnerability assessment to define the classes of the buildings evaluated. Therefore, they provide: (1) quantitative ranges of values whenever possible delimiting each parameter class; and (2) qualitative description of the classes that can be useful when doing the assessment in terms of simple visual inspections. The classifications provided in this chapter are specifically adapted to the evaluation of the seismic vulnerability of vernacular architecture, since the ranges of variation within each parameter are defined according to plausible ranges observed in vernacular buildings. Nonetheless, the definition of the classes using analytical methods can be also helpful to strengthen existing classifications in the literature by providing a numerical insight to those classifications that are usually solely based on empirical observations and expert judgment.

CHAPTER 5

DEFINITION OF SEISMIC VULNERABILITY ASSESSMENT PARAMETERS WEIGHTS

Chapter outline

- 5.1. [Introduction](#)
- 5.2. [Construction of the database for the seismic vulnerability assessment methods](#)
 - 5.2.1. [Methodology adopted for the seismic vulnerability parameters weights definition](#)
 - 5.2.2. [Methodology adopted for the development of the SAVVAS method](#)
 - 5.2.3. [Data analysis and extension of the database](#)
- 5.3. [Definition of the parameters weights based on statistical analysis](#)
 - 5.3.1. [Regression coefficients](#)
 - 5.3.2. [Vulnerability index weights](#)
- 5.4. [Definition of the parameters weights based on expert opinion](#)
 - 5.4.1. [Questionnaire survey and Analytical Hierarchy Process \(AHP\) methodology](#)
 - 5.4.2. [Definition of the weights](#)
 - 5.4.3. [Comparison with numerical results](#)
- 5.5. [Seismic vulnerability index for vernacular architecture \(SVIVA\) formulation](#)
- 5.6. [Conclusions](#)

5.1. Introduction

Following the definition of the ten key parameters presented in Chapter 3 and the corresponding seismic vulnerability classes presented in Chapter 4, the present chapter deals with the definition of the weights of each parameter. As explained in Chapter 3 (Table 3.1), the vulnerability index (I_v) is calculated as the weighted sum of the seismic vulnerability assessment parameters. The weights (p_i) are the coefficients that multiply the vulnerability class numeric value (C_{vi}) and, therefore, indicate the relative importance of each parameter in estimating the overall building seismic vulnerability. Parameters weights have been commonly assigned based on expert opinion. The present work proposes to specify the weights that are necessary to complete the SVIVA formulation following two different approaches: (1) statistical analysis; and (2) expert judgment.

The first statistical approach arises from the idea of taking advantage of the large amount of numerical data obtained from the parametric study carried out for the definition of the seismic vulnerability classes (Chapter 4). The information of the numerical models, as well as the results

from the parametric analyses performed on each of them were organized and structured in a wide database. The first section of the present chapter introduces the details of the construction of this database and its purpose, underlying its importance for the development of the two seismic vulnerability assessment methods for vernacular architecture proposed. Actually, it is noted that this database serves also as the basis for the development of the novel SAVVAS method, which is presented in Chapter 6. Therefore, since the database is common for the development of both methods, the present chapter introduces its role on: (a) the definition of the parameters weights for the SVIVA method; and (b) the development of the SAVVAS method.

The chapter then presents the details of the statistical procedure followed for the definition of the parameters weights. This approach consists of analyzing the large database previously assembled using multiple linear regression. This is intended to develop models that are able to estimate the load factors associated to the different limit states (LS), using as input data the seismic vulnerability classes of each parameter. One of the main outcomes of regression analysis is the obtainment of regression coefficients that can be further used to compare the relative strength of the parameters used in the calculation of the seismic vulnerability index. These coefficients can be then associated with the weights of the seismic vulnerability assessment parameters, which enables to their numerical definition.

The second approach followed is based on expert judgment. The importance of the expert opinion on the evaluation of the weights should not be disregarded, since they add an empirical judgment acquired on the basis of investigations of the effect of earthquakes in vernacular constructions. These post-earthquake observations can always complement the results obtained from an analytical approach. In order to collect information from experts on the influence of the selected parameters on the seismic performance of vernacular buildings, a questionnaire survey was developed and distributed to a group mainly formed by academics in the research field from all around the world. The data obtained from the respondents through the survey was analyzed using the Analytical Hierarchy Process (AHP) proposed by Saaty (1987), which allows quantifying the relative importance of the parameters based on subjective opinions. The relative strength of the parameters can again be associated with the weights of the seismic vulnerability assessment parameters and can lead to their numerical definition. As a result, two sets of seismic vulnerability parameters weight (p_i) are obtained following the two distinct approaches. A discussion comparing the results obtained using each approach is thus provided.

Finally, the Seismic Vulnerability Index for Vernacular Architecture (SVIVA) method proposed is considered complete after the definition of the parameters weight. Therefore, the information required to completely define the SVIVA method is summarized and provided at the end of the chapter, namely: (a) the selected parameters; (b) seismic vulnerability classes; (c) parameters weights; and (d) the SVIVA formulation.

5.2. Construction of the database for the seismic vulnerability assessment methods

The pushover parametric study performed and described in detail in Chapter 4 required the construction of more than 300 numerical models with varying geometrical, construction, material and structural characteristics. Subsequently, more than 400 pushover analyses were performed on the different models. The differing characteristics of the numerical models can be defined in terms of the ten key parameters selected. Additionally, the pushover analyses performed provided information about the seismic performance of the different buildings modelled, for different loading directions (X and Y). The seismic response of the buildings was described in terms of load factors that define each limit state expressed in terms of g (LS1, LS2, LS3 and LS4). These two pieces of information from each numerical model (building characteristics and results) were organized and structured for the construction of the database.

The idea behind the construction of a database with the numerical results is to understand the relationships between the parameters, as well as to investigate if these parameters can be used to predict the seismic response of the buildings. The process of extraction of useful information and knowledge from big amounts of data is known as knowledge discovery in databases (KDD) and one of the main steps of the process consists of the application of data mining (DM) algorithms to extract the models or patterns that explain relationships between variables (Fayyad et al. 1996). The employment of these tools can allow analyzing the complex database obtained from the numerical analyses performed, which presents a large number of variables and complex and unclear relationships among them.

The construction of a database for the application of KDD procedures was essential for the development of two tasks, which were carried out following the two clearly defined methodologies that are presented next. First of all, a methodology was defined for the definition of the parameters weights for the SVIVA method. A second methodology was defined for the construction of the regression models that determine the new proposed SAVVAS method.

5.2.1. Methodology adopted for the seismic vulnerability parameters weights definition

The first step of the methodology deals with the organization of the database. For the definition of the parameters weights (p_i), only the results in terms of load factors corresponding to the attainment of LS3 were taken into account. This was decided on the basis that this is the load factor depicting the maximum capacity of the model. Therefore, it was considered as the most determining when evaluating the seismic behavior of buildings. Additionally, after the definition of the seismic vulnerability classes for the ten parameters presented in Chapter 4, each model could be defined in terms of the class assigned to each parameter.

As a result, data can be structured in a database composed of 11 attributes: (a) ten variables associated to the parameters classes; and (b) one variable with the value of load factor associated

to LS3 obtained for each model. Since there are only four classes of increasing seismic vulnerability, the variables associated to the parameters are accordingly expressed in a discrete form, assuming only four countable numbers from 1 to 4, associated to the classes A to D, respectively. On the other hand the load factor defining LS3 is a continuous variables expressed in g , whose value typically ranges from 0 to 1. Table 5.1 presents the list of variables and organization of the database, showing as an example how the information was filled for three numerical models. The three models from the database used as an example are shown in Figure 5.1. These three models were created for the definition of the seismic vulnerability classes shown in Chapter 4. It is noted that the complete database used for the definition of the weights of the SVIVA method is presented in Annex A.

Table 5.1: List of variables and organization of the database for the definition of the SVIVA method weights

Model	Input variables										Output variable
	P1	P2	P3	P4	P5	P6	P7	P8	P9	P10	LS3
<i>Model name</i>	<i>[1-4]</i>										<i>(g)</i>
RE1F_s7h3t5_Y	1	3	4	1	4	1	1	1	1	4	0.39
RE2Fd1_3op4_X	1	1	4	1	1	1	3	3	1	2	0.42
STM3Fd2_Y	1	3	2	1	3	1	1	4	1	3	0.45

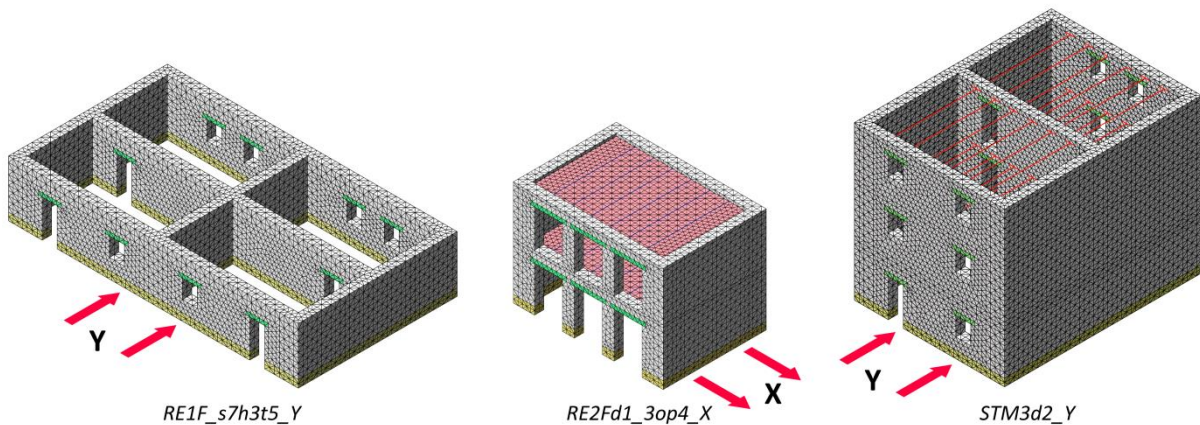


Figure 5.1: Numerical models used as an example of the fulfillment of the database

The DM technique that was applied to extract useful patterns from the database constructed is multiple linear regression (MR). Regression analysis is a popular statistical method used to study the relationships among variables (Kottegodo and Rosso 2008). It investigates the dependence of one variable (output variable) on one or more other variables (input variables). In this case, the ten parameter variables are the input variables, while LS3 is the output variable. The purpose is to formulate, evaluate and quantify these relationships through a mathematical model. More specifically, the objective is to evaluate the dependence of LS3 on the ten key seismic vulnerability assessment parameters and to define the relationship among them. A multiple regression model is required because there are several input variables (Montgomery et al. 2012).

The relationship between variables is often very complex and the simplest approach consists of fitting a multilinear equation to the data, which results in the following form:

$$Y = \beta_0 + \beta_1x_1 + \beta_2x_2 + \dots + \beta_kx_k + \varepsilon \quad (5.1)$$

where Y is the output variable and k is the number of input explanatory variables (x_k). The parameters β_k are called the regression coefficients and ε is the error. The resulting line defined by the regression equation (Eq. 5.1) describes how the response changes according to the explanatory variables. Therefore, each regression coefficient is a slope of the line and represents the expected change in the response per unit change in the input variable, when the remaining variables are held constant. For this reason, since they provide a measure of the amount of change, they can be used to compare the relative strength of the various predictor variables in the prediction of the dependent variable. This information precisely contributes to understand which parameters are more influential on determining the seismic vulnerability of vernacular buildings, which allows sorting the ten parameters by importance. Weights can thus be attributed to each parameter according to this arrangement, which enables their numerical definition. Figure 5.2 presents an overview of the steps followed for the definition of the parameters weights.

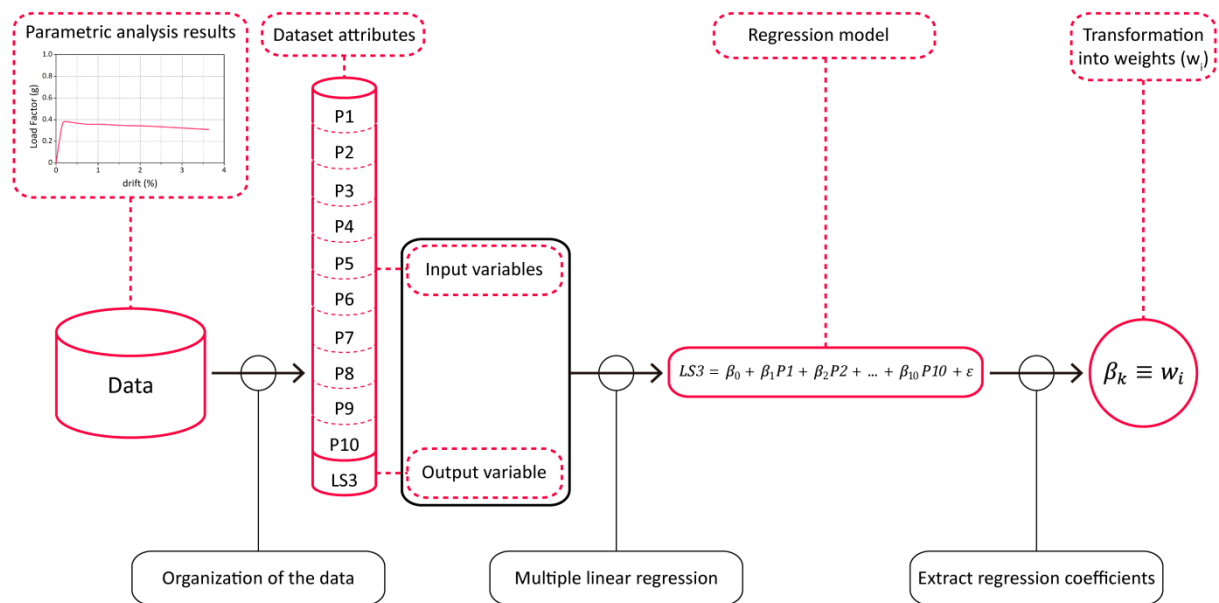


Figure 5.2: Methodology adopted for the definition of the seismic vulnerability assessment parameters weights

5.2.2. Methodology adopted for the development of the SAVVAS method

The SAVVAS method arises from the idea of using the regression models to directly estimate the load factors defining the different limit states. It is noted that the development of the SAVVAS method is shown in detail within Chapter 6. However, the general methodology followed is presented here, particularly focusing on the role of the database constructed for its development. Once again, the first step of the methodology concerns the organization of the database. In the

case of SAVVAS method, the target data does not only include the load factor corresponding to the attainment of LS3, but also the load factors defining the other two limit states (LS1 and LS2). The load factor defining LS4 is not taken into consideration because it is always by definition proportional in terms of load factor to LS3. These three load factors associated to the different LS are considered to define the seismic response of the buildings because they depict the seismic load (in terms of g) that would cause the building to reach different damage levels.

The regression models are thus intended to predict these three LS using as the input simple variables based on the previously selected parameters. Since the SAVVAS method relies directly upon the regression models, an effort was placed on increasing their prediction accuracy. Thus, while some of the parameters can be defined by the seismic vulnerability classes, others can be more precisely described using more specific quantitative attributes. For example, P2 (maximum wall span) can be directly defined by the span (in m), instead of by the vulnerability class. The same occurs for the wall slenderness (P1), wall openings (P7), the number of floors (P8) and the in-plane index (P10). Parameter P7 was also further divided into two parameters, aiming at distinguishing between the area of wall openings at the walls perpendicular to the loading direction (P7a) from the area of wall openings at the walls parallel to the loading direction (P7b). Other parameters, such as the type of material (P3), the quality of the wall-to-wall connections (P4), the horizontal diaphragms (P5), the roof thrust (P6) and the previous structural damage (P9), are defined using the classes, in qualitative terms. Thus, they are described in a discrete form, assuming four countable numbers from 1 to 4, associated to the classes A to D, respectively.

Other operations performed on the database to improve the prediction capabilities of the regression models of the SAVVAS method consisted of: (a) the transformation of the data attributes to better represent their effect in the seismic behavior of the building when the dependence between the output and input variables is not linear; and (b) exploring the interaction among the different parameters. The latter issue was detected in Chapter 4, where, for example, the greater influence of the area of wall openings when the building presents a rigid diaphragm was clearly observed. All these specificities of the SAVVAS method and details on how these issues were tackled are thoroughly discussed in Chapter 6.

As a result, data was structured in a database composed of 14 attributes: (a) eleven variables associated to the parameters; and (b) three variables with the values of load factor associated to LS1, LS2 and LS3 obtained for each model. The parameters variables are either: (1) expressed in a discrete form from 1 to 4 when the parameters are described by classes; or (2) expressed as continuous variables using different units depending on the parameter. The load factors are all continuous variables expressed in g , typically ranging from 0 to 1. Table 5.2 presents the organization of the database, showing as an example how the information was filled for the same three numerical models from the database shown in Figure 5.1. It is noted that the complete database used for developing the SAVVAS method is presented in Annex B.

Table 5.2: List of variables and organization of the database for the SAVVAS method

Model	Input variables										Output variables			
	P1	P2	P3	P4	P5	P6	P7a	P7b	P8	P9	P10	LS1	LS2	LS3
<i>Model name</i>	λ	s	[1-4]	[1-4]	[1-4]	[1-4]	$P7a$	$P7b$	N	[1-4]	γ_i	(g)		
<i>RE1F_s7h3t5_Y</i>	6	7	4	1	4	1	0.08	0	1	1	0.38	0.3	0.33	0.39
<i>RE2Fd1_3op4_X</i>	5.6	4.5	4	1	1	1	0	0.31	2	1	0.64	0.17	0.38	0.42
<i>STM3Fd2_Y</i>	5.45	7	2	1	3	1	0.08	0	3	1	0.5	0.27	0.38	0.45

In terms of applied DM algorithms, the SAVVAS method will explore the use of two different techniques to develop more reliable models, namely: (a) multiple linear regression (MR), which was already used for the SVIVA method; and (b) artificial neural networks (ANN). A brief literature review of the application of these DM techniques within the field of structural engineering is also provided in Chapter 6. The resulting regression models obtained are able to predict the seismic behavior of vernacular buildings based on the simple eleven parameters variables defined. They constitute the core of the SAVVAS method. Figure 5.3 presents an overview of the steps of the methodology adopted for the development of the SAVVAS method.

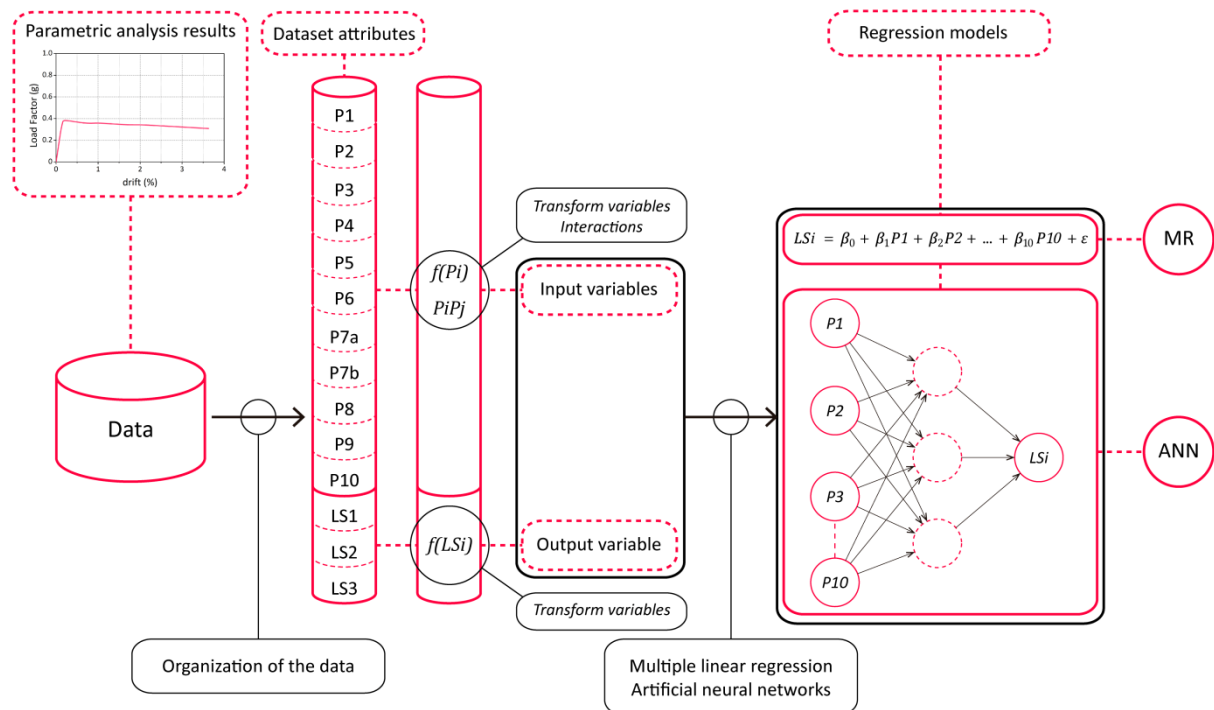


Figure 5.3: Methodology adopted for the development of the SAVVAS method

5.2.3. Data analysis and extension of the database

As previously mentioned, the big amount of data resulting from the numerical parametric analyses was used for the development of the regression models. However, a preliminary data analysis performed on the database, in terms of distribution, concluded that the population of

numerical models was not enough to perform a significant statistical analysis. In order to define a robust regression model that allows a confident estimation of the parameters weights, the database had to be strengthened by extending the numerical work. Therefore, additional numerical models had to be built, intending to have a more balanced distribution of buildings belonging to the different classes for each parameter and for it to be more comprehensive.

The database needed to be diverse and representative enough of all classes of each parameter. Considering the pattern of variability within each parameter variable (i.e. the distribution of buildings belonging to each class), a lack of balance (or asymmetry) was observed, which is an important limitation. Figure 5.4 presents the histograms for the eleven variables used in the database constructed for the SVIVA method, before and after the enlargement of the database. The input variables are divided into their four classes, while the output variable (LS3) is divided into five ranges of equal magnitude. It is clear that, due to the use of reference models showing similar initial conditions for the definition of the classes, some vulnerability classes are more frequent than others in each key parameter. As an example, in the case of parameter P1 (related to the wall slenderness), the height and the thickness of the walls of most of the models constructed did not vary when assessing other parameters. As a result, there is a clear unbalanced distribution of this parameter, where class A is clearly predominant, see Figure 5.4a.

Thus, the first step of the database extension process consisted of identifying those classes in each of the ten parameters that were less represented in the original database. The main criterion applied for the enlargement of the database was to ensure that there are a minimum of 25 models representing each parameter class, in order to contain a meaningful statistical amount for all of them. A total of 30 numerical models were built with particular geometrical, constructive and material features that can be associated to those vulnerability classes in each parameter that were observed to be insufficiently represented. Table 5.3 shows, for each parameter, the amount of models that were constructed assuming the different vulnerability classes. For example, with respect to parameter P9, which refers to the previous structural damage of the building, the great majority of the models constructed for the parametric study belong to class A (Figure 5.4i). Thus, most of the models from the new set of 30 models were analyzed assuming different initial levels of damage in order to represent the other classes (B, C and D).

For the preparation of the new models, the under-represented classes identified in each parameter were randomly combined. The diagram presented in Figure 5.3 shows an example on how these classes shown in Table 5.3 were combined to prepare one model. Figure 5.6 presents more examples of numerical models that were built for the database enlargement, showing also the seismic vulnerability classes assumed for each parameter. The precise information on all the new models prepared is included within the complete database for the SVIVA and SAVVAS methods shown in Annex A and B. It is noted that all the new models constructed were analyzed in both directions (X and Y) and the models with initial level of damage were also analyzed in the

undamaged condition. Thus, in total, 112 analyses were performed on the whole new set of models prepared for the enlargement of the database. This led to a final database composed of 530 results obtained from pushover analyses performed on the FE models. This enlargement of the original database was deemed satisfactory in terms of distribution within each parameter variable, complying with the previously established minimum condition of 25 models per vulnerability class in each parameter. This change in the distribution of the eleven variables after the extension of the dataset can also be observed in Figure 5.4.

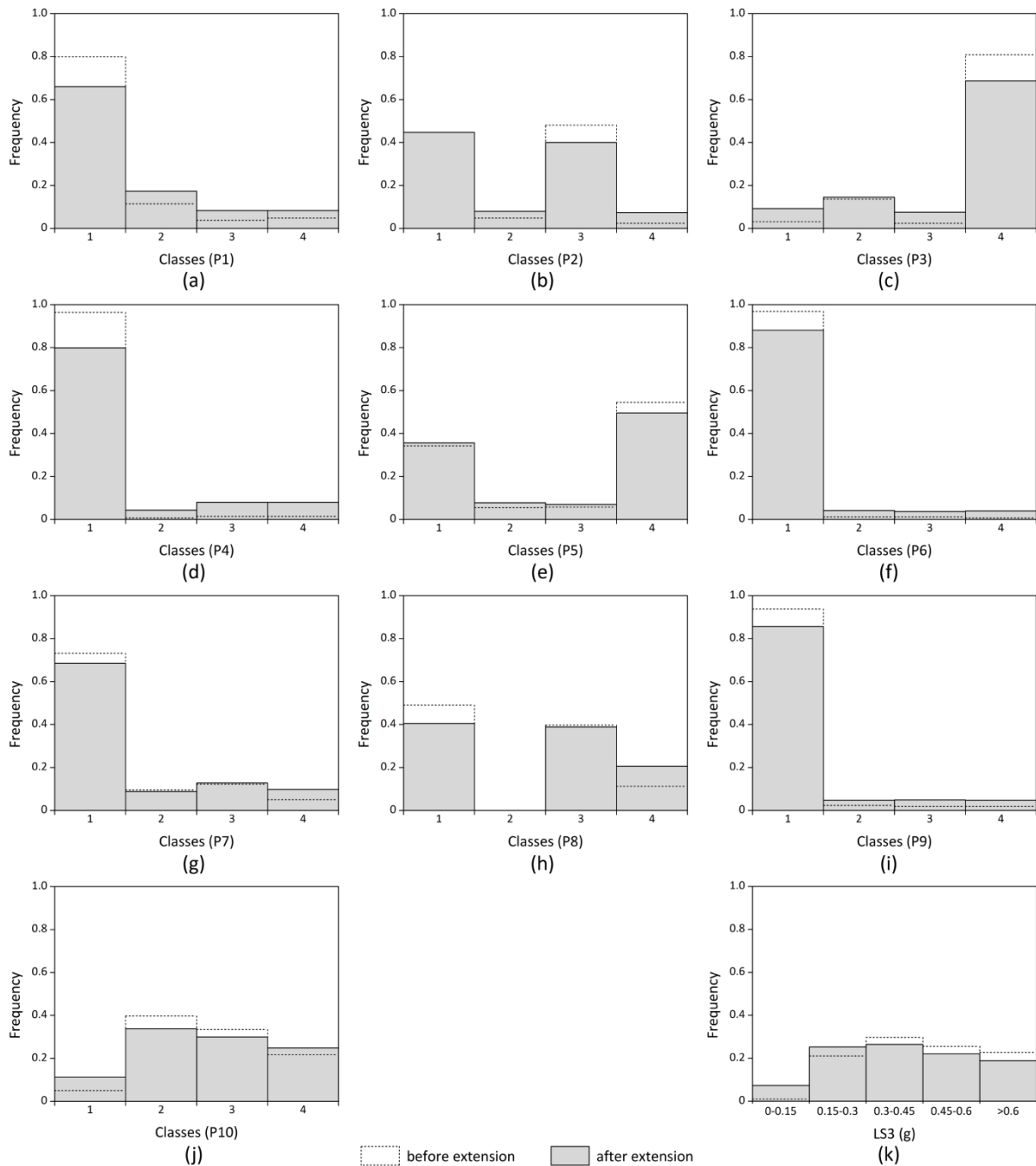


Figure 5.4: Histograms for the eleven variables in the database assembled for the SVIVA method

Table 5.3: Amount of models constructed assuming the different vulnerability classes in each parameter

Parameter	Class A	Class B	Class C	Class D
P1	4	12	8	6
P2	2	6	6	16
P3	10	5	8	7
P4	5	5	10	10
P5	12	6	7	5
P6	3	9	9	9
P7	2	5	4	19
P8	3	-	11	16
P9	5	7	10	8
P10	11	3	5	11

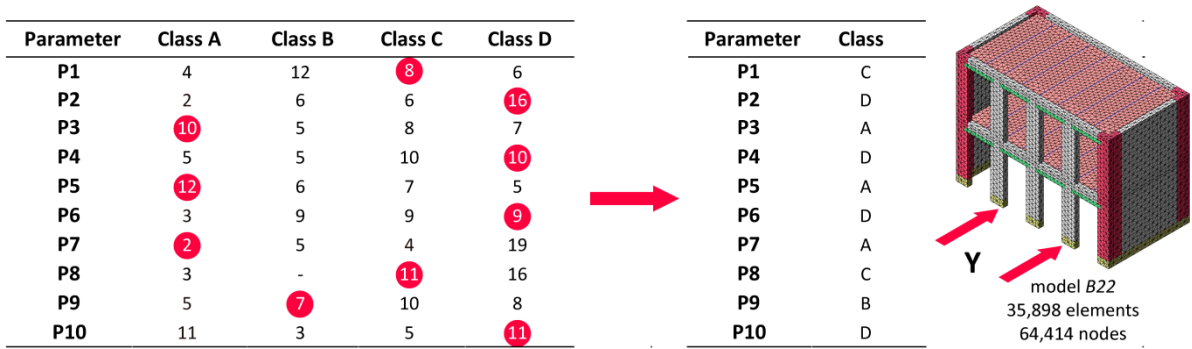


Figure 5.5: Procedure applied for the preparation of the new numerical models according to the lack of representation of some seismic vulnerability classes of the parameters

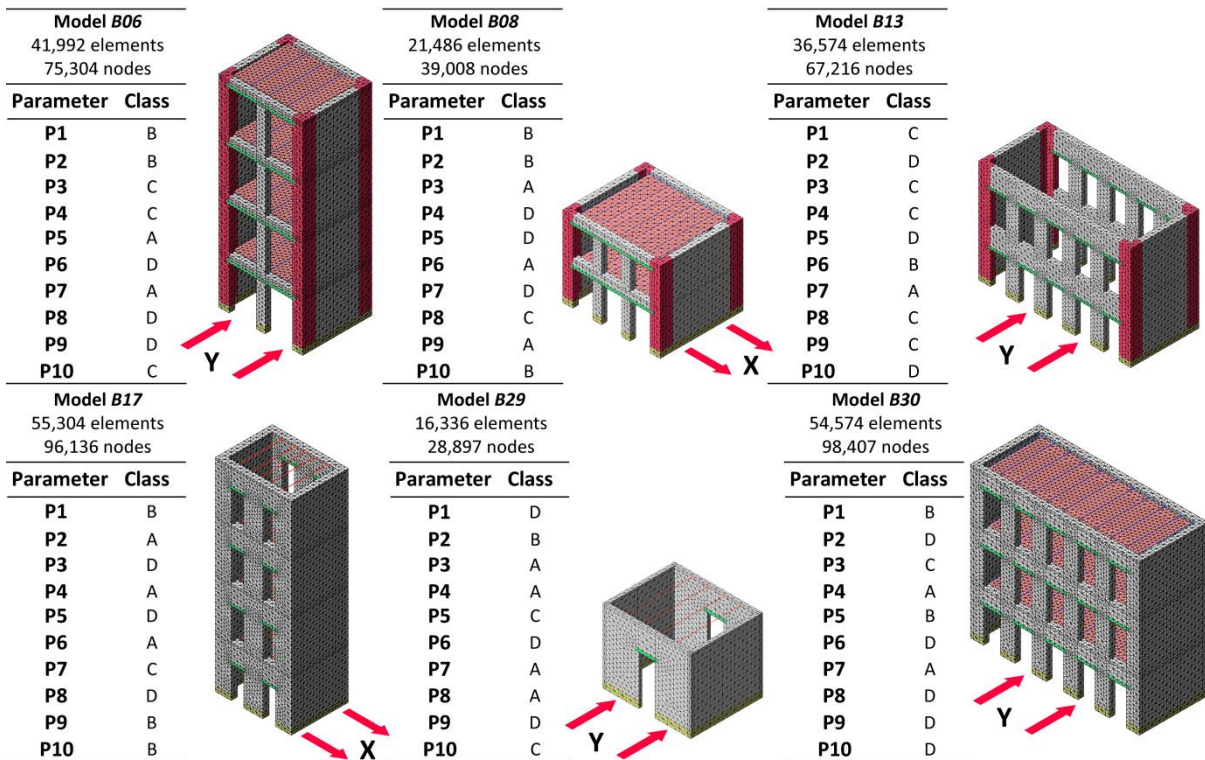


Figure 5.6: Examples of the numerical models built in order to extend the database with different combinations of the ten key parameters

Table 5.4 shows some statistical measures of the independent variables, particularly focused on central tendency and asymmetry of the data (skewness). It provides a deeper insight into the data from the total of 530 results from the analyses composing the database. It is noted that this section deals with the analysis of the database assembled for performing the regression statistical analysis aimed at the definition of the parameters weights (p_i), which is the main objective of the present chapter. The analysis of the database assembled for the development of the SAVVAS method is presented in Chapter 6.

Table 5.4: Statistical measures of the variables

	Variables	Minimum	Maximum	Mean	Median	Mode	STD	Skewness
Input	P1	1	4	1.59	1	1	0.95	1.48
	P2	1	4	2.1	2	1	1.06	0.17
	P3	1	4	3.36	4	4	1.04	-1.25
	P4	1	4	1.44	1	1	0.94	1.90
	P5	1	4	2.71	3	4	1.38	-0.27
	P6	1	4	1.24	1	1	0.70	3.04
	P7	1	4	1.64	1	1	1.04	1.29
	P8	1	4	2.39	3	1	1.21	-0.09
	P9	1	4	1.29	1	1	0.77	2.65
	P10	1	4	2.68	3	2	0.97	-0.08
Output	LS3 (g)	0.03	1.24	0.42	0.41	0.41	0.21	0.62

There is still an evident asymmetry in the distribution of the data in most parameters, despite the additional models constructed, which is clear looking at the histograms shown in Figure 5.4 after the extension of the database. Nevertheless, an asymmetry was expected since some classes are more typical than others in vernacular constructions. Thus, continuing with the same example above, the parameter P1 shows a clearly skewed distribution towards lower values of wall slenderness (Figure 5.4a). The vast majority of the values lie within class A and B, which implies values of slenderness $\lambda < 9$. This is considered to be reasonable because vernacular buildings rarely present greater values of wall slenderness. Also, it should be noted that there are no examples of class B for P8 because this class was removed and only three classes were considered in this parameter.

With respect to the output variable (LS3), it shows a more homogeneous and symmetric distribution (Figure 5.4k). There is a wide variability according to the different combinations of the parameters classes, which is in agreement with the results presented in the previous chapter that showed the clear influence of the different parameters selected on the seismic behavior of the buildings evaluated. This is the reason why a multiple regression analysis was envisaged, in order to examine the research question that arises on whether the seismic vulnerability key parameters variables can predict the load factor that defines the maximum seismic capacity of the building.

5.3. Definition of the parameters weights based on statistical analysis

The multiple regression analysis was performed using the R software (R Development Core Team 2008), which is the statistical tool selected to create the regression models. The regression model aims at predicting the load factor corresponding to LS3, which represents the attainment of the maximum capacity of the building and has a very clear physical meaning. Thus, the multiple linear regression model (*MRO*) measures the capacity of the ten parameters variables to predict LS3 adopting the simplest function as the structure:

$$MRO: LS3 \sim P1 + P2 + P3 + P4 + P5 + P6 + P7 + P8 + P9 + P10 \quad (5.2)$$

Model *MRO* is mainly meant to obtain the relative importance of the different parameters, which will be used to assist in the definition of the parameters weights (p_i) for the vulnerability index method (SVIVA). The regression equation that can be used for the prediction of LS3 is obtained after performing the multiple regression analysis and reads:

$$LS3 = 1.681 - 0.058 \times P1 - 0.017 \times P2 - 0.087 \times P3 - 0.04 \times P4 - 0.096 \times P5 - 0.032 \times P6 - 0.088 \times P7 - 0.093 \times P8 - 0.042 \times P9 - 0.026 \times P10 \quad (5.3)$$

Figure 5.7 illustrates the predicted versus observed LS3 values, showing the 45° line as a reference. The closer the plotted values lie near this line, the better behavior of the model. In summary, the model behaves well. All values are close to this line and most of them lie within the 45° +/- 0.1g lines also included in the graph. This indicates that the error between the predicted and the observed value obtained is lower than 0.1g for most cases. The behavior of the model is deemed very satisfactory, considering that the model predicts quite accurately the maximum capacity of the building, in terms of load factor, using as input merely the parameters classes.

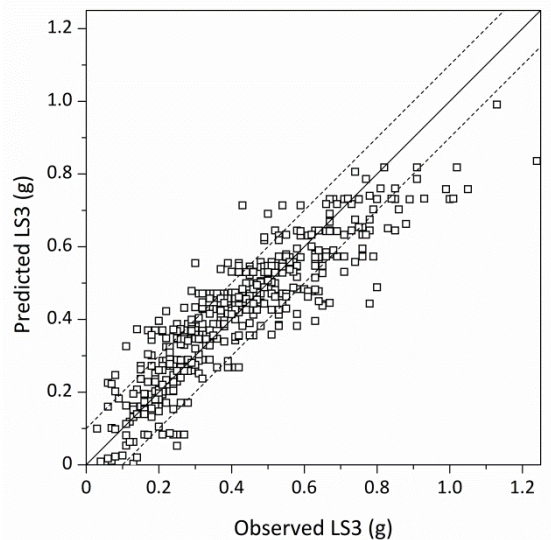


Figure 5.7: Predicted versus observed LS3 values for the regression model *MRO*

Table 5.5 shows some measurements of the performance of the model in terms of errors, coefficient of determination (R^2) and F-statistic. The errors relates to the difference between the predicted LS3 and the numerical (observed) LS3, using three measures: (1) maximum error observed (ϵ_{max}); (2) Mean Absolute Error (MAE); and (3) Root-Mean-Squared Error (RMSE). The coefficient of determination, R^2 , also denoted as R-squared, measures how well the model fits the actual data, and is very common in statistical applications. It lies within 0 and 1. The values close to 1 mean that the model explains all the observed variations in the dependent variable. It is noted that R^2 here refers to the adjusted R-squared, which is preferred for multiple regression analysis because it is stricter than R^2 , since it is penalized when some of the independent variables are not helpful in the prediction of the dependent variable. On the other hand, R^2 never decreases when an independent variable is added to the model, regardless of its influence on the prediction of the dependent variable (Montgomery et al. 2012). Finally, F-statistic is a common indicator of whether there is a relationship between the input and the output variables, which is verified for p-values close to 0. The value obtained confirms that there is a significant relationship between the set of predictors and the dependent variable. The performance in terms of adjusted R^2 is also deemed satisfactory, being close to 1 ($R^2 = 0.772$). Additionally, while the maximum error observed is large, both MAE and RMSE are below 0.1g, which can be considered small.

Table 5.5: Evaluation of the performance of the regression model *MRO*

R^2	ϵ_{max}	MAE	RMSE	F-statistic	
0.772	0.405g	0.075g	0.095g	180.2 on 10 and 519 Degrees of Freedom	p-value < 2.2e-16

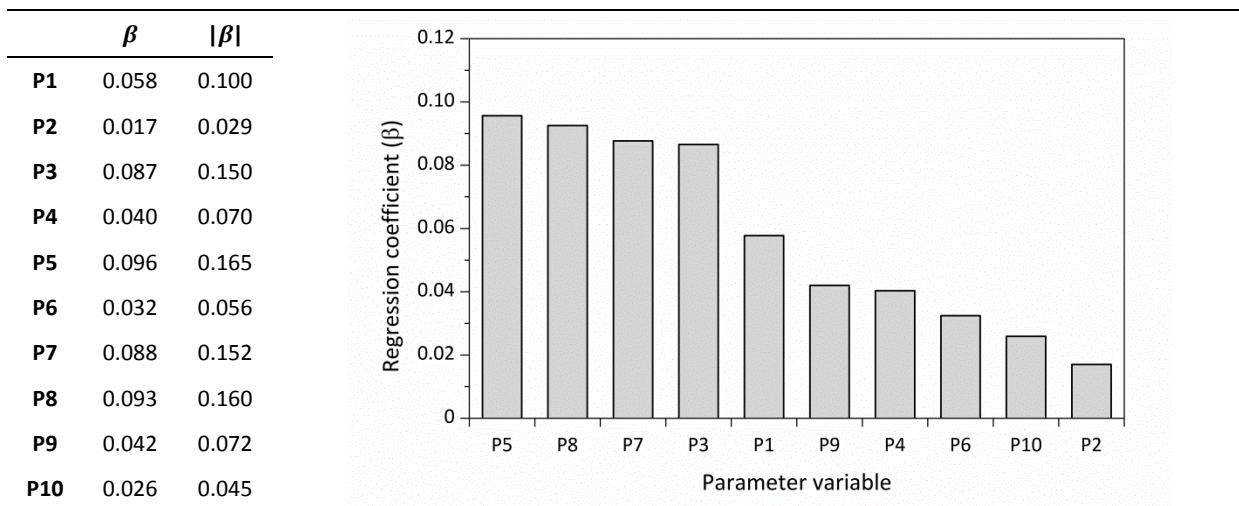
5.3.1. Regression coefficients

The results from the regression analysis confirm the ability of the multiple regression equation to estimate the load factor leading to the attainment of the damage limit state LS3. Subsequently, the ten key parameters selected are confirmed to be relevant predictors of the maximum seismic capacity of the building in terms of load factor. As a result, the regression equation is also considered satisfactory to be used for the estimation of the parameters weights. The regression coefficients (β_k) can be used to determine the magnitude of prediction of each variable and, thus, to evaluate independently the influence of each parameter. The regression coefficients can be obtained from Eq. 5.3. It is worth highlighting that all coefficients are negative because an increase in the parameter class leads to a decrease in the output variable. The physical meaning is clear, since an increase in the seismic vulnerability class will supposes a decrease in the capacity of the building in terms of load factor.

Although it is common practice to standardize the regression coefficients to interpret the relative strength of prediction of the variables because predictors are often measured in different units, this is not the case for the regression model under study. In this case, understanding a unit increase in a predictor is straightforward because it directly corresponds with an increase in the

vulnerability class, and all of the predictors are defined within the same range of classes, from 1 to 4 (associated to the classes A to D, respectively). For example, from Eq. 5.3 we can conclude that a unit increase in the seismic vulnerability class of P1 leads to a decrease in the maximum capacity of the building of 0.058g, but a unit increase in the class of P5 leads to a decrease in LS3 of 0.096g, which is almost the double. Therefore, these regression coefficients give a very good estimate of the relative importance of the different parameters. Table 5.6 compiles the absolute values of the regression coefficients obtained. It is noted that the higher the absolute values, the stronger influence of the variable in determining the load factor defining the maximum capacity of the building (LS3). The coefficients were also normalized so that they all sum to unity. The table shows these normalized absolute values ($|\beta|$) because they are the ones used for the numerical definition of the parameters weights. The coefficients are also displayed graphically and ordered by importance for a better visualization of their relative importance.

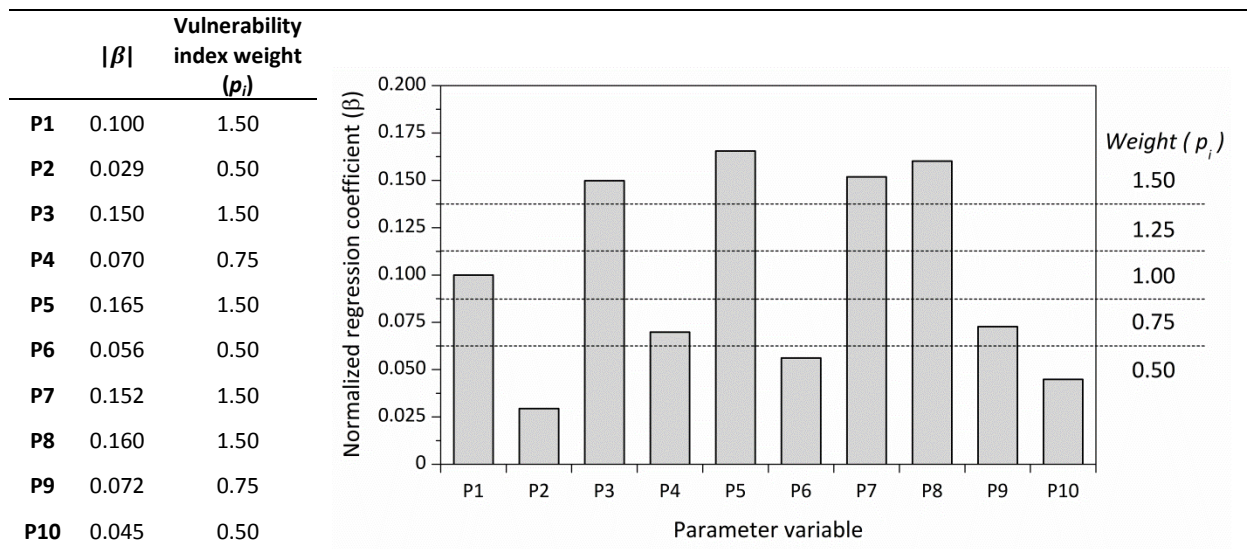
Table 5.6: Regression coefficients from *MRO* model in absolute value and parameter relative importance



5.3.2. Vulnerability index weights

The normalized regression coefficients resulting from *MRO* model shown in Table 5.6 were used for the definition of the parameters weights. Vulnerability index methods available in the literature (Benedetti and Petrini 1984; Vicente 2008; Boukri and Bensaibi 2008; Ferreira 2009; Shakya 2014) typically use weights for the parameters ranging from 0.50 to 1.50 in 0.25 intervals. Therefore, the criterion followed for the definition of the weights consisted of approximating the normalized regression coefficients to multiples of 0.025 establishing 0.050 and 0.150 as minimum and maximum respectively. Five ranges could be defined this way that could be directly associated to different weights: (a) $|\beta| < 0.0625 \equiv p_i = 0.50$; (b) $0.0625 < |\beta| < 0.0875 \equiv p_i = 0.75$; (c) $0.0875 < |\beta| < 0.1125 \equiv p_i = 1.00$; (d) $0.1125 < |\beta| < 0.1375 \equiv p_i = 1.25$; and (e) $|\beta| > 0.1375 \equiv p_i = 1.50$. Table 5.7 illustrates this process and shows the final weights adopted for the SVIVA method.

Table 5.7: Parameters weights definition



Finally, as a reference, the weights calculated numerically are compared with values proposed in the literature by other authors. Table 5.8 shows this comparison, acknowledging that the parameters are not exactly the same for all the methods, neither have the same exact physical meaning. There is an expected high variability among most of the weights, such as P4, P5 and P6. There is a noticeable disagreement in the case of wall openings (P7), which existing methods confer a minimal importance, but the parametric study proved that it can be a decisive parameter in some cases, particularly when coupled with rigid diaphragms. There is a general consensus among the methods on the importance of parameter P3, which refers to the type of material and particularly to its mechanical properties and strength. There is also agreement in giving moderate importance to the roof thrust (P6) and the previous structural damage in the building (P9). All methods also agree in conferring a reduced importance to the maximum wall span (P2).

Table 5.8: Comparison among the parameters weights proposed by different authors

Parameter	Vulnerability index weight (p_i)					
	Value adopted	Benedetti and Petrini (1984)	Vicente (2008)	Boukri and Bensaibi (2008)	Ferreira (2009)	Shakya (2014)
P1: Wall slenderness	1.00	-	-	-	0.50	-
P2: Maximum wall span	0.50	0.25	0.50	-	0.50	-
P3: Type of material	1.50	1.50	1.50	1.50	0.75	1.50
P4: Wall-to-wall connections	0.75	1.00	1.00	1.00	0.50	1.50
P5: Horizontal diaphragms	1.50	1.00	1.00	0.25	0.50	0.50
P6: Roof thrust	0.50	1.00	1.00	0.25	0.50	-
P7: Wall openings	1.50	-	0.50	-	0.50	1.00
P8: Number of floors	1.50	-	1.50	-	-	-
P9: Previous structural damage	0.75	1.00	1.00	1.00	0.75	1.00
P10: In-plane index	0.50	0.50	0.75	0.50	-	1.00

5.4. Definition of the parameters weights based on expert opinion

As aforementioned, besides the analytical procedure, the present chapter also introduces the expert point of view into the understanding and definition of the parameters weight for the SVIVA method. The weights obtained this way can be then compared with the values obtained with the statistical approach. The empirical knowledge obtained through post-earthquake damage observation can provide a different insight on the relative importance of the different parameters. The expert opinion was collected through a survey questionnaire carefully prepared. However, there is always a challenge in transforming subjective data into quantitative results that can be used for the numerical definition of the parameters weight. The questionnaire was prepared in order to be later processed using the Analytical Hierarchy Process (AHP) proposed by Saaty (1987). The details of this process are explained next, but it tackles the issue of quantifying the relative importance of the parameters based on subjective opinions expressed in terms of preferences and comparisons. This process has been employed for similar studies in other fields of civil engineering that required the definition of parameters weights based on expert judgment (Liu and Chen 2007; Pinheiro et al. 2015)

5.4.1. Questionnaire survey and Analytical Hierarchy Process (AHP) methodology

The questionnaire survey was prepared using the Google Forms digital platform. The survey was web based, which facilitated the distribution among experts throughout the world. The AHP is based on establishing pairwise comparisons among the parameters under evaluation in order to judge their relative importance in pairs. Thus, the survey asks the respondents to compare the relative importance of the parameters in a scale from 1 to 9, according to the fundamental scale defined by the AHP (see Table 5.9), where 1 means that they have equal importance, while 9 means that one factor is extremely more important than the other.

Table 5.9: The fundamental scale of AHP (Saaty 1987)

Intensity of importance	Definition	Explanation
1	Equal importance	Two parameters contribute equally to the objective
3	Moderate importance of one over another	Experience and judgment slightly favor one parameter over another
5	Essential or strong importance	Experience and judgment strongly favor one parameter over another
7	Very strong importance	A parameter is strongly favored and its dominance demonstrated in practice
9	Extreme importance	The evidence favoring one parameter over another is of the highest possible order of affirmation
2,4,6,8	Intermediate values between two adjacent judgments	When compromise is needed

A question of the survey was composed of two parts: (1) the first part proposes the pairwise comparison and asks the respondent to indicate which parameter is more important from the two presented, if any; and (2) the second part asks the respondent to rate this relative importance,

giving the AHP scale as a reference. Two different surveys were prepared with a different set of questions in each other. The complete survey can be found in Annex C. An example of the questions reads like:

(1) Please, indicate which of the following parameters you consider has a greater influence on the seismic behavior of vernacular buildings:

- *TYPE OF MATERIAL: Type of material used for the structural elements (load bearing walls) of the building (e.g. rammed earth, irregular stone masonry, dressed stone masonry, ect.)*
- *HORIZONTAL DIAPHRAGMS: Type of horizontal diaphragm (floors and roofs) and its connection to the load bearing walls*
- *Equal importance*

(2) Compare their relative importance in the provided scale from 1-9:

	1	2	3	4	5	6	7	8	9	
<i>Equal importance</i>	0	0	0	0	0	0	0	0	0	<i>Extreme importance of one parameter over the other</i>

The objective of using the AHP was to generate a pairwise comparison matrix of order n (where n is the number of parameters), from which the parameters can be arranged hierarchically in terms of importance for the definition of the weights. Since the matrix is reciprocal and the value of importance assigned to one parameter i when compared with parameter j is the reciprocal value assigned to j when compared with i (i.e. $a_{ji} = 1/a_{ij}$), the number of judgments required is $n(n-1)/2$. This would result in preparing 45 questions to consider the 10 parameters. However, the number of questions had to be reduced in order to avoid that the survey becomes repetitive and save the time of the respondents, encouraging their participation.

The problems of the incompleteness of the matrix could be tackled based on the method proposed by Harker (1987). The AHP includes redundancy in the answers, which plays a useful role because it allows the respondent to incorrectly answer a pairwise comparison without greatly affect the final weights. Thus, the comparisons should not be reduced either to the minimum $n-1$ needed to define the weights, in order to allow certain amount of redundancy. Therefore, there had to be a compromise in between the laborious task of completing 45 questions and the minimum of 9. At the end, the survey was composed of a total of 25 questions.

The process proposed by Harker (1987) is based on the fact that if the matrix is consistent, all entries can be derived for the relation $a_{ij} = a_{ik} \times a_{kj} \forall i, j, k$. However, the AHP expects and assumes the presence of inconsistencies, which can be measured with the consistency index (CI). A level of inconsistency is accepted within some proposed ranges, which depends on the number of elements in the matrix. Therefore, with the presence of inconsistencies, the abovementioned relation is not true for all the elements of the matrix and a_{ij} may differ when using different parameters k . Harker (1987) proposes to define the missing matrix elements by taking the geometric mean of the values obtained when taking different k . This process allows completing

the matrix and thus deriving the weights without the need to include the complete set of pairwise comparisons in the survey.

One of the most important considerations to take into account when carrying out a survey is the identification and selection of the respondents that will represent the expert opinion. In the present research, the survey was distributed and collected from a total of 50 experts working mainly in the field of seismic engineering and historical and vernacular masonry structures. The experts mainly belong to the academic environment and consist of professors, researchers and postgraduate students, including Ph.D and master's degree students from the Advanced Masters in Structural Analysis of Monuments and Historical Constructions program (SAHC). They can be grouped in three categories based on their assumed level of knowledge in the field: expert, high and regular knowledge. Professors and researchers are considered to have expert knowledge, Ph.D researchers are classified as high knowledge and the master's degree students as regular knowledge (Figure 5.8a). Nevertheless, the respondents were asked to rate their overall level of expertise on the matter in question, as a reference (Figure 5.8b). Even though there is a majority of respondents coming from Portugal, it is also worth highlighting that a particular emphasis was placed on distributing this survey among specialist from seismic prone regions all over the world, so that the particularities of the seismic behavior of vernacular constructions in different areas of the world are indirectly included within the survey. Among the surveyed, there were experts from countries such as Greece, Italy, Mexico, Peru, Chile, Iran, Nepal and India (Figure 5.8c).

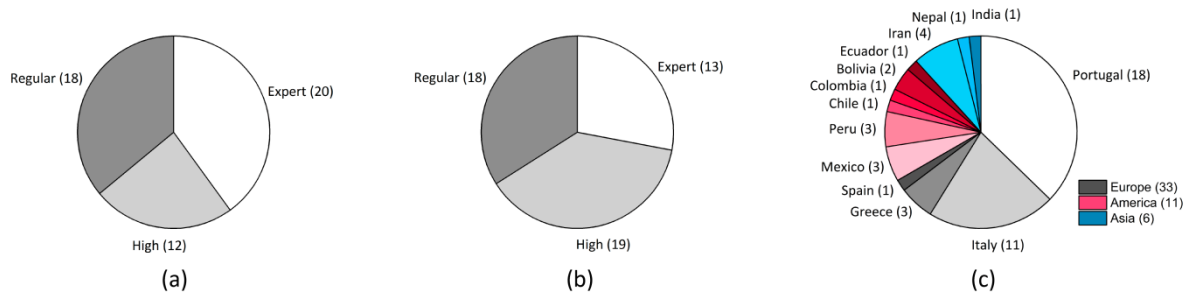


Figure 5.8: Respondents profile in terms of: (a) assumed expertise according to academic status; (b) self-evaluated expertise; and (c) country of origin

5.4.2. Definition of the weights

Following the AHP, the weights were derived using the eigenvector method. This method establishes that the attribute weights are equal to the components of the normalized principal eigenvector of the pairwise comparison matrix resulting from the survey. Thus, for each respondent of the survey, a matrix was composed using the answers provided and completing the missing elements of the matrix with the abovementioned method proposed by Harker (1987). As an example, Table 5.10 shows one complete matrix (A) of pairwise comparisons obtained from one of the respondents of the survey.

Table 5.10: Matrix A composed of a set of pairwise comparisons obtained from one of the respondents of the survey used for exemplification of the eigenvector method

	P1	P2	P3	P4	P5	P6	P7	P8	P9	P10
P1	1	1	3	2	1	3	4	1/2	1/2	1
P2	1	1	2	1	1/2	3	5	1/2	1	1/2
P3	1/3	1/2	1	1/2	1/3	2	1	1/5	1	1/2
P4	1/2	1	2	1	1	4	3	1/2	1	1
P5	1	2	3	1	1	4	3	1/2	2	2
P6	1/3	1/3	1/2	1/4	1/4	1	1	1/7	1/3	1/6
P7	1/4	1/5	1	1/3	1/3	1	1	1/4	1/2	1/4
P8	2	2	5	2	2	7	4	1	3	2
P9	2	1	1	1	1/2	3	2	1/3	1	1/3
P10	1	2	2	1	1/2	6	4	1/2	3	1

From the matrix A , the principal eigenvector (w) can be computed as:

$$Aw = \lambda_{max}w \tag{5.4}$$

where λ_{max} is the largest or principal eigenvalue of A . The principal eigenvector (w) obtained using Eq. 5.4 is then normalized. Finally, according to the AHP the components of the normalized principal eigenvector (\hat{w}) are directly associated with the parameters weights (p_i):

$$\hat{w} = (0.116, 0.096, 0.050, 0.100, 0.140, 0.029, 0.036, 0.214, 0.087, 0.133) \tag{5.5}$$

$$\hat{w}_{i,1} = p_i \tag{5.6}$$

According to Saaty (1984), calculating the eigenvector is the most appropriate method to synthesize the set of pairwise comparison and to obtain a vector of relative weights because it makes use of all the dominance information given in the matrix when it is not consistent. The consistency of the matrix can be measured with the CI (consistency index):

$$CI = (\lambda_{max} - n)/(n - 1) \tag{5.7}$$

Given the matrix A with n elements, $(\lambda_{max} - n)$ measures the deviation of the judgments from a perfectly consistent matrix, where $\lambda_{max} = n$. The closer λ_{max} is to n , the more consistent is the result. The AHP suggests a set of values denominated Random consistency index (RI), which depends on n , and, if the ratio $CI/RI \leq 0.1$, the judgments are taken as acceptable. For the case used as an example, where $n = 10$, $RI = 1.49$, and, thus, for the matrix A , $CI/RI = 0.03 \leq 0.1$.

This procedure was followed for the total of 50 answers collected, calculating the vector of relative weights for each answer. Table 5.11 shows the mean value of the relative weights obtained from all the answers. There is a great variety in the results, as shown by the standard

deviation (σ) and coefficient of variation (CV), which reaches in some cases values close to 1 for some parameters (such as P3). This depicts a wide discrepancy among the experts in identifying the most influential parameters and thus emphasizes the difficulty in assigning the weights based solely on empirical observations. Figure 5.9a shows the mean values of the parameters weights calculated independently for each level of knowledge assumed for the respondents, namely expert, high and regular. There are differences between the weights assigned by experts with different level of knowledge but, with the exception of P3, the relative difference among the parameters weights is similar for the three levels of knowledge. The weights shown in Table 5.11 were calculated assuming the same importance in the answers for the different levels of knowledge. However, in order to refine the definition of the weights taking into account the assumed level of knowledge of the respondents, two different scenarios were additionally considered and shown in Figure 5.9b: (1) increase in 20% the importance of the answers from the Expert level and decrease in the same proportion the importance of the answers obtained from the Regular level respondents; and (2) the same as in the previous case but considering a 50% variation between the knowledge levels. There are not significant differences among them.

Table 5.11: Relative weights considering the mean values from all answers

	\hat{w}_{mean}	σ	CV
P1	0.113	0.061	53.96%
P2	0.076	0.046	59.97%
P3	0.087	0.085	97.44%
P4	0.153	0.079	51.45%
P5	0.128	0.073	57.43%
P6	0.059	0.045	77.11%
P7	0.069	0.050	72.64%
P8	0.122	0.096	78.87%
P9	0.101	0.081	80.03%
P10	0.092	0.064	70.21%

According to the opinion of experts, the parameters that are more relevant on the seismic behavior of vernacular buildings are: P1 (wall slenderness), P4 (wall-to-wall connections), P5 (horizontal diaphragms) and P8 (number of floors). Figure 5.10 shows the frequency of the different parameters to be selected by the different respondents as the most or the least influential. This confirms that the majority of the respondents understand that the connection between perpendicular walls, the type of horizontal diaphragms and the number of floors are crucial in defining the seismic behavior of a building. On the other hand, it is worth highlighting that the type of material is considered by the significant majority of the respondents to be the least influential parameter in the seismic behavior, while around 10% consider this parameter to be the most important. This is in agreement with the great variability shown in Table 5.11,

recognizing a notable lack of consensus over the influence of this parameter. Nonetheless, Figure 5.9a shows that respondents with an expert knowledge concedes a significant importance to the type of material. Also, there is a quite uniform understanding that the maximum wall span (P2), the roof thrust (P6) and wall openings (P7) are among the least influential parameters.

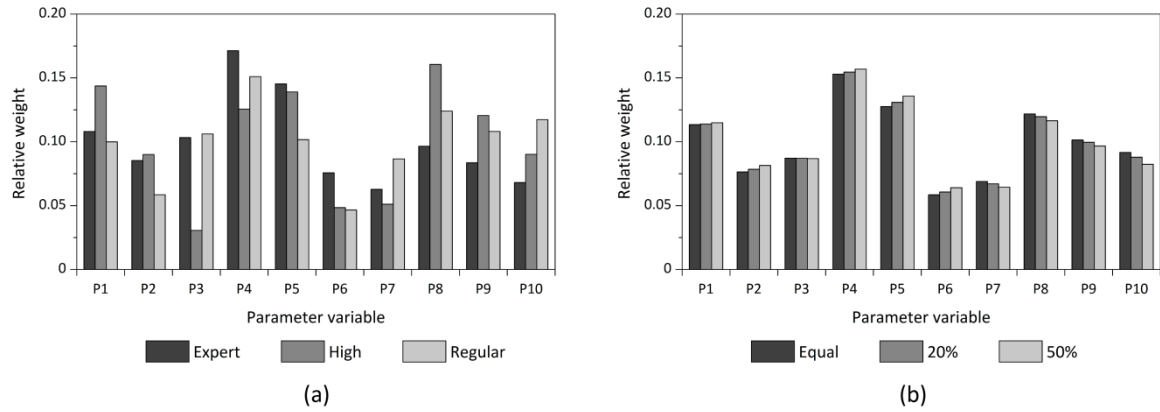


Figure 5.9: (a) Parameters weights according to the assumed level of knowledge of the respondents; and (b) different scenarios considered for the definition of the weights taking into account the levels of knowledge

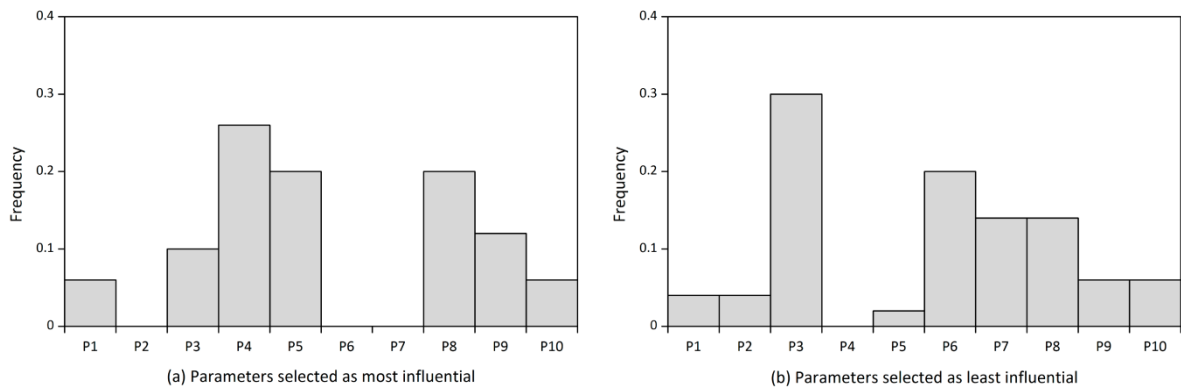


Figure 5.10: Frequency of the parameters being selected as: (a) the most; and (b) the least influential

5.4.3. Comparison with numerical results

Despite the variations in the answers to the questionnaire, results show consistency and are relevant, providing a good insight of the expert opinion on this matter. Nevertheless, there are important differences with the results obtained from the numerical analysis. Figure 5.11 shows a comparison among: (a) the weights calculated numerically from the normalized regression coefficients resulting from the multiple regression equation obtained to estimate the load factor leading to the attainment of the damage limit state LS3 (Table 5.6); and (b) the weights calculated based on expert judgment, which were established considering the scenario where the importance of the answers from the respondents assumed to have an expert level of knowledge is increased 50% (Figure 5.9b).

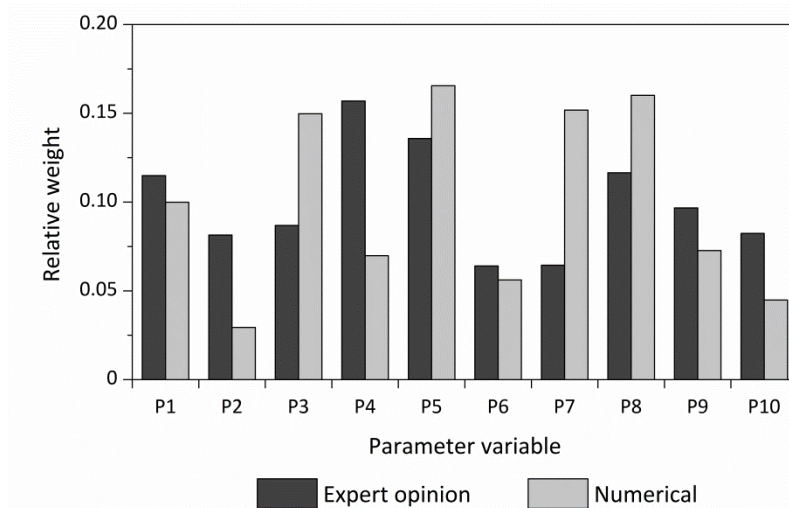


Figure 5.11: Comparison among the relative weights calculated based on expert opinion and numerically

The weight of some parameters is well matched and both experts and numerical results estimate their influence at a similar level, such as P5, which is always among the most influential parameters. This is the case also for P1, P6, P8 and P9. However, there is a remarkable difference for other parameters. For example, both the type of material (P3) and the wall openings (P7) have a significant influence according to the numerical results, while the survey respondents did not give them such an importance. In the case of the type of material, the discrepancy among the experts has already been discussed. Nevertheless, Table 5.8 showed that other vulnerability index methods agree on the importance of the mechanical properties and strength of the walls material (Benedetti and Petrini 1984; Vicente 2008; Boukri and Bensaibi 2008; Shakya 2014). Regarding wall openings, the difference may lie in the fact that the classes defined in the numerical results take into account the effect of wall openings when the building presents rigid diaphragms activating the in-plane response of the walls, which is the scenario for which this parameter has a greater influence. Vernacular constructions many times lack this positive diaphragm effect and seismic behavior mainly depends on the out-of-plane resistance of the walls, on which the area of wall openings has a minimum influence, as discussed in Chapter 4. Post-earthquake damage observations showing out-of-plane collapses may lead to the assumption that wall openings have a lesser influence, while, if presenting rigid diaphragms, they can have a crucial role. On the other hand, most experts judged as critical the importance of the connection among orthogonal walls (P4), whereas the numerical results granted it a more moderate influence. This difference is possibly due to the fact that a bad connection leading to an out-of-plane wall collapse is a very common post-earthquake damage pattern. Numerical results showed that damage usually arises at the connection between walls but the simulation of the reduction of the wall-to-wall integrity appears not to have such a strong effect on the seismic capacity of the building when compared with other parameters.

5.5. Seismic vulnerability index for vernacular architecture (SVIVA) formulation

Finally, the definition of the weights for the vulnerability index formulation adapted for vernacular architecture was based on the numerical results, using the correlation shown in Table 5.7 after the statistical analysis. As a result, Table 5.12 shows the proposed final formulation. The formulation is complete gathering the results from: (a) Chapters 3, where the parameters were selected; (b) Chapter 4, where the parameters classes were defined; and (c) the present chapter, which showed the determination of the parameters weights (p_i). The final formulation presented in Table 5.12 is thus a conclusion of this set of chapters, which have been primarily aimed at the development of the SVIVA method.

The vulnerability index that can be obtained through the application of the resulting formulation measures the lack of building seismic safety and, as described in Chapter 3, it can be related with the damage expected in a building for earthquakes of different intensities by means of empirically developed expressions, such as the one proposed by the macroseismic method. An example of the implementation of this vulnerability index formulation using the analytical expression from the macroseismic method in order to perform the damage and loss assessment by means of vulnerability and fragility curves is presented in Chapter 8.

Table 5.12: Vulnerability index formulation for vernacular architecture

Parameter	Class (C_{vi})				Weight (p_i)	Vulnerability index
	A	B	C	D		
P1. Wall slenderness	0	5	20	50	1.00	$I_V = \sum_{i=1}^{10} C_{vi} \times p_i$
P2. Maximum wall span	0	5	20	50	0.50	
P3. Type of material	0	5	20	50	1.50	
P4. Wall-to-wall connections	0	5	20	50	0.75	
P5. Horizontal diaphragms	0	5	20	50	1.50	
P6. Roof thrust	0	5	20	50	0.50	
P7. Wall openings	0	5	20	50	1.50	
P8. Number of floors	0	5	20	50	1.50	
P9. State of conservation	0	5	20	50	0.75	
P10. In-plane index	0	5	20	50	0.50	

5.6. Conclusions

The main objective of the present chapter has been the definition of the seismic vulnerability assessment parameters weights that are necessary to determine the vulnerability index formulation for the SVIVA method, adapted for vernacular architecture. For this, two approaches were followed with the goal of defining the parameters weight, namely: (a) statistical analysis (multiple linear regression); and (b) collection of expert opinion.

The first approach comes as a natural consequence of the extensive numerical study presented in the previous chapter. Based on the large number of numerical models constructed and analyzed, a wide database could be built that led to the possibility of performing a statistical regression analysis. Regression models were thus developed revealing a significant correlation between the parameters and the maximum seismic capacity of the building, in terms of load factor (LS3). The relative contribution of the parameters to determine this load factor depicting the maximum capacity of the building could be also quantified as a result of the regression analysis by means of the regression coefficients. These coefficients were associated with the parameters weight, which led to their numerical definition. The weights obtained are consistent with the results from the parametric study and the process presented within this chapter helps to understand better the contribution of the parameters to the load capacity of vernacular buildings under seismic loading.

Previous vulnerability index methods existing in the literature have based the definition of the parameters weight on the opinion of experts. The comparison among the weights obtained with the statistical approach with the weights proposed by other authors showed some significant disagreements. Nevertheless, there is a high variability among the weights defined by the different authors for the same parameters, which exemplifies the difficulty in defining the weights based solely on post-earthquake damage observation. The definition of the parameters weights based on numerical results can be considered innovative, since existing vulnerability index methods are typically defined on the basis of this empirical judgment and expert opinion.

However, the importance of validating analytical-based methods with empirical observations was acknowledged. That is why a second, more classical, approach based on expert opinion was followed for the definition of the parameters weight. In order to achieve this goal, a questionnaire survey was designed to gather this expert judgment in a systematic way. The answers were analyzed through a set of pairwise comparisons that could be later used to weight the relative importance of the parameters. Results proved again the difficulty of assessing the influence of the different parameters based on expert judgment. There is not a general agreement on which are the most influential parameters and the ranges of variation are very wide. Several discrepancies were observed when comparing the weights obtained from the statistical approach and the weights obtained from the expert opinion. The differences particularly involved the parameters related to the type of material (P3) and the area of wall openings (P7), whose importance appears to be underestimated by the experts. In any case, the discussion of the results provided a good insight of the general opinion of experts and it helped to validate some assumptions resulting from the numerical analysis, as there is some correspondence among the numerical and the expert-based results.

The SVIVA method was concluded by the adoption of the parameters weights obtained through the statistical analysis. It should be underlined that the proposed seismic vulnerability

assessment method is considered to be an easy tool, but it is a simplified approach. In fact, the seismic behavior of vernacular buildings is a complex matter that is difficult to explain using solely ten parameters. Moreover, the relationship between parameters is more complex than the one proposed by vulnerability index methods, where the influence of the parameters is considered individually. As shown in Chapter 4, the interaction between some parameters can be of great importance to effectively describe the seismic response of the building. This and other issues are tackled within the development of the SAVVAS method, which is presented in Chapter 6.

CHAPTER 6

DEVELOPMENT OF A NEW SEISMIC VULNERABILITY ASSESSMENT METHOD

Chapter outline

[6.1. Introduction](#)

[6.2. Development of the SAVVAS method](#)

[6.2.1. Analysis of the database and variables transformation](#)

[6.2.2. Multiple regression models](#)

[6.2.3. Artificial Neural Networks](#)

[6.2.4. ANN regression models and comparison among data mining techniques](#)

[6.3. Validation of the regression models](#)

[6.4. SAVVAS formulation](#)

[6.5. Conclusions](#)

6.1. Introduction

Chapter 5 introduced the idea behind the development of a novel method for the seismic vulnerability assessment of vernacular architecture. The extensive numerical simulation campaign carried out on different vernacular buildings with variations according to ten key parameters allowed constructing a reasonably robust database with the results of the pushover analyses. The results offered information about the seismic load capacity of the different buildings, which was defined in terms of load factors leading to the attainment of four damage limit states (LS1, LS2, LS3 and LS4). The regression analysis performed on this database led to the definition of the parameters weight presented in Chapter 5 and was the trigger for the development of the new seismic vulnerability assessment method. This new method is intended to estimate the seismic load capacity of vernacular buildings by means of regression models that use as input simple variables based on the ten key parameters. The development of the models is based on the results of the parametric numerical study used for the definition of the classes (shown in detail in Chapter 4).

The regression analysis shown in Chapter 5 proved to be an effective tool for extracting useful patterns from the vast amount of data derived from the parametric analysis, since the regression models constructed confirmed that the parameters selected are significant predictors of the

seismic load capacity of vernacular buildings. The new method proposed arises from the intention of delving more deeply into the research question of whether these parameters variables can quantitatively estimate the seismic load capacity of vernacular buildings. The final objective of the method is to calculate the seismic load factors (expressed in g) defining the different limit states (LS) that are associated with different degrees of structural damage suffered by the building. Thus, based on regression models, the proposed new method is able to directly estimate a value of a load factor that causes the structure to reach these specific levels of damage. As a result, these load factors can be directly compared with a seismic event expressed in terms of PGA, which allows skipping the middle steps of other seismic vulnerability assessment methods.

Chapter 5 started exploring knowledge discovery in databases (KDD) by means of multiple linear regression, but there are more data mining (DM) algorithms that can be applied for the desired deeper analysis in order to extract patterns explaining relationships between variables, such as artificial neural networks (ANN), support vector machines (SVM) and decision trees. There is an increasing amount of research in different fields that make use of the abovementioned techniques. This includes research in structural engineering where, for example, DM techniques have been widely applied to formulate models able to predict the mechanical properties of different materials based on experimental data. Among others, the ANN technique has been used to predict the tensile behavior of granite (Martins et al. 2014), the compressive and tensile strength of limestone (Baykasoglu et al. 2008) or the compressive strength of masonry prisms (Garzón-Roca et al. 2013a). Miranda et al. (2011) used multiple regression and ANN algorithms to develop models for the calculation of different strength and deformability parameters of rocks using large databases of geotechnical data. Moreover, DM has also been employed in assessing the structural behavior of different structural elements. Marques and Lourenço (2013) applied the SVM technique for the prediction of the shear strength of confined masonry walls subjected to lateral loadings. Similarly, ANN models have been developed to estimate the axial behavior and load-bearing capacity of unreinforced masonry walls (Garzón-Roca et al. 2013b; Sandoval et al. 2014), the shear strength of reinforced masonry walls (Aguilar et al. 2016) or the masonry failure surface under biaxial compressive stress (Plevris and Asteris 2014).

This brief overview on the use of DM techniques within the field of structural engineering shows that there is an increasing research focus on developing regression models for the prediction of the mechanical properties of different materials and the structural behavior of different structural elements. However, with the exception of Garzón-Roca et al. (2013), who used as the database for developing the ANN models the results of a parametric study with finite elements comprising 3700 models (Sandoval and Roca 2012), all abovementioned studies have developed the models based on large databases of experimental data.

This research work makes use of the database presented in Chapter 5, which is composed solely of numerical data obtained from the results of the nonlinear parametric study carried out.

The DM algorithms applied herein are based on: (a) multiple regression, which was already introduced and partially explored in the Chapter 5; and (b) ANN, whose concept and details will be briefly explained later within this chapter. Nevertheless, it is noted that the ANN models will be mainly developed for reference and comparison purposes, intended to show a research path open to further research, since the focus is placed on the multiple regression models, whose physical meaning is easier to interpret (Miranda et al. 2011).

In summary, the main goal of the present chapter is to use DM techniques to develop regression models able to predict the load factors associated to the different LS of vernacular buildings subjected to seismic action, using as input data simple variables based on the key seismic vulnerability parameters identified in Chapter 3. These models constitute the core of the new proposed seismic vulnerability assessment method, which has been denominated as Seismic Assessment of the Vulnerability of Vernacular Architecture Structures (SAVVAS), because it is specifically conceived to assess the structural performance of vernacular buildings under seismic loading. This new method is composed of three different expressions that allow estimating the load factors corresponding to the attainment of each limit state, namely LS1, LS2 and LS3. It is noted that the load factor associated to LS4 is not considered since, by definition, is always proportional to the load factor defining LS3. The input information of the models is always related with the ten key seismic vulnerability assessment parameters.

The chapter then shows the validation of the SAVVAS method, based on different numerical and experimental works dealing with the seismic analysis of traditional masonry constructions that were gathered from the literature. The examples were selected taking into account that there was enough information available regarding the geometry, construction and structural detailing of the buildings so that the regression models could be applied confidently. The available numerical and experimental works also had to provide results in terms of load factors or maximum capacity of the buildings so that they can be compared directly with the predicted values obtained by applying the regression models from the SAVVAS method. After validation, the SAVVAS method final formulation is presented at the end of the chapter, together with a summary of the steps to be followed in order to apply the new proposed method.

6.2. Development of the SAVVAS method

The database and the methodology used for the development of the SAVVAS method were already introduced in Chapter 5 (Figure 5.3). The data built was built based on the results of: (a) the pushover parametric analyses performed to define the seismic vulnerability classes (Chapter 4); and (b) the pushover analysis performed on the extra models that were constructed in order to extend the database to make it as much representative of vernacular buildings as possible

(Chapter 5). The database used for the development of the SAVVAS method is presented as a whole in Annex B.

The organization of the database into 14 attributes was also explained in detail in Chapter 5. The input variables had to be associated with the ten key seismic vulnerability assessment parameters, whose influence on the seismic behavior of vernacular buildings has been studied thoroughly within the present thesis. The main objective of the regression models developed for the SAVVAS method is to estimate the seismic load capacity of vernacular buildings in terms of values of load factor associated to different damage limit states (LS1, LS2 and LS3). Thus, the selection of the load factors that define each limit state, expressed in terms of gravity acceleration (g), as the target data set that is to be predicted was also clear.

Nevertheless, several operations can be applied on these selected attributes from the database, which can eventually help in improving the prediction capabilities of the regression models. There are many possibilities to represent these attributes that can help depending on the goal of the task (Fayyad et al. 1996). That is why, following a preliminary analysis of the data, this section reflects on possible transformations of the data attributes that can be applied in order to achieve better results. The operations evaluated include: (a) transformations of the input and output data attributes; and (b) interactions among the input variables. According to these operations considered, several regression models were built with different sets of input data. Two different DM techniques were considered to develop the regression models: (1) multiple regression models, which include the discussion on the use of different sets of input variables until obtaining the best model in terms of prediction capabilities; and (2) artificial neural networks (ANN) models. A brief overview and explanation of neural network modelling is provided before the development of the models. The statistical analysis and the definition of the regression models are carried out by using R open source software (R Development Core Team 2008). The different regression models will be compared and discussed in order to conclude with the final formulation of the SAVVAS method. The discussion of the results also allows a deeper understanding of the relationships among the parameters and their influence on the seismic behavior of vernacular buildings. The selection of the final expressions is based on a compromise between the accuracy in the prediction and the choice of patterns whose physical meaning is more understandable.

6.2.1. Analysis of the database and variables transformation

The database (presented in full in Annex B) contains a total of 530 results from the pushover analysis performed on models with varying values of the ten seismic vulnerability assessment parameters. In this way, the SAVVAS method makes use of the seismic vulnerability parameters and classes defined for the vulnerability index (SVIVA) method.

For the definition of the parameters weights (Chapter 5), the numerical models were simply described according to the class assigned to each parameter, thus presenting a discrete range of

values from 1 to 4, associated to classes A to D respectively. However, for the development of the SAVVAS method, some parameters could be more precisely defined using attributes different than the seismic vulnerability class. For example, P1 can be directly defined by the wall slenderness ratio (λ) instead of the vulnerability class. Therefore, a more precise quantitative description was considered for some parameters, using specific attributes: (1) P1 was defined by the wall slenderness (λ); (2) P2 was defined by the maximum wall span (s), expressed in m; (3) P8 was defined by the number of floors (N) of the building; and (4) P10 was defined by the in-plane index (γ_i). In the particular case of P7, which concerns the amount and area of walls openings, the parameter was divided into two: P7a and P7b. This distinction was made in order to differentiate the amount of walls openings observed in the walls perpendicular to the loading direction (P7a) from those present in the walls parallel to the loading direction (P7b). The classes were defined taking into account only the ratio of openings in the in-plane walls because the presence of openings mainly affects the in-plane resistance of the walls (Chapter 4). However, even if significantly lesser, the presence of wall openings in the walls perpendicular to the seismic load also has an influence in the seismic behavior. The parameter P7a is thus measured as a percentage of the total area of the considered wall (*P7a*). On the other hand, the parameter P7b refers to the area of wall openings in the in-plane walls, which accounts for the total area of wall openings observed in all the walls parallel to the loading direction, and is measured also as a percentage of the total area of all in-plane walls (*P7b*). The remaining five parameters (P3, P4, P5, P6 and P9) can only be described in qualitative terms. Thus, their definition is kept as a function of their class, being assigned with a discrete value from 1 to 4, depending on the vulnerability class A to D, respectively.

Besides the specification of the variable defined for each parameter in terms of a discrete or a continuous attribute, some data transformations were considered aiming at a better description of their effect in the seismic behavior of the building. Generally, multiple regression models depend linearly on predictors (input variables) but the dependence of the output variable on a specific predictor may be not linear, which can lead to errors in the prediction. Different transformations, such as logarithms and powers, can help to linearize this relationship and correct problems of prediction in the regression models. Therefore, based on the patterns of the load factor variations obtained for each parameter shown in Chapter 4, some transformations are considered and explored within different regression models, in order to assess if they can improve the correlation between the input and output variables. As an example, Figure 6.1a shows the variation of the load factor defining LS3 for a stone masonry building with flexible diaphragms and varying number of floors, obtained from the assessment of the influence of parameter P8 on the seismic behavior of vernacular buildings. This variation is not linear and a logarithmic trend line fits considerably better. Figure 6.1b shows how the logarithmic transformation of the variable can help to linearize the correlation among the load factor and the number of floors.

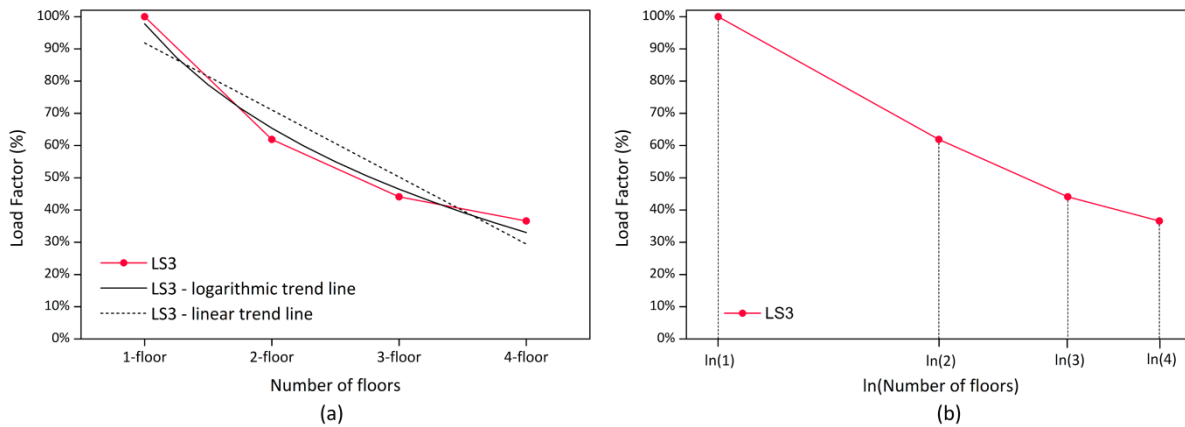


Figure 6.1: Variables linearization: (a) logarithmic and linear trend lines associated to the variation of the load factor defining LS3 for a stone masonry building with flexible diaphragms with varying number of floors; and (b) linearized correlation among number of floors and load factor after the log transformation

As a summary, the list of input variables considered, together with general statistical measurements, is presented in Table 6.1. It should be noted that the transformations of the variables results from a trial and error process. The intermediate transformations assumed from the patterns observed in the graphs showing the variations of the load factor were tested in different regression models, but this process is not discussed herein. Only those that revealed to have a notable influence in improving the prediction capabilities of the regression models are presented (Table 6.1).

With respect to the output variables, they also needed to be transformed in order to assure that the predicted values from the multiple linear regression models are always positive. The output variables are the load factors that measure the seismic action that causes the building to reach specific LS and they are expressed in terms of g . Therefore, as a measure of the seismic load, they cannot be negative. In some specific cases, as observed during Chapter 4, the load factor defining LS1 can be 0, if the building is assumed to present an initial level of structural damage because of the state of conservation or the roof thrust, but can never show values below 0. This led to the adoption of a logarithmic transformation of the three output variables (LS1, LS2 and LS3), since the predicted values from a log-transformed regression will never be negative, respecting the physical meaning of the variable. The logarithmic transformation involves the adoption of a natural logarithm of the output variables. It should be noted that, since there are zero values among the data of the variable LS1 and there is no logarithm of the value zero, a constant ($c = 0.01$) was added to all LS1 values before applying the log transformation. A small positive constant between 0 and the smallest non-zero observation that preserves the order of magnitudes of the data is usually recommended (McCune and Grace 2002; Field et al. 2012). The statistical measurements of the transformed output variables of the database are also presented in Table 6.1.

Table 6.1: List of variables and general statistical measures

Variables		Description	Minimum	Maximum	Mean	Median	Mode	STD
P1	λ	Ratio between the effective wall inter-story height (h) and its thickness (t)	4	22.5	7.34	6	5.6	3.43
	$\lambda^{-1/2}$	Power transformation of the variable	0.21	0.50	0.39	0.41	0.42	0.06
P2	s	Maximum wall span without intermediate supports, measured in meters (m)	2.5	12	5.90	5.25	7	1.87
	$\ln(s)$	Log transformation of the variable	0.92	2.48	1.73	1.66	1.95	0.30
P3	$P3$	Seismic vulnerability class of the building according to P3	1	4	3.36	4	4	1.04
	$\ln(P3)$	Log transformation of the variable	0	1.39	1.14	1.39	1.39	0.44
P4	$P4$	Seismic vulnerability class of the building according to P4	1	4	1.44	1	1	0.94
P5	$P5$	Seismic vulnerability class of the building according to P5	1	4	2.71	3	4	1.38
	$\ln(P5)$	Log transformation of the variable	0	1.39	0.82	1.10	1.39	0.64
Input P6	$P6$	Seismic vulnerability class of the building according to P6	1	4	1.24	1	1	0.70
	$P7a$	Ratio between the maximum area of wall openings in a wall perpendicular to the loading direction and the total area of the considered wall	0	0.7	0.09	0.06	0	0.16
P7	$P7b$	Ratio between the area of wall openings in all in-plane resisting walls and the total area of all in-plane resisting walls	0	0.69	0.12	0	0	0.18
	N	Number of floors	1	4	1.87	2	1	0.89
P8	$\ln(N)$	Log transformation of the variable	0	1.39	0.51	0.69	0	0.47
	$P9$	Seismic vulnerability class of the building according to P9	1	4	1.29	1	1	0.77
P9	$\ln(P9)$	Log transformation of the variable	0	1.39	0.15	0	0	0.39
	γ_i	Ratio between the in-plan area of earthquake resistant walls in the loading direction (A_w) and the total in-plan area of earthquake resistant walls (A_w)	0.26	0.79	0.53	0.50	0.50	0.11
LS1 (g)	$LS1 (g)$	Load factor associated to LS1	0	1	0.24	0.23	0	0.18
	$\ln(LS1+c)$	Log transformation of the variable	-4.61	0.01	-1.86	-1.43	-4.61	1.28
Output LS2 (g)	$LS2 (g)$	Load factor associated to LS2	0.02	1.01	0.36	0.35	0.38	0.19
	$\ln(LS2)$	Log transformation of the variable	-3.91	0.01	-1.17	-1.05	-0.97	0.62
LS3 (g)	$LS3 (g)$	Load factor associated to LS3	0.03	1.24	0.42	0.41	0.41	0.21
	$\ln(LS3)$	Log transformation of the variable	-3.51	0.22	-1.02	-0.89	-0.89	0.59

6.2.2. Multiple regression models

In this section, different regression models were prepared using always multiple regression analysis, but varying the input variables taken into consideration. The section then is meant to provide a comparison of the performance of the different models concerning their capability in predicting the load factors associated to the different limit states (LS). In total, 6 regression models are presented and discussed next. The first regression model used for comparison is the model used for the definition of the weights in Chapter 5 (*MR0*). A second regression model was built using continuous variables instead of classes for some parameters (*MR1*). Finally, four more regression models (*MR_I1*, *MR_I2*, *MR_I3* and *MR_I4*) are evaluated assuming different combinations of: (a) input variables; (b) transformations of the attributes; and (c) interactions

among the attributes. It is noted that, in a first step, all the regression models are constructed using LS3 as the output variable.

Thus, the first regression model that is mainly the same model used for the definition of the key parameters weights (*MR0*). The second model (*MR1*) also consists of a simple multiple regression model that evaluates the influence of the different parameters independently. However, in this case, the parameters variables for P1, P2, P7, P8 and P9 are described using the continuous variables presented in Table 6.1, instead of considering solely the parameters classes. In addition, this first model (*MR1*) uses the untransformed input variables, but the output variable is log-transformed. Therefore, model *MR1* reads:

$$MR1: \ln(LS3) \sim \lambda + s + P3 + P4 + P5 + P6 + P7a + P7b + N + P9 + \gamma_i \quad (6.1)$$

The adoption of more accurate attributes to define the parameter variables in *MR1*, together with the logarithmic transformation of the output variable, results in a significant improvement in its prediction performance in comparison with the *MR0* model constructed in Chapter 5. Figure 6.2 shows a comparison between the predicted versus observed LS3 values for both models. The improved behavior of the *MR1* model is evident. The plotted values of *MR1* lie notably closer to the 45° line than the plotted values of *MR0*, which is particularly visible for low LS3 values (below 0.2g). Values are thus more uniform and less scattered for the new model, showing a better prediction capacity. This represents a positive improvement of the model, since the biggest deviations take place for high values of LS3, approximately over 0.6g. Those buildings with $LS3 > 0.6g$ can be already considered to have low vulnerability so that the accuracy of the model is less critical. The main part of the dataset includes models with values of LS3 ranging from 0.15g to 0.6g (see Figure 6.2b), and is well matched.

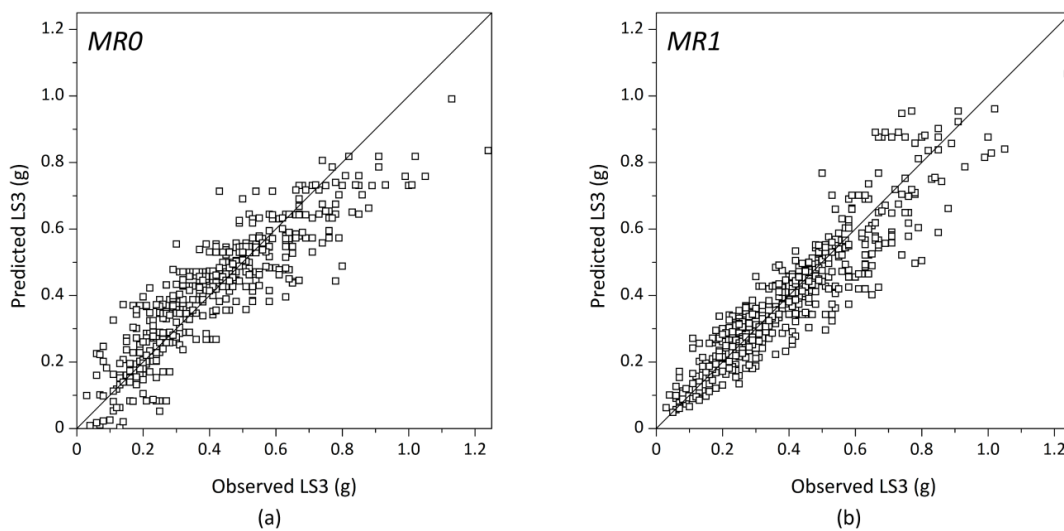


Figure 6.2: Comparison of predicted versus observed values for the regression models: (a) *MR0*; and (b) *MR1*

Table 6.2 shows a comparison between the performance of both models in terms of errors, coefficient of determination (R^2) and F-statistic. The error measures were notably reduced around 10-15% and also the maximum error was significantly reduced from around 0.4g to 0.3g. R^2 also increased by approximately 10%, up to 0.842. The regression equation obtained from *MR1* reads:

$$\ln(LS3) = 1.829 - 0.039 \times \lambda - 0.048 \times s - 0.239 \times P3 - 0.144 \times P4 - 0.218 \times P5 - 0.058 \times P6 + 0.223 \times P7a - 1.632 \times P7b - 0.368 \times N - 0.152 \times P9 + 0.85 \times \gamma_i \quad (6.2)$$

Table 6.2: Comparison of the performance of the first regression model constructed for the definition of the weights (*MRO*) and the new model *MR1*

Model	R^2	ε_{max}	MAE	RMSE	F-statistic	
<i>MRO</i>	0.772	0.405g	0.075g	0.095g	180.2 on 10 and 519 Degrees of Freedom	p-value < 2.2e-16
<i>MR1</i>	0.842	0.296g	0.064g	0.084g	257.7 on 11 and 518 Degrees of Freedom	p-value < 2.2e-16

Aiming at further improving the precision of the regression model, different models were built and tested by varying: (a) the input variables selected; (b) the transformations performed in the variables; and (b) the interaction among the different parameters. Different combinations were thus created using the attributes and transformations defined and presented in Table 6.1 and the interactions among them. This latter condition was considered as a very critical aspect because the results of the numerical parametric study confirmed the interaction between some of the parameters. For example, when the building presented a rigid diaphragm able to distribute the load among all structural elements (*P5*), the influence of the area of wall openings in the in-plane walls (*P7b*) is decisive. On the opposite, if the buildings present a flexible diaphragm, the failure of the building is typically controlled by the out-of-plane failure of the walls and, thus, the area of wall openings in the in-plane walls has a negligible effect on the response of the building. Therefore, the interaction between parameters that influence themselves mutually on their effect on the seismic behavior of vernacular buildings was introduced in the multiple regression models. This is intended to allow that the extent of the influence of some parameters in the output variable depends on other parameters. Considering the previous example, a new interaction term composed by the product $P5 \times P7b$ can be included in the regression models, keeping also the independent terms *P5* and *P7b*. With the new predictor term, the influence of *P7b* on the variation of LS3 is different for different values of the parameter *P5*, reflecting better what was observed in the numerical parametric study.

The results from numerical parametric study presented in Chapter 4 showed that the influence of some parameters is sensitive to the variations of other parameters. Therefore, many interactions between the parameters were tested in different regression models. It is noted that not all of them are herein discussed, but only those that confirmed to be significant predictors of the models: (1) area of wall openings in the in-plane walls (*P7b*) and number of floors (*P8* expressed in *N*), since the parametric study showed that the same percentage of wall openings

leads to greatest differences in terms of load factor when the building has more than one floor; (2) number of floors (N) and in-plane index (P10 expressed as γ_i), which is the result of taking also into account the height of the building (i.e. the mass) within the in-plan index, as proposed by Lourenço et al. (2013); (3) horizontal diaphragms (P5) and in-plane index (γ_i), which is also a direct consequence of the results of the parametric study that showed that the in-plane index has a decisive influence only when the building presents a rigid diaphragm; and (4) area of wall openings in the in-plane walls (P7b) and in-plane index (γ_i), because results showed that the presence of wall openings compromises the walls in-plane resistance, which may also affect the performance of the earthquake resisting walls parallel to the loading direction and thus jeopardizes the influence of the in-plane index on the seismic behavior of the building.

As a result, four different regression models with different sets of input variables and considering the different interactions among them are shown in Table 6.3. The table shows measurements of the predictive performance of the models in terms of errors and coefficient of determination (R^2). It is noted that the previously constructed models with no interactions (MR0 and MR1) are also included for comparison purposes. It is noted that it is not recommendable to compare the predictive accuracy of a model using the same data that is used for developing the model. Therefore, the k -fold cross-validation method, with $k = 10$, was used to assess the predictive capacity of the model. The k -fold cross-validation method is one of the most widely-used methods and is considered to be more robust than others like the holdout validation (Cortez 2010). The method consists of randomly partitioning the data into k sets of roughly the same size. A model is then trained using all the sets except the first subset, which is used for testing, calculating the prediction error and accuracy of the model. The same operation is repeated ten times (for each partition) and the performance of the model is evaluated by averaging the errors (MAE and RMSE) of the different test sets. Finally, once the most appropriate set of input variables and interactions is selected, the final models are developed using all the data.

Table 6.3: Different regression models constructed with measurements of their performance

Model	Variables		Interactions	R^2	ϵ_{max}	MAE	RMSE
	Output	Input					
MR0	LS3	P1; P2; P3; P4; P5; P6; P7; P8; P9; P10	-	0.772	0.405g	0.075g	0.095g
MR1	$\ln(LS3)$	λ ; s; P3; P4; P5; P6; P7a; P7b; N; P9; γ_i	-	0.842	0.296g	0.064g	0.084g
MR_I1	$\ln(LS3)$	λ ; s; P3; P4; P5; P6; P7a; P7b; N; P9; γ_i	P5:P7b	0.872	0.318g	0.057g	0.078g
MR_I2	$\ln(LS3)$	$\lambda^{-1/2}$; $\ln(s)$; $\ln(P3)$; P4; P5; P6; P7a; P7b; $\ln(N)$; $\ln(P9)$; γ_i	P5:P7b P7b: $\ln(N)$	0.875	0.320g	0.056g	0.076g
MR_I3	$\ln(LS3)$	$\lambda^{-1/2}$; $\ln(s)$; $\ln(P3)$; P4; P5; $\ln(P5)$; P6; P7a; P7b; $\ln(N)$; $\ln(P9)$; γ_i	P5:P7b P7b: $\ln(N)$ $\ln(N)$:P10 P5:P10 P7b:P10	0.891	0.345g	0.051g	0.069g
MR_I4	$\ln(LS3)$	$\lambda^{-1/2}$; $\ln(P3)$; P4; P5; P7b; $\ln(N)$; P9; γ_i	P5:P7b	0.865	0.338g	0.057g	0.077g

The models show different levels of complexity in order to find the abovementioned compromise between accuracy in the prediction and a clear and simple physical meaning. The four new models defined considering different parameter interactions showed an overall improvement with respect to the previous two models, reaching values of R^2 close to 0.9. The introduction of the interactions leads to an improvement in the prediction capability, reducing the errors, but the level of complexity of the formulation increases as well. This is the case of models *MR_I2* and *MRI_3*. The use of a robust cross-validation method reduces the risk of overfitting, i.e. the risk of creating excessively complex models that fit very well the data because of describing random error instead of the actual patterns of variability. However, the limitations of the database, such as the narrow range of variability within some parameters, may result in models that are very adequate for this dataset but are not so representative of scenarios outside of it. That is why, in the end, a more general expression was preferred. *MR_I4* tried to simplify the model to the maximum extent possible in terms of number of predictors, using only those showing the highest relative importance in the prediction. It shows a good performance, but it neglects some parameters that proved to be also influential in the parametric analyses and thus can be critical as well when evaluating other sets of data.

After evaluating the performance of the different models, as well as the compromise between simplicity and prediction capability, model *MR_I1* was adopted due to its relatively simple formulation. It uses all the untransformed input variables for the prediction, but adds the interaction between P5 and P7b that had an obvious influence and proves to have an important prediction weight. By adding this interaction term, the regression model reaches a R^2 of 0.877, explaining 88% of the variation of the output data, which is considered satisfactory. It should be mentioned that it provides a quite accurate value of LS3 based on the ten parameter variables and on one single simple interaction. The errors are also reduced with respect to models *MR0* and *MR1*, showing a maximum error of 0.318g. The predicted versus observed values obtained for this model are shown in Figure 6.3a. Figure 6.3b presents the predicted value with the residuals. The graph shows clearly that the highest deviations occur for higher values of LS3, as discussed for the *MR1* model. Besides, all values bounce over the 0 line, but the great majority of them lies between -0.1g and 0.1g. Only 16% of the models are outside this range, i.e. showed an absolute error higher than 0.1g. Thus, results were deemed acceptable to adopt *MR_I1* as the regression model. Figure 6.4 shows the predicted versus observed values obtained for the other three models with different sets of input variables and interactions. By comparing Figure 6.3a and Figure 6.4, it is clear that the performance of the different models is similar in terms of accuracy of the prediction, which justifies the selection of *MR_I1* as the final regression model, given its simpler formulation. The final regression equation obtained from *MR_I1* is:

$$\ln(LS3) = 2.162 - 0.041 \times \lambda - 0.053 \times s - 0.236 \times P3 - 0.156 \times P4 - 0.283 \times P5 - 0.082 \times P6 + 0.298 \times P7a - 2.794 \times P7b - 0.374 \times N - 0.154 \times P9 + 0.74 \times \gamma_i + 0.445 \times P5 \times P7b \quad (6.3)$$

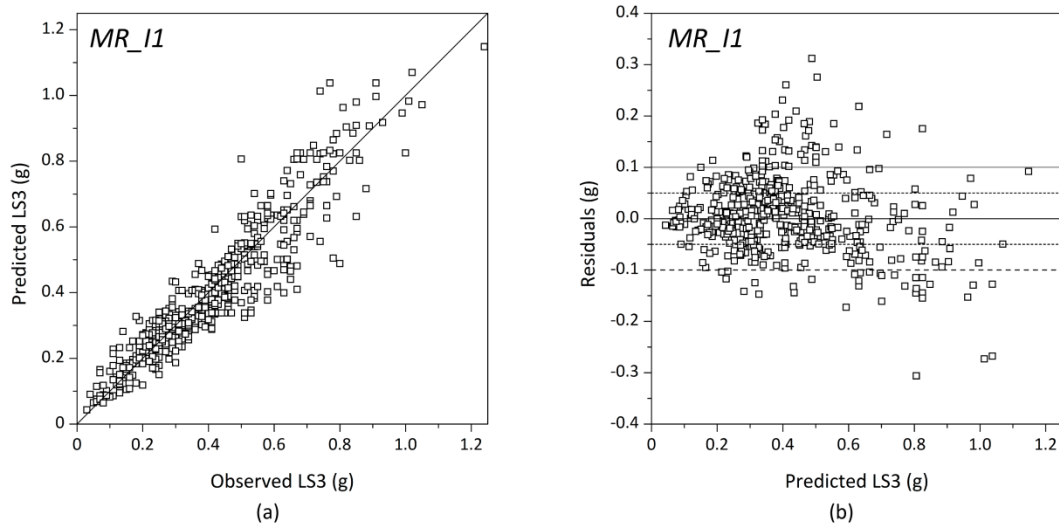


Figure 6.3: (a) Predicted versus observed values for the *MR_I1* model; and (b) residual versus fitted values

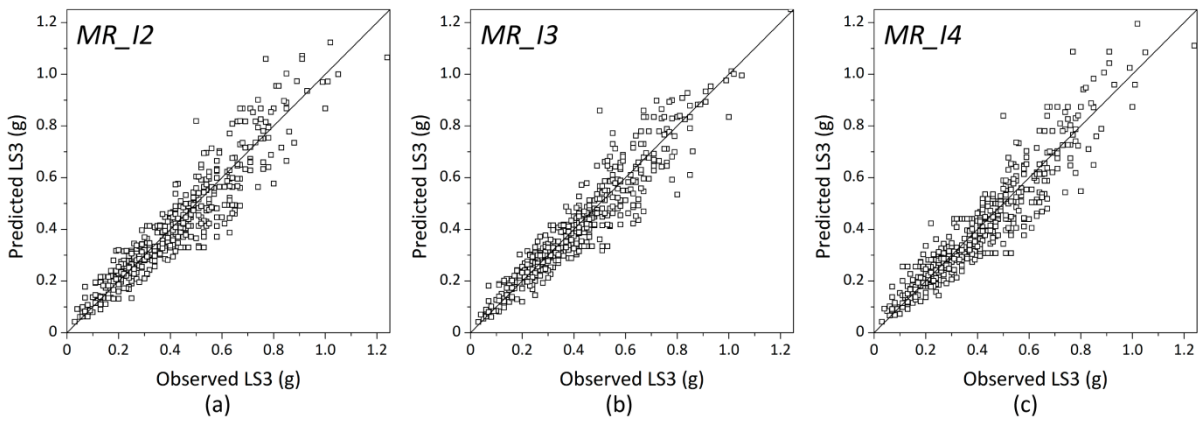


Figure 6.4: Predicted versus observed values for: (a) *MR_I2* model; (b) *MR_I3* model; and (c) *MR_I4* model

The regression models intended to predict the load factors corresponding to LS1 and LS2 were constructed following the same procedure previously explained for LS3. Only the final models adopted are presented and discussed. Figure 6.5 presents the predicted versus observed values of both models. Table 6.4 shows the variables used for the final models constructed and the measurements of the performance, in terms of errors (MAE and RMSE) and coefficient of determination (R^2). It also includes the results for the regression model constructed for the prediction of the load factor associated to LS3 (*MR_I1*), for comparison purposes.

In the case regression model prepared for the prediction of the load factor associated to LS1 (*MR_LS1*), different sets of input variables and different interactions were trained and tested until reaching the final formulation. As an example, particular attention was put in the use of the variables representing the seismic vulnerability parameters P6 (roof thrust) and P9 (previous structural damage), which can lead LS1 to take zero values for some classes. The logarithmic transformation of both variables allowed capturing properly this characteristic. The same

parameters interaction used for the selected *MR_I1* model for LS3 was also adopted for this model (*P5 × P7b*). The overall behavior of the model is considered quite acceptable for the relatively simple formulation obtained (Figure 6.5a), presenting low errors and a high R^2 of 0.811.

In the case of the regression model constructed for the prediction of the load factor associated to LS2, instead of using the parameter variables, the variables previously used as output (LS1 and LS3, expressed in *g*) are now used as the only input for the model. As previously discussed in Chapter 3, the definition of this damage limit state is originally based on LS1 and LS3, as it is calculated by assuming that the area below the three-linear curve formed by LS1, LS2 and LS3 coincides with the area below the pushover curve from LS1 to LS3. Therefore, it can be calculated using solely those two input variables. This simplified a lot its calculation and also led to very accurate predictions. Based solely on the values of LS3 and LS1, it shows an almost perfect correlation with much reduced errors (Figure 6.5b). The final regression equations obtained from both models are:

$$\ln(LS1 + c) = 1.968 - 0.058 \times \lambda - 0.102 \times s - 0.686 \times \ln(P3) - 0.142 \times P4 - 0.281 \times P5 - 0.389 \times \ln(P6) - 3.433 \times P7b - 0.821 \times \ln(N) - 2.274 \times \ln(P9) + 0.627 \times P5 \times P7b \quad (6.4)$$

$$LS2 = 0.161 \times LS1 + 0.776 \times LS3 \quad (6.5)$$

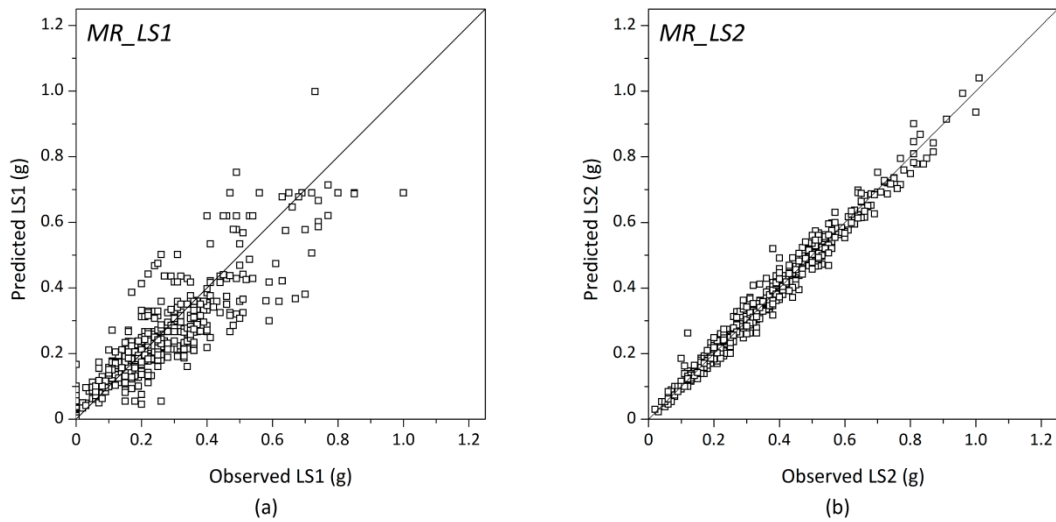


Figure 6.5: Predicted versus observed values for: (a) *MR_LS1* model; and (b) *MR_LS2* model

Table 6.4: Characteristics of the regression models constructed for the definition of LS1 and LS2

Model	Variables		Interactions	R^2	ϵ_{max}	MAE	RMSE
	Output	Input					
<i>MR_LS1</i>	$\ln(LS1+c)$	$\lambda; s; \ln(P3); P4; P5; \ln(P6); P7b; \ln(N); \ln(P9)$	<i>P5:P7b</i>	0.811	0.319g	0.057g	0.079g
<i>MR_LS2</i>	<i>LS2</i>	<i>LS1; LS3</i>	-	0.977	0.143g	0.022g	0.028g
<i>MR_I1</i>	$\ln(LS3)$	$\lambda; s; P3; P4; P5; P6; P7a; P7b; N; P9; \gamma_i$	<i>P5:P7b</i>	0.872	0.318g	0.057g	0.078g

6.2.3. Artificial Neural Networks

As aforementioned, another possible data mining technique that can be used for analyzing large databases, finding correlations between variables and eventually developing regression models able to predict output variables is artificial neural networks (ANN). An artificial neural network is a computational scheme whose basic unit are neurons organized in layers. Neurons receive a series of inputs, process the information and send an output. This process that takes place in each neuron of the system is schematized in Figure 6.6. First, the inputs received are multiplied by a previously defined weight and then linearly combined by adding a predetermined constant called bias or threshold to the sum. Finally, an activation function is applied, which, depending on the result of the previous combination, will send different outputs. Even though any function can be applied as the activation function, this work uses the sigmoid function, which is a particular case of logistic function that is commonly used within ANN architecture (Montgomery et al. 2012; Günther and Fritsch 2010;). It is noted that it is out of the scope of the present thesis to delve more deeply into inner details of the ANN architecture. More information on neural networks modelling and its conceptual basis can be found in many publications (Bishop 1995; Aleksander and Morton 1990; Haykin 1999).

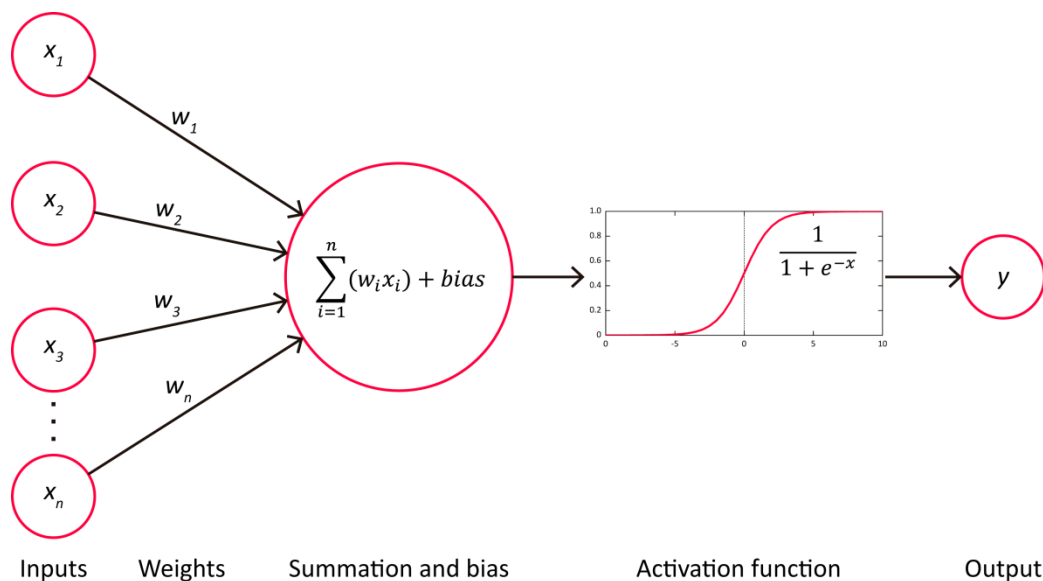


Figure 6.6: Single neuron working process

The most common neural networks are commonly composed by different parallel layers of neurons, i.e. multilayer networks (Miranda et al. 2011). Figure 6.7 shows a scheme of common neural network architecture. The first layer contains the input variables, the intermediate layer or layers are known as hidden layers, and the last layer contains the output and result of the network. Typically, besides the predefined input and output variables that are intended to be predicted, an ANN is also described by the number of hidden layers and the number of neurons in each hidden layer. Figure 6.7 shows as an example the functioning of a network with four input

variables, one output and one hidden layer with three neurons. It presents a feedforward network, which means that the connections always go from inputs to outputs (there is no connection between the neurons within the same layer) and there are no cycles in the network.

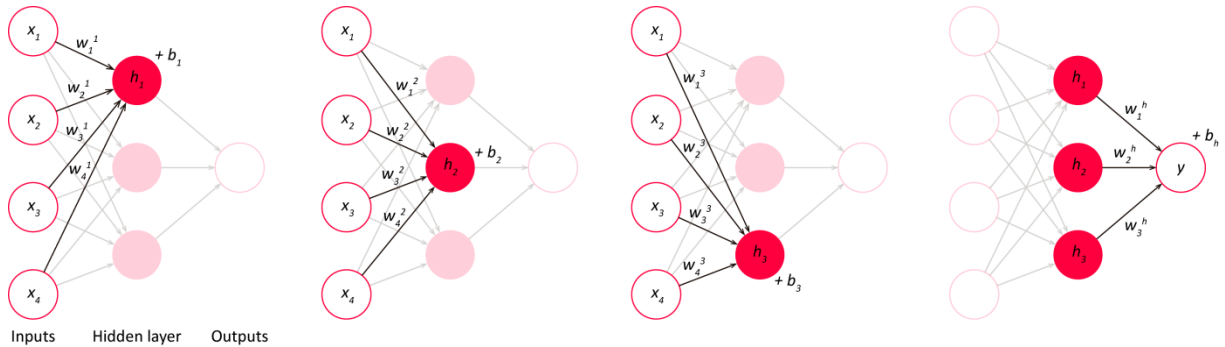


Figure 6.7: Feedforward neural network architecture functioning

Neural networks are capable of learning from trial and errors using algorithms like backpropagation, which is one of the most common ones and is also used for this study. The learning process from this method consists of setting initial random values for the weights and biases, leading to a specific output. The error is measured and propagated backwards in order to adjust the weights and biases. This process is repeated so that gradually the actual output from the model gets closer to the desired output after rounds of testing, until reaching a minimum error specified. The final architecture of the ANN model is defined by fixing the weights and biases that led to reach this minimum error.

6.2.4. ANN regression models and comparison among data mining techniques

The neuralnet package (Fritsch et al. 2016) for the R software was used for the preparation and training of the ANN models. ANN models are able to detect the interactions among the parameters and, since they are not based on a linear combination of the input variables, the transformations proposed for the input variables are no longer necessary either. However, the logarithmic transformation was still applied to the output variables in order to prevent them to reach negative values. Two models were prepared, each of them with one output variable: LS1 and LS3. The ANN model for LS2 was deemed unnecessary because the linear regression model already obtained, shown in Eq. 6.5, was considered accurate enough. The variables used as the input are those that proved to be significant predictors of LS1 and LS3 when preparing the multiple linear regression models, defined by the attributes presented in Table 6.1. This way, the models could also be directly compared. The ANN model selected is a multilayer feedforward with a unique hidden layer, whose number of neurons was determined by trial and error process. Even though there is no generally accepted rule to define the number of neurons in the hidden layer, it is usually recommended to be a number in between the number of input variables and outputs (Aguilar 2016). The final number of neurons used was four in both models, since they led to good

results in terms of performance. The 10-fold method previously described was also used for training and validating the models.

The results obtained showed that the ANN models slightly outperformed the multiple linear regression models. Figure 6.8 shows the predicted versus observed values in both models, showing the improvement in the behavior when compared to the predicted versus observed values obtained for the multiple regression models for LS1 (Figure 6.5a) and LS3 (Figure 6.3a). The results lie notably closer to the 45° line, even for the highest values of LS1 and LS3, which were less accurately estimated by the multiple regression models. Table 6.5 shows the variables adopted for each regression model and the measurements of performance of both models in terms of errors (MAE and RMSE) and coefficient of determination (R^2). The table also includes the measurements of performance of the multiple regression models constructed (MR_{I1} and MR_{LS1}), for comparison purposes. In comparison with the multiple regression models, the errors (MAE and RMSE) of the ANN models were reduced around 20% in both models, while the coefficient of determination also increased around 7% for the model predicting the load factor associated with LS1 and 5% for the model predicting the load factor associated with LS3.

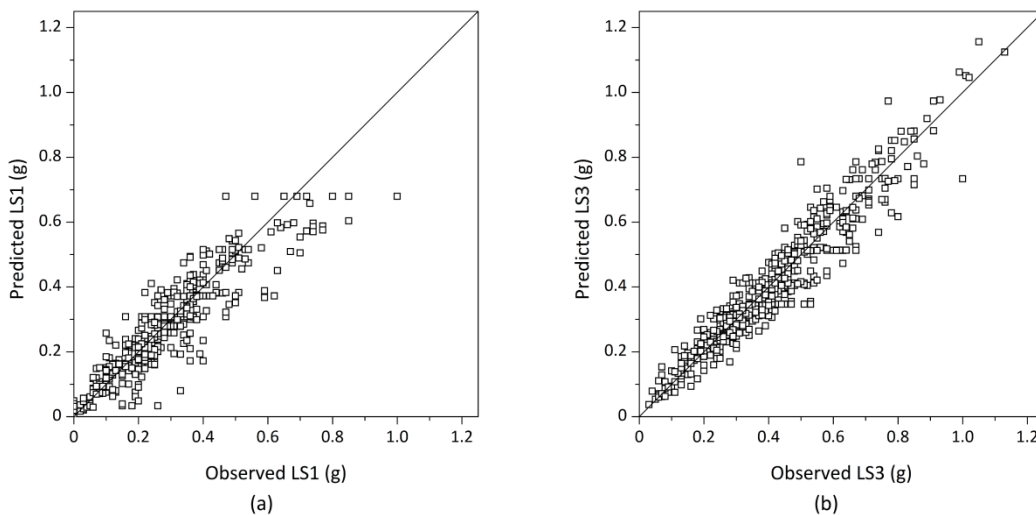


Figure 6.8: Predicted versus observed values for: (a) ANN_{LS1} model; and (b) ANN_{LS3} model

Table 6.5: Characteristics of the ANN regression models constructed for the definition of LS1 and LS3 compared with the multiple regression models

Model	Variables		Interactions	R^2	ϵ_{max}	MAE	RMSE
	Output	Input					
ANN_{LS1}	$\ln(LS1+c)$	$\lambda; s; \ln(P3); P4; P5; \ln(P6); P7b; \ln(N); \ln(P9)$	-	0.868	0.321g	0.044g	0.066g
MR_{LS1}	$\ln(LS1+c)$	$\lambda; s; \ln(P3); P4; P5; \ln(P6); P7b; \ln(N); \ln(P9)$	$P5:P7b$	0.811	0.319g	0.057g	0.079g
ANN_{LS3}	$\ln(LS3)$	$\lambda; s; P3; P4; P5; P6; P7a; P7b; N; P9; \gamma_i$	--	0.912	0.286g	0.048g	0.062g
MR_{I1}	$\ln(LS3)$	$\lambda; s; P3; P4; P5; P6; P7a; P7b; N; P9; \gamma_i$	$P5:P7b$	0.872	0.318g	0.057g	0.078g

The aforementioned improvement obtained with the ANN models is not considered significant enough to disregard the multiple regression models. ANN models have the disadvantage of not being so straightforward because the resulting formulation is not a simple equation such as the ones presented in Eq.6.3, Eq.6.4 and Eq.6.5, but a structure composed of hidden layers, multiple weights and inner functions, as previously explained. Thus, for practical matters, the complexity of the ANN architecture makes the MR models desirable for practical use. They are easy to implement and the assessment can be carried out with a simple spreadsheet, while keeping the robust prediction. It is noted that this method was conceived to provide a first seismic assessment that can be carried out in an expedited way, even for large numbers of buildings. Thus, it is preferable that it is based on simple visual inspection and simple formulations. That is why this work also proposes the development of a web application for the SAVVAS method, which can further help to easily apply the method during inspection.

Another main advantage of the multiple regression models is that they are easier to interpret. This is important because the method is also intended to allow performing an initial evaluation of the effect of different retrofitting strategies in reducing the seismic vulnerability of vernacular buildings. From the expressions provided in Eq.6.3, Eq.6.4 and Eq.6.5, assessing each parameter independently in order to understand their influence is possible. For instance, the term of Eq. 6.3 involving P4 is $(-0.156 \times P4)$, where P4 refers to the seismic vulnerability class of the building corresponding to the parameter P4 (wall-to-wall connections). Thus, the use of a strengthening solution that can improve the wall-to-wall connections and supposes an increase in the seismic vulnerability class from 4 to 1, leads to a quantifiable increase in the maximum capacity of the building (LS3) that can be easily calculated. This increase goes from $e^{(a-0.624)}$ up to $e^{(a-0.156)}$, where a represents the sum of the rest of the terms concerning the other variables and is kept constant. The strengthening is only applied at the level of the wall-to-wall connections. Since $e^{(a+b)} = e^a \times e^b$, $e^{(-0.624)} = 0.54$ and $e^{(-0.156)} = 0.86$, upgrading the class of P4 from 4 to 1, will suppose a significant increase of LS3, by the order of 1.6 times ($0.86/0.54$). This can be evaluated for every parameter, and it shows that the log transformation of the data adopted seemed to be enough for the multiple regression models to capture adequately the nonlinear relationships and interactions among the variables.

6.3. Validation of the regression models

This section was developed to validate the proposed regression models with examples gathered from the literature on numerical and experimental tests. It is noted that the regression models proposed are based on numerical simulations and, sometimes, the accuracy of the regression models might be biased with the intrinsic limitations of the database used for their development, which certainly cannot cover all possible cases. That is why some studies from the literature were reviewed and the experimental results are compared with the model predictions. They consist of

examples of the seismic assessment of different structures that could be considered vernacular because of their geometric, construction techniques and material characteristics. The following collection comprises both numerical and experimental studies that provide sufficient information about the buildings to perform the parameter survey and they inform about the maximum capacity of the buildings. In this way, the results from the studies can be compared in a straightforward way with the results obtained when applying the regression expressions. In total, six studies are here presented and discussed.

6.3.1. Seismic vulnerability of existing masonry buildings: nonlinear parametric study (Mendes and Lourenço 2015)

This example is a detailed numerical study that presents the seismic safety analysis of a representative stone masonry structure typology from Lisbon, in Portugal. The buildings belonging to this typology are commonly known as *gaioleiro* buildings, which were already discussed in Chapter 2. It represents an appropriate study because the building was studied by means of numerical modeling and pushover analysis, which were the analytical tools also applied for the development of the SAVVAS method. Additionally, the results of the maximum capacity of the building are given in terms of base shear coefficient or load factor, which is the same information that can be obtained after the application of the method and, thus, results can be directly compared. The numerical model and results of the study in terms of seismic coefficient versus displacements are shown in Figure 6.9.

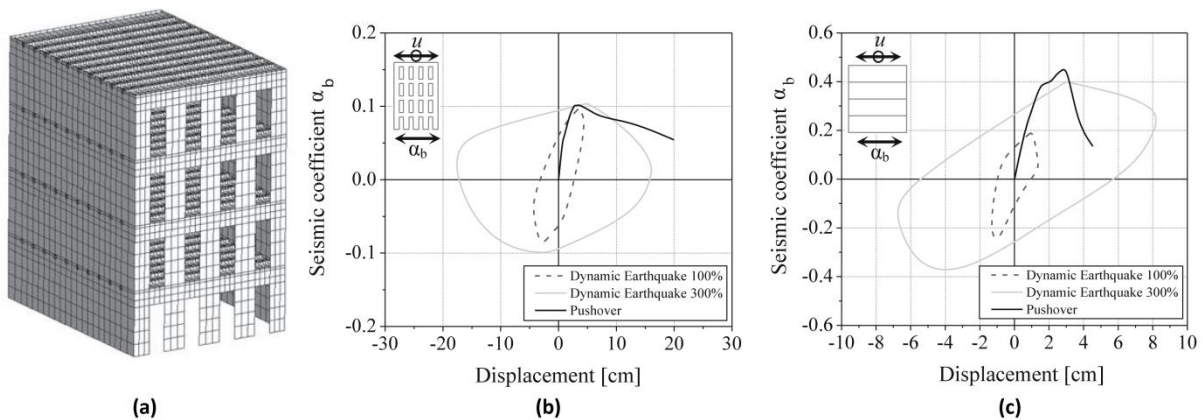


Figure 6.9: (a) Model of the analyzed structure; (b) results from the pushover analysis in the transversal direction; and (c) results from the pushover analysis in the longitudinal direction (Mendes and Lourenço 2015)

Since detailed information about the construction of the model is provided in the paper, the data from the parameters could be fulfilled in an unambiguous way. Table 6.6 shows: (1) the values adopted for each parameter, according to the attributes necessary to apply the regression models; (2) the numerical seismic coefficient provided by the paper; and (3) the estimated load factor associated to LS3 obtained using two different regression models: (a) *MR_II* model, which

was the multiple linear regression model finally selected for LS3; and (b) *ANN_LS3*, which is also provided for reference and comparison. Since there is no information about the onset of damage or other structural limit states, only the models aimed at the estimation of the maximum capacity of the building (LS3) were used.

Table 6.6: Application of the regression models to (Mendes and Lourenço 2015) and comparison of the results

Model	P1	P2	P3	P4	P5	P6	P7a	P7b	P8	P9	P10	LS3(g)		
												Literature	MR_I1	ANN_LS3
Transversal direction	7.06	12.45	3	1	1	1	0	0.33	4	1	0.46	0.10	0.12	0.14
Longitudinal direction	7.06	9.45	3	1	1	1	0.33	0	4	1	0.59	0.46	0.38	0.42

The SAVVAS method allows distinguishing the seismic behavior of the building in the two principal directions, which is not possible with other simplified formulations. The value of some parameters, such as the amount of wall openings in the in-plane walls or the in-plane index, depends on the evaluated direction. Thus, assessing each resisting direction, denominated as transversal and longitudinal using the terminology of the paper, leads to different values of the maximum capacity, which is in agreement with the reviewed study. The paper revealed that the capacity of the building is very different in each principal direction and this feature is well-captured by the SAVVAS method. There is a good correlation between the numerical seismic coefficient from the paper and the predicted load factor obtained from the method. The method also captures well the most vulnerable direction of the building. The reviewed paper also included a parametric analysis that consists of varying the material properties of the masonry walls. The results of this parametric study were also correlated with the results that the SAVVAS method by modifying parameter P3, assuming varying material quality of the masonry walls, see Table 6.7.

Table 6.7: Application of regression models following the parametric study from (Mendes and Lourenço 2015)

Model	P1	P2	P3	P4	P5	P6	P7a	P7b	P8	P9	P10	LS3(g)		
												Literature	MR_I1	ANN_LS3
Transversal direction (+)	7.06	12.45	2	1	1	1	0	0.33	4	1	0.46	0.15	0.16	0.17
Longitudinal direction (+)	7.06	9.45	2	1	1	1	0.33	0	4	1	0.59	0.51	0.48	0.56
Transversal direction (-)	7.06	12.45	4	1	1	1	0	0.33	4	1	0.46	0.07	0.10	0.12
Longitudinal direction (-)	7.06	9.45	4	1	1	1	0.33	0	4	1	0.59	0.29	0.30	0.31

A very good correlation between the results from the paper and the predicted load factor can be highlighted. The method is able to simulate accurately the variations in the parametric analysis simply by increasing or decreasing one vulnerability class in P3 (highlighted in bold in Table 6.7). Both models (MR and ANN) provide a good accuracy with a maximum difference of 0.08g but, in most cases, the difference is substantially lower.

6.3.2. Comparative analysis on the seismic behavior of unreinforced masonry buildings with flexible diaphragms (Betti et al. 2014)

This study presents the results of an experimental campaign carried out on a two-story unreinforced stone masonry building that was tested on a shaking table test at the CNR-ENEA research center of Casaccia, in Rome, Italy (Figure 6.10a). The results of the experimental analysis were replicated with finite element modelling and pushover analysis (Figure 6.10b-d). The building structural typology is adequate and there is enough information on the construction of the numerical model and the prototype tested in the laboratory to apply the SAVVAS method.

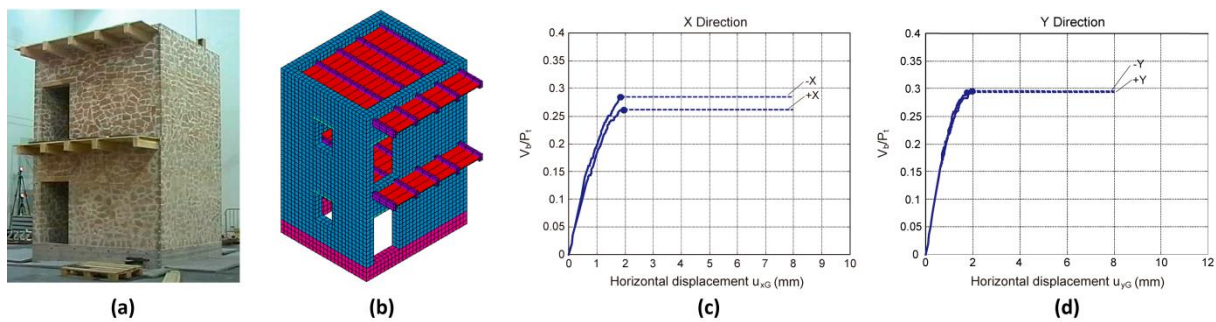


Figure 6.10: (a) Building prototype; (b) Numerical model of the analyzed structure; (c) results from the pushover analysis in Y direction; and (d) results from the pushover analysis in X direction (Betti et al. 2014)

The values adopted for each parameter could be easily assigned because there is sufficiently detailed data in the paper. Table 6.8 presents the values adopted for the parameters and the results obtained using the regression models. The method was also here applied in each main direction of the building, denominated as +/-X and +/-Y. The predicted load factors show again a very good agreement and very low errors. The regression models are also able to detect the most vulnerable direction, being the building slightly less resistant in -X direction.

Table 6.8: Application of the regression models to (Betti et al. 2014) and comparison of the results

Model	P1	P2	P3	P4	P5	P6	P7a	P7b	P8	P9	P10	LS3(g)		
												Literature	MR_I1	ANN_LS3
+X direction	9.10	3.75	4	1	4	1	0.06	0.22	2	1	0.50	0.27	0.23	0.26
-X direction	9.10	3.75	4	1	4	1	0	0.22	2	1	0.50	0.29	0.23	0.25
+Y direction	9.10	4.5	4	1	4	1	0.08	0.03	2	1	0.50	0.29	0.27	0.30
-Y direction	9.10	4.5	4	1	4	1	0.15	0.03	2	1	0.50	0.29	0.28	0.31

6.3.3. Shaking table test of strengthened full-scale stone masonry building with flexible diaphragms (Magenes et al. 2014)

The third example presents the results of another experimental test conducted at the EUCENTRE research center in Pavia, Italy. The test campaign consisted on shaking table tests

on two full-scale two-story unreinforced masonry buildings with timber floors. The first prototype was an unstrengthened reference prototype (URM) without seismic resistant detailing, while the second specimen introduced some reinforcement measures (RM). In this case, only the results of the experimental campaign are available so the results of the method were compared with the maximum resisted base shear coefficient. Again, the building typology is relevant for the application of the method and there is enough information on the construction of the specimens tested in laboratory. The prototype and the experimental results are shown in Figure 6.11.

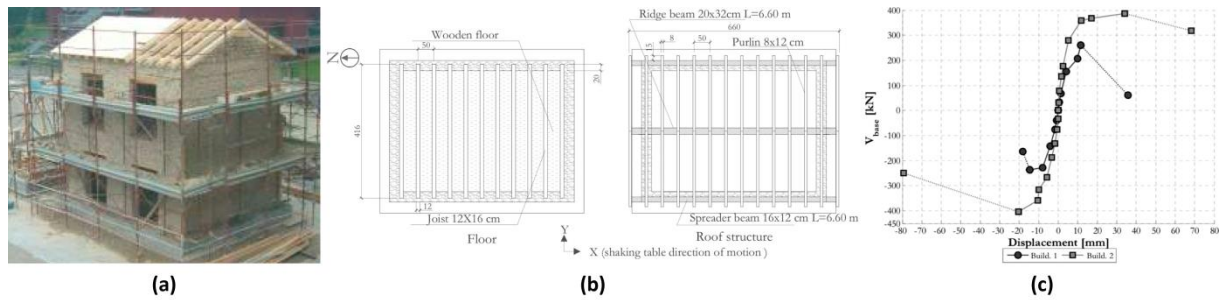


Figure 6.11: (a) Full scale building prototype (Magenes et al. 2010); (b) Detail of the floor and roof of the structure; and (c) results of the shaking table test in terms of base shear vs displacement (Magenes et al. 2014)

Even though detailed information about the construction of the two specimens is given in the paper, some of the qualitative parameters have to be assumed by the photos or by the descriptive qualitative information provided. For example, for the URM building, the type of horizontal diaphragm is considered as class D. According to the plans shown in Figure 6.11b, the beams are only connected to the walls by a partial embedment within the wall but there is no strengthened connection between the floor sheathing and the walls. This class was upgraded to class B for the RM buildings, since the strengthening interventions were destined to improve the wall-to-floor and wall-to-roof connections and to moderately improve the in-plane stiffness of the floor, aimed at preventing the occurrence of premature out-of-plane failure mechanisms. The undressed double-leaf stone masonry of the walls is considered as class B because of the assumed good workmanship at the laboratory. Also, the authors report that some damage took place on the RM building during the transportation phase, with observed cracks below 1 mm. Thus, a class B on the previous structural damage (P9) was adopted. Table 6.9 shows the values adopted for the parameters and the results obtained in the prediction of the seismic load factors associated with LS3. Although the table shows the results of the regression models in every direction, it should be noted that the uniaxial shaking table only imposed the base motion in +/- X direction. Thus, only these directions are directly comparable.

The regression models predict very accurately the maximum capacity of the building and capture very well the improvement in the seismic behavior when applying the strengthening intervention in the floors. The errors in the prediction of the multiple linear regression models are below 0.03g. The performance of the building was evaluated in all directions, including +/-Y,

because the regression models can estimate the weakest direction of the building. Thus, it is interesting to see how the method predicts that the unreinforced building, which is prone to out-of-plane collapse, is more vulnerable in Y direction while, after the intervention in the diaphragms, the building is more likely to fail in X direction. The method is thus able to show that reinforcing the diaphragms will have an effect in the failure mode of the building, leading to the development of in-plane resisting mechanisms. This change in the failure mode was also reported in the paper.

Table 6.9: Application of the regression models to (Magenes et al. 2014) and comparison of the results

Model	P1	P2	P3	P4	P5	P6	P7a	P7b	P8	P9	P10	LS3(g)		
												Literature	MR_I1	ANN_LS3
+Y direction (URM)	8.35	5.2	2	1	4	2	0.1	0.07	2	1	0.46	-	0.38	0.32
-Y direction (URM)	8.35	5.2	2	1	4	2	0.32	0.07	2	1	0.46	-	0.40	0.35
+X direction (URM)	8.35	3.75	2	1	4	1	0	0.22	2	1	0.61	0.43	0.41	0.36
-X direction (URM)	8.35	3.75	2	1	4	1	0.14	0.22	2	1	0.61	0.43	0.43	0.38
+Y direction (RM)	8.35	5.2	2	1	2	1	0.1	0.07	2	2	0.46	-	0.58	0.60
-Y direction (RM)	8.35	5.2	2	1	2	1	0.32	0.07	2	2	0.46	-	0.62	0.66
+X direction (RM)	8.35	3.75	2	1	2	1	0	0.22	2	2	0.61	0.54	0.51	0.58
-X direction (RM)	8.35	3.75	2	1	2	1	0.14	0.22	2	2	0.61	0.54	0.53	0.62

6.3.4. Dynamic tests on three leaf stone masonry building model before and after interventions (Mouzakis et al. 2012)

This example presents the results of an experimental campaign similar to the previous one carried out at the LEE/NTUA research center in Athens, Greece. Two reduced scaled (1:2) two-story unreinforced stone masonry buildings were tested on a bi-directional shaking table: one unstrengthened reference prototype (URM) and a second specimen with some reinforcement measures (RM). This study also just provides the results of the experimental campaign and thus the results obtained after the application of the regression models were compared with the values of maximum accelerations measured in g given by the paper. The laboratory specimen and the results of the campaign are presented in Figure 6.12.

Most of the information of the parameters was extracted from the detailed information about the construction of the specimen. However, as in the previous case, some assumptions had to be made for the definition of some of the qualitative parameters, based on the photos and description. For example, the walls were grouted in the RM building so the class of parameter P3 was upgraded from B to A. The floors were also reinforced, improving their connection to the walls, which resulted in a parameter upgrade from Class D to B. Table 6.10 shows the values adopted for all the parameters and the load factors associated to LS3 predicted using the regression models. The results show again a good correspondence and a good simulation of the

effect of the reinforcing techniques, presenting very low errors. The method is again able to correctly identify Y direction as the most vulnerable one, which is in agreement with the results obtained experimentally.

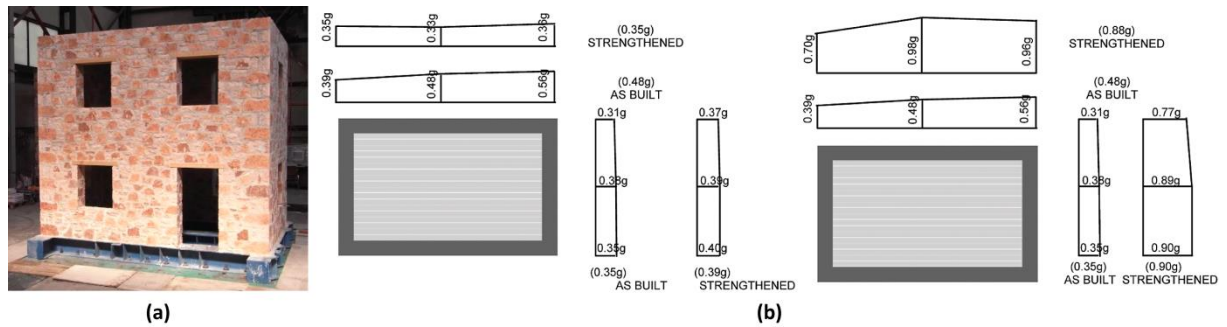


Figure 6.12: (a) Two-story building prototype (scale 1:2); and (b) results of the shaking table test reporting maximum accelerations recorded in X and Y direction for both URM and RM models (Mouzakis et al. 2012)

Table 6.10: Application of the regression models to (Mouzakis et al. 2012) and comparison of the results

Model	P1	P2	P3	P4	P5	P6	P7a	P7b	P8	P9	P10	LS3(g)		
												Literature	MR_I1	ANN_LS3
+Y direction (URM)	6.40	6.3	2	1	4	1	0.15	0.1	2	1	0.42	0.48	0.40	0.35
+X direction (URM)	6.40	3.6	2	1	4	1	0.1	0.15	2	1	0.67	0.48	0.52	0.42
+Y direction (RM)	6.40	6.3	1	1	2	1	0.15	0.1	2	1	0.42	0.88	0.81	0.72
+X direction (RM)	6.40	3.6	1	1	2	1	0.1	0.15	2	1	0.67	0.88	1.01	0.83

6.3.5. Shaking table tests on 24 simple masonry buildings (Benedetti et al. 1998)

This study presents the results of another experimental campaign of two-story unreinforced stone and brick masonry buildings tested on a shaking table by ISMES, in Bergamo, Italy and LEE/NTUA, in Athens, Greece. The results of the experimental campaign are provided in terms of maximum lateral force coefficients so they can be compared with the results provided by the SAVVAS method. The experimental campaign is very large and there is detailed information about the models, which include unstrengthened and strengthened prototypes. However, not all the models report values of maximum lateral force coefficients. Also, some of the qualitative parameters had to be assumed from descriptions and pictures provided in the paper. The plans of the typical laboratory specimen, as well as one of the brick masonry buildings and one stone masonry building, are shown in Figure XX, for reference.

Table 6.11 shows the values adopted for the parameters and the results that were given in terms of load coefficient for a stone masonry specimen (STM) and a brick specimen (BM). Also in this case, the predicted load factor associated with LS3 is in very good agreement with the experimental maximum lateral coefficient provided in the paper. The errors obtained are minimum, close to 0.01g.

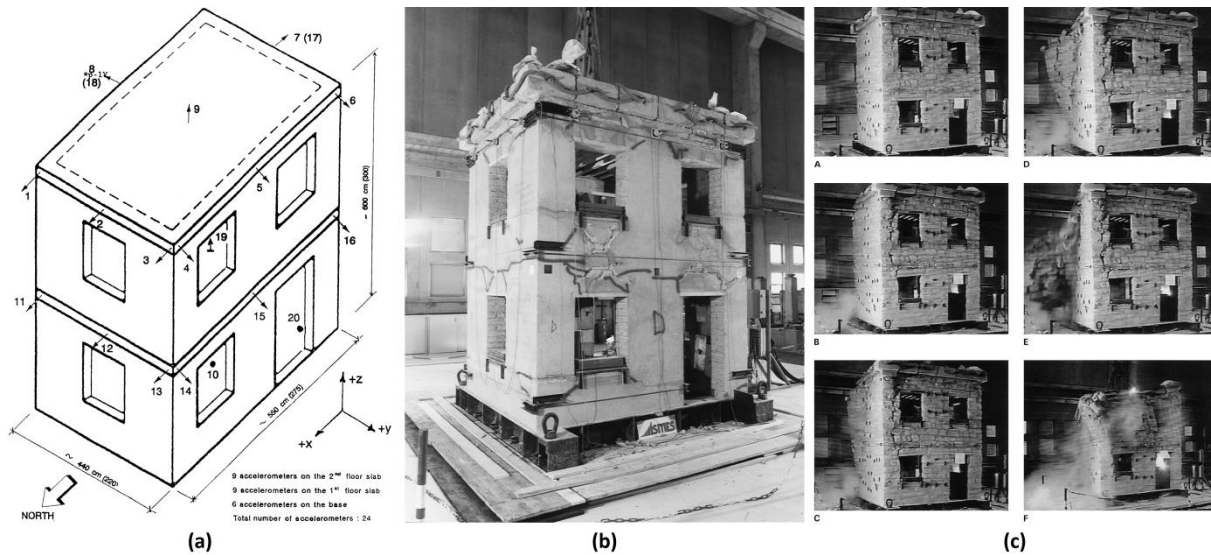


Figure 6.13: (a) Two-story building prototype; (b) brick masonry prototype before ultimate shock; and (c) collapse of one stone masonry building prototype (Benedetti et al. 1998)

Table 6.11: Application of the regression models to (Benedetti et al. 1998) and comparison of the results

Model	P1	P2	P3	P4	P5	P6	P7a	P7b	P8	P9	P10	LS3(g)		
												Literature	MR_I1	ANN_LS3
+Y direction (STM)	6.67	5.5	4	2	4	1	0.18	0.08	2	2	0.44	0.19	0.20	0.21
+X direction (STM)	6.40	4.4	4	2	4	1	0.08	0.2	2	2	0.56	0.19	0.20	0.20
+Y direction (BM)	6.67	5.5	3	1	4	1	0.18	0.08	2	2	0.44	0.3	0.29	0.29
+X direction (BM)	6.40	4.4	3	1	4	1	0.08	0.2	2	2	0.56	0.3	0.29	0.29

6.3.6. Shaking table test on a full-scale unreinforced clay masonry building with flexible diaphragms (Kallioras et al. 2018)

The sixth and last study included the results of an experimental campaign conducted at EUCENTRE research center in Pavia, Italy, consisting of a unidirectional shaking table test of a full-scale unreinforced clay brick masonry building. The study provides the results of the experimental campaign in terms of maximum accelerations measured in *g*, which were compared with the results obtained after the application of the regression models. The detailed information provided about the construction of the specimen, together with the qualitative descriptions and photos, allowed completing the definition of the different parameters for the application of the SAVVAS method.

The values finally adopted are presented in Table 6.12, which also presents the results of the experimental campaign and the results obtained from the regression models. The paper provided information about the base-shear coefficients (*BSC*) that led the building to reach different damage states, including: (a) the *BSC* corresponding to the onset of the first significant cracks, which can be correlated with the load factor related to the reaching of LS1; and (b) the maximum

attained overall *BSC* for the building, which can be correlated with the load factor related to the reaching of LS3. Thus, the two regression models aimed at the estimation of the load factors associated with LS1 and LS3 could be used and the results compared with the ones observed experimentally. Results for all limit states show a good agreement between the predicted values with the multiple regression models and the experimentally obtained values, with minimum errors, validating the results obtained with the two regression expressions. Errors are slightly higher for the ANN regression models.



Figure 6.14: (a) Two-story full-scale building prototype; (b) overall building response in terms of base shear coefficients (*BSC*) versus drift (Kallioras et al. 2018)

Table 6.12: Application of the regression models to (Kallioras et al. 2018) and comparison of the results

Model	P1	P2	P3	P4	P5	P6	P7a	P7b	P8	P9	P10	LS3(g)			LS1(g)		
												Lit.	MR_I1	ANN_LS3	Lit.	MR_LS1	ANN_LS1
+Y	13	4.04	1	1	3	1	0.20	0.18	2	1	0.54	0.54	0.54	0.41	0.39	0.35	0.34
-Y	13	4.91	1	1	3	1	0.18	0.18	2	1	0.54	0.54	0.52	0.39	0.39	0.32	0.31

6.3.7. Summary of the results

As a summary, Table 6.13 provides the most relevant results obtained for the validation of the regression models. All the results correspond to the load factor associated with LS3 because it could be calculated in the six cases. The prediction capability of the models was considered validated, given the low errors obtained, particularly for the multiple regression models.

Table 6.13: Summary of the results obtained for the application of the regression models to all the cases studied and comparison of the results

	LS3(g)												
	Mendes and Lourenço (2015)		Betti et al. (2014)				Magenes et al. (2014)		Mouzakis et al. (2012)		Benedetti et al. (1998)		Kallioras et al. (2018)
	Y	X	+X	-X	+Y	-Y	URM	RM	URM	RM	STM	BM	Y
Literature	0.10	0.46	0.27	0.29	0.29	0.29	0.43	0.54	0.48	0.88	0.19	0.3	0.54
MR_I1	0.12	0.38	0.23	0.23	0.27	0.28	0.43	0.53	0.52	1.01	0.20	0.29	0.54
ANN_LS3	0.14	0.42	0.26	0.25	0.30	0.31	0.38	0.62	0.42	0.83	0.20	0.29	0.41

6.4. SAVVAS formulation

The validation of the regression models with several examples available in the literature confirmed the reliability of the predictions of the regression models and the potential of the proposed method. As a consequence, a final formulation of the SAVVAS method is proposed, using the expressions for the three limit states shown in Eq.6.3, Eq.6.4 and Eq.6.5. Table 6.14 summarizes the process and provides the final formulation of the SAVVAS method. As observed during the validation process, the application of the method simply consists of three steps: (1) the first one involves the collection of the data related to the ten key seismic vulnerability assessment parameters. Depending on the parameter, they can be defined either by specifying different quantitative attributes or by assigning a seismic vulnerability class from 1 to 4, directly associated to the classification from A to D defined for the vulnerability index method; (2) in a second step, the regression models expressions are applied to determine the three different values of load factor defining each limit state (LS1, LS2 and LS3). With the obtainment of these values, it is possible to have an estimation of the seismic actions that can cause the building to reach the different structural limit states for each direction, expressed as an acceleration (in terms of g); (3) the third final step consists of providing an estimation of the minimum load that will cause the building to reach the different limit states. Since this method allows calculating a different load factor in each main direction of the building, the load factor representing the global vulnerability of the building is defined as the minimum value obtained among the four resisting directions.

Table 6.14: SAVVAS formulation and procedure

Step 1		Definition of the seismic vulnerability assessment parameters									
	P1	P2	P3	P4	P5	P6	P7		P8	P9	P10
	$\lambda (h/t)$	$s (m)$	$P3 [1-4]$	$P4 [1-4]$	$P5 [1-4]$	$P6 [1-4]$	$P7a$	$P7b$	N	$P9 [1-10]$	ν_i
Step 2		Calculation of the load factors associated to the limit states in each main direction i									
$LS1_i(g) = e^{(1.97-0.06\lambda-0.1s-0.68 \ln(P3)-0.14P4-0.28P5-0.39 \ln(P6)-3.43P7b-0.82 \ln(N)-2.27 \ln(P9)+0.63P5P7b) - c}$ $LS2_i(g) = 0.16 \times LS1(g) + 0.78 \times LS3(g)$ $LS3_i(g) = e^{(2.16-0.04\lambda-0.05s-0.24P3-0.16P4-0.28P5-0.08P6+0.3P7a-2.79P7b-0.37N-0.15P9+0.74\nu_i+0.44P5P7b)}$											
Step 3		Calculation of the global load factors defining the limit states of the building									
$LS1(g) = \min(LS1_i(g))$ $LS2(g) = \min(LS2_i(g))$ $LS3(g) = \min(LS3_i(g))$											

6.5. Conclusions

The main objective of the present chapter has been the definition of the new method for the seismic vulnerability assessment of vernacular architecture, named as Seismic Assessment of the Vulnerability of Vernacular Architecture Structures (SAVVAS). The method uses the common parameters and classes from the classical simplified seismic vulnerability index methods, but allows determining the seismic load factors associated with different damage limit states in terms of accelerations (g). This method considers the interaction between some of the parameters and distinguishes the different seismic behavior of the building in both orthogonal directions.

This new method has been developed on the basis of the extensive parametric study that made use of numerical finite element (FE) models and nonlinear static (pushover) analysis. In a second step, Knowledge discovery in databases (KDD) and data mining (DM) techniques were applied on the database resulting from the numerical campaign. The primary goal was to obtain new regression models able to predict the load factors corresponding to different structural limit states, having as predictors variables associated to the seismic vulnerability assessment parameters previously defined. Several multiple regression and ANN models were developed and proved to be reliable in their predictive capabilities. The regression models show a good behavior when used in the prediction of the seismic load factor of different masonry buildings experimentally and numerically assessed in the literature. The development of the models also allowed a better understanding of the role of the seismic vulnerability parameters on defining the seismic response of vernacular buildings in terms of load factors and helped to discover complex relationships among them. During the validation process, they were also confirmed to be useful in assessing the effect of some reinforcement techniques on the final seismic capacity of the building. Moreover, they also provide information about the capacity of the building in each main direction, which is another advantage of this method because it allows identifying the weakest direction and thus can help in making decisions about the retrofitting strategy that should be followed.

This method can be mainly considered analytical in its development because it relies on a solid numerical parametric study, even though the selection of the parameters was done through a combination of empirical observation and expert judgment. The robustness of the regression models is conditioned by the limitations and assumptions existing in nonlinear static analysis of masonry and earthen vernacular buildings. The results obtained when applying the regression expressions would simulate the results obtained as if we were performing a pushover analysis on a structure with such characteristics. The method is also conditioned by the size of the database which, even though is considered exhaustive, it cannot comprehend the vast amount of possibilities observed in vernacular buildings. Nonetheless, the results provided are deemed satisfactory, since the models showed to be able to provide a reliable first estimate of the seismic

capacity of a building based solely on limited information related to the ten key seismic vulnerability parameters.

Finally, it should be highlighted that another advantage of the SAVVAS method over more classical seismic vulnerability index approaches is that it results in the calculation of load factors that define different structural limit states of the building expressed as an acceleration (in terms of g). The load factors are directly related with structural limit states that are defined on the basis of damage descriptions and thus, the correlation between expected damage and the load factors can be achieved in a straightforward way. It should be mentioned that vulnerability index formulations calculate a vulnerability index (I_v), which is just an intermediate step to estimate the damage suffered by a building under an earthquake of a specific intensity, because empirically developed analytical expressions have to be later implemented to correlate I_v with damage. Therefore, the vulnerability functions resulting from the SAVVAS method are able to relate the seismic accelerations with structural limit states and, subsequently, with expected damage. This correlation is necessary in order to perform damage and loss assessments, which is an important part of seismic vulnerability assessment methods. This aspect will be later developed when implementing the method on a case study in Chapter 9.

It is finally noted that the development of the SAVVAS method formulation contributes to the completion of the second task of the present thesis and concludes one of its fundamental objectives: the development of a seismic vulnerability assessment method for vernacular architecture. Together with the vulnerability index method previously defined, two methods are finally proposed to this end.

CHAPTER 7

NUMERICAL EVALUATION OF TRADITIONAL EARTHQUAKES RESISTANT TECHNIQUES

Chapter outline

- [7.1. Introduction](#)
- [7.2. Traditional earthquake resistant techniques observed in the vernacular architecture](#)
 - [7.2.1. Ring beams](#)
 - [7.2.2. Corner braces](#)
 - [7.2.3. Quoins](#)
 - [7.2.4. Ties](#)
 - [7.2.5. Timber elements within the masonry](#)
 - [7.2.6. Wall subdivisions](#)
 - [7.2.7. Buttresses](#)
 - [7.2.8. Walls thickening](#)
 - [7.2.9. Summary](#)
- [7.3. Updated definition of the seismic vulnerability classes for P4](#)
- [7.4. Updated formulation of the SAVVAS method](#)
- [7.5. Conclusions](#)

7.1. Introduction

The main goal of this chapter is to respond to one of the objectives of the thesis, which consists of evaluating the efficiency of traditional strengthening solutions to mitigate the seismic vulnerability of vernacular architecture. The chapter presents the results of a detailed numerical study that follows a similar strategy than the one adopted for the quantification of the influence of the seismic vulnerability assessment parameters in the seismic behavior of vernacular buildings. Detailed FE models following the same macro-model approach were constructed, where the different traditional earthquake resistant techniques identified in Chapter 2 were simulated. Pushover analyses were performed on the different numerical models constructed and, therefore, similarly to the parametric study conducted within Chapter 4, the influence of each technique was quantitatively evaluated. Thus, the chapter is intended to respond to the primarily defined research objective 3, by means of numerical analysis. Additionally, it will contribute to a better understanding of the seismic behavior of traditional earthquake resistant solutions and their

structural role under seismic loading. These traditional techniques are typically the result of empirical knowledge transferred along generations. Therefore, for a better consistent assessment, a numerical evaluation and analytic comprehension of their possible beneficial effect in the seismic resistance of vernacular buildings is needed.

The chapter firstly introduces the eight different traditional earthquake resistant techniques identified in Chapter 2 that will be further evaluated through numerical analysis. Thereafter, the chapter is mainly structured in eight sections, revealing the individual assessment of the influence of each technique on the seismic behavior of vernacular buildings. All sections present the results according to the same structure. First, the numerical models prepared for the simulation of the different strengthening solutions are described in detail. Secondly, the discussion of the results is provided, in terms of: (a) variations on the damage patterns and failure mechanisms; (b) identification of the structural limit states and comparison of the capacity curves for the buildings with and without the different techniques; and (c) analysis of the load factor variations. Furthermore, an important part of this study consists of adapting the two seismic vulnerability assessment methods proposed so that they are able to consider the influence of different traditional strengthening solutions. Thus, the last part of each subsection is intended to discuss the ways to achieve this objective. A summary of the different approaches proposed to take into account the influence of each traditional seismic resistant solution is provided after the individual numerical studies. Finally, as a consequence of including the effect of some of the evaluated techniques, two specific updates concerning both seismic vulnerability assessment methods are summarized at the end of the chapter.

7.2. Traditional earthquake resistant techniques observed in the vernacular architecture

Previously, Chapter 2 presented a comprehensive overview of traditional earthquake resistant solutions resulting from a local seismic culture reported in the literature and, in some cases, also recognized within Portuguese vernacular architecture. The chapter particularly elaborated on the structural role and earthquake resisting concept of the different techniques. This chapter further addresses into this specific subject with the help of FE modeling and nonlinear analysis. All the identified traditional earthquake resistant techniques were summarized in Chapter 2 (Table 2.1). Table 7.1 presents those whose influence on the seismic behavior of vernacular buildings will be further studied in detail within this chapter. It should be noted that not all the techniques identified in Chapter 2 were considered for this additional numerical assessment because of different reasons that are explained below. Regardless of this, since all the techniques have an influence on the seismic behavior of vernacular buildings, the ways of taking them into account by the seismic vulnerability assessment methods are also discussed below. The following sections present the individual numerical studies conducted to evaluate the influence of the eight traditional solutions outlined in Table 7.1.

Table 7.1: Traditional earthquake resistant techniques that are numerically studied within this chapter

Traditional earthquake resistant techniques
Ring beams
Corner braces
Quoins
Ties
Timber elements within the masonry
Wall subdivision
Buttresses
Walls thickening

The main reason why no further analyses were deemed necessary for some of the techniques is that some of them are mainly intended to improve the characteristics of different structural elements whose influence on the seismic behavior of vernacular buildings was already evaluated within Chapter 4. For instance, the effect of reinforcing the diaphragm-to-wall connections or stiffening the diaphragms was thoroughly studied when evaluating P5. Chapter 4 already revealed how improving the diaphragmatic behavior has a crucial influence on the seismic resistance of vernacular buildings. This influence was also quantitatively evaluated. In order for the seismic vulnerability assessment methods to consider the influence of seismic strengthening solutions addressing the horizontal diaphragms, the seismic vulnerability class of the building for parameter P5 can be simply upgraded. As an example, if a building presenting very flexible diaphragms that are poorly connected to the walls is properly stiffened and its connections to the walls are notably improved, the class of P5 can be upgraded from D to A.

The same applies in the case of through-stones or ‘diatons’. Their influence was indirectly considered when evaluating P3 in Chapter 4. As a result, the classification of the vulnerability according to P3 provides a qualitative description of the type of material for the load bearing walls that belongs to each class. The presence or not of these transversal connection elements is included for the determination of the seismic vulnerability class. Therefore, the strengthening of the building through the application of this type of traditional element can result in the upgrade of the class for parameter P3.

Mended cracks and other post-earthquake repairs aimed at recovering the original integrity of the wall were not considered for further numerical evaluation. Their effect was also indirectly studied when assessing P9. When structural load bearing walls are repaired so that they do not present any cracks, their class can be considered again as class A, as if they were again in good original condition. With respect to reinforcing openings, they were not further evaluated because they were also taken into consideration when evaluating other parameters within Chapter 4. Some specific ways of reinforcing openings discussed in Chapter 2, such as the presence of discharging arches within the walls or the use of double timber window frames, can be considered as solutions that help to stabilize the structural walls and to transversally connect the walls

leaves. Thus, the seismic vulnerability class of P3 can be assigned by taken into account the presence of these reinforcing elements. Furthermore, the influence of openings was already studied in detail when evaluating P7. Another discussed typical traditional solution, consisting of the closing of the openings, has a direct implication on the assignment of a seismic vulnerability class for P7, since it changes the ratio of wall openings in the in-plane walls.

The analysis of structural timber frame walls as a strengthening technique is a different case. Their adoption as an efficient earthquake resistant construction system in many seismic prone regions in the world was widely discussed in Chapter 2. However, the present thesis has mainly focused on the study of the structural behavior of vernacular constructions systems consisting of unreinforced earthen and masonry load bearing walls. The seismic behavior of both structural typologies differs greatly. This chapter will actually deal with the numerical evaluation of the use of timber elements within the masonry or earthen walls as a reinforcing technique, but the numerical characterization of the structural behavior of timber frame walls is considered out of the scope of this research work. Nevertheless, the importance of this typical construction solution is acknowledged and further research is recommended. The numerical study of vernacular timber frame buildings can be eventually used for comparison with the results obtained in Chapter 4, when assessing P3. As a result, the four seismic vulnerability classes could be redefined in order to incorporate walls constructed with structural timber frames. In the same way, since the techniques discussed in Chapter 2 that are meant to have redundancy of structural elements always included timber frames structural systems, they are also out of the scope of the present research work.

Finally, reinforcing arches and other urban reinforcement elements were not further studied through numerical analysis. The main reason for this is the fact that reinforcing arches are principally aimed at achieving a collaborative action among neighboring construction, while the interaction between adjacent buildings was also left out of the scope of this thesis. Nonetheless, the resisting principle of these reinforcement elements is similar to the one of buttresses, whose behavior is indeed evaluated within this chapter. Since they are also meant to counteract horizontal loads and avoid the out-of-plane overturning of the walls, the effect of reinforcing arches on the seismic behavior of the building can be considered the same as buttresses.

7.2.1. Ring beams

Ring beams were identified as one of the most widespread traditional techniques used to improve the connections between structural elements. As explained in Chapter 2, ring or bond beams are a set of timber reinforcement elements, arranged in horizontal planes embedded within the walls, which usually run continuously along the length of the walls. Timber ring beams are commonly placed on the top of the walls and typically consist of a pair of longitudinal beams located at both edges of the walls and joined together with small transversal connectors, arranged like a ladder.

However, there are many possible configurations for the ring beams, which can vary according to: (a) the dimensions of the timber elements (axb); (b) the distance between transversal connectors (s); (c) the presence of diagonal bracing elements; (d) the number of longitudinal elements (n); or (e) their introduction at different levels within the height of the walls, namely at the floor level, at the lintel level or both. Therefore, different configurations according to these abovementioned variations were assumed. Figure 7.1 depicts the ring beams characteristics that will be modified in order to evaluate the influence of this traditional technique.

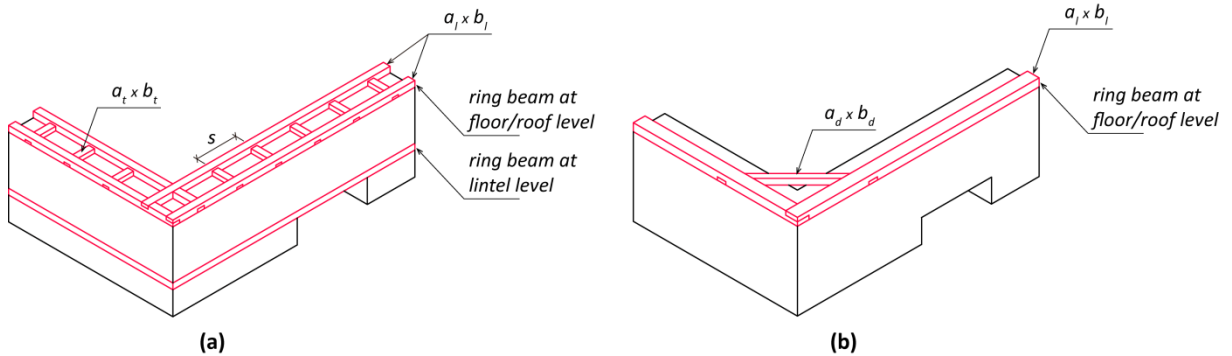


Figure 7.1: Ring beams characteristics subjected to variations showing two examples of the different configurations evaluated: (a) ring beams with two timbers in parallel at floor and lintel level; and (b) ring beam at the floor level with single timber band and diagonal brace at the corner

The different configurations and dimensions were established based on recommendations suggested by the Indian code (IS-13827 1993; IS-13828 1993), which contemplates the use of timber ring beams to improve the earthquake resistance of low strength masonry and earthen buildings. The guide for *bhatar* construction (a traditional construction system from Pakistan that also makes use of timber beams for reinforcing stone masonry walls) prepared by Schacher (2007), was also used as a reference for the specification of variations in the dimension of the timber elements. All the variations in the configuration of the ring beams were modeled in four reference models with varying number of floors and type of material, in order to evaluate the influence of this technique for different types of buildings: (a) one-floor rammed earth building (*RE1F*); (b) two-floor rammed earth building (*RE2F*); (c) two-floor stone masonry building (*STM2F*); and (d) three-floor stone masonry building (*STM3F*). The in-plan area of all models is $8 \times 5.5 \text{ m}^2$. All walls are 0.5 m thick and 3 m high. In all cases, the roof and floor loads are simply modeled as distributed load along the walls, simulating flexible diaphragms. Figure 7.2 shows some of the representative models constructed for the *RE2F* set of models. Table 7.2 presents the summary of the 29 models constructed in order to assess the influence of ring beams in the seismic behavior of vernacular buildings, specifying the variations in the dimensions and configuration of the ring beams elements. All models were subjected to a pushover analysis in the direction perpendicular to the walls presenting the maximum wall span (Y), since it is expected to be the most vulnerable direction of the building without reinforcement.

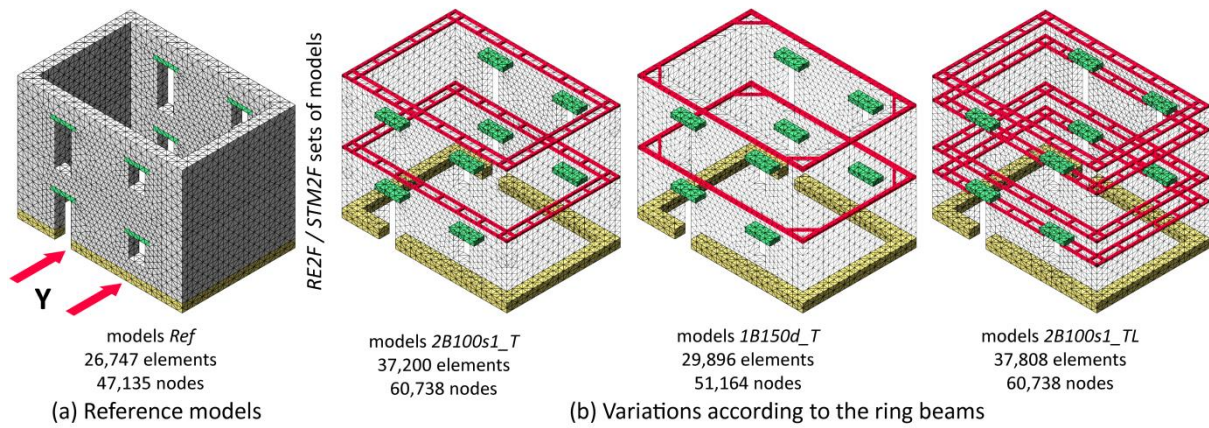


Figure 7.2: Numerical models built in order to assess the influence of timber ring beams in the seismic behavior of vernacular buildings

Table 7.2: Summary of the 29 models constructed for the evaluation of the influence of timber ring beams on the seismic behavior of vernacular buildings (dimensions in mm)

Model	Ring beam timber elements				Ring beam position						
	RE1F	RE2F	STM2F	STM3F	Longitudinal		Diagonal	Floor/roof level	Lintel level		
					Number (n)	Dimensions ($a_l \times b_l$)	Dimensions ($a_t \times b_t$)			Separation (s)	Dimensions ($a_d \times b_d$)
Ref	X	X	X	X	-	-	-	-	-		
2B100s0-5_T	X				2	100x75	75x50	500	-	X	-
2B100s1_T	X	X	X	X	2	100x75	75x50	1000	-	X	-
2B75s0-5_T	X				2	75x38	50x30	500	-	X	-
2B75s1_T	X				2	75x38	50x30	1000	-	X	-
1B150_T	X	X			1	150x100	-	-	-	X	-
1B150d_T	X	X			1	150x100	-	-	100x75	X	-
2B100s1_TL	X	X	X	X	2	100x75	75x50	1000	-	X	X
1B150d_TL	X	X	X	X	1	150x100	-	-	100x75	X	X
2B100s1d_T	X	X	X		2	100x75	75x50	1000	100x75	X	-
2B100s1d_TL	X	X	X		2	100x75	75x50	1000	100x75	X	X

As previously mentioned, the FE models were built following the same macromodel approach and adopting the same TSRCM material model discussed in Chapter 3, using DIANA software (TNO 2011). With respect to the modeling of the embedded timber ring beams, they are simulated using three-node 3D beam elements (CL18B), which also take shear deformation into account. The cross section of the different elements varies according to the values shown in Table 7.2. Concerning the material properties, the elastic mechanical properties shown in Chapter 3 (Table 3.3) were considered. Previously, all timber elements considered in the models were analyzed assuming linear elastic behavior. However, in this case, since the timber elements are meant to reinforce the wall, it was deemed necessary to assume that they are subjected to high stress and can also eventually experience failure. Thus, following the recommendations of Karanikoloudis

and Lourenço (2016), upper bounds on the ring beam timber elements' sectional resistance were specified, by means of adopting an ideal nonlinear plastic material model for tension. The value of the maximum tensile strength (f_t) adopted is 20.5 MPa and the Von Mises critical yield stress criterion was assumed. Only a tensile limit was applied because preliminary analyses showed that the highest stresses occur under tension. Even though modeling embedded timber elements in masonry is a very complex issue (particularly given the anisotropic nature of wood and the connections among the elements), this idealization of the nonlinear behavior of the timber was considered enough for this study to understand the effect that timber ring beams have on the seismic behavior of vernacular buildings and for the comparative analysis shown below.

7.2.1.1 Numerical results and discussion

The addition of a timber ring beam significantly affects the failure mode of the models, see Figure 7.3. The reference models showed the typical out-of-plane failure of the exterior wall (Figure 7.3a). However, when the ring beams are included, they are able to activate the box-behavior of the building and to transfer the load to the walls parallel to the horizontal load, which led to the development of relevant in-plane damage with characteristic diagonal shear cracking (Figure 7.3b-d). Most of the damage accumulates at the corners, where the transfer of forces takes place. When there is also a ring beam at the lintel level, the out-of-plane damage at the walls perpendicular to the loading direction is highly reduced and the in-plane resistance of the walls govern the global behavior of the building (Figure 7.3d).

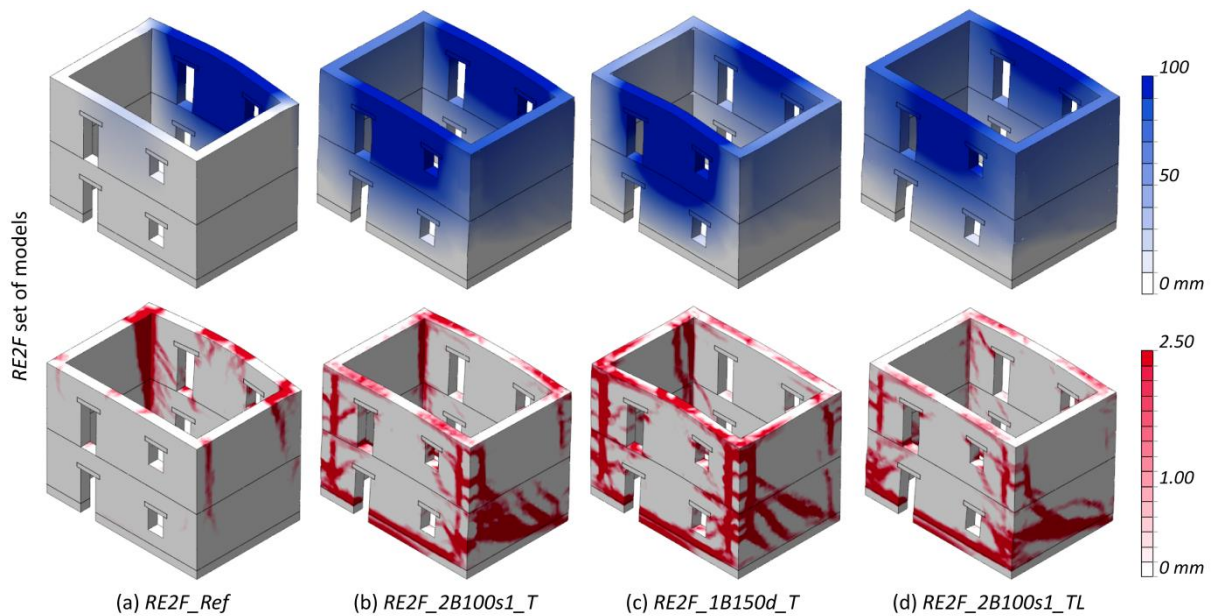


Figure 7.3: Representative failure modes at ultimate limit state (LS4) obtained for several models with different configurations of ring beams: (blue) maximum total displacements; and (red) crack pattern (crack width scale)

The level of stress at the timber elements was also controlled at the ultimate limit state. Figure 7.4 shows the axial forces (N) at the ultimate condition for the same two-floor buildings presented in Figure 7.3. As it could be expected, the maximum axial force values take place at the middle of the wall span perpendicular to the seismic load, because of the outward bending of that wall. However, the tensile stresses are always under the plastic limit adopted. Taking into account the dimensions of the beams cross section and the tensile strength plastic limit considered, the maximum axial force that the ring beams with two bands could resist is 150 kN, while the ring beam with one band could resist up to 300 kN. Figure 7.4c also shows that the use of a second ring beam at the lintel level helps to reduce the maximum stresses at the beam.

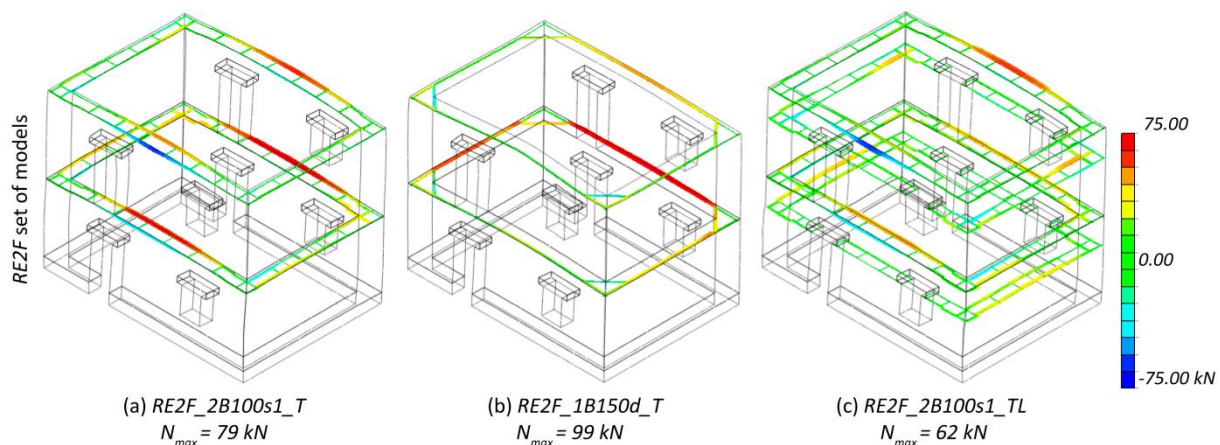


Figure 7.4: Axial forces (N) at the ring beams for the different models with different configurations at the ultimate limit state (LS4)

In order to clarify the influence of the axial capacity of the timber beams in the global response of the building, a small parametric analysis was carried out. Keeping the same ring beam configuration (model $2B100s0-5_T$), firstly the original plastic limit ($f_t = 20 \text{ MPa}$) was twice reduced two and four times. Secondly, the cross-section dimensions of the beams were also reduced (model $2B75s0-5_T$). Figure 7.5 presents the axial forces (N) at the ultimate condition for the four models constructed for the *RE1F* set of models. It shows how the maximum axial forces were also reduced according to the reductions of the plastic limit and cross section dimensions. For instance, when the plastic limit was reduced four times, the maximum load that the beams could resist was 37.5 kN. This was the maximum value obtained from the analysis (Figure 7.5c).

The reduction of the maximum capacity of the timber beams has a direct influence on the maximum capacity of the building. Figure 7.6 presents four-linear capacity curves constructed for the four buildings under analysis. The variations of the load factors defining each limit state are given in percentage, since they are normalized with the load factor obtained for the model with higher capacity ($2B100s0-5_T$). Results were also compared with the performance of the one-floor reference model with no ring beam. As discussed in Chapter 2, traditional timber ring beams could sometimes consist of rough timber pieces (trees trunks and branches) poorly connected and

arranged. The maximum capacity of the building increases approximately 2.5 times, when introducing a timber beam assuming the original maximum tensile strength, whereas the increase is around 1.7 times if the quality of the timber beam elements is considered poorer, assuming a tensile strength of around 5 MPa. The graph presented in Figure 7.6 also shows that the ring beams do not have the same influence defining LS1, which means that they do not prevent the appearance of damage.

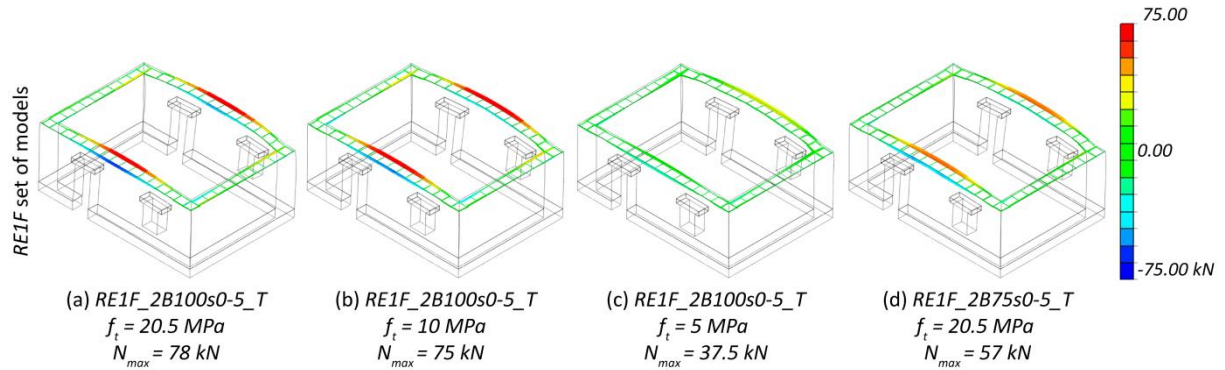


Figure 7.5: Axial forces (N) at the ultimate limit state (LS4) at the ring beams for the $RE1F$ set of models varying the plastic limit and the cross section dimensions of the ring beam elements

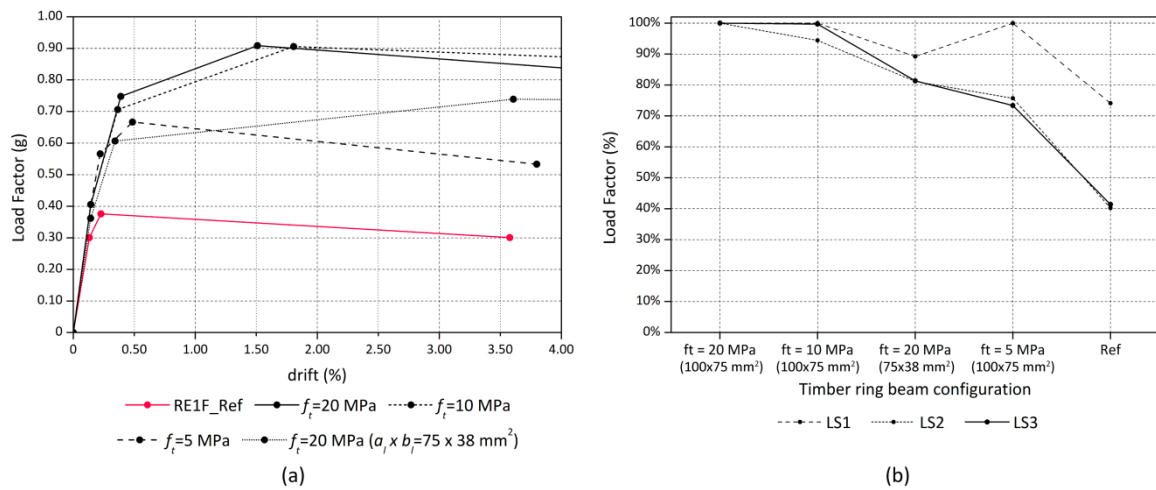


Figure 7.6: (a) Four-linear capacity curves constructed based on the computed limit states for the one-floor set of models; and (b) load factor variations obtained for each limit state for the one-floor set of models

The four-linear capacity curves constructed from the pushover analyses performed in the two-floor rammed earth models defined in Table 7.2 are shown in Figure 7.7a for the $RE2F$ set of models. Figure 7.7b shows the variations of the load factors defining each limit state obtained for the same set of models, taking into account the normalization based on the load factor obtained for the model showing the maximum capacity ($RE2F_2B100s1_TL$). The graphs in Figure 7.7 show again the favorable effect of the use of timber ring beams, which, in the best case, can increase the maximum capacity of the reference building approximately three times. The best

results are obtained for the model with ring beams at both the top and the lintel level, but the difference is not substantial with respect to the results from the building with the ring beam installed just at the top level. The ring beams with only one timber band are slightly less efficient than the ones with two bands, particularly if the diagonal bracing elements are not included. Figure 7.7b also reveals that the use of these diagonal elements has a significant effect on the definition of the load factor leading to LS1 and they actually help in delaying the initiation of damage. Figure 7.8 shows the variation of the load factor corresponding to the attainment of LS3 for the four sets of reference models. Very similar results can be observed for the sets of models considering stone masonry as the type of material for the walls and for different number of floors.

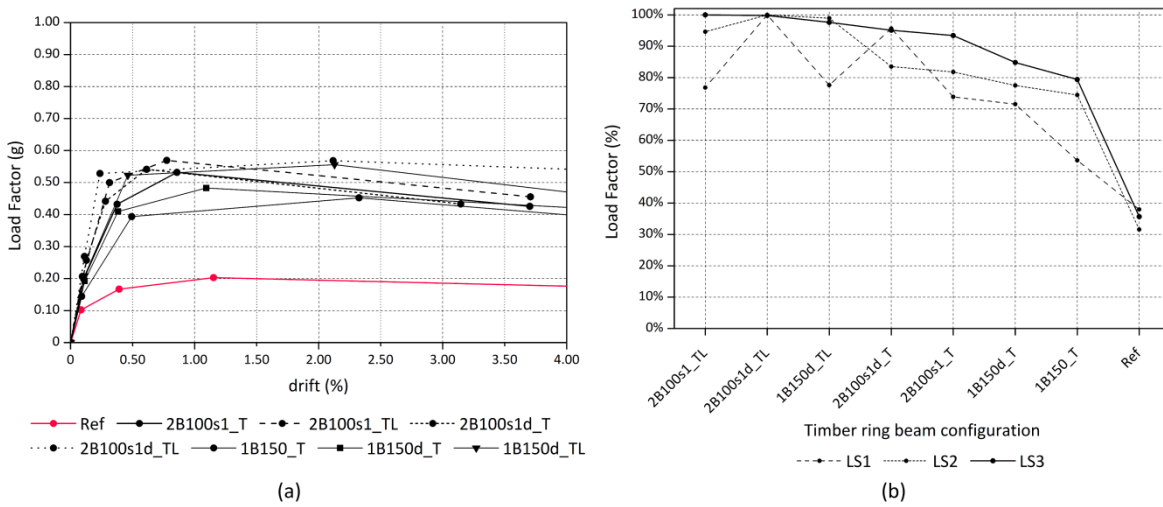


Figure 7.7: (a) Results in terms of four-linear capacity curves constructed based on the computed limit states for the two-floor models; and (b) load factor variations obtained for each limit state for the two-floor models

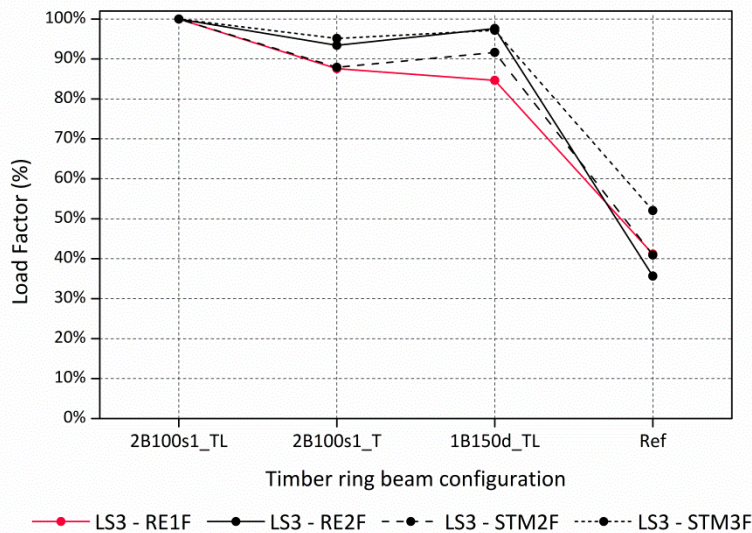


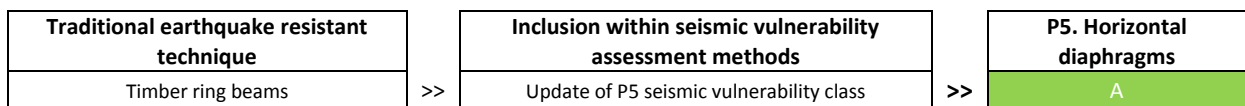
Figure 7.8: Variation of the load factor leading to the attainment of the maximum resistance (LS3) for the four sets of models evaluated according to the timber ring beam configuration

7.2.1.2 Inclusion within seismic vulnerability assessment methods

Results showed that timber ring beams are able to engage all the walls in the structural response of the building under seismic loading, thus activating its in-plane response. That is why they can significantly increase the maximum capacity of the building, by preventing the premature out-of-plane collapse of the walls. The effect of timber ring beams is similar to that of proper diaphragms, improving the connection between structural components by forming close contours in horizontal planes. To a greater or lesser extent, the same type of enhancement of the structural behavior of the building was achieved using the different ring beam configurations evaluated.

The influence of ring beams is quantitatively comparable to the influence of horizontal diaphragms. As shown in Chapter 4, when evaluating the influence of the type horizontal diaphragms, floors providing a proper diaphragmatic action also increase the maximum capacity of the reference building around three times. For this reason, the effect of ring beams on the seismic behavior of vernacular buildings is proposed to be taken into account by updating the P5 class. Therefore, if the building presents workmanlike built ring beams with timber bands at both the top and lintel level, P5 class should be considered as A. There can be exceptions according to the qualitative judgment of the person conducting the evaluation. For instance, if the ring beams are only present at the top level and are composed of single timber bands with no diagonal bracing, the class of P5 could just be considered as B. Other configurations that may indicate that ring beams will not be that beneficial, such as a poor construction quality or reduced cross sections dimensions, can result in updating P5 class to C. Table 7.3 summarizes the conclusions.

Table 7.3: Inclusion of timber ring beams within seismic vulnerability assessment methods



7.2.2. Corner braces

Based on the type of corner braces commonly observed in vernacular buildings presented in Chapter 2, a new set of models was prepared aimed at evaluating the structural influence of this technique in the seismic behavior of vernacular buildings. Among the many possibilities, three typical types of corner braces (C) were explored, consisting of: (1) a pair of longitudinal timber beams embedded within the walls at the corners, as a kind of partial ring beam; (2) addition of diagonal timber members to the first type; and (3) an independent diagonal corner brace, attached to the walls using timber wedges. The first two options were studied placing the corner braces at the top (T) and at the top and lintel level (TL), and the third option only at the top. The dimensions of the different timber elements were the ones adopted for the assessment of the timber ring beams. Additionally, another set of analysis was performed on buildings presenting an initial deterioration of the wall-to-wall connections integrity. Corner braces are assumed to be

particularly effective for walls showing a poor connection. This extra set of analyses is aimed at evaluating their efficiency in restoring the original strength of the building. The degraded wall-to-wall connections were simulated using the approach applied in Chapter 4 for the assessment of P4. Two different scenarios were thus prepared where the mechanical properties of the walls at the corners were reduced to 40% and 20%.

The three types of corner braces evaluated were modeled in three reference models with a varying number of floors and type of material, in order to evaluate the influence of this technique for different types of buildings: (a) one-floor rammed earth building (*RE1F*); (b) two-floor rammed earth building (*RE2F*); and (c) two-floor stone masonry building (*STM2F*). The same reference models used for the assessment of ring beams were used. Figure 7.9 shows some of the representative models constructed for the *RE2F* set of models. The same modeling strategy followed for the ring beams was adopted to model all corner brace timber elements, using 3D beam elements (CL18B) with a plastic limit in tension. The effect of the corner braces on walls with a degraded wall-to-wall connection was only evaluated for the *RE2F* set of models. Table 7.4 summarizes the 30 different models constructed to assess the effect of corner braces in the seismic response of vernacular buildings. All models were analyzed again in the direction perpendicular to the walls presenting the maximum wall span (Y), since it is expected to be the most vulnerable direction of the building without reinforcement.

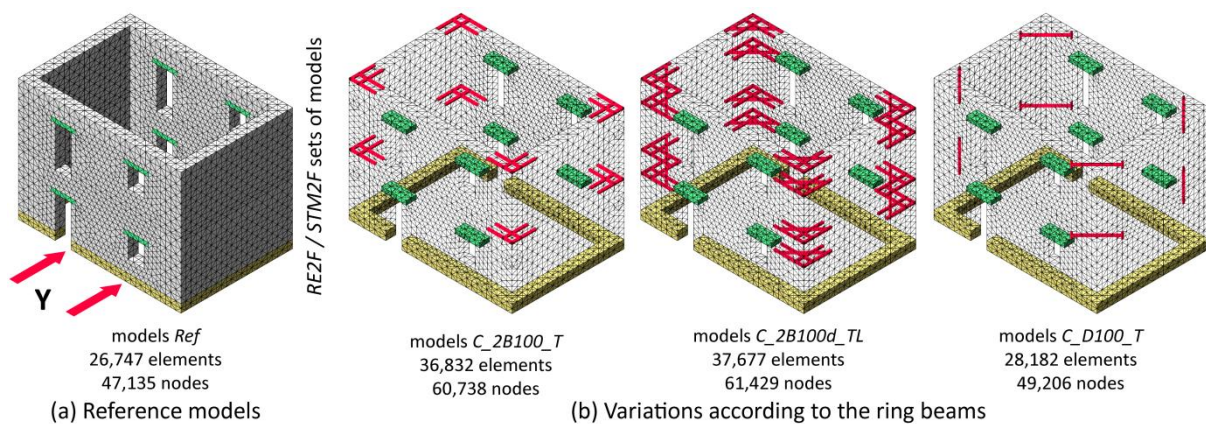


Figure 7.9: Numerical models built in order to assess the influence of timber corner braces in the seismic behavior of vernacular buildings

7.2.2.1 Numerical results and discussion

Figure 7.10 shows the failure modes observed for the *RE2F* set of models. The addition of the corner braces did not significantly affect the failure mode of the buildings, which still present the typical out-of-plane overturning of the exterior wall. However, the corner braces help to improve the connection between orthogonal walls. The failure modes observed in Figure 7.10b-d indicate that using a corner brace prevents damage at the corner, which now starts approximately at the

corner braces end within both orthogonal walls. Therefore, corner braces are able to engage the walls parallel to the seismic load in the building response, but their effect is limited to their length. Thus, they are not sufficient to activate the in-plane resistance of the walls parallel to the seismic load. The level of stress at the timber elements was also controlled at the ultimate limit state, which is displayed in Figure 7.11 in terms of axial forces (N). However, the stresses obtained are moderate and the timber elements are not prone to fail.

Table 7.4: Summary of the 30 models constructed for the evaluation of the influence of corner braces on the seismic behavior of vernacular buildings (dimensions in mm)

Name	Model					Corner brace type				Ring beam position	
	RE1F	RE2F	STM2F	RE2F (c = 40%)	RE2F (c = 20%)	Partial ring beam			Diagonal strut	Floor/roof level	Lintel level
						Longitudinal elements	Diagonal elements	Diagonal strut			
						Length (l)	Dimensions ($a_l \times b_l$)	Dimensions ($a_d \times b_d$)	Dimensions ($a_s \times b_s$)		
Ref	X	X	X	X	X	-	-	-	-	-	-
C_2B100_T	X	X	X	X	X	1250	100x75	-	-	X	-
C_2B100_TL	X	X	X	X	X	1250	100x75	-	-	X	X
C_2B100d_T	X	X	X	X	X	1500	100x75	100x75	-	X	-
C_2B100d_TL	X	X	X	X	X	1500	100x75	100x75	-	X	X
C_D100_T	X	X	X	X	X	-	-	-	100x75	X	-

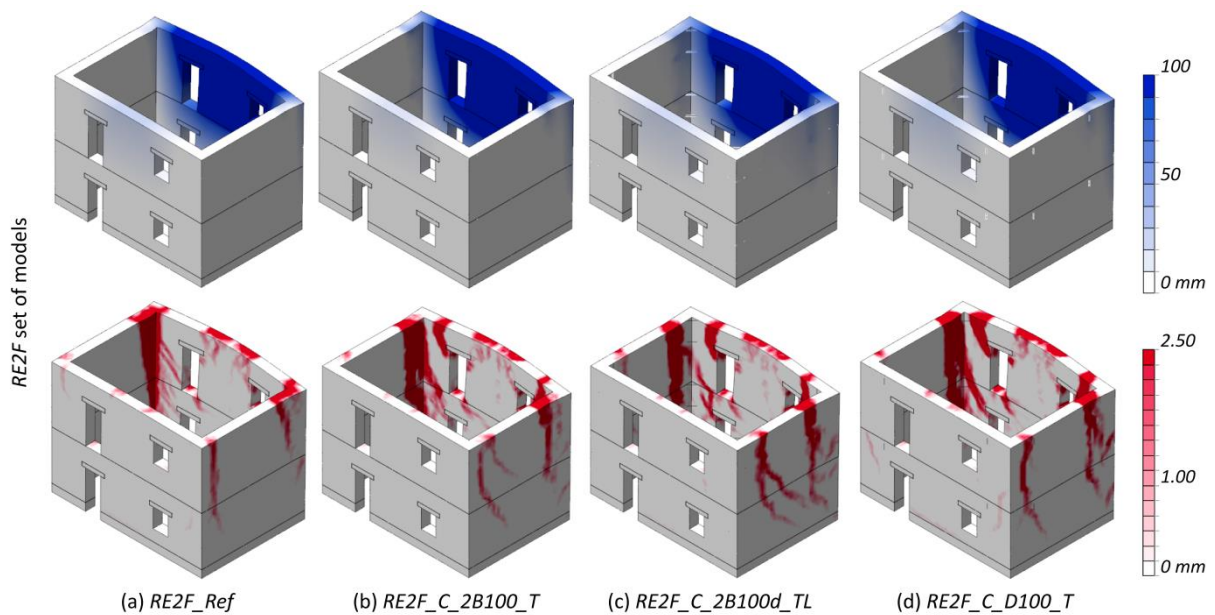


Figure 7.10: Representative failure modes at ultimate limit state (LS4) obtained for models with different types of corner braces: (blue) maximum total displacements; and (red) crack pattern (crack width scale)

Figure 7.12 shows the results in terms of damage pattern obtained for the *RE2F* set of models showing poor wall-to-wall connections. Results show that the introduction of corner braces effectively prevents the premature separation exhibited by the walls in the reference model with no braces. Besides, the great concentration of damage at the connection between perpendicular

walls is avoided with the use of corner braces, due to a better redistribution of stresses achieved. As a result, the out-of-plane bending damage at the center of the wall is more widespread and partial in-plane damage also takes place at the walls that are parallel to the seismic load, particularly at ground floor (Figure 7.12b,d).

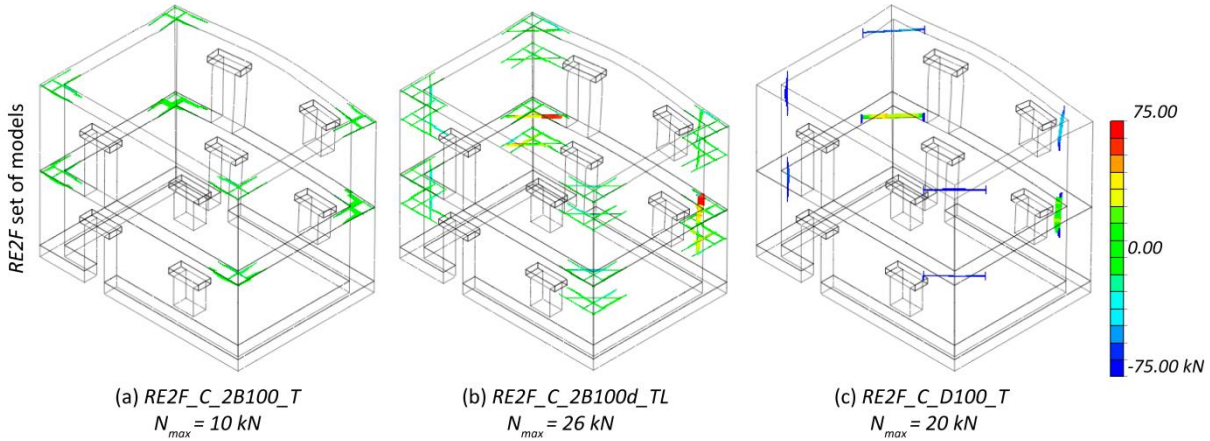


Figure 7.11: Axial forces (N) at the corner brace timber elements for the different models with different configurations at the ultimate limit state (LS4)

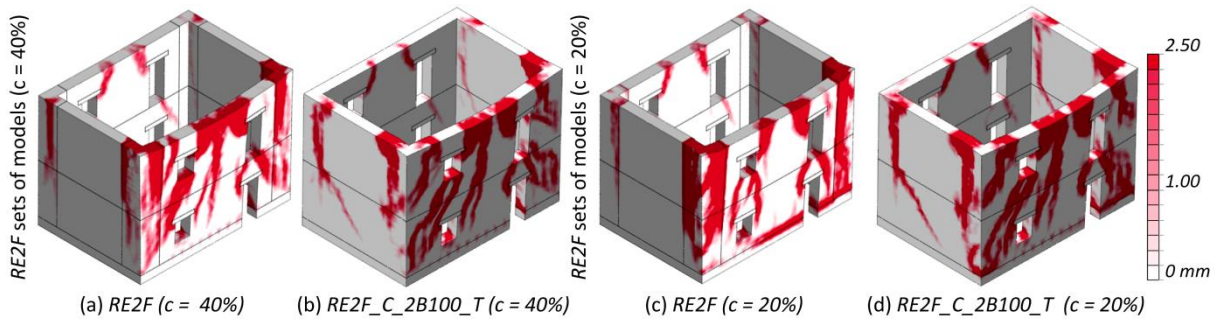


Figure 7.12: Damage crack pattern (crack width scale) at the ultimate limit state (LS4) obtained for the different models with deteriorated wall-to-wall connections and with or without corner braces

The four-linear capacity curves constructed from the pushover analyses performed in the two-floor rammed earth models are shown in Figure 7.13a. Figure 7.13b shows the variations of the load factors defining each limit state obtained for the same set of models, again in terms of percentage, normalized using load factors found for the model showing the maximum capacity. The abovementioned improved connection between orthogonal walls achieved with the corner braces is translated into a direct increment in the maximum capacity of the building. The increment varies for the different types of braces but the maximum almost reaches 30% for the corner brace consisting of a partial ring beam with a diagonal stiffener (model *RE2F_C_2B100dT*). Despite not being a great increase, this technique can prevent failure at the connection. It also has a greater influence in the attainment of LS1 because it avoids the early onset of damage due to a better redistribution of stresses at the corner of the building. The results

were very similar for the other two sets of reference models, as shown in Figure 7.14, where the variation of the load factor corresponding to the attainment of LS3 is displayed. Nonetheless, the influence is greater for the two-floor stone masonry buildings due to the combination with the better material properties of the stone masonry, allowing the engagement of the in-plane walls in the seismic response of the building, increasing its capacity.

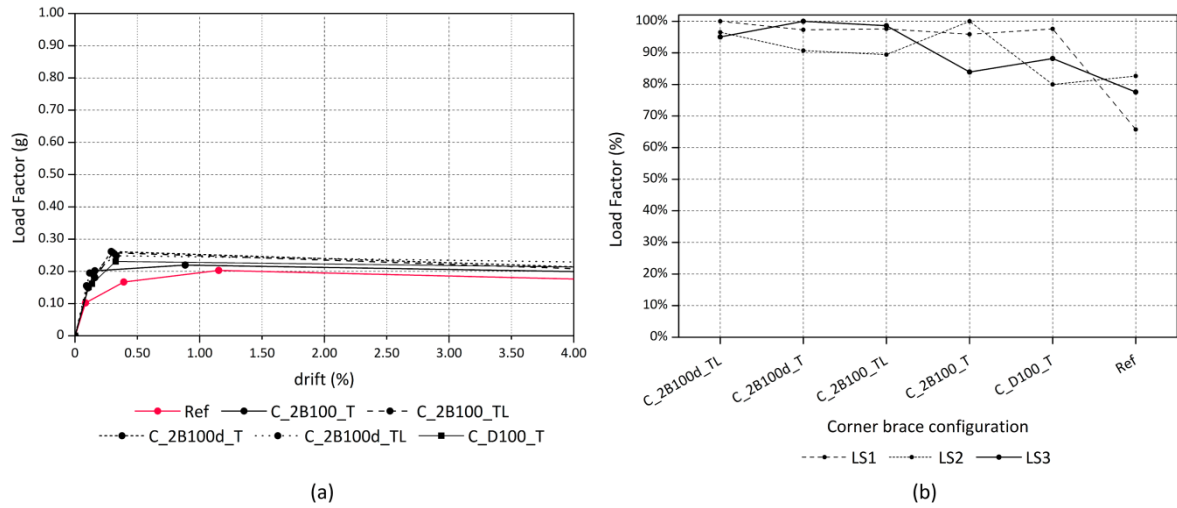


Figure 7.13: (a) Four-linear capacity curves constructed based on the computed limit states for the two-floor set of models; and (b) load factor variations obtained for each limit state for the two-floor set of models

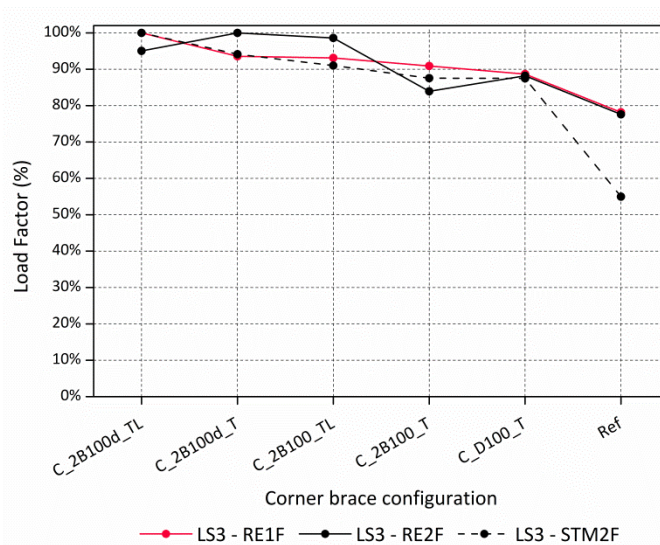


Figure 7.14: Variation of the load factor leading to the attainment of the maximum resistance (LS3) for the three set of models evaluated according to the different corner brace configurations

Figure 7.15a shows the four-linear capacity curves constructed from the pushover analyses on the *RE2F* set of models with deteriorated wall-to-wall connections, with and without the first type of corner brace (models *C_2B100_T*). The influence of the corner braces on the buildings with a deteriorated connection is clear, since they are able to restore almost completely the original

strength of the building, and they even outperform the seismic performance of the reference model assuming good wall-to-wall connection in terms of maximum capacity. Figure 7.15b shows the variation of the load factor corresponding to the attainment of LS3 when reducing the integrity of the wall-to-wall connection, with and without the different types of corner braces studied. The variations are studied for the same *RE2F* set of models, and are normalized using the results from the reference model with no corner brace. The previously discussed beneficial effect is very clear. The corner braces effectively ensure a proper wall-to-wall connection even if the original joint was compromised. Moreover, if the connection between walls was already good, corner braces also significantly enhance the seismic performance of the building. This effect highlights their potential as a seismic strengthening technique.

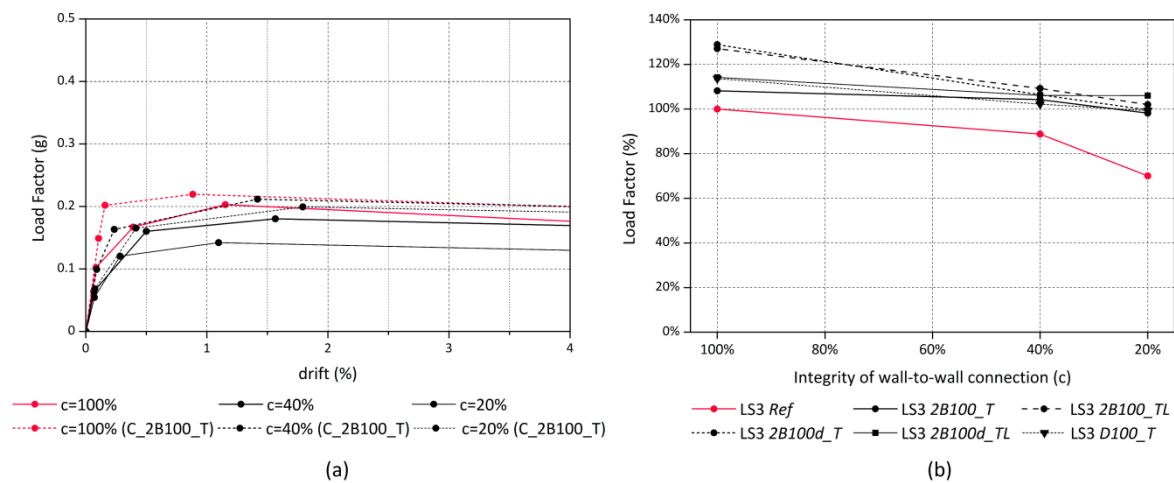


Figure 7.15: (a) Results in terms of four-linear capacity curves constructed based on the computed limit states for the *RE2F* models varying the wall-to-wall connection quality (with and without corner brace *C_2B100_T*); and (b) load factor variations obtained for LS3 for the *RE2F* models with and without different corner braces

7.2.2.2 Inclusion within seismic vulnerability assessment methods

Results showed that corner braces have an obvious influence in parameter P4, which refers to the quality of the wall-to-wall connections. They proved to be efficient in engaging orthogonal walls and avoiding damage at the connection. As a result, braces have a moderate effect in increasing the maximum resistance of the building. All the different corner braces configurations evaluated achieved a similar improvement in the structural behavior of the building under seismic loading, in terms of both damage pattern and maximum capacity. Results also showed that braces are efficient in restoring the integrity of poor wall-to-wall connections.

As a conclusion, the effect of the corner braces on the seismic behavior of vernacular buildings can be taken into account by means of increasing the vulnerability class of P4. However, as it can be observed in Chapter 4, class A from P4 includes buildings showing workmanlike built wall-to-wall connections and the presence of corner braces can further improve this condition. Thus, it

was deemed necessary to update the definition of P4 seismic vulnerability classes. Figure 7.16 presents the criteria followed for the redefinition of the four seismic vulnerability classes, which is the same previously used in Chapter 4, but including also the beneficial effect achieved with the application of corner braces. The average increase in the maximum capacity of the reference building obtained with the introduction of the different types of corner brace was used for the definition of the new classes. The classes are primarily defined using *RE1F* model, even though applying the same criterion to the two-floor model leads to a very similar definition of classes. It is noted that Figure 7.16 shows that the range and pattern of variation obtained for both sets of models is very similar. As a result, a new class A was introduced and the previously defined classes B and C were merged into a single class C. The previously defined class A is now established as class B and class D is kept the same. The resulting new classification is shown in Table 7.5. A new updated qualitative description is assigned to each vulnerability level.

Table 7.5: Redefinition of the seismic vulnerability classes according to the wall-to-wall connection

P4. Wall-to-wall connection	
Class	Description
A	Wall-to-wall connections are workmanlike built and enhanced with improved interlocking and the presence of timber or metallic connectors, such as timber corner braces
B	All wall-to-wall connections are workmanlike built. There might be elements related to Class A but only at some corners or orthogonal connections. There are no weakening signs or construction deficiencies. In case of masonry buildings, there is a good interlocking between the masonry units at the corners. In case of earthen buildings, there are no vertical joints at the corners
C	Some wall-to-wall connections are de deficient or degraded because of construction deficiencies, such as lack of efficient interlocking of the masonry units in case of masonry buildings or vertical joints in case of earthen construction. Connections can show also weakening signs, such as cracks or detachments
D	Wall-to-wall connections are barely non-existent because of poor construction practices or are highly degraded with important signs of separation and vertical cracks

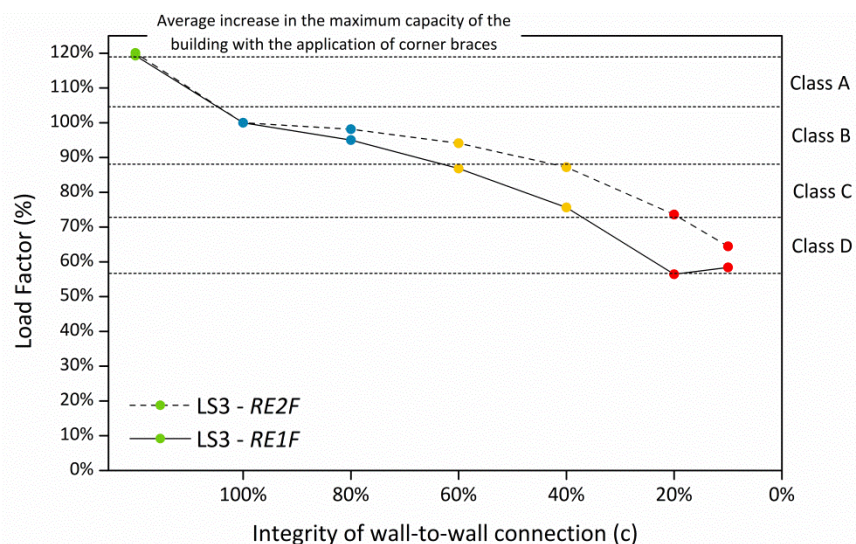


Figure 7.16: Variation of the load factor leading to the attainment of the maximum resistance (LS3) for the *RE1F* and *RE2F* set of models, evaluated modifying the conditions at the wall-to-wall connections

After the redefinition of P4 seismic vulnerability classes, the effect of the corner braces can be taken into account by the seismic vulnerability assessment methods according to Table 7.6.

Table 7.6: Inclusion of corner braces within seismic vulnerability assessment methods

Traditional earthquake resistant technique		Inclusion within seismic vulnerability assessment methods		P4. Wall-to-wall connection
Corner braces	>>	Update of P4 seismic vulnerability class	>>	A

7.2.3. Quoins

Quoins are a typical traditional technique applied to strengthen the buildings at the corners. They consist of using the best quality large squared stone ashlar at the corners, providing an efficient interlocking with the orthogonal walls. The modeling strategy adopted to quantitatively evaluate the structural influence of this technique in the seismic behavior of vernacular buildings consisted of increasing the mechanical properties of the walls at the corners. Five reference models were prepared with varying number of floors, type of diaphragm and type of material, in order to assess this technique for different types of buildings: (a) one-floor rammed earth building (*RE1F*); (b) two-floor rammed earth building (*RE2F*); (c) two-floor stone masonry building (*STM2F*); (d) three-floor stone masonry building (*STM3F*); and (e) two-floor rammed earth building with rigid diaphragm (*RE2Fd1*). The same reference models used for the assessment of the previous techniques were used. For the rammed earth buildings, the mechanical properties of the walls at the corners are increased twice 200% and 500%, in terms of percentage of the rammed earth material properties shown in Chapter 3 (Table 3.3). This is intended to simulate the use of rough stone masonry and ashlar masonry at the corners, respectively. For the stone masonry buildings, the properties at the corners were increased only 200% of the reference stone masonry properties from Table 3.3, simulating the use of ashlar at the corners. Table 7.7 presents the summary of the 13 models constructed in order to assess the influence of quoins in the seismic behavior of vernacular buildings. The same ratio (c) used in Chapter 4 represents the increase in the material properties assumed at the corners. Figure 7.17 shows the reference models constructed, marking the elements simulating the quoins in red. All the sets of models were analyzed in the direction perpendicular to the walls presenting the maximum wall span (Y).

Table 7.7: Summary of the 13 different models built in order to assess the influence of the quality of the wall-to-wall connections on the seismic behavior of vernacular buildings

Set of models	c (%)		
	100	200	500
<i>RE1F</i>	X (Ref)	X	X
<i>RE2F</i>	X (Ref)	X	X
<i>STM2F</i>	X (Ref)	X	
<i>STM3F</i>	X (Ref)	X	
<i>RE2Fd1</i>	X (Ref)	X	X

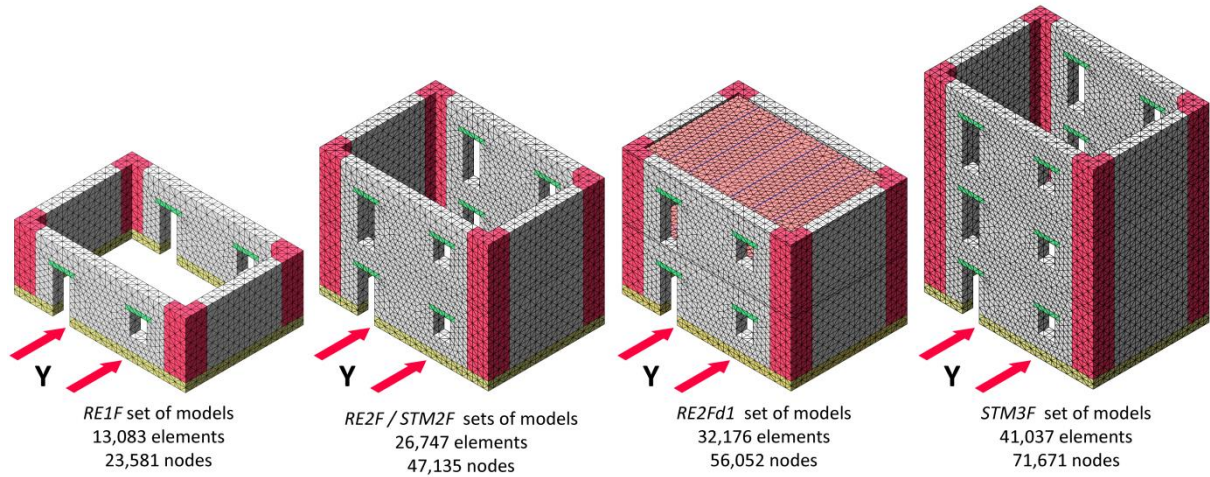


Figure 7.17: Numerical models built in order to assess the influence of quoins in the seismic behavior of vernacular buildings

7.2.3.1 Numerical results and discussion

The presence of quoins does not influence on the failure mode of the models, which consists of the out-of-plane overturning of the exterior wall for the models with flexible diaphragm, and the in-plane failure of the walls parallel to the seismic load for the two-floor model with rigid diaphragm. The failure modes for the *RE2F* set of models are shown in Figure 7.18. The quoins are nevertheless able to improve the wall-to-wall connection by preventing the onset of damage at the corner. In this case, the damage starts at the connection between the quoin and the rest of the wall (Figure 7.18b,c). The quoins thus are able to engage the walls parallel to the seismic load, but, when coupled with materials with low tensile strength, their effect can be limited.

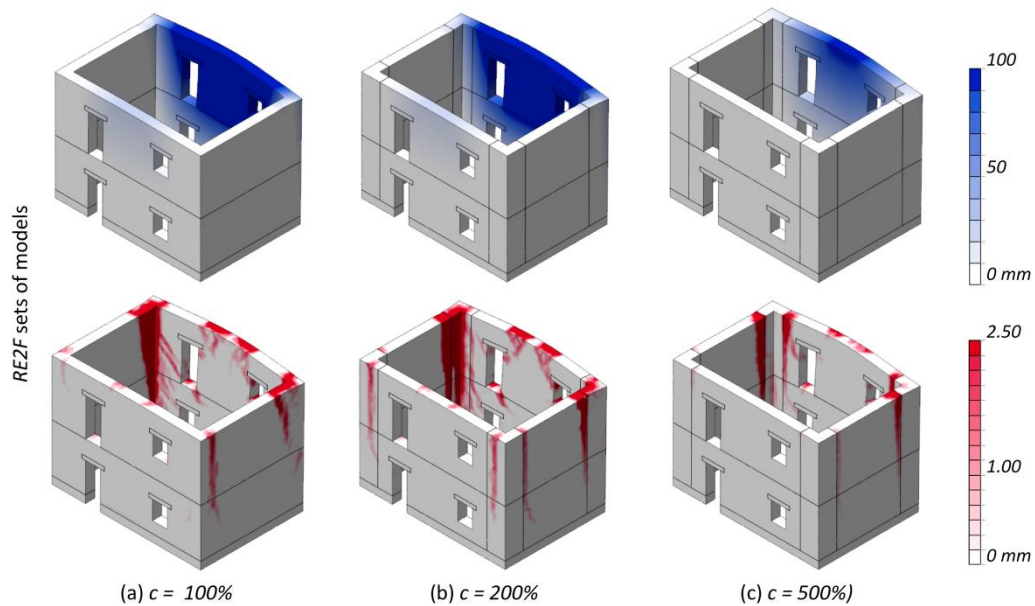


Figure 7.18: Representative failure modes at ultimate limit state (LS4) obtained for the *RE2F* set of models with and without quoins: (blue) maximum total displacements; and (red) crack pattern (crack width scale)

Results for the *RE2F* set of models are shown in Figure 7.19a, in terms of four-linear capacity curves constructed from the pushover analyses, and in Figure 7.19b, in terms of the variations of the load factors defining each limit state. The load factors are normalized using the results from the reference model. There is a clear increment in the maximum capacity of the building, reaching around 25% when good quality stone masonry is assumed at the quoins (500% increment of the material properties). However, the greatest variations occur for the load factor defining LS1, which almost doubles for the model with ashlar masonry at the corners. Quoins are thus efficient in delaying the onset of damage and preventing failure at the connection. Figure 7.20, shows the variations of the load factor corresponding to the attainment of LS3 for every set. Similar increasing patterns and range were observed on the other sets of reference models. However, results also show that quoins do not have an influence for the model presenting a rigid diaphragm, since the diaphragm is able by itself to redistribute the stresses among the walls and avoids the concentration of damage at the walls connection.

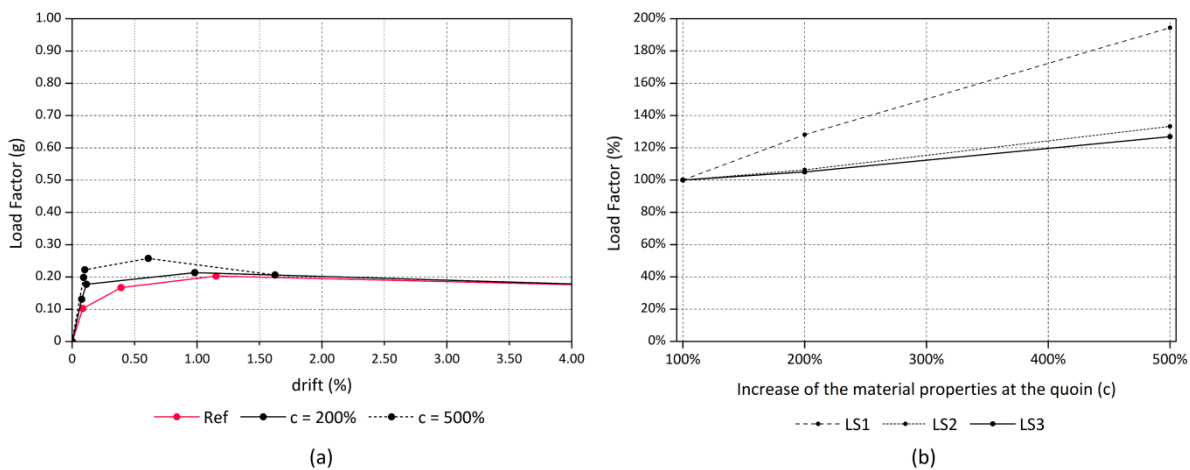


Figure 7.19: (a) Four-linear capacity curves constructed based on the computed limit states for the *RE2F* set of models; and (b) load factor variations obtained for each limit state for the *RE2F* set of models

7.2.3.2 Inclusion within seismic vulnerability assessment methods

Results showed that the effect of quoins can be directly associated with parameter P4, which addresses wall-to-wall connections. Similarly to the previously studied corner braces, they are efficient in engaging orthogonal walls and avoiding damage at the connection and, as a result, they are also able to increase the maximum resistance of the building. Their performance is also similar to corner braces quantitatively, as the increase achieved in the maximum capacity of the building with the use of quoins also lies within the 20-30% range.

Therefore, the effect of quoins on the seismic behavior of vernacular buildings can be also taken into consideration by means of increasing the vulnerability class of P4. The definition of class A from P4 had to be previously redefined to include also the effect of quoins, as shown in

Table 7.8. After this update, the effect of the quoins can be taken into account by the seismic vulnerability assessment methods by assuming class A for P4. Again, there can be exceptions according to the qualitative judgment of the person conducting the evaluation. For example, when quoins do not seem to be properly coupled with the orthogonal walls, the positive effect should not be taken into account. Table 7.9 summarizes these conclusions.

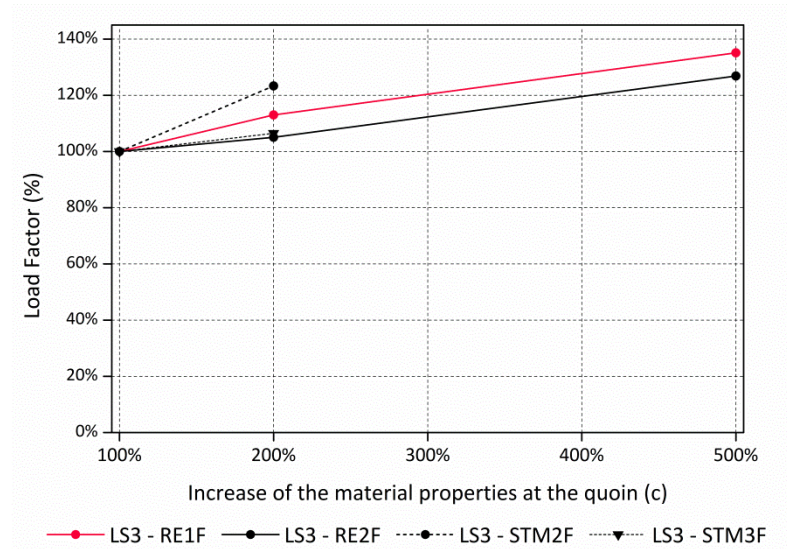
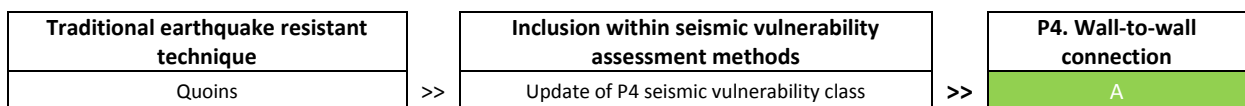


Figure 7.20: Variation of the load factor leading to the attainment of the maximum resistance (LS3) for the five sets of models evaluated with different type of quoins

Table 7.8: Redefinition of seismic vulnerability class A according to the wall-to-wall connection

P4. Wall-to-wall connection	
Class	Description
A	Wall-to-wall connections are workmanlike built and enhanced with improved interlocking, the use of better quality materials at the corners (i.e. quoins), and/or the presence of timber or metallic connectors, such as timber corner braces

Table 7.9: Inclusion of quoins within seismic vulnerability assessment methods



7.2.4. Ties

The widespread use of ties in vernacular architecture was reviewed in Chapter 2. Ties can be typically located at different locations of the building, intended to improve the connection among different structural elements. Ties connecting parallel walls or ties connecting floors or roofs to walls are intended to achieve a joint behavior from all the walls subjected to out-of-plane actions. This type of behavior was discussed when evaluating P5 in Chapter 4, where it was shown that modeling the timber beams, assuming a proper connection between the beams and the walls, improved the seismic resistance of vernacular buildings. Buildings presenting diaphragms of

negligible stiffness with beams well-connected to the walls were considered as Class C in the seismic vulnerability classification for P5. Thus, in order to consider the influence of ties, the seismic vulnerability class of the building according to P5 can be simply upgraded to C if they are properly coupling parallel walls or improving the beams-to-wall connection.

In this section, only the influence of ties connecting perpendicular walls will be numerically assessed. A simple steel tie rod of 20 mm diameter was modeled at the top part of the corners at a height of 2.7 m from the ground or the floor level. Only elastic properties were used, since the failure of the rod was not considered. A common elasticity modulus of 210 GPa was adopted. The ties were modeled as trusses, using three-node 3D truss elements (CL9TR), in order to be only subjected to axial forces. The ties were connected at the exterior part of the wall using a cross-shaped steel anchor modeled using 3D beam elements (CL18B). The embedment length of the tie was set at 1.25 m. Figure 7.21 shows the location of the ties at the one-floor and two-floor reference models. Preliminary analyses showed that ties barely have any influence in the seismic behavior of the buildings in terms of maximum capacity or damage pattern. Thus, in a second step, the ties were modelled in buildings with an initial deterioration of the integrity of the wall-to-wall connections, aiming at evaluating if ties can help in partially restoring their original strength. The compromised wall-to-wall connections were simulated using the approach used in Chapter 4 for the assessment of P4. The mechanical properties of the walls at the corners were reduced to 40% and to 20%. The effect of ties linking walls showing a degraded connection was evaluated using the same reference models used for the evaluation of the previous techniques with varying number of floors and type of material: (a) one-floor rammed earth building (*RE1F*); (b) two-floor rammed earth building (*RE2F*); and (c) two-floor stone masonry building (*STM2F*). The models were analyzed in the direction parallel to the direction of the tie (Y), to assess if the ties effectively prevent the out-of-plane mechanism. Table 7.10 presents the summary of the 29 models constructed in order to assess the influence of ties.

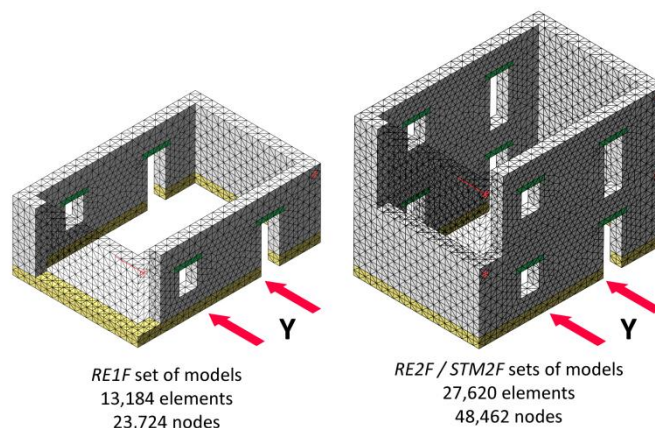


Figure 7.21: Position of the ties at the reference numerical models built in order to assess the influence of ties connecting perpendicular walls in the seismic behavior of vernacular buildings

Table 7.10: Summary of the 18 different models built in order to assess the influence of ties connecting perpendicular walls in the seismic behavior of vernacular buildings

Models	Ties		c (%)		
	Length (m)	Diameter (mm)	100	200	500
<i>RE1F_Ref</i>	-	-	X	X	X
<i>RE1F_t</i>	1.25	20	X	X	X
<i>RE2F_Ref</i>	-	-	X	X	X
<i>RE2F_t</i>	1.25	20	X	X	X
<i>STM2F_Ref</i>	-	-	X	X	X
<i>STM2F_t</i>	1.25	20	X	X	X

7.2.4.1 Numerical results and discussion

The presence of tie rods affected slightly the failure mode of the models since they helped in partially redistributing the stresses at the corner. Figure 7.22 presents representative failure modes for the two-floor buildings. After the introduction of ties, damage still mostly concentrates at the connection between perpendicular walls, showing their separation. Nevertheless, they are able to involve a bigger portion of the wall parallel to the seismic load, showing also significant damage at the location where the tie rod ends.

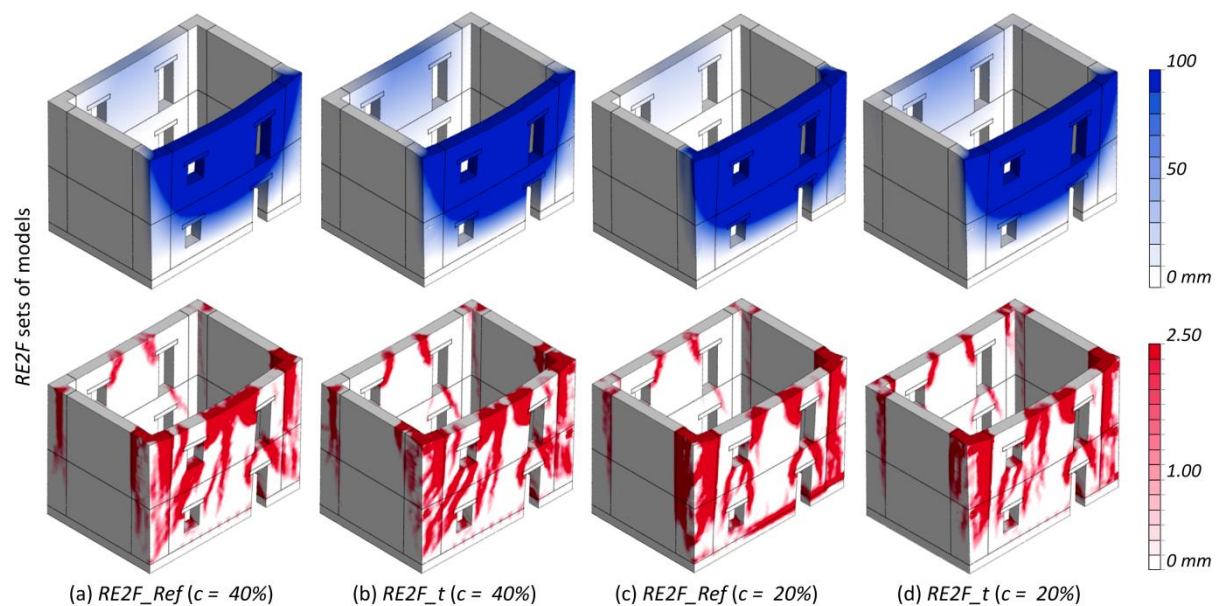


Figure 7.22: Representative failure modes at ultimate limit state (LS4) obtained for the *RE2F* models with different level of deterioration of the wall-to-wall connection (*c*) with and without ties: (blue) maximum total displacements; and (red) crack pattern (crack width scale)

This redistribution of stresses achieved by the ties has also a beneficial effect in the results in terms of maximum capacity. Figure 7.23a shows the four-linear capacity curves constructed from the pushover analyses for the *RE2F* set of models. Figure 7.23b shows the variation of the load factor corresponding to the attainment of LS3 when reducing the integrity of the wall-to-wall

connection, with and without ties, normalized using the results from the reference model with no ties. Even if the increment in the maximum capacity of the building is not high (around 10-15%), there is a noticeable beneficial effect. Ties mainly affected the seismic performance of the building in its inelastic range, as they always increased the capacity of undergoing larger deformations sustaining the same load-carrying capacity of the building. Only the variations in the load factor defining LS3 are evaluated because the ties are not effective in avoiding the formation of cracks and do not have a significant influence for LS1. Similar increasing trends and variations in the damage patterns can be observed in Figure 7.24, which shows the variations of the load factor defining LS3 for the other two sets of reference models, with and without ties.

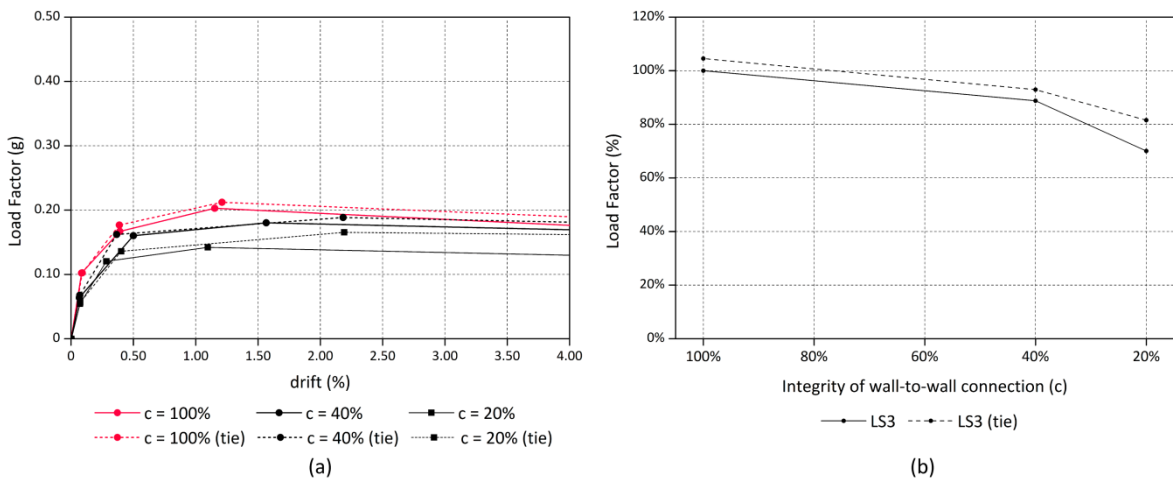


Figure 7.23: (a) Four-linear capacity curves constructed based on the computed limit states for the RE2F set of models; and (b) load factor variations obtained for LS3 for the RE2F set of models with and without ties

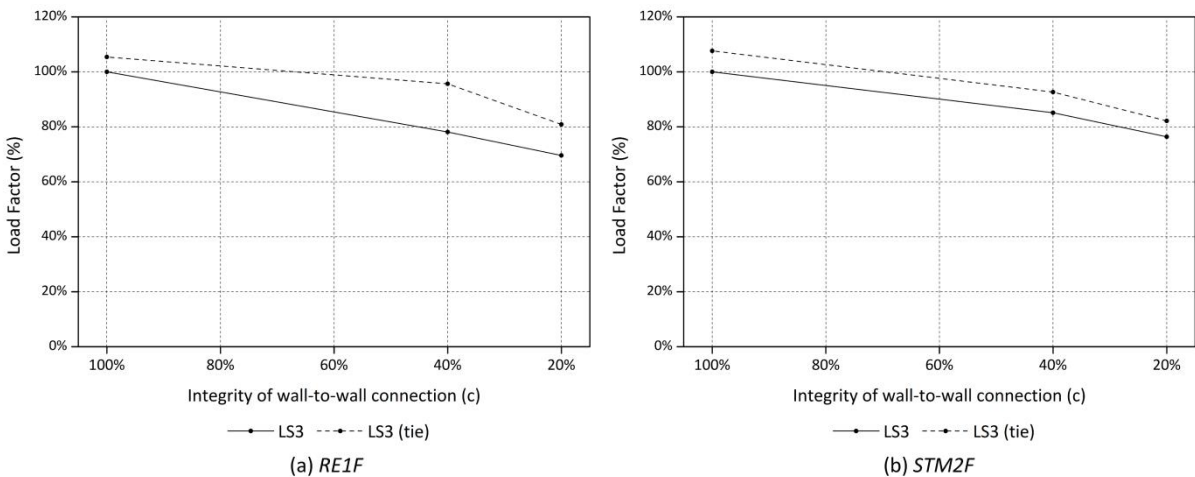


Figure 7.24: Variation of the load factor leading to the attainment of the maximum resistance (LS3) for: (a) RE1F; and (b) STM2F set of models; reducing the integrity of the wall-to-wall connection with or without ties

7.2.4.2 Inclusion within seismic vulnerability assessment methods

As previously discussed, the effect of ties connecting parallel walls or ties connecting floors or roofs to walls can be associated with parameter P5. They help to engage parallel walls subjected to out-of-plane actions in the seismic response of the building. As a result, they can be taken into consideration by means of increasing the vulnerability class of P5 to C, which refers to those buildings with flexible diaphragms but well-connected beams able to achieve the coupling action.

On the other hand, results showed that ties connecting perpendicular walls are efficient in partially restoring the integrity of the wall-to-wall connections that are deficient or degraded. The effect of this type of ties on the seismic behavior of vernacular buildings can thus be taken into consideration by means of increasing the vulnerability class of P4. Thus, if a building that could be considered as class D for P4 shows ties at the deficient connections, it can be upgraded to class C. This one-class upgrade was deemed sufficient given the results obtained in the parametric analysis. Nevertheless, it is acknowledged that there are many possible configurations for the ties that were not evaluated here. The shape of the tie or the type of embedment can help to improve its ability to redistribute the stresses and connect perpendicular walls, preventing their separation. It is up to the qualitative judgment of the person conducting the evaluation to eventually decide on the effect of the tie. Table 7.11 provides a summary of the conclusions.

Table 7.11: Inclusion of ties within seismic vulnerability assessment methods

Traditional earthquake resistant technique		Inclusion within seismic vulnerability assessment methods		P5. Horizontal diaphragms
Ties connecting parallel walls Ties connecting floor and roofs to walls	>>	Update of P5 seismic vulnerability class	>>	C
Traditional earthquake resistant technique		Inclusion within seismic vulnerability assessment methods		P4. Wall-to-wall connections
Ties connecting perpendicular walls	>>	Update of P4 seismic vulnerability class	>>	Upgrade 1 class

7.2.5. Timber elements within the masonry

The horizontal reinforcement of load bearing masonry walls with timber elements was also highlighted in Chapter 2 as one of the most common vernacular practices in many seismic prone regions. Following the same modeling approach used for the simulation of the ring beams, new numerical models were prepared inserting continuous timber bands along the height of the walls with a vertical spacing of 1 m. Only one configuration was considered. The horizontal reinforcement was arranged using two longitudinal beams joined together with small transversal connectors. The cross-section dimensions of the timber elements were 100x75 mm² for the longitudinal elements and 75x50 mm² for the transversal elements, which were placed each 1 m. This configuration was introduced in the same four reference models previously constructed with varying number of floors and type of material: (a) one-floor rammed earth building (*RE1F*); (b) two-floor rammed earth building (*RE2F*); (c) two-floor stone masonry building (*STM2F*); and (d)

three-floor stone masonry building (*STM3F*). The models were analyzed in the direction perpendicular to the walls presenting the maximum wall span (Y). Table 7.12 presents the summary of the 8 models constructed in order to assess the influence of introducing timber running timber beams within the walls in the seismic behavior of vernacular buildings, specifying the dimensions and configuration of the timber elements.

Table 7.12: Summary of the 8 different models built in order to assess the influence of timber reinforcement elements within the walls in the seismic behavior of vernacular buildings (dimensions in mm)

Set of models	RE1F	RE2F	STM2F	STM3F	Timber elements				
					Longitudinal		Transversal		Height
					Number (n)	Dimensions (a,x b)	Dimensions (a _t ,x b _t)	Separation (s)	Vertical spacing (h)
<i>Ref</i>	X	X	X	X	-	-	-	-	-
<i>Timber laced</i>	X	X	X	X	2	100x75	75x50	1000	1000

7.2.5.1 Numerical results and discussion

As expected, the presence of the timber reinforcement forming the timber laced walls had a crucial influence on the seismic behavior of the rammed earth building and its failure mode see Figure 7.25. It is noted that the failure mode of the *RE2F* building without reinforcement was shown in Figure 7.3a and consists of a clear out-of-plane failure of the exterior wall perpendicular to the loading direction. The timber elements are able to tie the walls, leading to an almost monolithic response. That is why the greatest damage concentrates at the base, promoting the rotation of the building as a block. At ultimate condition there is, in any case, extensive in-plane and out-of-plane damage widespread throughout the building, which remarks the efficiency of this technique to redistribute the stresses along the structure. The level of stress at the timber elements is also shown at Figure 7.25 at the ultimate state. The maximum axial force values occur at the mid span of the wall perpendicular to the seismic load, because of its outward bending, reaching around 75 kN, far below the plastic limit considered for the analysis.

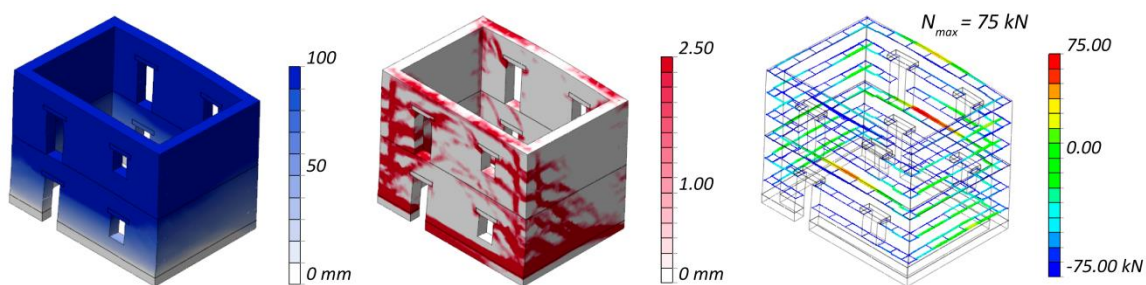


Figure 7.25: Failure modes at ultimate limit state (LS4) obtained for the *RE2F* model with the timber reinforcement: (blue) maximum total displacements; and (red) crack pattern (crack width scale)

The influence of this technique in the seismic behavior of the building is also very clear in terms of maximum capacity. Figure 7.26a shows the four-linear capacity curves constructed from

the pushover analyses for the *RE2F* model and Figure 7.26b shows the variation of the load factor defining each limit state. The introduction of the timber reinforcement increases the maximum capacity of the building up to approximately three times. Also, the use of timber lacing elements helps in delaying the crack propagation, showing a notable influence on the definition of LS1. The similarity in the results obtained when introducing this reinforcement in the other three models can be observed in Figure 7.27, in terms of the variation of the load factor corresponding to the attainment of LS3.

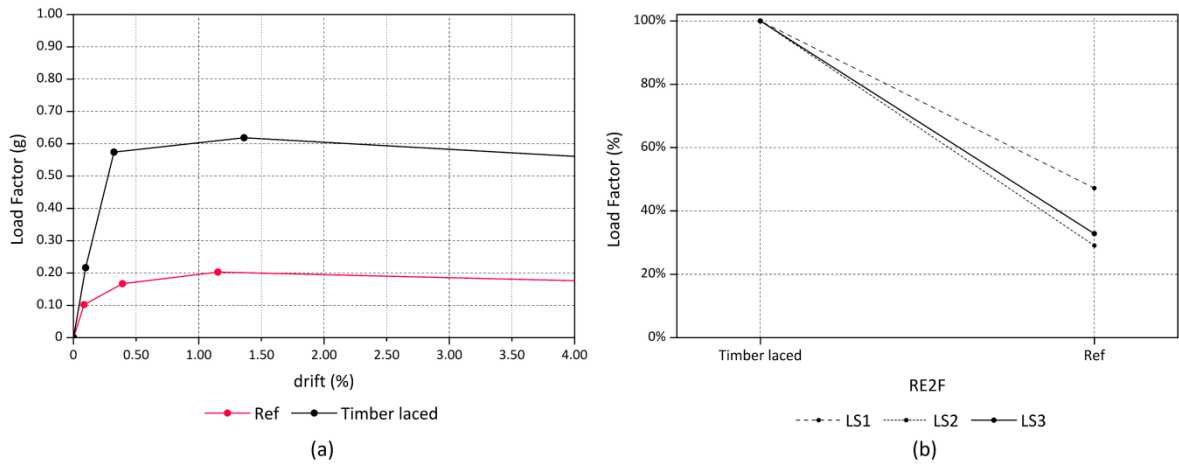


Figure 7.26: (a) Four-linear capacity curves constructed based on the computed limit states for the *RE2F* set of models; and (b) load factor variations obtained for each limit state for the *RE2F* set of models

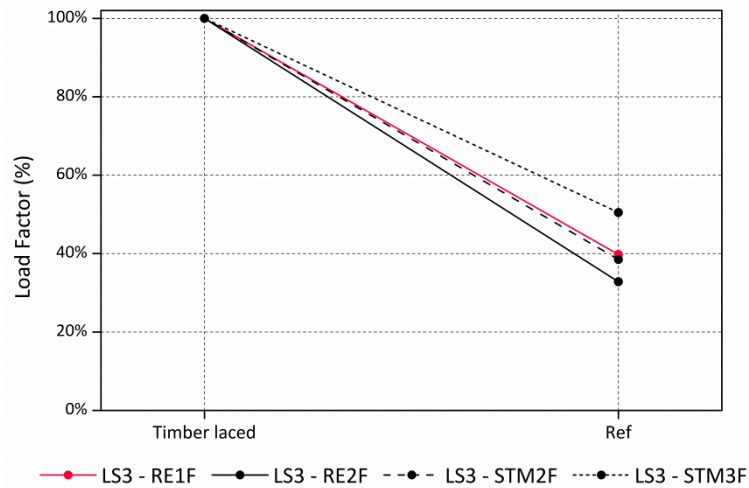


Figure 7.27: Variation of the load factor leading to the attainment of the maximum resistance (LS3) for the four set of models evaluated when introducing embedded timber elements within the walls

7.2.5.2 Inclusion within seismic vulnerability assessment methods

The numerical evaluation of the effect of introducing timber elements as continuous horizontal reinforcement embedded within the load bearing walls has a significant impact on the seismic

behavior of the building. The addition of timber laces is extremely efficient in tying the walls together and thus making the building respond as a unit. The effect is directly reflected in an increase of the maximum resistance of the building of approximately three times. This influence can be associated with parameter P3, which relates to the type of material composing the walls. When evaluating the influence of the type of material of the walls in Chapter 4, assuming a material with high material properties, such as dressed stone masonry, results in an increase the maximum capacity also close to three times with respect to the model with earthen walls. For this reason, a building presenting timber laced masonry walls is proposed to be considered as class A for P3. It is worth noting that exceptions may apply and a different upgrade may be adopted if, according to the qualitative judgment of the person conducting the evaluation, the embedded timber elements are considered to be in bad condition or are present only in some parts, not composing continuous horizontal bands. Table 7.13 summarizes these conclusions.

Table 7.13: Inclusion of timber elements within the masonry within seismic vulnerability assessment methods

Traditional earthquake resistant technique		Inclusion within seismic vulnerability assessment methods		P3. Type of material
Timber elements within the masonry	>>	Update of P3 seismic vulnerability class	>>	A

7.2.6. Wall subdivisions

The effect of the use of brick horizontal courses extending through the thickness of the walls on the seismic behavior of vernacular buildings was evaluated considering only one configuration, which was introduced in the same four reference models previously constructed with varying number of floors and type of material: (a) one-floor rammed earth building (*RE1F*); (b) two-floor rammed earth building (*RE2F*); (c) one-floor stone masonry building (*STM1F*); and (d) two-floor stone masonry building (*STM2F*). Brick courses were inserted each 1 m along the height of the walls assuming that the thickness of the courses is 0.2 m, simulating 2-3 layers of bricks. Figure 7.28 shows the reference models constructed, marking the elements simulating the brick courses in red. It is noted that two extra models were prepared assuming that the whole building is built in brick masonry: (e) one-floor brick masonry building (*BM1F*); and (f) two-floor brick masonry building (*BM2F*). This way, for each set, the performance of three different buildings can be compared: (1) reference building without brick bands; (2) reference building with brick bands; and (3) brick masonry building. The brick masonry horizontal courses were simulated using solid 3D elements (CTE30), adopting typical mechanical properties corresponding to solid brick masonry (NTC 2008), which are shown in Table 7.14. All sets of models were analyzed in the direction perpendicular to the walls presenting the maximum wall span (Y). Table 7.15 presents the summary of the 10 models finally prepared in order to assess the influence of subdividing the wall in the seismic behavior of vernacular buildings specifying the dimensions and configuration of the brick masonry horizontal courses.

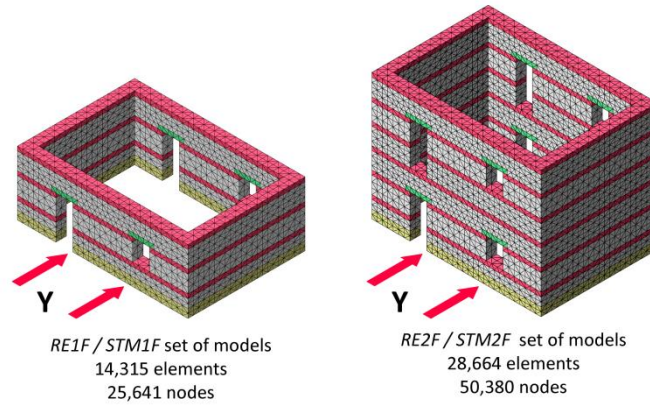


Figure 7.28: Numerical models built in order to assess the influence of subdividing the wall using brick horizontal courses in the seismic behavior of vernacular buildings

Table 7.14: Mechanical properties adopted for the brick masonry horizontal courses

Material	E (MPa)	ν	f_c (MPa)	G_{fc} (N/mm)	f_t (MPa)	G_{ft} (N/mm)	W (kN/m ³)
Brick masonry	2000	0.2	2	3.2	0.2	0.012	18

Table 7.15: Summary of the 10 different models built in order to assess the influence of brick masonry horizontal courses subdividing the walls in the seismic behavior of vernacular buildings (dimensions in m)

Set of models	RE1F	RE2F	STM1F	STM2F	BM1F	BM2F	Brick masonry horizontal courses		
							Dimensions		
							Height (h)	Thickness (t)	Vertical spacing (s)
Ref	X	X	X	X	X	X	-	-	-
BB	X	X	X	X			0.2	0.5	1

7.2.6.1 Numerical results and discussion

The brick bands are not as efficient as the previously studied embedded timber elements in lacing the building together and they do not change the failure mode of the building, which is driven by the out-of-plane failure of the exterior wall perpendicular to the seismic load. Nevertheless, the improvement in the material properties of the walls at the bands helps to slightly reduce the extension of the damage. Figure 7.29 presents the failure modes obtained for the two-floor rammed earth models with and without brick horizontal courses and the two-floor brick masonry model. The figure shows the evident progressive reduction of the damage when increasing the mechanical properties of the material composing the walls.

Figure 7.30a shows the four-linear capacity curves constructed from the pushover analyses performed in the same three models and Figure 7.30b shows the variation of the load factor defining each limit state. The influence of the introduction of brick bands is also clearly reflected in these graphs. The model with brick bands shows a performance in between the other two models, in terms of capacity, stiffness and ductility. However, since the rammed earth material is still predominant in the walls the response is still more similar to the one of the reference *RE2F*

model. Focusing on the variation of the load factor defining LS1, the variation is marginal, which suggests that the bands are not efficient in avoiding the development of cracks. Figure 7.31 shows the results for the other three models, in terms of the variation of the load factor corresponding to the attainment of LS3. The response of the building is always intermediate between the response of a building with walls built solely with the original material and the response of the building with brick masonry walls. Therefore, for the stone masonry model, whose material properties are more similar to the brick masonry properties, the influence is considerably lesser.

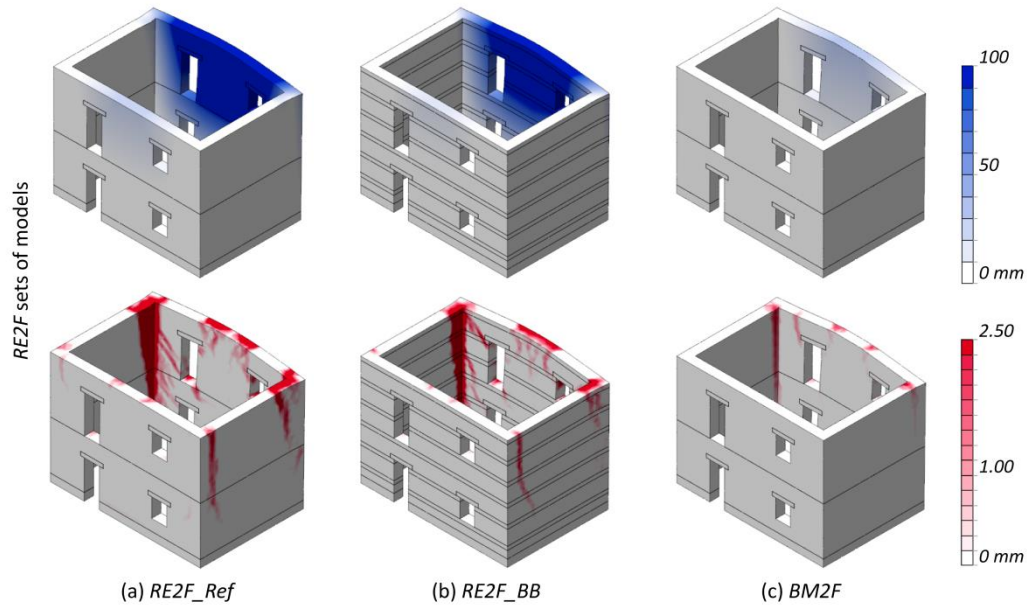


Figure 7.29: Failure modes at the ultimate limit state (LS4) obtained for the *RE2F* model with and without brick horizontal courses and for the *BM2F* model: (blue) maximum total displacements; and (red) crack pattern (crack width scale)

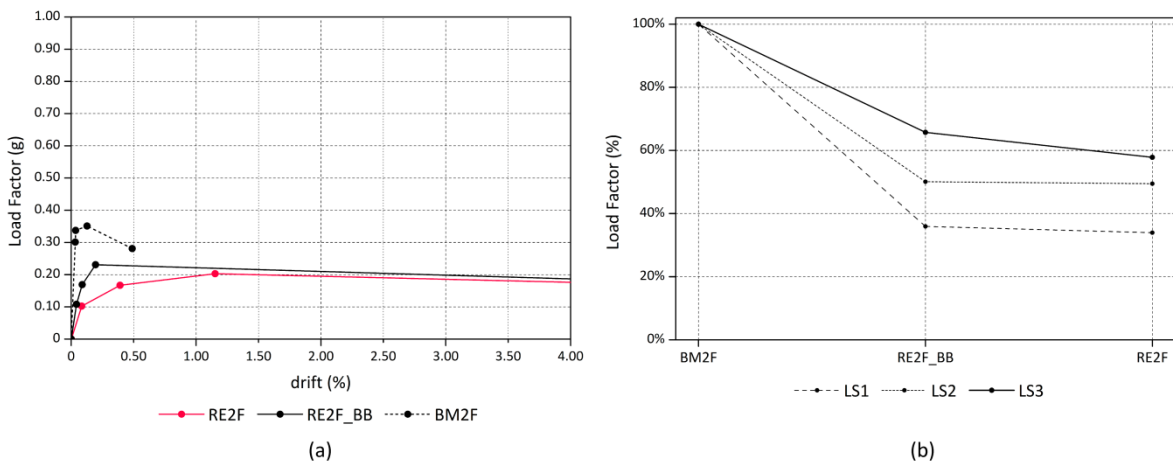


Figure 7.30: (a) Four-linear capacity curves constructed based on the computed limit states for the *RE2F_Ref*, *RE2F_BB* and *BM2F* models; and (b) load factor variations obtained for each limit state for the *RE2F_ref*, *RE2F_BB* and *BM2F* models

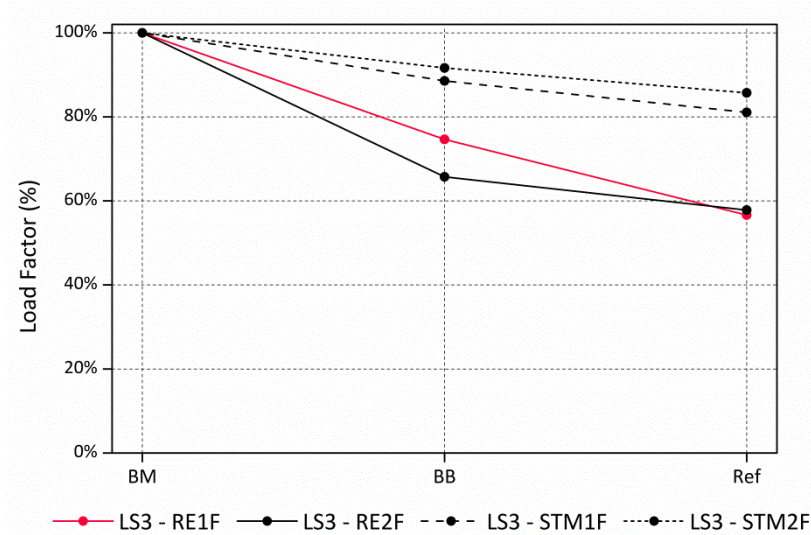
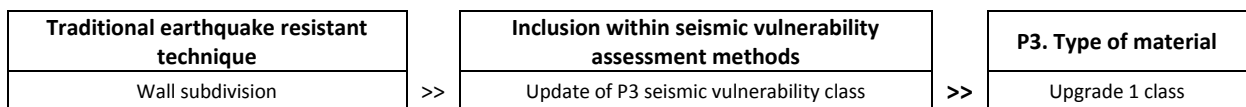


Figure 7.31: Variation of the load factor leading to the attainment of the maximum resistance (LS3) for the four sets of models evaluated when introducing horizontal brick masonry courses within the walls

7.2.6.2 Inclusion within seismic vulnerability assessment methods

The introduction of brick bands within the wall can be directly associated with changes on the parameter P3. Results showed that this technique allows enhancing the seismic behavior of the building a middle way between what would suppose constructing the walls entirely with the material used for the horizontal courses. Thus, the effect of these bands can be taken into account by increasing the vulnerability class of P3. This upgrade should vary according to the class of the materials used for the construction of both the walls and the bands. For instance, in the case of rammed earth walls, which belong to class D, with brick masonry horizontal bands, which belong to class B or A, the final class of the building can be considered as class C. As a general rule, a one-class upgrade can be assumed. It is acknowledged that this technique also helps in reducing the risk of delamination of masonry walls, and this effect is not taken into consideration by the numerical models. The classes for P3 defined in Chapter 4 already contemplated the beneficial action of brick bands and suggests considering as class B those masonry walls presenting horizontal stone or brick bands with dimensions similar to the wall thickness, so that they transversally connect the wall leaves by crossing the entire thickness at several points along the height of the walls. These conclusions are summarized in Table 7.16.

Table 7.16: Inclusion of the wall subdivision technique within seismic vulnerability assessment methods



7.2.7. Buttresses

Buttresses are one of the most common reinforcement techniques traditionally used in vernacular architecture. The main working resisting principle consisting of counteracting the rotation of the façade has always been very intuitive for vernacular builders and, as a result, buttresses were widely applied in most seismic prone regions. As previously discussed within Chapter 2, buttresses can show different configurations. Therefore, the evaluation of the effect of buttresses on the seismic behavior of the building is a complex matter, as there are many possible variables defining these elements. This section tries to provide a comprehensive analysis of the influence of buttresses focusing on the variations of two main characteristics: (a) dimensions; and (c) position within the building. With respect to the material composing the buttresses, the buttresses are assumed to be built using a low-quality irregular masonry class. Therefore, an elasticity modulus of 1000 MPa was initially considered. The compressive strength was estimated as 1/1000 of the elasticity modulus and the remaining nonlinear properties were computed directly from the compressive strength, based on recommendations given by Lourenço (2009), following the same approach discussed within Chapter 3. Preliminary analyses varying the initially considered material properties of the buttresses resulted in minimal variations of the seismic behavior of the models and thus, these properties were kept the same for the rest of the parametric analysis.

First of all, regarding the variations of the dimensions of the buttress (B), the thickness and length are modified. The initial dimensions were decided based on recommendations suggested by the Indian code (IS-13827 1993), which suggests the use of buttresses for walls longer than 10 times their thickness. The thickness of the buttress (t_b) is recommended to be equal to the wall thickness (t). The length of the buttress at the bottom (l_b) is suggested to be at least three times the thickness of the wall. This length is kept constant until the buttress is 0.4 m high and then it reduces progressively until reaching zero at the buttress maximum height (h_b).

With respect to the variations in the position of the buttress, two locations were considered: (1) within the span of the wall; and (2) at the corners. Concerning buttresses located within the span of long walls, aimed at stopping their out-of-plane rotation, two possibilities are evaluated: (a) buttresses located at an asymmetric position; and (b) buttresses located at the exact mid-span. Concerning buttresses located at the corners, aimed at preventing the walls separation, four different configurations are studied: (c) one buttress placed at one corner; (d) two buttress placed at both corners; (e) one buttress placed at one corner diagonally; and (f) two buttress placed at both corners diagonally. It is noted that the buttresses are modeled using the same solid 3D elements (CTE30) adopted for the walls and they are considered to be perfectly connected to the walls. It is acknowledged that this is not always the case in vernacular constructions but the ideal condition of the functioning of a buttress is addressed in this study. Figure 7.32 shows some of the most representative models constructed belonging to the different sets.

The variations in the characteristics and configuration of the buttresses were modeled in the same three reference models previously constructed for the evaluation of the other techniques, with varying number of floors and type of material, in order to evaluate their influence for different types of buildings: (a) one-floor rammed earth building (*RE1F*); (b) two-floor rammed earth building (*RE2F*); and (c) two-floor stone masonry building (*STM2F*). In order to better evaluate the influence of buttresses when located at different positions within the span of the wall, a new set of model was constructed: (d) one-floor rammed earth building with a longer wall of 10 m (*RE1F10*). The in-plan area of the models within this last set is 11x5.5 m² and the rest of the characteristics are kept the same. 7.2.7.1 presents the summary of the 29 different models constructed in order to assess the influence of buttresses in the seismic behavior of vernacular buildings, specifying the variations in the dimensions and configuration of the buttresses. All models described in 7.2.7.1 were always tested in the direction perpendicular to the walls presenting the maximum wall span (Y direction).

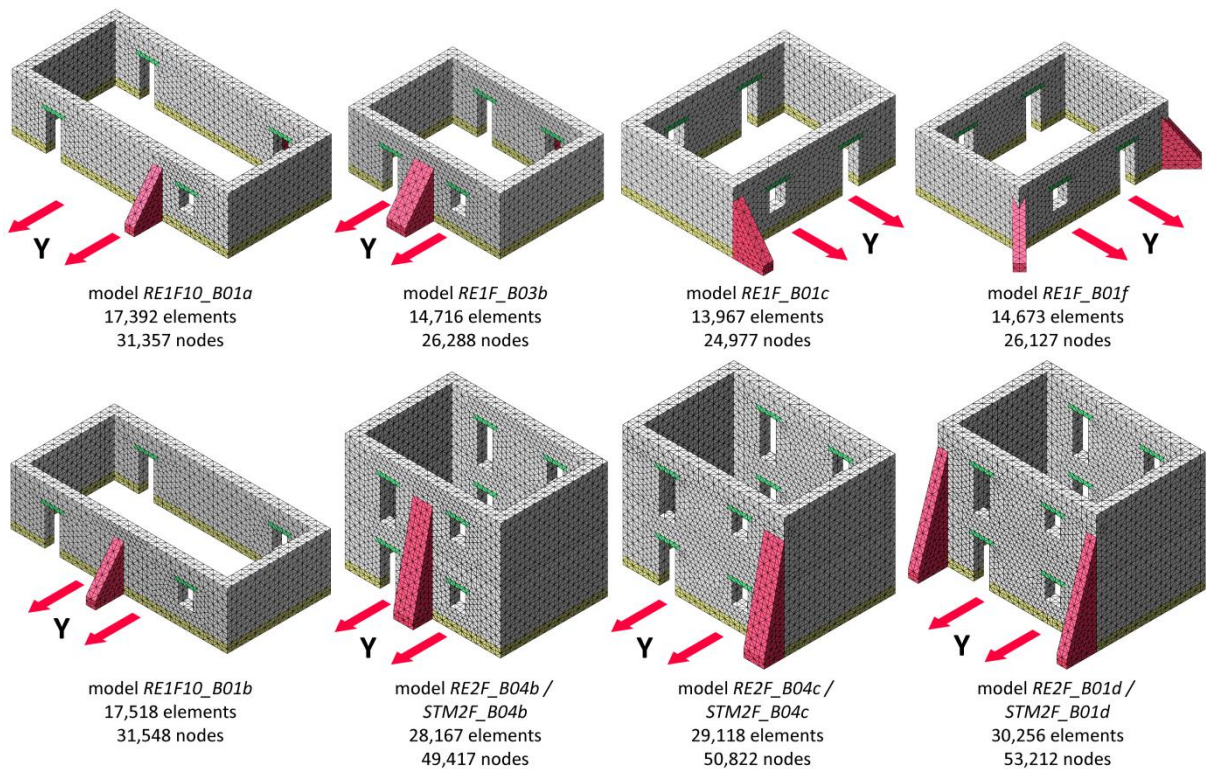


Figure 7.32: Representative numerical models built in order to assess the influence of buttresses in the seismic behavior of vernacular buildings

7.2.7.1 Numerical results and discussion

First of all, it should be noted that when the buttresses were modeled at the mid-span of the longest walls, the global failure of the building changed and was driven by the out-of-plane failure of the other wall perpendicular to the seismic load, which showed inward bending and overturned

towards the interior of the building. Since the buttresses are only meant to work by countering the rotation of the façade outwards, this initially obtained failure was prevented by not modeling the wall failing inwards. Figure 7.33 presents representative failure modes for the *RE1F10* model with the different positions of the buttresses along the wall span. The results are also compared with the failure modes of buildings with no buttresses presenting a maximum span of 5 and 7 m, which are the maximum free spans resulting after the addition of the buttresses. Buttresses do not change the initial out-of-plane failure of the wall, but are effective in avoiding the overturning of the exterior wall observed when the free span is 10 m (Figure 7.33a). The failure mode involves more bending damage widespread throughout the wall, which is no longer only accumulated at the connection between the walls and at the base (Figure 7.33b,c).

Table 7.17: Summary of the 29 models constructed for the evaluation of the influence of buttresses on the seismic behavior of vernacular buildings

Name	Models				Buttresses configuration									
	RE1F	RE1F10	RE2F	STM2F	Dimensions (m)			Location						
					Thickness (t_b)	Length (l_b)	Height (h_b)	Mid-span			Corners			
a	b	c	d	e	f									
<i>Ref</i>	X	X	X	X	-	-	-	-	-	-	-	-	-	-
<i>B01a</i>		X			0.5	1.5	2.4	X						
<i>B01b</i>	X	X	X	X	0.5	1.5	2.4 (5) ¹		X					
<i>B02b</i>	X	X			0.5	1	2.4		X					
<i>B03b</i>	X	X			1	1.5	2.4		X					
<i>B04b</i>	X	X	X	X	1	1	2.4 (5) ¹		X					
<i>B01c</i>	X		X	X	0.5	1.5	2.4 (5) ¹			X				
<i>B01d</i>	X		X	X	0.5	1.5	2.4 (5) ¹				X			
<i>B01e</i>	X				0.5	1.5	2.4					X		
<i>B01f</i>	X				0.5	1.5	2.4							X
<i>B04c</i>			X	X	1	1	5			X				
<i>B04d</i>			X	X	1	1	5				X			

¹ in parenthesis the height of the buttresses in the two-floor buildings

The effect of the addition of the buttress is also clearly reflected on the maximum capacity of the building. Figure 7.34 presents the four-linear capacity curves constructed for the *RE1F10* set of models and the variations of the load factors defining each limit state, in terms of percentage normalized using the results from the model with the buttress located at the mid-span of the wall. Results confirmed the efficiency of the buttress in avoiding the overturning and improving the seismic response of the building. The location of the buttress at the mid-span almost doubles the capacity of the reference model. Moreover, the maximum free spans resulting after the addition of the buttresses of model *RE1F10_B01b* is 5 m, which is also the maximum wall span of model *RE1F5_Ref*. However, the maximum capacity of the building with the buttress is around 20% greater. The same occurs with models *RE1F10_B01a* and *RE1F_Ref*. This exemplifies that the

addition of the buttresses leads to more restrictive boundary conditions of the walls when rotating out-of-plane, which increase the capacity of the building. The graph also shows that variations of the load factor defining LS1 are slightly smaller and, thus, buttresses do not have the same influence in preventing the onset of damage. In terms of the buttress dimensions, results show that, even though the biggest buttress (model *RE1F10_B03b*) leads to the best performance, the variation in the response according to the size is not critical.

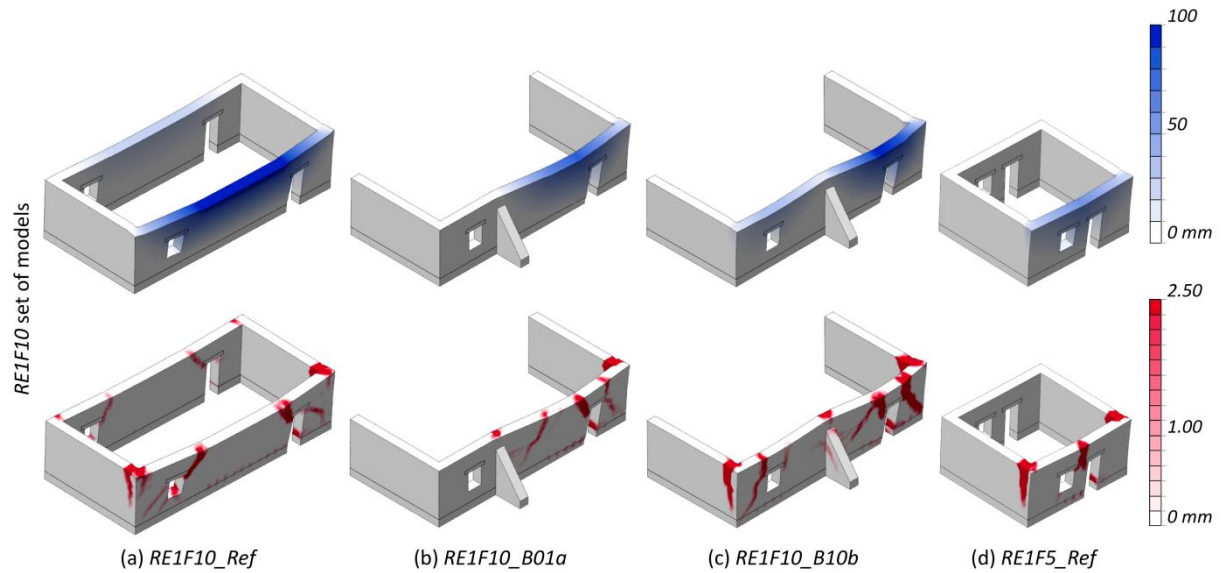


Figure 7.33: Representative failure modes at ultimate limit state (LS4) obtained for the several models within the *RE1F10* set with different locations of the buttress: (blue) maximum total displacements; and (red) crack pattern (crack width scale)

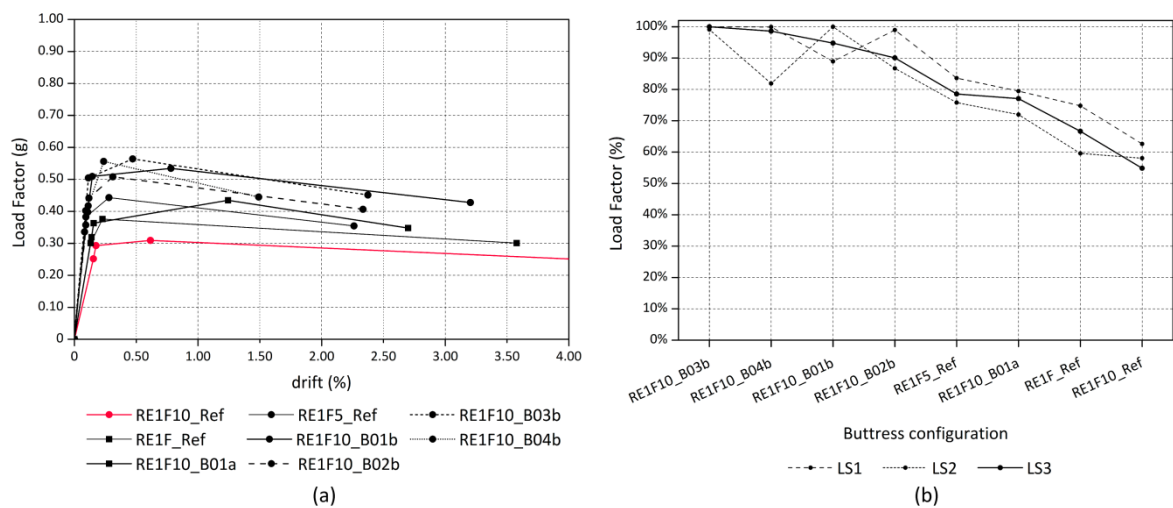


Figure 7.34: (a) Four-linear capacity curves constructed based on the computed limit states for the *RE1F10* set of models; and (b) load factor variations obtained for each limit state for the *RE1F10* set of models

The effect of buttresses located within the span of the wall was further explored on the remaining reference models. Figure 7.35 shows the failure modes for the *RE2F* models with

buttresses of different size placed at the same mid-position of the wall. Similarly to what was observed in Figure 7.33, reducing the maximum wall span with a buttress is translated into a much stiffer response of the building without modifying the original failure mode, always consisting of the out-of-plane bending failure of the wall perpendicular to the seismic load. Nevertheless, besides the widespread bending damage, an incipient out-of-plane collapse mechanism of the corner developed. Figure 7.36a presents the four-linear capacity curves constructed for the *RE2F* buildings and Figure 7.36b shows the variations of the load factor corresponding to the attainment of LS3 for the different sets of reference models. These results confirm that, with slight differences, the effect of buttresses of different size is similar for the different buildings, in terms of variation in the maximum capacity and damage patterns.

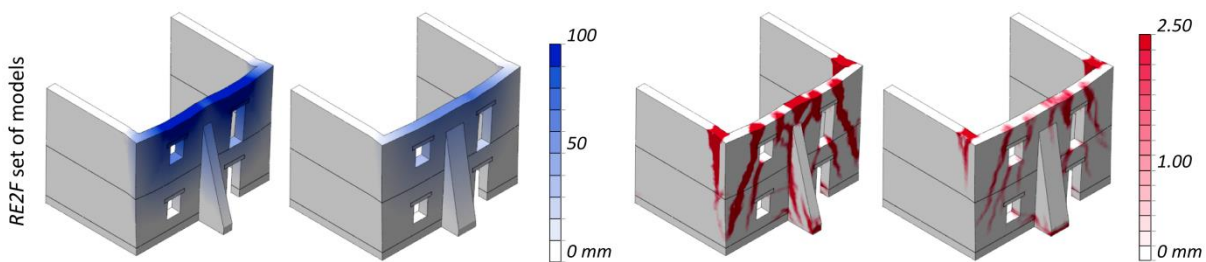


Figure 7.35: Failure modes in the transversal Y direction at ultimate limit state (LS4) obtained for the *RE2F* models with buttresses of different size at the mid-span: (blue) maximum total displacements; and (red) crack pattern (crack width scale in)

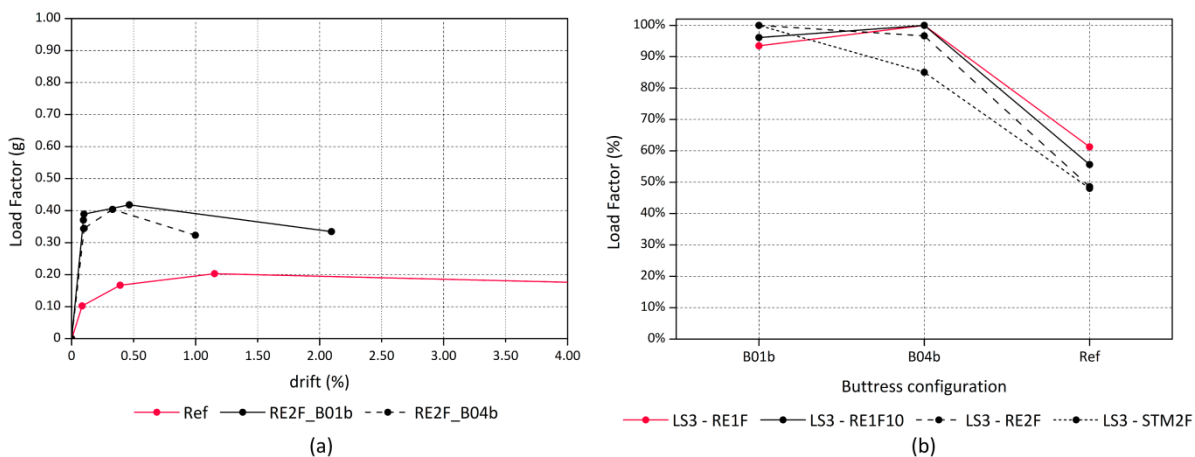


Figure 7.36: (a) Four-linear capacity curves constructed based on the computed limit states for the *RE2F* set of models; and (b) variation of the load factor leading to the attainment of the maximum resistance (LS3) for the different sets of models evaluated with buttresses of different size at the mid-span

Buttresses located at the corners of the building have a different structural role and are mainly intended to avoid the separation of perpendicular walls. They are indeed effective in limiting the damage at the connection, proving to be a successful solution, see Figure 7.37. Their influence on the seismic behavior of the building has also an impact in the capacity of the building

and the stiffness of its response, as it can be observed in the capacity curves resulting from the analysis in Figure 7.38a. Placing the buttresses at the corners leads to an increase in the maximum capacity of around 40%, see Figure 7.38b. Only by placing one buttress at one corner, there is a satisfactory improvement of the seismic response, but as expected, the best performance is shown by the building where the buttresses are placed at both corners.

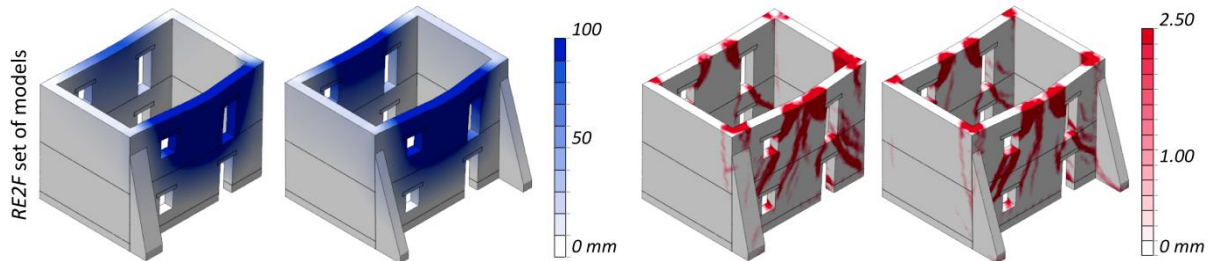


Figure 7.37: Representative failure modes at the ultimate limit state (LS4) obtained for the *RE2F* models with buttresses of different size at the corners: (blue) maximum total displacements; and (red) crack pattern (crack width scale)

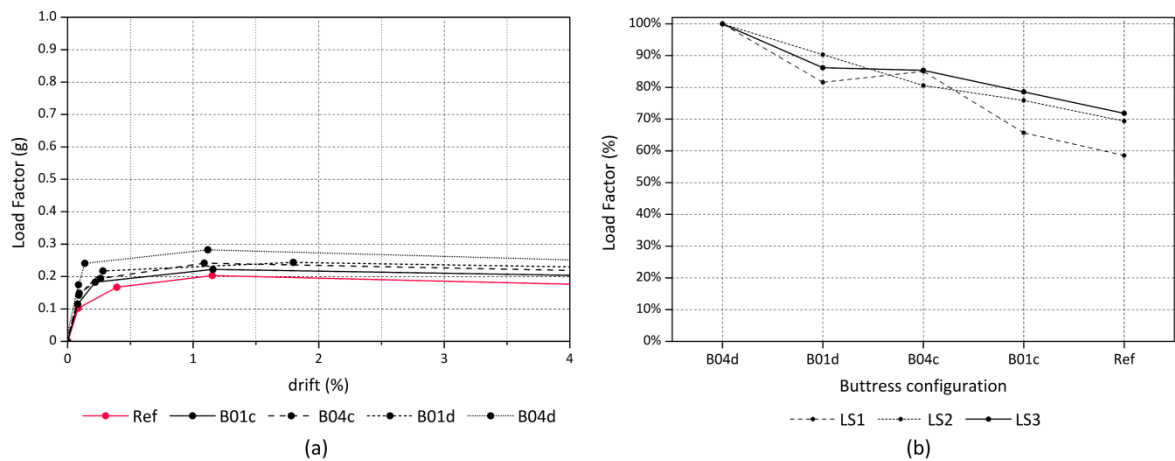


Figure 7.38: (a) Four-linear capacity curves constructed based on the computed limit states for the *RE2F* set of models; and (b) load factor variations obtained for each limit state for the *RE2F* set of models

The influence of placing buttresses at the corners was also evaluated on the remaining reference models. The use of diagonal buttress, for instance, was explored in the *RE1F* model. Results showed that their effect was the same as using buttresses perpendicular to the wall, see Figure 7.39a, which shows the capacity curves constructed for the *RE1F* models. Also, the results obtained for the *STM2F* models were very similar to the results obtained for the rammed earth models, as it can be observed in Figure 7.39b, which shows the comparison of the variation of the load factor corresponding to the attainment of LS3 for both models. It is noted that the influence of the size of the buttress is greater when they are placed at the corners, particularly concerning their thickness.

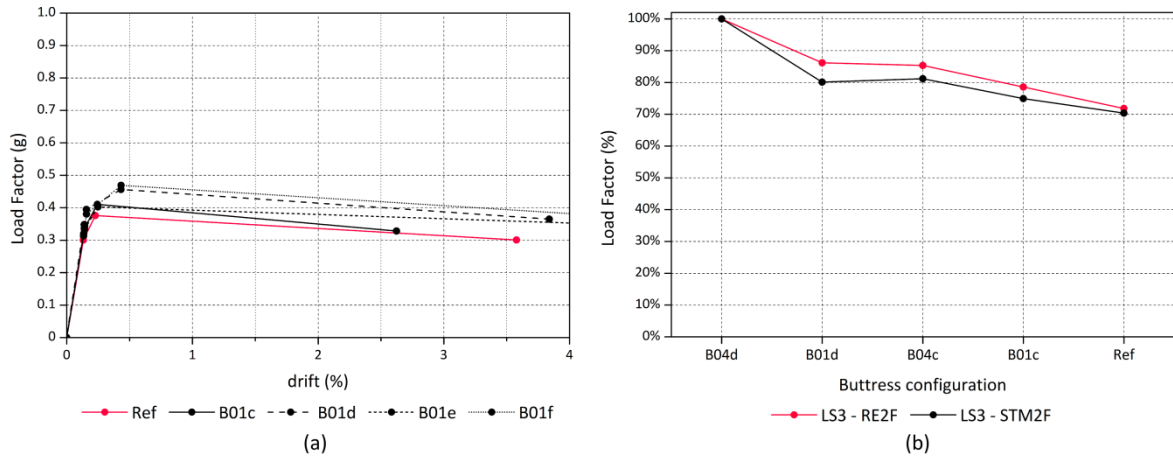


Figure 7.39: (a) Four-linear capacity curves constructed based on the computed limit states for the *RE1F* set of models; and (b) variation of the load factor leading to the attainment of the maximum resistance (LS3) for the *RE2F* and *STM2F* sets of models evaluated with buttresses of different size at the corners

Finally, another model was constructed based on some of the most typical retrofitting elements identified in Portuguese vernacular architecture within the Seismic-V project discussed in Chapter 2. A particular configuration observed was the simultaneous use of buttresses and stone plinths at the outer base of the walls. These traditional constructive elements were added to model *RE1F* in order to evaluate their influence on the seismic behavior of the building. Figure 7.40 shows the model and the results in terms of capacity curves, comparing the performance of the building with and without the new elements. The maximum capacity of the building almost doubles the original capacity. This assessment exemplifies how common traditional solutions, if well executed, can significantly reduce the seismic vulnerability of vernacular architecture.

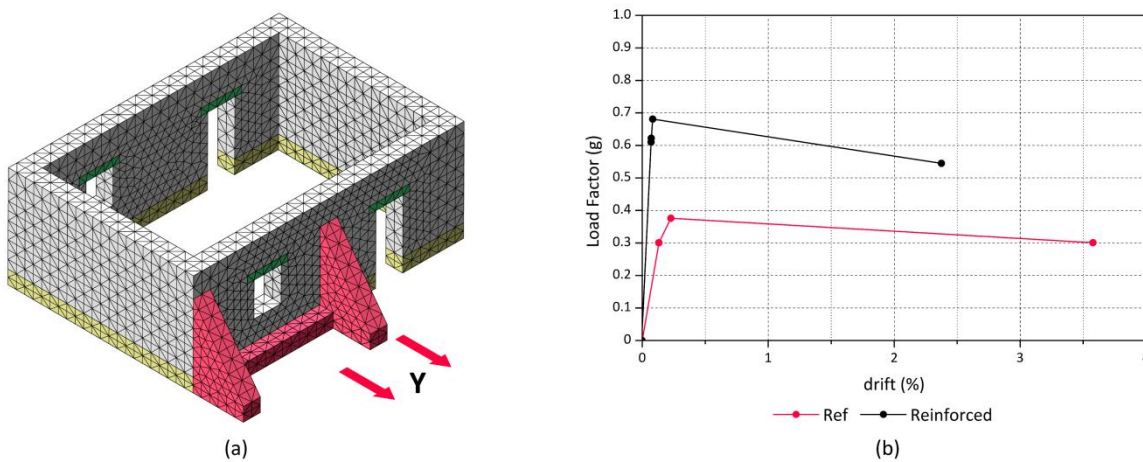


Figure 7.40: (a) Numerical model built in order to assess the influence of a typical configuration of different reinforcement elements observed in Portuguese vernacular architecture; and (b) results in terms of four-linear capacity curves constructed based on the computed limit states

7.2.7.2 Inclusion within seismic vulnerability assessment methods

In conclusion, the effect of buttresses located within the span of the wall mainly contributes to reduce effectively the maximum free span of the walls subjected to out-of-plane loading. Thus, they can be directly associated with P2. The most proper way to consider their influence using the two seismic vulnerability assessment methods would be to update P2 seismic vulnerability class according to the maximum free span resulting after the addition of the buttress. Even though it was observed that the effect of the buttress is stronger than simply reducing the maximum wall span, this upgrade of the class was deemed adequate, given the fact that the analyses performed always considered a perfect connection between buttress and wall, which is not always the case.

With respect to the buttress placed at the corners of the building, their effect directly addresses the quality of the wall-to-wall connections and, thus, they relate to parameter P4. Although the response of the building varied according to the size of the buttress, they were able to effectively improve the maximum capacity of the reference building, even when only one buttress was modeled. Therefore, the effect of buttresses located at the corners on the seismic behavior of vernacular buildings can be also taken into consideration by means of increasing the vulnerability class of P4 to class A. The conclusions are summarized in Table 7.18.

Table 7.18: Inclusion of buttresses within seismic vulnerability assessment methods

Traditional earthquake resistant technique		Inclusion within seismic vulnerability assessment methods		P2. Maximum wall span
Buttress within the span of the wall	>>	Update of P2 seismic vulnerability class	>>	According to the maximum free span resulting after the addition of the buttress
Traditional earthquake resistant technique		Inclusion within seismic vulnerability assessment methods		P4. Wall-to-wall connections
Buttress at the corner	>>	Update of P4 seismic vulnerability class	>>	A

7.2.8. Walls thickening

The final reinforcement that was assessed was the traditional thickening of the walls intended to lower the center of gravity of the buildings by adding mass to construct scarp walls with varying thickness. The reference models walls were modified geometrically to become inclined, with the thickness decreasing from the bottom to the top. Three configurations were evaluated varying the wall thickness at the bottom (t_1) and at the top (t_2): (a) $t_1 = 0.6\text{ m}$ and $t_2 = 0.4\text{ m}$; (b) $t_1 = 0.6\text{ m}$ and $t_2 = 0.5\text{ m}$; and (c) $t_1 = 0.5\text{ m}$ and $t_2 = 0.4\text{ m}$. These variations were introduced in two reference models with varying material: (a) one-floor rammed earth building (*REIF*); and (b) one-floor stone masonry building (*STMIF*). The models were analyzed in the direction perpendicular to the walls presenting the maximum wall span (Y). Table 7.19 presents the summary of the 12 models constructed in order to assess the influence of introducing thickening the walls in the seismic behavior of vernacular buildings, specifying the geometry of the final walls considered.

Table 7.19: Summary of the 12 different models built in order to assess the influence of thickening the walls in the seismic behavior of vernacular buildings (dimensions in m)

Set of models	Wall dimensions			
	Height (h)	span (s)	Thickness	
			t_1	t_2
<i>RE1F_Ref</i>	3	7	0.5	0.5
<i>RE1F_4</i>	3	7	0.4	0.4
<i>RE1F_6</i>	3	7	0.6	0.6
<i>RE1F_6-4</i>	3	7	0.6	0.4
<i>RE1F_6-5</i>	3	7	0.6	0.5
<i>RE1F_5-4</i>	3	7	0.5	0.4
<i>STM1F_Ref</i>	3	7	0.5	0.5
<i>STM1F_4</i>	3	7	0.4	0.4
<i>STM1F_6</i>	3	7	0.6	0.6
<i>STM1F_6-4</i>	3	7	0.6	0.4
<i>STM1F_6-5</i>	3	7	0.6	0.5
<i>STM1F_5-4</i>	3	7	0.5	0.4

7.2.8.1 Numerical results and discussion

The results showed clearly the beneficial effect of using scarp walls. The failure mode remains unchanged with respect to the reference building, as it is shown in Figure 7.41, but it occurs at a higher load. Figure 7.42a presents the capacity curves constructed for the *RE1F* models, showing clear variations in terms of maximum capacity and stiffness. Results are also compared with the performance of buildings with constant wall thickness of 0.4 and 0.6 m. The best results are obtained from the model that presents the greatest variation of the thickness along the height, which is due to the fact that the resisting cross section increases, while the mass at the top of the wall is reduced. The increment in the maximum capacity of the building with this configuration with respect to the capacity of the building with walls with a constant thickness of 0.6 m is 20%. Results are practically the same for the stone masonry model, see Figure 7.42b, which presents the variation of the load factor corresponding to the attainment of LS3 for both models.

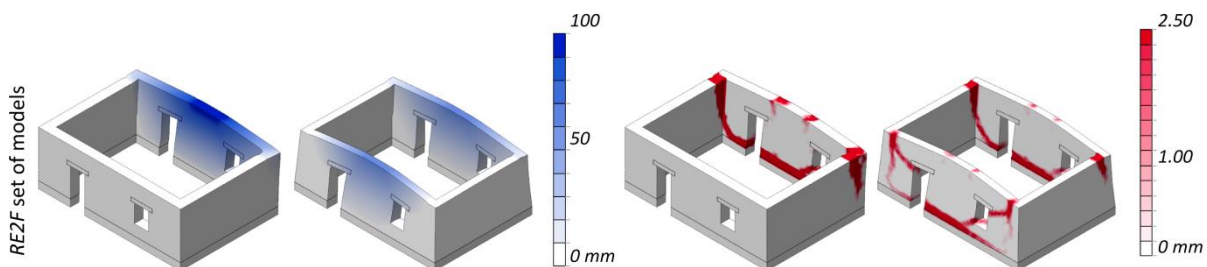


Figure 7.41: Failure modes at the ultimate limit state (LS4) obtained for the *RE1F* reference model and the model with scarp walls with varying thickness from 0.6 to 0.4 m: (blue) maximum total displacements; and (red) crack pattern (crack width scale in)

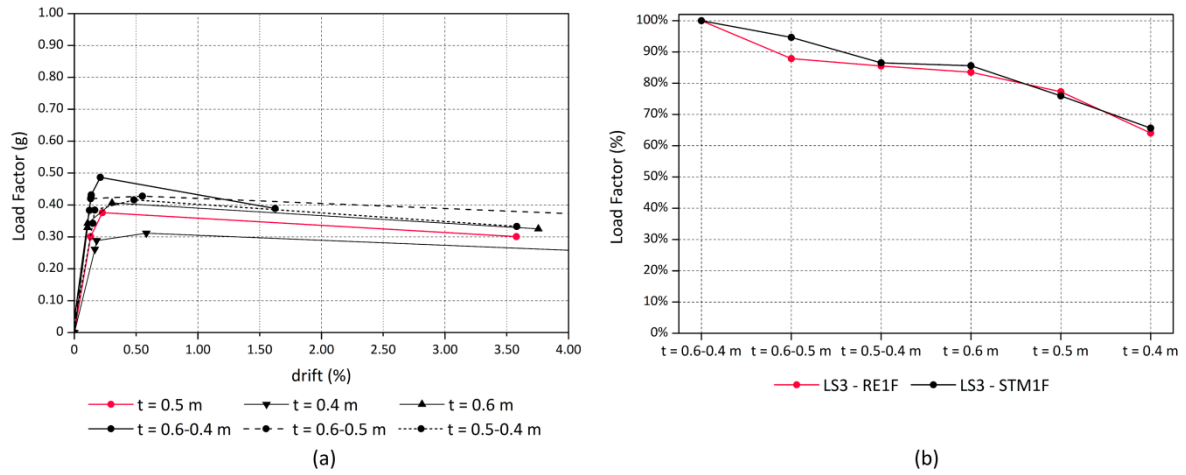
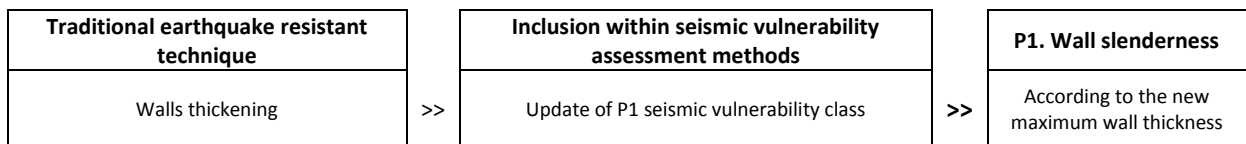


Figure 7.42: (a) Four-linear capacity curves constructed based on the computed limit states for the *RE1F* set of models; and (b) variation of the load factor leading to the attainment of the maximum resistance (LS3) for the *RE1F* and *STM1F* sets of models evaluated

7.2.8.2 Inclusion within seismic vulnerability assessment methods

The effect of thickening the wall is directly associated with the determination of the class for P1, as it involves a change in the wall slenderness. Therefore, the easiest way to take into account the effect of this technique consists of updating P1 seismic vulnerability class according to the new maximum wall thickness. In the case of scarp walls, the value of the wall thickness at the bottom (t_i) should be always adopted to calculate the new slenderness value. Even though results showed that the performance of the building is better when considering an inclined wall than having a wall with this value as the constant thickness, this upgrade of the class, despite conservative, was deemed enough to represent the new condition. Table 7.20 summarizes these conclusions.

Table 7.20: Inclusion of buttresses within seismic vulnerability assessment methods



7.2.9. Summary

All the decisions resulting from the individual numerical studies about how to include the effect of each traditional seismic resistant solution within the two proposed seismic vulnerability assessment methods are summarized in Table 7.21 for reference purposes.

Table 7.21: Summary of the proposed ways to include the effect of each traditional earthquake resistant technique within the seismic vulnerability assessment methods

Technique	Inclusion within seismic vulnerability assessment methods	
	Parameter updated	Update on the vulnerability class
Timber ring beams	P5	A
Corner braces	P4	A
Quoins	P4	A
Reinforced floor-to-wall and roof-to-wall connections	P5	According to the resulting type of horizontal diaphragm
Ties connecting parallel walls	P5	C
Ties connecting floor and roofs to walls	P5	C
Ties connecting perpendicular walls	P4	Upgrade 1 class
Timber elements within the masonry	P3	A
Wall subdivision	P3	Upgrade 1 class
Through-stones	P3	Considering the presence of transversal connection elements
Mended cracks	P9	A
Closing openings	P7	According to the new number of wall openings
Reinforcing openings	P3	Considering the presence of transversal connection elements
Stiffening floors and roofs	P5	According to the resulting type of horizontal diaphragm
Buttresses within the span of the wall	P2	According to the maximum free span resulting after the addition of the buttress
Buttresses at the corners	P4	A
Walls thickening	P1	According to the new maximum wall thickness
Urban reinforcing arches within the span of the wall	P2	According to the maximum free span resulting after the addition of the urban reinforcing arch
Urban reinforcing arches at the corners	P4	A

7.3. Updated definition of the seismic vulnerability classes for P4

As a result of the numerical study of some of the techniques aimed at improving the quality of wall-to-wall connections, the seismic vulnerability classes of P4 were updated. Primarily, a new class A was created considering a condition of the building where wall-to-wall connections are not only properly built but also improved by means of applying some of the reviewed techniques, such as quoins and corner braces. The final classification is shown in Table 7.22.

Table 7.22: Final vulnerability classes proposed according to the wall-to-wall connection

P4. Wall-to-wall connection	
Class	Description
A	Wall-to-wall connections are workmanlike built and enhanced with improved interlocking, the use of better quality materials at the corners (i.e. quoins), and/or the presence of timber or metallic connectors, such as timber corner braces
B	All wall-to-wall connections are workmanlike built. There might be elements related to Class A but only at some corners or orthogonal connections. There are no weakening signs or construction deficiencies. In case of masonry buildings, there is a good interlocking between the masonry units at the corners. In case of earthen buildings, there are no vertical joints at the corners
C	Some wall-to-wall connections are deficient or degraded because of construction deficiencies, such as lack of efficient interlocking of the masonry units in case of masonry buildings or vertical joints in case of earthen construction. Connections can show also weakening signs, such as cracks or detachments
D	Most wall-to-wall connections are barely non-existent because of poor construction practices or are highly degraded with important signs of separation and vertical cracks

7.4. Updated formulation of the SAVVAS method

As a consequence of updating P4 vulnerability classes in order to include the effect of some of the evaluated techniques, the formulation of the SAVVAS method needed to be updated considering these new classes instead of the original ones. For example, those buildings which were previously assigned a class A for P4, now belong to class B because they do not present a deficient wall-to-wall connection, but they do not have any of the reinforcement elements related to class A. This changes the parameter values for P4 considered in the database that was previously used for the development of the regression models previously proposed. A new database had thus to be prepared with the updated values for parameter P4 and then, following exactly the same approach shown in Chapter 6, new regression models were built. Both multiple regression and ANN models were again prepared. It is noted that 37 new numerical models were built to have a representative amount of buildings belonging to class A. For these new models, P4 seismic vulnerability class was kept as A, assuming that, for instance, the building presents well-constructed quoins, while the values of the remaining nine seismic vulnerability assessment parameters were varied. In the end, the results of the pushover analyses performed on a total of 567 models composed the final numerical database. The database presented in Annex B is the updated one. It is noted that the regression models prepared were validated with the same examples from the literature used in Chapter 6, confirming again the good prediction capability of the models. Just as in the previous chapter, the expressions considered for the formulation of the SAVVAS method are those resulting from the multiple regression analysis, and the ANN models are kept just for comparison. Table 7.23 provides the final updated formulation of the SAVVAS method, including the three steps necessary for its application, for reference purposes.

Table 7.23: Final SAVVAS formulation and procedure

Step 1											Definition of the seismic vulnerability assessment parameters
P1	P2	P3	P4	P5	P6	P7	P8	P9	P10		
$\lambda (h/t)$	$s (m)$	$P3 [1-4]$	$P4 [1-4]$	$P5 [1-4]$	$P6 [1-4]$	P7a	P7b	N	$P9 [1-10]$	γ_i	
Step 2											Calculation of the load factors associated to the limit states in each main direction i
$LS1_i(g) = e^{(2.2-0.06\lambda-0.1s-0.71\ln(P3)-0.16P4-0.29P5-0.52\ln(P6)-3.67P7b-0.85\ln(N)-2.31\ln(P9)+0.68P5P7b) - c}$ $LS2_i(g) = 0.15 \times LS1(g) + 0.78 \times LS3(g)$ $LS3_i(g) = e^{(2.52-0.04\lambda-0.06s-0.24P3-0.19P4-0.28P5-0.09P6+0.27P7a-2.83P7b-0.4N-0.16P9+0.68\gamma_i+0.44P5P7b)}$											
Step 3											Calculation of the global load factors defining the limit states of the building
$LS1(g) = \min(LS1_i(g))$ $LS2(g) = \min(LS2_i(g))$ $LS3(g) = \min(LS3_i(g))$											

7.5. Conclusions

This chapter has presented a numerical assessment of the efficiency of traditional strengthening solutions identified in the previous chapters in reducing the seismic vulnerability of vernacular architecture. Detailed FE models were prepared simulating the different techniques and possible variations. Pushover analyses were then conducted on the resulting model so that the influence of each technique could be quantitatively evaluated. Therefore, the extensive numerical study presented in this chapter mainly contributes to the deep understanding of the seismic behavior of these empirically developed traditional techniques. Results have primarily helped to validate the efficiency of the techniques. Some of them are extraordinarily efficient in increasing the capacity of vernacular buildings, particularly those meant to improve the connections between structural elements, such as ring beams, which, by tying the building and improving its 'box-behavior', led to increments of the building maximum capacity of around three times. The validation of these techniques is important because it can help to reintroduce them in the vernacular building culture for the preservation of the vernacular heritage. Gaining confidence on the use of these techniques can be also helpful in preventing the abandonment of vernacular buildings that are many times considered unsafe, since the loss of knowledge on traditional materials and construction techniques has commonly led to the demolition and reconstruction of the buildings using new modern materials, with the consequent invaluable loss of the heritage.

The second main goal of this chapter has been the incorporation of the evaluated techniques within the two new methods proposed for the seismic vulnerability assessment of vernacular architecture. The quantitative assessment of the influence of each different technique led to the proposal of different ways to take into account their effect by means of updating the seismic vulnerability classes of different parameters. The parameter updated depends on the structural goal of the technique applied. The upgrade depends on the numerical results and is mainly determined by the increment in the maximum capacity achieved after the application of the technique. As a result of the inclusion of the different techniques, both methods had to be updated, because of the introduction of a new seismic vulnerability class for P4. Thus, at the end of the chapter, three main outcomes have been provided: (a) a summary of the proposed ways suggested to include the effect of traditional strengthening solutions within both seismic vulnerability assessment methods; (b) the redefinition of the seismic vulnerability classes for P4; and (c) the final formulation of the SAVVAS method after the considered updates.

CHAPTER 8

CALIBRATION AND APPLICATION OF THE PROPOSED SEISMIC VULNERABILITY ASSESSMENT METHODS

Chapter outline

- 8.1. [Introduction](#)
- 8.2. [Calibration of the methods based on the damage data after the 1998 Azores earthquake](#)
 - 8.2.1. [Building stock characterization](#)
 - 8.2.2. [Damage classification](#)
 - 8.2.3. [Calibration and validation of the proposed methods](#)
 - 8.2.3.1. [Vulnerability index \(SVIVA\) method](#)
 - 8.2.3.2. [SAVVAS method](#)
 - 8.2.3.3. [Comparison between both methods](#)
- 8.3. [Application of the methods in Vila Real de Santo António](#)
 - 8.3.1. [Building characterization](#)
 - 8.3.2. [Seismic vulnerability assessment](#)
 - 8.3.2.1. [Vulnerability index \(SVIVA\) method](#)
 - 8.3.2.2. [SAVVAS method](#)
 - 8.3.2.3. [Historical vs current condition](#)
 - 8.3.2.4. [Mitigation of the seismic vulnerability with different building retrofitting strategies](#)
 - 8.3.3. [Loss assessment](#)
 - 8.3.3.1. [Collapsed and unusable buildings](#)
 - 8.3.3.2. [Human casualties and homelessness](#)
 - 8.3.3.3. [Economic loss and repair cost estimation](#)
- 8.4. [Conclusions](#)

8.1. Introduction

The seismic vulnerability assessment methods are mainly aimed at estimating the damage that a certain structure will suffer as a consequence of a seismic event of a given intensity. The two methods developed within this research work (SVIVA and SAVVAS) are intended to be applied to large scale assessments, comprising a large number of buildings within an urban center or a region. Both methods were conceived as first level approaches that can make use of simple more expedite inspections because they can rely on less detailed qualitative information related to a

few parameters. The present chapter deals with the application of the two methods using differentiated case studies and different purposes: (1) calibration and validation of the developed methods; and (2) estimation of damage scenarios and loss assessment of a historical city center for different earthquake events.

In the first case, the two methods are calibrated and validated through a wide set of damage data collected after the 1998 Azores earthquake, in Portugal. The use of post-earthquake information allowed the comparison of the damage estimated from the application of the two seismic vulnerability assessment methods with the observed damage after the earthquake. This exercise was extraordinarily helpful for a better understanding and training on the use of both methods for the seismic vulnerability assessment. More specifically, with regard to the SVIVA vulnerability index method, the calibration also led to the adjustment of the original analytical expression proposed by Lagomarsino and Giovinazzi (2006), which correlates the macroseismic intensity and mean damage grade, to fit better the new characteristics of the proposed method. Concerning the SAVVAS method, a correlation between the limit states (LS) calculated and the damage level is established and results are compared with the observed damage for its validation. The discussion of the advantages, drawbacks and limitations of each method is provided in detail.

In a second case, after the calibration and lessons gained in the previous application, the two methods are applied to the historical city center of Vila Real de Santo António (VRSA), in Portugal. The construction of VRSA at the end of the 18th century, after the 1755 earthquake, was planned with a high seismic awareness and, thus, it included the use of several seismic resistant measures, based on Pombalino construction principles. This is the main reason why it was selected as a case study. However, the historical city center of VRSA is highly altered and most of the original buildings have been replaced or suffered important modifications at the structural level. Two tasks were defined and carried out sequentially for this case study: (1) on-site inspection and collection of information about the existing buildings within the historical center; and (2) application of the two seismic vulnerability assessment methods on a set of buildings that were selected on the basis that their construction typology is included within the seismic vulnerability assessment methods developed, typically meaning that their structure is composed of load bearing walls and timber diaphragms. From the application of both methods, damage distributions in terms of vulnerability and fragility curves could be estimated. Given the detailed information available on the historical condition of the city in the literature, the seismic vulnerability assessment intends to be also carried out for the same buildings assuming the original historical state. Results will be compared with the current condition, discussing changes in the seismic vulnerability of the city center. Additionally, the seismic vulnerability of the buildings will be also evaluated after the proposal of different retrofitting strategies based on the previously studied traditional strengthening solutions (Chapter 7). A discussion on the possible level of reduction of the vulnerability using different strategies will be presented.

Finally, the study ends with the seismic loss assessment for the city center of VRSA using the results from the SAVVAS method. The loss assessment includes the estimation of the amount of collapsed and unusable buildings, number of casualties and homelessness, and the economic loss and repair costs. This loss estimation will be contrasted with the different scenarios of the evaluated building stock considered: (a) historical condition; (b) current condition; and (c) retrofitted condition. Particular focus will be placed on performing a cost analysis of the retrofitted scenario in order to later present an evaluation of the benefits related to the implementation of the strengthening techniques prior to a seismic event, instead of assuming the economic losses and repair costs resulting from the same earthquake occurring in the current unstrengthened condition.

8.2. Calibration of the methods based on the damage data after the 1998 Azores earthquake

The 1998 Azores earthquake struck the central group of the Azores Archipelago with a moment magnitude $M_w = 6.2$, mainly striking Faial, Pico and San Jorge islands. The earthquake reached high levels of destruction and affected more than 5000 people, causing 8 fatalities and leaving 1500 persons homeless (Matias et al. 2007). A Modified Mercalli Intensity (MMI) scale distribution map for the Faial Island was proposed by Zonno et al. (2010) based on post-earthquake damage survey campaigns, see Figure 8.1. Nevertheless, it is noted that the construction of this document is subjected to uncertainties and Zonno et al. (2010) argues that some locations might have been subjected to higher intensities than those plotted on the map.

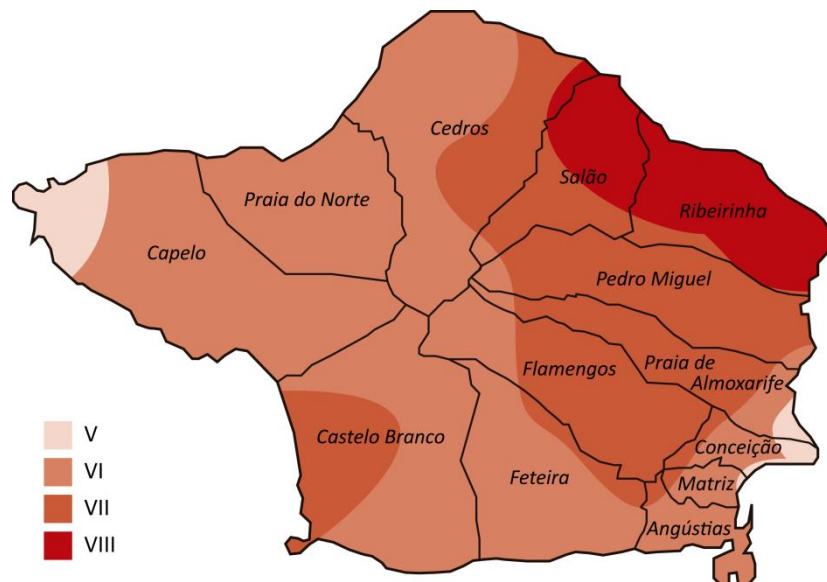


Figure 8.1: MMI scale distribution map of Faial Island indicating the administrative subdivision of the island into the different districts. Ferreira et al. (2017) adapted from Zonno et al. (2010)

8.2.1. Building stock characterization

The seismic event was followed by the collection of extensive data on the effects of the earthquake on the building stock of the islands. Neves et al. (2012) focused on the detailed characterization of the buildings in the Faial Island and particularly presented a detailed study of the construction systems that characterize the traditional architecture of the island, mainly composed of stone masonry load bearing walls, timber floor diaphragms and timber roof trusses. This is particularly adequate, given that the two seismic vulnerability assessment methods proposed were developed and are mainly addressed for this construction typology. Neves et al. (2012) also proposed a detailed damage classification for this traditional masonry building stock by identifying the main damage patterns surveyed. Moreover, the earthquake also attracted a significant amount of scientific research addressing the study of the structural behavior of these traditional construction techniques from the island (Costa 2002; Costa et al. 2011; Costa et al. 2013). This vast amount of information gathered and produced on the seismic performance of traditional Azorean masonry constructions after the 1998 earthquake makes this case study very appropriate for the calibration of the two seismic vulnerability assessment methods proposed. This is also why it has also been previously selected to perform and calibrate other seismic vulnerability assessments methods (Neves et al. 2012; Ferreira et al. 2017).

The same set of 88 masonry buildings used by Ferreira et al. (2017) was also selected for the application and calibration of the two methods proposed in this work. This selection includes comprehensive information on different representative traditional masonry construction types scattered throughout various villages in Faial Island. Both rural and urban building types are present in the selection, see Figure 8.2. The reader is referred to Costa and Arêde (2006) and Neves et al. (2012) for a more detailed description of these buildings in terms of construction systems and materials. The documentation available for each of these 88 buildings varied widely: from very detailed reports drafted during the reconstruction process with information of the original and retrofitted structure (including plans, damage reports and photographs) to very limited information with barely a damage report fulfilled on-site or a couple of photographs.

8.2.2. Damage classification

The selection of the set of 88 buildings was also meant to include buildings presenting a wide variation in terms of the observed grade of damage. The classification of the damage observed in each building is carried out according to the EMS-98 damage grade scale (Grünthal 1998), which is presented in Table 8.1 as a reference. It is noted that a sixth damage grade (Grade 0) is added to the scale, representing those buildings showing no damage. This damage classification was chosen because it is the scale used by the macroseismic method (Giovinazzi and Lagomarsino 2004), as discussed in Chapter 3. Thus, the mean damage grade (μ_D) that can be estimated using this method directly relates to the classification shown in Table 8.1.

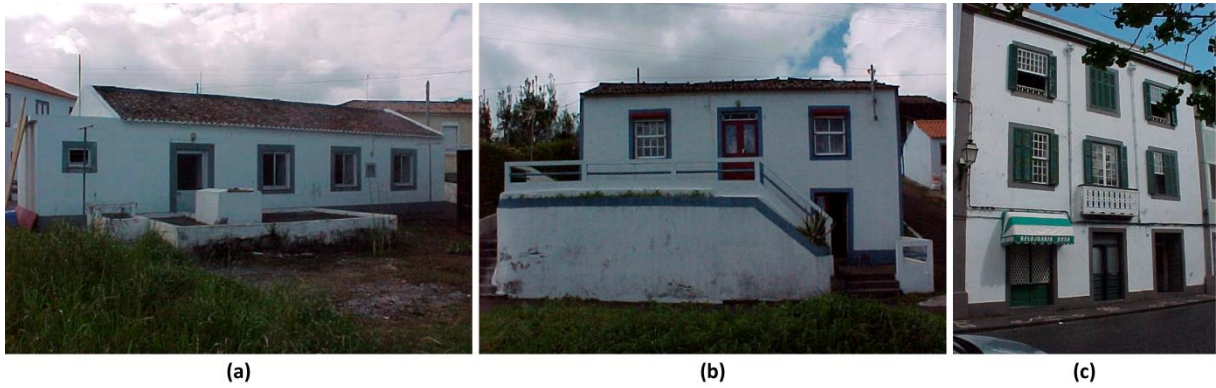


Figure 8.2: Examples of typical traditional Azorean masonry construction types in the island of Faial present in the selection: (a) one-floor rural building; (b) two-floor rural building; and (c) three-floor urban building

Table 8.1: Damage grades adopted for the study based on the EMS-98 scale (Grünthal 1998)

Damage grade	Description
0 No damage	No observed damage
1 Negligible to slight damage	No structural damage and/or slight non-structural damage: hairline cracks in very few walls, fall of small pieces of plaster, fall of loose stones from upper parts of buildings in very few cases
2 Moderate damage	Slight structural damage and/or moderate non-structural damage: cracks in many walls, fall of large pieces of plaster, partial collapse of chimneys
3 Substantial to heavy damage	Moderate structural damage and/or heavy non-structural damage: large and extensive cracks in most walls, roof tiles detach, chimneys fracture at the roof line, failure of individual non-structural elements (partitions or gable walls)
4 Very heavy damage	Heavy structural damage and/or very heavy non-structural damage: Serious failure of walls, partial structural failure of roofs and floors
5 Destruction	Very heavy structural damage: total or near total collapse

The buildings were thus classified in terms of damage using the data available. It is worth noting that a damage assessment is always qualitative, as it depends on the judgment of the evaluator. Besides, as previously stated, the existing information on the buildings is variable and, in some cases, limited. Therefore, in order to minimize uncertainties and to have a more robust and reliable assessment, four experts carried out the evaluation of the damage grades for the 88 buildings independently. The results were then analyzed and compared. The final damage classification adopted for each building was the mean value obtained from the four evaluations. This approach also provided the opportunity of obtaining mid-values in between the 6 damage grades (e.g. 3.25), which allowed a better comparison with the damage values resulting from the two seismic vulnerability assessment methods that express damage as a continuous variable.

Figure 8.3 shows several examples of buildings classified under the five damage grades. None of the buildings in the set was considered as grade 0, since all of them presented at least slight non-structural damage. The examples are compared with reference drawing provided by the EMS-98 scale. Finally, Figure 8.4 shows the distribution of the assessed buildings according to their estimated damage level. Damage levels in the graph are used as thresholds and include all buildings that have not reached the following damage level (i.e. buildings whose damage grade was estimated as 3.5 are included within damage grade 3). The graph shows that the majority of

the buildings (over 65%) did not reach damage grade 3 and, thus, did not present substantial structural damage.



Figure 8.3: Examples of evaluated buildings belonging to each damage grade from the EMS-98 scale

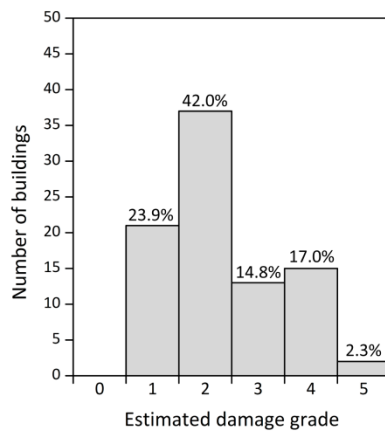


Figure 8.4: Distribution of the evaluated buildings according to the estimated damage level

8.2.3. Calibration and validation of the proposed methods

Prior to the application of the two seismic vulnerability assessment, some notes on the parameter classification should be outlined. First of all, the parameter survey is a crucial step for the application of the two proposed methods. The parameter classes for each building have to be defined and, in the case of the SAVVAS method, specific values for some of the parameters have to be assigned. It is worth highlighting that, just as with the damage classification, the damage data available for each building is not always complete enough to carry out a sound parameter survey. Therefore, some assumptions had to be made in order to decide the class for some of the parameters. The parameter survey is much dependent on the qualitative judgment of the person conducting the assessment, since different persons may reach to different classifications.

The definition of the classes can be particularly difficult for parameters that are not easily evaluated from the exterior, such as the quality of the wall-to-wall connections or the type of horizontal diaphragm. In this particular case, for example, it should be also noted that interpreting the class for parameter P9, which refers to the previous structural damage in the building, was very difficult, since all the pictures available correspond to the state of the buildings after the earthquake. Thus, it was decided to establish that all buildings fell within class A for parameter P9, so that this parameter does not have a relative influence in the results. As abovementioned, the information available for some of the buildings barely consisted of a brief damage report and a couple of photographs. For these buildings with limited information, the data obtained from other buildings from the set with more detailed information served as the basis for extrapolation. Also, the detailed construction characterization of the masonry walls, timber roofs and timber floors, conducted by Neves et al. (2012), was very helpful for the determination of some parameters classes.

8.2.3.1 Vulnerability index (SVIVA) method

The application of the new proposed vulnerability index formulation to the 88 buildings resulted in the vulnerability index distribution presented in Figure 8.5a. The mean value of the seismic vulnerability index (I_V) obtained is 43.22 with a standard deviation value (STD) of 7.1, which results in a coefficient of variation (CoV) of 16%. The minimum and maximum values of I_V are 21.5 and 55 respectively. The little variation within the index shows clearly that most of the buildings assessed belong to similar construction typologies. The main typological difference occurs between the rural and urban buildings. However, even between both construction types, the majority of the classification of the parameters coincides.

Figure 8.5b presents the class distribution for each parameter. The graph provides a clear insight on the typology of the buildings assessed. The structural typology of the great majority of the buildings consists of thick load bearing walls (class A for P1) constructed with stone masonry

of irregular quality (the class assigned for P3 to most of the buildings varies within C or D) and timber horizontal diaphragms that provide poor or no proper connection among the resisting walls (class D for P5). The connection between orthogonal walls is one of the parameters with the greatest variations. It is also a difficult parameter to evaluate based solely on exterior photographs. Nevertheless, some buildings were considered to present workmanlike built connections because of the observed use of better quality stones at the corners. However the majority of the buildings show weakening signs and lack of efficient interlocking (class C for P4). The roof type usually consists of timber rafters supported by a wall plate and provided with a rafter tie aimed at absorbing the thrust (class A for P6). Nevertheless, whenever the roof is considered to exert thrust, a class D is directly considered because of the heavy weight tile roofs that are characteristic from the island. In terms of geometry, the buildings are typically rectangular with a clear dominant direction (class C or D for P10), which makes the walls span large distances in many cases (class C and D for P2). The buildings present few openings (class A or B for P7) and mostly have one to two floors (class A or C for P8). Only those buildings located in the urban environment sometimes present three floors.

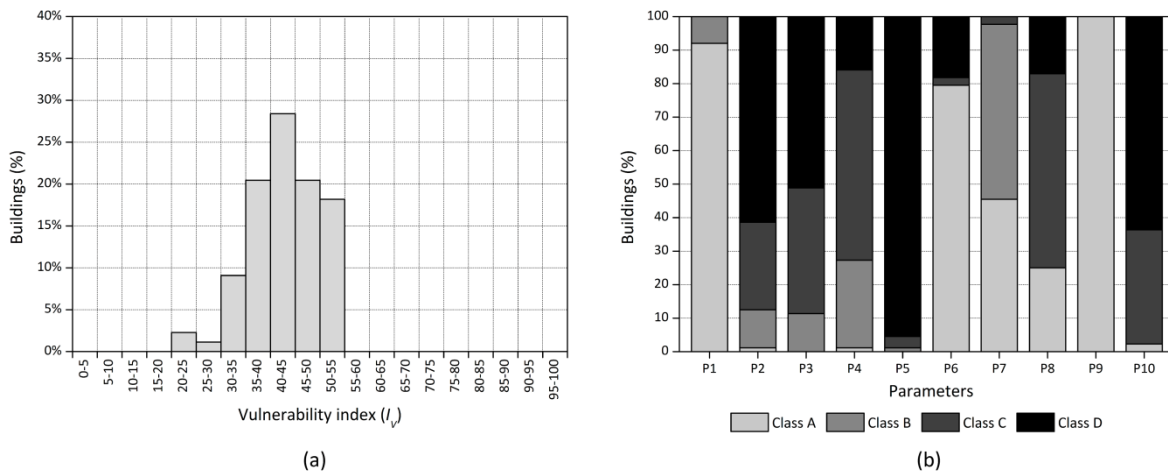


Figure 8.5: (a) Vulnerability index (I_v) distribution; and (b) parameter class distribution

Before the estimation of the mean damage grade (μ_D) for each building, the buildings were grouped by location and intensity, following the district subdivision shown in the intensity map (Figure 8.1). As previously mentioned in Chapter 3, the calculation of the damage grade requires using the European Macroseismic Intensity scale (EMS-98) as the input for the seismic intensity. Following the recommendations by Musson et al. (2010), the degrees from the MMI scale depicted in the intensity map can be directly correlated with the degrees from the EMS-98 scale, acknowledging a certain degree of subjectivity involved within this assumption (Ferreira et al. 2017). Thus, a scale V in MMI scale can be associated to a scale V in the EMS-98 scale.

Afterwards, the procedure described in Chapter 3 was followed. First, the vulnerability index (I_v) was transformed into the vulnerability index used in the macroseismic method (V), using the

analytical correlation (Eq. 3.5) proposed by Vicente (2008). Then, the analytical expression (Eq. 3.1) proposed by Lagomarsino and Giovinazzi (2006) to build vulnerability curves, correlating mean damage grade (μ_D), seismic intensity (I) and the vulnerability index (V), was applied to estimate the level of damage suffered by each of the 88 buildings. It is here noted that both expressions needed to be calibrated for the buildings under analysis. The initial results obtained using the original formulations were rather poor and a curve-fitting process was applied in order to find a better approximation between the damage observed-vulnerability index point cloud and the vulnerability curves (Figure 8.6).

The availability of post-earthquake damage data allows the comparison between the estimated and the observed damage. The fitting process was carried out using CurveExpert Pro software (Hyams 2017). This software automatizes the process of finding the best fit allowing the definition of a custom regression model based on the analytical expressions shown in Eq. 3.1 and Eq. 3.3. Subsequently, these two analytical expressions could be calibrated to better represent the seismic behavior observed for this particular type of buildings, by means of varying the coefficients that define both expressions. The resulting calibrated expressions are shown below, highlighting in bold the updated coefficients:

$$V = \mathbf{0.46} + \mathbf{0.012} \times I_V \quad (8.1)$$

$$\mu_D = 2.5 \left[1 + \tanh \left(\frac{I + \mathbf{6.25}V - \mathbf{12.7}}{Q} \right) \right] \quad (8.2)$$

The ductility index (Q) is empirical parameter and depends on the construction typology evaluated. In this study, a value of 2 is assumed based on recommendations of other authors dealing with load bearing masonry wall construction types (Ferreira et al. 2017; Shakya 2014). This factor defines the slope of the vulnerability curve and the value of 2 adopted also proved to provide the most accurate approximation. The fitting process resulted in a significant improvement in the correlation between the estimated and observed damage. Figure 8.6 illustrates this improvement by showing side by side plots of the mean damage grade observed (μ_D) versus the vulnerability index (I_V), with the corresponding vulnerability curves built using the original formulation and the calibrated one, for the three different macroseismic intensities registered in the island (*VI*, *VII* and *VIII*). It should be noted that, since only a few buildings within the set correspond to areas where the macroseismic intensity level registered was *VIII*, the improvement resulting from the fitting process is less optimized (Figure 8.6c). With regard to the partial distributions of I_V for each intensity level, a mean value of 41.1, 46.1 and 41.2 were obtained for $I_{EMS-98} = VI, VII$ and *VIII*, respectively. These similar values obtained confirmed the construction homogeneity of the set of buildings evaluated and showed that the fact that some

buildings suffered a greater level of damage, which should be associated to the greater accelerations registered in those areas.

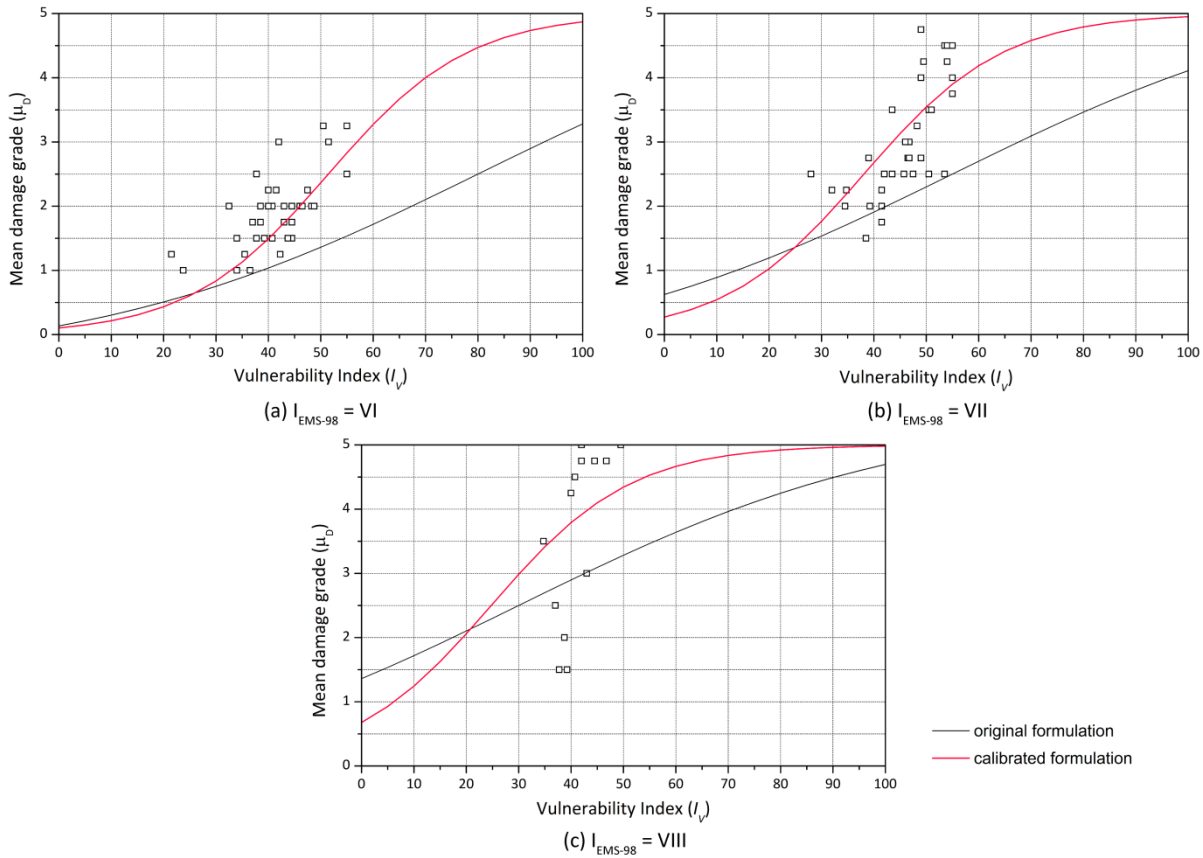


Figure 8.6: Observed damage versus mean damage grade estimated using the original and updated expressions for the construction of the vulnerability curves, grouped by the different macroseismic intensities

The damage estimation achieved using this new proposed vulnerability index formulation was considered satisfactory. The estimated versus observed damage plot is shown in Figure 8.7a, while Figure 8.7b presents the residual versus observed damage. The value of R^2 obtained reaches 0.605, which can be considered high for these simplified seismic vulnerability assessment methods. The errors are also low, showing a maximum error in the prediction of 2.24, but a MAE value of 0.56 and a RMSE value of 0.71. The graph from Figure 8.7b shows that the level of damage is predicted within a maximum difference of 1 level for the great majority of the buildings, with the exception of a few rare cases. Acknowledging the uncertainties inherent to the whole prediction process, namely the attribution of the macroseismic intensities, the assignment of a level of damage and the selection of the parameter classes to the different buildings, it should be highlighted that the results show a good prediction capability. The model is able to recognize the most vulnerable constructions and provide a good estimate of the damage that each building might suffer for earthquakes of different intensities.

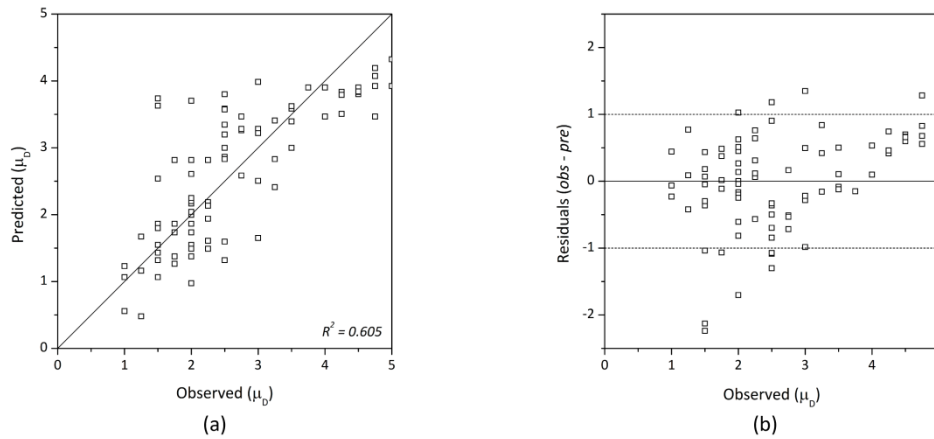


Figure 8.7: (a) Predicted versus observed damage grades; and (b) residuals versus observed damage grades

8.2.3.2 SAVVAS method

The application of the new proposed SAVVAS method requires a set of steps previously defined in Chapter 6 when this method was introduced. The three steps are finally established in Chapter 7 (Table 7.23), after the inclusion of the influence of traditional seismic earthquake resistant solutions. Part of the first step is common to both methods, namely the assignment of seismic vulnerability classes to the different parameters. Nevertheless, some of the parameters need to be defined directly through numeric values instead of classes. Moreover, the values adopted for each parameter are defined for the four main directions of the building (+/-X and +/-Y). This is intended to provide a more accurate description and understanding of the seismic behavior of the evaluated vernacular buildings, as well as a better estimation of their most vulnerable direction. Thus, the load factors associated to the three main limit states (LS1, LS2 and LS3) are calculated in each main direction but, in order to have a global assessment, the minimum values for each LS obtained among all directions are given as the global load factors defining the seismic vulnerability of the building.

As a result of the application of the SAVVAS procedure defined in detail in Table 7.23 (Chapter 7), the load factor distributions for the 88 buildings evaluated are presented in Figure 8.8. The mean values of the load factors obtained are 0.13g, 0.22g and 0.25g for LS1, LS2 and LS3 respectively, with a standard deviation (STD) value of 0.06g, 0.08g and 0.09g, which result in coefficients of variation (CoV) of 47%, 37% and 36%. These results show significantly greater variations than the ones obtained from the vulnerability index method, which suggests that this method is able to distinguish the capacity of the buildings that previously had the same vulnerability index (I_V). Therefore, the SAVVAS method seems to be able to detect more precisely the differences in the seismic performance of the different buildings, even though they belong to a very similar construction typology.

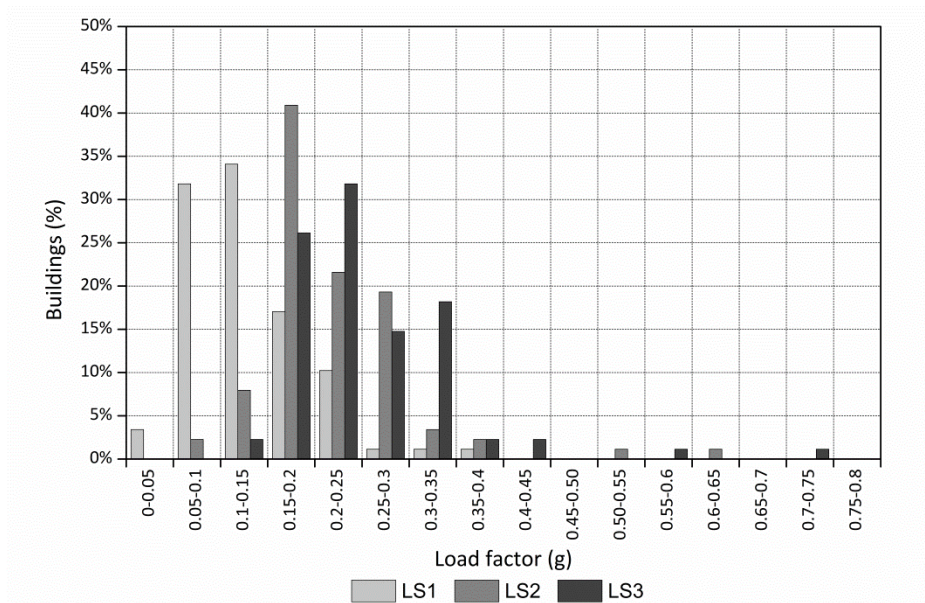


Figure 8.8: Load factor distributions for the three limit states: LS1, LS2 and LS3

A first seismic assessment of the buildings can be carried out just by comparing the seismic load factors obtained with the seismic demand established by the code. For Faial Island, the value of reference peak ground acceleration (PGA) is 0.25g (NP EN1998-1 2010). About 60% of the buildings present a load factor corresponding to LS3 below 0.25g, which means that their maximum capacity would be exceeded by the design load action of an earthquake with the characteristics defined by the code. This is a first indicator that reveals the vulnerability of the buildings in the island. Moreover, most of the buildings are prone to suffer structural damage. For 95% of the buildings evaluated, the load factor corresponding to LS1 obtained is considerably lower than 0.25g (Figure 8.8).

Table 8.2 shows the statistics obtained for the vulnerability parameters corresponding to the surveyed buildings. Table 8.2 also includes the statistics from the computed global load factors defining the three limit states. From the small variations found for parameters P1, P3 and P5, it is possible to confirm that the majority of the buildings belong to a similar construction type consisting of thick load bearing irregular masonry walls with flexible timber horizontal diaphragms. Some parameters show a greater variation than that observed for the vulnerability index method, which is attributed to: (a) the parameters are classified differently for each main direction; (b) parameters are more specifically classified and have a wider range of variation. For example, the variation observed for parameter P6 is due to the fact that, within the same building, some walls might be considered to receive the roof thrust while others do not. This is common when buildings have gable roofs (as is the case for most of the buildings under analysis), where only two walls can receive the possible thrust from the roof. Regarding parameter P2, walls get to span distances over 15 m in several cases, which also confirms a clear trend for the buildings in the island to be very slender in plan ($\gamma_i > 0.75$). The coefficient of variation (CoV) for

the two parameters addressing wall openings is very high because of the low value of the mean. However, the buildings typically present few openings, with some exception of those located in urban areas, which can show facades with up to 49% of wall openings. With respect to the number of floors, there is also a greater variation, which is associated mainly to the fact that many buildings are built in a slope. Therefore, different sides of the buildings can present different heights, which results also different values for this parameter within the same building.

Table 8.2: Statistics from the parametric survey and the estimated load factors defining each limit state

Variables		Units	Minimum	Maximum	Mean	Median	Mode	STD	CoV
Parameters	P1	λ	3.71	7.07	5.12	5.00	5.38	0.64	12.33%
	P2	m	2.85	17.40	7.38	6.52	4.50	3.30	44.74%
	P3	Class	2	4	3.47	4	4	0.66	19.04%
	P4	Class	1	4	2.90	3	3	0.67	23.00%
	P5	Class	2	4	3.68	4	4	0.49	13.42%
	P6	Class	1	4	1.33	1	1	0.92	69.43%
	P7a	$P7a$	0	0.49	0.09	0.06	0	0.10	110.64%
	P7b	$P7b$	0	0.36	0.07	0.06	0	0.06	96.43%
	P8	N	1	3	1.49	1	1	0.63	42.08%
	P9	Class	1	1	1	1	1	0	0.00%
P10	γ_i	0.19	0.71	0.39	0.40	0.45	0.10	24.34	
Load factor	LS1	g	0.04	0.38	0.13	0.12	-	0.06	46.67%
	LS2	g	0.09	0.63	0.22	0.20	-	0.08	36.72%
	LS3	g	0.11	0.74	0.25	0.23	-	0.09	36.13%

As abovementioned, it should be here noted that in cases where there is a limited amount of information available, some of the values assigned to each parameter had to be inferred just from a limited amount of pictures. The conditions observed in other buildings with more detailed information served as reference. However, there was no way to know if, for example, there were intermediate resisting walls that can reduce the span value adopted for P2 or, if the condition of the wall-to-wall connections was good. For these buildings, the analysis of the damage developed during the earthquake helped also to infer the classification of some of the parameters, taking into account that the damage is typically associated to deficiencies of the building. As an example, the photographs depicting the collapse of some walls allow detecting deficient wall-to-wall connections otherwise impossible to detect by a visual survey from the outside of the building.

The use of the real information available for this case study was in fact very useful to gain knowledge on how to carry out the parameter survey. The classification of some parameters was not straightforward in many cases. Some assumptions were considered in the present work that can be helpful for the future application of the method, including: (1) the wall slenderness might vary among the different walls of the building, the minimum observed was considered for all directions; (2) whenever walls showed different number of floors along their length because of being constructed in a slope, the maximum height was always considered; or (3) the value of the in-plane index considered in all directions was always the minimum calculated, unless the

building presents a class A or B type of diaphragm (P5), able to redistribute the load to the earthquake resistant walls in the loading direction. These assumptions were always aimed at taking into account the worst scenario. As a result of this calibration, some guidelines for the application of the SAVVAS method and the fulfillment of the parameter survey were outlined and presented in Annex D.

The next step after the application of the SAVVAS method consists of the estimation of damage grade based on the EMS-98 scale, correlated with the calculated load factors associated to the three limit states defined. In a first step, the SAVVAS method requires that the seismic input is expressed in terms of PGA instead of macroseismic intensity, so that it can be compared with the values of load factor. The existing data for the 1998 earthquake included strong-motion records and a large collection of post-earthquake damage in the building stock. Based on this information, Zonno et al. (2010) prepared possible PGA and MMI maps for the earthquake, according to possible epicenter locations (Figure 8.9).

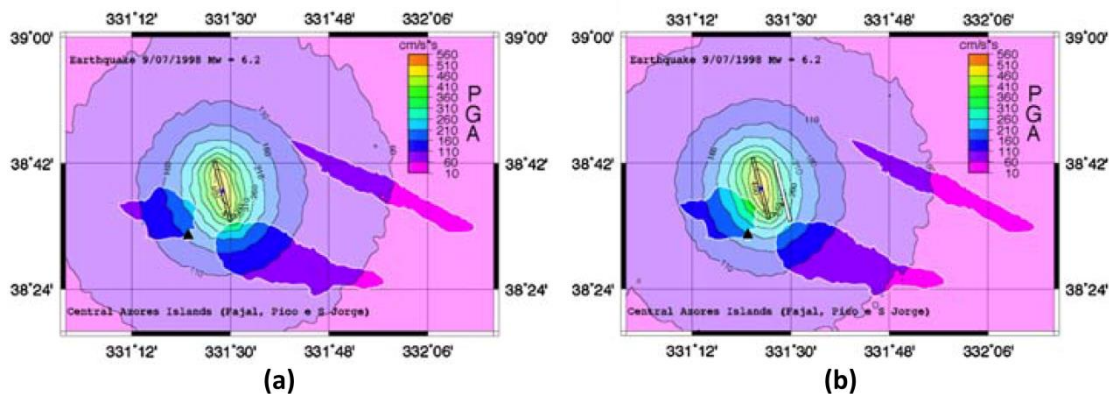


Figure 8.9: PGA maps computed by Zonno et al. (2010) for the 1998 Azores earthquake assuming two different possible epicenters

The previously shown MMI map (Figure 8.1) used for the application of the SVIVA method was constructed based on the surveyed damage data, as abovementioned. Subsequently, in order to have comparable results, the PGA values were inferred from the values of MMI shown in the map from Figure 8.1. There are several empirical relationships between seismic intensity and acceleration. Guagentini and Petrini (1989) and Margottini et al. (1992) derived their expressions based on post-earthquake observations in Italy. Zonno et al. (2010) used the relationship developed by Wald et al. (1999) for their work on the 1998 Faial earthquake. None of these expressions were derived based on previous earthquake data from Azores and all lead to different values of PGA, showing notable scatter. The values obtained using the expression from Guagentini and Petrini (1989) were deemed very low with respect to the two ground-shaking scenarios estimated by Zonno et al. (2010) for this earthquake, using two possible epicenter locations. This study adopts the mean values of PGA obtained using the two empirical

relationship proposed by Margottini et al. (1992) and Wald et al. (1999), see Table 8.3. The subjectivity of adopting the mean values is acknowledged. However, they were adopted because they are considered to be more approximated to the values of PGA computed by Zonno et al. (2010) shown in Figure 8.9, where the values of PGA range between 0.06 and 0.26g in Figure 8.9a and between 0.11 and 0.36g in Figure 8.9b.

Table 8.3: I-PGA relationships from the literature and final values of PGA adopted

MMI	PGA (g)		Mean value (adopted)
	Margottini et al. (1992) $PGA = 0.003353 \times 10^{0.2201 \times I_{MSK}}$	Wald et al. (1999) $MMI = 3.66 \times \log(PGA) - 1.66$	
6	0.07	0.13	0.10
7	0.12	0.24	0.18
8	0.19	0.44	0.32

After the definition of the seismic input, a correlation between seismic input, load factors (expressed in *g*) associated to the structural limit states and mean damage grade (μ_D) has to be defined. Results need to be expressed in terms of the same EMS-98 damage grade scale in order to enable the output of the SAVVAS method to be comparable with other seismic vulnerability assessment methods, such as the macroseismic method. Figure 8.10 shows the equivalence between the structural limit states defined from the pushover curve and EMS-98 damage grades.

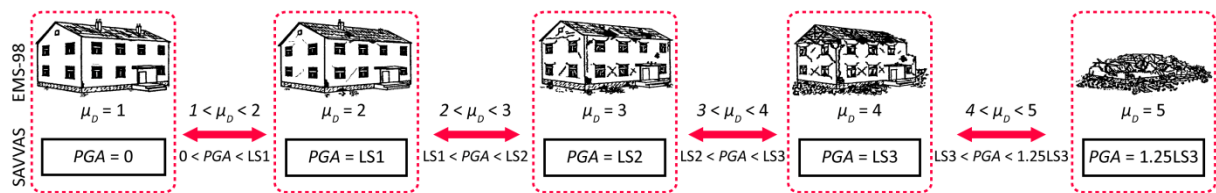


Figure 8.10: Correlation between the seismic input (PGA), SAVVAS limit states and EMS-98 damage grades

First of all, damage grade 0 was removed from the scale. Since the SAVVAS method does not detect non-structural damage, grade 0 and 1 are the same and both suppose the starting point of the scale representing no structural damage. The load factor defining LS1 (which represents the onset of cracking and end of the elastic behavior) delimits the point where the building reaches damage grade 2 and, thus, for values of PGA higher than LS1, the building is assumed to start presenting slight structural damage. Similarly, LS2 (which represents a transition point where the structure shows minor structural damage and a state where significant damage is visible) is associated to damage grade 3, and LS3 (which represents a point after which the building shows significant structural damage but retains some margin against collapse) with damage grade 4. The correlation with the 5th damage grade that refers to the total or near collapse of the structure was not straightforward. The ultimate limit state (LS4) related to the collapse of the building was defined from the pushover analysis but its calculation was not included within the SAVVAS method because it was defined in terms of displacement rather than load. An empirical

factor was established to define a load that would cause the collapse of the building and could be related to damage grade 5. This factor was calibrated using the post-earthquake damage data from the 1998 earthquake to fit better the collapse observed and was finally set as 1.25 times the value found for LS3. The final values for damage for intermediate values of PGA between limit states are obtained from simple linear interpolation in order to provide a continuous variable.

Once this correlation was established, the level of damage was assessed for the 88 buildings evaluated. The estimation of damage achieved using the SAVVAS method was deemed considerably accurate, clearly outperforming the prediction capability of the vulnerability index (SVIVA) method. Figure 8.11a shows the estimated versus observed damage plot, while Figure 8.11b presents the residual versus observed damage. The value of R^2 obtained from the correlation between observed and predicted damage reaches 0.802, which is quite high in comparison with other seismic vulnerability assessment methods. The errors are also reduced, showing a maximum error in the prediction of 2.33 but a MAE of 0.32 and a RMSE of 0.71. The graph from Figure 8.11b shows that the level of damage is predicted within a maximum difference of less than 0.5 in the damage level for the great majority of the buildings.

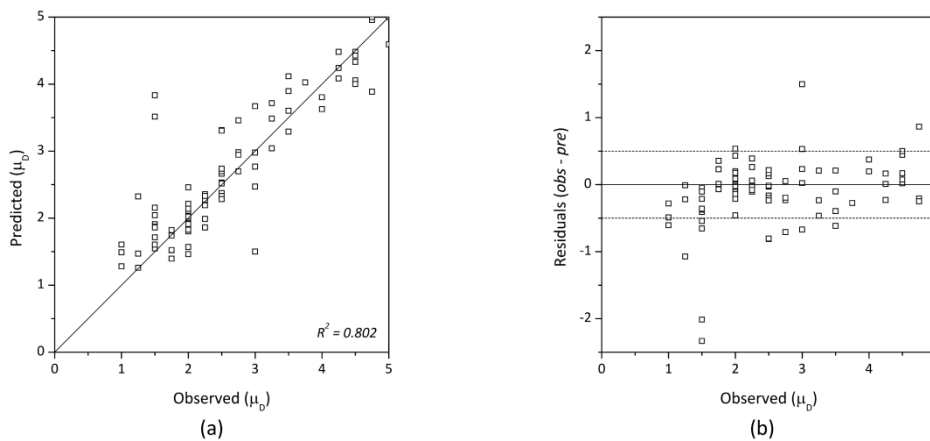


Figure 8.11: (a) Predicted versus observed damage grades; and (b) residuals versus observed damage grades

Figure 8.12 presents the vulnerability curves constructed using the SAVVAS method as a function of the load factor defining LS3. The damage observed-LS3 point cloud is also presented together for reference. The curves fit well the points representing the damage observed. Results are plotted for the three different PGA associated to the three different macroseismic intensities registered in the island. It should be noted that the estimation of damage depends not only on the load factor defining LS3, but also on LS1 and LS2, and the relative differences among them, as shown in Figure 8.10. Thus, the vulnerability curves constructed with the SAVVAS method may vary according to this. Four possible vulnerability curves are presented with varying difference between LS1 and LS3, which define the slope of the curves and can be related to the ductility of the structure. The mean difference between both limit states is 0.1g and that is why the vulnerability curve constructed using this difference is highlighted in red. The majority of the

points representing the damage observed lie within or very close to these curves, which confirms the good prediction capability of the SAVVAS method.

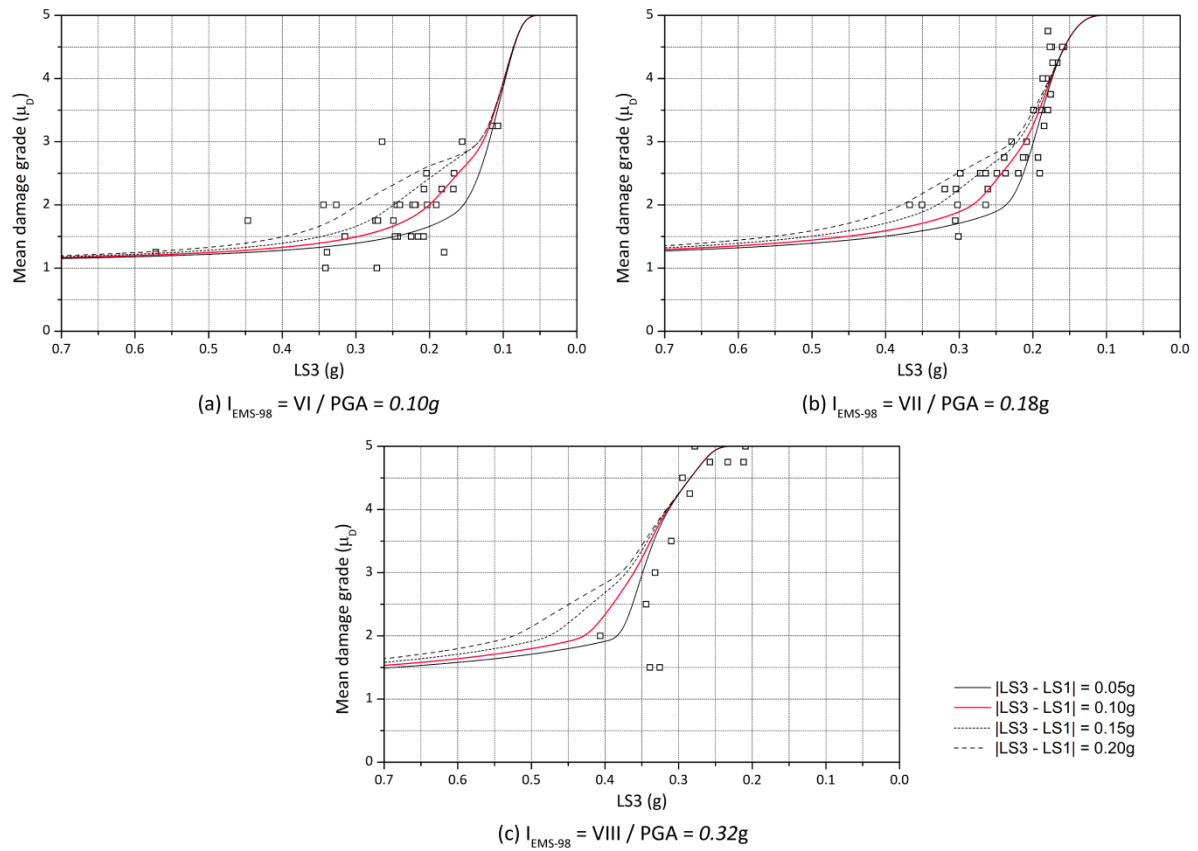


Figure 8.12: Observed damage versus mean damage grade estimated using the SAVVAS method for the construction of the vulnerability curves as a function of LS3, grouped by the different PGA

8.2.3.3 Comparison between both methods

Both seismic vulnerability assessment methods are evidently related since they are based on the same parameters and were developed using the same results from the numerical parametric study. The classes of the parameters are also common to both methods. Thus, a strong correlation between the vulnerability index (I_V) obtained with the SVIVA method and the load factors obtained with the SAVVAS method is observed. Figure 8.13 shows the correlation between the vulnerability index and the load factor corresponding to LS3 ($I_V - LS3$), as an example. However, it is noted that the SAVVAS method allows a more detailed seismic vulnerability assessment. The estimation of the numerical load factors based on numerical values adopted for the definition of some parameters enables to have a greater variation on the load factors when compared with the vulnerability index. For some buildings, the SAVVAS method provides very a different load factor defining LS3, while the vulnerability index remains unchangeable. This can be observed clearly in Figure 8.13, which shows buildings with $I_V = 39/LS3 = 0.21g$ and others with $I_V = 39/LS3 = 0.41g$. For the same vulnerability index, the predicted maximum capacity of the building doubles.

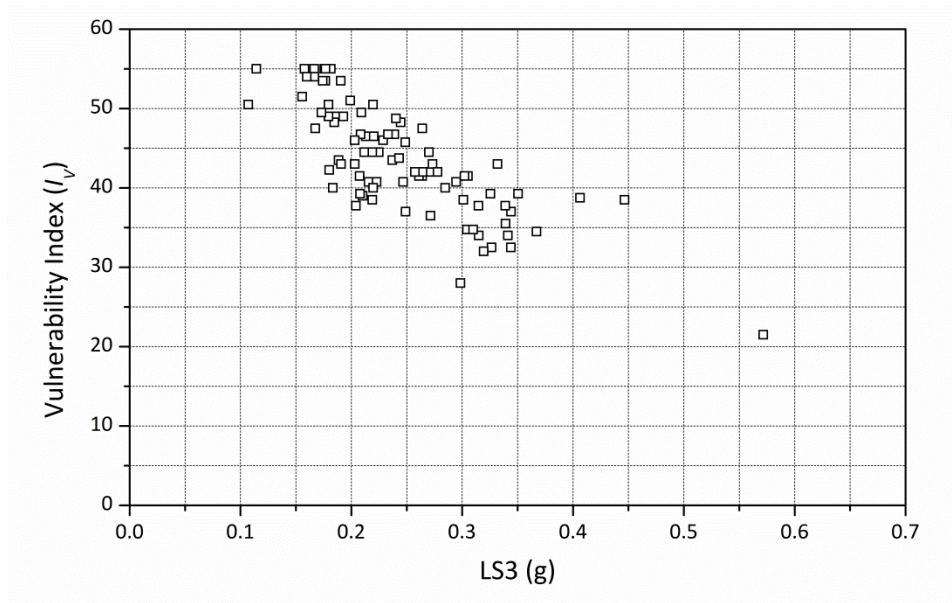


Figure 8.13: Correlation between vulnerability index (I_V) and $LS3(g)$

The more detailed seismic vulnerability assessment obtained from the SAVVAS method results in a commonly higher accuracy in the prediction of damage, as previously reported, showing also a significant reduction of the errors with respect to the damage observed (Figure 8.14). Besides, the requirement of numerical values does not generate an increment in the complexity of the application of the technique, since the parameters are defined by simple ratios that are usually also required for the definition of the classes for the vulnerability index method.

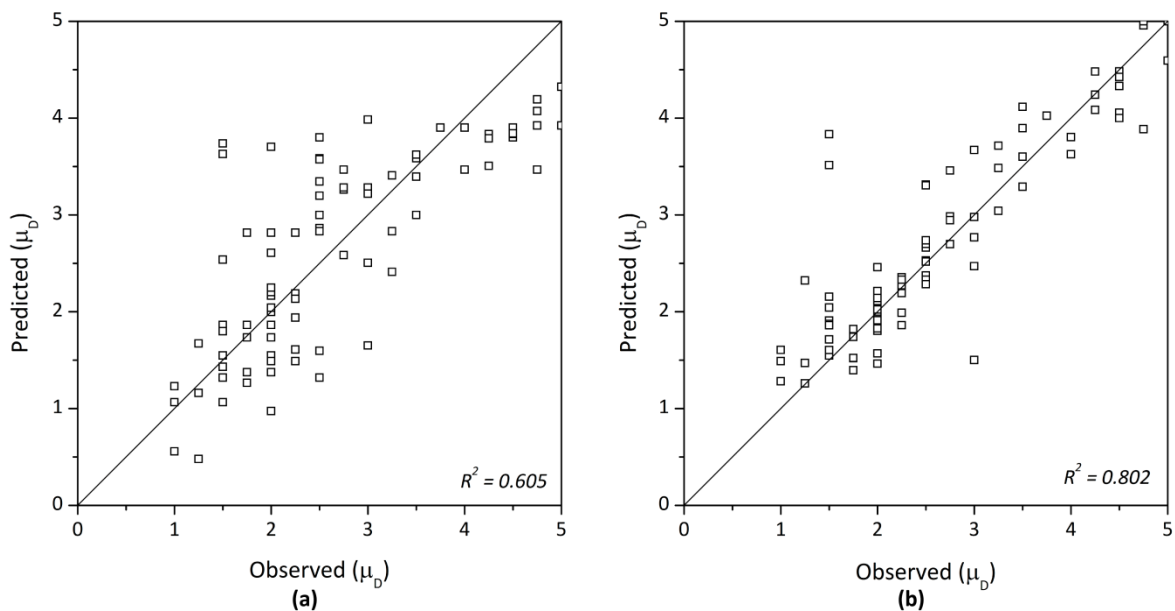


Figure 8.14: Comparison between predicted versus observed damage grades obtained with: (a) SVIVA vulnerability index method; and (b) SAVVAS method

Another main advantage of the SAVVAS method is the fact that it does not require the calibration of the vulnerability curves performed for the vulnerability index (SVIVA) method. The coefficients from the expression defined by the macroseismic method (Eq. 3.5) had to be redefined based on the observed damage in order to establish Eq. 8.1 and 8.2. As shown during the assessment performed (see Figure 8.6), the discrepancies can be quite high from using the original formulation and the calibrated ones. This is an important limitation when performing a seismic vulnerability assessment where an initial calibration is not possible. The SAVVAS method was in this sense applied blindly and provided good results from the beginning. In this method, just the factor of 1.25 defining the damage grade associated to the collapse of the building was calibrated, but its definition does not have such an influence on the results, since it only affects one level from the damage scale. In fact, the definition of the collapse is acknowledged as the main weakness of the SAVVAS method. The limit states LS1-LS3 are defined according to the numerical parametric study performed, based on loads. On the other hand, the limit state associated to the collapse (LS4) was initially defined in terms of displacement and cannot be determined using the SAVVAS method. Thus, the last damage grade has been here defined using this empirically devised factor of 1.25 that has been validated using this case study. Further research on the definition of the collapse for the SAVVAS method is recommended.

Another main difference among the SAVVAS and the SVIVA method concerns the seismic input. While the SVIVA method requires the definition of an earthquake scenario in terms of general macroseismic intensities, the SAVVAS method is carried out using values of PGA to define the seismic event. In the case study presented, the PGA scenario used is based on an already defined MMI scenario. However, this does not necessarily have to be always the case. A more detailed scenario can be defined based, for example, on the seismic microzonation of the area under study, which takes into account local effects. Therefore, the seismic vulnerability assessment can be carried out on the basis of more detailed seismic hazard scenario. Moreover, using the site response spectra and estimating the building natural frequency, the assessment can be carried out using specific accelerations adapted to each building and site. Further research is also recommended continuing with this research line.

In any case, besides these aspects related to the damage prediction potential of both methods, the biggest advantage of this type of seismic vulnerability assessment methods lies in their ability to detect possible deficiencies and strengths on the building stock under evaluation. Results are therefore particularly valuable in comparative terms, as they offer an expeditious and reliable evaluation on the buildings that are more vulnerable within a set, which is very useful to define and address structural retrofitting strategies at a regional or urban level.

Regarding this latter aspect, one advantage of the SAVVAS method is that, as previously shown in Chapter 6, this method allows evaluating the seismic load factors of the building in the four principal directions of the building. Therefore, when carrying out the seismic vulnerability

assessment, results did not only show a good correlation in terms of global damage, but were also able in many cases to identify the failure mode suffered by the building, as the most vulnerable direction identified matched the collapse observed at the earthquake. The evaluation of one building from the dataset is shown below as an example. Figure 8.15 shows the building plan and exterior and interior views depicting the damage suffered. Since the plans of the building were available, the quantitative parameters could be properly identified, leaving some uncertainty only for the classification of the qualitative parameters, namely the quality of the wall-to-wall connection (P4), type of material (P3), level of roof thrust (P6) and previous structural damage (P9). This case had sufficiently detailed data to fulfill the parameter survey easily, see Table 8.4. Besides the good correlation between the damage predicted and observed, the method is able to detect that the most vulnerable direction is +Y direction, which involves the gable wall that actually collapsed in reality, see Table 8.4. The building also suffered damage at the connection between the walls at the interior. The method also predicts that the building is prone to suffer structural damage for low values of acceleration ($LS1 = 0.14g$), matching the damage observed.



Figure 8.15: (a) Building plan and directions nomenclature; (b) main façade of the building; (c) collapsed gable wall; and (d) visible damage at the wall-to-wall connections from the interior of the building

Table 8.4: Parameter survey and results obtained per main resisting direction ($PGA = 0.18g$)

Direction	P1	P2	P3	P4	P5	P6	P7a	P7b	P8	P9	P10	LS1	LS2	LS3	Damage	
															Observed	Predicted
+X	4.79	12.99	4	4	3	1	0.03	0.02	1	1	0.29	0.14	0.19	0.22		
-X	4.79	12.99	4	4	3	1	0.30	0.02	1	1	0.29	0.14	0.21	0.24		
+Y	4.79	3.96	4	4	4	1	0.04	0.15	2	1	0.29	0.13	0.16	0.18	3.75	4.02
-Y	4.79	3.96	4	4	4	1	0.00	0.15	1	1	0.29	0.24	0.24	0.26		

8.3. Application of the methods in Vila Real de Santo António

Vila Real de Santo António (VRSA) is located in the southernmost region of Portugal, in the Algarve. This region was considerably affected by the 1755 earthquake and was practically abandoned at the time. However, the Marquis of Pombal considered that this region had a considerable economic potential and enacted an official recovery program during the 1760s and

1770s that included the setting-up of a completely new planned town (Correia 1997). The city was therefore erected *ex novo* at the end of the 18th Century, contemporary to the well-known reconstruction of Lisbon downtown, and followed similar urban, architectural and construction solutions, including the use of seismic resistant measures at an urban and architectural level. The main reason for planning an entire new city was the attempt to boost the Algarve local economy through industrial development (Mascarenhas 1996). It also aimed at controlling port transactions and being a display of political power, because of its strategic position, at the extreme South of the Algarve with the Spanish border (Correia 1997).

The new *Pombaline* city plan was formed by a rectangular area with one of the long sides placed along the Guadiana River, facing east, and consisted of a grid of seven by six urban blocks organized around a big central square, see Figure 8.16. The whole plan is characterized by its strong regularity, where all the blocks are approximately 53 m long and 22 m wide, with the exception of the central one, which is slightly longer, approximately 55 m. All the streets are 9 m wide. There are essentially four distinct architectural building types that defined a clear hierarchy at an urban level: (a) buildings in the riverfront, which have two main stories and a third attic floor; (b) buildings in the main square, which also have two main stories; (c) single story dwellings, characterized by their small scale and simplicity; and (d) single story factories and warehouses, which basically consists of a system of masonry arcades perpendicular to the façade walls and organized around a patio. Besides these strongly defined types, there are also some specific unique buildings, such as the Customs House, the church and the ‘towers’.



Figure 8.16: Original plan of VRSA city center and main building types (adapted from Rossa 2009)

In terms of construction and materials, a similar prefabrication process already applied for the Lisbon reconstruction plan, was also applied in the construction of VRSA. Ashlars for quins and opening frames arrived already cut and worked, ready to be placed, as well as the wooden components, such as doors, windows, beams and floorboards (Correia 1997). Load bearing exterior and party walls were built in stone masonry, and they are the main structural resisting elements

of all buildings. Timber was used for the roof rafters and trusses, floor beams and timber frame partition walls in upper floors. The roof was simply covered by wooden boards on which ceramic tiles were laid. Some ground floor rooms had vaulted ceilings supporting the first floor as a fire prevention measure, as in Lisbon (Mascarenhas 1996). Ground floor partition walls were usually built in solid brick masonry. The buildings were plastered with lime and sand and whitewashed. The most significant seismic resistant constructive solution applied was the inclusion of the timber frame partition *frontal* walls connecting the timber roof and the timber floor structures, analogous to the system developed for the reconstruction of Lisbon, known as *gaiola Pombalina*. Given the low height of the buildings in VRSA, the use of the whole seismic resistant construction system was not necessary but timber frame structural walls were used in those buildings with more than one floor. The seismic concern that emerged after the earthquake can be perceived in the generalized good quality and strength of the original buildings of VRSA (Oliveira 2009).

However, the great majority of the original buildings have nowadays either been substituted or are highly altered. Most of these alterations (addition of new floors, enlargement or addition of openings, substitution of floors and roofs, etc.) are a normal consequence of changes in the use of the buildings and the new needs of the users, but the deep mischaracterization of the built-up environment also reveals a loss of seismic awareness, as the initially adopted effective seismic resistant measures were abandoned. A research question arises whether or not and to what extent these changes on the original constructions have compromised the seismic resistance of the buildings. That is the main reason why VRSA was selected as a case study.

8.3.1. Building characterization

The transformation process that took place in the 1773 *Pombaline* core of VRSA motivated important research work promoted by the city hall (SGU 2008). The work consisted of an analysis carried out on a building by building basis intended to identify the remaining original *Pombaline* buildings and their morphological relationship with respect to the original design. According to Gonçalves (2005), results indicated that only 5% of the buildings still preserve unaltered original characteristics in terms of elevation and 8% in terms of volume. Moreover, 69% of the current buildings have no relationship at all with the original form in terms of elevation and 45% in terms of volume. The survey showed that even though stone masonry still is the construction system of the majority of the buildings, less than 20% of the buildings are the original *Pombaline* buildings constructed in the 18th century. Around 54% of the built-up fabric was constructed during the 20th century. These numbers clearly illustrate the significant alterations done in the historical built-up fabric and the degradation of the ideal originally designed plan. Even the best preserved buildings still show important alterations in relation to their original structure.

Generally, this transformation process has been characterized by a massive occupation of the blocks, leading to an extreme densification of the urban fabric, since patios were continuously

occupied by additional constructions. Two-story buildings located in the river front and the main square, together with the most significant buildings, present few alterations and preserve better their original design. On the contrary, the original ordinary dwellings have been more vulnerable to alterations. These single story buildings have been systematically exposed to demolitions, substitutions and large modifications, such as the addition of new floors. This is in fact one of the most typical alterations that can be observed and resulted in a significant increase in the average height of the buildings of the city. Modifications also commonly consisted of opening new windows and doors and the enlargement of the original openings. Other common important alteration reported by the previously commented study has been the substitution of the original roof typology, usually consisting of the replacement of the original hipped roofs by flat ones (SGU 2008). Modifications of the construction system and structural elements, such as floors, can also be expected in most of the constructions. Another systematic alteration that the buildings of VRSA have undergone is the elimination of the original *frontal* walls, revealing again a loss of seismic awareness by ignoring a distinctly seismic resistant feature of the original buildings. When buildings are reconstructed or rehabilitated, these *frontal* walls are obliterated or just kept as a vestige, ignoring the actual structural function as a seismic resistant element, which may have contributed to increase the seismic vulnerability of the buildings (Ortega et al. 2016a). Figure 8.17 shows examples of the deep alterations on the built-up environment that took place in the last century in VRSA and a comparison between the original and the current urban plan.

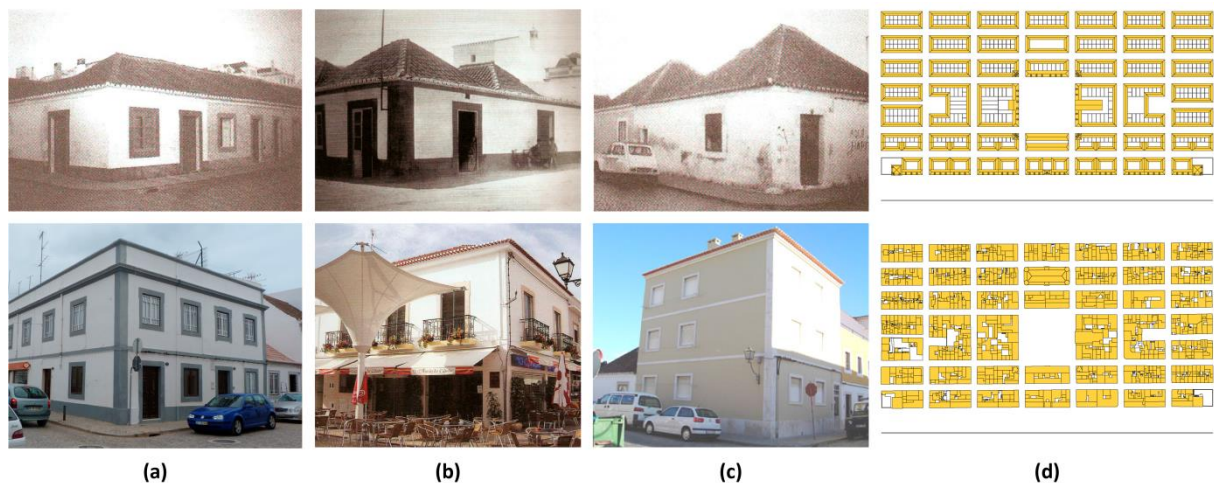


Figure 8.17: (a-c) Typical alterations occurred throughout the 20th century: original versus current condition (adapted from Gonçalves 2009); and (d) comparison between the original and current plan of VRSA city center

The data collected by SGU (2008) allowed identifying those buildings in the city center whose main construction system still consisted on stone masonry walls and timber floor and roof structures. From a total of 490 buildings located *Pombaline* core of VRSA, 284 stone masonry buildings were selected to perform the seismic vulnerability assessment. The remaining buildings either present R/C structures or mixed construction systems made them not applicable for the two

seismic vulnerability assessment methods for vernacular architecture developed. Among these 284 buildings, 7 buildings were identified as original unaltered buildings and 77 were constructed in the 18th century, but show significant structural alterations. The remaining 200 buildings are substitutions of the original buildings and were constructed during the 19th and 20th century. Figure 8.18 shows examples of the three types of buildings that were evaluated, classified according to their date of construction and altered condition. Figure 8.19 summarizes this data and shows the urban plan, identifying the buildings that were selected for the seismic vulnerability assessment.

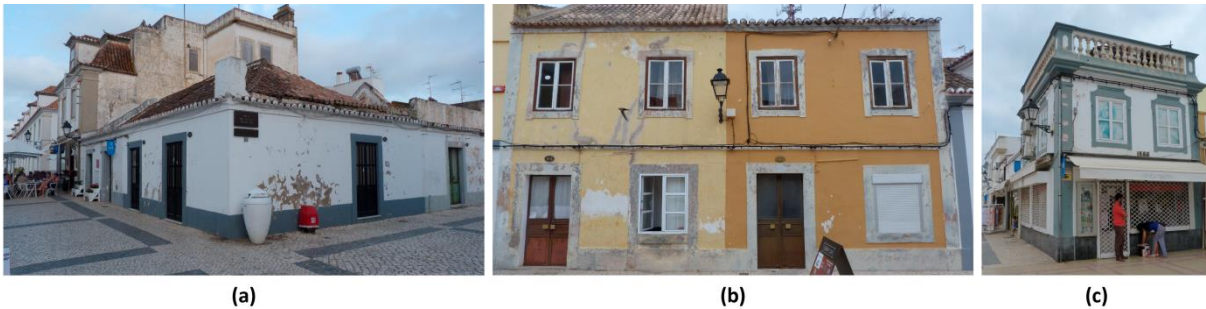


Figure 8.18: Examples of typical traditional stone masonry buildings in VRSA selected for the seismic vulnerability assessment: (a) original unaltered building; (b) original building with alterations (additional floors); and (c) non-original building constructed in the 19th century



Figure 8.19: Evaluated buildings in VRSA city center classified according to their date of construction and altered condition

The data available included urban plans and detailed reports on the construction characteristics and state of conservation of most of the buildings, including interior and exterior photographs. Additionally, a field visit was carried out, which allowed gathering more information from these buildings. Most of the buildings could only be inspected from the exterior, but some specific buildings could be surveyed more in detail, obtaining information of the

different structural elements (roof, floors, masonry walls, partition walls, etc.). As an example, the *Alfândega* or Customs House was thoroughly studied through historical survey, visual inspection and experimental in-situ dynamic identification, which allowed calibrating numerical models and estimate material properties (Ortega et al. 2016b). Because of the particularities of the construction process of VRSA, a great homogeneity in the building characteristics can be assumed, particularly for those buildings presenting original characteristics. Therefore, the data gathered from the buildings that were inspected in detail could be extrapolated to those buildings for which more limited information was available. Figure 8.20 shows typical examples of frequent structural elements that were observed throughout the buildings inspected.

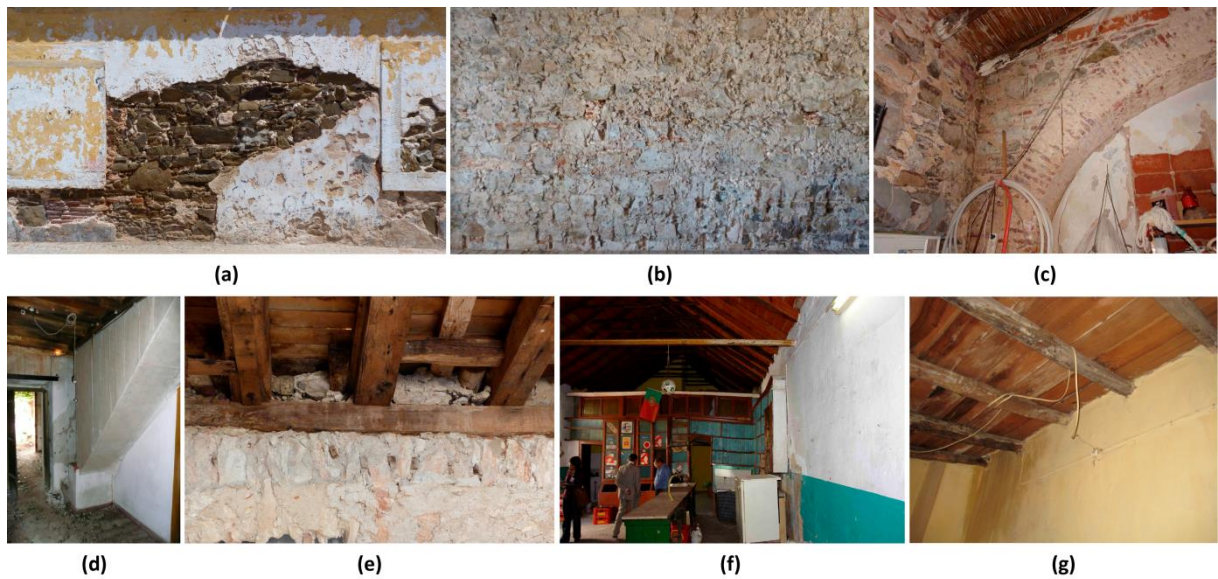


Figure 8.20: Typical construction characteristics of VRSA buildings: (a-b) stone masonry morphology; (c) timber roof connection with stone masonry walls (SGU 2008) (d) timber floor construction (SGU 2008); (e) timber floor connection with masonry walls; (f-g) roof timber construction and connection with masonry walls (SGU 2008)

8.3.2. Seismic vulnerability assessment

Sufficient amount of information was collected for the building characterization in order to perform the seismic vulnerability assessment of VRSA historical center. Since VRSA is located in the Algarve region, which is considered as one of the most seismic prone regions in Portugal, it was deemed as an appropriate case study for the application of the proposed seismic vulnerability assessment methods. Firstly, the assessment carried out using the vulnerability index (SVIVA) method with the new formulation proposed is presented. Then, the same assessment using the SAVVAS method is discussed, in order to compare the results and extract conclusions on the applicability of each method. The information collected included a wide set of data on the historical condition of the city, including detailed plans and construction details of the original buildings. This information could be used to perform a comparative analysis between the historical and current condition in terms of seismic vulnerability. In addition, several retrofitting

strategies based on traditional solutions (Chapter 2 and 7) are also studied and the level of reduction of the seismic vulnerability achieved with each of them is presented and discussed.

8.3.2.1 Vulnerability index (SVIVA) method

The SVIVA method was applied on the 284 buildings. A mean value of the vulnerability index (I_V) of 29.87 was obtained with a STD (σ_{I_V}) of 5.09 and a CoV of 17%. The minimum and maximum values of I_V are 21.75 and 49.75, respectively. The vulnerability index distribution obtained is presented in Figure 8.21a. The graph shows that less than 3% of the evaluated buildings present a vulnerability index value over 40 and more than half of the buildings present a value lower than 30, which can be considered low. The generalized small scale of the buildings in the city center contributes to the low values of vulnerability index. This can be more easily explained by looking at the class distribution for each parameter shown in Figure 8.21b.

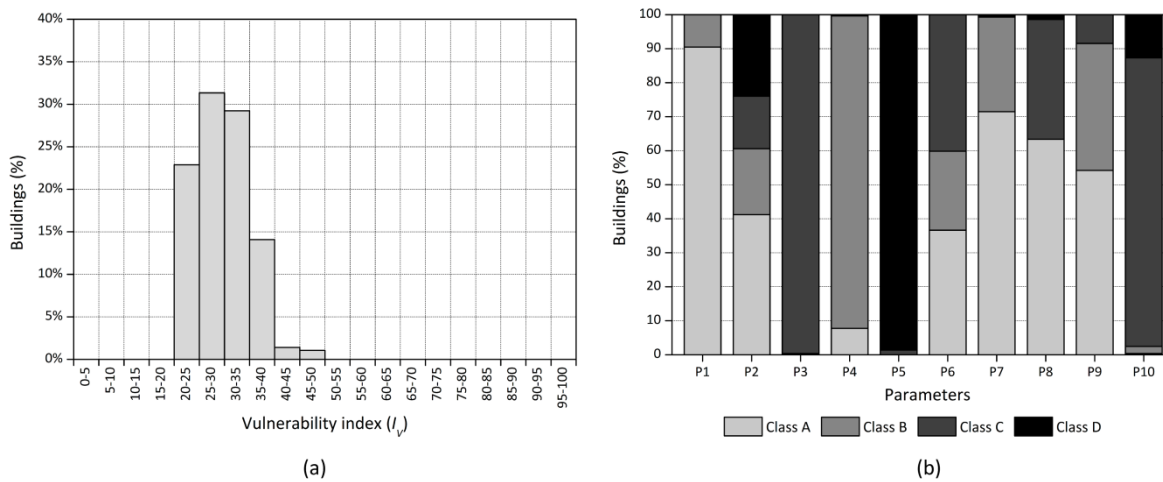


Figure 8.21: (a) Vulnerability index (I_V) distribution; and (b) parameter class distribution

The structural typology of most of the buildings consists of thick load bearing walls (class A for P1) constructed with irregular stone masonry walls shown in Figure 8.20 (class C for P3) and timber horizontal diaphragms that provide poor or no proper connection among the resisting walls (class D for P5). It should be noted that the class for the masonry was assigned based on the previously mentioned experimental investigation (Ortega et al. 2016), which was performed on a building that present the original walls. Thus, the type of material used for buildings constructed at a later stage (19th and 20th centuries) might not be the same. However, the same class was assumed for all buildings in the absence of more detailed information. The same criterion applies for other constructive parameters such as P1 and P5. Proper connection among orthogonal walls was considered for most of the buildings (class B for P4), since they were originally workmanlike constructed. Class A was considered for those buildings with a greater symbolic value, such as the riverfront buildings and the ‘towers’, because of the presence quoins. The roof type was quite variable since it is one of the structural elements that most often suffered alterations. Many

buildings present a flat roof (class A for P6), while the original typology is shown in Figure 8.20 and consists of timber rafters with no particular detailing at the connection with the walls that prevents the thrust. Class B or C was usually considered for P6 when pitched roofs were observed, depending on the inclination. In terms of geometry, the buildings are usually very regular with an almost square configuration (class C for P10). However, the extremely regular subdivision observed in the historical configuration has been lost. Many party walls have been demolished in order to join several buildings, and new buildings were constructed in the place previously occupied by two or more original buildings. As a result, some of the façade walls present large spans and, consequently parameter P2 shows a high variability. It is noted that the interior condition of these building could not be inspected in many cases and had to be assumed from the exterior. The buildings present few openings (class A or B for P7) and the great majority has one or two floors (class A or C for P8). The previous structural damage observed is also highly variable. There are several buildings that were considered as class B and C for P9, due to a clear lack of maintenance and abandonment. Some of the buildings inspected showed also big cracks that, according to the reports from SGU (2008), related with differential settlement.

Figure 8.22 shows the seismic vulnerability index distribution in VRSA historical center. The distribution was mapped using ArcGIS Pro (Esri 2017), a GIS application that allows mapping the different damage and loss scenarios calculated from the seismic vulnerability assessment, by associating information and structural characteristics to each building. These tools are very powerful for the management of data, since they can be easily updated, and allows for a rapid visualization, selection and search of buildings within a given study area (Vicente 2011). The resulting seismic vulnerability map shown in Figure 8.22 can be particularly useful for the detection of the most vulnerable buildings that should be recommended for a more detailed assessment for eventually defining the need of retrofitting or strengthening.

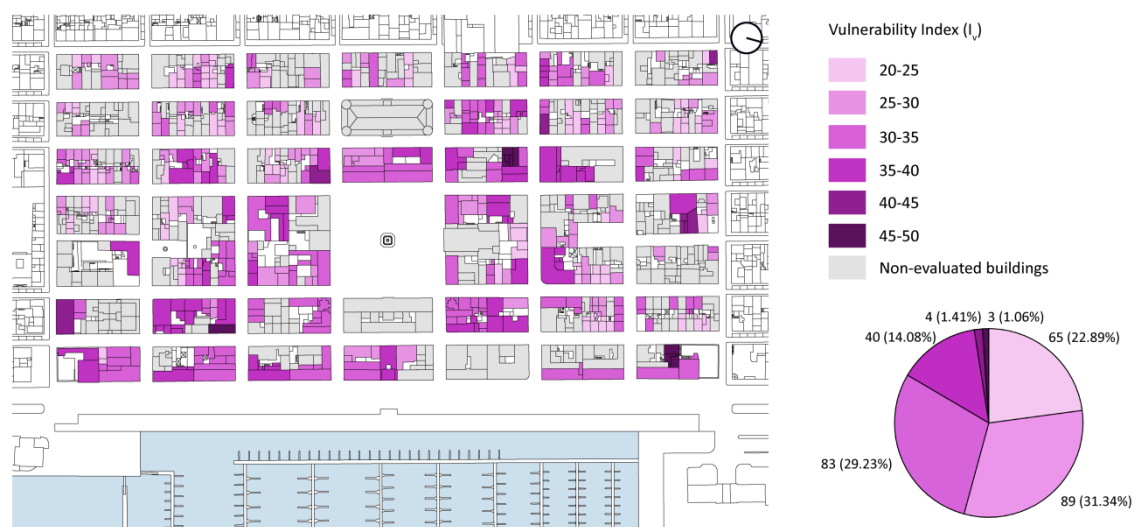


Figure 8.22: Vulnerability index distribution (I_v) in the city center of VRSA

The analytical expressions (Eq. 8.1 and 8.2) were applied to estimate the mean damage grade (μ_D) for different macroseismic intensities. As stated by Ferreira (2017), the results obtained with the seismic vulnerability assessment should be interpreted statistically. That is why vulnerability curves can be constructed for the mean value and for different upper and lower bounds of the vulnerability index defined according to the STD: (a) $\bar{I}_V - 2\sigma_{I_V}$; (b) $\bar{I}_V - \sigma_{I_V}$; (c) \bar{I}_V ; (d) $\bar{I}_V + \sigma_{I_V}$; and (e) $\bar{I}_V + 2\sigma_{I_V}$, see Figure 8.23. The GIS tool can be then used to present damage scenarios. Figure 8.24 shows the results for different earthquake intensities (I_{EMS-98}) from VII to IX. Damage mapping using GIS is an efficient tool for urban management and can help in defining protection strategies, since it allows a quick identification of the most vulnerable urban areas and buildings for which a more detailed evaluation is recommended. The maps show that few damage is expected for an earthquake of $I_{EMS-98} = VII$, for which only a reduced number of buildings would reach a state of severe damage ($\mu_D > 3$) and none shows values of damage close to potential collapse ($\mu_D > 4$). This is in agreement with the general low values of I_V obtained. As it could be expected, the risk highly increases for an earthquake scenario of $I_{EMS-98} = IX$, for which all buildings are expected to either show a state of severe damage or be close to potential collapse.

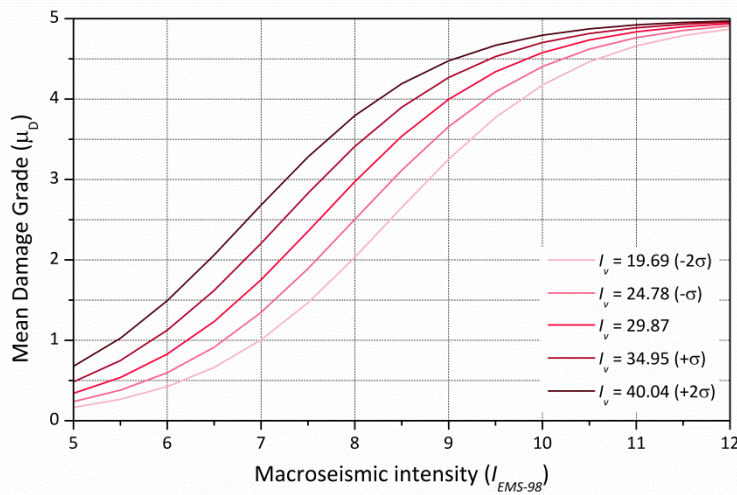


Figure 8.23: Vulnerability curves for the building stock of VRSA city center

As a final step, damage probability can be typically expressed using fragility curves. They define the probability ($P[D_k]$) that a specific building typology with a defined I_V exceeds a fixed damage grade D_k ($k \in [0,5]$), as a function of the earthquake macroseismic intensity. The probability p_k of having each damage grade can be evaluated assuming different types of damage distribution. The macroseismic method (Lagomarsino and Giovinazzi 2006) proposed to evaluate p_k for a certain mean damage grade (μ_D) according to the probability mass function (PMF) of the binomial distribution adopted to complete the physical damage grade distribution:

$$\text{PMF: } p_k = \frac{5!}{k!(5-k)!} \left(\frac{\mu_D}{5}\right)^k \left(1 - \frac{\mu_D}{5}\right)^{5-k} \quad (8.3)$$

where ! indicates the factorial operator. Since fragility curves express the probability ($P[D_k]$) that the expected damage of a structure exceeds a fixed damage grade during the ground shake, they can be obtained by calculating the cumulative probability:

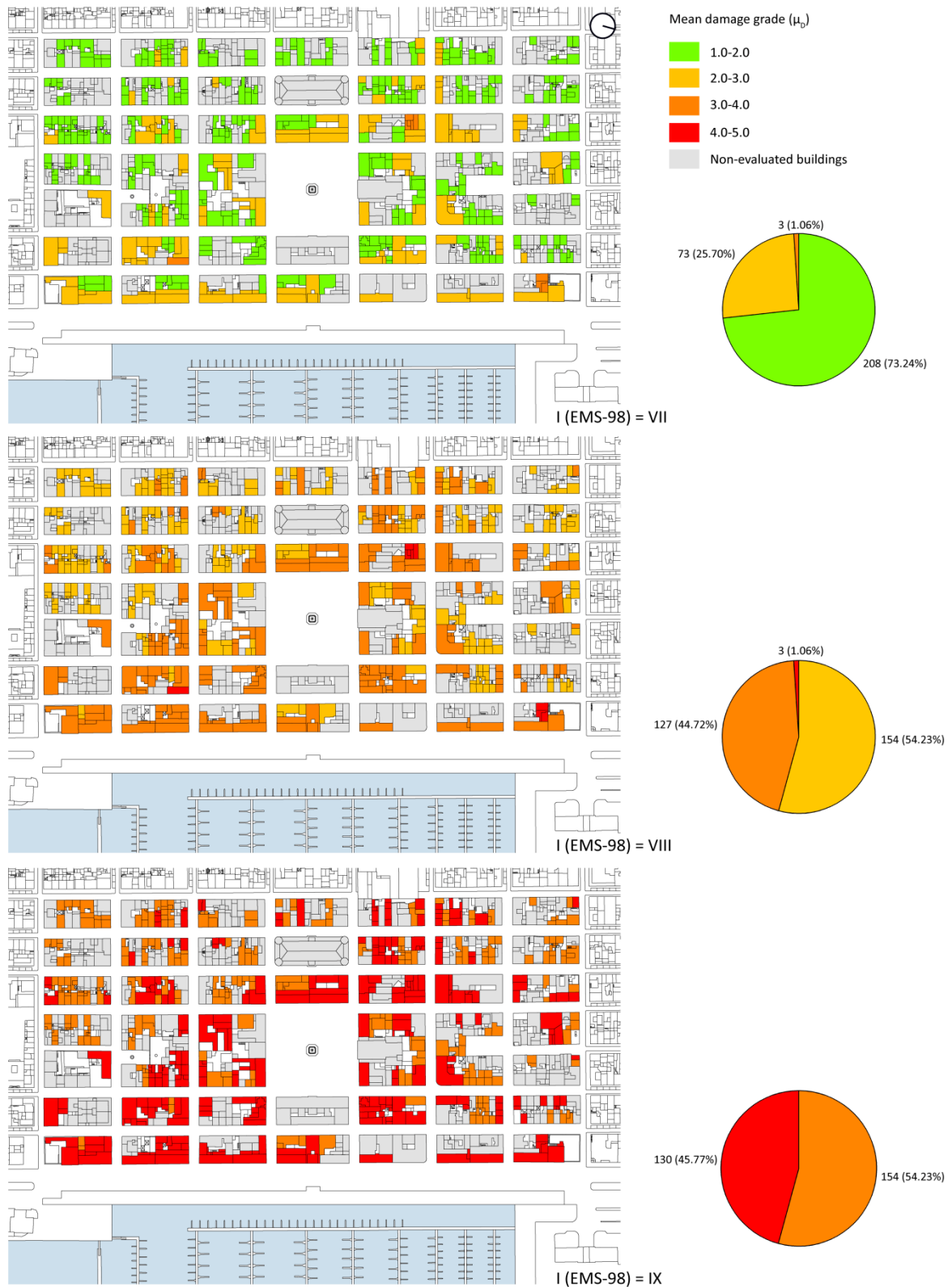


Figure 8.24: Damage scenarios for different macroseismic intensities (I_{EMS-98}): VII-IX

$$P[D_k] = \sum_{j=k}^5 p_j \quad (8.4)$$

where p_j is the probability associated to each damage grade ($j \in [0,5]$). The binomial distribution was selected after the good results obtained in the estimation of the damage observed during the 1980 Irpinia earthquake (Braga et al. 1982). Other authors, such as Vicente (2008), have instead assumed a beta distribution for the damage because of the high dispersion of the binomial distribution, which may lead to overestimate the number of buildings suffering high levels of damage for low values of μ_D (Giovinazzi 2005). The probability density function (PDF) of a beta distribution is expressed as:

$$\text{PDF: } p_\beta(x) = \frac{\Gamma(t)}{\Gamma(r)\Gamma(t-r)} \frac{(x-a)^{r-1}(b-x)^{t-r-1}}{(b-a)^{t-1}} \quad a \leq x \leq b \quad (8.5)$$

where t and r are the parameters defining the shape of the distribution, a and b are the parameters defining the range of the distribution and Γ is the gamma function. The values of a and b can be assumed as 0 and 5, respectively, representing the lower and upper bounds of the damage scale ($k \in [0,5]$). Parameters t and r characterize the scatter around the mean value, which can be reduced when increasing the value of t (Giovinazzi 2005). Parameter r can be obtained as a function of t and the mean damage grade (μ_D). Giovinazzi and Lagomarsino (2005) provides different values of t according to the building typology and uncertainty in the hazard assessment. Vicente et al. (2011) justifies the adoption of a unique value of $t = 8$ and the following relationship with parameter r :

$$r = t \times \frac{\mu_D}{5} \quad (8.6)$$

These values completely define the beta function. Therefore, the physical damage discrete distribution can be obtained evaluating the probability p_k associated with each damage grade D_k ($k \in [0,5]$), which can be defined as:

$$p_0 = \int_0^{0.5} \frac{\Gamma(t)}{\Gamma(r)\Gamma(t-r)} \frac{x^{r-1}(5-x)^{t-r-1}}{5^{t-1}} dx \quad (8.7)$$

$$p_k = \int_{k-0.5}^{k+0.5} \frac{\Gamma(t)}{\Gamma(r)\Gamma(t-r)} \frac{x^{r-1}(5-x)^{t-r-1}}{5^{t-1}} dx \quad 0 < k < 5 \quad (8.8)$$

$$p_5 = \int_{4.5}^5 \frac{\Gamma(t)}{\Gamma(r)\Gamma(t-r)} \frac{x^{r-1}(5-x)^{t-r-1}}{5^{t-1}} dx \quad (8.9)$$

In order to construct the fragility curves, the expression shown in Eq. 8.4 can be applied to obtain the probability ($P[D_k]$) that the expected damage of a structure exceeds a fixed damage

grade during the ground shake. Figure 8.25a presents the fragility curves constructed for the mean value of the vulnerability index ($I_V = 29.87$), both assuming a beta distribution and a binomial distribution for the damage. The reduction of the scatter around the mean is illustrated by the steeper slope of the curves assuming a beta distribution. However, given the overall similarity among the results obtained using both distributions and, for the sake of an easier implementation, the binomial distribution is adopted. It is noted that the binomial distribution has been widely employed for the development of fragility curves and, according to Giovinazzi (2005), it is almost equivalent to a beta distribution with $t = 7$. Figure 8.25b presents the fragility curves corresponding to a value of the vulnerability index of $\bar{I}_V + 2\sigma_{I_V} = 40.04$ with binomial distribution, which would represent the scenario with the greatest vulnerability.

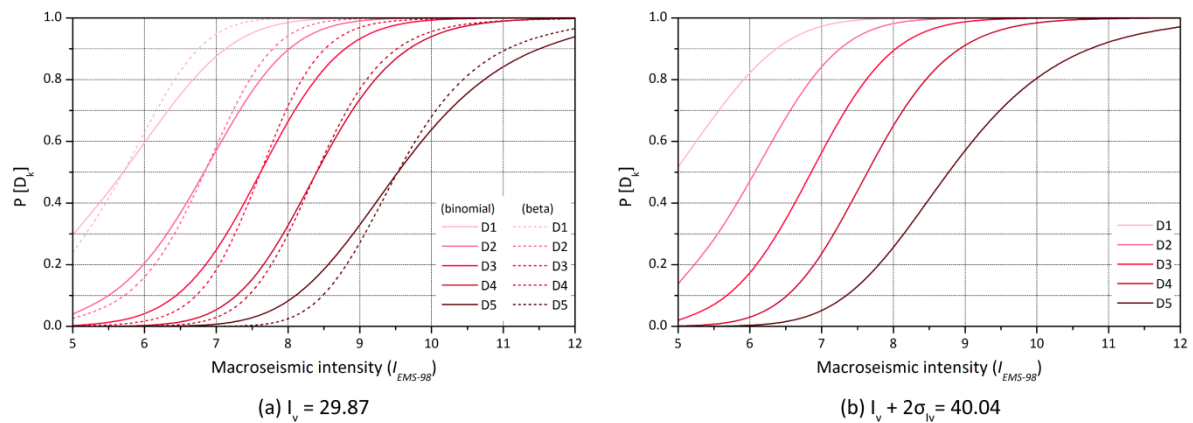


Figure 8.25: Fragility curves of the building stock in VRSA for: (a) $\bar{I}_V = 29.87$; and (b) $\bar{I}_V + 2\sigma_{I_V} = 40.04$

8.3.2.2 SAVVAS method

The SAVVAS method was also applied to the same building stock and the minimum load factors associated to the three main limit states (LS1, LS2 and LS3) were calculated for each building. The load factor distributions for the 284 buildings under analysis are presented in Figure 8.26. The mean values of the load factors obtained are 0.15g, 0.35g and 0.42g for LS1, LS2 and LS3 respectively, with a STD (σ_{LS}) of 0.14g, 0.13g and 0.14g, which result in CoV of 93%, 36% and 33%. The high variations obtained can be clearly observed in the widespread distribution shown in Figure 8.26. This illustrates how the SAVVAS method makes a greater distinction between the seismic performances of different buildings that may present similar vulnerability indexes. In order to have a primary idea of the vulnerability of the built-up fabric, the values obtained can be compared with the seismic demand from the code. For Vila Real de Santo António, the value of reference peak ground acceleration (PGA) is 0.17g (NP EN1998-1 2010). Only five buildings from the set present a load factor defining LS3 below 0.17g, i.e. their maximum capacity will be exceeded for an earthquake of the characteristics defined by the code. This fact also shows a generalized low vulnerability of the buildings in the historical city center, as previously discussed with the vulnerability index method. Most of the buildings are prone to suffer slight structural

damage, since the load factor defining LS1 for 60% of the buildings evaluated is below this limit of 0.17g. The great amount of buildings obtained with a very low load factor defining LS1 is due to the poor state of conservation of many buildings, which already show slight structural damage.

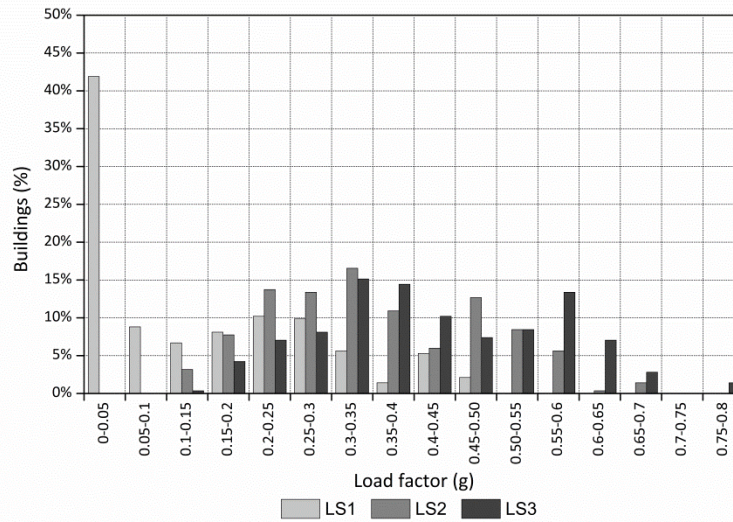


Figure 8.26: Load factor distributions for the three limit states: LS1, LS2 and LS3

In order to obtain a better understanding of the characteristics of the buildings evaluated, Table 8.5 shows the statistics from the values defining each parameter and the computed global load factors defining the three limit states. Given the low variations for parameters P1, P3 and P5, the table confirms that the main building structural typology evaluated is similar, consisting of thick load bearing irregular masonry walls coupled with flexible timber horizontal diaphragms. Low values for P2 and P8 confirm that the VRSA city center mainly comprises one-floor buildings of reduced scale. Buildings with two and three floors typically show a high amount of wall openings, in contrast with the few openings of single story buildings, reflecting high values of CoV for P7a and P7b. Results also show a high variability regarding the previous structural damage, which is the main responsible also for the extreme variability for LS1 and the reason why there is a significant amount of buildings showing initial slight structural damage (Figure 8.26).

Figure 8.27 shows the overall distribution of LS3 of the buildings within VRSA center, which is useful for the quick detection of the most vulnerable buildings, for example, those buildings with a load factor corresponding to LS3 below the seismic demand established by the code (0.17g). This map is the equivalent to the seismic vulnerability map shown in Figure 8.22. Thus, it is intended to detect the most vulnerable buildings that are recommended for a more detailed assessment in order to confirm the selection of the values defining each parameter and eventually decide on the need of retrofitting.

In order to estimate the EMS-98 mean damage grade (μ_D) based on the calculated load factors for different seismic inputs (in terms of PGA), the correspondence defined and presented in Figure 8.10 is applied. Following the same statistical approach used for the seismic vulnerability

index method, vulnerability curves can be constructed for the mean values of LS1, LS2 and LS3 obtained and for different upper and lower bounds defined according to the STD: (a) $\overline{LS} - 2\sigma_{LS}$; (b) $\overline{LS} - \sigma_{LS}$; (c) \overline{LS} ; (d) $\overline{LS} + \sigma_{LS}$; and (e) $\overline{LS} + 2\sigma_{LS}$, see Figure 8.28. It is noted that the scale starts at 0 because this method does not detect non-structural damage and thus grade 0 and 1 are the same and both represent that the buildings show no structural damage. The high variability previously observed results in great differences between the upper and the lower vulnerability curves, which present completely different behavior. While the most vulnerable scenario using $\overline{LS} - 2\sigma_{LS}$ predicts a mean damage grade of 5 for an earthquake with $PGA = 0.25g$, the scenario using $\overline{LS} + 2\sigma_{LS}$ predicts that μ_D will be below 2, which means that buildings will not even reach structural damage. This illustrates the difficulty to explain the seismic behavior of the building stock of VRSA center based solely on the mean values. Buildings are expected to show a very wide range of seismic performances and the SAVVAS method is aimed at detecting these differences.

Table 8.5: Statistics from the parametric survey and the estimated load factors defining each limit state

Variables	Units	Minimum	Maximum	Mean	Median	Mode	STD	CoV	
Parameters	P1	λ	4.55	6.82	5.15	5.30	5.30	0.50	9.71%
	P2	m	2.25	21.2	6.78	5.50	4.50	3.17	46.67%
	P3	Class	2	3	2.99	3	3	0.08	2.79%
	P4	Class	1	3	1.90	2	2	0.32	16.97%
	P5	Class	3	4	3.88	4	4	0.32	8.27%
	P6	Class	1	3	1.83	2	1	0.89	48.54%
	P7a	$P7a$	0	0.51	0.18	0.20	0	0.09	53.14%
	P7b	$P7b$	0	0.57	0.05	0.03	0	0.07	123.60%
	P8	N	1	3	1.37	1	1	0.50	36.47%
	P9	Class	1	3	1.59	1	0.66	0.66	41.28%
P10	γ_i	0.28	0.69	0.48	0.50	0.50	0.05	9.81%	
Load factor	LS1	g	0.00	0.50	0.15	0.09	0.03	0.14	93.21%
	LS2	g	0.10	0.69	0.35	0.34	0.27	0.13	35.88%
	LS3	g	0.13	0.79	0.42	0.40	0.33	0.14	33.03%



Figure 8.27: LS3 distribution in the city center of VRSA

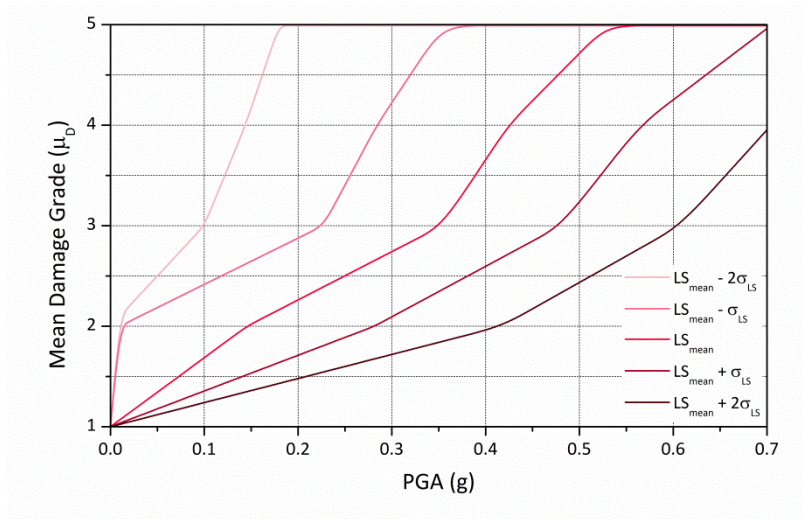


Figure 8.28: Vulnerability curves for the building stock of VRSA city center resulting from the SAVVAS method

The GIS tool is also used to present the damage scenarios. Figure 8.29 shows the results for three different earthquake inputs: (a) $PGA = 0.15g$; (b) $PGA = 0.25g$; and (c) $PGA = 0.35g$. These values were selected so that they could be comparable with the three earthquake inputs used in the previous assessment for the SVIVA method, which used $I_{EMS-98} = VII, VIII$ and IX . As previously discussed, the notable scatter observed in the literature for the transformation of macroseismic intensities into PGA is acknowledged (Guagentini and Petrini 1989; Margottini et al. 1992; Wald et al. 1999). That is why rounded values were selected that could be associated to the macroseismic intensities. In comparison with the results obtained using the vulnerability index method, a more scattered distribution of the damage is noted. Figure 8.24 showed that the level of damage increases almost homogeneously when increasing the seismic intensity. For example, the amount of buildings presenting damage (μ_D) between 2 and 3 for an earthquake of $I_{EMS-98} = VIII$ is the exactly same amount of buildings that present damage (μ_D) between 3 and 4 for an earthquake of $I_{EMS-98} = IX$. The SAVVAS method is able to individualize more the seismic behavior of each building and the maps show that there are several buildings presenting no structural damage even for an earthquake with $PGA = 0.35g$.

However, it should be mentioned that results obtained with the application of the SAVVAS method are overall in agreement with the main conclusions withdrawn after the application of the vulnerability index method concerning the general low vulnerability detected. Few damage is expected for an earthquake with $PGA = 0.15g$, for which only a reduced number of buildings would reach a state of severe damage ($\mu_D > 3$) and only one shows values of damage close to potential collapse ($\mu_D > 4$). As it could be expected, the risk highly increases for an earthquake scenario with $PGA = 0.35g$, for which the majority of the buildings are expected to either show a state of severe damage or be close to potential collapse.

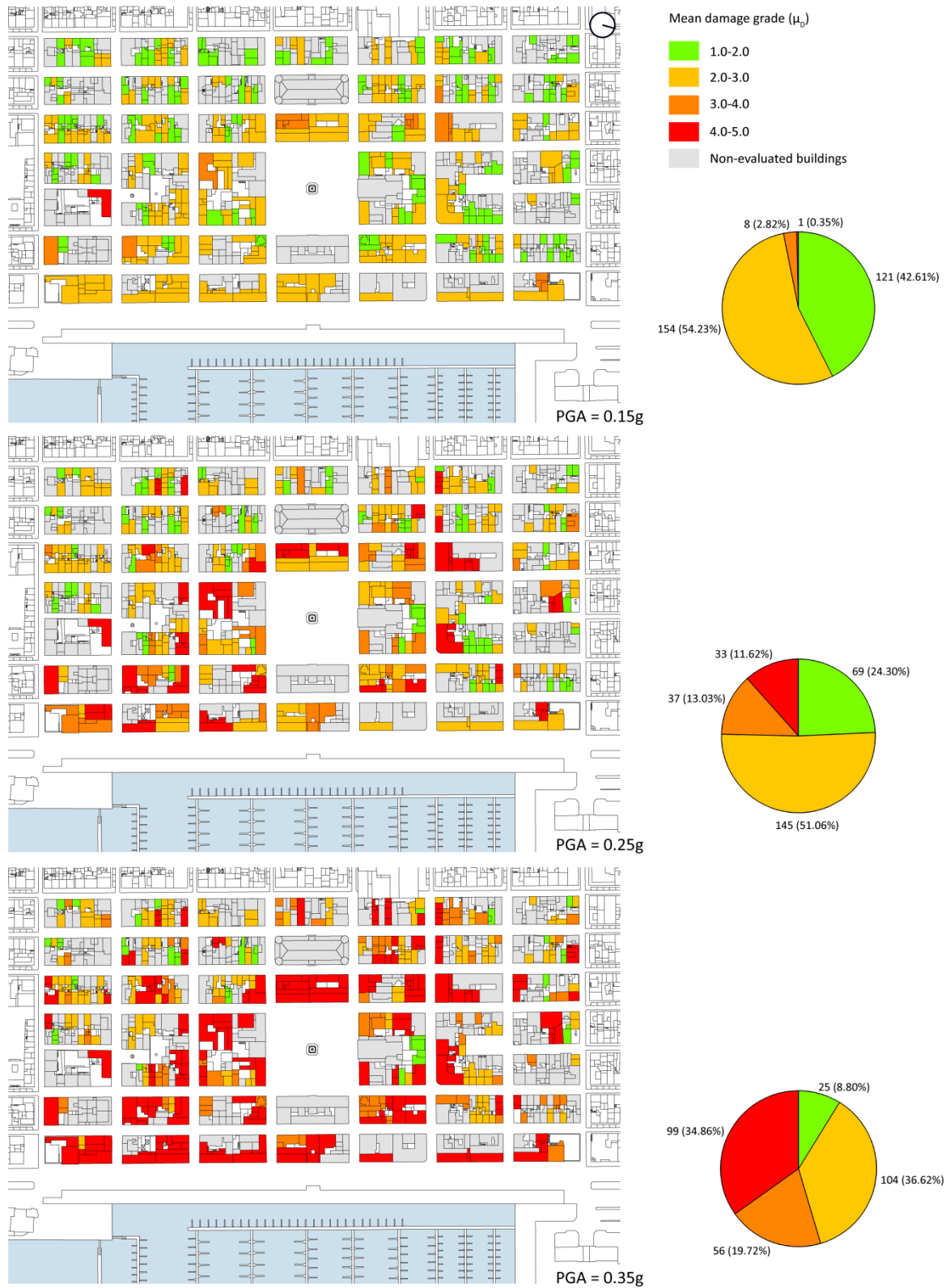


Figure 8.29: Damage scenarios for different seismic input in terms of PGA: (a) 0.15g; (b) 0.25g; and (c) 0.35g

Fragility curves can be also constructed with the results obtained with the SAVVAS method in order to express the damage probability. Figure 8.30 thus shows the probability ($P[D_k]$) of exceeding a fixed damage grade D_k ($k \in [1,5]$), as a function of the PGA (g) for: (a) mean values of

LS1, LS2 and LS3 (\overline{LS}); and (b) $\overline{LS} - \sigma_{LS}$, which represents a scenario with higher vulnerability. The probability mass function (PMF) of the binomial distribution shown in Eq. 8.3 is adopted to complete the physical damage grade distribution. Given the high variability in the results previously observed, the great difference among both scenarios is evident, showing that a fragility curve constructed using mean values may not be representative enough of the overall vulnerability of the buildings in VRSA city center.

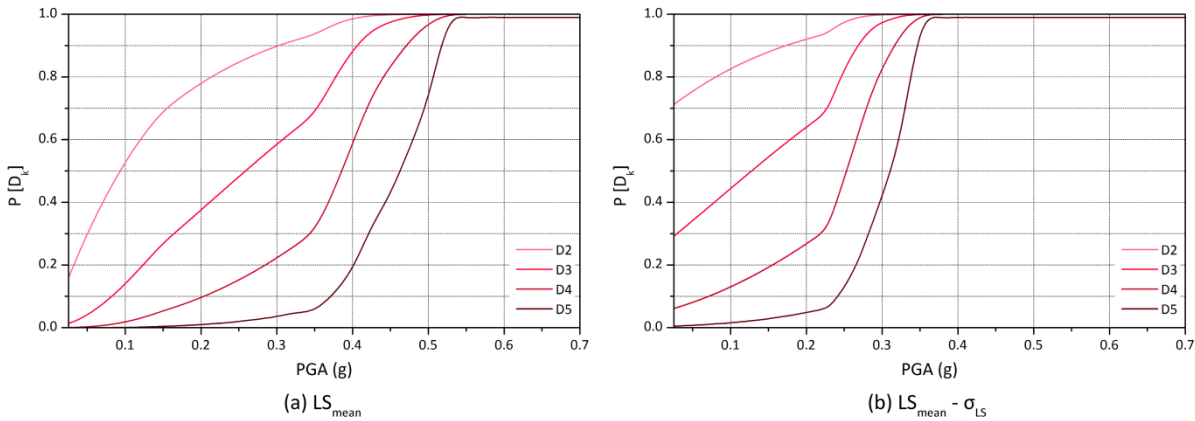


Figure 8.30: Fragility curves of the building stock in VRSA for: (a) \overline{LS} ; and (b) $\overline{LS} - \sigma_{LS}$

Due to this reason, another set of fragility curves were constructed aiming at obtaining a more accurate representation of the seismic response of the building stock in VRSA city center. Instead of adopting the statistical approach using mean values and upper and lower bounds and adopting a probability distribution to complete the physical damage grade distribution, the new curves are built using directly the results of μ_D obtained from all buildings. Firstly, Figure 8.31a shows the discrete mean damage grade distribution in terms of percentage of buildings (p_k) that are expected to reach each damage grade (D_k), as a function of the seismic input in terms of PGA. The criterion for belonging to each damage grade is the same defined in Eq. 8.7 to Eq. 8.9. Secondly, Figure 8.31b shows the cumulative distribution and, therefore, the percentage of buildings ($P[D_k]$) that are expected to exceed each damage grade (D_k), as a function of the seismic input in terms of PGA. The expression shown in Eq. 8.4 was applied for the construction of the curves. The latter curves can be compared with the fragility curves shown in Figure 8.30. These curves also confirm that for the previously mentioned earthquake defined by the code of $PGA = 0.17g$, less than 5% of the buildings are expected to present severe damage with potential risk of collapse ($\mu_D > 4$). However, slight structural damage is expected to occur even for earthquakes with low values of PGA ($PGA < 0.1g$), due to the poor state of conservation and previous structural damage observed in many buildings.

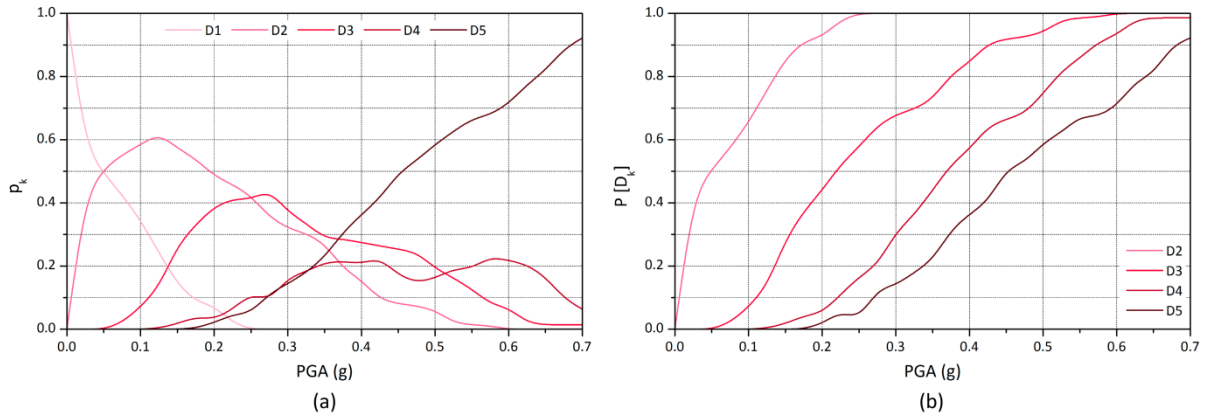


Figure 8.31: (a) Mean damage grade distribution for the building stock in VRSA; and (b) fragility curves

8.3.2.3 Historical vs current condition

An overall low vulnerability of VRSA city center was identified after the seismic vulnerability assessment. Nevertheless, as previously highlighted, VRSA was specifically conceived with high seismic awareness and seismic resistant measures were introduced at an urban and building level. Extensive and detailed information about the historical condition of the city was available in the literature (Mascarenhas 1996; Correia 1997; Figueiras 1999; SGU 2008; Rossa 2009; Gonçalves 2009), including plans of the original buildings and construction details (also in CAD format). Figure 8.32 shows examples of the historical information available. Thus, another seismic vulnerability assessment of VRSA was performed assuming the generic original building configuration. The objective of this study is to understand if the structural alterations done on the original constructions have increased their seismic vulnerability of the buildings.

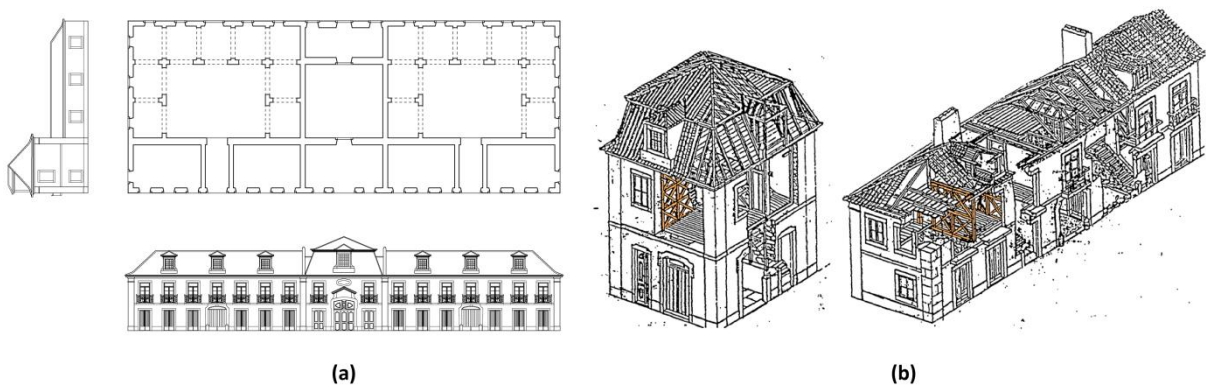


Figure 8.32: (a) Detailed CAD plans of the different original building types are available; and (b) extensive information on the construction details of the different building types (Mascarenhas 1996). The use of *frontal* walls in the two-story buildings of VRSA is highlighted

As shown in Figure 8.16, the original urban configuration was extremely homogeneous and was composed of essentially four distinct architectural typologies. The extensive information available allowed performing a detailed seismic vulnerability assessment of each building type.

The number of historical buildings evaluated was determined based on the 284 buildings evaluated for the current condition. The space occupied by the current building was compared with the original urban shape to determine the number of buildings to assess. Thus, if, for example, the current building occupies the space of three original single-story dwellings, three buildings of this type were selected for the historical seismic vulnerability assessment. As a result, a total of 403 buildings were considered for the historical condition seismic assessment. This already anticipated that the current buildings are of greater dimensions than the original ones and, thus, prone to be more vulnerable. From these 403 buildings, 8 different building types were identified (Figure 8.33): (A) single-story dwellings in the corner position of the urban block; (B) single-story dwellings in the mid position of the urban block; (C) the ‘towers’; (D) the *alfândega* or Customs House; (E) riverfront buildings; (F) salting factories and warehouses; (G) the square ‘towers’; and (H) the square buildings. Both the vulnerability index method and the SAVVAS method were applied to these buildings. Table 8.6 shows the results of the assessment and the number of buildings of each type (N).

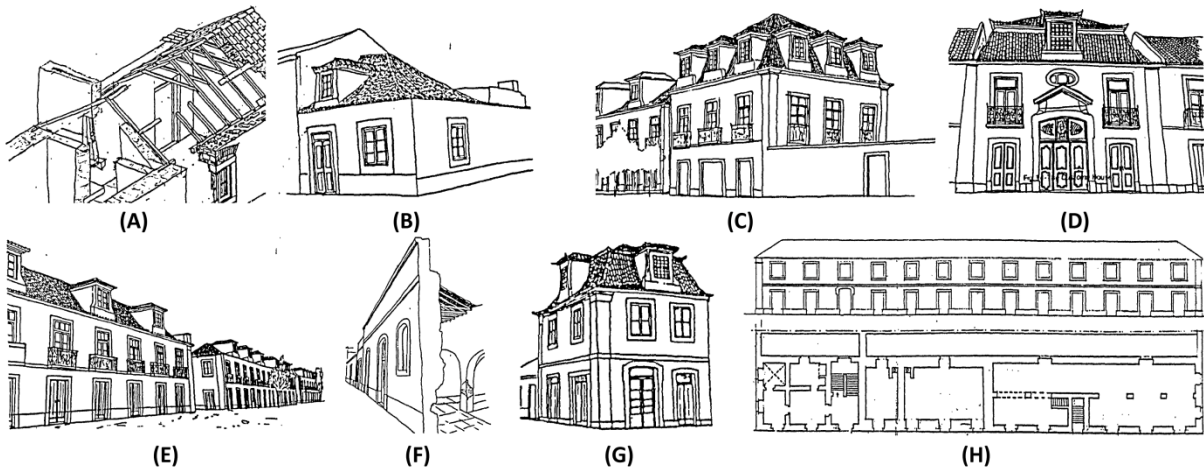


Figure 8.33: 8 different building types considered in the historical configuration (Mascarenhas 1996)

The comparison of these results with the ones obtained for the current condition confirms that the vulnerability of the historical VRSA city center was considerably lower than the current one (Table 8.6). Regarding the vulnerability index method, the mean value of I_V is reduced from 29.87 to 24.78. Since the great majority of the building in the historic downtown are single-story dwellings, the final mean value of I_V is much conditioned by the vulnerability index obtained for type A and B buildings. Given the small scale, good construction quality and regularity of the buildings, the overall vulnerability of VRSA historic city center is low. Following the same approach previously used, vulnerability curves were constructed for the mean value and for different upper and lower bounds of the vulnerability index defined according to the STD: (a) $\bar{I}_V - 2\sigma_{I_V}$; (b) $\bar{I}_V - \sigma_{I_V}$; (c) \bar{I}_V ; (d) $\bar{I}_V + \sigma_{I_V}$; and (e) $\bar{I}_V + 2\sigma_{I_V}$, see Figure 8.34a. Finally, Figure 8.34b shows a comparison in terms of vulnerability curves between the historical and the current condition, considering the mean value of the vulnerability index (\bar{I}_V).

Table 8.6 : Results of the seismic vulnerability assessment on the historical configuration of VRSA using the vulnerability index and the SAVVAS methods

Historic building type	Vulnerability index method		SAVVAS method		
	N	I_v	LS1 (g)	LS2 (g)	LS3 (g)
A	75	25.25	0.38	0.46	0.52
B	298	23.75	0.45	0.60	6.78
C	2	34	0.22	0.37	0.43
D	1	28.75	0.19	0.33	0.38
E	10	32.5	0.21	0.34	0.39
F	8	38.75	0.25	0.30	0.34
G	3	29	0.28	0.43	0.50
H	6	32.5	0.19	0.32	0.37
Mean		24.78	0.42	0.56	0.63
Minimum		23.75	0.19	0.30	0.34
Maximum		38.75	0.45	0.60	0.68
STD		2.77	0.06	0.08	0.10
CoV (%)		11.17	14.60	15.08	15.24

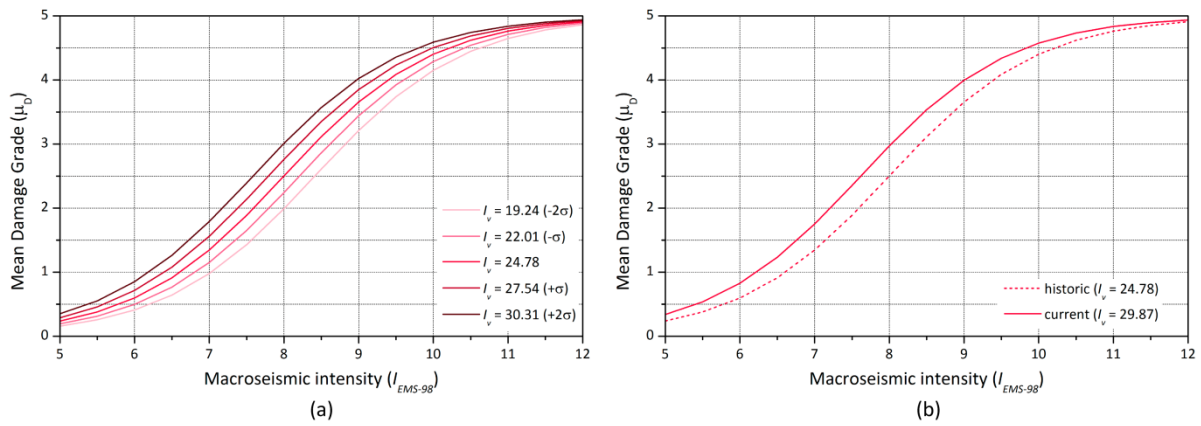


Figure 8.34: (a) Vulnerability curves of the historical building stock of VRSA city center; and (b) comparison between the historical vs current condition in terms of vulnerability curves constructed using \bar{I}_v

Even though Figure 8.34b shows the increase in the vulnerability of the current condition, the difference observed between both curves is not as significant as could be expected. On the other hand, the SAVVAS method was able to capture much greater differences among both scenarios. Firstly, the mean values of the load factors obtained are significantly higher than the ones obtained for the current condition: 0.42g, 0.56g and 0.63g in the historic condition against 0.15g, 0.35g and 0.42g in the current condition for LS1, LS2 and LS3, respectively. The vulnerability curves were also constructed for the mean value and for different upper and lower bounds of the vulnerability index defined according to the STD: (a) $\bar{L}S - 2\sigma_{LS}$; (b) $\bar{L}S - \sigma_{LS}$; (c) $\bar{L}S$; (d) $\bar{L}S + \sigma_{LS}$; and (e) $\bar{L}S + 2\sigma_{LS}$, see Figure 8.35a. Then, Figure 8.35b shows the comparison between the historic and the current condition in terms of vulnerability curves. The differences between the original and the current condition are clear.

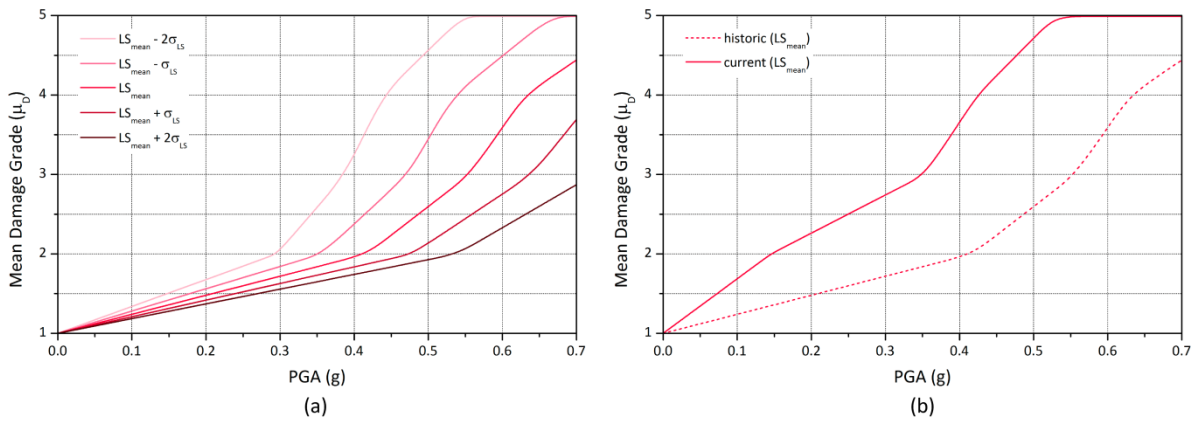


Figure 8.35: (a) Vulnerability curves of the historical building stock of VRSA city center; and (b) comparison between the historical vs current condition in terms of vulnerability curves constructed using \overline{LS}

A final comparison was performed using the results of the SAVVAS method in terms of fragility curves. The same approach used to build the fragility curves shown in Figure 8.31 is followed for the construction of the fragility curves for the historical condition, see Figure 8.36a. The curves are built using the results of μ_D obtained for the historical buildings. Since most of the buildings belong to the same typology, there are drastic changes in the curves. The percentage of buildings ($P[D_k]$) that is expected to exceed each damage grade (D_k) increases drastically after reaching specific values of PGA. The biggest change corresponds to the type B buildings because there are 298 buildings of this type. Figure 8.36b shows the comparison between the curves for the historical and the current condition. Even though the vulnerability of the current condition is considered relatively low, there has been a significant increase of the vulnerability with respect to the historical configuration. Only after values of PGA close to 0.4g, there would be buildings that are expected to present severe damage with potential risk of collapse ($\mu_D > 4$). Also, for the earthquake defined by the code of $PGA = 0.17g$, only around 7% of the historical buildings would be expected to present slight structural damage.

This study reflects clearly that the alterations carried out in the building stock have considerably influenced the seismic vulnerability of the buildings within VRSA historical city center. It should be also noted that the vulnerability assessment of the current condition has been carried out only for those buildings that still preserve the stone masonry skeleton and the timber diaphragms. Most buildings in VRSA city center show further level of intervention with poorly planned additions, new materials, alterations of the structural type, additions of parts structurally incompatible with the existing ones, etc. The increase in the overall seismic vulnerability in the city center can be even higher. That is why, as a future development, it is recommended to further evaluate the impact of structural alterations on existing vernacular construction. The numerical assessment of their influence should be carried out in the future in a

similar way as the one shown in the present research for other seismic vulnerability parameters. This way, their effect could be incorporated to both the SVIVA and the SAVVAS method.

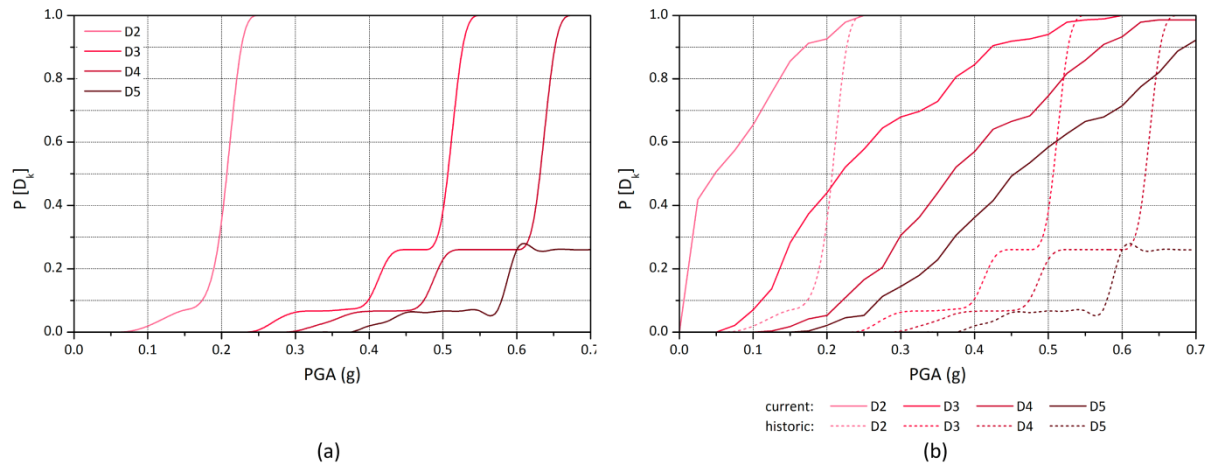


Figure 8.36: (a) fragility curves of the historical building stock of VRSA city center; and (b) comparison between the historical vs current condition in terms of fragility curves

8.3.2.4 Mitigation of the seismic vulnerability with different building retrofitting strategies

The last scenarios that are studied herein result from the application of different building retrofitting strategies, following the output from chapters 2 and 7, related with the traditional strengthening solutions and their effect in reducing the seismic vulnerability of vernacular constructions. This study is meant to serve as an example of the usefulness of seismic vulnerability assessment methods in the decision-making process involved in risk management and mitigation, and its capability as a general planning tool. The solutions considered are applied on the current building stock under study in VRSA, in order to assess the level of reduction of the vulnerability that can be achieved. The selection of the retrofitting strategies was done following three main steps: (1) selection of the most vulnerable buildings in which to implement the selected techniques according to the LS3 distribution shown in Figure 8.27; (2) identification of the parameters showing the worst classification according to the parameter class distribution of the evaluated buildings (Figure 8.21); and (3) selection of the most appropriate techniques that can be used to upgrade the seismic vulnerability classes of the previously identified parameters, according to the summary table presented in Chapter 7 (Table 7.21).

A total of 33 buildings were selected because of showing values of load factor associated to LS3 below 0.25g. The initial threshold of PGA considered was 0.17g, since this is the seismic demand established by the code (NP EN1998-1 2010). However, only five buildings from the set present a load factor defining LS3 below 0.17g, indicating that their maximum capacity will probably be exceeded for this earthquake. Thus, a final value of 0.25g was selected, which is the value of maximum reference peak ground acceleration for mainland Portugal (NP EN1998-1

2010). A common characteristic of the 33 buildings that show higher vulnerability is that they have greater dimensions than the typical buildings from VRSA city center. Most of them have two or more floors and/or have long facade walls presumably spanning large distances (high values for P2). It should be noted that, prior to the definition of a retrofitting strategy, a more detailed assessment is recommended, in order to confirm the real condition of the building. For instance, regarding P2, the interior configuration should be evaluated in detail to confirm that there are not intermediate supports well connected to the façade wall that can be considered as shear walls. In this case, the conditions assumed for the parameter survey are considered to be real in order to proceed with the definition of the retrofitting solutions. Figure 8.37 shows examples of some of the buildings showing higher vulnerability.



Figure 8.37: Examples of the 33 buildings in VRSA selected for the application of retrofitting solutions

Another common characteristic of the selected buildings is the use of timber horizontal diaphragms that provide poor or no proper connection among the resisting walls (class D for P5). The lack of proper connection between the roofs and the walls also results in assuming that the pitched roof types observed are exerting thrust on the walls (class B or C for P6). Finally, most of these buildings also present previous structural damage and significant cracks in the walls due to a poor state of conservation and even abandonment in some cases (class B or C for P6).

Taking the above into account, a first retrofitting strategy (A) could consist of directly addressing the horizontal diaphragms and improving their connection to the walls. According to Table 7.21 (Chapter 7), a common solution would consist of reinforcing the floor-to-wall and roof-to-wall connections and stiffening floors and roofs. A proper intervention of this type could result in upgrading the class of P5 to B in all directions. The reinforced roof-to-wall connection would also result in an upgrade of P6 class to A, since they would prevent the roof thrust. This retrofitting strategy and the followings should always include repairing the existing cracks and a proper conservation intervention of the structural elements in order to upgrade P9 class to A.

A second retrofitting strategy (B), more invasive towards the urban space, could consist of the construction of buttresses or urban reinforcing arches within the span of the wall. This strategy would aim at minimizing the façade free span. Finally, a third strategy (C) would be the application of the previous two techniques plus the addition of timber ring beams at the roof and floor levels of the buildings. This technique will upgrade the class of P5 to A. However, it is noted

that the implementation of this last strategy is more complex in terms of construction since it might require the raising and removal of the roof.

Table 8.7 shows the changes in the results using both methods. All retrofitting strategies have a clear impact on the overall vulnerability of the historical VRSA city center. Since the intervention is only considered for 33 buildings (12% of the total evaluated buildings), the changes in the mean values are not so evident. However, there is a significant difference concerning the minimum and maximum values. For instance, regarding the vulnerability index method, the maximum value of I_V (which represents the most vulnerable building) is reduced from 49.75 to 38.5 in the case of the solutions A and C. Solution C results in a minimum value of I_V of 9.25, which shows that the retrofitted buildings will gain significant seismic resistance. Similar conclusions can be extracted from the results obtained with the SAVVAS method. While the mean values do not show such a significant increase, the minimum value of LS3 is basically doubled from 0.13g to 0.25g using strategy A. Also, the retrofitted buildings using strategy C reach high values of LS3, exhibiting a high seismic resistance.

Table 8.7: Results of the seismic vulnerability assessment on the different retrofitted scenarios assumed for VRSA using the vulnerability index and the SAVVAS methods

Retrofitting strategy	Vulnerability index method					SAVVAS method					
	\bar{I}_V	Min	Max	STD	CoV (%)	$\bar{L}\bar{S}$	Min	Max	STD	CoV (%)	
Current	29.87	21.75	49.75	5.09	17.03	LS1 (g)	0.15	0.00	0.50	0.14	93.21
						LS2 (g)	0.35	0.10	0.69	0.13	35.88
						LS3 (g)	0.42	0.13	0.79	0.14	33.03
A	28.06	15.25	38.5	4.73	16.86	LS1 (g)	0.16	0.00	0.50	0.13	78.99
						LS2 (g)	0.38	0.20	0.69	0.11	29.76
						LS3 (g)	0.45	0.25	0.79	0.12	27.19
B	29.39	21.75	46.75	4.54	15.46	LS1 (g)	0.16	0.00	0.50	0.13	83.67
						LS2 (g)	0.37	0.15	0.69	0.11	30.58
						LS3 (g)	0.44	0.18	0.79	0.12	28.10
C	27.54	9.25	38.5	5.56	20.17	LS1 (g)	0.18	0.00	0.81	0.16	87.53
						LS2 (g)	0.41	0.20	1.08	0.16	37.68
						LS3 (g)	0.49	0.26	1.23	0.17	34.76

As previously noted, the differences in terms of mean values are not so significant. Thus, the vulnerability curves shown in Figure 8.38, constructed using the mean values of the four scenarios with both methods, do not show notable changes. The SAVVAS method vulnerability curves shows again to be more sensitive and the differences between the curves are higher.

Nevertheless, the differences are more visible in the fragility curves (Figure 8.39), which are constructed using the results of the SAVVAS method and following the approach previously presented. There is a notable reduction of the number of buildings ($P[D_k]$) that are expected to exceed each damage grade, particularly for values of $PGA < 0.25g$. The three retrofitting strategies are efficient in delaying the occurrence of severe damage with potential risk of collapse

($\mu_D > 4$). Strategy C is the most effective but also the costliest because requires a greater intervention. Strategy A, on the contrary, only intervenes at the diaphragm level, and proves to effectively reduce the seismic risk. For instance, for the earthquake defined by the code of $PGA = 0.17g$, none of the buildings is expected to show severe damage and risk of collapse. The process followed to define the retrofiting scenarios can be applied to define others in order to assess the efficiency of other traditional strengthening solutions. Also, in order to further reduce the seismic vulnerability of VRSA historical city center, the number of buildings intervened can be enlarged up to a satisfactory result.

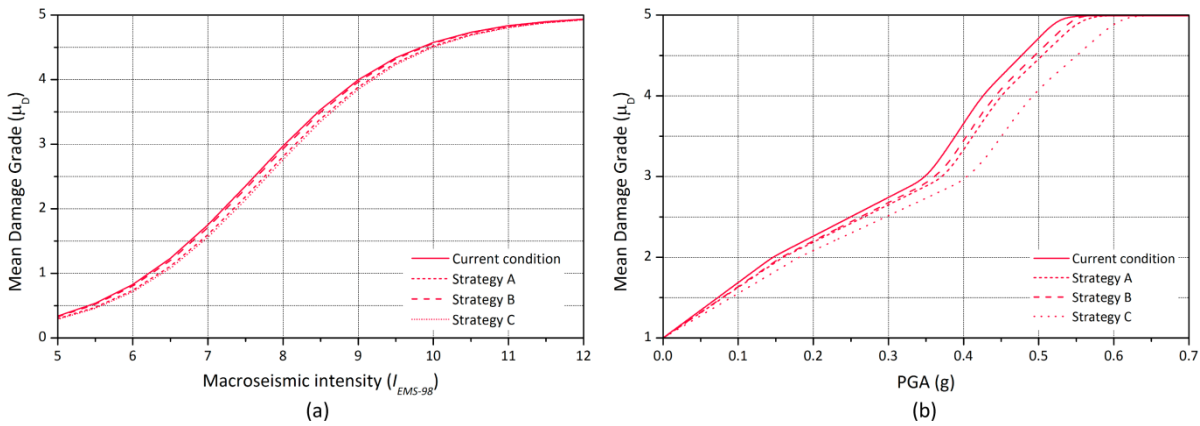


Figure 8.38: Vulnerability curves for the four different scenarios considered for VRSA city center: (a) vulnerability index method; and (b) SAVVAS method

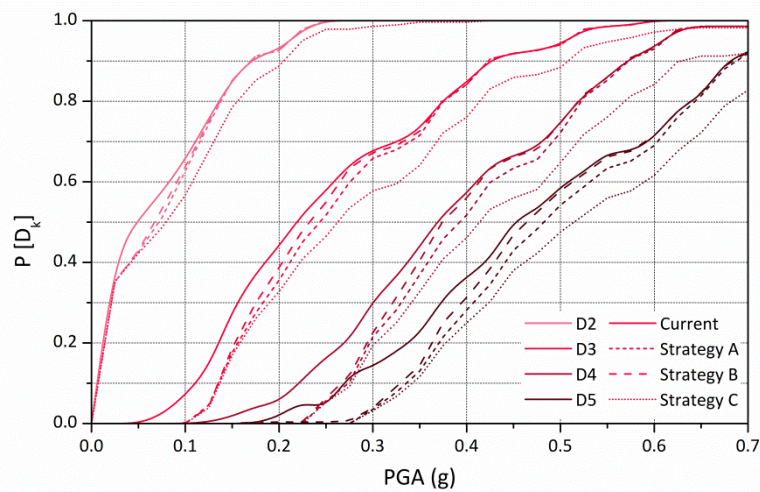


Figure 8.39: Comparison between the fragility curves constructed for the four different scenarios considered

Results obtained with the SAVVAS method are also presented in Figure 8.40 using the GIS tool, showing the damage scenarios for an earthquake with $PGA = 0.25g$ considering the three different retrofiting strategies. They can be compared with the same scenario for the current

condition shown in Figure 8.29 in order to see how the collapse of several buildings is avoided. No buildings are expected to suffer collapse considering the retrofitting strategies A and C.



Figure 8.40: Damage scenarios for an earthquake with $PGA = 0.25g$ considering the three retrofitting strategies

8.3.3. Loss assessment

Finally, this last section deals with the loss assessment for the buildings evaluated for the historical city center of Vila Real de Santo António. Since the loss estimation depends on the physical damage grade distribution, the assessment was carried out using the results of μ_D obtained from all buildings obtained from the SAVVAS method. Results will be also presented using the GIS tool to visualize the loss scenarios. The losses are estimated as a function of the probability of exceedance of certain damage grades using methodologies available in the literature and previously applied in similar seismic vulnerability assessments. It is noted that the discussion of the expressions applied for the loss assessment is out of the scope of this work. The loss estimation obtained for the current condition is also contrasted with the historical and retrofitted condition, in order to better understand: (a) the effects of the alterations undergone by VRSA city center in terms of losses; and (b) the impact of the retrofitting strategies in the reduction of human and economic losses.

8.3.3.1 Collapsed and unusable buildings

The loss estimation models used for assessing the probability of building collapse and loss of functionality are based on the work developed by Bramerini et al. (1995) after post-earthquake damage observation. The probability is thus calculated by using multiplier factors ranging from 0 to 1 on the probability (p_k) associated to certain damage grades D_k ($k \in [0,5]$):

$$P_{collapse} = p_5 \quad (8.10)$$

$$P_{unusable} = 0.4 \times p_3 + 0.6 \times p_4 \quad (8.11)$$

The factors 0.4 and 0.6 are adopted from Vicente et al. (2011). Figure 8.41a depicts the probability of collapsed and unusable buildings based on the percentage of buildings that are expected to exceed each damage grade shown in Figure 8.31b. Figure 8.41b shows the comparison between the current, historic and retrofitted scenario (considering the application of strategy A). Figure 8.42 shows the results for the current condition of VRSA, mapped using the GIS tool and considering a seismic event with $PGA = 0.25g$. Finally, overall results for different seismic events with increasing PGA and for the three different scenarios are summarized in Table 8.8, where it is worth highlighting the low vulnerability of the historical condition.

Table 8.8: Number of collapsed and unusable buildings for the three different scenarios considered

$N = 284$	Current condition				Historical condition				Retrofitted condition			
	PGA (g)				PGA (g)				PGA (g)			
	0.15	0.25	0.35	0.45	0.15	0.25	0.35	0.45	0.15	0.25	0.35	0.45
Collapsed	0	15	65	140	0	0	0	6	0	0	37	122
Unusable	33	66	69	58	0	0	10	23	19	60	79	67

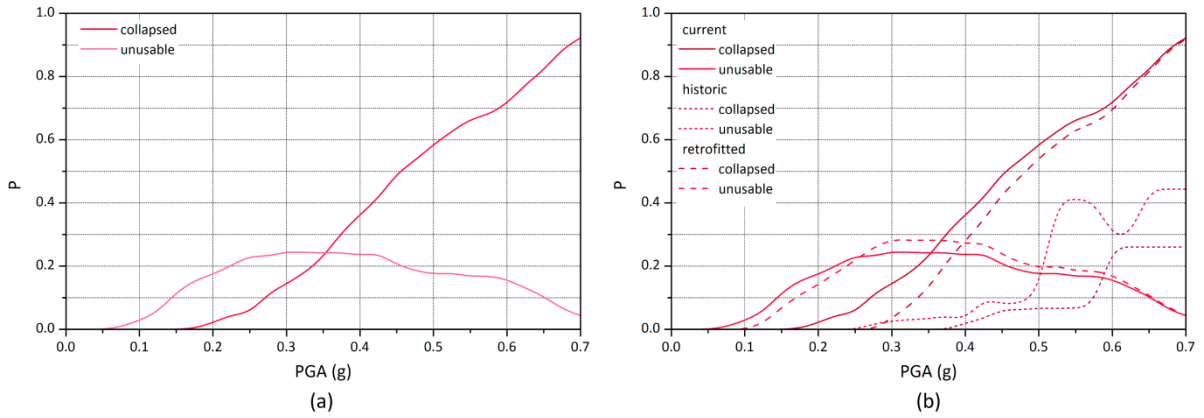


Figure 8.41: (a) Probability of collapsed and unusable buildings in the current condition; and (b) comparison with the historic and retrofitted condition (strategy A)

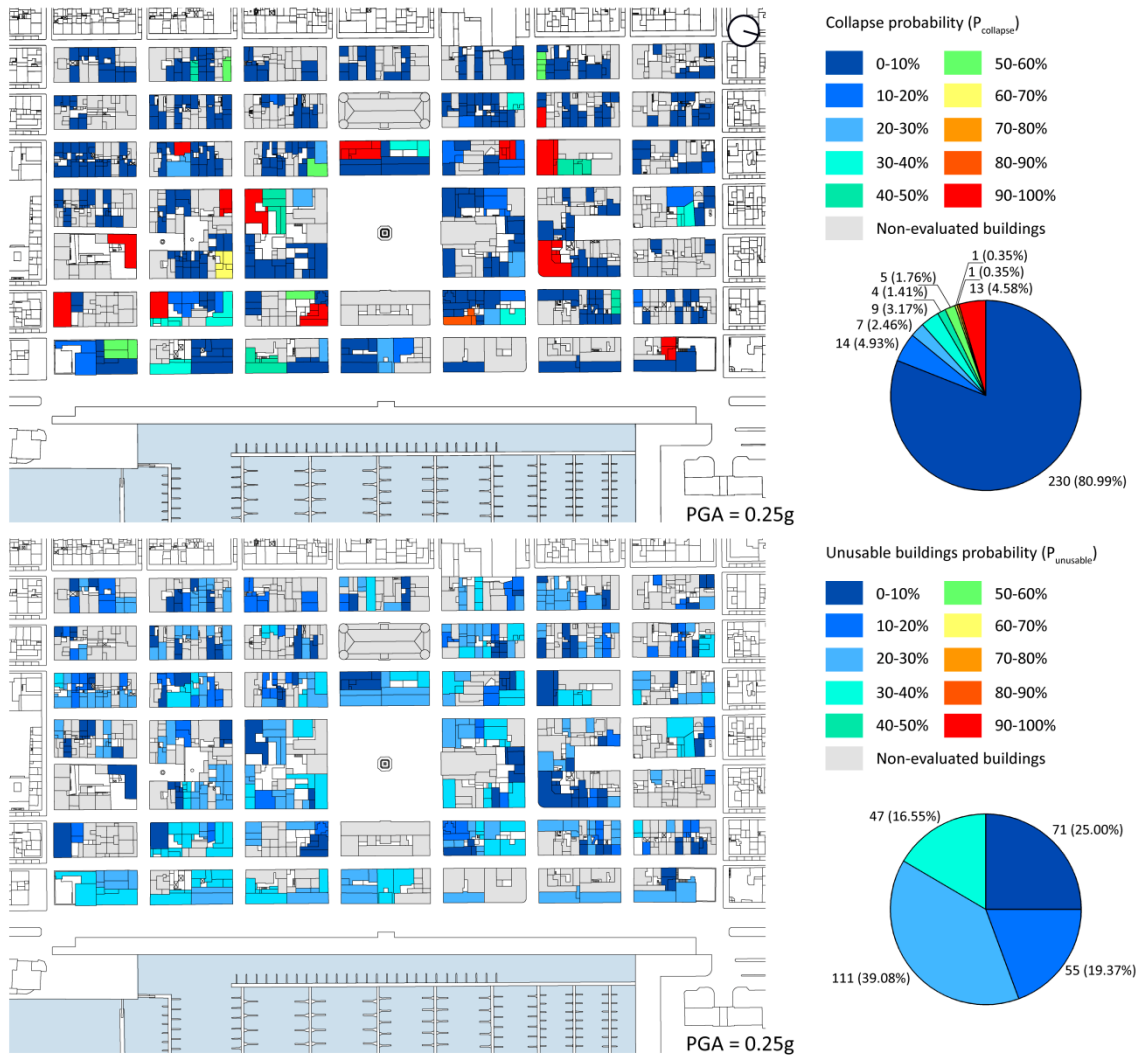


Figure 8.42: Collapsed and unusable buildings loss scenarios in the current condition for a seismic event of $PGA = 0.25g$

8.3.3.2 Human casualties and homelessness

The work developed by Bramerini et al. (1995) served also as a basis for the loss estimation models used for assessing the casualty rates (deaths and severely injured) and homelessness. The multiplier factors adopted were also adopted from Vicente et al. (2011). The casualty rates are considered as being 30% of the residents of collapsed buildings (Eq. 8.12). The amount of homeless people that will require shelter after the event is estimated using Eq. 8.13:

$$P_{dead\ and\ severely\ injured} = 0.3 \times p_5 \tag{8.12}$$

$$P_{homeless} = 0.4 \times p_3 + 0.6 \times p_4 + 0.7 \times p_5 \tag{8.13}$$

Figure 8.43a depicts the estimation of the number of casualty rates and homeless based again on the percentage of buildings that are expected to exceed each damage grade shown in Figure 8.31b, while Figure 8.43b shows the comparison with the historic and the retrofitted scenario A. Figure 8.44 shows these results mapped using the GIS tool and considering a seismic event with an expected $PGA = 0.25g$. Finally, overall results for different seismic events with increasing PGA and for the three different scenarios are summarized in Table 8.9. The total number of inhabitants living in the 284 buildings evaluated was considered as 1784. The reduction of the number of casualties for the retrofitted scenario is significant, particularly for a seismic event with a $PGA = 0.25g$, where the number of dead or severed injured is reduced from 28 to 0.

Table 8.9: Number of dead or severely injured and homeless people for the three scenarios considered

$N = 1784$	Current condition				Historical condition				Retrofitted condition			
	PGA (g)				PGA (g)				PGA (g)			
	0.15	0.25	0.35	0.45	0.15	0.25	0.35	0.45	0.15	0.25	0.35	0.45
Dead or severely injured	0	28	122	264	0	0	0	5	0	0	70	230
Homeless	207	481	718	981	0	0	10	35	121	379	660	959

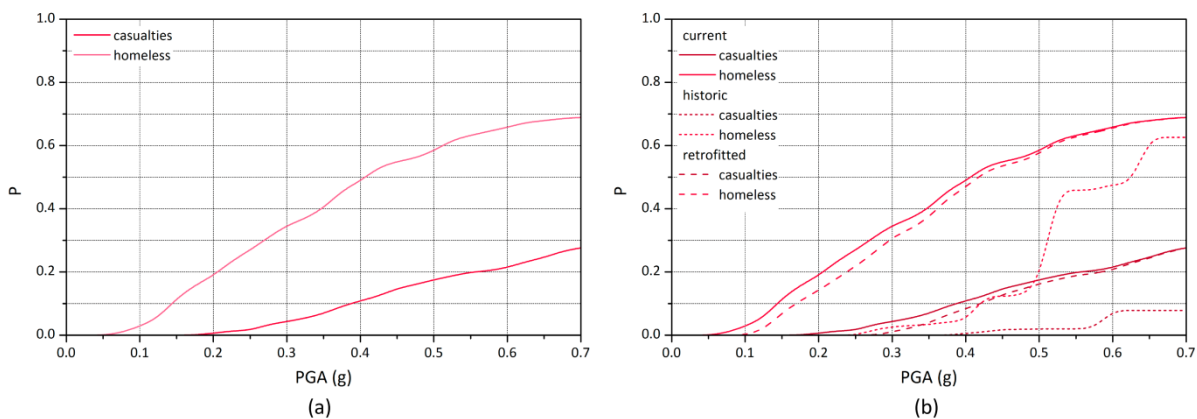


Figure 8.43: (a) Probability of casualties and homeless in the current condition; and (b) comparison with the historic and retrofitted condition (strategy A)

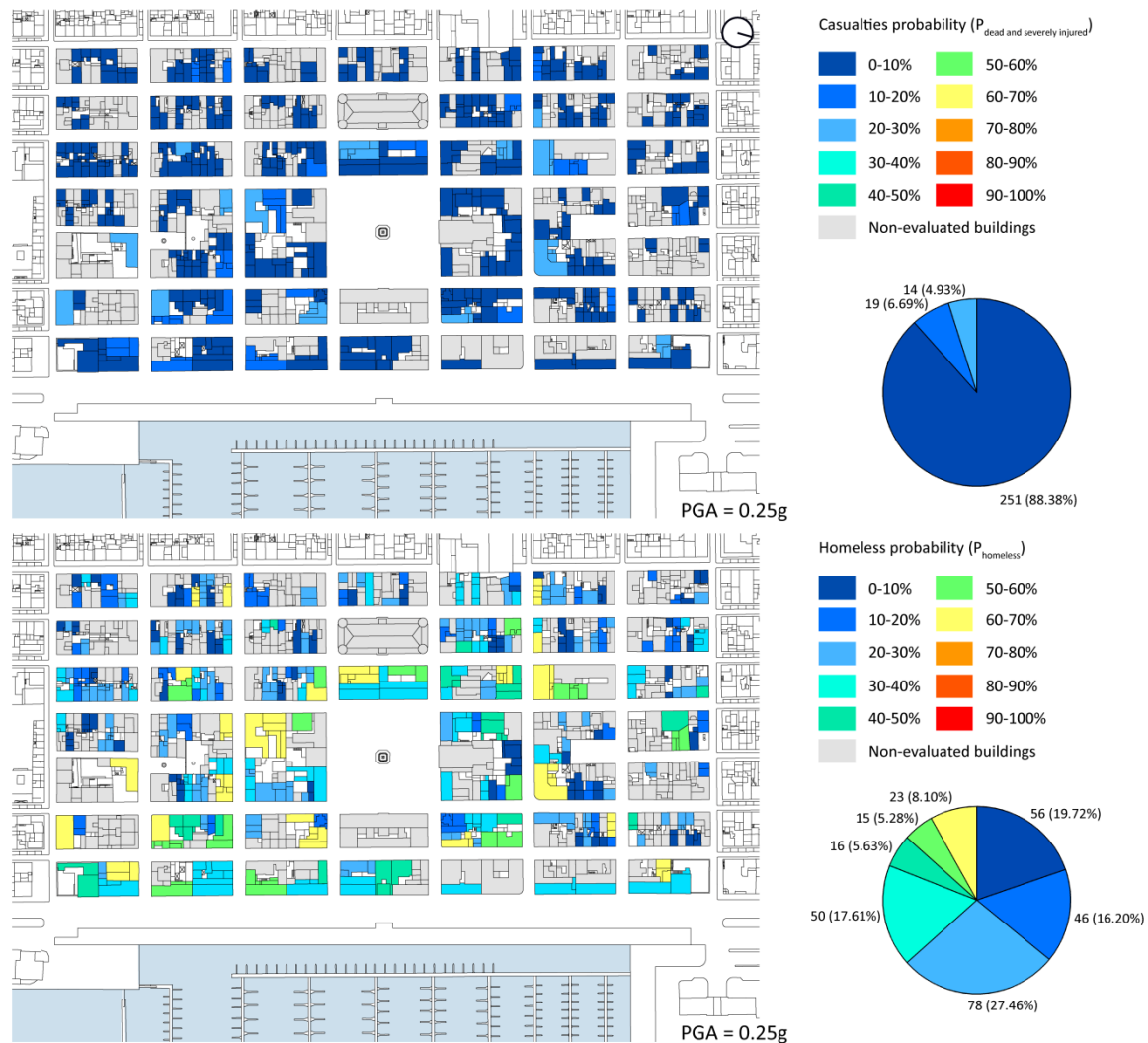


Figure 8.44: Casualties and homeless estimation scenarios in the current condition for a seismic event of $PGA = 0.25g$

8.3.3.3 Economic loss and repair cost estimation

The economic loss estimation models used in the present study are based on establishing a correlation between the damage grades (D_k) and the estimated repair and rebuilding costs, expressed in terms of an economic damage index, following the approach suggested by Vicente et al. (2011). As presented in Chapter 3, Benedetti and Petrini (1984) introduced the use of an economic damage index instead of damage grades in order to create the vulnerability functions for the vulnerability index method (Figure 3.1). This index can be defined as the ratio between the repair cost and the replacement cost of the building. Several correlations between damage grades and economic damage index exist in the literature and are typically established after post-seismic investigation. The one applied in this study was established by Dolce et al. (2005), calibrated after the Umbria Marche (1997) and Pollino (1998) earthquakes. The correlation between damage grades and damage economical index is shown in Table 8.10.

Table 8.10: Correlation between damage grades D_k and damage index

Damage grade (D_k)	0	1	2	3	4	5
Dolce et al. (2005)	0.005	0.035	0.145	0.305	0.800	0.950

The probability of repair costs (expressed in terms of the economic index ranging from 0 to 1) that would be required after an earthquake (P_{repair}) can be estimated by multiplying the conditional probability of the repair costs for each damage level ($P[R|D_k]$), using the values shown in Table 8.10, with the probability (p_k) associated to the different damage grades:

$$P_{repair} = \sum_{k=1}^5 P[R|D_k] \times p_k \quad (8.14)$$

It is noted that damage grade 0 is not included because the SAVVAS method considers that damage grades 0 and 1 are the same, since it does not detect non-structural damage. The estimated cost of repairing the building stock of VRSA city center was calculated by considering an average cost value of 800 €/m² as the replacement cost of the buildings. The resulting estimated repairing cost can be expressed as a function of the seismic input in terms of PGA, see Figure 8.45a. The figure also includes the costs estimated for the retrofitted scenario A, which shows that the difference in the repair costs can be significant by making a preventive intervention in 33 buildings and can reach up to 2.5 million of euros for a seismic event with $PGA = 0.25g$.

Figure 8.45b presents the return of the investment (ROI) of the retrofitting strategy A as a function of PGA. Diz et al. (2015) estimated the cost of the retrofitting solution included in strategy A, consisting of strengthening the diaphragm-to-wall connections, at 23€/m². This value was increased up to 50€/m² considering additional costs associated to the intervention, such as the stiffening of the diaphragms and the repairing of cracks. This value is in line with other values shown in the literature based on strengthening works carried out in Azores after 1998 earthquake (Costa et al. 2013). The graph shows that the initial costs of the intervention are rapidly compensated economically. This fact, together with the reduced loss in terms of collapse buildings and human casualties shown in Table 8.8 and Table 8.9, justifies the need of preventive action regarding seismic protection including the retrofitting of the existing building stock. It should be noted that this simplified cost-benefit analysis is primarily aimed at showing the potentialities of using this tool for making decisions regarding risk management and control. A deeper study of the implementation costs of the different traditional solutions to perform a more robust cost-benefit analysis is out of the scope of this work, but left for future work. Finally, overall results for different seismic events with increasing PGA and for the current and retrofitted scenarios are summarized in Table 8.11.

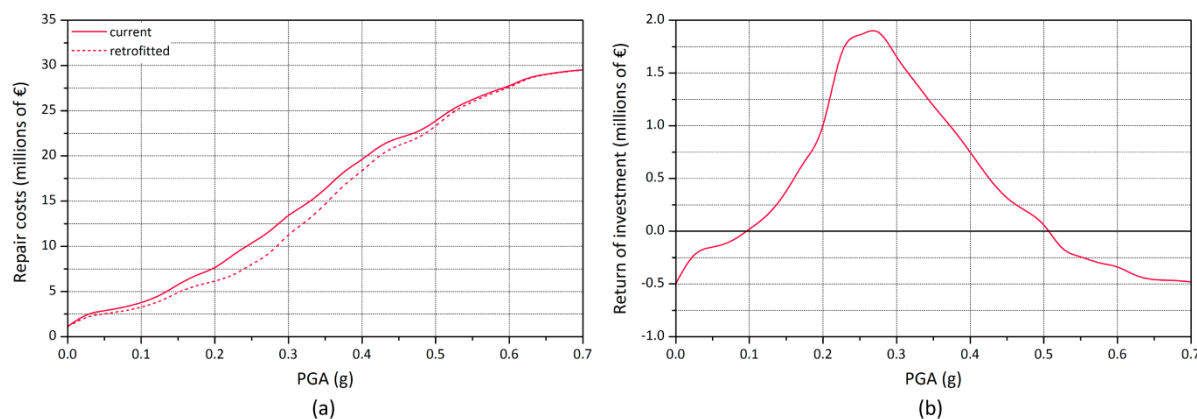


Figure 8.45: (a) Estimation of repair costs for the current and retrofitted condition (strategy A); and (b) return of the investment of the retrofitting strategy A as a function of the seismic event in terms of PGA

Table 8.11: Estimation of the repair costs for the current and retrofitted scenarios considered

$N = 284$	Current condition				Retrofitted condition			
	PGA (g)				PGA (g)			
	0.15	0.25	0.35	0.45	0.15	0.25	0.35	0.45
Repair costs (in millions of €)	5.8	10.37	16.28	22.04	4.94	8.03	14.60	21.24

8.4. Conclusions

The present chapter has dealt with the calibration and application of the two seismic vulnerability assessment methods developed in the present thesis. The calibration of the methods was carried out based on post-earthquake damage data on a set of 88 buildings taken from reports from the island of Faial in Azores, after the 1998 earthquake. Since the damage suffered by the buildings is known, the application of the two seismic vulnerability assessment methods in this case study was very valuable mainly for their calibration. The calibration process is particularly important for the vulnerability index (SVIVA) method because it led to the adjustment of the analytical expression that correlates the vulnerability index with the macroseismic intensity and mean damage grade, and is used for the construction of the vulnerability curves. In the case of SAVVAS method, the correlation between the seismic input in terms of PGA and the EMS-98 damage grades was established and validated using the available damage data. The application of both methods led to very good results in terms of predicted versus observed damage grades, confirming the validity of both methods as first level approaches. Using few data, mostly qualitative, of the buildings related to 10 parameters, both provided a good estimation of the damage that the buildings would experience when subjected to an earthquake with different intensities.

It should be noted that the SAVVAS method provided some novelties with respect to the vulnerability index method. First of all, the prediction capability of the method was very accurate and showed very low values for the errors. Since the data used for the application is slightly more

specific, it allows a significantly more detailed assessment. Besides, one of the main advantages of the SAVVAS method is the fact that it did not require the initial calibration of the expression required by the vulnerability index method, and the correlation between damage and seismic input could be applied directly. Additionally, the method calculates the vulnerability of the building in different directions, which represents a great advantage in accurately assessing the most vulnerable direction and thus detecting more accurately the possible deficiencies of the building under evaluation. The method proved to identify the failure mode suffered by the building in many cases.

In a second stage, the two methods were applied in the historical city center of Vila Real de Santo António, in the South of Portugal. A complete seismic vulnerability assessment of the city center was performed with both methods, showing their applicability to large scale analysis. Results were presented in terms of damage distribution, vulnerability and fragility curves. The use of a GIS tool allowed the storage of the results associated to the urban plan of the city. Thus, results could be presented in different maps, allowing an easy visualization and the quick detection of the most vulnerable buildings. The most important uncertainties of both methods are related to the input information and the inspection phase. Since not all the buildings could be inspected in detail, not all the data required to complete the parameter survey is completely reliable. However, the available information included sufficiently detailed reports and photographs of enough buildings to be confident on the results obtained. A general low level of damage was estimated for the buildings of VRSA using both methods, which was attributed to a generalized reduced scale of the buildings. With this respect, the SAVVAS method allowed identifying a significant amount of buildings that show a worrisome vulnerability and were recommended for a more detailed assessment. It is noted that the SAVVAS method allowed differentiating better the vulnerability level of the buildings.

Two extra scenarios were considered for the seismic vulnerability assessment. Firstly, the vulnerability of the historical condition of the city at the moment of its construction was evaluated, since detailed information was available. The objective was to understand if the structural alterations undergone by the buildings in VRSA city center have resulted in an increase of the seismic vulnerability, and to measure this increment. Although the vulnerability of the current condition is low, there has been a notable increase of the vulnerability with respect to the historical configuration, whose resistance to seismic actions is very high. Secondly, several retrofitting strategies were defined based on traditional strengthening techniques studied in the previous chapters and applied to a total of 33 buildings of VRSA, which were identified as the most vulnerable to seismic actions. The reduction of the overall vulnerability of the city center was then evaluated and proved to be efficient in reducing the number of buildings that are expected to exceed the different damage levels defined, particularly for earthquakes with values of PGA lower than 0.25g.

The final section of the chapter presents the seismic loss assessment for the city center of VRSA using the results from the SAVVAS method, including the estimation of the amount of collapsed and unusable buildings, number of casualties and homelessness, and the economic loss and repair costs. The losses were also estimated for the historic and retrofitted condition in order to further investigate the differences among the three scenarios. Particularly with respect to the retrofitted scenario, results show that investing in retrofitting using traditional strengthening solutions would result in economic benefits in the event of an earthquake. More importantly, it would also provide a significant reduction of the number of collapsed buildings and possible human casualties.

In summary, this chapter provides a deep insight of the capabilities of large scale seismic vulnerability assessment in managing seismic risk and making decisions on rehabilitation strategies of old urban areas. It also validates the applicability of the novel SAVVAS method for this matter.

CHAPTER 9

CONCLUSIONS AND FUTURE RESEARCH

Chapter outline

[9.1. Introduction](#)

[9.2. Summary of conclusions](#)

[9.2.1. Quantitative evaluation of the seismic behavior of representative examples of Portuguese vernacular architecture \(Research objective 1\)](#)

[9.2.2. Development of a seismic vulnerability assessment method for vernacular architecture \(Research objective 2\)](#)

[9.2.3. Assessment of the efficiency of traditional strengthening solutions to mitigate the seismic vulnerability of vernacular architecture \(Research objective 3\)](#)

[9.2.4. Recommendations of traditional strengthening solutions to reduce the seismic vulnerability of in-use vernacular architecture \(Research objective 4\)](#)

[9.2.5. Thesis outcomes](#)

[9.3. Future](#)

9.1. Introduction

The present thesis is primarily aimed at providing tools for the protection of the vernacular heritage located in earthquake prone areas. In order to accomplish this, the work carried out has followed two complementary lines of investigation: (1) the identification of traditional strengthening solutions and the numerical evaluation of their efficiency in reducing the seismic vulnerability of vernacular buildings; and (2) the development of two seismic vulnerability assessment methods for vernacular architecture. The process followed has allowed obtaining a better understanding of the seismic behavior of vernacular architecture. The combination of both approaches has also provided specific tools that can be used for: (a) the assessment of existing vernacular architecture earthquake preparedness; and (b) the evaluation of the adequacy of applying different traditional strengthening solutions to reduce the seismic vulnerability of vernacular architecture.

The present chapter is mainly intended to summarize the conclusions drawn from the research work developed. The chapter firstly provides a general description of the work developed

and then outlines the most relevant conclusions, with a particular focus on providing an answer to the four fundamental objectives specified in Chapter 1. The present thesis has also provided a series of quantitative outcomes that are also outlined in this chapter. Finally, the chapter and the thesis concludes by acknowledging the limitations of the research work carried out and by providing suggestions for new continuing research lines that have been identified in the scope of the protection of the vernacular heritage.

9.2. Summary of conclusions

The thesis was structured according to the four tasks, previously defined and described in Chapter 1, which were consecutively performed in order to accomplish the thesis objectives. First of all, in Chapter 2, and based on the literature review, the most common strengthening techniques traditionally used around the world as part of a local seismic culture were identified. Based on field observations, these solutions were also recognized in several seismic prone Portuguese regions. The second task is fulfilled in chapters 3 through 6 and consisted of the development of the two new seismic vulnerability assessment methods, based on: (a) literature review; (b) an extensive numerical campaign; (c) statistical analysis; and (d) expert opinion. The third task is accomplished in Chapter 7 and consisted of the use of numerical analysis for the evaluation of the effect of the previously identified traditional strengthening techniques on the seismic behavior of vernacular buildings. The fourth task is completed in Chapter 8 and included the application of the seismic vulnerability assessment methods on two selected case studies. The first case study was the island of Faial, in Azores (Portugal), and the methods were applied on a set of buildings damaged by the 1998 earthquake. The obtained results were confronted with the post-earthquake observations, in order to calibrate and validate the methods. The second case study was the historical city center of Vila Real de Santo António (Portugal). For the second case, the information was collected from historical research and on-site observations. The two methods were then applied in order to show an example of their applicability. Different building retrofitting strategies were also explored in order to understand the possibilities of the methods developed for decision-making on seismic strengthening planning at an urban level. The study of these strategies, together with the individual numerical studies of traditional strengthening solutions carried out in the third task, allowed drawing some conclusions regarding their efficiency in reducing the vulnerability of in-use vernacular architecture. The most relevant conclusions drawn within the abovementioned process are outlined next, arranged according to the four fundamental objectives of the thesis.

9.2.1. Quantitative evaluation of the seismic behavior of representative examples of Portuguese vernacular architecture (Research objective 1)

The accomplishment of the first research objective comes as a consequence of the process followed for the development of the two seismic vulnerability assessment methods for vernacular architecture. The development of these methods required a deep knowledge of the seismic behavior of characteristic Portuguese vernacular buildings. Therefore, an extensive parametric numerical study based on detailed finite element modeling and nonlinear static analysis was planned and carried out. This numerical campaign provided the desired thorough understanding on the seismic response of vernacular building.

The reference models prepared for the parametric study were based on representative vernacular rammed earth rural constructions commonly found in the South Portuguese region of Alentejo. However, the initial reference model was partially modified within the parametric analysis to cover a wider range of vernacular architecture, with variations in the geometrical, material, construction and structural characteristics. Eventually, it is considered that the results obtained are sufficiently comprehensive to have a better understanding of the structural behavior of many representative Portuguese vernacular architectural heritage typologies under seismic loading. Moreover, Portuguese vernacular buildings share many characteristics with other vernacular constructions throughout the world and, therefore, the results obtained in this work can also be representative for other similar structures outside Portugal.

The results of the parametric study have been thoroughly presented within Chapter 4, which is the mainly contributor for accomplishing the first research objective. Results were provided in terms of: (a) variations in the damage patterns and failure mechanisms; (b) capacity curves that offer information on the seismic capacity, stiffness and ductility of the buildings; and (c) load factor variations. These load factors were previously associated to four different performance levels or structural limit states. Therefore, they are an indicator of the seismic performance of vernacular buildings, as they reflect the load capacity of the structure before reaching specific damage limit states. In conclusion, the advanced numerical analysis performed on the many models constructed showing different constructive, geometrical and material characteristics that can be typically observed on vernacular structures contributes to accomplish the objective by providing the desired better insight of the seismic structural behavior of vernacular buildings.

9.2.2. Development of a seismic vulnerability assessment method for vernacular architecture (Research objective 2)

Two seismic vulnerability assessment methods for vernacular architecture have been: (1) developed; (2) calibrated; (3) validated; and (4) applied on real case studies within the present thesis. The first method is referred as Seismic Vulnerability Index for Vernacular Architecture

(SVIVA) method, and it is an adaptation of the existing methods to the characteristics of the vernacular architecture under study, following a standard vulnerability index formulation. The second method was named as Seismic Assessment of the Vulnerability of Vernacular Architecture Structures (SAVVAS) method, and is considered innovative because, while being also based on existing methods, it proposes a new formulation that allows correlating the seismic capacity of the building expressed in terms of load factors defining different structural limit states with simple seismic vulnerability assessment parameters. Since these load factors are expressed as acceleration (in terms of g) and are related with structural limit states that are defined on the basis of damage descriptions, the SAVVAS method can directly correlate the peak ground acceleration (PGA) with the expected damage.

From the wide range of seismic vulnerability assessment methods existing in the literature, the present thesis used as main references and as the basis for development of the new methods the vulnerability index method and the macroseismic method. Both methods are expedited simplified approaches that rely on empirical basis, involving post-earthquake damage observation and expert judgment. Vulnerability index methods correlate the vulnerability of a structure with different parameters related to simple geometric and constructive characteristics. Thus, they provide the possibility of performing a primary seismic safety assessment and of obtaining an indicator of the seismic performance of a building or group of buildings, based on expedited surveys that can be carried out even solely by means of visual inspection. That is why they are practical when addressing large numbers of buildings or, when the necessary amount of resources cannot be assigned to the assessment of the targeted buildings, which is generally the case when dealing with the study of vernacular constructions.

As abovementioned, the development of the two proposed methods was based on obtaining a comprehensive understanding of the seismic behavior of vernacular architecture, by means of detailed finite element modeling and nonlinear static analysis. A set of geometric, material and construction parameters were selected based on literature review and, according to those parameters, an extensive parametric study was performed to evaluate and quantify numerically their influence on the seismic performance of vernacular buildings. The influence of the different parameters was thus validated through numerical analysis and the results were used to provide a quantitative definition of four seismic vulnerability classes for each parameter. The use of an analytical procedure for the definition of the seismic vulnerability assessment classes helps to strengthen the reliability of the existing simplified methods that typically rely solely on empirical knowledge obtained from post-earthquake damage observation. The vulnerability classes proposed are overall in line with the classifications available in the literature, but are adapted to the evaluation of the seismic vulnerability of vernacular buildings.

The completion of the vulnerability index formulation also required the determination of the parameters weights, which indicate the relative importance of each parameter in estimating the

overall seismic vulnerability of the building. The thesis presented two approaches for their definition: (a) statistical; and (b) expert judgment. With respect to the statistical approach, all models built for the parametric analysis composed an extensive database that was used to perform a regression analysis. This allowed obtaining regression coefficients that were used to compare the relative importance of the parameters to estimate the seismic behavior of the models. These coefficients were then associated with the weights of the seismic vulnerability assessment parameters. The second approach was mostly intended to perceive the overall view of experts from different seismic prone regions throughout the world on the topic, and to compare their empirical judgment with the results obtained from the numerical campaign. The high scatter observed in their answers confirmed the difficulty of assessing the influence of the different parameters based solely on expert judgment and post-earthquake damage observations. This fact also justified the use of an analytical-based approach for enhancing the comprehension of the contribution of the parameters to the structural response of vernacular buildings under seismic loading. In the end, a comparison between the weights obtained through the statistical and expert judgment approaches was provided and discussed. The final weights were also compared with the weights already used by similar methods available in the literature.

The results obtained highlighted the complexity of the matter and the difficulty to explain the seismic behavior of vernacular buildings only by considering the influence of ten independent parameters. The interaction among the different parameters revealed to be of great importance to effectively describe the seismic response of the building. The SAVVAS method tries to overcome these encountered limitations. Moreover, it tries to provide a quantitative estimation of the seismic behavior of vernacular buildings, instead of the traditional qualitative indicators that can be achieved with the vulnerability index method. Data mining techniques (namely multiple linear regression and artificial neural networks) and regression analysis were the tools applied on the database resulting from the numerical campaign for the determination of the SAVVAS formulation. The method was validated with its application on numerical and experimental examples found in the literature, revealing a very good correlation between the predicted and the observed seismic load factors. Besides the abovementioned advantages, the SAVVAS method also provides information about the capacity of the building in different loading directions. The method is also able to predict possible failure mechanisms of the building, which can be particularly useful in order to identify deficiencies at the structure before deciding on strengthening interventions.

Both developed methods were calibrated using the case study of Faial Island, in Azores (Portugal), and the available post-earthquake damage data for making a comparison between predicted and observed damage. Both methods provided a good estimation of the damage experienced by the buildings, solely on the basis of few data, mostly qualitative, related to the ten parameters previously selected. The SAVVAS method outperformed the vulnerability index

method in terms of prediction capabilities. Furthermore, it did not require the calibration of the empirical coefficients from the expressions that are used in the vulnerability index method to correlate damage, seismic intensity and the vulnerability index. The correlation between damage and seismic input could be applied directly.

The applicability and the ease of use of both methods for a large scale analysis were further illustrated with a second case study, which consisted of the historical city center of Vila Real de Santo António, in Portugal. The seismic vulnerability and loss assessment was carried out, presenting results in terms of damage distribution, vulnerability and fragility curves and loss scenarios considering earthquakes with different intensities. Besides the reliable prediction potential shown by both methods, results are particularly valuable in comparative terms, because they can identify the buildings that are more vulnerable within the whole evaluated set. This part is critical because: (a) since this type of methods take into account possible uncertainties related to the input information collected at the expeditious inspection phase, it allows detecting the need for more detailed assessment of the most vulnerable elements at risk; and (b) it allows defining and optimizing the structural retrofitting strategies at an urban level, since it highlights the buildings where the biggest efforts should be concentrated on, which helps in managing the seismic risk of the city. With respect to the latter aspect, the applicability of the SAVVAS method was also validated when performing a cost-benefit analysis of different urban retrofitting strategies based on traditional strengthening techniques.

9.2.3. Assessment of the efficiency of traditional strengthening solutions to mitigate the seismic vulnerability of vernacular architecture (Research objective 3)

The most common seismic strengthening solutions traditionally used in vernacular architecture associated with a local seismic culture have been: (a) identified through literature review; (b) recognized through on-site visits to several regions in Portugal; (c) analyzed in terms of construction principles; and finally (d) numerically evaluated. As a result, their effect on the seismic performance of vernacular structures has been quantitatively assessed, as well as the determination of the increment in the maximum capacity of the building achieved after the application of the technique. This quantification of their effect also allowed incorporating the evaluated techniques within the two new methods proposed for the seismic vulnerability assessment of vernacular architecture. Different ways were proposed on how to take into account their effect by means of updating the seismic vulnerability classes of different parameters.

The numerical assessment included detailed FE models that simulated the different techniques and possible variations, which contributed to gain knowledge on the structural behavior of these empirically developed traditional techniques. The thorough analysis carried out helped to understand not only the efficiency of the different techniques in improving the seismic capacity of vernacular buildings, but also which structural aspect of the building can be improved

with their application and how. The results from the numerical studies thus included: (1) ranges of increase of the maximum strength of the building; (2) structural improvement; and (3) applicability (or ease of use) of the different techniques. This can eventually be of help in making decisions on seismic strengthening strategies for the vernacular heritage.

Even though most of the techniques evaluated were proved to reduce the seismic vulnerability of vernacular buildings, the techniques that are able to provide a proper diaphragmatic action to the building, by engaging all the walls in the seismic response of the building, were the ones showing the most significant improvements. These techniques, such as ring beams and reinforced floor-to-wall connections, allow improving the 'box-behavior' of the building, and led to the increase of the maximum capacity of the buildings up to almost three times. They can also transform the failure mode of the building from the characteristic local out-of-plane to an in-plane one, which is usually preferred. Other techniques such as buttresses are also effective in avoiding the out-of-plane failure of the walls by reducing the maximum free span and can thus significantly increase the overall strength of the building.

With respect to the reflection on the existence of a local seismic culture in the country, most of the techniques identified and evaluated within the present research work can also be identified in Portugal. Thus, although scarce and essentially abandoned, there are signs of a seismic culture that was active in the past. However, the loss of seismic awareness of the population resulting from the large periods of time without earthquakes has led to its abandonment. The signs of this past Portuguese local seismic culture mostly consist of the remains of the reactive response of the people to earthquakes right after the event, when the seismic concern was high. That is why the numerical validation carried out is important, since gaining confidence on the efficiency of these techniques can encourage reintroducing them in the vernacular building culture in order to reduce the seismic vulnerability of their constructions. The loss of knowledge on traditional materials and construction techniques that are many times considered unsafe has commonly led to their abandonment and substitution by modern ones. Therefore, the re-adoption of traditional techniques for the seismic strengthening of existing in-use vernacular architecture can also help to preserve this heritage in terms of compatibility and authenticity.

9.2.4. Recommendations of traditional strengthening solutions to reduce the seismic vulnerability of in-use vernacular architecture (Research objective 4)

The results obtained during the completion of the thesis have provided a deeper understanding regarding the seismic behavior of vernacular architecture and traditional strengthening solutions. Their effect on the seismic response of vernacular buildings has been studied at building and at urban level, which contributes to provide some general recommendations on how to apply traditional strengthening techniques to mitigate the seismic vulnerability of the in-use vernacular heritage.

As abovementioned, there is a range of techniques intended to improve the connection between structural elements that enhance the global behavior of the structure, by forming close contours in vertical and horizontal planes. Forces can be thus properly transmitted from one element to another, even through large deformations. Many are particularly aimed at improving wall-to-wall connections and, among them, ring beams are particularly effective because they are placed running continuously at the floor or lintel level, tying the building and the walls together, improving its 'box-behavior'. This technique was proved to engage all walls in the seismic response of the building, activating the in-plane response of load bearing walls, which can lead to significant increases of the maximum strength of the building.

Other techniques aimed at improving the wall-to-wall connections of the building are also efficient in engaging orthogonal walls and avoiding damage at the connection, but revealed a more moderate increase of the maximum capacity of the building. They are also not able to transform the failure mode of the building and, thus, do not significantly vary its seismic performance. For instance, the role of corner braces and quoins is similar in quantitative terms. However, quoins are practically impossible to implement other than at the time of construction or during partial reconstruction, while corner braces can be more easily applied for strengthening. Ties connecting perpendicular walls do not improve so significantly the maximum capacity of the building, but results show that they are efficient in partially restoring the integrity of the wall-to-wall connections that are deficient or degraded. This highly beneficial effect was also observed for the corner braces.

Several ways of reinforcing floor-to-wall and roof-to-wall connections using traditional solutions were presented and discussed, such as the use of wooden wedges or ties. The influence of the horizontal diaphragm in the seismic response of vernacular buildings was thoroughly evaluated. Particularly, results show the great importance of having a proper connection between walls and diaphragms in order to enhance the seismic behavior of the building. Even if the diaphragm is flexible, if properly connected, it can involve more elements in the seismic response of the building and, even partially, it can activate the walls in-plane response, altering the failure mode of the building and significantly enhancing its seismic behavior.

There is another type of techniques that are intended to stabilize the different structural elements of the building, such as the stiffening of floors and roofs. The parametric numerical analysis showed that the type of diaphragm was one of the parameters with the greatest influence on the seismic behavior of the building and on defining its maximum capacity. Results showed that the maximum load capacity obtained for a building presenting a rigid diaphragm properly connected to the wall can be up to three times the maximum load capacity obtained for a building presenting a very flexible diaphragm poorly connected to the load bearing walls. Thus, an efficient retrofitting strategy can always consist of addressing the horizontal diaphragms, by:

(a) improving their connection to the walls; and (b) stiffening them through diagonal bracing, triangulation or additional layers of sheathing boards.

The insertion of timber elements within the masonry was also evaluated and confirmed to have a significant impact on the seismic behavior of the building. This is a widespread traditional earthquake resistant technique that effectively ties the wall together and makes the building respond as a unit. Its effect is directly reflected in an increase of the maximum resistance of the building of approximately three times. However, its application as a strengthening technique is again difficult. A similar evaluated technique is the introduction of brick courses and the subdivision of the wall, which also modifies the wall typology aiming at its stabilization. It also improves the seismic behavior of the building, but more moderately. It is acknowledged that both techniques also help in reducing the risk of delamination of the walls leaves in the case of masonry walls, even though this effect was not taken into consideration by the numerical models.

The type and quality of the material used for the construction of the walls was also confirmed to be one of the most influential parameters in defining the seismic response of the building. That is why those solutions that help in improving the quality of the masonry fabric can be very efficient in strengthening the walls. For example, using through-stones or other types of transversal connectors helps to prevent the delamination or separation of the wall leaves, improving its monolithic behavior. The presence of transversal connection elements can significantly improve the cross-section morphology and, thus, the stability of the wall. Several traditional ways of reinforcing the openings were explored that can also provide this function. For example, the use of embedded discharging arches or properly linked double timber window frames. Besides, these elements lead to a better distribution of the load and avoid stress concentration at the openings.

Vernacular buildings showing a poor state of conservation or even abandoned will result in a compromising structural performance in the event of an earthquake. The presence of structural damage in structural walls will accelerate the formation of damage and significantly decrease the maximum capacity of the building. That is why any retrofitting strategy should always include the repairing of existing cracks, aimed at recovering their original integrity, together with the proper conservation intervention of all the structural elements, such as floors and roofs.

Another identified and discussed technique was the use of timber frames as the earthquake resistant construction system for the building, but its numerical evaluation was out of the scope of the present research work. Nonetheless, the good seismic performance of timber frame traditional structures was reported and their use was identified in many seismic prone regions throughout the world. Particular types of timber frame walls are also used as secondary structural systems in some vernacular buildings, in order to introduce structural redundancy and thus allowing the partial collapse and failure of certain members. In all cases, timber frame

construction typologies have to be implemented at the time of the construction of the building. Otherwise, new structural elements have to be introduced in the building, which can result in a rather invasive intervention.

The last type of traditional techniques evaluated during this research are those intended to directly counteract the horizontal loads exerted by the buildings during the shaking by adding extra resistance through the introduction of new typically massive structural elements on the façade. Buttresses are the most common earthquake resistant technique of this type, but other similar elements that can fulfill the same function are, for example, urban reinforcing arches. The latter are a typical option in those buildings set in an urban environment. When these elements are located within the span of the wall, they mainly contribute to reduce effectively the maximum free span of the walls subjected to out-of-plane loading. However, they have to be properly connected to the walls. Otherwise, their effect could be counterproductive and could even introduce a new source of loading, as they could be prone to rock against the existing wall. Nevertheless, if properly connected and placed, the parametric analysis showed that these elements can almost double the overall resistance of the building. With respect to buttresses placed at the corners of the building, their effect directly addresses the quality of the wall-to-wall connections and can also improve the maximum capacity of the building, but less notably. The last traditional technique discussed and numerically evaluated consisted of thickening the walls and increasing the resisting cross-section, which results in a reduction of the wall slenderness and thus in an increase of the maximum capacity of the building. Results showed that the performance of the building is better when considering an inclined wall, since the cross-section increases, while the mass at the top is reduced, lowering the center of gravity of the wall.

Certainly, the preparation of guidelines on how to address a proper seismic strengthening intervention in existing vernacular buildings is necessarily a simplification, given the complexity of the matter. That is why this research thesis focused more on the understanding of the structural concept behind the different traditional techniques. To detect the seismic deficiencies of the building is a first step, in order to identify the need of reinforcing a particular construction aspect. In this case, the geometrical, structural and material parameters that seem to have the greatest influence on the seismic behavior of vernacular buildings were thoroughly studied. Results have shown how the seismic response of the building varies with the variations of these parameters and how improving the seismic vulnerability classification of these parameters results in a better seismic performance of the building. Once the particular parameter that needs to be ameliorated is identified, there will be always several different ways of addressing the retrofitting. This work has particularly presented many examples of traditional solutions that served as an illustration of how vernacular builders have approached these issues in several regions throughout the world that usually suffer the effect of earthquakes. They are the result of a local seismic culture and the work has shown that the empirical understanding of local

communities is most of the times correct, since these solutions are actually efficient in mitigating the seismic vulnerability of vernacular constructions.

9.2.5. Thesis outcomes

Besides the main conclusions outlined and the answer to the research objectives provided, the present thesis also contributes to the protection of the vernacular heritage by generating several quantitative outcomes. The following outcomes are considered ready-to-use tools that can be helpful for the seismic vulnerability assessment of existing vernacular architecture earthquake preparedness:

SVIVA method: even though the Seismic Vulnerability Index for Vernacular Architecture (SVIVA) method is mainly an adaptation of existing vulnerability index methods, the seismic vulnerability parameters, classes and weights have been determined on the basis of numerical and statistical analysis. This helped to strengthen the robustness of previous existing methods.

SAVVAS method: the Seismic Assessment of the Vulnerability of Vernacular Architecture Structures (SAVVAS) method can be considered as the main quantitative outcome of the thesis. It is considered as a novel method for the assessment of vernacular structures and it has been validated and calibrated with several case studies.

Numerical database: the extensive numerical parametric study carried out has resulted in a database composed by the results of the pushover analyses performed on a total of 567 models. This database was the basis for the preparation of the expressions from the SAVVAS method. However, it can be considered as a starting point, since it can be enlarged in the future with more results. The addition of more results can lead to increase the comprehensiveness and the precision of the models developed for the SAVVAS method. It is noted that the database is provided entirely in Annex B.

Guidelines for the application of the SAVVAS method: the buildings survey required for the application of both the SVIVA and the SAVVAS methods is one of the most important steps in order to obtain proper results. The calibration and application of the methods allowed withdrawing some conclusions on how to carry out this survey. As a result, some guidelines particularly addressing the application of the SAVVAS method were prepared and are provided in Annex D.

SAVVAS method application: Finally, it is worth highlighting that the SAVVAS method is a ready-to-use tool for technicians and decisions makers to perform risk assessment and management in urban areas. It can help for example in the definition of public safety policies related with building rehabilitation and population awareness, among others. A website application is under development for an easier implementation of the SAVVAS method by the decision makers, which can use it to define strategies and intervention priorities. It is noted that

this application is intended to be used for *in-situ* seismic assessment at the building level. Thus, this application can become very helpful and eventually can be distributed and promoted among city councils, regional authorities and professionals, together with the guidelines of application.

9.3. Future research

The present thesis dealt with the assessment of the vernacular architecture earthquake preparedness and the mitigation of its seismic vulnerability using traditional earthquake resistant solutions, which is an exceptionally wide area of research. The current work addressed the response to the research objectives raised at the beginning, but several new continuing research lines were identified during its development. The present thesis set the basis for further research that can improve the knowledge regarding the two most important aspects of the study: (1) a better understanding of traditional seismic resistant solutions; and (2) new seismic vulnerability assessment methods.

With respect to the understanding of the structural behavior of traditional earthquake resistant techniques, the current knowledge is still limited. Experimental work is recommended for this matter. The different traditional solutions identified and recognized should be characterized *in-situ*. An experimental campaign can also be planned in order to replicate and test the different techniques at the laboratory. This approach can be used to further confirm and validate the numerical results.

The research work has focused on the study of a common vernacular typology that consists of buildings that present timber diaphragms as the horizontal structural element coupled with earthen and stone masonry load bearing walls, which are the main vertical resisting elements of the structure. Thus, some vernacular typologies, such as timber frame constructions, which were recognized as a widespread seismic resistant solution, were out of the scope of the thesis. Further research is recommended on this typology and on some particular solutions that involve timber frames, such as those that are meant to achieve redundancy of structural elements. The results of this numerical research can eventually serve also to introduce this typology within the seismic vulnerability assessment methods developed.

Additionally, an assessment of the efficiency of current seismic strengthening solutions on vernacular constructions is also recommended. The findings could be compared in terms of their efficiency in increasing the seismic capacity of the building with respect to the results obtained using the traditional solutions identified within this research. This comparison should also be done in economic terms, obtaining a more accurate understanding of the implementation costs of different traditional and modern traditional solutions. This can lead to perform a more robust cost-benefit analysis that the one shown as an example in the present work.

With respect to the seismic vulnerability assessment methods developed in the present thesis, continuing lines of research were also detected mainly related to the enhancement of the SAVVAS method, which is the innovative method presented. The first research line identified involves the two methods developed within the thesis and consists of the extension of the parameters selected. Particularly, the parameters related with the interaction between neighboring buildings were left out of the scope of the research work because of time limitations. However, they are considered to have an important role in defining the seismic behavior of urban buildings. Several parameters related to them were identified for future research, namely: (a) the position of the building within the aggregate; (b) the relative height of the building within the aggregate; (c) the presence of staggered floors; (d) the typological heterogeneity among adjacent units; and (e) the difference in percentage of opening areas among adjacent façades. Following the same numerical approach shown within this research, the effect of these parameters on the seismic behavior of vernacular buildings should be evaluated and included within the seismic vulnerability assessment methods that were proposed.

Another important parameter that could be further numerically evaluated for future inclusion within the seismic vulnerability assessment methods is the one addressing structural alterations. Vernacular constructions are continuously subjected to modifications because of the new needs of the users along the years. The effect of these alterations in the seismic vulnerability of the building can be of great importance, because it involves the consideration of new construction and structural aspects. The most common structural alterations identified in vernacular architecture should be characterized, such as the replacement of existing floors and roofs with concrete slab and the enlargement of openings. These alterations were systematically recognized, for example, in Vila Real de Santo António. The quantitative assessment of their influence can then be carried out in a similar way as the one shown in the present research.

Concerning the particularities and limitations of the SAVVAS method, the research highlighted that it was conceived to predict the results that would be obtained in the same way as if when performing a pushover analysis on a structure with the same characteristics. Therefore, the method has the same limitations and assumptions existing for the pushover analyses. Despite being a simplified procedure because of simulating the earthquake loading as a set of equivalent static forces, pushover analyses were selected due to the relatively low computation demand in comparison with other methods, such as nonlinear dynamic analysis. Nonetheless, different types of analyses can also be recommended to be carried out to strengthen the reliability of the method proposed and for further validation. Moreover, the database used for the development of the method can always be further enlarged with more results in order to make it more comprehensive.

Also, the definition of the collapse was identified as one of the main limitations of the SAVVAS method. The method is determined on the basis of load factors that can be directly

associated to equivalent static horizontal actions that the buildings can withstand before reaching specific structural limit states, regardless of the type of failure that the building would suffer. It is acknowledged the limitations of considering loads instead of displacements for the seismic assessment, since some aspects, such as the ductility of the structure, are not considered. However, loads provide a good representative indicator of the maximum building's seismic capacity in different loading directions. Besides this, certain limit states corresponding to damage levels can be associated to specific values of load factors. These limit states are defined taking into consideration the overall damage state of the building and not only individual structural elements composing the buildings. Thus, the load factors are representative of the global behavior of the buildings under analysis and establish the basis of comparison between the different buildings in order to define which are more vulnerable than others. The definition of the different limit states could only be done directly based on the results of the numerical parametric study for the limit states associated to light damage (LS1), damage limitation (LS2) and life safety (LS3). The limit state associated to the collapse (LS4) was initially defined in terms of displacement and could not be determined in terms of loads for the SAVVAS method. Therefore, LS4 was defined using an empirically devised factor of 1.25 of the maximum load factor corresponding to LS3. This approach was validated with the results of the application of the method on the case study of Faial Island, in Azores. However, further research on these issues is recommended.

In summary, the entailed research contributed not only for knowledge, but also for the protection of the vernacular heritage, opening important future lines of research. Continuing with these research lines is fundamental, since the findings have an important impact in society and, therefore, in people's life, by providing a safer built environment regarding in-use vernacular architecture, which is inhabited by a significant percentage of the planet's population.

REFERENCES

- AIS (2005) Manual para la rehabilitación de viviendas construidas en adobe y tierra pisada, Asociación Colombiana de Ingeniería Sísmica (AIS)
- Aguilar V, Sandoval C, Adam JM, Garzón-Roca J, Valdebenito G (2016) Prediction of the shear strength of reinforced masonry walls using a large experimental database and artificial neural networks, *Structure and Infrastructure Engineering* 12 (12): 1661-1674
- Aleksander I, Morton H (1990) An introduction to neural computing, Chapman & Hall
- Angulo-Ibáñez Q, Mas-Tomás Á, Galvañ-Llopis V, Sántolaria-Montesinos JL (2012) Traditional braces of earth constructions, *Construction and Building Materials* 30: 389-399
- ATC-13 (1985) Earthquake damage evaluation data for California, Applied Technology Council (ATC), Redwood City, California, USA
- ATC-40 (1996) Seismic evaluation and retrofit of concrete buildings, Applied Technology Council (ATC), Redwood City, California, USA
- Audefroy JF (2011) Haiti: post-earthquake lessons learned from traditional construction, *Environment and Urbanization* 23 (2): 447-462
- Azizi-bondarabadi H, Mendes N, Lourenço PB, Sadeghi NH (2016) Empirical seismic vulnerability analysis for masonry buildings based on school buildings survey in Iran, *Bulletin of Earthquake Engineering* 14 (11): 3195-3229
- Benouar D, Foufa AA (2008) Investigation of the 1716 Algiers (Algeria) Earthquake and the traditional seismic preventive measures from historical document sources, in: Proc. of the 14th World Conference on Earthquake Engineering, Beijing, China
- Barbat A, EERI M, Yépez Moya F, Canas JA (1996) Damage Scenarios Simulation for Seismic Risk Assessment in Urban Zones, *Earthquake Spectra* 12 (3): 371-394
- Barbisan U, Laner F (1995) Wooden floors: part of historical antiseismic building systems, in: Bosch, Funicello, Guidoboni & Rovelli (eds), *Earthquakes in the past. Multidisciplinary approaches*, *Annals of Geophysics* 38: 775-784
- Baykasoglu A, Güllü H, Çanakçı H, Özbakir L (2008) Prediction of compressive and tensile strength of limestone via genetic programming, *Expert Systems with Applications* 35: 111-123

- Benedetti D, Petrini V (1984) Sulla Vulnerabilità Di Edifici in Muratura: Proposta Di Un Metodo Di Valutazione, *L'industria delle Costruzioni* 149 (1): 66-74
- Benedetti D, Carydis P, Pezzoli P (1998) Shaking table tests on 24 simple masonry buildings, *Earthquake Engineering and Structural Dynamics* 27: 67-90
- Betti M, Vignoli A (2011) Numerical assessment of the static and seismic behaviour of the basilica of Santa Maria all'Impruneta (Italy), *Construction and Building Materials* 25 (12): 4308-4324
- Betti M, Galano L, Vignoli A (2014) Comparative analysis on the seismic behaviour of unreinforced masonry buildings with flexible diaphragms, *Engineering Structures* 61: 195-208
- Binda L, Penazzi D (2000) Classification of masonry cross sections and of typologies of historic buildings, Technical Report, Book of Commission RILEM MMM
- Binda L, Saisi A (2001) State of the Art of Research on Historic Structures in Italy, Department of Structural Engineering, Politecnico di Milano, Milan, Italy
- Bishop CM (1995) *Neural Networks for Pattern Recognition*, Clarendon Press, Oxford
- Blondet M, Villa García GM, Brzev S, Rubiños A (2011) Earthquake-resistant construction of adobe buildings: a tutorial, Earthquake Engineering Research Institute (EERI), Oakland, California, USA
- Bothara J, Hiçyılmaz K (2008) General observations of building behaviour during the 8th October 2005 Pakistan earthquake, *Bulletin of the New Zealand Society for Earthquake Engineering* 41 (4): 209-233
- Bothara J, Brzev S (2012) A tutorial: improving the seismic performance of stone masonry buildings, Earthquake Engineering Research Institute (EERI), Oakland, California, USA
- Boukri M, Bensaïbi M (2008) Vulnerability Index of Algiers Masonry Buildings, in: Proc. of 14th World Conference on Earthquake Engineering, Beijing, China
- Braga F, Dolce M, Liberatore O (1982) A statistical study on damaged buildings review of the MSK-76 scale, in: Proc. of the Conference of the European Association of Earthquake Engineering, Athens, Greece
- Braga A, Estevão J (2010) Os Sismos e a Construção em Taipa no Algarve, in: Proc. of Sísmica 2010 – 8º Congresso de Sismologia e Engenharia Sísmica, Aveiro, Portugal
- Bramerini F, Di Pasquale G, Orsini A, Pugliese A, Romeo R, Sabetta F (1995) Rischio sismico del territorio italiano. Proposta per una metodologia e risultati preliminary, Rapporto tecnico del Servizio Sismico Nazionale (SSN), Roma, Italy
- Brignola A, Podestà S, Pampanin S (2008) In-plane stiffness of wooden floor, in: Proc. of New Zealand Society for earthquake engineering conference

- Brignola A, Pampanin S, Podestà S (2012) Experimental evaluation of the in-plane stiffness of timber diaphragms, *Earthquake Spectra* 28 (4): 1687-1709
- Bui QB, Morel JC, Hans S, Meunier N (2008) Compression behaviour of non-industrial materials in civil engineering by three scale experiments: the case of rammed earth, *Materials and Structures* 42 (8): 1101-1116
- Calvi GM (1999) A Displacement-Based Approach for Vulnerability Evaluation of Classes of Buildings, *Journal of Earthquake Engineering* 3 (3): 411-438
- Calvi GM, Pinho R, Magenes G, Bommer JJ, Restrepo-Vélez LF, Crowley H (2006) Development of seismic vulnerability assessment methodologies over the past 30 years, *ISET Journal of Earthquake Technology* 34 (472): 75-104
- Cardani G, Giaimi P, Belluco P, Binda L (2015) A simplified method of analysis to define the seismic vulnerability of complex buildings in historic centres, in: *Proc. of 12th North American Masonry Conference, Denver, Colorado*
- Cardoso R, Lopes M, Bento R (2004) Earthquake resistant structures of Portuguese old 'Pombalino' buildings, in: *Proc. of the 13th World Conference on Earthquake Engineering, Vancouver BC, Canada*
- Cheng Vong U (2016) Assessment of Seismic Vulnerability of Vernacular Buildings in Urban Centers: The Case Study of Vila Real de Santo Antonio, M.Sc. thesis, Universidade do Minho, Guimarães, Portugal
- Correia J (1997) Vila Real de Santo António. Urbanismo e Poder na Política Pombalina, Ph.D. thesis, Faculdade de Arquitectura da Universidade de Porto, Portugal
- Correia M, Merten J (2001) Preliminary report of the local seismic culture in Portugal, in: *Taversism project – Atlas of local seismic cultures, European University Centre for Cultural Heritage (EUCCH), Ravello, Italy*
- Correia M (2002) A habitação vernácula rural no Alentejo, Portugal, in: *Memorias del IV Seminario Iberoamericano sobre vivienda rural y calidad de vida en los asentamientos rurales, Santiago del Chile, Chile*
- Correia M (2007) *Taipa no Alentejo, Argumentum, Lisboa, Portugal*
- Correia M, Carlos G, Rocha S, Lourenço PB, Vasconcelos G, Varum H (2014) SEISMIC-V: vernacular seismic culture in Portugal, in: *Correia, Carlos & Rocha (eds), Vernacular heritage and earthen architecture: contributions for sustainable development, pp. 663-668, Taylor & Francis Group, London, UK*
- Correia M, Carlos G (2015) *Cultura sísmica local em Portugal. Local seismic culture in Portugal, Argumentum, Lisboa, Portugal*

- Correia M, Lourenço PB, Varum H (2015) *Seismic Retrofitting: Learning from Vernacular Architecture*, Taylor & Francis Group, London, UK
- Correia M (2017) Experiences from past for today's challenges, in: *The road to sustainable development. Chapter 6 – Traditional and generational change*, La fábrica, Fundación Contemporánea, Madrid, Spain
- Cortez P (2010) Data Mining with Neural Networks and Support Vector Machines Using the R/rminer Tool, in: *Proc. of 10th Industrial Conference, ICDM 2010*, Berlin, Germany
- Costa A (2002) Determination of mechanical properties of traditional masonry walls in dwellings of Faial Island, Azores, *Earthquake Engineering and Structural Dynamics* 31 (7): 1361-1382
- Costa A, Arêde A (2006) Strengthening of structures damaged by the Azores earthquake of 1998, *Construction and Building Materials* 20 (4): 252-268
- Costa AA, Arêde A, Costa A, Oliveira CS (2011) In situ cyclic tests on existing stone masonry walls and strengthening solutions, *Earthquake Engineering and Structural Dynamics* 40 (4): 449-471
- Costa AA, Arêde A, Campos Costa A, Penna A, Costa A (2013) Out-of-plane behaviour of a full scale stone masonry façade. Part 1: specimen and ground motion selection, *Earthquake Engineering and Structural Dynamics* 42: 2081-2095
- Cutter S (1996) Vulnerability to environmental hazards, *Progress in Human Geography* 20 (4): 529-539
- D'Ayala DF, Speranza E (2003) Definition of Collapse Mechanisms and Seismic Vulnerability of Historic Masonry Buildings, *Earthquake Spectra* 19 (3): 479-509
- D'Ayala DF, Paganoni S (2011) Assesment and analysis of damage in L'Aquila historic city centre after 6th April 2009, *Bulletin of Earthquake Engineering* 9 (1): 81-104
- D'Ayala DF (2014) Conservation principles and performance based strengthening of heritage buildings in post-event reconstruction, in: Ansal (ed), *Perspectives on European Earthquake Engineering and Seismology*, Volume 1: 489-514, Springer
- De Felice G (2011) Out-of-plane seismic capacity of masonry depending on wall section morphology, *International Journal of Architectural Heritage. Conservation, Analysis and Restoration* 5 (4-5): 466-482
- Degg MR, Homan J (2005) Earthquake vulnerability in the Middle East, *Geography* 90 (1): 54-66
- Di Pasquale G, Orsini G, Romeo RW (2005) New developments in seismic risk assessment in Italy, *Bulletin of Earthquake Engineering* 3: 101-128

- Diz S, Costa A, Costa AA (2015) Efficiency of strengthening techniques assessed for existing masonry buildings, *Engineering Structures* 101: 205-215
- Dolce M, Masi A, Marino M, Vona M (2003) Earthquake Damage Scenarios of the Building Stock of Potenza (Southern Italy) Including Site Effects, *Bulletin of Earthquake Engineering* 1 (1): 115-140
- Dolce M, Kappos A, Masi A, Penelis G, Vona M (2006) Vulnerability assessment and earthquake damage scenarios of the building stock of Potenza (southern Italy) using Italian and Greek methodologies, *Engineering Structures* 28 (3): 357-371
- Dubois D, Parade H (1980) *Fuzzy sets and systems*, Academic Pres, New York, USA
- Erberick MA (2008) Generation of fragility curves for Turkish masonry buildings considering in-plane failure modes, *Earthquake Engineering and Structural Dynamics* 37: 387-405
- Esri (2017) *Environmental Systems Research Institute (ESRI), Inc.*
- Fajfar P (1999) Capacity spectrum method based on inelastic demand spectra. *Earthquake Engineering and Structural Dynamics* 28: 979-993
- Fayyad U, Piatetsky-Shapiro G, Smyth P (1996) From Data Mining to Knowledge Discovery in Databases, *AI Magazine* 17 (3): 37-54
- Fernandes J, Mateus R (2012) Energy efficiency principles in Portuguese vernacular architecture, in: *Proc. of International Conference BSA, Porto, Portugal*
- Ferreira TM (2009) *Avaliação da vulnerabilidade sísmica das paredes de fachada de edifícios em alvenaria*, M.Sc. thesis, Universidade de Aveiro, Aveiro, Portugal
- Ferreira TM, Vicente R, Varum H, Costa A, Costa AA (2012) Out-of-plane seismic response of stone masonry walls: Experimental and analytical study of real piers, in: *Proc. of the 15th world conference on earthquake engineering, Lisbon, Portugal*
- Ferreira TM, Santos C, Vicente R, Mendes JAR (2013a) Caracterização arquitectónica e construtiva do património edificado do núcleo urbano do antigo Seixal, *Conservar Património* 17: 21-38
- Ferreira TM, Vicente R, Mendes da Silva JAR, Varum H, Costa A (2013b) Seismic vulnerability assessment of historical urban centres: case study of the old city centre in Seixal, Portugal, *Bulletin of Earthquake Engineering* 11 (5): 1753-1773
- Ferreira TM, Vicente R, Varum H (2014) Seismic vulnerability assessment of masonry facade walls: development, application and validation of a new scoring method, *Structural Engineering and Mechanics* 50 (4): 541-561

- Ferreira TM (2014) Out-of-plane seismic performance of stone masonry walls: experimental and analytical assessment, Ph.D. thesis, Universidade do Aveiro, Aveiro, Portugal
- Ferreira TM, Maio R, Vicente R (2017) Seismic vulnerability assessment of the old city centre of Horta, Azores: calibration and application of a seismic vulnerability index method, *Bulletin of Earthquake Engineering* 15 (7): 2879-2899
- Ferrigni F (1990) S. Lorenzello, à la recherche des anomalies qui protègent, Conseil de l'Europe et Centre universitaire européen pour les biens culturels, Ravello, Italy
- Ferrigni F, Helly B, Mauro A, Mendes Victor L, Pierotti P, Rideaud A, Teves Costa P (2005) Ancient buildings and earthquakes. The local seismic culture approach: principles, methods, potentialities, Centre universitaire européen pour les biens culturels, Edipuglia srl, Ravello, Italy
- Field A, Miles J, Field Z (2012) *Discovering Statistics Using R*, SAGE Publishing
- Figueiras R (1999) Vila Pombalina: Vila Real de Santo António, Câmara Municipal de Vila Real de Santo António, Vila Real de Santo António, Portugal
- Formisano A, Florio G, Landolfo R, Mazzolani FM (2011) Numerical Calibration of a Simplified Procedure for the Seismic Behaviour Assessment of Masonry Building Aggregates, in: *Proc. of the 13th Int. Conf. Civil, Struct. Environ. Eng. Comput.* Stirlingshire, Scotland
- Foufa AA, Benouar D (2005) Atlas of earthquake-resistant traditional techniques in Algeria: the case of the Casbah of Algiers, *European Earthquake Engineering J.* 2 (5): 23-39
- Fritsch S, Günther F, Suling M, Müller S (2016) Package 'neuralnet', R manual
- Gallego R, Arto I (2014) Evaluation of seismic behaviour of rammed earth structures, in: Mileto, Vegas, Soriano & Cristini (eds), *Earthen architecture: past, present and future*, Taylor & Francis Group, London, UK
- Garnier P, Moles O (2012) *Natural hazards, disasters and local development. Cultures constructives et développement durable*, CRAterre Éditions, Grenoble, France
- Garzón-Roca J, Marco C, Adam JM (2013a) Compressive strength of masonry made of clay bricks and cement mortar: Estimation based on neural networks and fuzzy logic, *Engineering Structures* 48: 21-27
- Garzón-Roca J, Adam JM, Sandoval C, Roca P (2013b) Estimation of the axial behavior of masonry walls based on artificial neural networks, *Computers and Structures* 125: 145-152
- Gautam D, Prajapati J, Paterno KV, Bhetwal KK, Neupane P (2016) Disaster resilient vernacular housing technology in Nepal, *Geoenvironmental Disasters* 3 (1)
- Giardini D, Grünthal G, Shedlock KM, Zhang P (1999) The GSHAP global seismic hazard map, *Annals of Geophysics* 42 (6): 1225-1230

- Giongo I, Dizhur D, Tomasi R, Ingham J (2014) Field testing of flexible timber diaphragms in an existing vintage URM building, *Journal of Structural Engineering* 141 (1), Special issue: field testing of bridges and buildings
- Giovinazzi S, Lagomarsino S (2004) A macroseismic model for the vulnerability assessment of buildings, in: *Proc. of 13th world conference on earthquake engineering*, Vancouver BC, Canada
- Giovinazzi S (2005) The vulnerability assessment and the damage scenario in seismic risk analysis, Ph.D. thesis, University of Florence (Italy) and Technical University Carolo-Wilhelmina at Braunschweig (Germany)
- Giovinazzi S, Lagomarsino S (2005) Fuzzy-random approach for a seismic vulnerability model, in: *Proc. of International Conference on Structural Safety and Reliability*, pp. 2853-2861
- Giuffrè (1993) *Sicurezza en conservazione dei centri storici: Il caso Ortigia*, Editrice Laterza, Bari, Italy
- GNDT (1994) Scheda di esposizione e vulnerabilità e di rilevamento danni di primo livello e secondo livello (muratura e cemento armato), Gruppo Nazionale per la Difesa dai Terremoti (GNDT), Rome, Italy
- Gomes MI, Lopes M, de Brito J (2011) Seismic resistance of earth construction in Portugal, *Engineering Structures* 33 (3): 932-941
- Gonçalves A (2005) Caracterização do Núcleo Pombalino, *ECDJ* 9: 18-35, Universidade de Coimbra, Portugal
- Gonçalves A (2009) Vila Real de Santo António. Planeamento de pormenor e salvaguarda em desenvolvimento, *Monumentos* (30): 40-53
- Grünthal G (1998) European Macroseismic Scale 1998 (EMS-98), European Seismological Commission, Subcommission on Engineering Seismology. Working Group Macroseismic Scales, *Cahiers du Centre Européen de Géodynamique et de Séismologie* 15
- Guagenti E, Petrini V (1989) Il caso delle vecchie costruzioni: verso una legge danni-intensità, in: *Proc. of 4th Italian National Conference on Earthquake Engineering*, pp. 145-153, Milan, Italy
- Gülhan D, Gürney İÖ (2000) The behaviour of traditional building systems against earthquakes and its comparison to reinforced concrete frame systems: experiences of Marmara earthquake damage assessment studies in Kocaeli and Sakarya, in: *Proc. of the International Conference on the Seismic Performance of Traditional Buildings*, Istanbul, Turkey
- Günther F, Fritsch S (2010) neuralnet: Training of Neural Networks, *The R Journal* 2 (1): 30-38
- Halvorson SJ, Hamilton JP (2009) Vulnerability and the erosion of seismic culture in mountainous Central Asia, *Mountain Research and Development* 27 (4): 322-330

- Harker PT (1987) Incomplete pairwise comparisons in the analytic hierarchy process, *Mathematical Modelling* 9 (11): 837-848
- Haykin S (1999) *Neural Networks – A comprehensive Foundation*, Prentice-Hall, New Jersey, USA
- HAZUS (1999) *HAZUS earthquake loss estimation methodology: technical manual, Vol. 1*, Federal Emergency Management Agency (FEMA), Washington D.C., USA
- Homan J (2004) *Seismic cultures: myth or reality?*, in: *Proc. of Second International conference on post-disaster reconstruction: planning for reconstruction*, Coventry University, UK
- Hughes R (2000) *Cator and Cribbage construction in Northern Pakistan*, in: *Proc. of the International Conference on the Seismic Performance of Traditional Buildings*, Istanbul, Turkey
- Hurd J (2009) *Observing and applying ancient repair techniques to piers and adobe in seismic regions of Central Asia and Trans-Himalaya*, in: *Proc. of the Getty Seismic Adobe Project 2006 Colloquium*, Getty Conservation Institute (GCI), Los Angeles, USA
- Hyams DG (2017) *CurveExpert Professional Documentation, Release 2.6.4.*, Hyams Development
- ICOMOS (1964) *The Venice Charter*, International Council of Monuments and Sites (ICOMOS), Venice, Italy
- ICOMOS (1999) *Charter on the built vernacular heritage*, International Council of Monuments and Sites (ICOMOS), ICOMOS 12th General Assembly, Mexico
- Inan Z (2014) *Runner beams as building element of masonry walls in Eastern Anatolia, Turkey*, in: *Correia, Carlos & Rocha (eds), Vernacular heritage and earthen architecture: contributions for sustainable development*, pp. 721-726, Taylor & Francis Group, London, UK
- IS-13287 (1993) *Improving earthquake resistance of earthen buildings – Guidelines*, Bureau of Indian Standards (BIS), New Delhi, India
- IS-13288 (1993) *Improving earthquake resistance of low strength masonry building – Guidelines*, Bureau of Indian Standards (BIS), New Delhi, India
- Jaquin P (2008) *Analysis of historic rammed earth construction*, Ph.D. thesis, Durham University, UK
- Jain S (1998) *Indian earthquakes: an overview*, *Indian Concrete Journal* 72 (11): 555-562
- Jaiswal K, Aspinall W, Perkins D, Wald D, Porter KA (2012) *Use of expert judgement to estimate seismic vulnerability of selected building types*, in: *Proc. of 15th World Conference on Earthquake Engineering*, Lisbon, Portugal

- Jigyasu R (2002) Reducing disaster vulnerability through local knowledge and capacity. The case of earthquake prone rural communities in India and Nepal, Ph.D. thesis, Norwegian University of Science and Technology, Trondheim, Norway
- Kallioras S, Guerrini G, Tomassetti U, Marchesi B, Penna A, Graziotti F (2018) Experimental seismic performance of a full-scale unreinforced clay-masonry building with flexible timber diaphragms, *Engineering Structures* 161: 231-249
- Karakostas C, Lekidis V, Makarios T, Salonikios T, Sous I, Demosthenus M (2005), Seismic response of structures and infrastructures facilities during the Lefkada, Greece earthquake of 14/8/2003, *Engineering Structures* 27 (2): 213-227
- Karanikoloudis G, Lourenço PB (2016) Seismic assessment of Kuño Tambo Church (strengthening proposal), Peru, Technical Report 2016-DEC/E-10, Universidade do Minho, Guimarães, Portugal
- Kottegodo N, Rosso R (2008) *Applied Statistics for Civil and Environmental Engineers*, Blackwell Publishing, New Jersey, USA
- Lagomarsino S, Giovinazzi S (2006) Macro seismic and mechanical models for the vulnerability assessment of current buildings, *Bulletin of Earthquake Engineering* 4 (4): 415-433
- Lagomarsino S, Penna A, Galasco A, Cattari S (2013) TREMURI program: An equivalent frame model for the nonlinear seismic analysis of masonry buildings, *Engineering Structures* 56: 1787-1799
- Langenbach R (2007) From 'Opus Craticium' to the 'Chicago Frame': Earthquake-Resistant Construction, *International Journal of Architectural Heritage. Conservation, Analysis and Restoration* 1 (1): 29-59
- Langenbach R (2009) Don't tear it down! Preserving the earthquake resistant vernacular architecture of Kashmir, UNESCO, New Delhi, India
- Langenbach R, Kelly S, Sparks P, Rowell K, Hammer M, Julien OJ (2010) Preserving Haiti's Gingerbread Houses. 2010 Earthquake and Mission Report, World Monuments Fund, New York, USA
- Lantada N, Pujades LG, Barbat AH (2004) Risk Scenarios for Barcelona, Spain, in: Proc. of 13th World Conference on Earthquake Engineering, Vancouver BC, Canada
- Liu YC, Chen CS (2007) A new approach for application of rock mass classification on rock slope stability assessment, *Engineering Geology* 89 (1-2): 129-143
- LNEC (1986) A sismicidade histórica e a revisão do catálogo sísmico, Laboratório Nacional de Engenharia Civil (LNEC), Lisboa, Portugal

- Lopes dos Santos V (1994) O sistema construtivo Pombalino em Lisboa em edifícios urbanos agrupados de habitação colectiva – estudo de um legado humanista da segunda metade do séc. XVIII, Ph.D. thesis, FAUTL, Lisboa, Portugal
- Lourenço PB, Krakowiak F, Fernandes FM, Ramos LF (2007) Failure analysis of Monastery of Jerónimos, Lisbon: how to learn from sophisticated numerical models, *Engineering Failure Analysis* 14: 280-300
- Lourenço PB (2009) Recent advances in masonry structures: micromodelling and homogenization, in: Galvanetto & Ferri Aliabadi (eds), *Multiscale modeling in solid mechanics: computational approaches*, pp. 280-300, Imperial College Press, London, UK
- Lourenço PB, Mendes N, Ramos LF, Oliveira DV (2011) Analysis of masonry structures without box-behavior, *International Journal of Architectural Heritage. Conservation, Analysis and Restoration* 5 (4-5): 369-382
- Lourenço PB, Oliveira DV, Leite JC, Ingham JM, Modena C, Porto F (2013) Simplified indexes for the seismic assessment of masonry buildings: International database and validation, *Engineering Failure Analysis* 34: 585-605
- Lourenço PB, Karanikoloudis G, Mendes N, Corallo C (2015) Assessment of the South aisle in Canterbury, in: *Proc. of the 2nd International conference on preservation, maintenance and rehabilitation of historical buildings and structures*, Porto, Portugal
- Lourenço PB, Karanikoloudis G, Greco F (2016) In situ testing and modeling of cultural heritage buildings in Peru, in: *Proc. of the 10th International conference on structural analysis of historical constructions (SAHC 2016)*, Leuven, Belgium
- Lozano G, Lozano A (1995) Curso de técnicas de intervención en el patrimonio arquitectónico. Tomo 1. Reestructuración en madera, Ed. Cons. Técn. de Contrucción CB, Gijón, Spain
- Magenes G, Penna A, Senaldi IE, Rota M, Galasco A (2014) Shaking Table Test of a Strengthened Full-Scale Stone Masonry Building with Flexible Diaphragms, *International Journal of Architectural Heritage. Conservation, Analysis and Restoration* 8: 349-375
- Mallardo V, Malvezzi R, Milani E, Milani G (2008) Seismic vulnerability of historical masonry buildings: a case study in Ferrara, *Engineering Structures* 30: 2223-2241
- Marahatta P (2008) Earthquake vulnerability and Newari buildings: a study of indigenous knowledge in traditional building technology, *Vaastu: the Annual Journal of Architecture* 10
- Margottini C, Molin D, Serva L (1992) Intensity versus ground motion: a new approach using Italian data, *Engineering Geology* 33: 45-58
- Marques R, Lourenço PB (2013) A model for pushover analysis of confined masonry structures: implementation and validation, *Bulletin of Earthquake Engineering* 11: 2133-2150

- Martins F, Vasconcelos G, Miranda T (2014) The performance of ultrasonic pulse velocity on the prediction of tensile granite behaviour: a study based on artificial neural networks, in: Proc. of 9th International Masonry Conference, Guimarães, Portugal
- Mascarenhas JMD (1996) A study of the design and construction of buildings in the Pombaline quarter, Ph.D. thesis, University of Glamorgan, UK
- Masciotta MG, Ramos LF, Lourenço PB, Matos JAC (2016) Development of Key Performance Indicators for the Structural Assessment of Heritage Buildings, in: Proc. of 8th European Workshop on Structural Health Monitoring (EWSHM 2016), Bilbao, Spain
- Matias L, Dias NA, Morais I, Vales D, Carrilho F, Madeira J, Gaspar JL, Senos L, Silveira AB (2007) The 9th of July 1998 Faial Island (Azores, North Atlantic) seismic sequence, *Journal of Seismology* 11 (3): 275-298
- May J (2010) *Handmade houses & other buildings: the world of vernacular architecture*, Thames & Hudson, London, UK
- McCune B, Graces J (2002) *Analysis of Ecological Communities*, MjM Software Design, Gleneden, USA
- Medvedev SV (1962) *Engineering seismology*, Israel Program for Scientific Translations
- Mendes N, Lourenço PB (2010) Seismic assessment of masonry 'Gaioleiro' buildings in Lisbon, Portugal, *Journal of Earthquake Engineering* 14: 80-101
- Mendes N, Lourenço PB (2015) Seismic vulnerability of existing masonry buildings: nonlinear parametric analysis, in: Psycharis, Pantazopoulou & Papadrakakis (eds), *Seismic assessment, behavior and retrofit of heritage buildings and monuments. Computational methods in applied sciences*, Vol. 37, Springer
- Miccoli L, Oliveira DV, Silva R, Müller U, Schueremans L (2014) Static behaviour of rammed earth: experimental testing and finite element modelling, *Materials and Structures* 48 (10): 3443-3456
- Michiels T (2015) Seismic retrofitting techniques for historic adobe buildings, *International Journal of Architectural Heritage. Conservation, Analysis and Restoration* 9 (8): 1059-1068
- Miranda T, Correia AG, Santos M, Ribeira e Sousa L, Cortez P (2011) New Models for Strength and Deformability Parameter Calculation in Rock Masses Using Data-Mining Techniques, *International Journal of Geomechanics* 11 (1): 44-58
- Mogollón J (2002) Bahareque: a local seismic culture of the Colombian coffee region, in: Proc. of the International workshop on the role of bamboo in disaster avoidance, INBAR, Guayaquil, Ecuador

- Montgomery DC, Peck EA, Vining GG (2012) Introduction to linear regression analysis, John Wiley & Sons, Inc., New Jersey, USA
- Mouyiannou A, Rota M, Penna A, Magenes G (2014) Identification of suitable limit states from nonlinear dynamic analyses of masonry structures, *Journal of Earthquake Engineering* 18 (2): 231-263
- Mouzakis C, Vintzileou E, Adam CE, Karapitta L (2012) Dynamic tests on three leaf stone masonry building model before and after interventions, in: *Proc. of Structural Analysis of Historical Constructions, SAHC 2012, Wroclaw, Poland*
- Musson R, Grünthal G, Stucchi M (2010) The comparison of macroseismic intensity scales, *Journal of Seismology* 14 (2): 413-428
- Naderzadeh A (2009) Application of seismic base isolation technology in Iran, *Menshin* 63 (2): 40-47
- NBC-203 (1994) Guidelines for earthquake resistant building construction: low strength masonry, Government of Nepal, Kathmandu, Nepal
- NBC-204 (1994) Guidelines for earthquake resistant building construction: earthen building, Government of Nepal, Kathmandu, Nepal
- Neves F, Costa A, Vicente R, Oliveira CS, Varum H (2012) Seismic vulnerability assessment and characterization of the buildings on Faial Island, Azores, *Bulletin of Earthquake Engineering* 10 (1): 27-44
- Niglio O, Olivieri D (2005) Vernacular architecture and 'historical seismography' yearly research experience, in: Modena, Lourenço and Roca (eds), *Structural analysis of historical constructions*, pp. 203-212, Taylor & Francis Group, London, UK
- NP EN1998-1 (2010) Eurocódigo 8 – Projecto de estruturas para resistência aos sismos–Parte 1: Regras gerais, acções sísmicas e regras para edificios (Anexo Nacional), CEN
- NTC (2008) Norme Tecniche per le Costruzioni. D.M. 14 gennaio 2008, S.O. No. 30, G.U. No. 29/2008, Rome, Italy
- Okubo T (2016) Traditional wisdom for disaster mitigation in history of Japanese architectures and historic cities, *Journal of Cultural Heritage* 20: 715-724, *Cultural HELP 2014 Special Issue*
- Oliveira CS, Ferreira MA, Mota de Sá F (2004) Seismic Vulnerability and Impact Analysis: Elements for Mitigation Policies, XI Congresso Nazionale "L'ingegneria Sismica in Italia", Genova, Italy

- Oliveira CS, Mota de Sá F, Ferreira MA (2005) Application of Two Different Vulnerability Methodologies to Assess Seismic Scenarios in Lisbon, in: Proc. of International conference 250th anniversary of the 1755 Lisbon earthquake, Lisbon, Portugal
- Oliveira A (2009) Casa da Câmara de Vila Real de Santo António. Levantamento arqueológico, Monumentos (30): 54-61
- Oliver P (1997) Encyclopedia of vernacular architecture of the world, Cambridge University Press, Cambridge, UK
- Ortega J, Vasconcelos G, Rodrigues H, Correia M (2016a) Local Seismic Cultures: the use of timber frame structures in the South of Portugal, in: Cruz, Saporiti, Machado, Campos Costa, Xavier Candeias, Ruggieri & Manuel Catarino (eds), Historical earthquake-resistant timber framing in the Mediterranean Area, pp. 101-111, Springer International Publishing
- Ortega J, Vasconcelos G, Rodrigues H, Correia M (2016b) Seismic behavior of an old masonry building in Vila Real de Santo António, Portugal, in: Proc. of the 10th International Conference on Structural Analysis of Historical Constructions, SAHC 2016, Leuven, Belgium
- Pasticier L, Amadio C, Fragiocomo M (2008) Non-linear seismic analysis and vulnerability evaluation of a masonry building by means of the SAP2000 V. 10 code, Earthquake Engineering and Structural Dynamics 37: 467-485
- Pierotti P, Uliveri D (2001) Culture sismiche locali, Edizioni plus, Università di Pisa, Pisa, Italy
- Pinheiro M, Sanches S, Miranda T, Neves A, Tinoco J, Ferreira A, Correia AG (2015) A new empirical system for rock slope stability analysis in exploitation stage, International Journal of Rock Mechanics and Mining Sciences 76: 182-191
- Plevris V, Asteris PG (2014) Modeling of masonry failure surface under biaxial compressive stress using neural networks, Construction and Building Materials 55: 447-461
- Porphyrios D (1971) Traditional earthquake-resistant construction on a Greek island, Journal of the Society of Architectural Historians 30 (1): 31-39
- R Development Core Team (2008) R: A language and environment for statistical computing, R Foundation for Statistical Computing, Vienna, Austria
- Rapoport A (1969) House, form and culture, Prentice-Hall, Englewoods Cliffs, USA
- Roca A, Goula X, Susagna T, Chávez J, González M, Reinoso E (2006) A simplified method for vulnerability assessment of dwelling buildings and estimation of damage scenarios in Catalonia, Spain, Bulletin of Earthquake Engineering 4: 141-158
- Rossa W (2009) Cidades da razão: Vila Real de Santo António e arredores, Monumentos (30): 16-31

- Rota M, Penna A, Strobbia C (2006) Typological Fragility Curves from Italian Earthquake Damage Data, in: Proc. of First European Conference on Earthquake Engineering and Seismology, Geneva, Switzerland
- Rota M, Penna A, Magenes G (2010) A methodology for deriving analytical fragility curves for masonry buildings based on stochastic nonlinear analyses, *Engineering Structures* 32: 1312-1323
- Rudofsky B (1964) *Architecture without architects – a short introduction to non-pedigreed architecture*, Museum of Modern Art, New York, USA
- Saaty RW (1987) The analytic hierarchy process – what it is and how it is used, *Mathematical Modelling* 9 (3-5): 161-176
- Sabetta F, Goretti A, Lucantoni A (1998) Empirical Fragility Curves from Damage Surveys and Estimated Strong Ground Motion, in: Proc. of 11th European Conference on Earthquake Engineering, Paris, France
- Saloustros S, Pelà L, Roca P, Portal J (2014) Numerical analysis of structural damage in the church of the Poblet Monastery, *Engineering Failure Analysis* 48: 41-61
- Sandoval C, Roca P, Adam JM, Garzón-Roca J (2014) Modelling of buckling failure of load bearing walls, in: Proc. of 9th International masonry conference, Guimarães, Portugal
- Sandoval C, Roca P (2012) Study of the influence of different parameters on the buckling behaviour of masonry walls, *Construction and Building Materials* 35: 888-899
- Schacher T (2007) *Bhatar construction: an illustrated guide for craftsmen*, Swiss Agency for Development and Cooperation SDC, Mansehra, NWFP, Pakistan
- Sepe V, Speranza E, Viskovic A (2008) A method for large-scale vulnerability assessment of historic towers, *Journal of Structural Control and Health Monitoring* 15: 389-415
- SGU (2008) *Plano de Pormenor de Salvaguarda do Núcleo Pombalino de Vila Real de Santo António*, Sociedade de Gestão Urbana (SGU) de Vila Real de Santo António
- Shakya M (2014) *Seismic vulnerability assessment of slender masonry structures*, Ph.D. thesis, Universidade de Aveiro, Aveiro, Portugal
- Sousa G (2015) Portuguese historical seismicity, in: Correia, Lourenço & Varum (eds), *Seismic Retrofitting: Learning from Vernacular Architecture*, Taylor & Francis Group, London, UK
- Spence RJS, Coburn AW, Pomonis A, Sakai S (1992) Correlation of ground motion with building damage: The definition of a new damage-based seismic intensity scale, in: Proc. of 10th Conference on Earthquake Engineering, Madrid, Spain
- Spence RJS, D'Ayala D (1999) Damage assessment and analysis of the 1997 Umbria-Marche earthquakes, *Structural Engineering International* 9 (3): 229-233

- Tarque N (2008) Seismic risk assessment of adobe dwellings, M.Sc. thesis, Università degli Studi di Padova, Padua, Italy
- Tavares A, D'Ayala D, Costa A, Varum H (2014) Construction systems, in: Costa, Guedes & Varum (eds), Structural rehabilitation of old buildings, Vol. 2: 1-35, Springer
- Timchenko I (2002) Seismic vulnerability assessment of buildings on the basis of numerical analyses, in: Proc. of 12th European Conference on Earthquake Engineering, London, UK
- Tiwari PSR (1998) Traditional architecture of Kathmandu Valley, in: Workshop on seismic design of buildings, organized by CEC, Institute of Engineering, Pulchowk, Lalitpur, Nepal
- TNO (2011) DIplacement method ANALyser. User's manual, release 9.4.4., Netherlands
- Tolles EL, Kimbro E, Webster F, Ginell W (2000) Seismic stabilization of historic adobe structures: final report of the Getty Seismic Adobe Project, GCI Scientific Program Reports, The Getty Conservation Institute (GCI), Los Angeles, USA
- Tomazevic M (1999) Earthquake-resistant design of masonry buildings, Imperial College Press, London, UK
- Touliatos PG (1992) Traditional aseismic techniques in Greece, in: Mendes Victor (ed), Proc. of the International Workshop "Les systèmes nationaux faces aux séismes majeurs", Lisbon, Portugal
- Touliatos PG (2001) The box framed entity and function of the structures: the importance of wood's role, in: Proc. of International seminar of restoration of historic buildings in seismic areas: the case of settlements in Aegean, Lesvos Island, Greece
- Vasconcelos G, Lourenço PB (2009a) Experimental characterization of stone masonry in shear and compression, *Construction and Building Materials* 23 (11): 3337-3345
- Vasconcelos G, Lourenço PB (2009b) In-plane experimental behavior of stone masonry walls, *Journal of Structural Engineering (ASCE)* 135 (10): 1269-1278
- Vargas J, Blondet M, Cancino C (2009) Research on the use of mud-based grouts in the repair of structural cracks in adobe walls, in: Proc. of MEDITERRA, Cagliari, Italy
- Varum H, Figueiredo A, Silveira D, Martins T, Costa A (2011) Outputs from the research developed at the university of Aveiro regarding the mechanical characterization of existing adobe constructions in Portugal, *Revista Informes de la Construcción* 63 (523): 127-142
- Vicente R (2008) Estratégias e metodologias para intervenções de reabilitação urbana. Avaliação da vulnerabilidade e do risco sísmico do edificado da Baixa de Coimbra, Ph.D. thesis, Universidade do Aveiro, Aveiro, Portugal

- Vicente R, Parodi S, Lagomarsino S, Varum H, Mendes da Silva JAR (2011) Seismic vulnerability and risk assessment: a case study of the historic city centre of Coimbra, Portugal, *Bulletin of Earthquake Engineering* 9 (4): 1067-1096
- Vieira RS (2009) Do terramoto de 23 de Abril de 1909 à reconstrução da Vila de Benavente. Um processo de reformulação e expansão urbana, Câmara Municipal de Benavente, Benavente, Portugal
- Vintzileou E (2008) Effect of timber ties on the behavior of historic masonry, *Journal of Structural Engineering* 134 (6): 961-972
- Vintzileou E (2011) Timber-reinforced structures in Greece: 2500 BC-1900 AD, in: *Proc. of the Institution of Civil Engineers (ICE) – Structures and Buildings* 164 (SB3): 167-180
- Wald DJ, Quitoriano V, Heaton TH, Kanamori H (1999) Relationships between peak ground acceleration, peak ground velocity, and modified Mercalli intensity in California, *Earthquake Spectra* 15: 557-564
- Whitman RV, Reed JW, Hong ST (1974) Earthquake Damage Probability Matrices, in: *Proc. of the 5th World Conference on Earthquake Engineering*, Rome, Italy
- Whitney R, Agrawal A (2015) Seismic performance of flexible timber diaphragms: damping, force-displacement and natural period, *Engineering Structures* 101: 583-590
- Wilson A, Quenneville P, Ingham J (2013) Natural period and seismic idealization of flexible timber diaphragms, *Earthquake Spectra* 29 (3): 1003-1019
- Zhiping Z (2000) Traditional Chinese buildings and their performance in earthquake, in: *Proc. of the International Conference on the Seismic Performance of Traditional Buildings*, Istanbul, Turkey
- Zonno G, Oliveira CS, Ferreira MA, Musacchio G, Meroni F, Mota-de-Sá F, Neves F (2010) Assessing seismic damage through stochastic simulation of ground shaking: The case of the 1998 Faial earthquake (Azores Islands), *Surveys in Geophysics* 31 (3): 361-381

ANNEX A

DATABASE FOR THE SVIVA METHOD

The complete database is composed with the 530 results obtained from the extensive numerical parametric carried out. It was used for the definition of the seismic vulnerability assessment parameters weights and is shown in Table A.1. Data is structured in a database composed of 11 attributes (Figure A.1):

(1) Input variables: ten variables are used as the input, related to the parameters classes, assuming only four countable numbers from 1 to 4, associated to the four classes of increasing vulnerability A to D;

(2) Output variable: one variable with the value of load factor associated to LS3 obtained for each model, whose value typically ranges from 0 to 1.

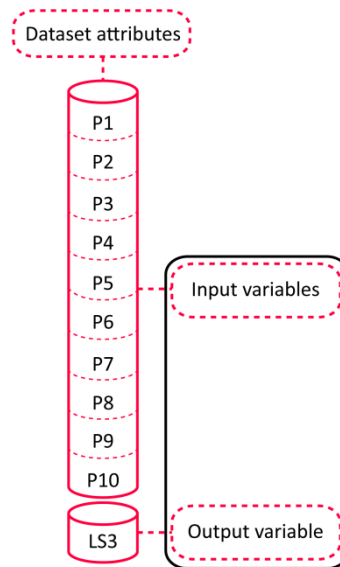


Figure A.1: Organization of the database

Table A.1: Database constructed for the definition of the SVIVA method weights

Model	Input variables										Output variable
	P1	P2	P3	P4	P5	P6	P7	P8	P9	P10	LS3
RE1F_Y	1	3	4	1	4	1	1	1	1	3	0.38
RE2F_Y	1	3	4	1	4	1	1	3	1	3	0.24
RE3F_Y	1	3	4	1	4	1	1	4	1	3	0.17
STM1F_Y	1	3	2	1	4	1	1	1	1	3	0.58
STM2F_Y	1	3	2	1	4	1	1	3	1	3	0.36
STM3F_Y	1	3	2	1	4	1	1	4	1	3	0.26
STM4F_Y	1	3	2	1	4	1	1	4	1	3	0.21
RE1F_kc1_Y	1	3	4	1	4	1	1	1	1	3	0.43
RE2F_kc1_Y	1	3	4	1	4	1	1	3	1	3	0.26
RE3F_kc1_Y	1	3	4	1	4	1	1	4	1	3	0.21
STM1F_kc1_Y	1	3	2	1	4	1	1	1	1	3	0.64
STM2F_kc1_Y	1	3	2	1	4	1	1	3	1	3	0.43
STM3F_kc1_Y	1	3	2	1	4	1	1	4	1	3	0.33
STM4F_kc1_Y	1	3	2	1	4	1	1	4	1	3	0.28
RE1F_kc5_Y	1	3	4	1	3	1	1	1	1	3	0.54
RE2F_kc5_Y	1	3	4	1	3	1	1	3	1	3	0.38
RE3F_kc5_Y	1	3	4	1	3	1	1	4	1	3	0.32
STM1F_kc5_Y	1	3	2	1	3	1	1	1	1	3	0.78
STM2F_kc5_Y	1	3	2	1	3	1	1	3	1	3	0.57
STM3F_kc5_Y	1	3	2	1	3	1	1	4	1	3	0.45
STM4F_kc5_Y	1	3	2	1	3	1	1	4	1	3	0.41
RE1Fd1_kc5_Y	1	3	4	1	2	1	1	1	1	3	0.88
RE2Fd1_kc5_Y	1	3	4	1	2	1	1	3	1	3	0.64
RE3Fd1_kc5_Y	1	3	4	1	2	1	1	4	1	3	0.53
STM1Fd1_kc5_Y	1	3	2	1	2	1	1	1	1	3	1.24
STM2Fd1_kc5_Y	1	3	2	1	2	1	1	3	1	3	0.83
STM3Fd1_kc5_Y	1	3	2	1	2	1	1	4	1	3	0.64
STM4Fd1_kc5_Y	1	3	2	1	2	1	1	4	1	3	0.54
STM3F_B3_Y	1	3	3	1	4	1	1	4	1	3	0.22
STM3F_C3_Y	1	3	4	1	4	1	1	4	1	3	0.18
STM3F_23_Y	1	3	2	1	4	1	1	4	1	3	0.27
STM3F_55_Y	1	3	2	1	4	1	1	4	1	3	0.29
RE1F_kc0d0_Y	2	3	4	1	4	1	1	1	1	4	0.28
RE1F_kc1d0_Y	2	3	4	1	4	1	1	1	1	4	0.36
RE1F_kc6d0_Y	2	3	4	1	3	1	1	1	1	4	0.48
RE1F_kc6d1_Y	2	3	4	1	1	1	1	1	1	4	0.74
RE1F_kc6d6_Y	2	3	4	1	2	1	1	1	1	4	0.55
RE1F_kc6d1_kdc0_Y	2	3	4	1	2	1	1	1	1	4	0.67
RE1F_kc1d1_kdc0_Y	2	3	4	1	3	1	1	1	1	4	0.58
RE1F_kc1d6_Y	2	3	4	1	3	1	1	1	1	4	0.52
RE1F_kc1d1_Y	2	3	4	1	2	1	1	1	1	4	0.63
RE1F_kc1d6_kdc0_Y	2	3	4	1	3	1	1	1	1	4	0.46
RE1F_kc6d6_kdc0_Y	2	3	4	1	3	1	1	1	1	4	0.60

Model	Input variables										Output variable
	P1	P2	P3	P4	P5	P6	P7	P8	P9	P10	LS3
RE1F_kc6d2_Y	2	3	4	1	2	1	1	1	1	4	0.66
RE1F_kc6d3_Y	2	3	4	1	1	1	1	1	1	4	0.78
RE1F_0op_Y	1	3	4	1	4	1	1	1	1	3	0.34
RE1F_1op_Y	1	3	4	1	4	1	1	1	1	3	0.38
RE1F_3op1_Y	1	3	4	1	4	1	1	1	1	3	0.36
RE1F_3op2_Y	1	3	4	1	4	1	1	1	1	3	0.46
RE1F_3op3_Y	1	3	4	1	4	1	1	1	1	3	0.45
RE1F_3op4_Y	1	3	4	1	4	1	1	1	1	3	0.38
RE1F_3op5_Y	1	3	4	1	4	1	1	1	1	3	0.37
RE2F_0op_Y	1	3	4	1	4	1	1	3	1	3	0.21
RE2F_1op_Y	1	3	4	1	4	1	1	3	1	3	0.22
RE2F_3op1_Y	1	3	4	1	4	1	1	3	1	3	0.22
RE2F_3op2_Y	1	3	4	1	4	1	1	3	1	3	0.25
RE2F_3op3_Y	1	3	4	1	4	1	1	3	1	3	0.28
RE2F_3op4_Y	1	3	4	1	4	1	1	3	1	3	0.27
RE2F_3op5_Y	1	3	4	1	4	1	1	3	1	3	0.31
RE1F_c100_Y	1	3	4	1	4	1	1	1	1	4	0.39
RE1F_c80_Y	1	3	4	2	4	1	1	1	1	4	0.37
RE1F_c60_Y	1	3	4	3	4	1	1	1	1	4	0.34
RE1F_c40_Y	1	3	4	3	4	1	1	1	1	4	0.29
RE1F_c20_Y	1	3	4	4	4	1	1	1	1	4	0.22
RE1F_c10_Y	1	3	4	4	4	1	1	1	1	4	0.23
RE1F_R0_Y	1	3	4	1	4	1	1	1	1	4	0.54
RE1F_R1_Y	1	3	4	1	4	2	1	1	1	4	0.46
RE1F_R2_Y	1	3	4	1	4	2	1	1	1	4	0.41
RE1F_R3_Y	1	3	4	1	4	3	1	1	1	4	0.38
RE1F_R4_Y	1	3	4	1	4	3	1	1	1	4	0.31
RE1F_R5_Y	1	3	4	1	4	4	1	1	1	4	0.22
RE1F_2op_LS1_Y	1	3	4	1	4	1	1	1	2	3	0.42
RE1F_2op_LS2_Y	1	3	4	1	4	1	1	1	2	3	0.42
RE1F_2op_LS3_Y	1	3	4	1	4	1	1	1	2	3	0.41
RE1F_2op_LS3a_Y	1	3	4	1	4	1	1	1	3	3	0.36
RE1F_2op_LS4_Y	1	3	4	1	4	1	1	1	4	3	0.34
RE1F_3op_LS1_Y	1	3	4	1	4	1	1	1	2	3	0.43
RE1F_3op_LS2_Y	1	3	4	1	4	1	1	1	2	3	0.41
RE1F_3op_LS3_Y	1	3	4	1	4	1	1	1	3	3	0.36
RE1F_3op_LS4_Y	1	3	4	1	4	1	1	1	4	3	0.32
RE2F_3op_LS1_Y	1	3	4	1	4	1	1	3	2	3	0.25
RE2F_3op_LS2_Y	1	3	4	1	4	1	1	3	3	3	0.24
RE2F_3op_LS3_Y	1	3	4	1	4	1	1	3	3	3	0.19
RE2F_3op_LS4_Y	1	3	4	1	4	1	1	3	4	3	0.13
RE2F_3op1_LS1_Y	1	3	4	1	4	1	1	3	2	3	0.25
RE2F_3op1_LS2_Y	1	3	4	1	4	1	1	3	3	3	0.23
RE2F_3op1_LS3_Y	1	3	4	1	4	1	1	3	4	3	0.20

Model	Input variables										Output variable
	P1	P2	P3	P4	P5	P6	P7	P8	P9	P10	LS3
RE2F_3op1_LS4_Y	1	3	4	1	4	1	1	3	4	3	0.19
RE1F_s4t5_Y	1	1	4	1	4	1	1	1	1	3	0.48
RE1F_s5t5_Y	1	2	4	1	4	1	1	1	1	3	0.46
RE1F_s6t5_Y	1	2	4	1	4	1	1	1	1	4	0.41
RE1F_s8t5_Y	1	3	4	1	4	1	1	1	1	4	0.37
RE1F_s9t5_Y	1	4	4	1	4	1	1	1	1	4	0.35
RE1F_s10t5_Y	1	4	4	1	4	1	1	1	1	4	0.34
RE1F_s11t5_Y	1	4	4	1	4	1	1	1	1	4	0.33
RE1F_s12t5_Y	1	4	4	1	4	1	1	1	1	4	0.32
RE1F_s4t4_Y	2	1	4	1	4	1	1	1	1	3	0.46
RE1F_s5t4_Y	2	2	4	1	4	1	1	1	1	3	0.4
RE1F_s6t4_Y	2	2	4	1	4	1	1	1	1	4	0.38
RE1F_s7t4_Y	2	3	4	1	4	1	1	1	1	4	0.38
RE1F_s8t5_Y	2	3	4	1	4	1	1	1	1	4	0.35
RE1F_s9t5_Y	2	4	4	1	4	1	1	1	1	4	0.32
RE1F_s10t5_Y	2	4	4	1	4	1	1	1	1	4	0.3
RE1F_s4t3_Y	3	1	4	1	4	1	1	1	1	3	0.45
RE1F_s5t3_Y	3	2	4	1	4	1	1	1	1	4	0.41
RE1F_s6t3_Y	3	2	4	1	4	1	1	1	1	4	0.36
RE1F_s7t3_Y	3	3	4	1	4	1	1	1	1	4	0.33
RE1F_q1_1-1_Y	1	3	4	1	4	1	1	1	1	3	0.35
RE1F_q1_1-2_Y	1	3	4	1	4	1	1	1	1	3	0.43
RE1F_q1_2-1_Y	1	3	4	1	4	1	1	1	1	3	0.35
RE1F_q1_2-2_Y	1	3	4	1	4	1	1	1	1	3	0.31
RE1F_q1_2-3_Y	1	3	4	1	4	1	1	1	1	3	0.32
RE1F_q1_3_Y	1	3	4	1	4	1	1	1	1	3	0.42
RE1F_q1_4-1_Y	1	3	3	1	4	1	1	1	1	3	0.51
RE1F_q1_4-2_Y	1	3	3	1	4	1	1	1	1	3	0.48
RE1F_q1_4-3_Y	1	3	3	1	4	1	1	1	1	3	0.54
RE1F_q2_1-1_Y	1	3	4	1	4	1	1	1	1	3	0.36
RE1F_q2_1-2_Y	1	3	4	1	4	1	1	1	1	3	0.35
RE1F_q2_2-2_Y	1	3	4	1	4	1	1	1	1	3	0.42
RE1F_q2_3-1_Y	1	3	4	1	4	1	1	1	1	3	0.51
RE1F_q2_3-2_Y	1	3	4	1	4	1	1	1	1	3	0.48
RE1F_q2_3-3_Y	1	3	4	1	4	1	1	1	1	3	0.54
RE1F_q3_1-1_Y	1	3	4	1	4	1	1	1	1	3	0.36
RE1F_q3_1-2_Y	1	3	4	1	4	1	1	1	1	3	0.42
RE1F_q3_2-1_Y	1	3	4	1	4	1	1	1	1	3	0.42
RE1F_q3_2-2_Y	1	3	4	1	4	1	1	1	1	3	0.43
RE1F_q3_3-1_Y	1	3	3	1	4	1	1	1	1	3	0.51
RE1F_q3_3-2_Y	1	3	3	1	4	1	1	1	1	3	0.51
RE1F_q3_3-3_Y	1	3	3	1	4	1	1	1	1	3	0.57
RE1F_q3_4_Y	1	3	2	1	4	1	1	1	1	3	0.58
RE1F_q4_1_Y	1	3	2	1	4	1	1	1	1	3	0.58

Model	Input variables										Output variable
	P1	P2	P3	P4	P5	P6	P7	P8	P9	P10	LS3
RE1F_q4_2-1_Y	1	3	2	1	4	1	1	1	1	3	0.63
RE1F_q4_2-2_Y	1	3	2	1	4	1	1	1	1	3	0.64
RE1F_q4_2-3_Y	1	3	1	1	4	1	1	1	1	3	0.8
RE1F_q4_3_Y	1	3	1	1	4	1	1	1	1	3	0.68
RE1F_q5_1_Y	1	3	1	1	4	1	1	1	1	3	0.67
RE1F_q5_2-1_Y	1	3	1	1	4	1	1	1	1	3	0.75
RE1F_q5_2-2_Y	1	3	1	1	4	1	1	1	1	3	0.67
RE1F_q5_2-3_Y	1	3	1	1	4	1	1	1	1	3	0.85
RE1F_q5_3_Y	1	3	1	1	4	1	1	1	1	3	0.8
RE1F_q6_6-1_Y	1	3	1	1	4	1	1	1	1	3	0.8
RE1F_q6_6-2_Y	1	3	1	1	4	1	1	1	1	3	0.71
RE1F_q6_6-3_Y	1	3	1	1	4	1	1	1	1	3	1
RE1F_s7h3_5t5_Y	2	3	4	1	4	1	1	1	1	4	0.29
RE1F_s7h4t5_Y	2	3	4	1	4	1	1	1	1	4	0.25
RE1F_s7h3_5t4_Y	2	3	4	1	4	1	1	1	1	4	0.32
RE1F_s7h4t4_Y	3	3	4	1	4	1	1	1	1	4	0.27
RE1F_s7h3_5t3_Y	3	3	4	1	4	1	1	1	1	4	0.27
RE1F_s7h4t3_Y	4	3	4	1	4	1	1	1	1	4	0.23
RE1F_s7h4_5t3_Y	4	3	4	1	4	1	1	1	1	4	0.21
RE1F_s7h3t2_Y	4	3	4	1	4	1	1	1	1	4	0.24
RE1F_s7h3_5t2_Y	4	3	4	1	4	1	1	1	1	4	0.21
RE1F_s7h4t2_Y	4	3	4	1	4	1	1	1	1	4	0.18
RE1F_s7h4_5t2_Y	4	3	4	1	4	1	1	1	1	4	0.15
RE1F_s5h4t3_Y	4	2	4	1	4	1	1	1	1	4	0.28
RE1F_s5h3t2_Y	4	2	4	1	4	1	1	1	1	4	0.34
RE1F_s5h4t3_Y	4	2	4	1	4	1	1	1	1	4	0.25
STM3F_t4	2	3	2	1	4	1	1	4	1	3	0.23
STM3F_t3	3	3	2	1	4	1	1	4	1	3	0.19
RE2F_2op_a_Y	1	3	4	1	1	1	1	3	1	4	0.58
RE2F_3op4_a_Y	1	3	4	1	1	1	1	3	1	4	0.65
RE1F_3op3_a_y	1	3	4	1	1	1	1	1	1	4	1.01
RE1F_s7h3t5_X	1	1	4	1	4	1	1	1	1	2	0.49
RE1F_s7h3t4_X	2	1	4	1	4	1	1	1	1	2	0.47
RE1F_s7h3t3_X	3	1	4	1	4	1	1	1	1	2	0.41
RE1F_s7h3_5t5_X	2	1	4	1	4	1	1	1	1	2	0.46
RE1F_s7h4t5_X	2	1	4	1	4	1	1	1	1	2	0.4
RE1F_s7h3_5t4_X	2	1	4	1	4	1	1	1	1	2	0.41
RE1F_s7h4t4_X	3	1	4	1	4	1	1	1	1	2	0.37
RE1F_s7h3_5t3_X	3	1	4	1	4	1	1	1	1	2	0.39
RE1F_s7h4t3_X	4	1	4	1	4	1	1	1	1	2	0.32
RE1F_s7h4_5t3_X	4	1	4	1	4	1	1	1	1	2	0.3
RE1F_s7h3t2_X	4	1	4	1	4	1	1	1	1	2	0.33
RE1F_s7h3_5t2_X	4	1	4	1	4	1	1	1	1	2	0.3
RE1F_s7h4t2_X	4	1	4	1	4	1	1	1	1	2	0.27

Model	Input variables										Output variable
	P1	P2	P3	P4	P5	P6	P7	P8	P9	P10	LS3
RE1F_s7h4_5t2_X	4	1	4	1	4	1	1	1	1	2	0.25
RE1Fd1_s7h3t5_X	1	1	4	1	1	1	1	1	1	2	0.91
RE1Fd1_s7h3_5t5_X	2	1	4	1	1	1	1	1	1	2	0.85
RE1Fd1_s7h4t5_X	2	1	4	1	1	1	1	1	1	2	0.81
RE1Fd1_s7h3_5t4_X	2	1	4	1	1	1	1	1	1	2	0.85
RE1Fd1_s7h4t4_X	3	1	4	1	1	1	1	1	1	2	0.79
RE1Fd1_s7h3_5t3_X	3	1	4	1	1	1	1	1	1	2	0.86
RE1Fd1_s7h4t3_X	4	1	4	1	1	1	1	1	1	2	0.78
RE1Fd1_s7h4_5t3_X	4	1	4	1	1	1	1	1	1	2	0.73
RE1Fd1_s7h3_5t2_X	4	1	4	1	1	1	1	1	1	2	0.85
RE1Fd1_s7h4t2_X	4	1	4	1	1	1	1	1	1	2	0.67
RE1Fd1_s7h4_5t2_X	4	1	4	1	1	1	1	1	1	2	0.52
RE1F_X	1	1	4	1	4	1	1	1	1	2	0.41
RE2Fd1_3op4_X	1	1	4	1	1	1	3	3	1	2	0.42
RE2Fd1_q1_2-1_X	1	1	4	1	1	1	3	3	1	2	0.41
RE2Fd1_q1_4-1_X	1	1	3	1	1	1	3	3	1	2	0.48
RE2Fd1_q2_1-2_X	1	1	4	1	1	1	3	3	1	2	0.37
RE2Fd1_q2_2_X	1	1	4	1	1	1	3	3	1	2	0.43
RE2Fd1_q2_3-2_X	1	1	4	1	1	1	3	3	1	2	0.44
RE2Fd1_q3_3-2_X	1	1	3	1	1	1	3	3	1	2	0.51
RE2Fd1_q3_4_X	1	1	2	1	1	1	3	3	1	2	0.53
RE2Fd1_q4_1_X	1	1	2	1	1	1	3	3	1	2	0.59
RE2Fd1_q4_2-1_X	1	1	2	1	1	1	3	3	1	2	0.61
RE2Fd1_q5_2-1_X	1	1	1	1	1	1	3	3	1	2	0.66
RE2Fd1_q5_3_X	1	1	1	1	1	1	3	3	1	2	0.69
RE2Fd1_q6_1-3_X	1	1	1	1	1	1	3	3	1	2	0.73
RE2Fd1_c100_X	1	1	4	1	1	1	2	3	1	2	0.49
RE2Fd1_c80_X	1	1	4	2	1	1	2	3	1	2	0.48
RE2Fd1_c60_X	1	1	4	3	1	1	2	3	1	2	0.46
RE2Fd1_c40_X	1	1	4	3	1	1	2	3	1	2	0.45
RE2Fd1_c20_X	1	1	4	4	1	1	2	3	1	2	0.4
RE2Fd1_c10_X	1	1	4	4	1	1	2	3	1	2	0.37
RE1F_kc0d0_X	2	1	4	1	4	1	1	1	1	1	0.44
RE1F_kc1d0_Y	2	1	4	1	4	1	1	1	1	1	0.48
RE1F_kc6d0_X	2	1	4	1	4	1	1	1	1	1	0.44
RE1F_kc6d1_X	2	1	4	1	1	1	1	1	1	1	0.77
RE1F_kc6d6_X	2	1	4	1	2	1	1	1	1	1	0.5
RE1F_kc6d1_kdc0_X	2	1	4	1	4	1	1	1	1	1	0.52
RE1F_kc1d1_kdc0_X	2	1	4	1	4	1	1	1	1	1	0.47
RE1F_kc1d6_X	2	1	4	1	3	1	1	1	1	1	0.58
RE1F_kc1d1_X	2	1	4	1	3	1	1	1	1	1	0.76
RE1F_kc1d6_kdc0_X	2	1	4	1	4	1	1	1	1	1	0.45
RE1F_kc6d6_kdc0_X	2	1	4	1	4	1	1	1	1	1	0.44
RE1F_kc6d2_X	2	1	4	1	2	1	1	1	1	1	0.67

Model	Input variables										Output variable
	P1	P2	P3	P4	P5	P6	P7	P8	P9	P10	LS3
RE1F_kc6d3_X	2	1	4	1	1	1	1	1	1	1	0.91
RE1F_0op_X	1	1	4	1	4	1	1	1	1	2	0.41
RE1F_1op_X	1	1	4	1	4	1	1	1	1	2	0.4
RE1F_3op1_X	1	1	4	1	4	1	2	1	1	2	0.41
RE1F_3op2_X	1	1	4	1	4	1	2	1	1	2	0.42
RE1F_3op3_X	1	1	4	1	4	1	3	1	1	2	0.46
RE1F_3op4_X	1	1	4	1	4	1	4	1	1	2	0.41
RE1F_3op5_X	1	1	4	1	4	1	4	1	1	2	0.36
RE2F_0op_X	1	1	4	1	4	1	1	3	1	2	0.25
RE2F_1op_X	1	1	4	1	4	1	1	3	1	2	0.25
RE2F_3op1_X	1	1	4	1	4	1	2	3	1	2	0.25
RE2F_3op2_X	1	1	4	1	4	1	2	3	1	2	0.28
RE2F_3op3_X	1	1	4	1	4	1	3	3	1	2	0.27
RE2F_3op4_X	1	1	4	1	4	1	4	3	1	2	0.27
RE2F_3op5_X	1	1	4	1	4	1	4	3	1	2	0.25
RE1Fd1_2op_X	1	1	4	1	1	1	2	1	1	2	0.89
RE1Fd1_0op_X	1	1	4	1	1	1	1	1	1	2	1.02
RE1Fd1_3op2_X	1	1	4	1	1	1	2	1	1	2	0.75
RE1Fd1_3op3_X	1	1	4	1	1	1	3	1	1	2	0.69
RE1Fd1_3op4_X	1	1	4	1	1	1	3	1	1	2	0.66
RE1Fd1_3op5_X	1	1	4	1	1	1	3	1	1	2	0.67
RE1Fd1_3op2_b_X	1	1	4	1	1	1	3	1	1	2	0.59
RE1Fd1_3op3_b_X	1	1	4	1	1	1	4	1	1	2	0.42
RE1Fd1_3op4_b_X	1	1	4	1	1	1	4	1	1	2	0.39
RE1Fd1_3op5_b_X	1	1	4	1	1	1	4	1	1	2	0.3
RE1Fd0_3op2_X	1	1	4	1	4	1	3	1	1	2	0.46
RE1Fd0_3op3_X	1	1	4	1	4	1	4	1	1	2	0.42
RE1Fd0_3op4_X	1	1	4	1	4	1	4	1	1	2	0.39
RE1Fd0_3op5_X	1	1	4	1	4	1	4	1	1	2	0.3
RE2Fd1_2op_X	1	1	4	1	1	1	2	3	1	2	0.58
RE2Fd1_0op_X	1	1	4	1	1	1	1	3	1	2	0.76
RE2Fd1_3op2_X	1	1	4	1	1	1	2	3	1	2	0.49
RE2Fd1_3op3_X	1	1	4	1	1	1	3	3	1	2	0.43
RE2Fd1_3op4_X	1	1	4	1	1	1	3	3	1	2	0.42
RE2Fd1_3op5_X	1	1	4	1	1	1	3	3	1	2	0.4
RE2Fd1_3op2_b_X	1	1	4	1	1	1	3	3	1	2	0.41
RE2Fd1_3op3_b_X	1	1	4	1	1	1	4	3	1	2	0.27
RE2Fd1_3op4_b_X	1	1	4	1	1	1	4	3	1	2	0.24
RE2Fd1_3op5_b_X	1	1	4	1	1	1	4	3	1	2	0.17
RE2Fd0_3op2_X	1	1	4	1	4	1	3	3	1	2	0.26
RE2Fd0_3op3_X	1	1	4	1	4	1	4	3	1	2	0.24
RE2Fd0_3op4_X	1	1	4	1	4	1	4	3	1	2	0.21
RE2Fd0_3op5_X	1	1	4	1	4	1	4	3	1	2	0.16
RE2F_X	1	1	4	1	4	1	1	3	1	2	0.25

Model	Input variables										Output variable
	P1	P2	P3	P4	P5	P6	P7	P8	P9	P10	LS3
STM3F_X	1	1	2	1	4	1	1	4	1	2	0.43
STM4Fd1_kc5_X	1	1	2	1	1	1	1	4	1	2	0.43
STM3Fd1_kc5_X	1	1	2	1	1	1	1	4	1	2	0.54
RE3Fd1_kc5_X	1	1	4	1	1	1	1	4	1	2	0.42
STM2Fd1_kc5_X	1	1	2	1	1	1	1	3	1	2	0.74
RE2Fd1_kc5_X	1	1	4	1	1	1	1	3	1	2	0.55
STM1Fd1_kc5_X	1	1	2	1	1	1	1	1	1	2	1.13
RE1Fd1_kc5_X	1	1	4	1	1	1	1	1	1	2	0.82
STM3F_23_X	1	1	2	1	4	1	2	4	1	2	0.38
STM3F_55_X	1	1	2	1	4	1	3	4	1	2	0.31
RE2Fd1_2op_LS1_X	1	1	4	1	1	1	2	3	2	2	0.51
RE2Fd1_2op_LS2_X	1	1	4	1	1	1	2	3	3	2	0.42
RE2Fd1_2op_LS3_X	1	1	4	1	1	1	2	3	4	2	0.42
RE2Fd1_3op4_LS1_X	1	1	4	1	1	1	3	3	2	2	0.34
RE2Fd1_3op4_LS2_X	1	1	4	1	1	1	3	3	3	2	0.26
RE2Fd1_3op4_LS3_X	1	1	4	1	1	1	3	3	4	2	0.26
RE1Fd1_3op4_LS1_X	1	1	4	1	1	1	3	1	2	2	0.62
RE1Fd1_3op4_LS2_X	1	1	4	1	1	1	3	1	3	2	0.63
RE1Fd1_3op4_LS3_X	1	1	4	1	1	1	3	1	4	2	0.58
RE1Fd1_3op4_t6_X	1	1	4	1	1	1	3	1	1	1	0.67
RE1Fd1_3op4_t4_X	2	1	4	1	1	1	3	1	1	2	0.66
RE1Fd1_3op4_t3_X	3	1	4	1	1	1	3	1	1	2	0.65
RE2Fd1_2op_t3_X	3	1	4	1	1	1	2	3	1	2	0.55
RE2Fd1_2op_t4_X	2	1	4	1	1	1	2	3	1	2	0.57
RE2Fd1_2op_t6_X	1	1	4	1	1	1	2	3	1	1	0.56
RE2Fd1_3op4_t6_X	1	1	4	1	1	1	3	3	1	1	0.43
RE2Fd1_3op4_t4_X	2	1	4	1	1	1	3	3	1	2	0.41
RE2Fd1_3op4_t3_X	3	1	4	1	1	1	3	3	1	2	0.41
RE2Fd1_s5_5t5_X	1	2	4	1	1	1	2	3	1	2	0.54
RE2Fd1_s5_5t3_X	3	2	4	1	1	1	2	3	1	2	0.53
RE2Fd1_s5_5t4_X	2	2	4	1	1	1	2	3	1	2	0.55
RE2Fd1_s5_5t6_X	1	2	4	1	1	1	2	3	1	2	0.52
RE2Fd1_s2_5_X	1	1	4	1	1	1	2	3	1	1	0.64
RE2Fd1_s3_5_X	1	1	4	1	1	1	2	3	1	1	0.59
RE2Fd1_s6_5_X	1	2	4	1	1	1	2	3	1	2	0.5
RE2Fd1_s2_5_2C_X	1	1	4	1	1	1	2	3	1	1	0.63
RE2Fd1_s3_5_2C_X	1	1	4	1	1	1	2	3	1	2	0.58
RE2Fd1_s4_5_2C_X	1	1	4	1	1	1	2	3	1	2	0.54
RE2Fd1_s5_5_2C_X	1	2	4	1	1	1	2	3	1	3	0.51
RE2Fd1_s6_5_2C_X	1	2	4	1	1	1	2	3	1	3	0.48
RE2Fd1_0op_2C_X	1	1	4	1	1	1	1	3	1	2	0.71
RE2Fd1_3op2_2C_X	1	1	4	1	1	1	2	3	1	2	0.45
RE2Fd1_3op3_2C_X	1	1	4	1	1	1	3	3	1	2	0.39
RE2Fd1_3op4_2C_X	1	1	4	1	1	1	3	3	1	2	0.38

Model	Input variables										Output variable
	P1	P2	P3	P4	P5	P6	P7	P8	P9	P10	LS3
RE2Fd1_3op5_2C_X	1	1	4	1	1	1	4	3	1	2	0.34
RE2Fd1_2op_Y	1	3	4	1	1	1	1	3	1	4	0.58
RE2Fd1_s2_5_Y	1	3	4	1	1	1	1	3	1	4	0.42
RE2Fd1_s3_5_Y	1	3	4	1	1	1	1	3	1	4	0.51
RE2Fd1_s5_5_Y	1	3	4	1	1	1	1	3	1	3	0.66
RE2Fd1_s6_5_Y	1	3	4	1	1	1	1	3	1	3	0.71
RE2Fd1_s4_5_2C_Y	1	3	4	1	1	1	1	3	1	3	0.71
RE2Fd1_s3_5_2C_Y	1	3	4	1	1	1	1	3	1	3	0.69
RE2Fd1_s5_5_2C_Y	1	3	4	1	1	1	1	3	1	3	0.79
RE2Fd1_s5_5L4_Y	1	1	4	1	1	1	1	3	1	2	0.77
RE2Fd1_s5_5L5_Y	1	2	4	1	1	1	1	3	1	3	0.68
RE2Fd1_s5_5L6_Y	1	2	4	1	1	1	1	3	1	3	0.64
RE2Fd1_s5_5L8_Y	1	3	4	1	1	1	1	3	1	4	0.52
RE1Fd1_2op_Y	1	3	4	1	1	1	1	1	1	4	0.93
RE1Fd1_s2_5_Y	1	3	4	1	1	1	1	1	1	4	0.72
RE1Fd1_s3_5_Y	1	3	4	1	1	1	1	1	1	4	0.84
RE1Fd1_s5_5_Y	1	3	4	1	1	1	1	1	1	3	0.99
RE1Fd1_s6_5_Y	1	3	4	1	1	1	1	1	1	3	1.05
RE2Fd1_IP35_L4_Y	1	1	4	1	1	1	3	3	1	3	0.32
RE2Fd1_IP35_L5_Y	1	1	4	1	1	1	3	3	1	2	0.34
RE2Fd1_IP35_L6_Y	1	1	4	1	1	1	3	3	1	2	0.37
RE2Fd1_IP35_L8_Y	1	1	4	1	1	1	3	3	1	1	0.46
RE2Fd1_IP55_L4_Y	1	1	4	1	1	1	4	3	1	3	0.18
RE2Fd1_IP55_L5_Y	1	1	4	1	1	1	4	3	1	2	0.21
RE2Fd1_IP55_L6_Y	1	1	4	1	1	1	4	3	1	2	0.19
RE2Fd1_IP55_L8_Y	1	1	4	1	1	1	4	3	1	1	0.20
B01_X	1	2	3	1	1	1	4	4	1	1	0.14
B01_Y	1	4	3	1	1	4	1	4	1	4	0.41
B01_X1	1	2	3	1	1	1	4	4	4	1	0.08
B01_Y1	1	4	3	1	1	4	1	4	4	4	0.18
B01b_X	1	2	3	1	1	1	4	4	1	2	0.25
B01c_X	1	2	3	1	1	1	4	4	1	2	0.3
B02_X	3	2	1	2	4	1	4	4	1	4	0.1
B02_Y	3	4	1	2	3	3	1	4	1	4	0.39
B02_X1	3	2	1	2	4	1	4	4	4	1	0.09
B02_Y1	3	4	1	2	3	3	1	4	3	4	0.21
B03_X	2	1	2	4	2	1	4	4	1	1	0.08
B03_Y	2	4	2	4	2	2	1	4	1	4	0.17
B03_X1	2	1	2	4	2	1	4	4	2	1	0.06
B03_Y1	2	4	2	4	2	2	1	4	2	4	0.15
B04_X	2	1	4	4	1	1	3	4	1	3	0.15
B04_Y	2	1	4	4	1	3	1	4	1	3	0.29
B04_X1	2	1	4	4	1	1	3	4	2	3	0.12
B04_Y1	2	1	4	4	1	3	1	4	2	3	0.25

Model	Input variables										Output variable
	P1	P2	P3	P4	P5	P6	P7	P8	P9	P10	LS3
B05_X	2	1	4	2	4	1	4	4	1	1	0.06
B05_Y	2	4	4	2	4	1	1	4	1	4	0.11
B05_X1	2	1	4	2	4	1	4	4	2	1	0.05
B05_Y1	2	4	4	2	4	1	1	4	2	4	0.07
B06_X	2	1	3	3	1	1	4	4	1	2	0.06
B06_Y	2	2	3	3	1	4	1	4	1	3	0.25
B06_X1	2	1	3	3	1	1	4	4	4	2	0.03
B06_Y1	2	2	3	3	1	4	1	4	4	3	0.07
B07_X	3	2	1	4	4	1	4	4	1	1	0.08
B07_Y	3	4	1	4	3	2	1	4	1	4	0.32
B07_X1	3	2	1	4	4	1	4	4	3	1	0.07
B07_Y1	3	4	1	4	3	2	1	4	3	4	0.24
B08_X	2	2	1	4	4	1	4	3	1	2	0.2
B08_Y	2	2	1	4	3	3	1	3	1	3	0.58
B09_X	2	1	3	4	1	1	2	3	1	1	0.63
B09_Y	2	4	3	4	1	3	1	3	1	4	0.29
B09_X1	2	1	3	4	1	1	2	3	4	1	0.34
B09_Y1	2	4	3	4	1	3	1	3	4	4	0.24
B10_X	1	1	4	2	1	1	2	3	1	1	0.71
B10_Y	1	3	4	2	1	3	1	3	1	4	0.65
B10_X1	1	1	4	2	1	1	2	3	3	1	0.48
B10_Y1	1	3	4	2	1	3	1	3	3	4	0.51
B11_X	4	1	1	4	4	1	4	1	1	1	0.29
B11_Y	4	3	1	4	4	3	1	1	1	4	0.33
B11_X1	4	1	1	4	4	1	4	1	2	1	0.24
B11_Y1	4	3	1	4	4	3	1	1	2	4	0.31
B12_X	3	1	2	3	1	1	3	4	1	1	0.25
B12_Y	3	3	2	3	1	2	1	4	1	4	0.29
B12_X1	3	1	2	3	1	1	3	4	2	1	0.11
B12_Y1	3	3	2	3	1	2	1	4	2	4	0.18
B13_X	3	1	3	3	4	1	3	3	1	1	0.23
B13_Y	3	4	3	3	4	2	1	3	1	4	0.07
B13_X1	3	1	3	3	4	1	3	3	3	1	0.13
B13_Y1	3	4	3	3	4	2	1	3	3	4	0.06
B14_X	4	1	1	4	4	1	4	4	1	3	0.13
B14_Y	4	1	1	4	2	2	1	4	1	3	0.41
B14_X1	4	1	1	4	4	1	4	4	3	3	0.1
B14_Y1	4	1	1	4	2	2	1	4	3	3	0.26
B15_X	2	2	2	1	4	1	4	3	1	1	0.14
B15_Y	2	4	2	1	3	1	1	3	1	4	0.47
B15_X1	2	2	2	1	4	1	4	3	4	1	0.11
B15_Y1	2	4	2	1	3	1	1	3	4	4	0.34
B16_X	2	1	4	3	1	1	1	3	1	2	0.47
B16_Y	2	2	4	3	1	4	1	3	1	3	0.42

Model	Input variables										Output variable
	P1	P2	P3	P4	P5	P6	P7	P8	P9	P10	LS3
B16_X1	2	1	4	3	1	1	1	3	4	2	0.29
B16_Y1	2	2	4	3	1	4	1	3	4	3	0.24
B17_X	2	1	4	1	4	1	3	4	1	2	0.14
B17_Y	2	1	4	1	4	3	1	4	1	3	0.2
B17_X1	2	1	4	1	4	1	3	4	2	2	0.15
B17_Y1	2	1	4	1	4	3	1	4	2	3	0.13
B18_X	2	1	4	2	2	1	3	3	1	1	0.23
B18_Y	2	4	4	2	2	4	1	3	1	4	0.26
B18_X1	2	1	4	2	2	1	3	3	3	1	0.2
B18_Y1	2	4	4	2	2	4	1	3	3	4	0.18
B19_X	2	1	3	3	1	1	3	3	1	1	0.27
B19_Y	2	4	3	3	1	1	1	3	1	4	0.29
B20_X	3	1	3	3	4	1	2	4	1	1	0.17
B20_Y	3	4	3	3	4	2	1	4	1	4	0.04
B21_X	1	1	1	3	4	1	4	3	1	1	0.26
B21_Y	1	3	1	3	3	4	1	3	1	4	0.65
B21_X1	1	1	1	3	4	1	4	3	3	1	0.24
B21_Y1	1	3	1	3	3	4	1	3	2	4	0.63
B22_X	3	1	1	4	1	1	3	3	1	1	0.5
B22_Y	3	4	1	4	1	4	1	3	1	4	0.44
B22_X1	3	1	1	4	1	1	3	3	3	1	0.22
B22_Y1	3	4	1	4	1	4	1	3	3	4	0.24
B23_X	3	2	1	3	4	1	4	4	1	1	0.12
B23_Y	3	4	1	3	3	2	1	4	1	4	0.23
B23_X1	3	2	1	3	4	1	4	4	4	1	0.07
B23_Y1	3	4	1	3	3	2	1	4	4	4	0.16
B24_X	3	1	1	4	1	1	3	4	1	1	0.4
B24_Y	3	4	1	4	1	3	1	4	1	4	0.2
B25_X	4	1	3	2	2	1	4	3	1	1	0.16
B25_Y	4	4	3	2	2	2	1	3	1	4	0.3
B25_X1	4	1	3	2	2	1	4	3	2	1	0.13
B25_Y1	4	4	3	2	2	2	1	3	2	4	0.22
B26_X	4	1	2	4	1	1	4	4	1	1	0.09
B26_Y	4	3	2	4	1	4	1	4	1	4	0.15
B26_X1	4	1	2	4	1	1	4	4	3	1	0.08
B26_Y1	4	3	2	4	1	4	1	4	3	4	0.13
B27_X	4	1	2	3	1	1	4	4	1	2	0.2
B27_Y	4	2	2	3	1	4	1	4	1	3	0.3
B27_X1	4	1	2	3	1	1	4	4	3	2	0.11
B27_Y1	4	2	2	3	1	4	1	4	3	3	0.19
B28_X	1	1	4	1	2	1	3	1	1	1	0.53
B28_Y	1	3	4	1	2	3	1	1	1	4	0.55
B29_X	4	1	1	1	4	1	2	1	1	2	0.49
B29_Y	4	2	1	1	3	4	1	1	1	3	0.55

Model	Input variables										Output variable
	P1	P2	P3	P4	P5	P6	P7	P8	P9	P10	LS3
B29_X1	4	1	1	1	4	1	2	1	4	2	0.31
B29_Y1	4	2	1	1	3	4	1	1	4	3	0.32
B30_X	2	1	3	3	4	1	3	4	1	1	0.25
B30_Y	2	4	3	3	2	2	1	4	1	4	0.28
B30_X1	2	1	3	3	4	1	3	4	4	1	0.13
B30_Y1	2	4	3	3	2	2	1	4	4	4	0.18
RE1F_s7h3t6_Y	1	3	4	1	4	1	1	1	1	4	0.45
RE1F_s7h2_4t6_Y	1	3	4	1	4	1	1	1	1	4	0.67
RE1F_s5h3t6_Y	1	2	4	1	4	1	1	1	1	3	0.49
RE1F_s5h2_4t6_Y	1	2	4	1	4	1	1	1	1	3	0.8
RE1F_s7h3t6_X	1	1	4	1	4	1	1	1	1	2	0.57
RE1F_s7h2_4t6_X	1	1	4	1	4	1	2	1	1	2	0.78
RE2F_c100_Y	1	3	4	1	4	1	1	3	1	4	0.21
RE2F_c80_Y	1	3	4	2	4	1	1	3	1	4	0.21
RE2F_c60_Y	1	3	4	3	4	1	1	3	1	4	0.2
RE2F_c40_Y	1	3	4	3	4	1	1	3	1	4	0.19
RE2F_c20_Y	1	3	4	4	4	1	1	3	1	4	0.16
RE2F_c10_Y	1	3	4	4	4	1	1	3	1	4	0.14
RE2F_kc6d3_Y	1	3	4	1	1	1	1	3	1	3	0.76
RE2F_kc6d1_Y	1	3	4	1	1	1	1	3	1	3	0.71
RE2F_kc1d1_Y	1	3	4	1	2	1	1	3	1	3	0.64
RE2F_kc6d1_kdc0_Y	1	3	4	1	2	1	1	3	1	3	0.62
RE2F_kc6d6_Y	1	3	4	1	2	1	1	3	1	3	0.61
RE2F_kc1d6_Y	1	3	4	1	3	1	1	3	1	3	0.58
RE2F_kc6d6_kdc0_Y	1	3	4	1	3	1	1	3	1	3	0.53
RE2F_kc1d1_kdc0_Y	1	3	4	1	3	1	1	3	1	3	0.48
RE2F_kc1d6_kdc0_Y	1	3	4	1	3	1	1	3	1	3	0.43
RE2F_kc6d3_X	1	1	4	1	1	1	1	3	1	2	0.62
RE2F_kc1d1_X	1	1	4	1	2	1	1	3	1	2	0.56
RE2F_kc6d1_kdc0_X	1	1	4	1	4	1	1	3	1	2	0.31
RE2F_kc6d6_X	1	1	4	1	2	1	1	3	1	2	0.45
RE2F_kc1d6_X	1	1	4	1	3	1	1	3	1	2	0.46
RE2F_kc6d6_kdc0_X	1	1	4	1	4	1	1	3	1	2	0.27
RE2F_kc1d1_kdc0_X	1	1	4	1	4	1	1	3	1	2	0.28
RE2F_kc1d6_kdc0_X	1	1	4	1	4	1	1	3	1	2	0.26
RE2F_kc5_X	1	1	4	1	4	1	1	3	1	2	0.26
RE2F_kc1_X	1	1	4	1	4	1	1	3	1	2	0.26
STM3F_kc6d3_Y	1	3	2	1	1	1	1	4	1	3	0.76
STM3F_kc6d1_Y	1	3	2	1	1	1	1	4	1	3	0.75
STM3F_kc1d1_Y	1	3	2	1	2	1	1	4	1	3	0.74
STM3F_kc6d1_kdc0_Y	1	3	2	1	2	1	1	4	1	3	0.74
STM3F_kc6d6_Y	1	3	2	1	2	1	1	4	1	3	0.56
STM3F_kc1d6_Y	1	3	2	1	3	1	1	4	1	3	0.55
STM3F_kc6d6_kdc0_Y	1	3	2	1	3	1	1	4	1	3	0.61

Model	Input variables										Output variable
	P1	P2	P3	P4	P5	P6	P7	P8	P9	P10	LS3
STM3F_kc1d1_kdc0_Y	1	3	2	1	3	1	1	4	1	3	0.61
STM3F_kc1d6_kdc0_Y	1	3	2	1	3	1	1	4	1	3	0.52
STM3F_kc6d3_X	1	1	2	1	1	1	1	4	1	2	0.59
STM3F_kc1d1_X	1	1	2	1	2	1	1	4	1	2	0.53
STM3F_kc6d1_kdc0_X	1	1	2	1	4	1	1	4	1	2	0.53
STM3F_kc6d6_X	1	1	2	1	2	1	1	4	1	2	0.49
STM3F_kc1d6_X	1	1	2	1	3	1	1	4	1	2	0.45
STM3F_kc6d6_kdc0_X	1	1	2	1	4	1	1	4	1	2	0.47
STM3F_kc1d1_kdc0_X	1	1	2	1	4	1	1	4	1	2	0.51
STM3F_kc1d6_kdc0_X	1	1	2	1	4	1	1	4	1	2	0.47
STM3F_kc5_X	1	1	2	1	4	1	1	4	1	2	0.45
STM3F_kc1_X	1	1	2	1	4	1	1	4	1	2	0.44
RE2F_R1_Y	1	3	4	1	4	2	1	3	1	4	0.19
RE2F_R2_Y	1	3	4	1	4	2	1	3	1	4	0.17
RE2F_R3_Y	1	3	4	1	4	3	1	3	1	4	0.16
RE2F_R4_Y	1	3	4	1	4	3	1	3	1	4	0.13
RE2F_R5_Y	1	3	4	1	4	4	1	3	1	4	0.11
RE2F_kc6d1_Y	1	3	4	1	1	1	1	3	1	4	0.63
RE1F_2op_a_X	1	1	4	1	4	1	2	1	1	2	0.49
RE1F_0op_a_X	1	1	4	1	4	1	1	1	1	2	0.46
RE1F_3op2_a_X	1	1	4	1	4	1	2	1	1	2	0.46
RE1F_3op3_a_X	1	1	4	1	4	1	3	1	1	2	0.45
RE1F_3op4_a_X	1	1	4	1	4	1	3	1	1	2	0.42
RE1F_3op5_a_X	1	1	4	1	4	1	3	1	1	2	0.35
RE2F_2op_a_X	1	1	4	1	4	1	2	3	1	2	0.25
RE2F_0op_a_X	1	1	4	1	4	1	1	3	1	2	0.27
RE2F_3op2_a_X	1	1	4	1	4	1	2	3	1	2	0.27
RE2F_3op3_a_X	1	1	4	1	4	1	3	3	1	2	0.28
RE2F_3op4_a_X	1	1	4	1	4	1	3	3	1	2	0.26
RE2F_3op5_a_X	1	1	4	1	4	1	3	3	1	2	0.22
RE2Fd1_R1_Y	1	3	4	1	1	2	1	3	1	4	0.63
RE2Fd1_R2_Y	1	3	4	1	1	3	1	3	1	4	0.63
RE2Fd1_R3_Y	1	3	4	1	1	4	1	3	1	4	0.64
RE1Fd0_c100_Y	1	3	4	1	4	1	1	1	1	4	0.38
RE2Fd0_c100_Y	1	3	4	1	4	1	1	3	1	4	0.2
STM2Fd0_c100_Y	1	3	2	1	4	1	1	3	1	4	0.3
RE2Fd3_c100_Y	1	3	4	1	1	1	1	3	1	4	0.51
STM3Fd0_c100_Y	1	3	2	1	4	1	1	4	1	4	0.28
RE2Fd3_c200_Y	1	3	4	1	1	1	1	3	1	4	0.5
RE2Fd3_c500_Y	1	3	4	1	1	1	1	3	1	4	0.51
STM3Fd0_LW_Y	1	3	3	1	4	1	1	4	1	3	0.29
STM3Fd1_23_X	1	1	2	1	1	1	2	4	1	2	0.49
STM3Fd1_55_X	1	1	2	1	1	1	3	4	1	2	0.37
RE2F_2op_L9_Y	1	4	4	1	1	1	1	3	1	4	0.5

Annex A. Database for the SVIVA method

	Input variables										Output variable
Model	P1	P2	P3	P4	P5	P6	P7	P8	P9	P10	LS3
<i>RE2F_2op_L10_Y</i>	1	4	4	1	1	1	1	3	1	4	0.46
<i>RE2F_2op_L11_Y</i>	1	4	4	1	1	1	1	3	1	4	0.44
<i>RE2F_2op_L12_Y</i>	1	4	4	1	1	1	1	3	1	4	0.42

ANNEX B

DATABASE FOR THE SAVVAS METHOD

The final database used for the development of the SAVVAS method is composed with the 567 results obtained from the extensive numerical parametric carried out. The database is shown in Table B.1. Data is structured in a database composed of 14 attributes (Figure B.1):

(1) Input variables: eleven variables are used as the input, related to the parameters classes, assuming which can be: (a) expressed in a discrete form from 1 to 4, associated to the four classes of increasing vulnerability A to D; or (b) expressed as continuous variables using different units depending on the parameter;

(2) Output variables: three variables with the values of load factors associated to LS1, LS2 and LS3 obtained for each model, whose values typically range from 0 to 1.

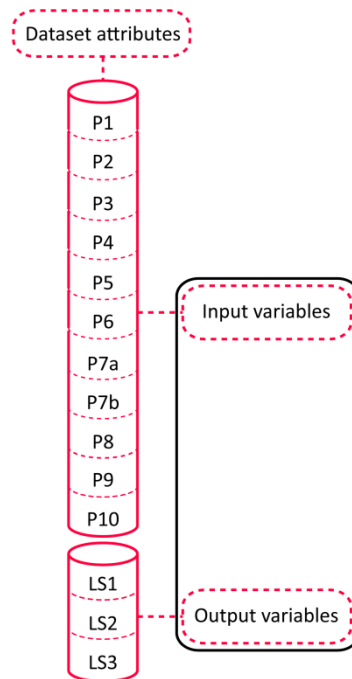


Figure B.1: Organization of the database

Table B.1: Database constructed for the development of the SAVVAS method

Model	Input variables										Output variable			
	P1	P2	P3	P4	P5	P6	P7a	P7b	P8	P9	P10	LS1	LS2	LS3
	λ	s	[1-4]	[1-4]	[1-4]	[1-4]	P7a	P7b	N	[1-4]	γ_i	(g)		
RE1F_Y	6	7	4	2	4	1	0.08	0	1	1	0.5	0.32	0.36	0.38
RE2F_Y	5.6	7	4	2	4	1	0.08	0	2	1	0.5	0.11	0.21	0.24
RE3F_Y	5.45	7	4	2	4	1	0.08	0	3	1	0.5	0.1	0.13	0.17
STM1F_Y	6	7	2	2	4	1	0.08	0	1	1	0.5	0.46	0.56	0.58
STM2F_Y	5.6	7	2	2	4	1	0.08	0	2	1	0.5	0.22	0.28	0.36
STM3F_Y	5.45	7	2	2	4	1	0.08	0	3	1	0.5	0.19	0.21	0.26
STM4F_Y	5.4	7	2	2	4	1	0.08	0	4	1	0.5	0.19	0.2	0.21
RE1F_kc1_Y	6	7	4	2	4	1	0.08	0	1	1	0.5	0.34	0.38	0.43
RE2F_kc1_Y	5.6	7	4	2	4	1	0.08	0	2	1	0.5	0.15	0.22	0.26
RE3F_kc1_Y	5.45	7	4	2	4	1	0.08	0	3	1	0.5	0.13	0.19	0.21
STM1F_kc1_Y	6	7	2	2	4	1	0.08	0	1	1	0.5	0.45	0.6	0.64
STM2F_kc1_Y	5.6	7	2	2	4	1	0.08	0	2	1	0.5	0.24	0.31	0.43
STM3F_kc1_Y	5.45	7	2	2	4	1	0.08	0	3	1	0.5	0.21	0.28	0.33
STM4F_kc1_Y	5.4	7	2	2	4	1	0.08	0	4	1	0.5	0.22	0.25	0.28
RE1F_kc5_Y	6	7	4	2	3	1	0.08	0	1	1	0.5	0.37	0.51	0.54
RE2F_kc5_Y	5.6	7	4	2	3	1	0.08	0	2	1	0.5	0.21	0.27	0.38
RE3F_kc5_Y	5.45	7	4	2	3	1	0.08	0	3	1	0.5	0.19	0.28	0.32
STM1F_kc5_Y	6	7	2	2	3	1	0.08	0	1	1	0.5	0.51	0.73	0.78
STM2F_kc5_Y	5.6	7	2	2	3	1	0.08	0	2	1	0.5	0.31	0.4	0.57
STM3F_kc5_Y	5.45	7	2	2	3	1	0.08	0	3	1	0.5	0.27	0.38	0.45
STM4F_kc5_Y	5.4	7	2	2	3	1	0.08	0	4	1	0.5	0.28	0.34	0.41
RE1Fd1_kc5_Y	6	7	4	2	2	1	0.08	0	1	1	0.5	0.24	0.73	0.88
RE2Fd1_kc5_Y	5.6	7	4	2	2	1	0.08	0	2	1	0.5	0.16	0.54	0.64
RE3Fd1_kc5_Y	5.45	7	4	2	2	1	0.08	0	3	1	0.5	0.15	0.45	0.53
STM1Fd1_kc5_Y	6	7	2	2	2	1	0.08	0	1	1	0.5	0.49	1.01	1.24
STM2Fd1_kc5_Y	5.6	7	2	2	2	1	0.08	0	2	1	0.5	0.27	0.68	0.83
STM3Fd1_kc5_Y	5.45	7	2	2	2	1	0.08	0	3	1	0.5	0.25	0.56	0.64
STM4Fd1_kc5_Y	5.4	7	2	2	2	1	0.08	0	4	1	0.5	0.25	0.44	0.54
STM3F_B3_Y	5.45	7	3	2	4	1	0.08	0	3	1	0.5	0.1	0.18	0.22
STM3F_C3_Y	5.45	7	4	2	4	1	0.08	0	3	1	0.5	0.06	0.15	0.18
STM3F_23_Y	5.45	7	2	2	4	1	0.23	0	3	1	0.5	0.22	0.24	0.27
STM3F_55_Y	5.45	7	2	2	4	1	0.55	0	3	1	0.5	0.26	0.29	0.29
RE1F_kc0d0_Y	7.2	7	4	2	4	1	0.06	0	1	1	0.38	0.2	0.22	0.28
RE1F_kc1d0_Y	7.2	7	4	2	4	1	0.06	0	1	1	0.38	0.2	0.32	0.36
RE1F_kc6d0_Y	7.2	7	4	2	3	1	0.06	0	1	1	0.38	0.24	0.38	0.48
RE1F_kc6d1_Y	7.2	7	4	2	1	1	0.06	0	1	1	0.38	0.49	0.68	0.74
RE1F_kc6d6_Y	7.2	7	4	2	2	1	0.06	0	1	1	0.38	0.29	0.53	0.55
RE1F_kc6d1_kdc0_Y	7.2	7	4	2	2	1	0.06	0	1	1	0.38	0.44	0.56	0.67
RE1F_kc1d1_kdc0_Y	7.2	7	4	2	3	1	0.06	0	1	1	0.38	0.3	0.47	0.58
RE1F_kc1d6_Y	7.2	7	4	2	3	1	0.06	0	1	1	0.38	0.22	0.46	0.52
RE1F_kc1d1_Y	7.2	7	4	2	2	1	0.06	0	1	1	0.38	0.46	0.54	0.63
RE1F_kc1d6_kdc0_Y	7.2	7	4	2	3	1	0.06	0	1	1	0.38	0.25	0.42	0.46

Model	Input variables										Output variable			
	P1	P2	P3	P4	P5	P6	P7a	P7b	P8	P9	P10	LS1	LS2	LS3
	λ	s	[1-4]	[1-4]	[1-4]	[1-4]	$P7a$	$P7b$	N	[1-4]	ν_i	(g)		
RE1F_kc6d6_kdc0_Y	7.2	7	4	2	3	1	0.06	0	1	1	0.38	0.36	0.53	0.60
RE1F_kc6d2_Y	7.2	7	4	2	2	1	0.06	0	1	1	0.38	0.32	0.58	0.66
RE1F_kc6d3_Y	7.2	7	4	2	1	1	0.06	0	1	1	0.38	0.7	0.74	0.78
RE1F_0op_Y	6	7	4	2	4	1	0	0	1	1	0.5	0.3	0.33	0.34
RE1F_1op_Y	6	7	4	2	4	1	0.04	0	1	1	0.5	0.32	0.34	0.38
RE1F_3op1_Y	6	7	4	2	4	1	0.11	0	1	1	0.5	0.32	0.34	0.36
RE1F_3op2_Y	6	7	4	2	4	1	0.23	0	1	1	0.5	0.3	0.39	0.46
RE1F_3op3_Y	6	7	4	2	4	1	0.34	0	1	1	0.5	0.28	0.38	0.45
RE1F_3op4_Y	6	7	4	2	4	1	0.55	0	1	1	0.5	0.24	0.35	0.38
RE1F_3op5_Y	6	7	4	2	4	1	0.7	0	1	1	0.5	0.16	0.34	0.37
RE2F_0op_Y	5.6	7	4	2	4	1	0	0	2	1	0.5	0.1	0.17	0.21
RE2F_1op_Y	5.6	7	4	2	4	1	0.04	0	2	1	0.5	0.1	0.16	0.22
RE2F_3op1_Y	5.6	7	4	2	4	1	0.11	0	2	1	0.5	0.12	0.19	0.22
RE2F_3op2_Y	5.6	7	4	2	4	1	0.23	0	2	1	0.5	0.12	0.21	0.25
RE2F_3op3_Y	5.6	7	4	2	4	1	0.34	0	2	1	0.5	0.12	0.26	0.28
RE2F_3op4_Y	5.6	7	4	2	4	1	0.55	0	2	1	0.5	0.12	0.25	0.27
RE2F_3op5_Y	5.6	7	4	2	4	1	0.7	0	2	1	0.5	0.1	0.24	0.31
RE1F_c500_Y	6	7	4	1	4	1	0.08	0	1	1	0.38	0.37	0.45	0.52
RE1F_c200_Y	6	7	4	1	4	1	0.08	0	1	1	0.38	0.38	0.42	0.43
RE1F_c100_Y	6	7	4	2	4	1	0.08	0	1	1	0.38	0.3	0.33	0.39
RE1F_c80_Y	6	7	4	2	4	1	0.08	0	1	1	0.38	0.28	0.3	0.37
RE1F_c60_Y	6	7	4	3	4	1	0.08	0	1	1	0.38	0.25	0.33	0.34
RE1F_c40_Y	6	7	4	3	4	1	0.08	0	1	1	0.38	0.22	0.25	0.29
RE1F_c20_Y	6	7	4	4	4	1	0.08	0	1	1	0.38	0.2	0.2	0.22
RE1F_c10_Y	6	7	4	4	4	1	0.08	0	1	1	0.38	0.07	0.21	0.23
RE1F_R0_Y	4.8	7	4	2	4	1	0.05	0	1	1	0.39	0.48	0.5	0.54
RE1F_R1_Y	4.8	7	4	2	4	2	0.05	0	1	1	0.39	0.4	0.43	0.46
RE1F_R2_Y	4.8	7	4	2	4	2	0.05	0	1	1	0.39	0.36	0.38	0.41
RE1F_R3_Y	4.8	7	4	2	4	3	0.05	0	1	1	0.39	0.33	0.34	0.38
RE1F_R4_Y	4.8	7	4	2	4	3	0.05	0	1	1	0.39	0.13	0.22	0.31
RE1F_R5_Y	4.8	7	4	2	4	4	0.05	0	1	1	0.39	0	0.21	0.22
RE1F_2op_LS1_Y	6	7	4	2	4	1	0.08	0	1	2	0.5	0.18	0.35	0.42
RE1F_2op_LS2_Y	6	7	4	2	4	1	0.08	0	1	2	0.5	0.26	0.31	0.42
RE1F_2op_LS3_Y	6	7	4	2	4	1	0.08	0	1	2	0.5	0.15	0.31	0.41
RE1F_2op_LS3a_Y	6	7	4	2	4	1	0.08	0	1	3	0.5	0	0.33	0.36
RE1F_2op_LS4_Y	6	7	4	2	4	1	0.08	0	1	4	0.5	0	0.31	0.34
RE1F_3op_LS1_Y	6	7	4	2	4	1	0.23	0	1	2	0.5	0	0.37	0.43
RE1F_3op_LS2_Y	6	7	4	2	4	1	0.23	0	1	2	0.5	0	0.38	0.41
RE1F_3op_LS3_Y	6	7	4	2	4	1	0.23	0	1	3	0.5	0	0.33	0.36
RE1F_3op_LS4_Y	6	7	4	2	4	1	0.23	0	1	4	0.5	0	0.29	0.32
RE2F_3op_LS1_Y	5.6	7	4	2	4	1	0.34	0	2	2	0.5	0	0.23	0.25
RE2F_3op_LS2_Y	5.6	7	4	2	4	1	0.34	0	2	3	0.5	0	0.22	0.24

Model	Input variables										Output variable			
	P1	P2	P3	P4	P5	P6	P7a	P7b	P8	P9	P10	LS1	LS2	LS3
	λ	s	[1-4]	[1-4]	[1-4]	[1-4]	P7a	P7b	N	[1-4]	γ_i	(g)		
RE2F_3op_LS3_Y	5.6	7	4	2	4	1	0.34	0	2	3	0.5	0	0.17	0.19
RE2F_3op_LS4_Y	5.6	7	4	2	4	1	0.34	0	2	4	0.5	0	0.12	0.13
RE2F_3op1_LS1_Y	5.6	7	4	2	4	1	0.55	0	2	2	0.5	0	0.21	0.25
RE2F_3op1_LS2_Y	5.6	7	4	2	4	1	0.55	0	2	3	0.5	0	0.21	0.23
RE2F_3op1_LS3_Y	5.6	7	4	2	4	1	0.55	0	2	4	0.5	0	0.16	0.2
RE2F_3op1_LS4_Y	5.6	7	4	2	4	1	0.55	0	2	4	0.5	0	0.12	0.19
RE1F_s4t5_Y	6	4	4	2	4	1	0.13	0	1	1	0.52	0.36	0.36	0.48
RE1F_s5t5_Y	6	5	4	2	4	1	0.11	0	1	1	0.46	0.32	0.32	0.46
RE1F_s6t5_Y	6	6	4	2	4	1	0.09	0	1	1	0.41	0.28	0.29	0.41
RE1F_s8t5_Y	6	8	4	2	4	1	0.07	0	1	1	0.35	0.26	0.28	0.37
RE1F_s9t5_Y	6	9	4	2	4	1	0.06	0	1	1	0.32	0.26	0.26	0.35
RE1F_s10t5_Y	6	10	4	2	4	1	0.05	0	1	1	0.30	0.26	0.33	0.34
RE1F_s11t5_Y	6	11	4	2	4	1	0.05	0	1	1	0.28	0.25	0.32	0.33
RE1F_s12t5_Y	6	12	4	2	4	1	0.04	0	1	1	0.26	0.25	0.31	0.32
RE1F_s4t4_Y	7.5	4	4	2	4	1	0.13	0	1	1	0.52	0.37	0.4	0.46
RE1F_s5t4_Y	7.5	5	4	2	4	1	0.11	0	1	1	0.45	0.3	0.37	0.4
RE1F_s6t4_Y	7.5	6	4	2	4	1	0.09	0	1	1	0.41	0.26	0.29	0.38
RE1F_s7t4_Y	7.5	7	4	2	4	1	0.08	0	1	1	0.37	0.26	0.34	0.38
RE1F_s8t4_Y	7.5	8	4	2	4	1	0.07	0	1	1	0.35	0.26	0.33	0.35
RE1F_s9t4_Y	7.5	9	4	2	4	1	0.06	0	1	1	0.32	0.25	0.31	0.32
RE1F_s10t4_Y	7.5	10	4	2	4	1	0.05	0	1	1	0.30	0.24	0.3	0.3
RE1F_s4t3_Y	10	4	4	2	4	1	0.13	0	1	1	0.51	0.29	0.37	0.45
RE1F_s5t3_Y	10	5	4	2	4	1	0.11	0	1	1	0.44	0.24	0.35	0.41
RE1F_s6t3_Y	10	6	4	2	4	1	0.09	0	1	1	0.41	0.21	0.33	0.36
RE1F_s7t3_Y	10	7	4	2	4	1	0.08	0	1	1	0.36	0.21	0.27	0.33
RE1F_q1_1-1_Y	6	7	4	2	4	1	0.08	0	1	1	0.5	0.22	0.34	0.35
RE1F_q1_1-2_Y	6	7	4	2	4	1	0.08	0	1	1	0.5	0.37	0.38	0.43
RE1F_q1_2-1_Y	6	7	4	2	4	1	0.08	0	1	1	0.5	0.26	0.34	0.35
RE1F_q1_2-2_Y	6	7	4	2	4	1	0.08	0	1	1	0.5	0.21	0.24	0.31
RE1F_q1_2-3_Y	6	7	4	2	4	1	0.08	0	1	1	0.5	0.3	0.31	0.32
RE1F_q1_3_Y	6	7	4	2	4	1	0.08	0	1	1	0.5	0.35	0.39	0.42
RE1F_q1_4-1_Y	6	7	3	2	4	1	0.08	0	1	1	0.5	0.37	0.43	0.51
RE1F_q1_4-2_Y	6	7	3	2	4	1	0.08	0	1	1	0.5	0.22	0.43	0.48
RE1F_q1_4-3_Y	6	7	3	2	4	1	0.08	0	1	1	0.5	0.47	0.49	0.54
RE1F_q2_1-1_Y	6	7	4	2	4	1	0.08	0	1	1	0.5	0.32	0.34	0.36
RE1F_q2_1-2_Y	6	7	4	2	4	1	0.08	0	1	1	0.5	0.22	0.34	0.35
RE1F_q2_2-2_Y	6	7	4	2	4	1	0.08	0	1	1	0.5	0.35	0.39	0.42
RE1F_q2_3-1_Y	6	7	4	2	4	1	0.08	0	1	1	0.5	0.37	0.43	0.51
RE1F_q2_3-2_Y	6	7	4	2	4	1	0.08	0	1	1	0.5	0.22	0.43	0.48
RE1F_q2_3-3_Y	6	7	4	2	4	1	0.08	0	1	1	0.5	0.47	0.49	0.54
RE1F_q3_1-1_Y	6	7	4	2	4	1	0.08	0	1	1	0.5	0.32	0.34	0.36
RE1F_q3_1-2_Y	6	7	4	2	4	1	0.08	0	1	1	0.5	0.37	0.4	0.42

Model	Input variables											Output variable		
	P1	P2	P3	P4	P5	P6	P7a	P7b	P8	P9	P10	LS1	LS2	LS3
	λ	s	[1-4]	[1-4]	[1-4]	[1-4]	$P7a$	$P7b$	N	[1-4]	γ_i	(g)		
RE1F_q3_2-1_Y	6	7	4	2	4	1	0.08	0	1	1	0.5	0.35	0.39	0.42
RE1F_q3_2-2_Y	6	7	4	2	4	1	0.08	0	1	1	0.5	0.4	0.41	0.43
RE1F_q3_3-1_Y	6	7	3	2	4	1	0.08	0	1	1	0.5	0.37	0.43	0.51
RE1F_q3_3-2_Y	6	7	3	2	4	1	0.08	0	1	1	0.5	0.44	0.45	0.51
RE1F_q3_3-3_Y	6	7	3	2	4	1	0.08	0	1	1	0.5	0.51	0.52	0.57
RE1F_q3_4_Y	6	7	2	2	4	1	0.08	0	1	1	0.5	0.46	0.56	0.58
RE1F_q4_1_Y	6	7	2	2	4	1	0.08	0	1	1	0.5	0.49	0.51	0.58
RE1F_q4_2-1_Y	6	7	2	2	4	1	0.08	0	1	1	0.5	0.54	0.56	0.63
RE1F_q4_2-2_Y	6	7	2	2	4	1	0.08	0	1	1	0.5	0.34	0.54	0.64
RE1F_q4_2-3_Y	6	7	1	2	4	1	0.08	0	1	1	0.5	0.8	0.8	0.8
RE1F_q4_3_Y	6	7	1	2	4	1	0.08	0	1	1	0.5	0.56	0.61	0.68
RE1F_q5_1_Y	6	7	1	2	4	1	0.08	0	1	1	0.5	0.65	0.65	0.67
RE1F_q5_2-1_Y	6	7	1	2	4	1	0.08	0	1	1	0.5	0.69	0.7	0.75
RE1F_q5_2-2_Y	6	7	1	2	4	1	0.08	0	1	1	0.5	0.47	0.63	0.67
RE1F_q5_2-3_Y	6	7	1	2	4	1	0.08	0	1	1	0.5	0.85	0.85	0.85
RE1F_q5_3_Y	6	7	1	2	4	1	0.08	0	1	1	0.5	0.72	0.75	0.8
RE1F_q6_6-1_Y	6	7	1	2	4	1	0.08	0	1	1	0.5	0.72	0.75	0.8
RE1F_q6_6-2_Y	6	7	1	2	4	1	0.08	0	1	1	0.5	0.47	0.69	0.71
RE1F_q6_6-3_Y	6	7	1	2	4	1	0.08	0	1	1	0.5	1	1	1
RE1F_s7h3_5t5_Y	7	7	4	2	4	1	0.07	0	1	1	0.38	0.21	0.24	0.29
RE1F_s7h4t5_Y	8	7	4	2	4	1	0.06	0	1	1	0.38	0.16	0.19	0.25
RE1F_s7h3_5t4_Y	8.75	7	4	2	4	1	0.07	0	1	1	0.37	0.18	0.27	0.32
RE1F_s7h4t4_Y	10	7	4	2	4	1	0.06	0	1	1	0.37	0.14	0.22	0.27
RE1F_s7h3_5t3_Y	11.7	7	4	2	4	1	0.07	0	1	1	0.36	0.15	0.19	0.27
RE1F_s7h4t3_Y	13.3	7	4	2	4	1	0.06	0	1	1	0.36	0.11	0.2	0.23
RE1F_s7h4_5t3_Y	15	7	4	2	4	1	0.05	0	1	1	0.36	0.1	0.16	0.21
RE1F_s7h3t2_Y	15	7	4	2	4	1	0.08	0	1	1	0.35	0.15	0.23	0.24
RE1F_s7h3_5t2_Y	17.5	7	4	2	4	1	0.07	0	1	1	0.35	0.11	0.16	0.21
RE1F_s7h4t2_Y	20	7	4	2	4	1	0.06	0	1	1	0.35	0.08	0.14	0.18
RE1F_s7h4_5t2_Y	22.5	7	4	2	4	1	0.05	0	1	1	0.35	0.06	0.15	0.15
RE1F_s5h4t3_Y	13.3	5	4	2	4	1	0.08	0	1	1	0.44	0.16	0.22	0.28
RE1F_s5h3t2_Y	15	5	4	2	4	1	0.11	0	1	1	0.43	0.17	0.28	0.34
RE1F_s5h4t3_Y	20	5	4	2	4	1	0.08	0	1	1	0.43	0.12	0.19	0.25
STM3F_t4	5.45	7	2	2	4	1	0.08	0	3	1	0.5	0.16	0.21	0.23
STM3F_t3	5.45	7	2	2	4	1	0.08	0	3	1	0.5	0.13	0.17	0.19
RE2F_2op_a_Y	5.6	7	4	2	1	1	0.08	0	2	1	0.44	0.35	0.46	0.58
RE2F_3op4_a_Y	5.6	7	4	2	1	1	0.55	0	2	1	0.44	0.4	0.52	0.65
RE1F_3op3_a_y	6	7	4	2	1	1	0.34	0	1	1	0.44	0.53	0.83	1.01
RE1F_s7h3t5_X	6	3.5	4	2	4	1	0	0.09	1	1	0.63	0.46	0.46	0.49
RE1F_s7h3t4_X	7.5	3.65	4	2	4	1	0	0.09	1	1	0.62	0.36	0.4	0.47
RE1F_s7h3t3_X	10	3.8	4	2	4	1	0	0.09	1	1	0.6	0.28	0.36	0.41
RE1F_s7h3_5t5_X	7	3.5	4	2	4	1	0	0.08	1	1	0.63	0.4	0.42	0.46

Model	Input variables											Output variable		
	P1	P2	P3	P4	P5	P6	P7a	P7b	P8	P9	P10	LS1	LS2	LS3
	λ	s	[1-4]	[1-4]	[1-4]	[1-4]	P7a	P7b	N	[1-4]	γ_i	(g)		
RE1F_s7h4t5_X	8	3.5	4	2	4	1	0	0.07	1	1	0.63	0.38	0.39	0.4
RE1F_s7h3_5t4_X	8.75	3.65	4	2	4	1	0	0.08	1	1	0.62	0.32	0.36	0.41
RE1F_s7h4t4_X	10	3.65	4	2	4	1	0	0.07	1	1	0.62	0.3	0.32	0.37
RE1F_s7h3_5t3_X	11.7	3.8	4	2	4	1	0	0.08	1	1	0.6	0.25	0.32	0.39
RE1F_s7h4t3_X	13.3	3.8	4	2	4	1	0	0.07	1	1	0.6	0.22	0.28	0.32
RE1F_s7h4_5t3_X	15	3.8	4	2	4	1	0	0.06	1	1	0.6	0.21	0.28	0.3
RE1F_s7h3t2_X	15	3.95	4	2	4	1	0	0.09	1	1	0.58	0.2	0.27	0.33
RE1F_s7h3_5t2_X	17.5	3.95	4	2	4	1	0	0.08	1	1	0.58	0.16	0.23	0.3
RE1F_s7h4t2_X	20	3.95	4	2	4	1	0	0.07	1	1	0.58	0.15	0.19	0.27
RE1F_s7h4_5t2_X	22.5	3.95	4	2	4	1	0	0.06	1	1	0.58	0.15	0.19	0.25
RE1Fd1_s7h3t5_X	6	3.5	4	2	1	1	0	0.09	1	1	0.63	0.85	0.87	0.91
RE1Fd1_s7h3_5t5_X	7	3.5	4	2	1	1	0	0.08	1	1	0.63	0.74	0.84	0.85
RE1Fd1_s7h4t5_X	8	3.5	4	2	1	1	0	0.07	1	1	0.63	0.66	0.75	0.81
RE1Fd1_s7h3_5t4_X	8.75	3.5	4	2	1	1	0	0.08	1	1	0.63	0.74	0.82	0.85
RE1Fd1_s7h4t4_X	10	3.5	4	2	1	1	0	0.07	1	1	0.63	0.64	0.77	0.79
RE1Fd1_s7h3_5t3_X	11.7	3.5	4	2	1	1	0	0.08	1	1	0.62	0.72	0.81	0.86
RE1Fd1_s7h4t3_X	13.3	3.5	4	2	1	1	0	0.07	1	1	0.62	0.61	0.76	0.78
RE1Fd1_s7h4_5t3_X	15	3.5	4	2	1	1	0	0.06	1	1	0.62	0.51	0.67	0.73
RE1Fd1_s7h3_5t2_X	17.5	3.5	4	2	1	1	0	0.08	1	1	0.61	0.58	0.7	0.85
RE1Fd1_s7h4t2_X	20	3.5	4	2	1	1	0	0.07	1	1	0.61	0.49	0.56	0.67
RE1Fd1_s7h4_5t2_X	22.5	3.5	4	2	1	1	0	0.06	1	1	0.61	0.4	0.52	0.52
RE1F_X	6	4.5	4	2	4	1	0	0.09	1	1	0.57	0.35	0.36	0.41
RE2Fd1_3op4_X	5.6	4.5	4	2	1	1	0	0.31	2	1	0.64	0.17	0.38	0.42
RE2Fd1_q1_2-1_X	5.6	4.5	4	2	1	1	0	0.31	2	1	0.64	0.16	0.37	0.41
RE2Fd1_q1_4-1_X	5.6	4.5	3	2	1	1	0	0.31	2	1	0.64	0.17	0.38	0.48
RE2Fd1_q2_1-2_X	5.6	4.5	4	2	1	1	0	0.31	2	1	0.64	0.16	0.33	0.37
RE2Fd1_q2_2_X	5.6	4.5	4	2	1	1	0	0.31	2	1	0.64	0.18	0.34	0.43
RE2Fd1_q2_3-2_X	5.6	4.5	4	2	1	1	0	0.31	2	1	0.64	0.13	0.35	0.44
RE2Fd1_q3_3-2_X	5.6	4.5	3	2	1	1	0	0.31	2	1	0.64	0.2	0.42	0.51
RE2Fd1_q3_4_X	5.6	4.5	2	2	1	1	0	0.31	2	1	0.64	0.2	0.44	0.53
RE2Fd1_q4_1_X	5.6	4.5	2	2	1	1	0	0.31	2	1	0.64	0.21	0.51	0.59
RE2Fd1_q4_2-1_X	5.6	4.5	2	2	1	1	0	0.31	2	1	0.64	0.21	0.53	0.61
RE2Fd1_q5_2-1_X	5.6	4.5	1	2	1	1	0	0.31	2	1	0.64	0.26	0.6	0.66
RE2Fd1_q5_3_X	5.6	4.5	1	2	1	1	0	0.31	2	1	0.64	0.26	0.61	0.69
RE2Fd1_q6_1-3_X	5.6	4.5	1	2	1	1	0	0.31	2	1	0.64	0.31	0.66	0.73
RE2Fd1_c100_X	5.6	4.5	4	2	1	1	0	0.19	2	1	0.64	0.25	0.44	0.49
RE2Fd1_c80_X	5.6	4.5	4	2	1	1	0	0.19	2	1	0.64	0.25	0.43	0.48
RE2Fd1_c60_X	5.6	4.5	4	3	1	1	0	0.19	2	1	0.64	0.25	0.41	0.46
RE2Fd1_c40_X	5.6	4.5	4	3	1	1	0	0.19	2	1	0.64	0.25	0.39	0.45
RE2Fd1_c20_X	5.6	4.5	4	4	1	1	0	0.19	2	1	0.64	0.22	0.29	0.4
RE2Fd1_c10_X	5.6	4.5	4	4	1	1	0	0.19	2	1	0.64	0.11	0.3	0.37
RE1F_kc0d0_X	7.2	3.5	4	2	4	1	0	0.07	1	1	0.69	0.39	0.39	0.44

Model	Input variables											Output variable		
	P1	P2	P3	P4	P5	P6	P7a	P7b	P8	P9	P10	LS1	LS2	LS3
	λ	s	[1-4]	[1-4]	[1-4]	[1-4]	$P7a$	$P7b$	N	[1-4]	γ_i	(g)		
RE1F_kc1d0_Y	7.2	3.5	4	2	4	1	0	0.07	1	1	0.69	0.38	0.41	0.48
RE1F_kc6d0_X	7.2	3.5	4	2	4	1	0	0.07	1	1	0.69	0.4	0.4	0.44
RE1F_kc6d1_X	7.2	3.5	4	2	1	1	0	0.07	1	1	0.69	0.63	0.64	0.77
RE1F_kc6d6_X	7.2	3.5	4	2	2	1	0	0.07	1	1	0.69	0.41	0.45	0.5
RE1F_kc6d1_kdc0_X	7.2	3.5	4	2	4	1	0	0.07	1	1	0.69	0.38	0.43	0.52
RE1F_kc1d1_kdc0_X	7.2	3.5	4	2	4	1	0	0.07	1	1	0.69	0.39	0.44	0.47
RE1F_kc1d6_X	7.2	3.5	4	2	3	1	0	0.07	1	1	0.69	0.41	0.49	0.58
RE1F_kc1d1_X	7.2	3.5	4	2	3	1	0	0.07	1	1	0.69	0.63	0.64	0.76
RE1F_kc1d6_kdc0_X	7.2	3.5	4	2	4	1	0	0.07	1	1	0.69	0.39	0.44	0.45
RE1F_kc6d6_kdc0_X	7.2	3.5	4	2	4	1	0	0.07	1	1	0.69	0.39	0.39	0.44
RE1F_kc6d2_X	7.2	3.5	4	2	2	1	0	0.07	1	1	0.69	0.5	0.57	0.67
RE1F_kc6d3_X	7.2	3.5	4	2	1	1	0	0.07	1	1	0.69	0.68	0.87	0.91
RE1F_0op_X	6	4.5	4	2	4	1	0	0.05	1	1	0.57	0.36	0.37	0.41
RE1F_1op_X	6	4.5	4	2	4	1	0	0.06	1	1	0.57	0.36	0.39	0.4
RE1F_3op1_X	6	4.5	4	2	4	1	0	0.11	1	1	0.57	0.36	0.36	0.41
RE1F_3op2_X	6	4.5	4	2	4	1	0	0.21	1	1	0.57	0.36	0.39	0.42
RE1F_3op3_X	6	4.5	4	2	4	1	0	0.31	1	1	0.57	0.35	0.39	0.46
RE1F_3op4_X	6	4.5	4	2	4	1	0	0.42	1	1	0.57	0.33	0.39	0.41
RE1F_3op5_X	6	4.5	4	2	4	1	0	0.5	1	1	0.57	0.25	0.31	0.36
RE2F_0op_X	5.6	4.5	4	2	4	1	0	0.04	2	1	0.57	0.22	0.24	0.25
RE2F_1op_X	5.6	4.5	4	2	4	1	0	0.06	2	1	0.57	0.22	0.24	0.25
RE2F_3op1_X	5.6	4.5	4	2	4	1	0	0.12	2	1	0.57	0.25	0.25	0.25
RE2F_3op2_X	5.6	4.5	4	2	4	1	0	0.21	2	1	0.57	0.2	0.25	0.28
RE2F_3op3_X	5.6	4.5	4	2	4	1	0	0.31	2	1	0.57	0.15	0.2	0.27
RE2F_3op4_X	5.6	4.5	4	2	4	1	0	0.41	2	1	0.57	0.12	0.22	0.27
RE2F_3op5_X	5.6	4.5	4	2	4	1	0	0.49	2	1	0.57	0.1	0.21	0.25
RE1Fd1_2op_X	6	4.5	4	2	1	1	0	0.11	1	1	0.64	0.74	0.81	0.89
RE1Fd1_0op_X	6	4.5	4	2	1	1	0	0.04	1	1	0.64	0.77	0.91	1.02
RE1Fd1_3op2_X	6	4.5	4	2	1	1	0	0.19	1	1	0.64	0.5	0.65	0.75
RE1Fd1_3op3_X	6	4.5	4	2	1	1	0	0.26	1	1	0.64	0.4	0.62	0.69
RE1Fd1_3op4_X	6	4.5	4	2	1	1	0	0.31	1	1	0.64	0.37	0.6	0.66
RE1Fd1_3op5_X	6	4.5	4	2	1	1	0	0.38	1	1	0.64	0.33	0.6	0.67
RE1Fd1_3op2_b_X	6	4.5	4	2	1	1	0	0.27	1	1	0.64	0.46	0.55	0.59
RE1Fd1_3op3_b_X	6	4.5	4	2	1	1	0	0.4	1	1	0.64	0.34	0.41	0.42
RE1Fd1_3op4_b_X	6	4.5	4	2	1	1	0	0.51	1	1	0.64	0.31	0.38	0.39
RE1Fd1_3op5_b_X	6	4.5	4	2	1	1	0	0.64	1	1	0.64	0.23	0.26	0.3
RE1Fd0_3op2_X	6	4.5	4	2	4	1	0	0.27	1	1	0.64	0.38	0.38	0.46
RE1Fd0_3op3_X	6	4.5	4	2	4	1	0	0.4	1	1	0.64	0.34	0.37	0.42
RE1Fd0_3op4_X	6	4.5	4	2	4	1	0	0.51	1	1	0.64	0.34	0.37	0.39
RE1Fd0_3op5_X	6	4.5	4	2	4	1	0	0.64	1	1	0.64	0.25	0.26	0.3
RE2Fd1_2op_X	5.6	4.5	4	2	1	1	0	0.11	2	1	0.64	0.36	0.51	0.58
RE2Fd1_0op_X	5.6	4.5	4	2	1	1	0	0.02	2	1	0.64	0.47	0.65	0.76

Model	Input variables											Output variable		
	P1	P2	P3	P4	P5	P6	P7a	P7b	P8	P9	P10	LS1	LS2	LS3
	λ	s	[1-4]	[1-4]	[1-4]	[1-4]	P7a	P7b	N	[1-4]	γ_i	(g)		
RE2Fd1_3op2_X	5.6	4.5	4	2	1	1	0	0.19	2	1	0.64	0.25	0.44	0.49
RE2Fd1_3op3_X	5.6	4.5	4	2	1	1	0	0.26	2	1	0.64	0.17	0.34	0.43
RE2Fd1_3op4_X	5.6	4.5	4	2	1	1	0	0.31	2	1	0.64	0.17	0.38	0.42
RE2Fd1_3op5_X	5.6	4.5	4	2	1	1	0	0.38	2	1	0.64	0.16	0.36	0.4
RE2Fd1_3op2_b_X	5.6	4.5	4	2	1	1	0	0.28	2	1	0.64	0.2	0.32	0.41
RE2Fd1_3op3_b_X	5.6	4.5	4	2	1	1	0	0.41	2	1	0.64	0.11	0.23	0.27
RE2Fd1_3op4_b_X	5.6	4.5	4	2	1	1	0	0.51	2	1	0.64	0.11	0.2	0.24
RE2Fd1_3op5_b_X	5.6	4.5	4	2	1	1	0	0.63	2	1	0.64	0.08	0.14	0.17
RE2Fd0_3op2_X	5.6	4.5	4	2	4	1	0	0.28	2	1	0.64	0.2	0.24	0.26
RE2Fd0_3op3_X	5.6	4.5	4	2	4	1	0	0.41	2	1	0.64	0.12	0.22	0.24
RE2Fd0_3op4_X	5.6	4.5	4	2	4	1	0	0.51	2	1	0.64	0.11	0.18	0.21
RE2Fd0_3op5_X	5.6	4.5	4	2	4	1	0	0.63	2	1	0.64	0.07	0.13	0.16
RE2F_X	5.6	4.5	4	2	4	1	0	0.09	2	1	0.57	0.23	0.24	0.25
STM3F_X	5.45	4.5	2	2	4	1	0	0.09	3	1	0.57	0.31	0.38	0.43
STM4Fd1_kc5_X	5.4	4.5	2	2	1	1	0	0.09	4	1	0.57	0.2	0.4	0.43
STM3Fd1_kc5_X	5.45	4.5	2	2	1	1	0	0.09	3	1	0.57	0.3	0.51	0.54
RE3Fd1_kc5_X	5.45	4.5	4	2	1	1	0	0.09	3	1	0.57	0.22	0.37	0.42
STM2Fd1_kc5_X	5.6	4.5	2	2	1	1	0	0.09	2	1	0.57	0.48	0.67	0.74
RE2Fd1_kc5_X	5.6	4.5	4	2	1	1	0	0.09	2	1	0.57	0.37	0.52	0.55
STM1Fd1_kc5_X	6	4.5	2	2	1	1	0	0.09	1	1	0.57	0.73	0.96	1.13
RE1Fd1_kc5_X	6	4.5	4	2	1	1	0	0.09	1	1	0.57	0.77	0.78	0.82
STM3F_23_X	5.45	4.5	2	2	4	1	0	0.2	3	1	0.57	0.25	0.35	0.38
STM3F_55_X	5.45	4.5	2	2	4	1	0	0.38	3	1	0.57	0.12	0.23	0.31
RE2Fd1_2op_LS1_X	5.6	4.5	4	2	1	1	0	0.11	2	2	0.64	0	0.43	0.51
RE2Fd1_2op_LS2_X	5.6	4.5	4	2	1	1	0	0.11	2	3	0.64	0	0.31	0.42
RE2Fd1_2op_LS3_X	5.6	4.5	4	2	1	1	0	0.11	2	4	0.64	0	0.33	0.42
RE2Fd1_3op4_LS1_X	5.6	4.5	4	2	1	1	0	0.31	2	2	0.64	0	0.33	0.34
RE2Fd1_3op4_LS2_X	5.6	4.5	4	2	1	1	0	0.31	2	3	0.64	0	0.24	0.26
RE2Fd1_3op4_LS3_X	5.6	4.5	4	2	1	1	0	0.31	2	4	0.64	0	0.25	0.26
RE1Fd1_3op4_LS1_X	6	4.5	4	2	1	1	0	0.26	1	2	0.64	0	0.49	0.62
RE1Fd1_3op4_LS2_X	6	4.5	4	2	1	1	0	0.26	1	3	0.64	0	0.5	0.63
RE1Fd1_3op4_LS3_X	6	4.5	4	2	1	1	0	0.26	1	4	0.64	0	0.47	0.58
RE1Fd1_3op4_t6_X	5	4.5	4	2	1	1	0	0.31	1	1	0.65	0.4	0.59	0.67
RE1Fd1_3op4_t4_X	7.5	4.5	4	2	1	1	0	0.31	1	1	0.63	0.36	0.59	0.66
RE1Fd1_3op4_t3_X	10	4.5	4	2	1	1	0	0.31	1	1	0.63	0.33	0.51	0.65
RE2Fd1_2op_t3_X	9.35	4.5	4	2	1	1	0	0.11	2	1	0.63	0.35	0.51	0.55
RE2Fd1_2op_t4_X	7	4.5	4	2	1	1	0	0.11	2	1	0.63	0.38	0.5	0.57
RE2Fd1_2op_t6_X	4.65	4.5	4	2	1	1	0	0.11	2	1	0.65	0.39	0.53	0.56
RE2Fd1_3op4_t6_X	4.65	4.5	4	2	1	1	0	0.31	2	1	0.65	0.18	0.39	0.43
RE2Fd1_3op4_t4_X	7	4.5	4	2	1	1	0	0.31	2	1	0.63	0.18	0.38	0.41
RE2Fd1_3op4_t3_X	9.35	4.5	4	2	1	1	0	0.31	2	1	0.63	0.18	0.37	0.41
RE2Fd1_s5_5t5_X	5.6	5.5	4	2	1	1	0	0.11	2	1	0.59	0.35	0.47	0.54

Model	Input variables											Output variable		
	P1	P2	P3	P4	P5	P6	P7a	P7b	P8	P9	P10	LS1	LS2	LS3
	λ	s	[1-4]	[1-4]	[1-4]	[1-4]	$P7a$	$P7b$	N	[1-4]	γ_i	(g)		
RE2Fd1_s5_5t3_X	9.35	5.5	4	2	1	1	0	0.11	2	1	0.58	0.35	0.46	0.53
RE2Fd1_s5_5t4_X	7	5.5	4	2	1	1	0	0.11	2	1	0.59	0.35	0.46	0.55
RE2Fd1_s5_5t6_X	4.65	5.5	4	2	1	1	0	0.11	2	1	0.60	0.36	0.47	0.52
RE2Fd1_s2_5_X	5.6	2.5	4	2	1	1	0	0.11	2	1	0.76	0.44	0.6	0.64
RE2Fd1_s3_5_X	5.6	3.5	4	2	1	1	0	0.11	2	1	0.70	0.41	0.47	0.59
RE2Fd1_s6_5_X	5.6	6.5	4	2	1	1	0	0.11	2	1	0.55	0.34	0.44	0.5
RE2Fd1_s2_5_2C_X	5.6	2.5	4	2	1	1	0	0.11	2	1	0.71	0.41	0.56	0.63
RE2Fd1_s3_5_2C_X	5.6	3.5	4	2	1	1	0	0.11	2	1	0.63	0.35	0.52	0.58
RE2Fd1_s4_5_2C_X	5.6	4.5	4	2	1	1	0	0.11	2	1	0.57	0.31	0.49	0.54
RE2Fd1_s5_5_2C_X	5.6	5.5	4	2	1	1	0	0.11	2	1	0.52	0.3	0.45	0.51
RE2Fd1_s6_5_2C_X	5.6	6.5	4	2	1	1	0	0.11	2	1	0.48	0.26	0.42	0.48
RE2Fd1_0op_2C_X	5.6	4.5	4	2	1	1	0	0.03	2	1	0.57	0.52	0.66	0.71
RE2Fd1_3op2_2C_X	5.6	4.5	4	2	1	1	0	0.22	2	1	0.57	0.24	0.4	0.45
RE2Fd1_3op3_2C_X	5.6	4.5	4	2	1	1	0	0.31	2	1	0.57	0.19	0.35	0.39
RE2Fd1_3op4_2C_X	5.6	4.5	4	2	1	1	0	0.37	2	1	0.57	0.2	0.33	0.38
RE2Fd1_3op5_2C_X	5.6	4.5	4	2	1	1	0	0.46	2	1	0.57	0.19	0.31	0.34
RE2Fd1_2op_Y	5.6	7	4	2	1	1	0.11	0	2	1	0.44	0.35	0.46	0.58
RE2Fd1_s2_5_Y	5.6	7	4	2	1	1	0.11	0	2	1	0.33	0.26	0.38	0.42
RE2Fd1_s3_5_Y	5.6	7	4	2	1	1	0.11	0	2	1	0.39	0.31	0.44	0.51
RE2Fd1_s5_5_Y	5.6	7	4	2	1	1	0.11	0	2	1	0.48	0.39	0.51	0.66
RE2Fd1_s6_5_Y	5.6	7	4	2	1	1	0.11	0	2	1	0.52	0.42	0.63	0.71
RE2Fd1_s4_5_2C_Y	5.6	7	4	2	1	1	0.11	0	2	1	0.50	0.43	0.64	0.71
RE2Fd1_s3_5_2C_Y	5.6	7	4	2	1	1	0.11	0	2	1	0.45	0.38	0.55	0.69
RE2Fd1_s5_5_2C_Y	5.6	7	4	2	1	1	0.11	0	2	1	0.54	0.5	0.71	0.79
RE2Fd1_s5_5L4_Y	5.6	4	4	2	1	1	0.11	0	2	1	0.58	0.53	0.66	0.77
RE2Fd1_s5_5L5_Y	5.6	5	4	2	1	1	0.11	0	2	1	0.52	0.45	0.57	0.68
RE2Fd1_s5_5L6_Y	5.6	6	4	2	1	1	0.11	0	2	1	0.48	0.4	0.52	0.64
RE2Fd1_s5_5L8_Y	5.6	8	4	2	1	1	0.11	0	2	1	0.41	0.28	0.47	0.52
RE1Fd1_2op_Y	6	7	4	2	1	1	0.11	0	1	1	0.44	0.46	0.77	0.93
RE1Fd1_s2_5_Y	6	7	4	2	1	1	0.11	0	1	1	0.33	0.4	0.64	0.72
RE1Fd1_s3_5_Y	6	7	4	2	1	1	0.11	0	1	1	0.39	0.45	0.72	0.84
RE1Fd1_s5_5_Y	6	7	4	2	1	1	0.11	0	1	1	0.48	0.49	0.81	0.99
RE1Fd1_s6_5_Y	6	7	4	2	1	1	0.11	0	1	1	0.52	0.54	0.81	1.05
RE2Fd1_IP35_L4_Y	5.6	4.5	4	2	1	1	0	0.35	2	1	0.53	0.11	0.29	0.32
RE2Fd1_IP35_L5_Y	5.6	4.5	4	2	1	1	0	0.35	2	1	0.57	0.13	0.3	0.34
RE2Fd1_IP35_L6_Y	5.6	4.5	4	2	1	1	0	0.35	2	1	0.61	0.15	0.27	0.37
RE2Fd1_IP35_L8_Y	5.6	4.5	4	2	1	1	0	0.33	2	1	0.67	0.17	0.4	0.46
RE2Fd1_IP55_L4_Y	5.6	4.5	4	2	1	1	0	0.55	2	1	0.53	0.06	0.16	0.18
RE2Fd1_IP55_L5_Y	5.6	4.5	4	2	1	1	0	0.53	2	1	0.57	0.1	0.18	0.21
RE2Fd1_IP55_L6_Y	5.6	4.5	4	2	1	1	0	0.55	2	1	0.61	0.1	0.17	0.19
RE2Fd1_IP55_L8_Y	5.6	4.5	4	2	1	1	0	0.55	2	1	0.67	0.1	0.19	0.2
B01_X	4.8	5	3	2	1	1	0	0.58	4	1	0.69	0.05	0.12	0.14

Model	Input variables											Output variable		
	P1	P2	P3	P4	P5	P6	P7a	P7b	P8	P9	P10	LS1	LS2	LS3
	λ	s	[1-4]	[1-4]	[1-4]	[1-4]	P7a	P7b	N	[1-4]	γ_i	(g)		
B01_Y	4.8	10	3	2	1	4	0.58	0	4	1	0.38	0.22	0.33	0.41
B01_X1	4.8	5	3	2	1	1	0	0.58	4	4	0.69	0	0.07	0.08
B01_Y1	4.8	10	3	2	1	4	0.58	0	4	4	0.38	0	0.11	0.18
B01b_X	4.8	5	3	2	1	1	0	0.43	4	1	0.62	0.05	0.22	0.25
B01c_X	4.8	5	3	2	1	1	0	0.41	4	1	0.62	0.19	0.26	0.3
B02_X	11.7	5	1	2	4	1	0	0.69	3	1	0.66	0.05	0.09	0.1
B02_Y	11.7	9	1	2	3	3	0.69	0	3	1	0.38	0.17	0.35	0.39
B02_X1	11.7	5	1	2	4	1	0	0.69	3	4	0.66	0	0.08	0.09
B02_Y1	11.7	9	1	2	3	3	0.69	0	3	3	0.38	0	0.11	0.21
B03_X	7	4	2	4	2	1	0	0.65	4	1	0.73	0.03	0.06	0.08
B03_Y	7	10	2	4	2	2	0.65	0	4	1	0.33	0.09	0.15	0.17
B03_X1	7	4	2	4	2	1	0	0.65	4	2	0.73	0	0.05	0.06
B03_Y1	7	10	2	4	2	2	0.65	0	4	2	0.33	0	0.13	0.15
B04_X	7.5	4	4	4	1	1	0	0.27	3	1	0.55	0.09	0.13	0.15
B04_Y	7.5	4	4	4	1	3	0.27	0	3	1	0.55	0.22	0.26	0.29
B04_X1	7.5	4	4	4	1	1	0	0.27	3	2	0.55	0	0.1	0.12
B04_Y1	7.5	4	4	4	1	3	0.27	0	3	2	0.55	0	0.17	0.25
B05_X	7	4.5	4	2	4	1	0	0.64	4	1	0.74	0.02	0.06	0.06
B05_Y	7	12	4	2	4	1	0.64	0	4	1	0.31	0.03	0.07	0.11
B05_X1	7	4.5	4	2	4	1	0	0.64	4	2	0.74	0	0.05	0.05
B05_Y1	7	12	4	2	4	1	0.64	0	4	2	0.31	0	0.04	0.07
B06_X	8.75	4	3	3	1	1	0	0.65	4	1	0.59	0.02	0.05	0.06
B06_Y	8.75	5	3	3	1	4	0.65	0	4	1	0.49	0.15	0.22	0.25
B06_X1	8.75	4	3	3	1	1	0	0.65	4	4	0.59	0	0.03	0.03
B06_Y1	8.75	5	3	3	1	4	0.65	0	4	4	0.49	0	0.05	0.07
B07_X	11.7	5	1	4	4	1	0	0.69	3	1	0.66	0.04	0.06	0.08
B07_Y	11.7	9	1	4	3	2	0.69	0	3	1	0.38	0.08	0.3	0.32
B07_X1	11.7	5	1	4	4	1	0	0.69	3	3	0.66	0	0.06	0.07
B07_Y1	11.7	9	1	4	3	2	0.69	0	3	3	0.38	0	0.17	0.24
B08_X	7.5	5	1	4	4	1	0	0.56	2	1	0.58	0.12	0.16	0.2
B08_Y	7.5	6	1	4	3	3	0.56	0	2	1	0.49	0.31	0.53	0.58
B09_X	8.75	4.5	3	4	1	1	0	0.1	2	1	0.74	0.3	0.5	0.63
B09_Y	8.75	12	3	4	1	3	0.1	0	2	1	0.31	0.17	0.26	0.29
B09_X1	8.75	4.5	3	4	1	1	0	0.1	2	4	0.74	0	0.27	0.34
B09_Y1	8.75	12	3	4	1	3	0.1	0	2	4	0.31	0	0.21	0.24
B10_X	4.8	4	4	2	1	1	0	0.13	2	1	0.69	0.5	0.57	0.71
B10_Y	4.8	8	4	2	1	3	0.13	0	2	1	0.38	0.33	0.54	0.65
B10_X1	4.8	4	4	2	1	1	0	0.13	2	3	0.69	0	0.44	0.48
B10_Y1	4.8	8	4	2	1	3	0.13	0	2	3	0.38	0	0.46	0.51
B11_X	17.5	4	1	4	4	1	0	0.6	1	1	0.68	0.21	0.23	0.29
B11_Y	17.5	8	1	4	4	3	0.6	0	1	1	0.35	0.12	0.23	0.33
B11_X1	17.5	4	1	4	4	1	0	0.6	1	2	0.68	0	0.18	0.24

Model	Input variables											Output variable		
	P1	P2	P3	P4	P5	P6	P7a	P7b	P8	P9	P10	LS1	LS2	LS3
	λ	s	[1-4]	[1-4]	[1-4]	[1-4]	P7a	P7b	N	[1-4]	γ_i	(g)		
B11_Y1	17.5	8	1	4	4	3	0.6	0	1	2	0.35	0	0.2	0.31
B12_X	10	3.5	2	3	1	1	0	0.36	3	1	0.72	0.13	0.2	0.25
B12_Y	10	8	2	3	1	2	0.36	0	3	1	0.35	0.2	0.25	0.29
B12_X1	10	3.5	2	3	1	1	0	0.36	3	2	0.72	0	0.08	0.11
B12_Y1	10	8	2	3	1	2	0.36	0	3	2	0.35	0	0.17	0.18
B13_X	10	4.5	3	3	4	1	0	0.34	2	1	0.72	0.12	0.21	0.23
B13_Y	10	11	3	3	4	2	0.34	0	2	1	0.33	0	0.07	0.07
B13_X1	10	4.5	3	3	4	1	0	0.34	2	3	0.72	0	0.08	0.13
B13_Y1	10	11	3	3	4	2	0.34	0	2	3	0.33	0	0.06	0.06
B14_X	15	4	1	4	4	1	0	0.56	3	1	0.52	0.05	0.11	0.13
B14_Y	15	4	1	4	2	2	0.56	0	3	1	0.52	0.21	0.38	0.41
B14_X1	15	4	1	4	4	1	0	0.56	3	3	0.52	0	0.08	0.1
B14_Y1	15	4	1	4	2	2	0.56	0	3	3	0.52	0	0.2	0.26
B15_X	8	5	2	2	4	1	0	0.58	2	1	0.67	0.07	0.13	0.14
B15_Y	8	9	2	2	3	1	0.58	0	2	1	0.40	0.15	0.36	0.47
B15_X1	8	5	2	2	4	1	0	0.58	2	4	0.67	0	0.07	0.11
B15_Y1	8	9	2	2	3	1	0.58	0	2	4	0.40	0	0.12	0.34
B16_X	8.75	4	4	3	1	1	0	0.05	2	1	0.59	0.36	0.45	0.47
B16_Y	8.75	5	4	3	1	4	0	0	2	1	0.49	0.34	0.38	0.42
B16_X1	8.75	4	4	3	1	1	0	0.05	2	4	0.59	0	0.2	0.29
B16_Y1	8.75	5	4	3	1	4	0	0	2	4	0.49	0	0.22	0.24
B17_X	8	3.5	4	2	4	1	0	0.25	4	1	0.63	0.05	0.11	0.14
B17_Y	8	5	4	2	4	3	0.25	0	4	1	0.47	0.06	0.14	0.2
B17_X1	8	3.5	4	2	4	1	0	0.25	4	2	0.63	0	0.1	0.15
B17_Y1	8	5	4	2	4	3	0.25	0	4	2	0.47	0	0.1	0.13
B18_X	8	4	4	2	2	1	0	0.33	2	1	0.71	0.1	0.19	0.23
B18_Y	8	9	4	2	2	4	0.33	0	2	1	0.36	0.05	0.18	0.26
B18_X1	8	4	4	2	2	1	0	0.33	2	3	0.71	0	0.18	0.2
B18_Y1	8	9	4	2	2	4	0.33	0	2	3	0.36	0	0.13	0.18
B19_X	8	4	3	3	1	1	0	0.39	2	1	0.73	0.08	0.25	0.27
B19_Y	8	10	3	3	1	1	0.18	0	2	1	0.33	0.1	0.25	0.29
B20_X	11.7	4.5	3	3	4	1	0	0.23	3	1	0.74	0	0.12	0.17
B20_Y	11.7	12	3	3	4	2	0.23	0	3	1	0.30	0	0.02	0.04
B21_X	4.8	4	1	3	4	1	0	0.61	2	1	0.70	0.22	0.23	0.26
B21_Y	4.8	8	1	3	3	4	0.61	0	2	1	0.40	0.36	0.55	0.65
B21_X1	4.8	4	1	3	4	1	0	0.61	2	3	0.70	0	0.22	0.24
B21_Y1	4.8	8	1	3	3	4	0.61	0	2	2	0.40	0.2	0.38	0.63
B22_X	11.7	4.5	1	4	1	1	0	0.35	2	1	0.68	0.16	0.42	0.5
B22_Y	11.7	9	1	4	1	4	0.16	0	2	1	0.36	0.24	0.37	0.44
B22_X1	11.7	4.5	1	4	1	1	0	0.35	2	3	0.68	0	0.18	0.22
B22_Y1	11.7	9	1	4	1	4	0.16	0	2	3	0.36	0	0.1	0.24
B23_X	10	5	1	3	4	1	0	0.56	4	1	0.70	0.03	0.09	0.12

Model	Input variables											Output variable		
	P1	P2	P3	P4	P5	P6	P7a	P7b	P8	P9	P10	LS1	LS2	LS3
	λ	s	[1-4]	[1-4]	[1-4]	[1-4]	P7a	P7b	N	[1-4]	γ_i	(g)		
B23_Y	10	11	1	3	3	2	0.56	0	4	1	0.35	0.15	0.21	0.23
B23_X1	10	5	1	3	4	1	0	0.56	4	4	0.70	0	0.05	0.07
B23_Y1	10	11	1	3	3	2	0.56	0	4	4	0.35	0	0.15	0.16
B24_X	10	3.5	1	4	1	1	0	0.34	3	1	0.79	0.19	0.34	0.4
B24_Y	10	12	1	4	1	3	0.15	0	3	1	0.26	0.18	0.2	0.2
B25_X	20	4	3	2	2	1	0	0.56	2	1	0.74	0.07	0.13	0.16
B25_Y	20	11	3	2	2	2	0.56	0	2	1	0.29	0.08	0.25	0.3
B25_X1	20	4	3	2	2	1	0	0.56	2	2	0.74	0	0.09	0.13
B25_Y1	20	11	3	2	2	2	0.56	0	2	2	0.29	0	0.17	0.22
B26_X	13.3	4	2	4	1	1	0	0.53	4	1	0.68	0.03	0.08	0.09
B26_Y	13.3	8	2	4	1	4	0.53	0	4	1	0.37	0.06	0.13	0.15
B26_X1	13.3	4	2	4	1	1	0	0.53	4	3	0.68	0	0.06	0.08
B26_Y1	13.3	8	2	4	1	4	0.53	0	4	3	0.37	0	0.1	0.13
B27_X	13.3	4.5	2	3	1	1	0	0.4	3	1	0.59	0.06	0.18	0.2
B27_Y	13.3	6	2	3	1	4	0.18	0	3	1	0.46	0.17	0.28	0.3
B27_X1	13.3	4.5	2	3	1	1	0	0.4	3	3	0.59	0	0.06	0.11
B27_Y1	13.3	6	2	3	1	4	0.18	0	3	3	0.46	0	0.16	0.19
B28_X	4.8	3.5	4	2	2	1	0	0.34	1	1	0.73	0.42	0.5	0.53
B28_Y	4.8	8	4	2	2	3	0.18	0	1	1	0.37	0.39	0.52	0.55
B29_X	22.5	4	1	2	4	1	0	0.13	1	1	0.57	0.47	0.47	0.49
B29_Y	22.5	5	1	2	3	4	0.13	0	1	1	0.47	0.41	0.44	0.55
B29_X1	22.5	4	1	2	4	1	0	0.13	1	4	0.57	0	0.22	0.31
B29_Y1	22.5	5	1	2	3	4	0.13	0	1	4	0.47	0	0.23	0.32
B30_X	8.75	4	3	3	4	1	0	0.37	3	1	0.75	0.15	0.2	0.25
B30_Y	8.75	11	3	3	2	2	0.37	0	3	1	0.30	0.2	0.25	0.28
B30_X1	8.75	4	3	3	4	1	0	0.37	3	4	0.75	0	0.12	0.13
B30_Y1	8.75	11	3	3	2	2	0.37	0	3	4	0.30	0	0.16	0.18
RE1F_s7h3t6_Y	5	7	4	2	4	1	0.08	0	1	1	0.39	0.35	0.38	0.45
RE1F_s7h2_4t6_Y	4	7	4	2	4	1	0.1	0	1	1	0.39	0.59	0.65	0.67
RE1F_s5h3t6_Y	5	5	4	2	4	1	0.11	0	1	1	0.48	0.4	0.43	0.49
RE1F_s5h2_4t6_Y	4	5	4	2	4	1	0.13	0	1	1	0.48	0.67	0.72	0.8
RE1F_s7h3t6_X	5	3.65	4	2	4	1	0	0.09	1	1	0.63	0.51	0.53	0.57
RE1F_s7h2_4t6_X	4	3.65	4	2	4	1	0	0.11	1	1	0.63	0.7	0.74	0.78
RE2F_c100_Y	5.6	7	4	2	4	1	0.11	0	2	1	0.44	0.11	0.18	0.21
RE2F_c80_Y	5.6	7	4	2	4	1	0.11	0	2	1	0.44	0.1	0.18	0.21
RE2F_c60_Y	5.6	7	4	3	4	1	0.11	0	2	1	0.44	0.09	0.17	0.2
RE2F_c40_Y	5.6	7	4	3	4	1	0.11	0	2	1	0.44	0.07	0.17	0.19
RE2F_c20_Y	5.6	7	4	4	4	1	0.11	0	2	1	0.44	0.06	0.14	0.16
RE2F_c10_Y	5.6	7	4	4	4	1	0.11	0	2	1	0.44	0.08	0.12	0.14
RE2F_kc6d3_Y	5.6	7	4	2	1	1	0.08	0	2	1	0.5	0.62	0.65	0.76
RE2F_kc6d1_Y	5.6	7	4	2	1	1	0.08	0	2	1	0.5	0.39	0.64	0.71
RE2F_kc1d1_Y	5.6	7	4	2	2	1	0.08	0	2	1	0.5	0.4	0.5	0.64

Model	Input variables											Output variable		
	P1	P2	P3	P4	P5	P6	P7a	P7b	P8	P9	P10	LS1	LS2	LS3
	λ	s	[1-4]	[1-4]	[1-4]	[1-4]	$P7a$	$P7b$	N	[1-4]	γ_i	(g)		
RE2F_kc6d1_kdc0_Y	5.6	7	4	2	2	1	0.08	0	2	1	0.5	0.35	0.49	0.62
RE2F_kc6d6_Y	5.6	7	4	2	2	1	0.08	0	2	1	0.5	0.11	0.48	0.61
RE2F_kc1d6_Y	5.6	7	4	2	3	1	0.08	0	2	1	0.5	0.12	0.55	0.58
RE2F_kc6d6_kdc0_Y	5.6	7	4	2	3	1	0.08	0	2	1	0.5	0.24	0.46	0.53
RE2F_kc1d1_kdc0_Y	5.6	7	4	2	3	1	0.08	0	2	1	0.5	0.25	0.34	0.48
RE2F_kc1d6_kdc0_Y	5.6	7	4	2	3	1	0.08	0	2	1	0.5	0.16	0.35	0.43
RE2F_kc6d3_X	5.6	4.5	4	2	1	1	0	0.09	2	1	0.57	0.37	0.48	0.62
RE2F_kc1d1_X	5.6	4.5	4	2	2	1	0	0.09	2	1	0.57	0.37	0.52	0.56
RE2F_kc6d1_kdc0_X	5.6	4.5	4	2	4	1	0	0.09	2	1	0.57	0.24	0.26	0.31
RE2F_kc6d6_X	5.6	4.5	4	2	2	1	0	0.09	2	1	0.57	0.26	0.38	0.45
RE2F_kc1d6_X	5.6	4.5	4	2	3	1	0	0.09	2	1	0.57	0.26	0.41	0.46
RE2F_kc6d6_kdc0_X	5.6	4.5	4	2	4	1	0	0.09	2	1	0.57	0.25	0.26	0.27
RE2F_kc1d1_kdc0_X	5.6	4.5	4	2	4	1	0	0.09	2	1	0.57	0.22	0.25	0.28
RE2F_kc1d6_kdc0_X	5.6	4.5	4	2	4	1	0	0.09	2	1	0.57	0.23	0.24	0.26
RE2F_kc5_X	5.6	4.5	4	2	4	1	0	0.09	2	1	0.57	0.22	0.25	0.26
RE2F_kc1_X	5.6	4.5	4	2	4	1	0	0.09	2	1	0.57	0.22	0.26	0.26
STM3F_kc6d3_Y	5.45	7	2	2	1	1	0.08	0	3	1	0.5	0.59	0.69	0.76
STM3F_kc6d1_Y	5.45	7	2	2	1	1	0.08	0	3	1	0.5	0.35	0.63	0.75
STM3F_kc1d1_Y	5.45	7	2	2	2	1	0.08	0	3	1	0.5	0.32	0.62	0.74
STM3F_kc6d1_kdc0_Y	5.45	7	2	2	2	1	0.08	0	3	1	0.5	0.38	0.62	0.74
STM3F_kc6d6_Y	5.45	7	2	2	2	1	0.08	0	3	1	0.5	0.22	0.43	0.56
STM3F_kc1d6_Y	5.45	7	2	2	3	1	0.08	0	3	1	0.5	0.19	0.47	0.55
STM3F_kc6d6_kdc0_Y	5.45	7	2	2	3	1	0.08	0	3	1	0.5	0.3	0.54	0.61
STM3F_kc1d1_kdc0_Y	5.45	7	2	2	3	1	0.08	0	3	1	0.5	0.3	0.56	0.61
STM3F_kc1d6_kdc0_Y	5.45	7	2	2	3	1	0.08	0	3	1	0.5	0.22	0.41	0.52
STM3F_kc6d3_X	5.45	4.5	2	2	1	1	0	0.09	3	1	0.57	0.31	0.55	0.59
STM3F_kc1d1_X	5.45	4.5	2	2	2	1	0	0.09	3	1	0.57	0.29	0.5	0.53
STM3F_kc6d1_kdc0_X	5.45	4.5	2	2	4	1	0	0.09	3	1	0.57	0.3	0.4	0.53
STM3F_kc6d6_X	5.45	4.5	2	2	2	1	0	0.09	3	1	0.57	0.29	0.41	0.49
STM3F_kc1d6_X	5.45	4.5	2	2	3	1	0	0.09	3	1	0.57	0.28	0.38	0.45
STM3F_kc6d6_kdc0_X	5.45	4.5	2	2	4	1	0	0.09	3	1	0.57	0.28	0.45	0.47
STM3F_kc1d1_kdc0_X	5.45	4.5	2	2	4	1	0	0.09	3	1	0.57	0.29	0.4	0.51
STM3F_kc1d6_kdc0_X	5.45	4.5	2	2	4	1	0	0.09	3	1	0.57	0.28	0.39	0.47
STM3F_kc5_X	5.45	4.5	2	2	4	1	0	0.09	3	1	0.57	0.33	0.44	0.45
STM3F_kc1_X	5.45	4.5	2	2	4	1	0	0.09	3	1	0.57	0.33	0.41	0.44
RE2F_R1_Y	5.6	7	4	2	4	2	0.11	0	2	1	0.44	0.07	0.16	0.19
RE2F_R2_Y	5.6	7	4	2	4	2	0.11	0	2	1	0.44	0.07	0.15	0.17
RE2F_R3_Y	5.6	7	4	2	4	3	0.11	0	2	1	0.44	0	0.12	0.16
RE2F_R4_Y	5.6	7	4	2	4	3	0.11	0	2	1	0.44	0	0.11	0.13
RE2F_R5_Y	5.6	7	4	2	4	4	0.11	0	2	1	0.44	0	0.09	0.11
RE2F_kc6d1_Y	5.6	7	4	2	1	1	0.11	0	2	1	0.44	0.36	0.52	0.63
RE1F_2op_a_X	6	4.5	4	2	4	1	0	0.11	1	1	0.64	0.36	0.39	0.49

Model	Input variables											Output variable		
	P1	P2	P3	P4	P5	P6	P7a	P7b	P8	P9	P10	LS1	LS2	LS3
	λ	s	[1-4]	[1-4]	[1-4]	[1-4]	P7a	P7b	N	[1-4]	γ_i	(g)		
RE1F_0op_a_X	6	4.5	4	2	4	1	0	0.04	1	1	0.64	0.36	0.39	0.46
RE1F_3op2_a_X	6	4.5	4	2	4	1	0	0.19	1	1	0.64	0.37	0.39	0.46
RE1F_3op3_a_X	6	4.5	4	2	4	1	0	0.26	1	1	0.64	0.35	0.41	0.45
RE1F_3op4_a_X	6	4.5	4	2	4	1	0	0.31	1	1	0.64	0.35	0.39	0.42
RE1F_3op5_a_X	6	4.5	4	2	4	1	0	0.38	1	1	0.64	0.25	0.32	0.35
RE2F_2op_a_X	5.6	4.5	4	2	4	1	0	0.11	2	1	0.64	0.25	0.25	0.25
RE2F_0op_a_X	5.6	4.5	4	2	4	1	0	0.02	2	1	0.64	0.25	0.25	0.27
RE2F_3op2_a_X	5.6	4.5	4	2	4	1	0	0.19	2	1	0.64	0.2	0.23	0.27
RE2F_3op3_a_X	5.6	4.5	4	2	4	1	0	0.26	2	1	0.64	0.14	0.21	0.28
RE2F_3op4_a_X	5.6	4.5	4	2	4	1	0	0.31	2	1	0.64	0.11	0.2	0.26
RE2F_3op5_a_X	5.6	4.5	4	2	4	1	0	0.38	2	1	0.64	0.1	0.19	0.22
RE2Fd1_R1_Y	5.6	7	4	2	1	2	0.11	0	2	1	0.44	0.36	0.52	0.63
RE2Fd1_R2_Y	5.6	7	4	2	1	3	0.11	0	2	1	0.44	0.36	0.51	0.63
RE2Fd1_R3_Y	5.6	7	4	2	1	4	0.11	0	2	1	0.44	0.36	0.57	0.64
RE1Fd0_c100_Y	6	7	4	2	4	1	0.11	0	1	1	0.44	0.3	0.3	0.38
RE1Fd0_c200_Y	6	7	4	1	4	1	0.11	0	1	1	0.44	0.32	0.34	0.42
RE1Fd0_c500_Y	6	7	4	1	4	1	0.11	0	1	1	0.44	0.4	0.44	0.51
RE2Fd0_c100_Y	6	7	4	2	4	1	0.11	0	2	1	0.44	0.1	0.17	0.2
RE2Fd0_c200_Y	6	7	4	1	4	1	0.11	0	2	1	0.44	0.13	0.18	0.21
RE2Fd0_c500_Y	6	7	4	1	4	1	0.11	0	2	1	0.44	0.2	0.22	0.26
STM2Fd0_c100_Y	6	7	2	2	4	1	0.11	0	2	1	0.44	0.21	0.27	0.3
STM2Fd0_c200_Y	6	7	2	1	4	1	0.11	0	2	1	0.44	0.31	0.34	0.37
RE2Fd3_c100_Y	6	7	4	2	1	1	0.11	0	2	1	0.44	0.32	0.4	0.51
RE2Fd3_c200_Y	6	7	4	1	1	1	0.11	0	2	1	0.44	0.34	0.47	0.5
RE2Fd3_c500_Y	6	7	4	1	1	1	0.11	0	2	1	0.44	0.38	0.45	0.51
STM3Fd0_c100_Y	6	7	2	2	4	1	0.11	0	3	1	0.44	0.2	0.2	0.28
STM3Fd0_c200_Y	6	7	2	1	4	1	0.11	0	3	1	0.44	0.28	0.28	0.3
RE1F_h3t4_c500_Y	7.5	7	4	1	4	1	0.11	0	1	1	0.43	0.34	0.4	0.41
RE1F_h4t4_c500_Y	10	7	4	1	4	1	0.11	0	1	1	0.43	0.23	0.27	0.32
RE1F_h4t3_c500_Y	13.3	7	4	1	4	1	0.11	0	1	1	0.42	0.19	0.23	0.24
RE1F_s5_c500_Y	6	5	4	1	4	1	0.11	0	1	1	0.52	0.45	0.58	0.74
RE1F_s8_c500_Y	6	8	4	1	4	1	0.11	0	1	1	0.41	0.32	0.38	0.42
RE1F_s10_c500_Y	6	10	4	1	4	1	0.11	0	1	1	0.35	0.27	0.32	0.35
BM1F_c150_Y	6	7	2	1	4	1	0.11	0	1	1	0.44	0.57	0.6	0.69
STM1F_c200_Y	6	7	2	1	4	1	0.11	0	1	1	0.44	0.52	0.54	0.65
IRR_STM1F_c200_Y	6	7	3	1	4	1	0.11	0	1	1	0.44	0.45	0.49	0.56
RE2Fd2_c500_Y	6	7	4	1	2	1	0.11	0	2	1	0.44	0.17	0.4	0.42
RE2Fd1_c500_Y	6	7	4	1	3	1	0.11	0	2	1	0.44	0.23	0.28	0.4
RE1F_R1_c500_Y	6	7	4	1	4	2	0.11	0	1	1	0.44	0.35	0.38	0.42
RE1F_R2_c500_Y	6	7	4	1	4	3	0.11	0	1	1	0.44	0.3	0.33	0.38
RE1F_R3_c500_Y	6	7	4	1	4	4	0.11	0	1	1	0.44	0	0.12	0.3
RE2F_3op2_c500_Y	6	7	4	1	4	1	0.23	0	2	1	0.44	0.18	0.24	0.33

Model	Input variables											Output variable		
	P1	P2	P3	P4	P5	P6	P7a	P7b	P8	P9	P10	LS1	LS2	LS3
	λ	s	[1-4]	[1-4]	[1-4]	[1-4]	$P7a$	$P7b$	N	[1-4]	γ_i	(g)		
RE2F_3op3_c500_Y	6	7	4	1	4	1	0.34	0	2	1	0.44	0.16	0.27	0.35
RE2F_3op4_c500_Y	6	7	4	1	4	1	0.55	0	2	1	0.44	0.16	0.29	0.32
RE2Fd3_2op_c500_Y	6	4.5	4	1	1	1	0	0.11	2	1	0.64	0.37	0.54	0.6
RE2Fd3_3op2_c500_Y	6	4.5	4	1	1	1	0	0.19	2	1	0.64	0.22	0.44	0.51
RE2Fd3_3op4a_c500_Y	6	4.5	4	1	1	1	0	0.31	2	1	0.64	0.07	0.41	0.44
RE2Fd3_3op4b_c500_Y	6	4.5	4	1	1	1	0	0.51	2	1	0.64	0.03	0.23	0.27
RE3F_c500_Y	6	7	4	1	4	1	0.11	0	3	1	0.44	0.17	0.18	0.2
RE1F_LS1_c500_Y	6	7	4	1	4	1	0.11	0	1	2	0.44	0	0.39	0.45
RE1F_LS2_c500_Y	6	7	4	1	4	1	0.11	0	1	3	0.44	0	0.38	0.39
RE1F_LS3_c500_Y	6	7	4	1	4	1	0.11	0	1	4	0.44	0	0.35	0.37
RE2Fd3_s3_5_c500_Y	6	7	4	1	1	1	0.11	0	2	1	0.39	0.36	0.42	0.45
RE2Fd3_s5_5_c500_Y	6	7	4	1	1	1	0.11	0	2	1	0.48	0.44	0.55	0.61
RE2Fd3_L5_c500_Y	6	4.5	4	1	1	1	0	0.35	2	1	0.57	0.08	0.3	0.35
RE2Fd3_L8_c500_Y	6	4.5	4	1	1	1	0	0.33	2	1	0.67	0.15	0.41	0.46
STM3Fd0_LW_Y	5.45	7	3	2	4	1	0.08	0	3	1	0.5	0.2	0.26	0.29
STM3Fd1_23_X	5.45	4.5	2	2	1	1	0	0.2	3	1	0.57	0.24	0.42	0.49
STM3Fd1_55_X	5.45	4.5	2	2	1	1	0	0.38	3	1	0.57	0.16	0.33	0.37
RE2F_2op_L9_Y	5.6	9	4	2	1	1	0.09	0	2	1	0.38	0.25	0.4	0.5
RE2F_2op_L10_Y	5.6	10	4	2	1	1	0.08	0	2	1	0.35	0.22	0.43	0.46
RE2F_2op_L11_Y	5.6	11	4	2	1	1	0.07	0	2	1	0.33	0.2	0.4	0.44
RE2F_2op_L12_Y	5.6	12	4	2	1	1	0.06	0	2	1	0.31	0.17	0.32	0.42

ANNEX C

EXPERT SURVEY

A questionnaire surveys was prepared to collect the opinion of experts on the influence of the selected seismic vulnerability assessment parameters on the seismic performance of vernacular buildings. This survey was distributed to a group mainly formed by academics in the research field from all around the world and is presented here in full.

Seismic vulnerability assessment methodology for vernacular architecture: Parameter weight definition I

Dear colleague,

As part of a research project from the Institute for Sustainability and Innovation (ISISE) of the University of Minho, we are developing a simplified methodology for the seismic vulnerability assessment of vernacular architecture. The proposed simplified methodology is based on the vulnerability index formulation, which focuses on the identification of those constructive aspects and parameters that influence the most the seismic behavior of the building.

Specifically, the research primarily addresses Portuguese vernacular architecture, where the most common traditional construction materials used are stone, wood and earth. Stone masonry or earth are used to build the walls. Timber is mostly used for floors and roofs. Thus, the common Portuguese vernacular architecture typology consists of timber diaphragms as the common horizontal structural elements coupled with earthen and stone masonry load bearing walls, which are the main vertical resisting elements of the structure.

We have identified ten parameters that we consider critical in defining the seismic response of this type of buildings. As a next step, since the influence of each parameter in the seismic vulnerability of a building is not the same, we are weighting the different parameters according to their relative importance. In order to define these weights, we would like to have your opinion, as an expert in this field.

In the following survey, we ask you to compare the relative importance of the parameters in a scale from 1 to 9. A set of pairwise comparisons will be presented where 1 means that they have equal importance, while 9 means that one factor has an extremely higher importance than the other. The results will be processed using the Analytic Hierarchy Process Method (Saaty, 1987). Please, refer to the following paper if you want to find out more about this methodology:

<http://www.sciencedirect.com/science/article/pii/0270025587904738>

A total of 25 questions were prepared and we expect that it will not take you more than ten minutes of your time to complete the survey.

Thank you very much for your time and for sharing with us your valuable insight.

*Required

1. Email address *

Survey

The questionnaire is presented below. The ten parameters considered for the methodology are listed below together with a brief description for each of them. For reference purposes, a typical range of variation within the parameter is also provided. This list is just intended as a reference if some clarification on the parameters is needed during the survey.

P1. WALL SLENDERNESS: This parameter can be defined as the ratio between the height of the wall and its thickness (i.e. h/t). Given the traditional materials commonly used for the walls (stone and earth), vernacular buildings typically presents low slenderness ratio below 9, and is rare to find ratios over 12.

P2. MAXIMUM WALL SPAN: This parameter takes into account the maximum length of a wall prone to out-of-plane movements, which is a wall spanning between two in-plane earthquake resistant walls. Typically, values might range between 4 and 10 meters.

P3. TYPE OF MATERIAL: This parameter takes into account the type of material used for the vertical structural elements of the building. In the cases included in the study, only earthen and masonry (brick and stone) materials are considered, while the type of structure of the buildings always consists of load bearing walls. Materials can vary from adobe masonry or irregular not worked stone masonry to carefully worked dressed stone masonry.

P4. WALL-TO-WALL CONNECTION: This parameter takes into account the quality of the connection between the structural walls. The quality may vary from visible separation between orthogonal walls to workmanlike built connections with good interlocking between the masonry units at the corners in case of masonry buildings.

P5. HORIZONTAL DIAPHRAGMS: This parameter takes into account the type of horizontal diaphragm (floors and roofs), focusing on the quality of its connection to the load bearing walls and its in-plane stiffness. Typically, the diaphragms may vary from diaphragms of negligible stiffness with beams poorly connected to the walls to rigid timber diaphragm well-connected to the walls.

P6. ROOF THRUST: This parameter takes into account the possible thrust that the roof may exert to the load bearing walls. Roofs may vary from thrusting roof types with considerable weight and low inclination to non-thrusting roof types.

P7. WALL OPENINGS: This parameter takes into account the total area of wall openings that can be observed in the load bearing structural walls, as a percentage of the total area of the walls. Typically, vernacular buildings may present a reduced area of wall openings (below 20%), but large areas (over 50%) can also be observed.

P8. NUMBER OF FLOORS: This parameter takes into account the number of floors of the studied building. Vernacular buildings rarely presents more than four stories.

P9. STATE OF CONSERVATION: This parameter takes into account the state of conservation of the building and the existing damage that can be observed, mainly focused on the state of degradation of the structural elements of the building. Previous damage may vary from a severe deterioration of the materials and widespread cracking to walls in good conditions with no visible damage.

P10. IN-PLANE INDEX: This parameter can be defined as the ratio between the in-plan area of earthquake resistant walls in each main direction and the total in-plan area of earthquake resistant walls. This ratio provides direct information about the in-plane stiffness of the structure along each main direction. Values that deviate significantly from 0.5 will indicate that one direction is clearly predominant and that there is an asymmetry in the amount of earthquake resistant walls in each main direction

Before getting started, the following figure shows typical vernacular buildings for which this methodology is intended.



1/25

2. Please, indicate which of the following parameters you consider has a greater influence on the seismic behavior of vernacular buildings:

Mark only one oval.

- WALL SLENDERNESS: Ratio between the height of the wall and its thickness (h/t)
- TYPE OF MATERIAL: Type of material used for the structural elements (load bearing walls) of the building (e.g. rammed earth, irregular stone masonry, dressed stone masonry, etc.)
- Equal importance

3. Compare their relative importance in the provided scale from 1-9

1: Equal importance / 3: Moderate importance of one over another / 5: Essential or strong importance / 7: Very strong importance / 9: Extreme importance / 2,4,6,8: Intermediate values between adjacent judgments

Mark only one oval.

	1	2	3	4	5	6	7	8	9	
Equal importance	<input type="radio"/>	<input type="radio"/>	<input type="radio"/>	<input type="radio"/>	<input type="radio"/>	<input type="radio"/>	<input type="radio"/>	<input type="radio"/>	<input type="radio"/>	Extreme importance of one parameter over the other

2/25

4. Please, indicate which of the following parameters you consider has a greater influence on the seismic behavior of vernacular buildings:

Mark only one oval.

- WALL SLENDERNESS: Ratio between the height of the wall and its thickness (h/t)
- STATE OF CONSERVATION: Degree of deterioration of the building and existing damage
- Equal importance

5. Compare their relative importance in the provided scale from 1-9

1: Equal importance / 3: Moderate importance of one over another / 5: Essential or strong importance / 7: Very strong importance / 9: Extreme importance / 2,4,6,8: Intermediate values between adjacent judgments

Mark only one oval.

	1	2	3	4	5	6	7	8	9	
Equal importance	<input type="radio"/>	<input type="radio"/>	<input type="radio"/>	<input type="radio"/>	<input type="radio"/>	<input type="radio"/>	<input type="radio"/>	<input type="radio"/>	<input type="radio"/>	Extreme importance of one parameter over the other

3/25

6. Please, indicate which of the following parameters you consider has a greater influence on the seismic behavior of vernacular buildings:

Mark only one oval.

- MAXIMUM WALL SPAN: Maximum length of a wall prone to out-of-plane movement
- ROOF THRUST: Type of roof according to the thrust that it exerts to the load bearing walls
- Equal importance

7. Compare their relative importance in the provided scale from 1-9

1: Equal importance / 3: Moderate importance of one over another / 5: Essential or strong importance / 7: Very strong importance / 9: Extreme importance / 2,4,6,8: Intermediate values between adjacent judgments

Mark only one oval.

	1	2	3	4	5	6	7	8	9	
Equal importance	<input type="radio"/>	<input type="radio"/>	<input type="radio"/>	<input type="radio"/>	<input type="radio"/>	<input type="radio"/>	<input type="radio"/>	<input type="radio"/>	<input type="radio"/>	Extreme importance of one parameter over the other

4/25

8. Please, indicate which of the following parameters you consider has a greater influence on the seismic behavior of vernacular buildings:

Mark only one oval.

- TYPE OF MATERIAL: Type of material used for the structural elements (load bearing walls) of the building (e.g. rammed earth, irregular stone masonry, dressed stone masonry, etc.)
- NUMBER OF FLOORS: Number of floors (or stories) of the building
- Equal importance

9. Compare their relative importance in the provided scale from 1-9

1: Equal importance / 3: Moderate importance of one over another / 5: Essential or strong importance / 7: Very strong importance / 9: Extreme importance / 2,4,6,8: Intermediate values between adjacent judgments

Mark only one oval.

	1	2	3	4	5	6	7	8	9	
Equal importance	<input type="radio"/>	<input type="radio"/>	<input type="radio"/>	<input type="radio"/>	<input type="radio"/>	<input type="radio"/>	<input type="radio"/>	<input type="radio"/>	<input type="radio"/>	Extreme importance of one parameter over the other

5/25

10. Please, indicate which of the following parameters you consider has a greater influence on the seismic behavior of vernacular buildings:

Mark only one oval.

- MAXIMUM WALL SPAN: Maximum length of a wall prone to out-of-plane movement
- IN-PLANE INDEX: Ratio between the in-plan area of earthquake resistant walls in each main direction and the total in-plan area of earthquake resistant walls
- Equal importance

11. Compare their relative importance in the provided scale from 1-9

1: Equal importance / 3: Moderate importance of one over another / 5: Essential or strong importance / 7: Very strong importance / 9: Extreme importance / 2,4,6,8: Intermediate values between adjacent judgments

Mark only one oval.

	1	2	3	4	5	6	7	8	9	
Equal importance	<input type="radio"/>	<input type="radio"/>	<input type="radio"/>	<input type="radio"/>	<input type="radio"/>	<input type="radio"/>	<input type="radio"/>	<input type="radio"/>	<input type="radio"/>	Extreme importance of one parameter over the other

6/25

12. Please, indicate which of the following parameters you consider has a greater influence on the seismic behavior of vernacular buildings:

Mark only one oval.

- WALL-TO-WALL CONNECTION: Quality of the connection between the main vertical structural elements (i.e. load bearing walls)
- WALL OPENINGS: Number and area of wall openings observed in the load bearing walls
- Equal importance

13. Compare their relative importance in the provided scale from 1-9

1: Equal importance / 3: Moderate importance of one over another / 5: Essential or strong importance / 7: Very strong importance / 9: Extreme importance / 2,4,6,8: Intermediate values between adjacent judgments

Mark only one oval.

	1	2	3	4	5	6	7	8	9	
Equal importance	<input type="radio"/>	<input type="radio"/>	<input type="radio"/>	<input type="radio"/>	<input type="radio"/>	<input type="radio"/>	<input type="radio"/>	<input type="radio"/>	<input type="radio"/>	Extreme importance of one parameter over the other

7/25

14. Please, indicate which of the following parameters you consider has a greater influence on the seismic behavior of vernacular buildings:

Mark only one oval.

- HORIZONTAL DIAPHRAGMS: Type of horizontal diaphragm (floors and roofs) and its connection to the load bearing walls
- IN-PLANE INDEX: Ratio between the in-plan area of earthquake resistant walls in each main direction and the total in-plan area of earthquake resistant walls
- Equal importance

15. Compare their relative importance in the provided scale from 1-9

1: Equal importance / 3: Moderate importance of one over another / 5: Essential or strong importance / 7: Very strong importance / 9: Extreme importance / 2,4,6,8: Intermediate values between adjacent judgments

Mark only one oval.

	1	2	3	4	5	6	7	8	9	
Equal importance	<input type="radio"/>	<input type="radio"/>	<input type="radio"/>	<input type="radio"/>	<input type="radio"/>	<input type="radio"/>	<input type="radio"/>	<input type="radio"/>	<input type="radio"/>	Extreme importance of one parameter over the other

8/25

16. Please, indicate which of the following parameters you consider has a greater influence on the seismic behavior of vernacular buildings:

Mark only one oval.

- WALL-TO-WALL CONNECTION: Quality of the connection between the main vertical structural elements (i.e. load bearing walls)
- NUMBER OF FLOORS: Number of floors (or stories) of the building
- Equal importance

17. Compare their relative importance in the provided scale from 1-9

1: Equal importance / 3: Moderate importance of one over another / 5: Essential or strong importance / 7: Very strong importance / 9: Extreme importance / 2,4,6,8: Intermediate values between adjacent judgments

Mark only one oval.

	1	2	3	4	5	6	7	8	9	
Equal importance	<input type="radio"/>	<input type="radio"/>	<input type="radio"/>	<input type="radio"/>	<input type="radio"/>	<input type="radio"/>	<input type="radio"/>	<input type="radio"/>	<input type="radio"/>	Extreme importance of one parameter over the other

9/25

18. Please, indicate which of the following parameters you consider has a greater influence on the seismic behavior of vernacular buildings:

Mark only one oval.

- ROOF THRUST: Type of roof according to the thrust that it exerts to the load bearing walls
- WALL OPENINGS: Number and area of wall openings observed in the load bearing walls
- Equal importance

19. Compare their relative importance in the provided scale from 1-9

1: Equal importance / 3: Moderate importance of one over another / 5: Essential or strong importance / 7: Very strong importance / 9: Extreme importance / 2,4,6,8: Intermediate values between adjacent judgments

Mark only one oval.

	1	2	3	4	5	6	7	8	9	
Equal importance	<input type="radio"/>	<input type="radio"/>	<input type="radio"/>	<input type="radio"/>	<input type="radio"/>	<input type="radio"/>	<input type="radio"/>	<input type="radio"/>	<input type="radio"/>	Extreme importance of one parameter over the other

10/25

20. Please, indicate which of the following parameters you consider has a greater influence on the seismic behavior of vernacular buildings:

Mark only one oval.

- HORIZONTAL DIAPHRAGMS: Type of horizontal diaphragm (floors and roofs) and its connection to the load bearing walls
- WALL OPENINGS: Number and area of wall openings observed in the load bearing walls
- Equal importance

21. Compare their relative importance in the provided scale from 1-9

1: Equal importance / 3: Moderate importance of one over another / 5: Essential or strong importance / 7: Very strong importance / 9: Extreme importance / 2,4,6,8: Intermediate values between adjacent judgments

Mark only one oval.

	1	2	3	4	5	6	7	8	9	
Equal importance	<input type="radio"/>	<input type="radio"/>	<input type="radio"/>	<input type="radio"/>	<input type="radio"/>	<input type="radio"/>	<input type="radio"/>	<input type="radio"/>	<input type="radio"/>	Extreme importance of one parameter over the other

11/25

22. Please, indicate which of the following parameters you consider has a greater influence on the seismic behavior of vernacular buildings:

Mark only one oval.

- NUMBER OF FLOORS: Number of floors (or stories) of the building
- STATE OF CONSERVATION: Degree of deterioration of the building and existing damage
- Equal importance

23. Compare their relative importance in the provided scale from 1-9

1: Equal importance / 3: Moderate importance of one over another / 5: Essential or strong importance / 7: Very strong importance / 9: Extreme importance / 2,4,6,8: Intermediate values between adjacent judgments

Mark only one oval.

	1	2	3	4	5	6	7	8	9	
Equal importance	<input type="radio"/>	<input type="radio"/>	<input type="radio"/>	<input type="radio"/>	<input type="radio"/>	<input type="radio"/>	<input type="radio"/>	<input type="radio"/>	<input type="radio"/>	Extreme importance of one parameter over the other

12/25

24. Please, indicate which of the following parameters you consider has a greater influence on the seismic behavior of vernacular buildings:

Mark only one oval.

- WALL SLENDERNESS: Ratio between the height of the wall and its thickness (h/t)
- WALL-TO-WALL CONNECTION: Quality of the connection between the main vertical structural elements (i.e. load bearing walls)
- Equal importance

25. Compare their relative importance in the provided scale from 1-9

1: Equal importance / 3: Moderate importance of one over another / 5: Essential or strong importance / 7: Very strong importance / 9: Extreme importance / 2,4,6,8: Intermediate values between adjacent judgments

Mark only one oval.

	1	2	3	4	5	6	7	8	9	
Equal importance	<input type="radio"/>	<input type="radio"/>	<input type="radio"/>	<input type="radio"/>	<input type="radio"/>	<input type="radio"/>	<input type="radio"/>	<input type="radio"/>	<input type="radio"/>	Extreme importance of one parameter over the other

13/25

26. Please, indicate which of the following parameters you consider has a greater influence on the seismic behavior of vernacular buildings:

Mark only one oval.

- MAXIMUM WALL SPAN: Maximum length of a wall prone to out-of-plane movement
- HORIZONTAL DIAPHRAGMS: Type of horizontal diaphragm (floors and roofs) and its connection to the load bearing walls
- Equal importance

27. Compare their relative importance in the provided scale from 1-9

1: Equal importance / 3: Moderate importance of one over another / 5: Essential or strong importance / 7: Very strong importance / 9: Extreme importance / 2,4,6,8: Intermediate values between adjacent judgments

Mark only one oval.

	1	2	3	4	5	6	7	8	9	
Equal importance	<input type="radio"/>	<input type="radio"/>	<input type="radio"/>	<input type="radio"/>	<input type="radio"/>	<input type="radio"/>	<input type="radio"/>	<input type="radio"/>	<input type="radio"/>	Extreme importance of one parameter over the other

14/25

28. Please, indicate which of the following parameters you consider has a greater influence on the seismic behavior of vernacular buildings:

Mark only one oval.

- TYPE OF MATERIAL: Type of material used for the structural elements (load bearing walls) of the building (e.g. rammed earth, irregular stone masonry, dressed stone masonry, etc.)
- IN-PLANE INDEX: Ratio between the in-plan area of earthquake resistant walls in each main direction and the total in-plan area of earthquake resistant walls
- Equal importance

29. Compare their relative importance in the provided scale from 1-9

1: Equal importance / 3: Moderate importance of one over another / 5: Essential or strong importance / 7: Very strong importance / 9: Extreme importance / 2,4,6,8: Intermediate values between adjacent judgments

Mark only one oval.

	1	2	3	4	5	6	7	8	9	
Equal importance	<input type="radio"/>	<input type="radio"/>	<input type="radio"/>	<input type="radio"/>	<input type="radio"/>	<input type="radio"/>	<input type="radio"/>	<input type="radio"/>	<input type="radio"/>	Extreme importance of one parameter over the other

15/25

30. Please, indicate which of the following parameters you consider has a greater influence on the seismic behavior of vernacular buildings:

Mark only one oval.

- ROOF THRUST: Type of roof according to the thrust that it exerts to the load bearing walls
- STATE OF CONSERVATION: Degree of deterioration of the building and existing damage
- Equal importance

31. Compare their relative importance in the provided scale from 1-9

1: Equal importance / 3: Moderate importance of one over another / 5: Essential or strong importance / 7: Very strong importance / 9: Extreme importance / 2,4,6,8: Intermediate values between adjacent judgments

Mark only one oval.

	1	2	3	4	5	6	7	8	9	
Equal importance	<input type="radio"/>	<input type="radio"/>	<input type="radio"/>	<input type="radio"/>	<input type="radio"/>	<input type="radio"/>	<input type="radio"/>	<input type="radio"/>	<input type="radio"/>	Extreme importance of one parameter over the other

16/25

32. Please, indicate which of the following parameters you consider has a greater influence on the seismic behavior of vernacular buildings:

Mark only one oval.

- WALL SLENDERNESS: Ratio between the height of the wall and its thickness (h/t)
- HORIZONTAL DIAPHRAGMS: Type of horizontal diaphragm (floors and roofs) and its connection to the load bearing walls
- Equal importance

33. Compare their relative importance in the provided scale from 1-9

1: Equal importance / 3: Moderate importance of one over another / 5: Essential or strong importance / 7: Very strong importance / 9: Extreme importance / 2,4,6,8: Intermediate values between adjacent judgments

Mark only one oval.

	1	2	3	4	5	6	7	8	9	
Equal importance	<input type="radio"/>	<input type="radio"/>	<input type="radio"/>	<input type="radio"/>	<input type="radio"/>	<input type="radio"/>	<input type="radio"/>	<input type="radio"/>	<input type="radio"/>	Extreme importance of one parameter over the other

17/25

34. Please, indicate which of the following parameters you consider has a greater influence on the seismic behavior of vernacular buildings:

Mark only one oval.

- MAXIMUM WALL SPAN: Maximum length of a wall prone to out-of-plane movement
- WALL OPENINGS: Number and area of wall openings observed in the load bearing walls
- Equal importance

35. Compare their relative importance in the provided scale from 1-9

1: Equal importance / 3: Moderate importance of one over another / 5: Essential or strong importance / 7: Very strong importance / 9: Extreme importance / 2,4,6,8: Intermediate values between adjacent judgments

Mark only one oval.

	1	2	3	4	5	6	7	8	9	
Equal importance	<input type="radio"/>	<input type="radio"/>	<input type="radio"/>	<input type="radio"/>	<input type="radio"/>	<input type="radio"/>	<input type="radio"/>	<input type="radio"/>	<input type="radio"/>	Extreme importance of one parameter over the other

18/25

36. Please, indicate which of the following parameters you consider has a greater influence on the seismic behavior of vernacular buildings:

Mark only one oval.

- WALL-TO-WALL CONNECTION: Quality of the connection between the main vertical structural elements (i.e. load bearing walls)
- ROOF THRUST: Type of roof according to the thrust that it exerts to the load bearing walls
- Equal importance

37. Compare their relative importance in the provided scale from 1-9

1: Equal importance / 3: Moderate importance of one over another / 5: Essential or strong importance / 7: Very strong importance / 9: Extreme importance / 2,4,6,8: Intermediate values between adjacent judgments

Mark only one oval.

	1	2	3	4	5	6	7	8	9	
Equal importance	<input type="radio"/>	<input type="radio"/>	<input type="radio"/>	<input type="radio"/>	<input type="radio"/>	<input type="radio"/>	<input type="radio"/>	<input type="radio"/>	<input type="radio"/>	Extreme importance of one parameter over the other

19/25

38. Please, indicate which of the following parameters you consider has a greater influence on the seismic behavior of vernacular buildings:

Mark only one oval.

- HORIZONTAL DIAPHRAGMS: Type of horizontal diaphragm (floors and roofs) and its connection to the load bearing walls
- NUMBER OF FLOORS: Number of floors (or stories) of the building
- Equal importance

39. Compare their relative importance in the provided scale from 1-9

1: Equal importance / 3: Moderate importance of one over another / 5: Essential or strong importance / 7: Very strong importance / 9: Extreme importance / 2,4,6,8: Intermediate values between adjacent judgments

Mark only one oval.

	1	2	3	4	5	6	7	8	9	
Equal importance	<input type="radio"/>	<input type="radio"/>	<input type="radio"/>	<input type="radio"/>	<input type="radio"/>	<input type="radio"/>	<input type="radio"/>	<input type="radio"/>	<input type="radio"/>	Extreme importance of one parameter over the other

20/25

40. Please, indicate which of the following parameters you consider has a greater influence on the seismic behavior of vernacular buildings:

Mark only one oval.

- MAXIMUM WALL SPAN: Maximum length of a wall prone to out-of-plane movement
- TYPE OF MATERIAL: Type of material used for the structural elements (load bearing walls) of the building (e.g. rammed earth, irregular stone masonry, dressed stone masonry, etc.)
- Equal importance

41. Compare their relative importance in the provided scale from 1-9

1: Equal importance / 3: Moderate importance of one over another / 5: Essential or strong importance / 7: Very strong importance / 9: Extreme importance / 2,4,6,8: Intermediate values between adjacent judgments

Mark only one oval.

	1	2	3	4	5	6	7	8	9	
Equal importance	<input type="radio"/>	<input type="radio"/>	<input type="radio"/>	<input type="radio"/>	<input type="radio"/>	<input type="radio"/>	<input type="radio"/>	<input type="radio"/>	<input type="radio"/>	Extreme importance of one parameter over the other

21/25

42. Please, indicate which of the following parameters you consider has a greater influence on the seismic behavior of vernacular buildings:

Mark only one oval.

- WALL SLENDERNESS: Ratio between the height of the wall and its thickness (h/t)
- ROOF THRUST: Type of roof according to the thrust that it exerts to the load bearing walls
- Equal importance

43. Compare their relative importance in the provided scale from 1-9

1: Equal importance / 3: Moderate importance of one over another / 5: Essential or strong importance / 7: Very strong importance / 9: Extreme importance / 2,4,6,8: Intermediate values between adjacent judgments

Mark only one oval.

	1	2	3	4	5	6	7	8	9	
Equal importance	<input type="radio"/>	<input type="radio"/>	<input type="radio"/>	<input type="radio"/>	<input type="radio"/>	<input type="radio"/>	<input type="radio"/>	<input type="radio"/>	<input type="radio"/>	Extreme importance of one parameter over the other

22/25

44. Please, indicate which of the following parameters you consider has a greater influence on the seismic behavior of vernacular buildings:

Mark only one oval.

- STATE OF CONSERVATION: Degree of deterioration of the building and existing damage
- IN-PLANE INDEX: Ratio between the in-plan area of earthquake resistant walls in each main direction and the total in-plan area of earthquake resistant walls
- Equal importance

45. Compare their relative importance in the provided scale from 1-9

1: Equal importance / 3: Moderate importance of one over another / 5: Essential or strong importance / 7: Very strong importance / 9: Extreme importance / 2,4,6,8: Intermediate values between adjacent judgments

Mark only one oval.

	1	2	3	4	5	6	7	8	9	
Equal importance	<input type="radio"/>	<input type="radio"/>	<input type="radio"/>	<input type="radio"/>	<input type="radio"/>	<input type="radio"/>	<input type="radio"/>	<input type="radio"/>	<input type="radio"/>	Extreme importance of one parameter over the other

23/25

46. Please, indicate which of the following parameters you consider has a greater influence on the seismic behavior of vernacular buildings:

Mark only one oval.

- WALL OPENINGS: Number and area of wall openings observed in the load bearing walls
- NUMBER OF FLOORS: Number of floors (or stories) of the building
- Equal importance

47. Compare their relative importance in the provided scale from 1-9

1: Equal importance / 3: Moderate importance of one over another / 5: Essential or strong importance / 7: Very strong importance / 9: Extreme importance / 2,4,6,8: Intermediate values between adjacent judgments

Mark only one oval.

	1	2	3	4	5	6	7	8	9	
Equal importance	<input type="radio"/>	<input type="radio"/>	<input type="radio"/>	<input type="radio"/>	<input type="radio"/>	<input type="radio"/>	<input type="radio"/>	<input type="radio"/>	<input type="radio"/>	Extreme importance of one parameter over the other

24/25

48. Please, indicate which of the following parameters you consider has a greater influence on the seismic behavior of vernacular buildings:

Mark only one oval.

- TYPE OF MATERIAL: Type of material used for the structural elements (load bearing walls) of the building (e.g. rammed earth, irregular stone masonry, dressed stone masonry, etc.)
- STATE OF CONSERVATION: Degree of deterioration of the building and existing damage
- Equal importance

49. Compare their relative importance in the provided scale from 1-9

1: Equal importance / 3: Moderate importance of one over another / 5: Essential or strong importance / 7: Very strong importance / 9: Extreme importance / 2,4,6,8: Intermediate values between adjacent judgments

Mark only one oval.

	1	2	3	4	5	6	7	8	9	
Equal importance	<input type="radio"/>	<input type="radio"/>	<input type="radio"/>	<input type="radio"/>	<input type="radio"/>	<input type="radio"/>	<input type="radio"/>	<input type="radio"/>	<input type="radio"/>	Extreme importance of one parameter over the other

25/25

50. Please, indicate which of the following parameters you consider has a greater influence on the seismic behavior of vernacular buildings:

Mark only one oval.

- WALL-TO-WALL CONNECTION: Quality of the connection between the main vertical structural elements (i.e. load bearing walls)
- IN-PLANE INDEX: Ratio between the in-plan area of earthquake resistant walls in each main direction and the total in-plan area of earthquake resistant walls
- Equal importance

51. Compare their relative importance in the provided scale from 1-9

1: Equal importance / 3: Moderate importance of one over another / 5: Essential or strong importance / 7: Very strong importance / 9: Extreme importance / 2,4,6,8: Intermediate values between adjacent judgments

Mark only one oval.

	1	2	3	4	5	6	7	8	9	
Equal importance	<input type="radio"/>	<input type="radio"/>	<input type="radio"/>	<input type="radio"/>	<input type="radio"/>	<input type="radio"/>	<input type="radio"/>	<input type="radio"/>	<input type="radio"/>	Extreme importance of one parameter over the other

Personal details

To conclude, we would like to ask you for some personal details that will help us to weigh the survey, thank you.

52. Name

53. Professional position *

Mark only one oval.

- Professional
- University Professor
- Postdoc Researcher
- PhD Researcher
- Student

54. How would you rate your overall level of expertise on the matter in question on a scale of one to five? *

Mark only one oval.

	1	2	3	4	5
Low	<input type="radio"/>	<input type="radio"/>	<input type="radio"/>	<input type="radio"/>	<input type="radio"/>

Send me a copy of my responses.

ANNEX D

GUIDELINES FOR APPLICATION OF THE SAVVAS METHOD

This section presents some guidelines prepared for an easier application of the SAVVAS method and the fulfillment of the parameter survey.

P1. Wall slenderness

The wall slenderness (λ) is a geometrical parameter that can be defined as the ratio between the effective wall inter-story height (h) and its thickness (t). Both variables are measured in meters. The slenderest elements are always more vulnerable to the seismic action.

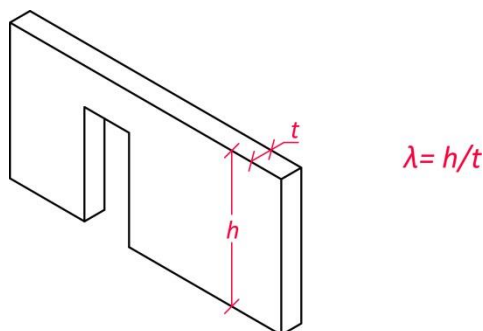


Figure P1-1: Definition of the wall inter-story height (h) and wall thickness (t)

Table P1-1: Seismic vulnerability classes according to the wall slenderness (λ)

P1. Wall slenderness	
Class	Description
A	$\lambda \leq 6$
B	$6 < \lambda \leq 9$
C	$9 < \lambda \leq 12$
D	$\lambda > 12$

Given the traditional materials commonly used for the walls (stone and earth), the walls of vernacular buildings are typically very thick. They are rarely thinner than 0.45-0.5 m and can easily reach 0.6-0.7 m thick. The maximum wall height is more variable, even though vernacular buildings tend to be rather compact and present small dimensions. Taking into account these aspects, vernacular constructions typically presents low slenderness ratios (below 9) and is rare to find ratios over 12.

Since the slenderness particularly affects the out-of-plane behavior of the walls, the value adopted for this method should be the slenderness value of the slenderest wall perpendicular to the direction assessed, which is the wall most prone to suffer an out-of-plane failure.

The following diagrams show some recommendations on how to consider the values for this parameter for different conditions. It is noted that the final value adopted will ultimately depend on the qualitative judgment of the person conducting the assessment. Discrepancies and differences between the values adopted by different evaluators are expected. Additionally, this set of recommendations does not cover all the possibilities and it will be up to the evaluator, the final decision on how to determine the final value of slenderness.

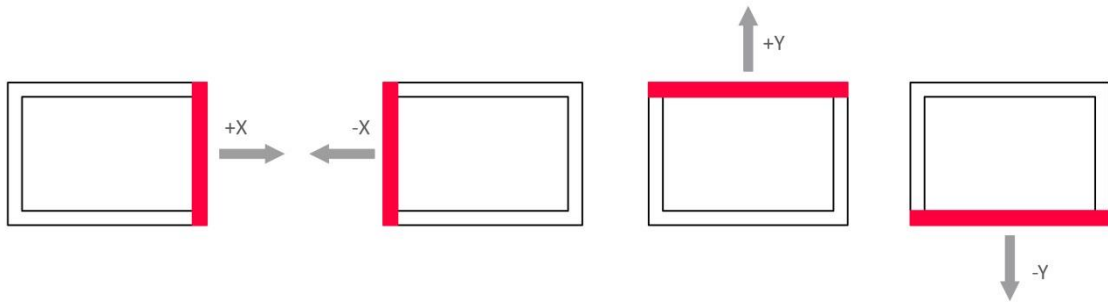


Figure P1-2: Wall to consider according to the loading direction evaluated (plan view)

In general for the assessment of a building, a direction should not be considered if there is an adjacent building blocking the possible out-of-plane rotation of the wall perpendicular to the loading direction evaluated.

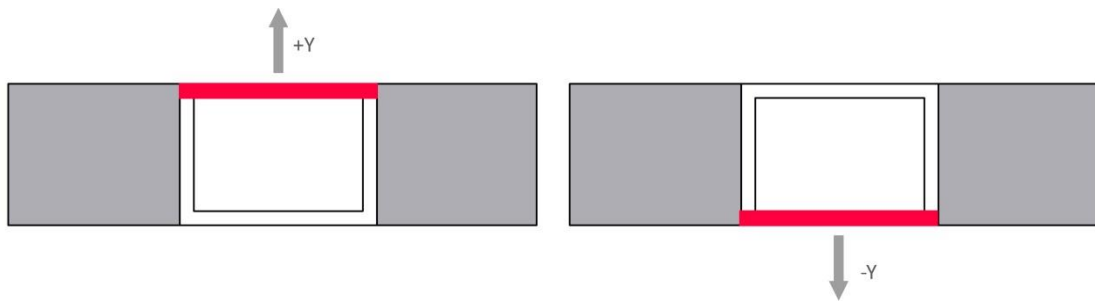


Figure P1-3: In the case above, only the direction +Y and -Y should be evaluated because walls perpendicular to loading direction +X and -X are not likely to fail out-of-plane because of the presence of an adjacent building (plan view)

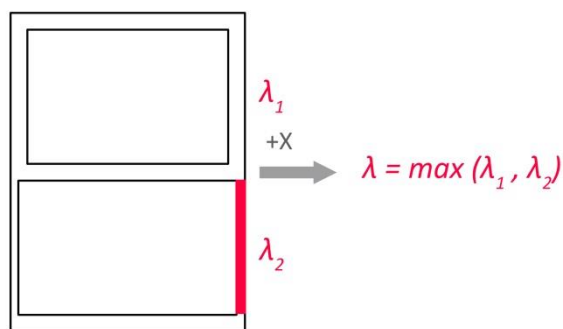


Figure P1-4: In the case of different slenderness values for different walls in the same direction, the maximum value of slenderness should be adopted (plan view)

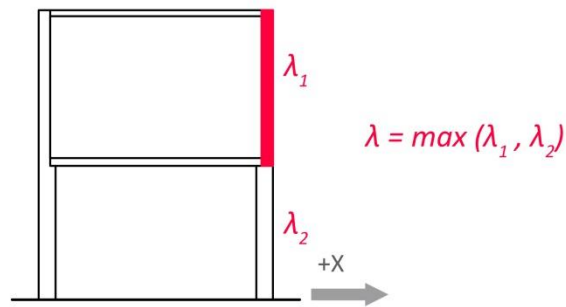


Figure P1-5: Similarly, in the case of different values of slenderness in the same direction along the height of the building, the maximum value should be adopted (section view)

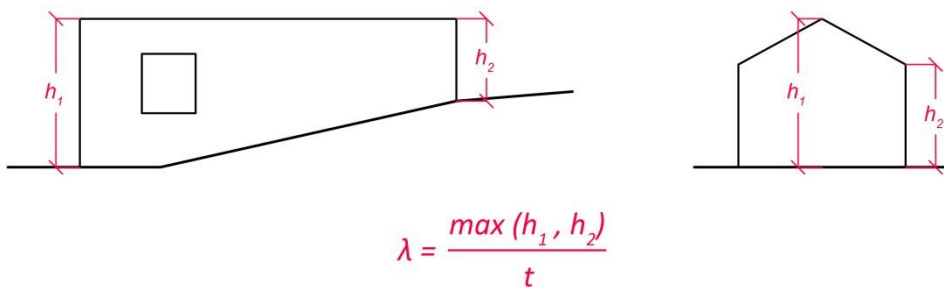


Figure P1-6: In the case of difference in height along the wall length, the value of height leading to the maximum value of slenderness should be adopted. This is particularly common in case of gable walls (elevation view)

P2. Maximum wall span

The maximum wall span (s) is a geometrical parameter that takes into account the maximum length of a wall prone to out-of-plane movements, which is the wall spanning the maximum distance between two in-plane earthquake resistant walls. This variable is measured in meters. The longest elements without intermediate support can be particularly vulnerable to the seismic action and increase the probability of occurrence of out-of-plane collapse.

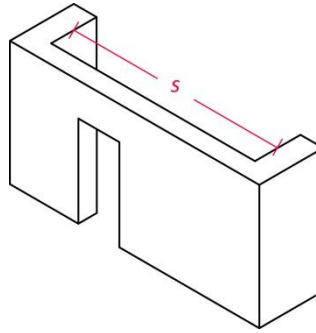


Figure P2-1: Definition of the maximum wall span (s)

Table P2-1: Seismic vulnerability classes according to the maximum wall span (s)

P2. Maximum wall span	
Class	Description (values in m)
A	$s_{max} < 5$
B	$5 \leq s_{max} < 7$
C	$7 \leq s_{max} < 9$
D	$s_{max} \geq 9$

The maximum wall span is much variable for vernacular buildings, even though vernacular buildings tend to have small dimensions. Since the maximum wall span governs the out-of-plane response of the walls, the value adopted for this method should be the maximum wall span presented by the walls perpendicular to the direction assessed, which will be the wall more prone to suffer an out-of-plane failure.

The following diagrams show some recommendations on how to consider the values for this parameter for different conditions. It is noted that the final value adopted will ultimately depend on the qualitative judgment of the person conducting the assessment. Discrepancies and differences between the values adopted by different evaluators are expected. Additionally, this set of recommendations does not cover all the possibilities and it will be up to the evaluator, the final decision on how to determine the final value of maximum wall span.

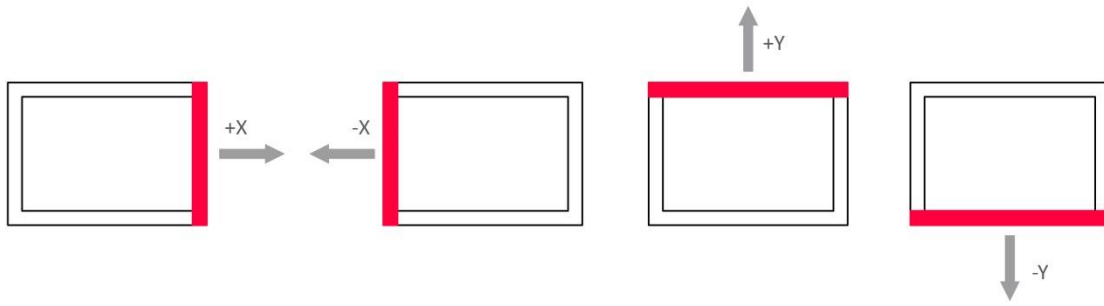


Figure P2-2: Wall to consider according to the loading direction evaluated (plan view)

In general for the assessment of a building, a direction should not be considered if there is an adjacent building blocking the possible out-of-plane rotation of the wall perpendicular to the loading direction evaluated.

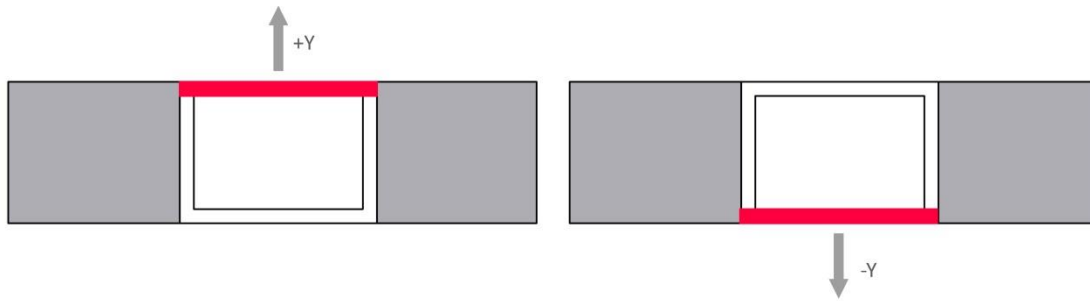


Figure P2-3: In the case above, only the direction +Y and -Y should be evaluated because walls perpendicular to loading direction +X and -X are not likely to fail out-of-plane because of the presence of an adjacent building (plan view)

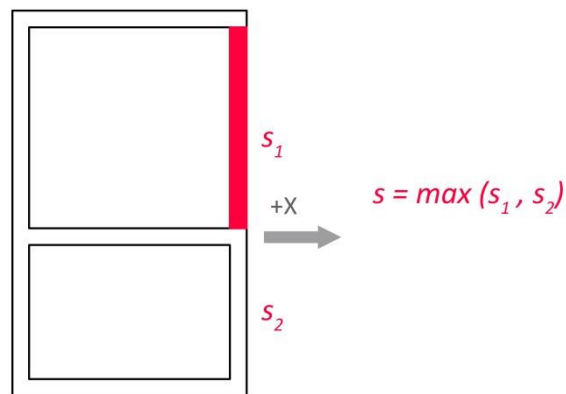


Figure P2-4: For a specific direction, always the maximum wall span should be adopted (plan view)

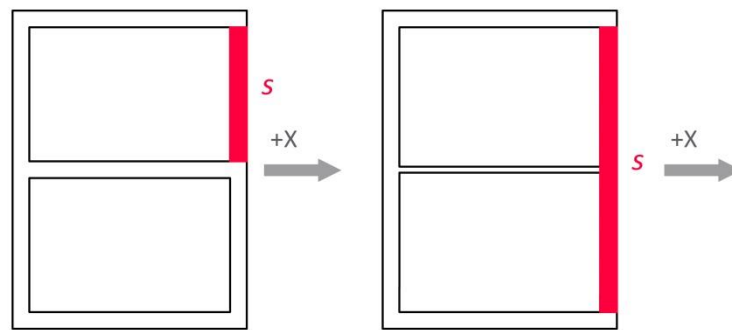


Figure P2-5: Intermediate walls should be only considered as earthquake resistant walls when they present enough dimensions to fulfill this function (plan view)

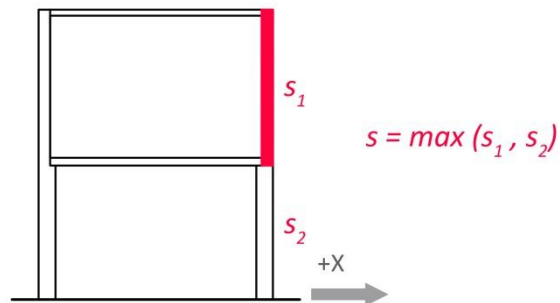


Figure P2-6: In the case of different values of maximum wall span in the same direction along the height of the building, the maximum value should be adopted (section view)

P3. Type of material

This parameter takes into account the type of material used to build the walls, which are the main vertical load bearing elements of vernacular buildings. This method is particularly prepared for buildings with walls built in masonry (stone and brick) or earthen materials.

Table P3-1: Seismic vulnerability classes according to the type of material

P3. Type of material				
Class	Description	Reference material properties		
		E (MPa)	f_c (MPa)	f_t (MPa)
A	Stone masonry consisting of well-cut homogeneous units in terms of material and dimensions with parallelepiped shape. Carefully worked horizontal courses with not-aligned mortar head joints. The mortar has good quality and properly fills vertical and horizontal joints. Proper transversal connection among wall leaves using through-stones or stones or brick bands crossing the entire wall thickness. Brick masonry with well-arranged vertical and horizontal joints and good quality mortar	2000-3000	2-4	0.1-0.6
B	Non-homogeneous stone masonry in terms of materials and dimensions but well-arranged longitudinally and transversally with generally respected horizontal courses, not-aligned mortar head joints and good quality mortar. Proper transversal connection among the wall leaves using through-stones or stone or brick bands crossing the entire wall thickness. Brick masonry with well-arranged joints and average quality mortar	1500-2000	1.5-2	0.1-0.4
C	Coarsely carved stone masonry irregularly shaped with poor arrangement of the stones and weak or average quality mortar. Few or no transversal connection elements. The core of multiple-leaf walls has a reasonably consistency.	1000-1500	1-1.5	0.05-0.3
D	Irregular not worked stone masonry of low quality, with not respected horizontal courses or aligned mortar head joints. Poor quality mortar. There are no transversal connection elements. Multi-leaf masonry with partially unstable empty core showing voids. Adobe masonry and rammed earth walls are also included within this class	150-1000	0.6-1.5	0.05-0.2

The classification mainly addresses qualitative aspects of the wall typology and provides a qualitative description of the material. This classification is thus intended to be determined on the basis of simple visual inspection. Nevertheless, since this classification was made according to the variations of the material properties, a range of material properties is given as a reference for the four classes defined. This can be useful in case that an experimental campaign can also be performed along with the survey and quantitative data is available. Among them, the Young's modulus was observed to be particularly influential in defining the seismic behavior of a building. There are several aspects that determine the quality of the walls and, thus, the capacity of the building to withstand horizontal forces resulting from the seismic load:

Constituent material

Wall typologies primarily differ in the constituent material. The vernacular buildings that are addressed with this method usually present walls built in stone, brick, adobe and rammed earth. The material affects the seismic performance of the building under an earthquake, since the mechanical properties of the materials may vary highly from one another and they have an important role in the seismic performance of the structure.

Masonry wall morphology

Masonry walls can present significant variations on the type, shape and size of the masonry units: ashlar stone masonry, irregular rubble stone masonry, roughly shaped stone masonry, brick masonry, etc.

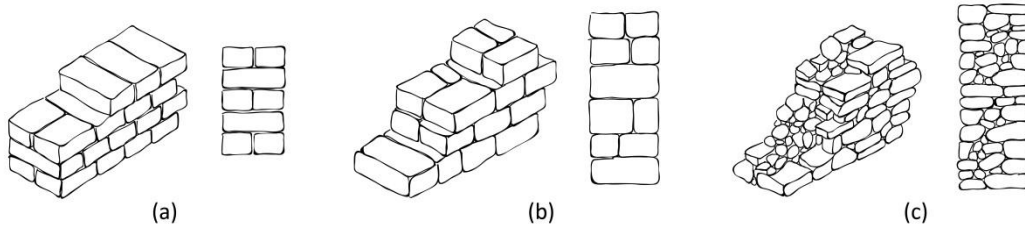


Figure P3-1: Different masonry units (view and cross-section): (a) brick masonry; (b) ashlar stone masonry; and (c) irregular stone masonry (adapted from NIKER 2010)

The masonry can differ because of presenting: irregular or regular horizontal courses:

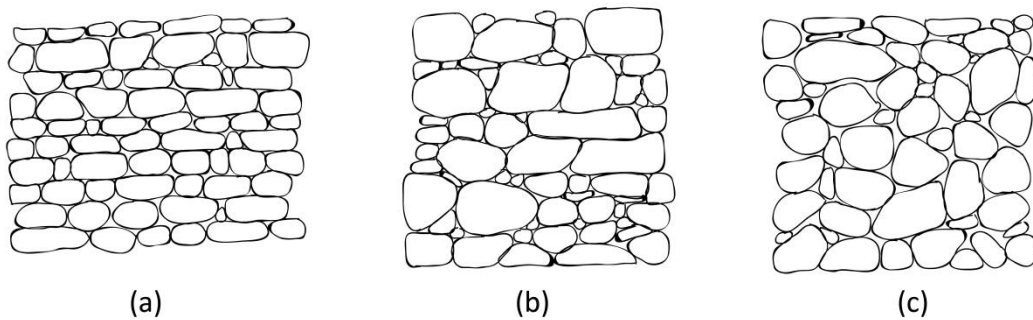


Figure P3-2: Different masonry arrangement (wall elevation): (a) respected horizontal courses; (b) partially respected horizontal courses; and (c) no horizontal courses (adapted from NIKER 2010)

The cross-section masonry morphology can also present several leaves and good or poor connection among them. This is a very important aspect defining the mechanical behavior of masonry walls.

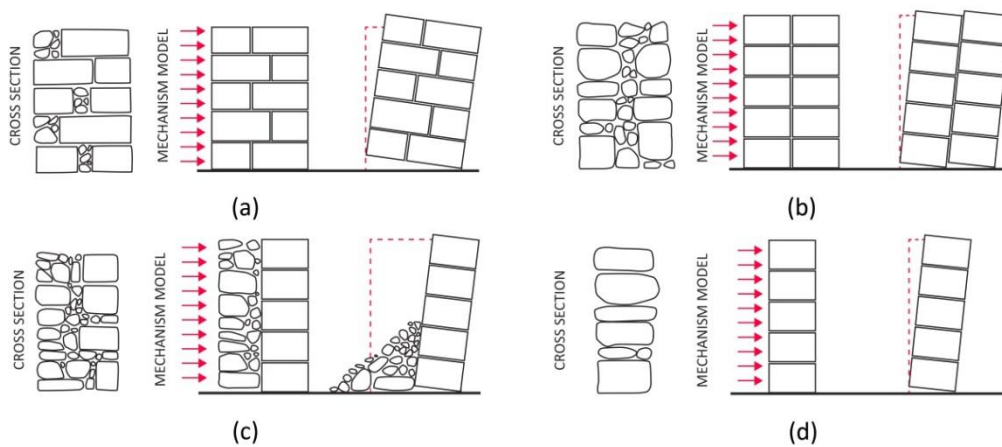


Figure P3-3: Structural behavior of multiple-leaf stone masonry walls according to the quality of transversal connection among leaves (adapted from Binda 2009)

The masonry can differ also in the type of mortar used for the construction, if any. The following figure shows an example of a wall survey that can be carried out according to the morphology:

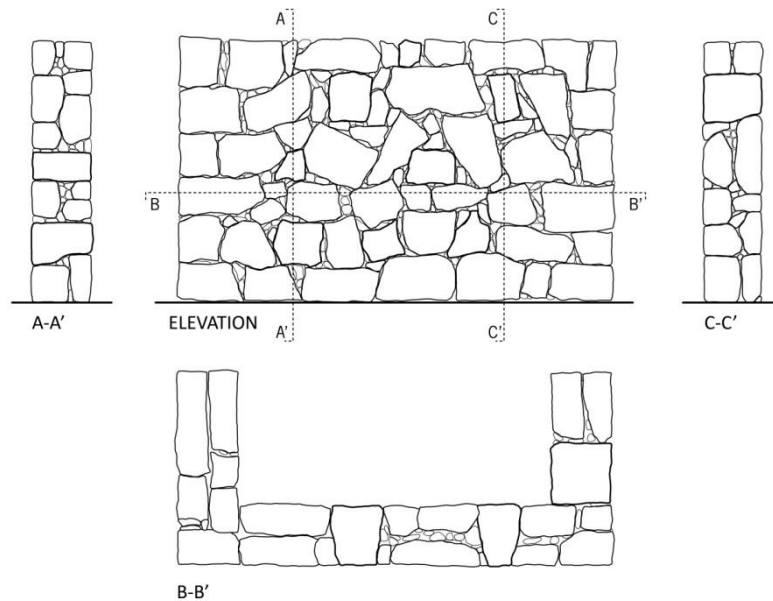


Figure P3-4: Irregularly shaped stone units of varying size. Poor arrangement of the stones with not-respected horizontal courses. Two leaves with several through-stones as transversal connection elements. No mortar. Because of the above survey, this masonry could be classified as class C

It is acknowledged that, many times, some morphological aspects, such as the presence of transversal connection elements cannot be detected with the naked eye. The classification should be thus carried out on the basis of information of other similar buildings in the regions, if existing. In the case of no information, it is recommended to assume the worst case scenario.

The class assigned to this parameter is global for all directions, in order to take into account its influence in both the in-plane behavior and the out-of-plane behavior of the walls. Therefore, some recommendations on how to evaluate this parameter for different conditions are given below. It is noted that the final value adopted will ultimately depend on the qualitative judgment of the person conducting the assessment. Discrepancies and differences between the values adopted by different evaluators are expected. Additionally, this set of recommendations does not cover all the possibilities and the final decision on how to classify the parameter is up to the evaluator.

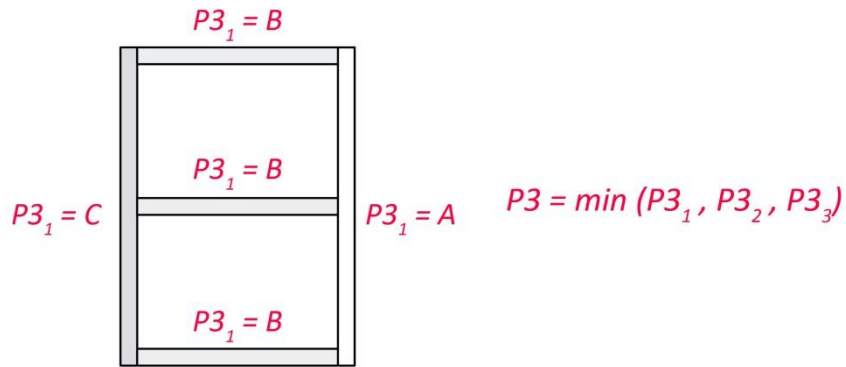


Figure P3-5: In the case of different types of masonry for different walls, the worst class for the type of material should be adopted (plan view)

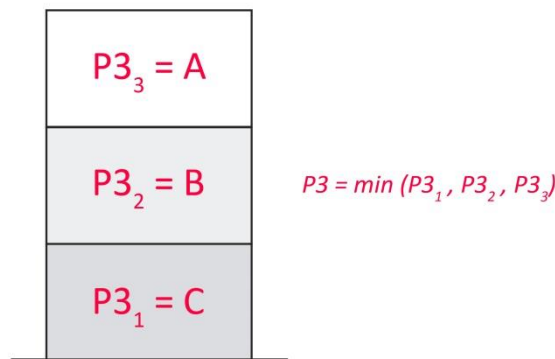


Figure P3-6: In the case of different types of masonry for different walls along the height of the building, the worst class for the type of material should be adopted (elevation view)

Binda (2009) *A classification of structures and masonries for the adequate choice of repair*. Repair Mortars for Historic Masonry, RILEM, Delft, Netherlands: 20-34

NIKER (2010) *Inventory of earthquake-induced failure mechanisms related to construction types, structural elements and materials (Report D3.1)*. Italy: New Integrated Knowledge Based Approaches to the Protection of Cultural Heritage from Earthquake-Induced Risk (NIKER) project

P4. Wall-to-wall connections

This parameter takes into account the organization of the vertical structural system and, in particular, the quality and the level of connection between orthogonal walls. The quality may vary from visible separation between orthogonal walls to efficiently built connections improved by means of applying traditional reinforcing techniques, such as quoins and corner braces.

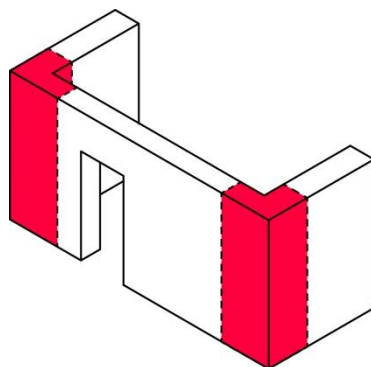


Figure P4-1: Quality of the wall-to-wall connections

Table P4-1: Seismic vulnerability classes according to the wall-to-wall connections

P4. Wall-to-wall connections	
Class	Description
A	All wall-to-wall connections are workmanlike built. There is no weakening signs or construction deficiencies. In case of masonry buildings, there is a good interlocking between the masonry units at the corners. In case of earthen buildings, there are no vertical joints at the corners
B	Some wall-to-wall connections show either construction deficiencies, such as lack of efficient interlocking of the masonry units in case of masonry buildings or vertical joints in case of earthen construction, or weakening signs
C	Many wall-to-wall connections are deficient or degraded because of construction deficiencies, such as vertical joints, and/or weakening signs, such as cracks or detachments
D	Most wall-to-wall connections are barely non-existent because of poor construction practices or are highly degraded with important signs of separation and vertical cracks

Post-earthquake damage observation has shown how the failure mode of vernacular buildings is many times characterized by vertical cracks at the wall intersections, leading to the out-of-plane overturning of the walls. This proves that the quality of the wall-to-wall connections is a key parameter governing the seismic behavior of vernacular buildings.

The low tensile strength of stone masonry and rammed earth results in the detachment of the façade walls from the transversal walls. Particularly, concerning stone masonry buildings, the level of interlocking between the stones at the corner, mainly defined by the size and arrangement of the units, may have a decisive influence in advancing or delaying the formation of a failure mechanism consisting of the separation of the walls at the corners. The traditional technique applied to achieve proper wall-to-wall connections consist of using the best quality large squared stone blocks at the corners, carefully bonded to the orthogonal walls by creating an efficient overlapping of the ashlar with the rest of the masonry. However, the efficacy of quoins is

limited when coupled with poor fabric or internally unconnected masonry which tend to become loose.

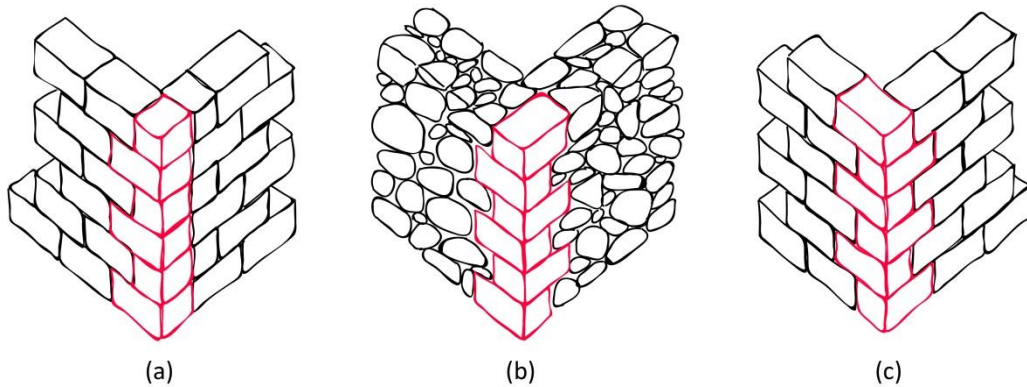


Figure P4-2: Quality of the wall-to-wall connections: (a) absence of interlocking; (b) ineffective constraints because of poor fabric; and (c) traditional ashlar masonry quoin (adapted from NIKER 2010)

Nevertheless, when performing visual inspection, particular care should be paid to the identification of quoins. Frequently, decorative stone elements at the corner can be easily confused with quoins. These elements do not extend in the depth of the wall and have no structural connection with it.

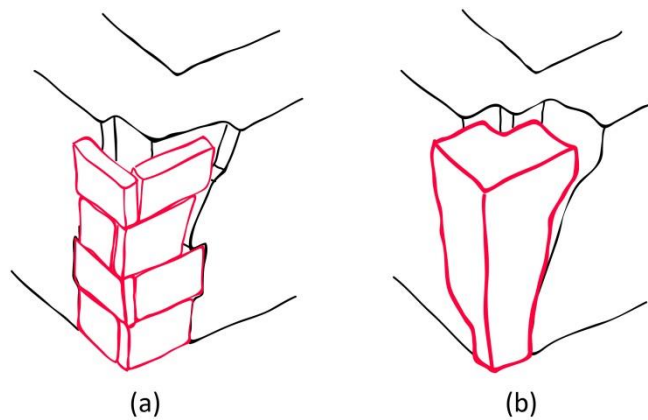


Figure P4-3: The stone blocks at the wall connections can be: (a) only decorative elements; or (b) only superficial (adapted from Doglioni 2007)

In the case of rammed earth buildings, typical weak connections arise from the difficulty of creating corners inside the frameworks and poor joints with vertical recess solution. Because of this, the presence of stones or other elements bracing perpendicular walls is typical in vernacular buildings. For example, pieces of schist or timber can be found within rammed earth buildings at the corners. Traditional timber corner braces or keys are also very common. They consist of timber-stiffening elements placed usually diagonally at the corners that help to reinforce the wall-

to-wall connections of the building. The use of ties for making effective links to hold together orthogonal walls is another typical vernacular practice.

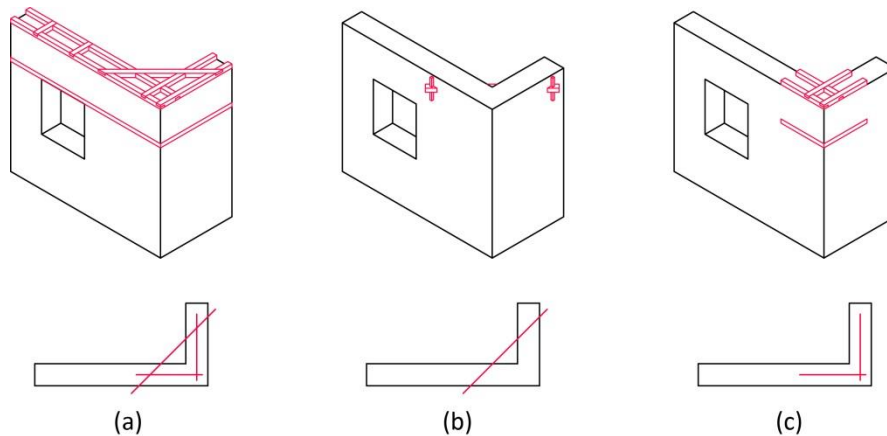


Figure P4-4: Different types of corner braces traditionally used in vernacular architecture: (a) ring beams with diagonal stiffener; (b) independent corner brace attached to the wall with wedges; and (c) partial ring beam at the corner (Ortega et al. 2017)

It is acknowledged that, many times, some of the mentioned aspects, such as the depth of the quoins and the level of connection between orthogonal walls is difficult to assess by means of only visual inspection. The classification should be thus carried out on the basis of information of other similar buildings in the regions, if existing. In the case of no information, it is recommended to assume the worst case scenario.

The class assigned to this parameter is global for all directions, since a poor wall-to-wall connection will compromise the out-of-plane behavior of both connected walls. The classification shown above provides a qualitative indication on how to determine the class based on the number of wall-to-wall connections of a specific type in linguistic terms: "all", "most" or "some". Therefore, it is noted that the final value adopted will ultimately depend on the qualitative judgment of the person conducting the assessment. Discrepancies and differences between the values adopted by different evaluators are expected. Additionally, this set of recommendations does not cover all the possibilities and the final decision on how to classify the parameter is up to the evaluator.

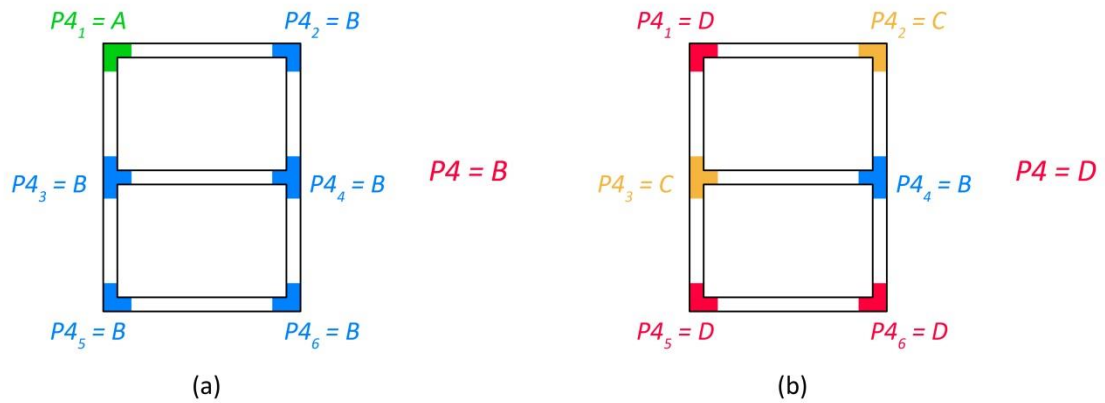


Figure P4-5: In the case of different quality of wall-to-wall connections in the building, the classification provides a qualitative indication on how to classify. As an example: (a) this case shows a building with all workmanlike built wall-to-wall connections with some elements that are related to class A, but not enough to classify as A; and (b) this case shows a very heterogeneous construction, but where most wall-to-wall connections seem to be poor or highly degraded so it was classified as D (plan view)

Doglioni F, Mazzotti P (2007) *Codice di pratica per gli interventi di miglioramento sismico nel restauro del patrimonio architettonico*. Regione Marche, Italy

NIKER (2010) *Inventory of earthquake-induced failure mechanisms related to construction types, structural elements and materials (Report D3.1)*. Italy: New Integrated Knowledge Based Approaches to the Protection of Cultural Heritage from Earthquake-Induced Risk (NIKER) project

Ortega J, Vasconcelos G, Rodrigues H, Correia M, Lourenço PB (2017) *Traditional earthquake resistant techniques for vernacular architecture and local seismic culture: a literature review*. *Journal of Cultural Heritage* 27: 181-196

P5. Horizontal diaphragms

This parameter addresses the construction solutions and materials used to build the horizontal structural elements of vernacular buildings. Timber floors are the most common horizontal diaphragms used in vernacular architecture. They have a critical role in transmitting the lateral earthquake loads to the vertical resisting elements of the structure. Thus, the seismic response of vernacular buildings is strongly dependent on the characteristics of timber diaphragms.

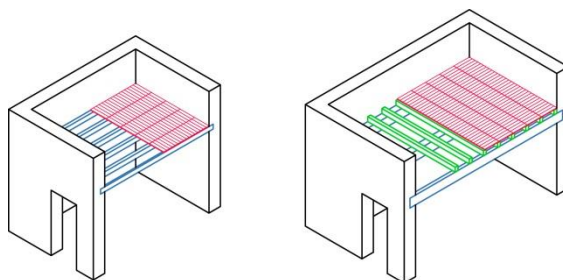


Figure P5-1: Typical layout of traditional timber diaphragms in vernacular buildings: (a) wooden beams covered with cross board sheathing; and (b) two-way traditional timber floor with secondary set of timber joists (Ortega et al. 2018)

Table P5-1: Seismic vulnerability classes according to the type of horizontal diaphragm

P5. Horizontal diaphragms				
Class	Description	Beam-to-wall connection (k_c)	Diaphragm connection (k_{dc})	Diaphragm stiffness (k_d)
A	Rigid diaphragm well-connected to the walls	Good	Good	Rigid
B	Flexible diaphragm well-connected to the walls. Rigid diaphragm well-connected to the walls but beams poorly coupled with the walls. Rigid diaphragm poorly connected to the walls but beams properly coupled with the walls. Poor connections can be either due to construction deficiencies or because of signs of deterioration and decay of the timber elements, such as rotting or biological attacks	Good	Good	Flexible
		Poor	Good	Rigid
		Good	Poor	Rigid
C	Flexible diaphragm well-connected to the walls but beams poorly coupled with the walls. Rigid and flexible diaphragms poorly connected to the walls with beams poorly coupled with the walls. Flexible diaphragms poorly connected to the walls but beams properly coupled with the walls. Diaphragms of negligible stiffness with beams well-connected to the walls achieving a coupling effect. Poor connections can be either due to construction deficiencies or because of signs of deterioration and decay of the timber elements, such as rotting or biological attacks	Poor	Good	Flexible
		Poor	Poor	Rigid
		Good	Poor	Flexible
		Poor	Poor	Flexible
D	Diaphragms of negligible stiffness with beams poorly connected to the walls. Poor connections can be either due to construction deficiencies or because of signs of deterioration and decay of the timber elements, such as rotting or biological attacks	Poor	-	-

The classification shown provides a qualitative description of the type of horizontal diaphragm that belongs to each class. Three aspects are particularly taken into consideration for the classification of the type of horizontal diaphragm: (a) the quality of the connection the beams and the load bearing walls; (b) the quality of the connection between the diaphragms and the load

bearing walls; and (c) the in-plane stiffness of timber diaphragms. As shown in Fig. P5-1, timber floor construction in vernacular architecture is usually very simple, consisting of wooden beams covered with cross boards directly nailed to the beams composing the sheathing. When larger spans are required, two-way floors are commonly used, which add a secondary set of timber joists perpendicular to the main contribution of the flexural and shear deformation of the single cross boards and the rigid rotation beams. The overall in-plane flexibility of this type of single sheathing timber floors results from the contribution of the flexural and shear deformation of the single cross boards and the rigid rotation of the board due to nail slip.

Since timber beams are the main structural element composing traditional horizontal diaphragms, the behavior of the diaphragm is clearly different in the two orthogonal directions: perpendicular and parallel to the main beam axis. That is why a different class can be considered according to the loading direction under evaluation. In terms of construction, there are different ways of achieving a proper diaphragm-to-wall connection in both directions. Primary beams are usually only linked with the perpendicular walls by means of partial embedment of the timber beams within the masonry or rammed earth walls. Nevertheless, there are different traditional ways of ensuring a tight connection between both elements.

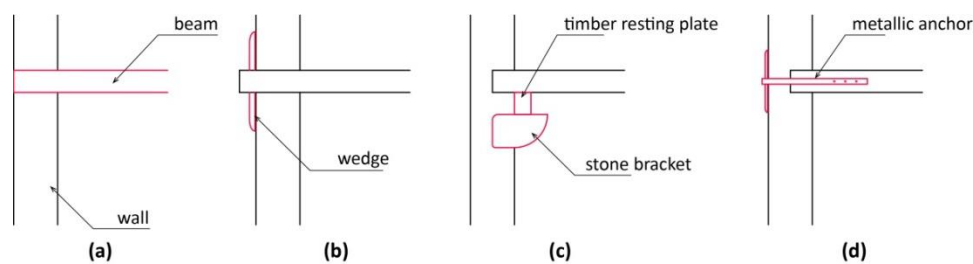


Figure P5-2: Different types of reinforced beam-to-wall connections: (a) timber beam resting on the whole width of the wall; (b) timber wedges; (c) timber resting plates and stone brackets; and (d) metallic anchoring devices (Ortega et al. 2017)

Proper detailing is also required to ensure shear transfer connection between the diaphragm and the load bearing walls parallel to the primary timber beams. Many times, the connection between both elements is barely nonexistent. A beam is placed adjacent to the wall, but there is no structural element linking diaphragm and wall. Their connection relies solely on friction. Metallic anchor keys and ties have been traditionally applied with the purpose of connecting two or three consecutive beams to the walls. Perimeter steel elements can also further or alternatively ensure the diaphragm-to-wall connection. In cases where there is a change in the section of the wall, the beam can typically rest on the set-back, which provides a better support and helps to transfer the shear through friction. For two-way floors, the secondary set of timber joists perpendicular to the main beams can be properly connected to the walls by means of partial embedment or by any of the solutions shown in Fig. P5-2 for connecting beams to perpendicular walls.

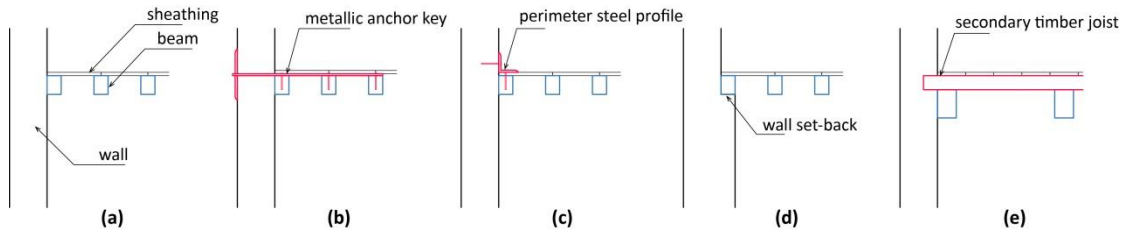


Figure P5-3: (a) Lack of connection between the beams and the parallel walls; (b) metallic anchor keys anchoring the beams to the walls; (c) use of perimeter steel profiles; (d) beams resting on the set-back of the wall; and (e) secondary timber joists partially embedded in the wall (Ortega et al. 2018)

The overall stiffness of the diaphragm can be thus considered as the combination of the in-plane stiffness of the diaphragm and the stiffness of the connection between the diaphragm and the walls. The quality of the diaphragm-to-wall connection can be evaluated based on the typical structural solutions previously discussed. Taking into account that vernacular diaphragm structural systems typically consist of wooden beams and timber board sheathing, the influence of the quality of the connection between the main beams and the perpendicular walls and between the whole diaphragm and the perimeter walls can be assessed independently. Table P5-1 is prepared taking into account different combinations of these different aspects.

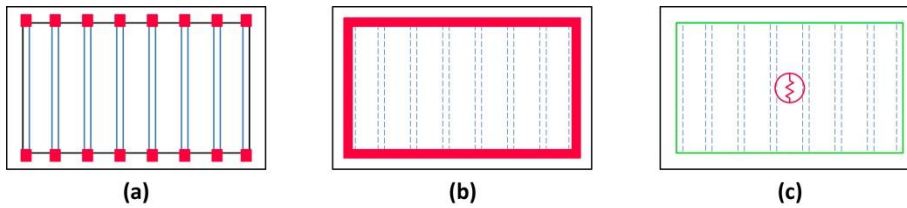


Figure P5-4: Construction aspects taken into consideration for the classification of the type of horizontal diaphragm: (a) level of connection between timber beams and walls; (b) level of connection between the diaphragm and the walls; and (c) stiffness of the diaphragm (Ortega et al. 2018)

It is acknowledged that, many times, some construction aspects, such as the level of connection between the structural elements cannot be detected with the naked eye. The classification should be thus carried out on the basis of information of other similar buildings in the region, if existing. In the case of no information, it is recommended to assume the worst case scenario. The following diagrams show some recommendations on how to consider the values for this parameter for different conditions. It is noted that the final value adopted will ultimately depend on the qualitative judgment of the person conducting the assessment. Discrepancies and differences between the values adopted by different evaluators are expected. Additionally, this set of recommendations does not cover all the possibilities and it will be up to the evaluator, the final decision on how to determine the final class for the horizontal diaphragms. A different class can be considered according to the direction evaluated because of the abovementioned characteristics of vernacular timber diaphragms:

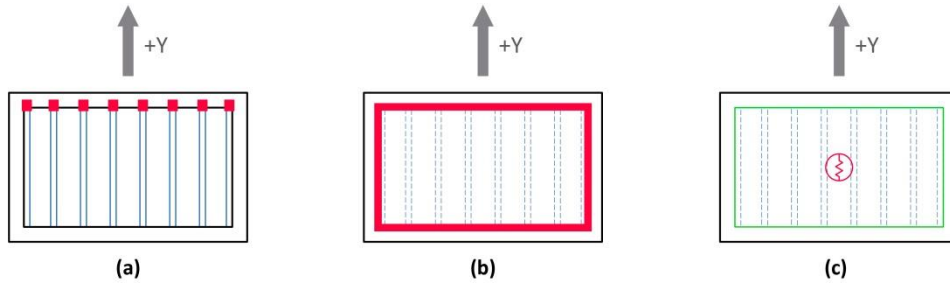


Figure P5-5: In the case above, when evaluating loading direction +Y, which is parallel to the beams direction, the quality of the beam-to-wall connection is crucial, together with the quality of the diaphragm-to-wall connection and the diaphragm stiffness

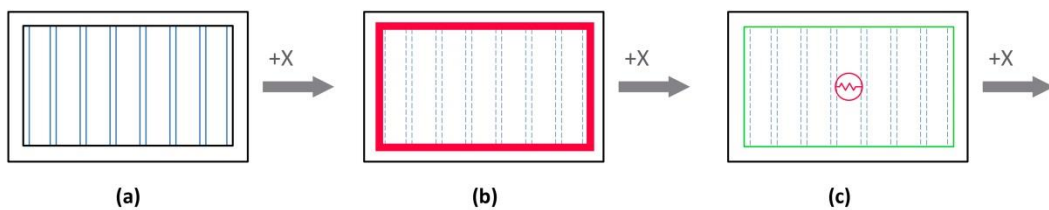
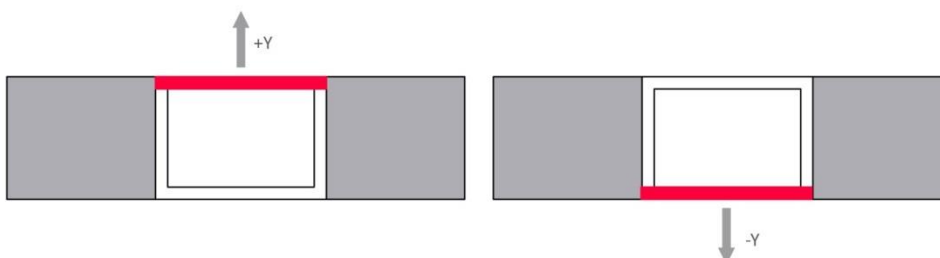


Figure P5-6: On the other hand, in the case above when evaluating loading direction +X, which is perpendicular to the beams direction, the quality of the beam-to-wall connection is negligible, since they do not have such an influence in distributing the load to the in-plane walls. In this direction, only the quality of the diaphragm-to-wall connection and the diaphragm stiffness will determine the class for the horizontal diaphragm

Let's assume that in the example in the diagrams above the diaphragm is simply composed by beams well connected to the walls and single board sheathing of negligible stiffness poorly connected to the walls. When evaluating +/-Y direction, a class C could be considered, while when evaluating +/-X direction, a class D should be considered because the beneficial coupling effect of the beams does not take place in this direction.

In general for the assessment of a building, a direction should not be considered if there is an adjacent building blocking the possible out-of-plane rotation of the wall perpendicular to the loading direction evaluated.



P5-7: In the case above, only the direction +Y and -Y should be evaluated because walls perpendicular to loading direction +X and -X are not likely to fail out-of-plane because of the presence of an adjacent building (plan view)

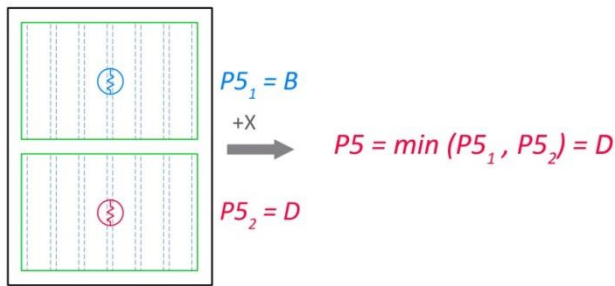


Figure P5-8: In the case of different types of horizontal diaphragms along the building, the worst class should be adopted (plan view)

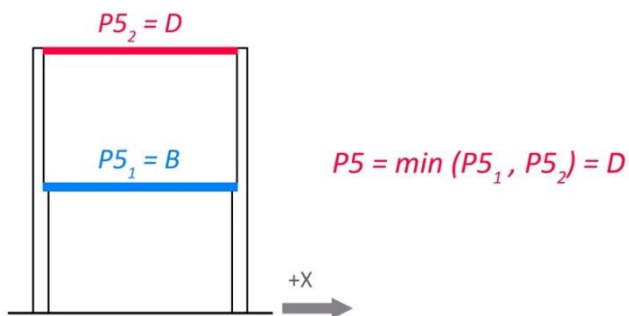


Figure P5-9: In the case of different types of horizontal diaphragms along the height of the building, the worst class should be adopted (section view)

Ortega J, Vasconcelos G, Rodrigues H, Correia M, Lourenço PB (2017) *Traditional earthquake resistant techniques for vernacular architecture and local seismic culture: a literature review*. Journal of Cultural Heritage 27: 181-196

Ortega J, Vasconcelos G, Rodrigues H, Correia M (2018) *Assessment of the influence of horizontal diaphragms on the seismic performance of vernacular buildings*. Bulletin of Earthquake Engineering

P6. Roof thrust

This parameter evaluates the influence of the type of roofing system, specifically taking into account the thrust exerted by the roof, which may anticipate the out-of-plane collapse mechanism of the load bearing walls supporting the roof. There are particular types of roofing structural systems that can be observed in vernacular buildings that exert lateral thrust. This thrust-exerting roof types are mainly composed by rafters with no intermediate support, whose feet are fixed at a wall plate, but are not properly connected among them at the ridge. Thus, rafters subjected to vertical loads push the supporting walls at their top.

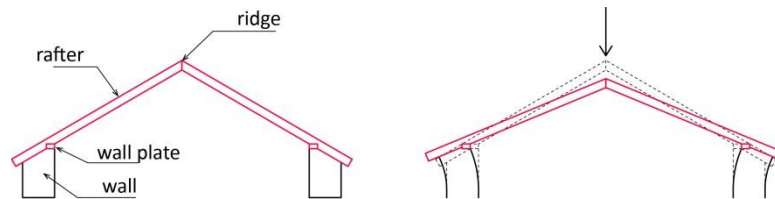


Figure P6-1: Common behavior of thrust-exerting roofing structural systems

Table P6-1: Seismic vulnerability classes according to the type of horizontal diaphragm

P6. Roof thrust	
Class	Description
A	Non-thrusting roof types and semi-thrusting roof types with light-weight and high inclination
B	Thrusting roof types with light-weight ($w < 0.9 \text{ kN/m}^2$) and high inclination ($\alpha > 35^\circ$). Semi-thrusting roof types with light-weight and low inclination ($\alpha < 20^\circ$) or heavy roof types ($w > 0.9 \text{ kN/m}^2$) with high inclination ($\alpha > 35^\circ$)
C	Thrusting roof types with light-weight ($w < 0.9 \text{ kN/m}^2$) and medium inclination ($20^\circ < \alpha < 35^\circ$) or heavy roof types ($w > 0.9 \text{ kN/m}^2$) with high inclination ($\alpha > 35^\circ$). Semi-thrusting heavy roof types ($w > 0.9 \text{ kN/m}^2$) with medium-high inclination ($20^\circ < \alpha < 35^\circ$)
D	Thrusting roof types with light-weight ($w < 0.9 \text{ kN/m}^2$) and low inclination ($\alpha < 20^\circ$) or heavy roof types ($w > 0.9 \text{ kN/m}^2$) with medium-high inclination ($\alpha < 35^\circ$)

The classification shown provides a qualitative description of the type of roofing structural system according to the: (a) thrusting nature of the roofing system; (b) roof weight; (c) roof inclination. All these aspects can be usually determined by means of exterior visual inspection. Regarding the thrusting nature, some roof structural types do not exert lateral thrust simply because of their geometry or because of the addition of specific structural elements. Collar roofs with tie beams or ceiling joists can make use of horizontal roof elements to absorb the horizontal thrust. Truss roofs use the structural framework and the different diagonal and horizontal elements to exert only vertical loads on the supporting walls. Shed roofs or single roof systems composed only by rafters, but having an intermediate support can also highly reduce the thrust because of the proper vertical support at the ridge. The presence of other structural elements, such as ring beams at the top of the wall, tying the rafters together, can also help in reducing the detrimental effects of thrust-exerting roof types.

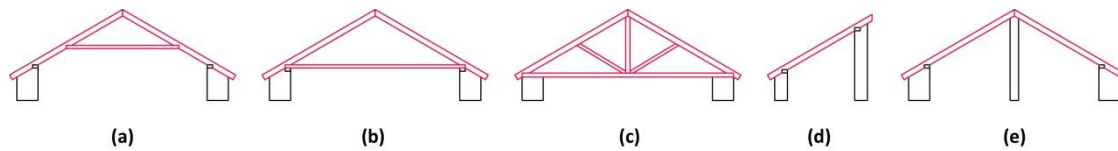


Figure P6-2: (a-c) Different non-thrust exerting roofing types and (d-e) semi-thrusting roof types

Post-earthquake damage observation has shown how the failure mode of the buildings many times involves the out-of-plane bending failure of exterior walls. The additional horizontal load created by an incorrectly designed roof can certainly anticipate this failure. This horizontal loading can also increase the stresses at the corners and induce damage at these points. Therefore, the type of roof and its ability to exert or not thrust onto the supporting walls is a key aspect regarding the seismic behavior of vernacular buildings. Roof may vary from thrusting types with considerable weight and low inclination to non-thrusting types. Semi-thrusting roof types are also included in the classification as a middle ground between non-thrust exerting and exerting roofing systems.

The roof type (mono-pitched roof, dual-pitched or gable roof, hipped roof, etc.) also causes that some walls may receive the roof thrust while others do not. That is why a different class can be considered according to the loading direction under evaluation.

It is acknowledged that, many times, some construction aspects, such as the existence of collar beams or horizontal roof elements absorbing the horizontal thrust cannot be detected with the naked eye. The classification should be thus carried out on the basis of information of other similar buildings in the region, if existing. In the case of no information, it is recommended to assume the worst case scenario.

The following diagrams show some recommendations on how to consider the values for this parameter for different conditions. It is noted that the final value adopted will ultimately depend on the qualitative judgment of the person conducting the assessment. Discrepancies and differences between the values adopted by different evaluators are expected. Additionally, this set of recommendations does not cover all the possibilities and it will be up to the evaluator, the final decision on how to determine the final class for the roof thrust.

A different class can be thus considered according to the direction evaluated because of the abovementioned different shapes that vernacular roofs present. The class adopted for each direction should finally depend on the thrust considered to be applied on the walls perpendicular to the direction assessed, which will be the walls more prone to suffer an out-of-plane failure.

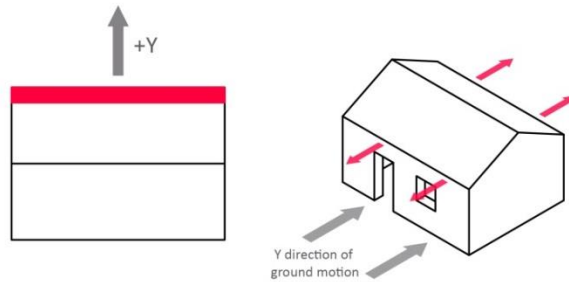


Figure P6-3: In the case above, when evaluating loading direction +Y, which is parallel to the slope direction of the roof, the wall perpendicular to the loading direction is subjected to both the seismic action and the possible roof thrust (plan and 3D view)

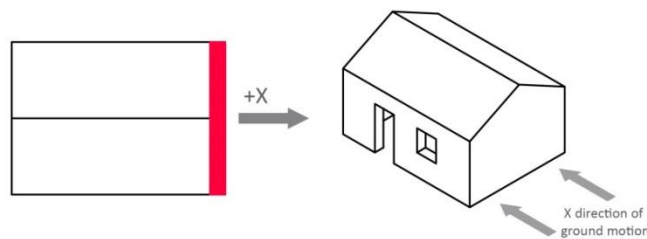


Figure P6-4: On the other hand, in the case above, when evaluating loading direction +X, which is perpendicular to the slope direction of the roof, the wall perpendicular to the loading direction is only subjected to the seismic. The possible roof thrust does not affect the wall under consideration, neither anticipates its possible out-of-plane failure (plan and 3D view)

Let's assume that in the example above, the roof type is considered to be thrust-exerting and is lightweight with low inclination. When evaluating +/-Y direction, a class C could be considered, while when evaluating +/-X, a class A should be considered because the roof exert no thrust in this direction.

In general for the assessment of a building, a direction should not be considered if there is an adjacent building blocking the possible out-of-plane rotation of the wall perpendicular to the loading direction evaluated.

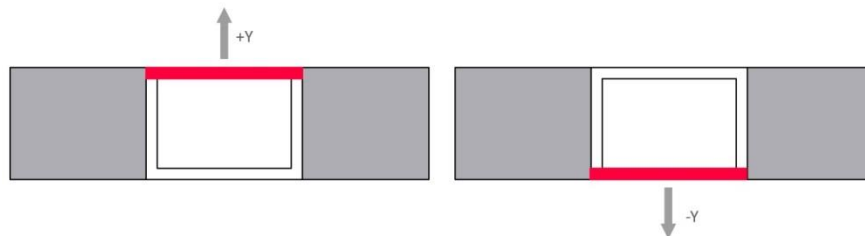


Figure P6-5: In the case above, only the direction +Y and -Y should be evaluated because walls perpendicular to loading direction +X and -X are not likely to fail out-of-plane because of the presence of an adjacent building (plan view)

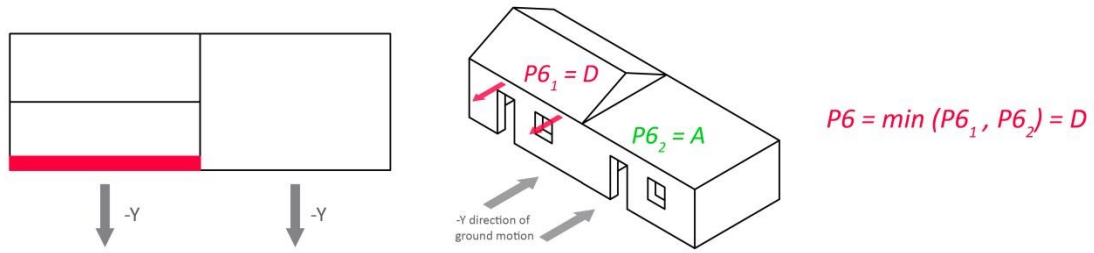


Figure P6-6: In the case of different types of roof along the building, the worst class should be adopted (plan and 3D view)

P7a. Wall openings (out-of-plane)

The parameter that take into account the number and area of wall openings was divided into two: P7a and P7b. This distinction is made in order to differentiate the amount of wall openings observed in the walls perpendicular to the loading direction from those present in the walls parallel to the loading direction. Both parameters are measured as a ratio between the area of wall openings and the area of the walls, ranging between 0 and 1. However, the classes are defined taking into account only the ratio of openings in the in-plane walls because the presence of openings mainly affects the in-plane resistance of the walls.

The presence of wall openings in the walls perpendicular to the seismic load has a lesser influence, but was also taken into account. Therefore, P7a addresses this aspect and accounts for the maximum area of wall openings observed in a wall perpendicular to the loading direction, and is measured as a percentage of total area of the considered wall.

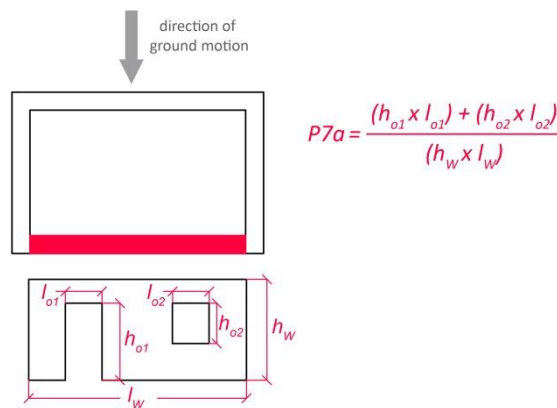


Figure P7a-1: Definition of the ratio P7a concerning the area of wall openings in the walls perpendicular to the loading direction

Vernacular buildings in rural areas generally present a reduced area of wall openings, but it is very variable. The area of wall openings can increase significantly if the building is located in an urban environment. Since one of the most important factors controlling the out-of-plane response of the walls is their mass, models with a greater area of wall openings and subsequent lighter walls typically behave better against horizontal loading.

The following diagrams show some recommendations on how to consider the values for this parameter for different conditions. It is noted that the final value adopted will ultimately depend on the qualitative judgment of the person conducting the assessment. Discrepancies and differences between the values adopted by different evaluators are expected. Additionally, this set of recommendations does not cover all the possibilities and it will be up to the evaluator, the final decision on how to determine the final value of the area wall openings in the walls perpendicular to the loading direction.

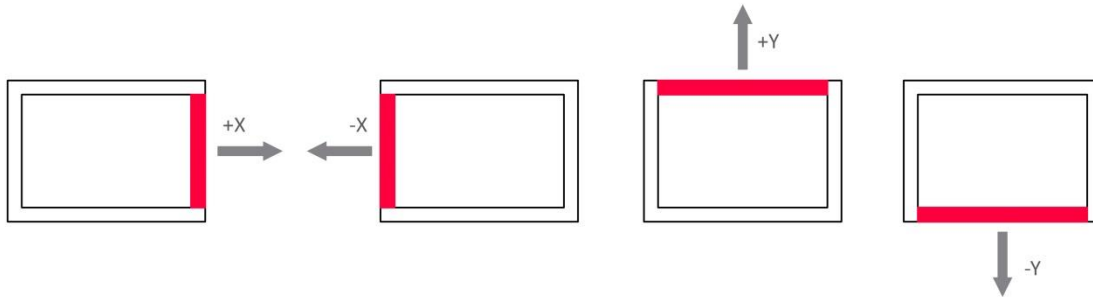


Figure P7a-2: Wall to consider according to the loading direction evaluated (plan view)

In general for the assessment of a building, a direction should not be considered if there is an adjacent building blocking the possible out-of-plane rotation of the wall perpendicular to the loading direction evaluated.

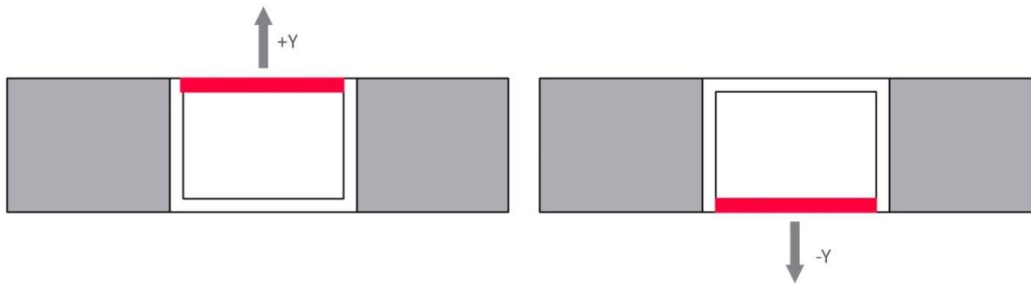


Figure P7a-3: In the case above, only the direction +Y and -Y should be evaluated because walls perpendicular to loading direction +X and -X are not likely to fail out-of-plane because of the presence of an adjacent building (plan view)

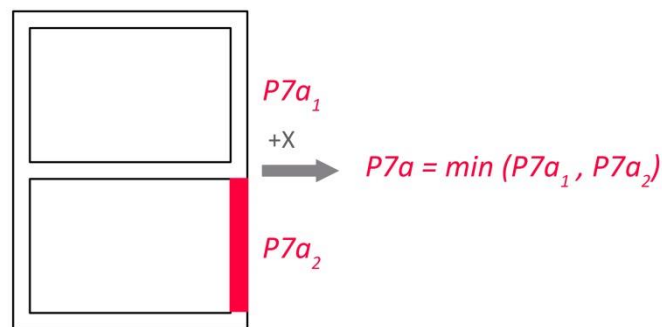


Figure P7a-4: In the case of walls presenting different ratio P7a of wall openings in a specific direction, the minimum value should be adopted in order to be on the safe side (plan view)

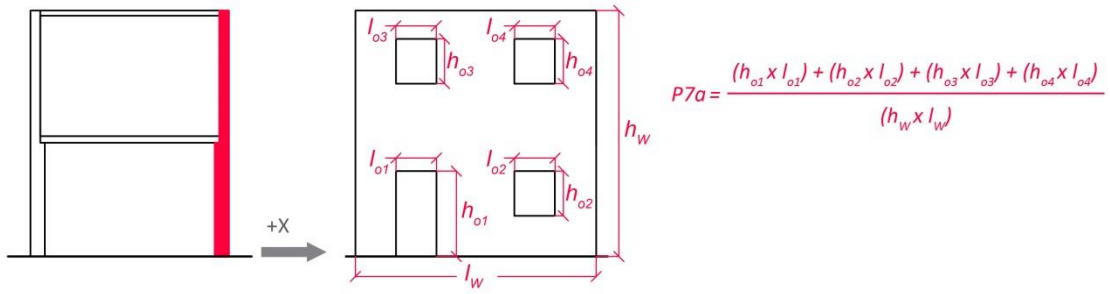


Figure P7a-5: When evaluating buildings with more than one floor, the ratio P7a of wall openings can be obtained by taking into account the whole height of the wall (section and elevation view)

P7b. Wall openings (in-plane)

This parameter that take into account the number and area of wall openings was divided into two: P7a and P7b. This distinction is made in order to differentiate the amount of wall openings observed in the walls perpendicular to the loading direction from those present in the walls parallel to the loading direction. Both parameters are measured as a ratio between the area of wall openings and the area of the walls, ranging between 0 and 1. However, the classes are defined taking into account only the ratio of openings in the in-plane walls because the presence of openings mainly affects the in-plane resistance of the walls.

P7b thus refers to the area of wall openings in the in-plane walls, which accounts for the total area of wall openings observed in all the walls parallel to the loading direction, and is measured also as a percentage of the total surface area of all in-plane walls.

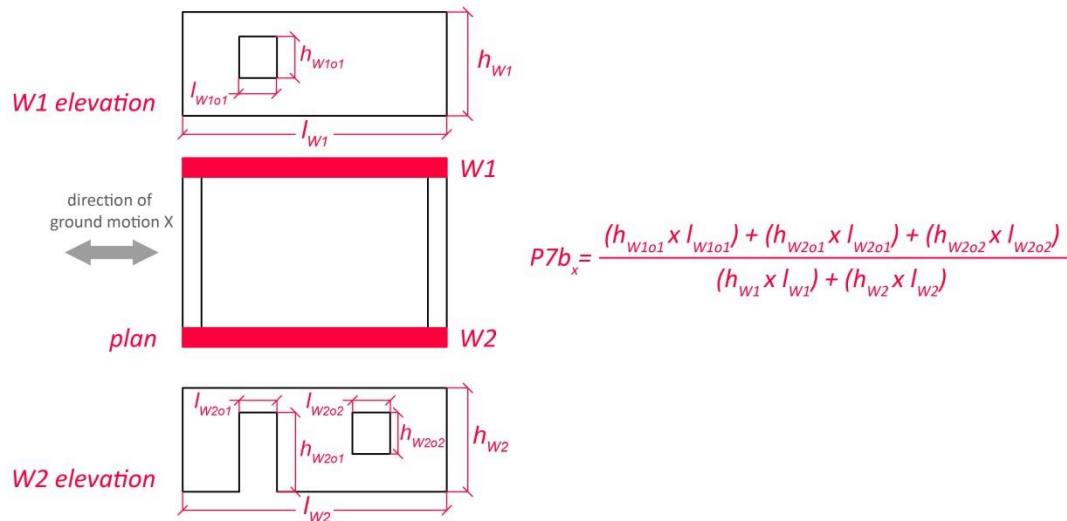


Figure P7b-1: Definition of the ratio P7b concerning the area of wall openings in the walls parallel to the loading direction

Table P7b-1: Seismic vulnerability classes according to the wall openings (P7b)

P7. Wall openings	
Class	Description
A	$IP < 10\%$
B	$10\% \leq IP < 25\%$
C	$25\% \leq IP < 40\%$
D	$IP \geq 40\%$

The presence of wall openings can be particularly influential on the seismic behavior of vernacular buildings when they are prone to suffer in-plane damage, such as when presently sufficiently stiff diaphragms able to avoid premature out-of-plane collapses. Damage patterns

observed after earthquakes show that the crack lines often follow the distribution of the façade openings, revealing the vulnerability induced by these elements. Vernacular buildings in rural areas generally present a reduced area of wall openings, but it is very variable. The area of wall openings can increase significantly if the building is located in an urban environment.

The following diagrams show some recommendations on how to consider the values for this parameter for different conditions. It is noted that the final value adopted will ultimately depend on the qualitative judgment of the person conducting the assessment. Discrepancies and differences between the values adopted by different evaluators are expected. Additionally, this set of recommendations does not cover all the possibilities and it will be up to the evaluator, the final decision on how to determine the final value of the area wall openings in the walls parallel to the loading direction.

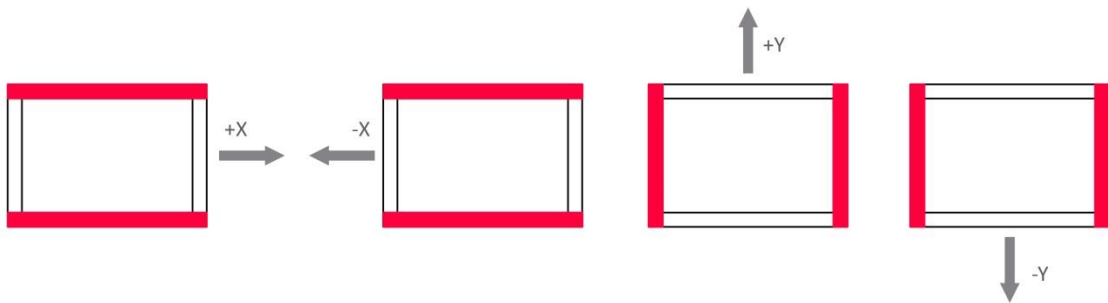


Figure P7b-2: Walls to consider according to the loading direction evaluated (plan view)

In general for the assessment of a building, a direction should not be considered if there is an adjacent building blocking the possible out-of-plane rotation of the wall perpendicular to the loading direction evaluated.

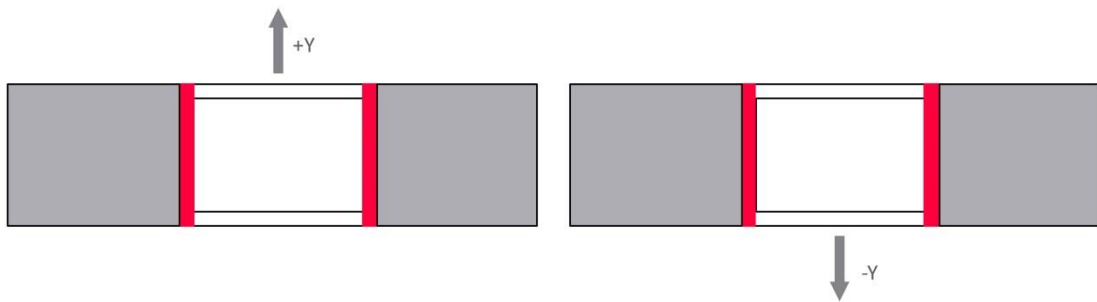


Figure P7b-3: In the case above, only the direction +Y and -Y should be evaluated because walls perpendicular to loading direction +X and -X are not likely to fail out-of-plane because of the presence of an adjacent building (plan view)

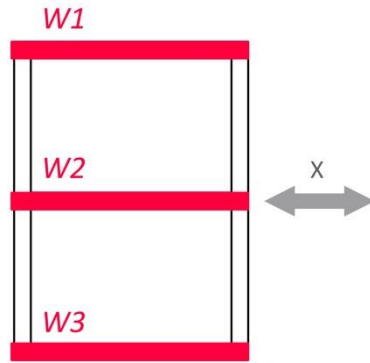


Figure P7b-4: All earthquake resistant walls in the main direction under evaluation and the total area of wall openings in them should be taken into account (plan view)

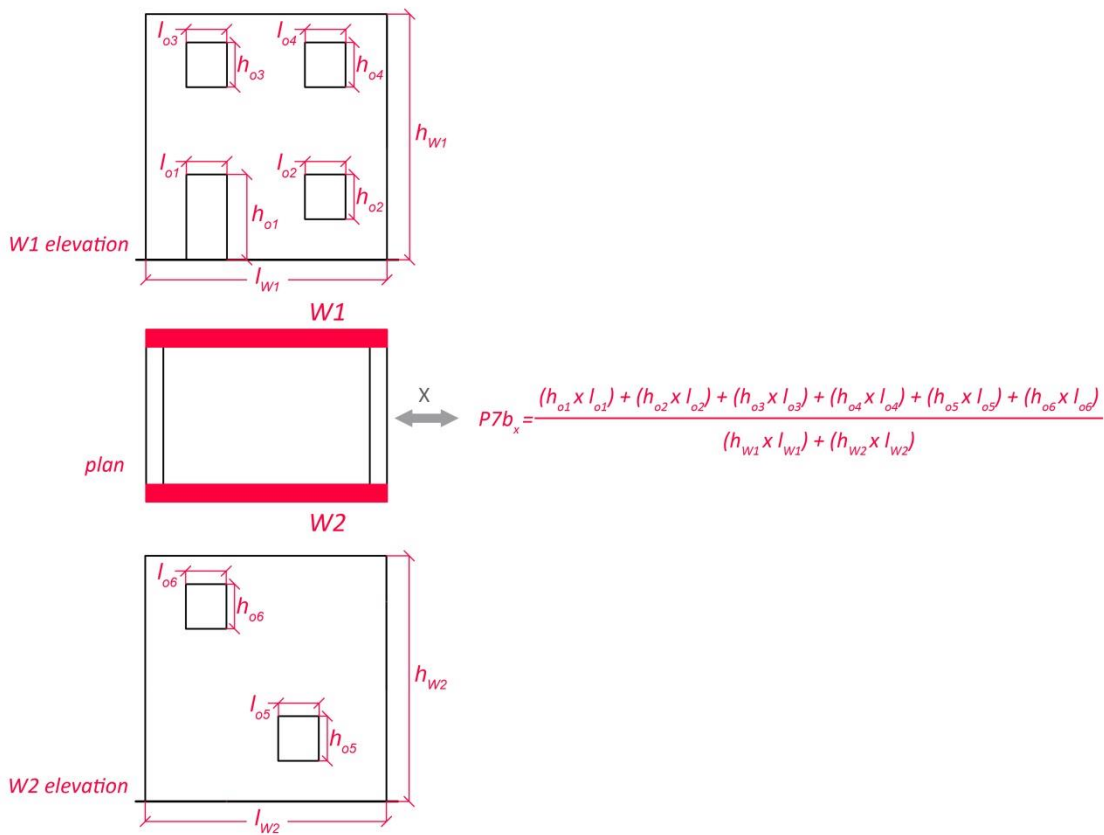


Figure P7b-5: When evaluating buildings with more than one floor, the ratio P7b of wall openings can be obtained by taking into account the whole height of the wall (plan and elevation view)

P8. Number of floors

This parameter takes into account the number of floors (N) of the studied buildings. Taller buildings tend to be more vulnerable to earthquakes because the center of gravity is raised and, thus, the lateral loads on the bearing walls increase during the seismic action.

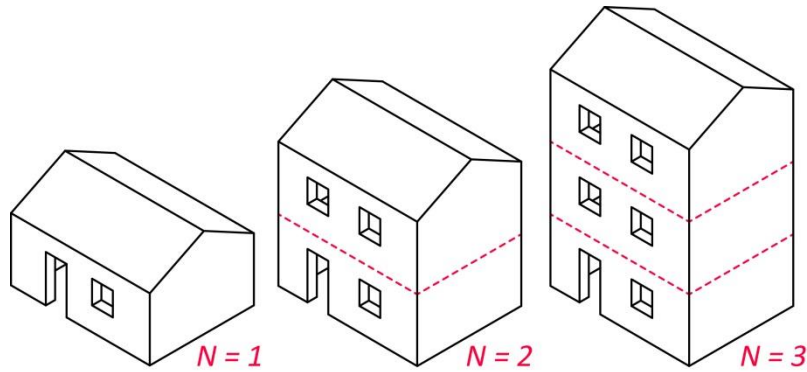


Figure P8-1: Definition of the number of floors (N)

Table P8-1: Seismic vulnerability classes according to the number of floors (N)

P8. Number of floors	
Class	Description
A	1 floor
B	-
C	2 floors
D	≥ 3 floors

Vernacular buildings are typically not too high. In the rural environment, rammed earth constructions usually extend horizontally and are composed by a single story, but in the urban context they rarely present more than two stories. Stone masonry vernacular buildings in the urban context can easily present up to four stories, particularly when arranged in aggregates, such as in most European historical city centers. Since the seismic vulnerability of two-floor vernacular buildings typically present a highly reduced maximum capacity when compared with one-floor buildings, there is no Class B for this parameter.

The following diagrams show some recommendations on how to consider the values for this parameter for different conditions. It is noted that the final value adopted will ultimately depend on the qualitative judgment of the person conducting the assessment. Discrepancies and differences between the values adopted by different evaluators are expected. Additionally, this set of recommendations does not cover all the possibilities and it will be up to the evaluator, the final decision on how to determine the final value of number of floors.

The number of floors may vary when evaluating different loading directions because of buildings being constructed in a slope or because of ground level differences on the site. That is why this parameter is also evaluated for the four main directions.

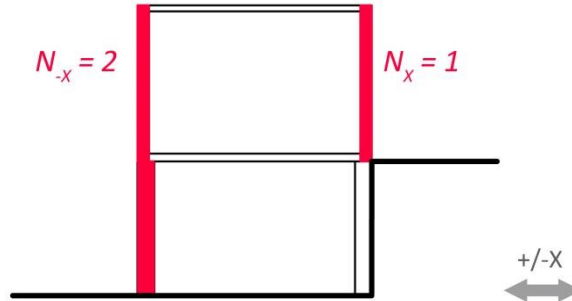


Figure P8-2: When there are ground level differences or the building is built in a slope, the number of floors may vary depending on the loading direction under evaluation (section view)

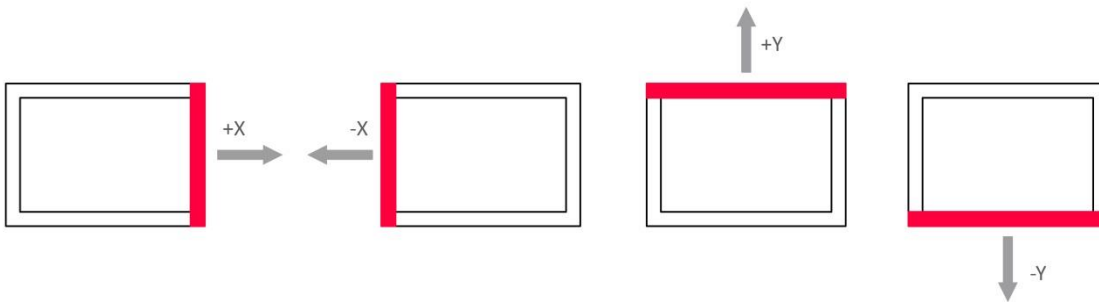


Figure P8-3: Wall to consider according to the loading direction evaluated (plan view)

In general for the assessment of a building, a direction should not be considered if there is an adjacent building blocking the possible out-of-plane rotation of the wall perpendicular to the loading direction evaluated.

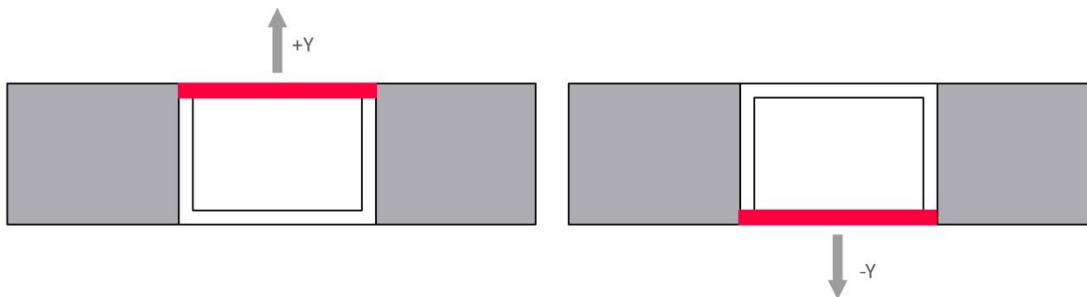


Figure P8-4: In the case above, only the direction +Y and -Y should be evaluated because walls perpendicular to loading direction +X and -X are not likely to fail out-of-plane because of the presence of an adjacent building (plan view)

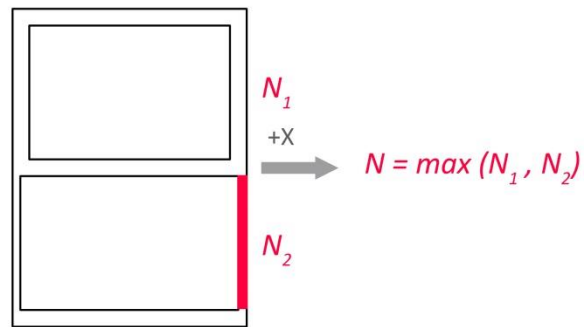


Figure P8-5: In the case of difference in the number of floors for different walls in the same direction because of ground level differences, the maximum value should be adopted (plan view)

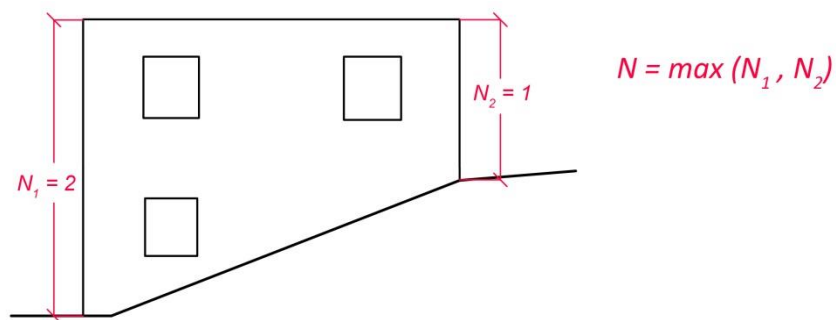


Figure P8-6: In the case of difference in height along the wall length because of the building being built in a slope, the maximum number of floors observed in the wall should be adopted (elevation view)

P9. Previous structural damage

This parameter takes into account the state of conservation of the building, but focuses on the existing damage that can be observed, mainly addressing the degree of degradation of the structural elements of the building (i.e. the walls). Generally, a critical reason for the vernacular heritage to be so vulnerable to earthquakes is the fact that they are in an advanced state of deterioration, as a result of poor maintenance and abandonment. Weakening signs in the structural load bearing walls of the building, such as cracks and deformations, may aggravate damage in the event of an earthquake, increasing its vulnerability.

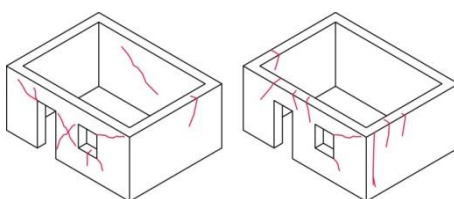


Figure P9-1: Existing structural damage and visible cracks in the building

Table P9-1: Seismic vulnerability classes according to the previous structural damage

P9. Previous structural damage	
Class	Description
A	Structural load bearing walls are in good condition with no visible damage
B	Structural load bearing walls present not widespread hairline and small cracks (≈ 1 mm or less) , and/or slight signs of deformation in the structural elements (drifts below 0.1%)
C	Structural load bearing walls present a poor state of conservation showing moderate cracks ($\approx 1-5$ mm) and/or relevant signs of deformation in the structural elements (drifts between 0.1-0.5%)
D	Structural load bearing walls present a state of severe deterioration with widespread damage. There are large structurally compromising cracks (> 5 mm) at critical locations, such as near the corners, indicating a sign of disconnection between orthogonal walls. There are severe signs of deformation in the structural elements, such as out-of-plumb walls or bulging of the load bearing walls (drifts over 0.5%)

A poor maintenance and abandonment is common in many vernacular buildings, which may present an advanced state of deterioration of the materials and often results in previous structural damage going unrepaired, such as widespread cracking at the walls. Existing cracks increase the vulnerability of specific parts of the structure and can anticipate the failure of the structure. This parameter is specifically focused on the state of degradation of the load bearing walls of the building. This method proposes to measure the degree of damage according to the maximum crack size, following recommendations by Masciotta et al. (2016):

Table P9-2: Classification of damage according to existing cracks (Masciotta et al. 2016)

Degree of damage	Description	Crack width
No visible damage	No visible damage	-
Slight damage	Hairline and fine cracks	~ 1 mm
Moderate damage	Moderate cracks	~ 1 mm to 5 mm
Severe damage	Large cracks impairing functionality	> 5 mm

The vulnerability classes are defined in terms of the visible damage observed in the buildings and on the estimation of the cracks opening. Therefore, a visual inspection of the buildings should be complemented with a detailed damage survey, particularly focused on the cracking state of the structural elements.

It is acknowledged that, many times, this detailed damage survey is not possible and only an exterior visual inspection can be carried out. The classification should be thus carried out on the basis of information of other similar buildings in the region, if existing. Nonetheless, in cases of doubt, it is recommended to assume the worst case scenario.

The class assigned to this parameter is global and represents the state of conservation of the whole building, since previous damage can compromise both the out-of-plane and in-plane behavior of the building. It is noted that the final value adopted will ultimately depend on the qualitative judgment of the person conducting the assessment. Discrepancies and differences between the values adopted by different evaluators are expected. Additionally, this set of recommendations does not cover all the possibilities and the final decision on how to classify the parameter is up to the evaluator.

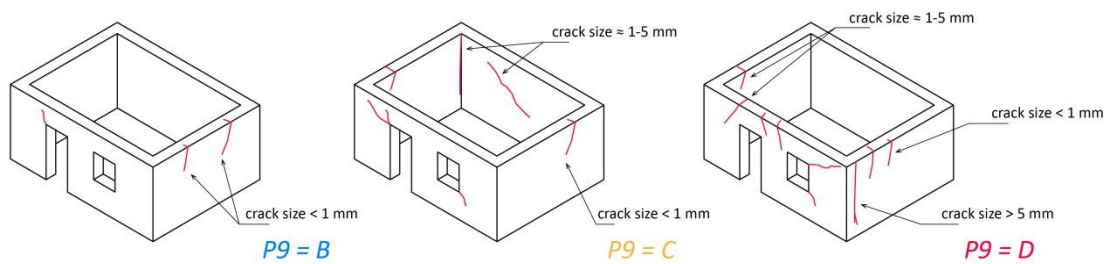


Figure P9-2: Examples of recommendations on how to consider different classes according to the maximum crack size observed in the building (3D view)

Masciotta MG, Ramos LF, Lourenço PB, Matos JAC (2016) *Development of key performance indicators for the structural assessment of heritage buildings*. In Proc. of 8th European Workshop on Structural health monitoring (EWSHM 2016), 5-8 July, Bilbao, Spain

P10. In-plane index

This parameter is defined by the in-plane ratio (γ_i), which provides information about the in-plane stiffness of the structure along each main axis. γ_i is defined as the ratio between the in-plan area of the earthquake resistant walls (length x thickness) in each main direction and the total in-plan area of the earthquake resistant walls. The ratio thus ranges between 0 and 1. Values close to 0.5 indicate that the in-plan configuration of the building is well-balanced. On the other hand, values deviating significantly from 0.5 will indicate that one direction is clearly predominant and that there is an asymmetry in the amount of earthquake resistant walls in each main direction. As a result, the building may present a weaker direction.

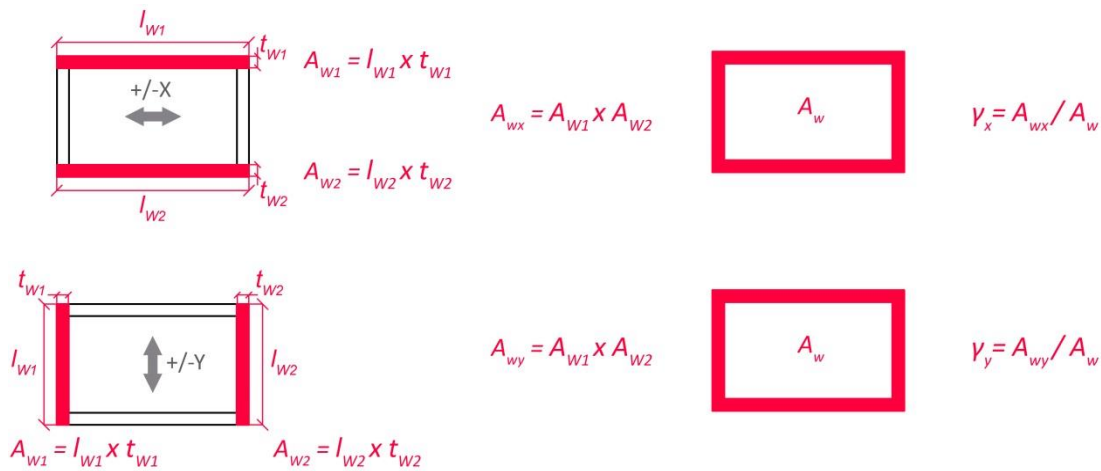


Figure P10-1: Definition of the in-plan area of earthquake resistant walls in each main direction (A_{wi}) that defines the in-plane ratio (γ_i)

Table P10-1: Seismic vulnerability classes according to the in-plane index (γ_i)

P10. In-plane index	
Class	Description
A	$\gamma_i \geq 0.65$
B	$0.55 \leq \gamma_i < 0.65$
C	$0.45 \leq \gamma_i < 0.55$
D	$\gamma_i < 0.45$

The in-plane index (γ_i) addresses the conventional shear strength of the walls by taking into account their distribution in the in-plan configuration of the building. The seismic capacity of a building may be jeopardized when it presents an unbalanced area of resisting walls in the two orthogonal directions. This parameter thus gives a measure of the in-plane stiffness of the structure in each main direction and can be considered as an indicator of the feasible seismic performance of the building (Lourenço et al. 2013). Since this index provides an estimation of the shear strength in each orthogonal direction, it can also be considered as an indicator of the in-

plan irregularity of the building. It is noted that the classification according to this parameter only requires knowing roughly the geometry of the building, which can be obtained by means of simple visual inspection.

The in-plane index (γ_i) intends to characterize the ability of a vernacular building to resist the seismic action through the development of in-plane resisting mechanisms of the shear walls. However, shear walls are only effective in contributing to the global seismic resistance of the building if premature out-of-plane failure mechanisms are prevented. Typically, this is only the case when the building presents sufficiently stiff diaphragms that can ensure an adequate transmission of the seismic action among the different structural elements of the building.

The following diagrams show some recommendations on how to consider the values for this parameter for different conditions. It is noted that the final value adopted will ultimately depend on the qualitative judgment of the person conducting the assessment. Discrepancies and differences between the values adopted by different evaluators are expected. Additionally, this set of recommendations does not cover all the possibilities and it will be up to the evaluator, the final decision on how to determine the final value of the in-plane index (γ_i) in each main direction.

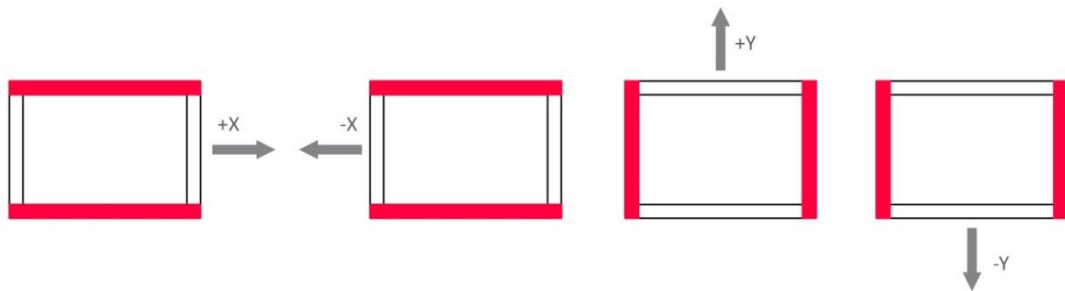


Figure P10-2: Walls to consider according to the loading direction evaluated (plan view)

In general for the assessment of a building, a direction should not be considered if there is an adjacent building blocking the possible out-of-plane rotation of the wall perpendicular to the loading direction evaluated.

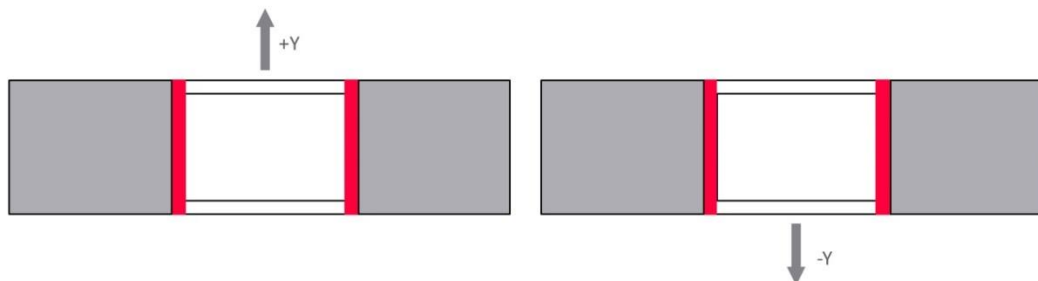


Figure P10-3: In the case above, only the direction +Y and -Y should be evaluated because walls perpendicular to loading direction +X and -X are not likely to fail out-of-plane because of the presence of an adjacent building (plan view)

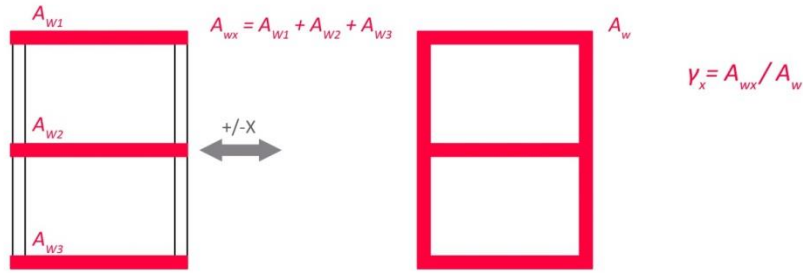


Figure P10-4: All earthquake resistant walls in the main direction under evaluation should be taken into account (plan view)

As previously discussed, the in-plane index (γ_i) is particularly influential on the seismic behavior of vernacular buildings when they are prone to suffer in-plane damage, such as when presently sufficiently stiff diaphragms able to avoid a premature out-of-plane collapse of the building. That is why this parameter should classify differently when presenting different types of horizontal diaphragm. The value of the in-plane index considered in all directions should be the minimum calculated, unless the building presents class A or B types of diaphragm (P5), able to redistribute the load to the earthquake resistant walls in the loading direction. This recommendation is aimed at taking into account the worst possible scenario in order to be on the safe side. Therefore, if there is no rigid diaphragm, the possible beneficial contribution of the in-plane walls on the seismic response of the building should not be taken into account.

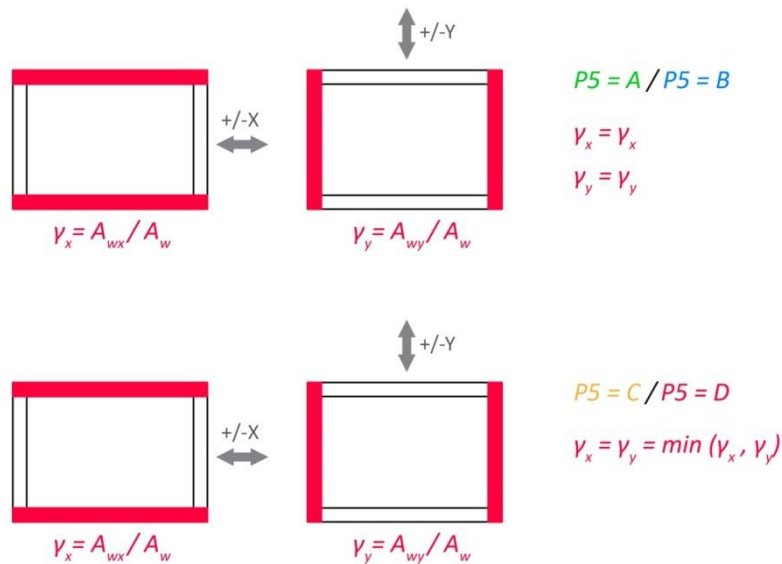


Figure P10-5: When evaluating buildings with type C or D horizontal diaphragm, the in-plane index (γ_i) should be the minimum obtained from two directions (plan view)